## Related titles

*The Transport Properties of Concrete*
(ISBN 978-1-78242-306-5)

*Eco-Efficient Construction and Building Materials*
(ISBN 978-0-85709-767-5)

*Understanding the Tensile Properties of Concrete*
(ISBN 978-0-85709-045-4)

Woodhead Publishing Series in Civil and Structural Engineering: Number 64

# Marine Concrete Structures

## Design, Durability and Performance

*Edited by*

*Mark G. Alexander*



AMSTERDAM • BOSTON • CAMBRIDGE • HEIDELBERG
LONDON • NEW YORK • OXFORD • PARIS • SAN DIEGO
SAN FRANCISCO • SINGAPORE • SYDNEY • TOKYO
Woodhead Publishing is an imprint of Elsevier



Woodhead Publishing is an imprint of Elsevier
The Officers' Mess Business Centre, Royston Road, Duxford, CB22 4QH, UK
50 Hampshire Street, 5th Floor, Cambridge, MA 02139, USA
The Boulevard, Langford Lane, Kidlington, OX5 1GB, UK

Copyright © 2016 Elsevier Ltd. All rights reserved.

No part of this publication may be reproduced or transmitted in any form or by any means, electronic or mechanical, including photocopying, recording, or any information storage and retrieval system, without permission in writing from the publisher. Details on how to seek permission, further information about the Publisher's permissions policies and our arrangements with organizations such as the Copyright Clearance Center and the Copyright Licensing Agency, can be found at our website: www.elsevier.com/permissions.

This book and the individual contributions contained in it are protected under copyright by the Publisher (other than as may be noted herein).

**Notices**
Knowledge and best practice in this field are constantly changing. As new research and experience broaden our understanding, changes in research methods, professional practices, or medical treatment may become necessary.

Practitioners and researchers must always rely on their own experience and knowledge in evaluating and using any information, methods, compounds, or experiments described herein. In using such information or methods they should be mindful of their own safety and the safety of others, including parties for whom they have a professional responsibility.

To the fullest extent of the law, neither the Publisher nor the authors, contributors, or editors, assume any liability for any injury and/or damage to persons or property as a matter of products liability, negligence or otherwise, or from any use or operation of any methods, products, instructions, or ideas contained in the material herein.

**British Library Cataloguing-in-Publication Data**
A catalogue record for this book is available from the British Library

**Library of Congress Cataloging-in-Publication Data**
A catalog record for this book is available from the Library of Congress

ISBN: 978-0-08-100905-5 (print)
ISBN: 978-0-08-100084-7 (online)

For information on all Woodhead Publishing publications visit our website at https://www.elsevier.com/




*Publisher:* Matthew Deans
*Acquisition Editor:* Gwen Jones
*Editorial Project Manager:* Charlotte Cockle
*Production Project Manager:* Omer Mukthar
*Designer:* Matthew Limbert

Typeset by TNQ Books and Journals

# List of contributors

**P.-C. Aïtcin** Université de Sherbrooke, Quebec, Canada

**M.G. Alexander** University of Cape Town, South Africa

**S.N. Allen** Former Managing Director of specialist marine construction company Stefanutti Stocks Marine (Pty) Ltd, Cape Town, South Africa

**C. Andrade** Institute of Construction Science "Eduardo Torroja"-IETcc-CSIC, Spain

**M. Baz** GUPC: Grupo Unidos por el Canal (Sacyr)

**M.W. Braestrup** Ramboll, Denmark

**Z. Fan** CCCC 4th Harbor Research Institute, Guangzhou, China

**O.E. Gjørv** Formerly of Norwegian University of Science and Technology - NTNU, Trondheim, Norway

**J. Gulikers** Ministry of Infrastructure and the Environment, Rijkswaterstaat-GPO, Utrecht, the Netherlands

**K. Heath** Clough Murray & Roberts, Cape Town, South Africa

**W.S. Langley** Concrete & Materials Technology, Inc, Lower Sackville, Nova Scotia, Canada

**K. Li** Tsinghua University, Beijing, China

**Q. Li** Tsinghua University, Beijing, China

**K.P. Mackie** Keith Mackie Consulting Coastal & Harbour Engineer, South Africa

**S. Mindess** University of British Columbia, Vancouver, British Columbia, Canada

**G.A.C. Moore** Specialist Marine Civil Engineering Consultant, Cape Town, South Africa

**G. Nganga** University of Cape Town, South Africa

**M. Otieno** University of the Witwatersrand, Johannesburg, South Africa

**R. Pérez** GUPC: Grupo Unidos por el Canal (Sacyr)

**N. Rebolledo** Institute of Construction Science "Eduardo Torroja"-IETcc-CSIC, Spain

**M. Santhanam** Indian Institute of Technology Madras, Chennai, India

**P.E. Smith** Prestedge Retief Dresner Wijnberg (Pty) Ltd

**F. Tavares** Institute of Construction Science "Eduardo Torroja"-IETcc-CSIC, Spain

**M. Thomas** University of New Brunswick, Fredericton, Canada

# Woodhead Publishing Series in Civil and Structural Engineering

1 **Finite element techniques in structural mechanics**
*C. T. F. Ross*
2 **Finite element programs in structural engineering and continuum mechanics**
*C. T. F. Ross*
3 **Macro-engineering**
*F. P. Davidson, E. G. Frankl and C. L. Meador*
4 **Macro-engineering and the earth**
*U. W. Kitzinger and E. G. Frankel*
5 **Strengthening of reinforced concrete structures**
*Edited by L. C. Hollaway and M. Leeming*
6 **Analysis of engineering structures**
*B. Bedenik and C. B. Besant*
7 **Mechanics of solids**
*C. T. F. Ross*
8 **Plasticity for engineers**
*C. R. Calladine*
9 **Elastic beams and frames**
*J. D. Renton*
10 **Introduction to structures**
*W. R. Spillers*
11 **Applied elasticity**
*J. D. Renton*
12 **Durability of engineering structures**
*J. Bijen*
13 **Advanced polymer composites for structural applications in construction**
*Edited by L. C. Hollaway*
14 **Corrosion in reinforced concrete structures**
*Edited by H. Böhni*
15 **The deformation and processing of structural materials**
*Edited by Z. X. Guo*
16 **Inspection and monitoring techniques for bridges and civil structures**
*Edited by G. Fu*
17 **Advanced civil infrastructure materials**
*Edited by H. Wu*
18 **Analysis and design of plated structures Volume 1: Stability**
*Edited by E. Shanmugam and C. M. Wang*

19 **Analysis and design of plated structures Volume 2: Dynamics**
*Edited by E. Shanmugam and C. M. Wang*
20 **Multiscale materials modelling**
*Edited by Z. X. Guo*
21 **Durability of concrete and cement composites**
*Edited by C. L. Page and M. M. Page*
22 **Durability of composites for civil structural applications**
*Edited by V. M. Karbhari*
23 **Design and optimization of metal structures**
*J. Farkas and K. Jarmai*
24 **Developments in the formulation and reinforcement of concrete**
*Edited by S. Mindess*
25 **Strengthening and rehabilitation of civil infrastructures using fibre-reinforced polymer (FRP) composites**
*Edited by L. C. Hollaway and J. C. Teng*
26 **Condition assessment of aged structures**
*Edited by J. K. Paik and R. M. Melchers*
27 **Sustainability of construction materials**
*J. Khatib*
28 **Structural dynamics of earthquake engineering**
*S. Rajasekaran*
29 **Geopolymers: Structures, processing, properties and industrial applications**
*Edited by J. L. Provis and J. S. J. van Deventer*
30 **Structural health monitoring of civil infrastructure systems**
*Edited by V. M. Karbhari and F. Ansari*
31 **Architectural glass to resist seismic and extreme climatic events**
*Edited by R. A. Behr*
32 **Failure, distress and repair of concrete structures**
*Edited by N. Delatte*
33 **Blast protection of civil infrastructures and vehicles using composites**
*Edited by N. Uddin*
34 **Non-destructive evaluation of reinforced concrete structures Volume 1: Deterioration processes**
*Edited by C. Maierhofer, H.-W. Reinhardt and G. Dobmann*
35 **Non-destructive evaluation of reinforced concrete structures Volume 2: Non-destructive testing methods**
*Edited by C. Maierhofer, H.-W. Reinhardt and G. Dobmann*
36 **Service life estimation and extension of civil engineering structures**
*Edited by V. M. Karbhari and L. S. Lee*
37 **Building decorative materials**
*Edited by Y. Li and S. Ren*
38 **Building materials in civil engineering**
*Edited by H. Zhang*
39 **Polymer modified bitumen**
*Edited by T. McNally*
40 **Understanding the rheology of concrete**
*Edited by N. Roussel*
41 **Toxicity of building materials**
*Edited by F. Pacheco-Torgal, S. Jalali and A. Fucic*

42 **Eco-efficient concrete**
*Edited by F. Pacheco-Torgal, S. Jalali, J. Labrincha and V. M. John*
43 **Nanotechnology in eco-efficient construction**
*Edited by F. Pacheco-Torgal, M. V. Diamanti, A. Nazari and C. Goran-Granqvist*
44 **Handbook of seismic risk analysis and management of civil infrastructure systems**
*Edited by F. Tesfamariam and K. Goda*
45 **Developments in fiber-reinforced polymer (FRP) composites for civil engineering**
*Edited by N. Uddin*
46 **Advanced fibre-reinforced polymer (FRP) composites for structural applications**
*Edited by J. Bai*
47 **Handbook of recycled concrete and demolition waste**
*Edited by F. Pacheco-Torgal, V. W. Y. Tam, J. A. Labrincha, Y. Ding and J. de Brito*
48 **Understanding the tensile properties of concrete**
*Edited by J. Weerheijm*
49 **Eco-efficient construction and building materials: Life cycle assessment (LCA), eco-labelling and case studies**
*Edited by F. Pacheco-Torgal, L. F. Cabeza, J. Labrincha and A. de Magalhães*
50 **Advanced composites in bridge construction and repair**
*Edited by Y. J. Kim*
51 **Rehabilitation of metallic civil infrastructure using fiber-reinforced polymer (FRP) composites**
*Edited by V. Karbhari*
52 **Rehabilitation of pipelines using fiber-reinforced polymer (FRP) composites**
*Edited by V. Karbhari*
53 **Transport properties of concrete: Measurement and applications**
*P. A. Claisse*
54 **Handbook of alkali-activated cements, mortars and concretes**
*F. Pacheco-Torgal, J. A. Labrincha, C. Leonelli, A. Palomo and P. Chindaprasirt*
55 **Eco-efficient masonry bricks and blocks: Design, properties and durability**
*F. Pacheco-Torgal, P. B. Lourenço, J. A. Labrincha, S. Kumar and P. Chindaprasirt*
56 **Advances in asphalt materials: Road and pavement construction**
*Edited by S.-C. Huang and H. Di Benedetto*
57 **Acoustic emission (AE) and related non-destructive evaluation (NDE) techniques in the fracture mechanics of concrete: Fundamentals and applications**
*Edited by M. Ohtsu*
58 **Nonconventional and vernacular construction materials: Characterisation, properties and applications**
*Edited by K. A. Harries and B. Sharma*
59 **Science and technology of concrete admixtures**
*Edited by P.-C. Aïtcin and R. J. Flatt*
60 **Textile fibre composites in civil engineering**
*Edited by T. Triantafillou*
61 **Corrosion of steel in concrete structures**
*Edited by A. Poursaee*
62 **Innovative developments of advanced multifunctional nanocomposites in civil and structural engineering**
*Edited by K. J. Loh and S. Nagarajaiah*
63 **Biopolymers and biotech admixtures for eco-efficient construction materials**
*Edited by F. Pacheco-Torgal, V. Ivanov, N. Karak and H. Jonkers*

64 **Marine concrete structures: Design, durability and performance**
*Edited by M. G. Alexander*
65 **Recent trends in cold-formed steel construction**
*Edited by C. Yu*
66 **Start-up creation: The smart eco-efficient built environment**
*F. Pacheco-Torgal, E. Rasmussen, C.G. Granqvist, V. Ivanov, A. Kaklauskas and S. Makonin*
67 **Characteristics and uses of steel slag in building construction**
*I. Barisic, I. Netinger Grubesa, A. Fucic and S. S. Bansode*
68 **The utilization of slag in civil infrastructure construction**
*G. Wang*

# Preface and acknowledgements

This book should be a valuable resource for professionals involved in provision of coastal infrastructure, and specifically for coastal or marine infrastructure engineers involved in planning, designing and constructing marine concrete facilities. It is the combined efforts of 17 authors, who in their respective fields are highly knowledgeable and experienced professionals. The authors come from nine countries, indicating the wide scope of expertise drawn upon. A fair number of these authors are from South Africa, but their experience is international.

The title, "Marine Concrete Structures: Design, Durability and Performance," suggests that the major concern of the book is durability of marine concrete infrastructure and performance of this infrastructure in service. Marine structures can be exposed to some of the harshest environments on the planet. Despite this, many perform adequately for decades and longer, which is a testimony to their design, construction and the materials used to build them. Nevertheless, with the likely increase in construction of marine concrete infrastructure in the future, it is timely that a book like this should be concerned with these important aspects.

The book is unique in that it brings together in three parts aspects such as design and specification, construction methodologies and challenges; performance and properties, including durability and deterioration; and a comprehensive collection of case studies of significant marine concrete structures. These include, inter alia, the Confederation Bridge in Canada, Danish Strait Crossings, marinas in the Gulf region, large and small harbor structures and the new Panama Canal.

I am hugely indebted to all the authors who gave unstintingly of their time and expertise in writing the specialist chapters for this book. Their names are given in the respective chapters. I also acknowledge Dr. James Mackechnie for valuable information that he provided on the Simonstown Jetty in Chapter 14.

Lastly, I wish to thank the Woodhead editorial and production team: Gwen Jones, Kate Hardcastle and Charlotte Cockle.

# Introduction: importance of marine concrete structures and durability design

1

*M.G. Alexander, G. Nganga*
University of Cape Town, South Africa

## 1.1 Introduction

This book is about the design, durability, and performance of marine concrete structures, which come in many different types and shapes. Some are mass unreinforced concrete structures; others are reinforced to withstand the forces and actions that bear upon them. Concrete in its various forms permits the construction of coastal facilities, including docks and harbours, quays, jetties, wharves, seawalls, pipelines, tunnels, and so on, which in turn facilitate on-shore and near-shore developments such as cities, industrial areas, recreational sites, and many other needed developments. The demand for human development worldwide continues to grow, and much of this development will occur in marine areas in the future because of the great advantages of coastal localities in terms of trade and transport opportunities, areas suitable for human habitation and recreation, and accessibility. Thus, it is extremely important that engineers and designers understand the requirements of marine concrete structures, and particularly how they perform over the long-term in regard to their durability. This book links the concepts of design, durability, and performance, recognising that a durable concrete structure that performs acceptably over its intended lifespan begins with appropriate design and specification, although clearly construction and execution are also critical. This latter aspect is also covered in the book.

Three commonly used terms require definition.

**Marine** is an adjective usually applied to things or aspects relating to the sea, for example, marine biology, marine geology, and marine structures. It almost always refers exclusively to seawater environments.
**Maritime** is usually an adjective that describes objects or activities relating to the sea, most often activities such as shipping and sailing.[a]
**Coastal** refers to a zone where interaction of sea and land processes occurs.

In this book, the term ‘marine’ will be used frequently since it is a broad term relating to the sea or ocean; it will mostly be used in relation to ‘marine structures’,

[a] ‘Maritime’ is also used occasionally as a noun, as in Maritime meaning a climate type, or The Maritimes, meaning certain East Coast Canadian provinces.

**Marine Concrete Structures.** http://dx.doi.org/10.1016/B978-0-08-100081-6.00001-5
Copyright © 2016 Elsevier Ltd. All rights reserved.

that is, structures in or in very close proximity to the sea or in contact with the sea. However, 'coastal' will also be used on occasions.

### 1.1.1 Importance of concrete in the marine environment

Concrete is widely used in the marine environment, as evidenced by the vast stock of concrete structures near, in, or under the sea. Fig. 1.1 shows a selection of a port, a bridge, a high-rise building, and an oil platform, all in marine environments. There are good reasons for the extensive use of concrete. First, concrete is highly versatile, and it can be cast and moulded into useful shapes or made in factory environments for inclusion in subsequent construction. Second, concrete is a cost-effective material with inherent mechanical and durability properties that make it attractive for use, especially in severe environments such as the marine environment. Concrete is also increasingly understood as a relatively 'low-carbon footprint' material, contrary to uninformed perceptions, and research effort is increasingly being put toward further reducing its carbon footprint. The reality is that concrete will continue to be the construction material of choice for use in marine environments, as well as




**Figure 1.1** (a) Avonmouth docks, Port of Bristol, England. *(https://commons.wikimedia.org/wiki/File:Avonmouth_Docks.jpg.)* (b) Megyeri Bridge, Hungary. *(https://commons.wikimedia.org/wiki/Cable-stayed_bridges#/media/File:Civertanmegyeri4.jpg.)* (c) Metung-Wharf-Pano, Victoria, Australia. *(https://commons.wikimedia.org/wiki/File:Metung-Wharf-Pano,-Vic.jpg.)* (d) Troll A Platform, Norway. *(Photograph taken from South East, viewed November 2015. https://en.wikipedia.org/wiki/Troll_A_platform.)*

in a range of other demanding environments, into the foreseeable future. At this stage, there is simply no other viable alternative (Scrivener, 2014).

Concrete, as a material and as applied in different structural forms, is continually undergoing improvements that will render it even more cost-effective, durable, environmentally friendly, and long-lasting in the future. For example, it is now possible to make highly durable concretes that have such low chloride diffusion coefficients as to be almost impenetrable to chlorides. Interestingly, this is achieved not by greater use of the primary binder, Portland cement, but by engineered use of supplementary cementitious materials (SCMs) in appreciable proportions, which also reduces concrete's carbon footprint. The aggressive marine environment also gives rise to substantial physical and mechanical forces acting on concrete structures, such as severe abrasion, wave loading, and occasional accidental ship impact loading, and in this respect, concrete is eminently suitable, being of sufficient self-weight and robustness to withstand these effects.

The current (2015) global population is approximately 7.3 billion, of which approximately 44% is estimated to live within 150 km of the sea (UN Atlas, 2010). Thus, a vast number of people are affected directly or indirectly in their daily lives by the sea, and this includes the structures in which they live and work, or those that are provided by way of urban or industrial infrastructure. Marine infrastructure takes many various forms such as ports and harbours for trade, tourist and recreational attractions, residential and commercial buildings, and many others. Over the years, there has been growth in the number and size of ports, particularly in the developing world such as in China, India, Indonesia, and South Africa, as well as in the developed world such as Japan, Hong Kong, and Europe (Hinrichsen, 1999). This growth in ports and coastal facilities is accompanied by an increase in economic activities and job opportunities that lead to further increase in the human population along coastal regions. Therefore, major infrastructure development will occur in coastal and marine areas into the future, with concrete continuing to be the dominant construction material.

Considering future challenges for marine concrete construction, global warming and related effects of climate change are likely to be among the most serious. Already, there are rising temperatures and sea levels and increases in extreme weather events around the globe. These are particularly destructive and damaging when they impact coastal infrastructure. Coupled with the likely growth of populations in coastal localities, this poses a major challenge for designers, constructors, and operators of marine concrete infrastructure. Greater robustness and resilience will be needed from this infrastructure, and demands for increased durability are likely to multiply. Further, with increasing pressure on land-based space, underwater construction for cities and other uses is almost certain to occur. Chapter 16 'Durability design of new concrete infrastructure for future development of Singapore city' in this book deals with just such a case study—that of Singapore and its need for additional space for development. Such challenges will also bring opportunities for future development of newer cements more suited to marine environments.

## 1.2 Definition and characteristics of the marine environment

The marine environment is defined in somewhat different ways depending on the problem in hand (Chapters 'Deterioration of concrete in the marine environment', 'Design and durability of marine concrete structures', and 'Concrete durability in small harbours – the southern African experience' in this book give fuller definitions of the marine environment and marine exposures, including the seashore zone). Here, the marine environment is defined in terms of its *interaction with concrete structures*—an environment in which a concrete structure is *in contact with the sea or the immediate influence of the sea*. This definition therefore encompasses environments in which structures may be (1) in-shore (sometimes called atmospheric zone) but subject to marine spray and salt deposition from wind, such as coastal residential, commercial, or industrial buildings, and coastal bridges; (2) partially submerged in the sea (therefore exposed to tidal and splash actions), such as jetties, wharves, sea defences, breakwaters and harbour structures, and parts of oil drilling platforms; or (3) permanently submerged beneath the sea, such as undersea pipelines, submarine tunnels, and submerged parts of oil rigs. All these structures are exposed to very harsh conditions, and at the same time, they are required to be highly robust and offer good service life and structural reliability.

'Loading' on marine structures can be either mechanical, physical, or environmental. Mechanical loads upon marine structures include those from wind and waves, impacts and traction from maritime vessels, loads from cranes and adjacent railways and roads, other live loads imposed on marine deck structures, and the pressure of soil on retaining walls such as sheet-pile or sheet-anchor walls. Physical attack may arise from freeze—thaw in the ocean, or abrasion from heavy sediment-laden wave action. Environmental loads involve chemical attack on the concrete itself, which may apply to mass (unreinforced) concrete structures or to reinforced concrete structures. (Chapter 'Deterioration of concrete in the marine environment' deals with attack of concrete by seawater.) For reinforced concrete (RC) structures, chlorides in the seawater generally pose the greatest risk to structural durability and serviceability due to potential corrosion of the reinforcing steel.

All these different 'loads' impact on the serviceability and durability of marine structures, and a thorough knowledge is required of not only the environment, but the material itself, to carry out appropriate design, construction, and operation for any given project. This book is intended to give guidance on these important aspects.

The fact that marine concrete structures can be in-shore, on-shore, or underwater structures implies that different types of concrete mixtures and construction techniques will be needed. Underwater concreting is required for subsea structures, and these mixes require special proportioning and placing techniques to prevent washout of fines and to deal with seawater temperatures that might vary from near-freezing to mild or warm. (Chapter 'Construction methodologies and challenges for marine concrete structures' deals with underwater concreting in more detail.) Further, seawalls that retain earth on one face and seawater on the other are particularly challenging for durable construction. As illustrated in Fig. 1.2 (see later), several different transport

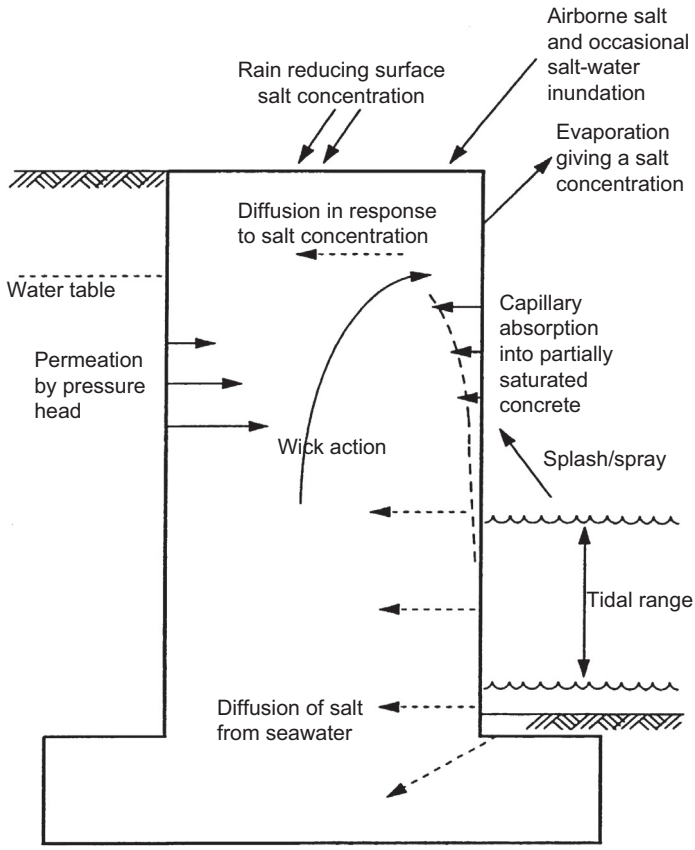



**Figure 1.2** Transport process and movement of salts in a seawall.
Based on BS 6349-1, 2000. Maritime Structures Part 1: Code of Practice for General Criteria. British Standards, London.

mechanisms operate simultaneously in such structures, making them very susceptible to deterioration. Also, they are frequently subjected to heavy mechanical loads. Construction of all such structures is challenging from the durability perspective since the possibility of concrete contamination is always present, and constructing in or under the sea is very challenging. In this respect, precast construction offers distinct advantages since the concrete elements can be manufactured off-site in controlled factory conditions and then transported to site and built in. Doubtless, more of this type of construction can be expected in the future.

### *1.2.1 Marine exposure classes*

Different concrete design standards around the world give guidance on exposure classes for concrete structures, including marine concrete structures. These exposure classes attempt to 'define' the environment, using a classification system that considers the severity of exposure, mainly in regard to chloride-induced corrosion. They

therefore represent environments in which concrete structures must operate and for which they need to be designed.

In many cases, these definitions are overly simplistic and not always helpful. Nevertheless, it is instructive to consider the provisions from a number of the more prominent concrete codes internationally; see Table 1.1.

Similar descriptions of exposure conditions are given in the different standards considered. The severity depends on the location of a structure with the most severe condition being in the tidal and spray zones. Additional descriptions of the exposure conditions consider freeze−thaw conditions in temperate climates (CSA, 2009) and the influence of wave action in abrasion (EN 206-1, 2013).

This aspect of marine exposure zones and exposure classes (or classification) is covered in Chapter 'Deterioration of concrete in the marine environment', which contains an Appendix on the comparison of the major durability requirements from different design codes in relation to the marine environment. Also, Chapter 'Design and durability of marine concrete structures' critiques the simplistic nature of the current provisions.

### 1.2.2 Mass transport processes in concrete in marine environments

Chapter 'Deterioration of concrete in the marine environment' in this book gives a description of mass transport processes in concrete in the marine environment. A useful summary is given in Fig. 1.2 (BS 6349, 2000), which shows the influence of seawater on a marine concrete earth-retaining structure also subjected to seawater on one face. The range of transport mechanisms shown in the figure is very varied: permeation, diffusion, wick action, capillary absorption, and convection due to evaporation. Together, these all represent a very severe environment for a concrete structure. The most severe attack of seawater on concrete tends to occur just above the level of high tide due to wetting and drying cycles, salt deposition and crystalization, and sufficient access of oxygen to any embedded reinforcing steel to cause corrosion.

Fig. 1.2 indicates that all of these transport processes may act simultaneously on a given marine concrete structure, and in general, their effects will be cumulative. This again illustrates the severity of the marine environment.

## 1.3 Fundamental requirements for marine concrete structures

The fundamental requirements for marine structures are similar to other types of concrete structures, that is, structural robustness and reliability, meaning that the structure is sufficiently stable and strong to resist various types of loading without undue risk of failure; adequate serviceability to ensure that the structure can carry out the required functions properly; and excellent durability so that it can continue to fulfil its functions for a considerable period of time. For concrete structures in marine environments,

**Table 1.1 Exposure classes for marine structures in different standards**

| Country | Standard/ design code | Exposure class | Description |
|---|---|---|---|
| USA | ACI 318 (2008) | C0: Negligible | Concrete dry and protected from moisture |
| | | C1: Moderate | Concrete exposed to moisture, no external source of chlorides |
| | | C2: Severe | Concrete exposed to moisture, and an external source of chlorides |
| India | IS 456 (2000) | III: Severe | Concrete completely immersed in seawater |
| | | | Concrete exposed to coastal environment |
| | | IV: Very severe | Concrete exposed to seawater spray |
| | | V: Extreme | Surface of members in tidal zone |
| Canada | CSA A23.1/ 23.2 (2009) | C-XL | Extreme chloride |
| | | Exposure to chlorides: C-1 | With or without freeze−thaw |
| | | C-2 | With freeze−thaw |
| | | C-3 | Continuously submerged concrete exposed to chlorides but no freeze−thaw |
| Europe | EN 206-1 (2013) | XS1: Exposed to airborne salt but not in direct contact with seawater | Surfaces near to or on the coast |
| | | XS2: Permanently submerged | Parts of marine structures |
| | | XS3: Tidal, splash and spray zone | Parts of marine structures |
| Australia | AS 3600 (2009) | B-1: Near coastal | 1−50 km from coastline |
| | | B-2: Coastal | Up to 1 km from coastline excluding tidal and splash zone |
| | | B-2: Seawater | Permanently submerged |
| | | C: Seawater | Tidal and splash zones |

durability considerations largely govern the choice of constituent materials, with strength being a secondary but not unimportant consideration; the physical shape and form of the structure also contribute substantially to robustness and reliability. These concepts are illustrated in Fig. 1.3(a) and (b), which shows two marine concrete bridges—the one more conventional but eminently robust, the other very aesthetic and designed with strict durability considerations in mind.

(a)



(b)



**Figure 1.3** (a) Little Bay bridge, New Hampshire, US. *(Photograph, viewed November 2015 https://en.wikipedia.org/wiki/Little_Bay_Bridge.)* (b) Storebæltsbroen (Great Belt Fixed Link, Denmark) *(https://upload.wikimedia.org/wikipedia/commons/0/00/GreatBeltBridgeTRJ1.JPG.)*

### 1.3.1 Materials selection and concrete specifications for durability

Selection of the mix constituents for marine concretes is crucial in obtaining needed durability. Modern concretes can comprise multiple different constituents, including multi-blend cements, several different aggregates, admixtures and additives, and possibly fibres. With modern cements, it is usually not difficult to achieve adequate strength, and for marine concrete structures that tend to be massive, strength is not necessarily the overriding concern. Also, there is generally now widespread availability of SCMs, superplasticizers, and various other admixtures. These may be very useful in obtaining durable concrete, but conversely they may also result in the undesirable situation of these concretes being less 'forgiving' than previous simpler mixtures. Modern binders and concretes are much more sensitive to the binder and concrete chemistry and to construction factors such as mixing and placing and particularly curing, making the concrete more susceptible to durability problems. The selection of the particular constituents and their relative proportions (mixture design) should be handled by an experienced materials engineer with a keen understanding of deterioration mechanisms and long-term performance of concrete in the marine environment. (Chapters 'Design and specification of marine concrete structures' and 'The durability of concrete for marine construction: materials and properties' in this book have information on constituents and mixtures for marine concretes, and the case study chapters [Chapters 8–16] contain a wealth of material on concretes used in different marine environments.)

From a durability point of view, it is important to distinguish between marine structures of mass concrete, for example, coastal armouring elements such as dolosse, and those made with RC. Mass concrete structures will primarily be subject to mechanical and physical deterioration mechanisms, although chemical attack on the surface skin may occur. However, since these are usually massive, gravity-stable structures, some surface deterioration is generally not a problem, unless the concrete is particularly porous and permeable, in which case it is likely not to have the necessary mechanical strength. RC marine structures pose a far greater durability problem because of the possible corrosion of the embedded reinforcing steel. In this case, durability design is largely around avoidance or control of corrosion. Several options are available: selection of suitable binders which limit chloride ingress together with an appropriate cover depth to give an acceptable service life; use of galvanised or stainless steel reinforcing rather than black steel; use of integral corrosion inhibitors such as calcium nitrite; and cathodic prevention or cathodic protection, depending upon the objectives of the cathodic system applied. In the case of cathodic protection, there are the options of sacrificial anode systems or impressed current systems. Even with this limited list, it is obvious that a range of protection or prevention measures are available to enhance durability, and knowledge and experience are needed to select and apply the right system for a particular situation.

Concretes which are cast underwater require special properties in comparison with normal land-based concreting, or concreting 'in the dry'. Special anti-washout admixtures are needed, and the concrete must be sufficiently flowable to be placed without undue effort and without the need for compaction under water. Temperature rise due to

heat of hydration in large underwater concrete sections in relation to the sea temperature must also be considered to avoid undue thermal cracking. The case study chapters later in this book cover many of these issues.

Specifications for marine concrete are also generally similar to those for other types of concrete structures, although usually there is, or should be, emphasis on the need for durability and robustness. Most specifications still tend to be prescriptive, with requirements for minimum cement content, maximum water/cement ratio, minimum strength, and so on. However, it is increasingly being realised that this approach is restrictive and hinders innovation, while also not always producing durable concrete structures. As an example, undue emphasis is often put on compressive strength and possibly maximum water/cement ratio, and the crucial aspect of binder chemistry and selection can be overlooked.

Therefore, there is a move toward performance-based specifications in which the desired performance of the structure in its various stages of construction and operation is clearly specified without unnecessarily restricting materials, methods, or construction techniques. In any performance-based methodology, the performance parameters and criteria for the structure must be explicitly defined, and a scheme set up to verify these parameters in practice and to ensure the criteria are met. According to the US National Ready Mixed Concrete Association, 'A performance specification is a set of instructions that outlines the functional requirements for hardened concrete depending on the application. The instructions should be clear, achievable, measurable and enforceable. Performance specifications should avoid requirements for means and methods and should avoid limitations on the ingredients or proportions of the concrete mixture' (Lobo et al., 2005). (This definition should really include requirements for fresh concrete as well.)

It is not possible within the scope of this chapter to deal comprehensively with performance specifications, for which there is a growing literature (see, eg, Bickley et al., 2006). Briefly, features of performance specifications are:

1. functional requirements should be clearly defined to ensure correct interpretation by all parties (owner, concrete producers, and contractors) involved in the implementation
2. compositional and proportioning requirements should be left largely to the concrete producer and/or constructor, who must show evidence that the final mix and materials selection will meet the specified fresh and hardened requirements
3. a scheme should be set up for verification of compliance using tests that are reliable, repeatable, accurate, and preferably applicable on site
4. there should be the means to enforce compliance with the specifications

It will take years if not decades for performance-based specifications to become common practice in concrete construction generally, and marine concrete construction particularly, but one can expect to see more of this in the near future.

### 1.3.2 Structural selection and form

As mentioned, marine concrete structures must be particularly robust to withstand actions of the sea and sea-going vessels, as well as the harsh environments to which

they are subjected. Frequently, this robustness is achieved by sufficient mass and bulk, for example, seawalls, breakwaters, and wharves. Other special structures that must be robust are wave-deflecting or energy-dispersing structures, coastal protection structures, lighthouses, offshore oil rigs, and so on. Many of these types of structures are dealt with elsewhere in this book.

However, the need for robustness does not preclude the design and construction of relatively slender and elegant structures in the marine environment, particularly if they are for commercial or residential purposes. Fig. 1.3(b) shows a marvellously aesthetic marine bridge structure in Norway, which is also robust and highly durable. For slender or smaller structures, robustness and durability must be provided by other means, typically by protecting the structure from excessive wave action and providing sufficient corrosion protection.

## 1.4 Standards and guidelines for design and construction of marine concrete structures

National standards for design of concrete structures generally contain provisions for marine concrete structures in relation to exposure conditions (see Table 1.1). However, these are necessarily brief and often too simplistic. Also, design codes of practice are usually aimed at 'normal' building structures, not marine structures that are subjected to very different types of loads, operating conditions, and exposure environments. Consequently, more detailed guides and 'standards' are needed for marine concrete structures. This book is aimed at providing much of this knowledge, but other sources are mentioned briefly below.

CIRIA (Dupray et al., 2010) provides a useful guide to good practice in the use of concrete in marine engineering. This guide was developed from research and practical experience obtained with the use of concrete infrastructure in marine environments in the United Kingdom and France. The various topics considered in the guide are:

1. different maritime concrete structures and elements
2. asset management of marine concrete structures
3. the design process and optimisation for marine structures, cost considerations, and environmental considerations and sustainability
4. environmental agents that cause deterioration in marine concrete structures
5. design of concrete mixtures for marine structures
6. durability design of marine structures, considering prescriptive and performance-based approaches
7. testing of concrete elements using either destructive or nondestructive tests, quality control requirements, and course of action in the event of noncompliance
8. construction of marine structures, which considers precast units, underwater construction, works in tidal/splash zones, concrete over water, and floating structures
9. inspection and monitoring of structures to determine the concrete condition and assess deterioration, which facilitates design of an appropriate repair and maintenance program
10. maintenance and repair options, protection, rehabilitation, and upgrading of structures

PIANC (2015), a world association for waterborne transport infrastructure, is concerned with design, development, and maintenance of ports, waterways, and coastal areas. It consists of various commissions and working groups with international experts who conduct short-term studies (24 months) and research on current problems, to ensure a quick response. The commission outputs are published in a technical report in either English or French. Examples of technical reports from the marine commission are as follows: design and maintenance of container terminal pavements; life cycle management of port structures (recommended practice and implementation); seismic design guidelines for port structures; floating breakwaters (a practical guide for design and construction); and development of modern marine terminals.

BS 6349-1-4 (2013) provides recommendations for materials in the design and construction of structures in marine environments. The code of practice is divided into four parts which consider planning and design for operations, assessment of actions such as protective measures and maintenance, geotechnical design, and materials for construction which may include concrete, steel, timber, or stone for protection works.

## 1.5 Book outline

This book comprises three parts, in addition to the introductory chapter; its purpose is to cover fundamental aspects of marine concrete structures, their environments and materials, and durability and performance before dealing with a series of informative case studies highlighting notable marine concrete structures and their durability.

The first part of the book, Chapters 'Types of marine concrete structures' to 'Construction methodologies and challenges for marine concrete structures', deals with issues around design, specification, construction, and maintenance of marine concrete structures. It also deals with specific types of marine concrete structures to give a general background to these structures and to indicate the wide range of such structures that exist. (Chapter 'Concrete durability in small harbours – the southern African experience' also deals with a range of marine concrete structures, mainly smaller harbour structures.)

The second part of the book, Chapters 'Deterioration of concrete in the marine environment' to 'Marine exposure environments and marine exposure sites', covers the important subject of deterioration mechanisms of concrete in marine environments, including how such materials perform in the sea. This leads on to a consideration of the durability of marine concrete from the perspective of the constituent materials and required properties. Last, there is a chapter on marine exposure environments and marine exposure sites.

The third part of the book (Chapters 8–16) comprises a series of case studies on marine concrete structures and durability-based design and performance. It covers structures in all the major environmental zones of the world, from cold or temperate to hot and dry or moist. Some iconic concrete structures are described, including the Confederation Bridge in Canada and the bridges of the Danish Strait Crossings.

Some projects still under construction are also covered, such as the Hong Kong–Zhuhai–Macau sea link project, China.

The book provides useful information on many of the important aspects of marine concrete structures and reinforces these in the informative case studies.

## References

ACI 318, 2008. Building Code Requirements for Structural Concrete and Commentary. American Concrete Institute, Farmington Hills, Michigan.

AS 3600, 2009. Australian Standard, Concrete Structures. Standards Australia Limited, Sydney.

BS 6349-1, 2000. Maritime Structures – Part 1: Code of Practice for General Criteria. British Standards, London.

BS 6349-1-4, 2013. Maritime Works. General. Code of Practice for Materials. British Standards, London.

Bickley, J., Hooton, R.F., Hover, K.C., 2006. Preparation of a Performance-based Specification for Cast-in-place Concrete. RMC Research Foundation, 2006.

CSA, 2009. A23.1/23.2. Concrete Materials and Methods of Concrete Construction/Test Methods and Standard Practices for Concrete. Canadian Standards Association, Toronto.

Dupray, S., Knights, J., Robertshaw, G., Simm, J., Wimpenny, D., Ballard, B.W., 2010. The Use of Concrete in Maritime Engineering – A Guide to Good Practice. CIRIA, London.

EN 206-1, 2013. Concrete – Part 1: Specification, Performance, Production and Conformity. European Committee for Standardization (CEN), Brussels.

Hinrichsen, D., 1999. The coastal population explosion. Available from: http://oceanservice.noaa.gov/websites/retiredsites/natdia_pdf/ctrends_proceed.pdf. Retrieved November 2015.

IS (Indian Standard) 456, 2000. Plain and Reinforced Concrete – Code of Practice (4th Revision). Bureau of Indian Standards, New Delhi.

Lobo, C., Lemay, L., Obla, K., 2005. Performance-based specifications for concrete. The Indian Concrete Journal 79 (12), 13–17.

PIANC, 2015. The World Association for Waterborne Transport Infrastructure. Available from: http://www.pianc.org/. Retrieved October 2015.

Scrivener, K., 2014. Options for the future of cement. The Indian Concrete Journal 88 (7), 11–21.

UN Atlas, 2010. 44 Percent of us Live in the Coastal Areas. Available from: http://coastalchallenges.com. Retrieved November 2015.

# Types of marine concrete structures

2

*P.E. Smith*
Prestedge Retief Dresner Wijnberg (Pty) Ltd

This chapter describes the various types of marine structures and works in which concrete is utilised. Many of the examples relate to Southern African marine structures by virtue of the experience and locality of operation of the authors; however, other international examples are also given. Concrete is used in a wide variety of applications in a diverse range of marine structures.

The largest and more obvious marine concrete structures are port structures, such as quay walls and jetties, but concrete is also used in less noticeable applications such as tidal pools and boat ramps. In the marine environment, concrete can form the main structural components, or serve another role such as a weight coating providing stability for a submarine pipeline, or as a protective cladding to prevent corrosion.

The marine environment varies from sheltered ports with relatively still water to the open ocean with heavy swells and possible abrasion such as sediment and sea ice. One factor that is common for all marine structures is the aggressiveness of the seawater.

Another important factor that has a large influence on the configuration of marine structures and the use of concrete in the sea is the frequent difficulty and impracticability of constructing concrete components in the water or underwater. It is difficult to place the concrete, to compact it and to ensure that a quality product is achieved in such conditions. Wherever possible, therefore, some form of precast or prefabricated element is used to construct the immersed portions of a structure that is positioned in the water. Once the structure has risen above the water level, normal concrete construction practices can be used, but again the use of precast elements is often preferred to ease the condition of working over water.

## 2.1 Port structures

One of the most important categories of marine structures is that of port structures, which are used for the berthing and load transfer of marine vessels. Port structures are an essential component of the maritime transport infrastructure and are a major capital investment. The following sections describe some of the more important port structures.

### *2.1.1 Quay walls*

Very often, an area of land is required behind the berth for the handling and stacking of the cargo of marine vessels, and this necessitates a quay wall against which to moor the

**Marine Concrete Structures.** http://dx.doi.org/10.1016/B978-0-08-100081-6.00002-7
Copyright © 2016 Elsevier Ltd. All rights reserved.

vessel and which will itself retain the fill for the land area. A variety of quay wall types have been developed, and these are described in the following. The choice of wall type depends not only on cost and durability but also on the prevailing site conditions. A quay wall type that is suitable for a harbour basin that is to be dug out in the dry may be impractical to construct in a wet site in an established harbour basin, or vice versa. Particular geotechnical conditions can exclude certain wall types; for example, sheet-piled structures are unsuitable where hard rock exists at shallow depth.

#### *2.1.1.1 Blockwork walls*

Blockwork walls are typically constructed in wet sites, and the underwater section is constructed from mass (plain) concrete blocks with an in-situ concrete cap for the upper section of the structure. The precast blocks are typically founded on a stone bed and terminate in the tidal zone. The cap is constructed in-situ, working tidally in the dry, and it is used to tie the block stacks together and spread the berthing and mooring loads. The horizontal and vertical placing tolerances of the block stacks is typically larger than that normally used for in-situ works, and the in-situ cap serves to accommodate the variation in block position and to create an accurate edge.

Blockwork walls are among some of the oldest quay structures in existence, due largely to the use of plain concrete (or even occasionally large blocks of rock). The oldest quay walls in the Victoria Basin of the Victoria & Alfred Waterfront in Cape Town date from the late 19th Century, and they were some of the earliest marine structures constructed in South Africa (Fig. 2.1). These blockwork walls are still in service today and are testament to the durability of plain concrete in the marine environment. Another example of a blockwork wall in the Victoria Basin is shown in schematic cross-section in Fig. 2.2.

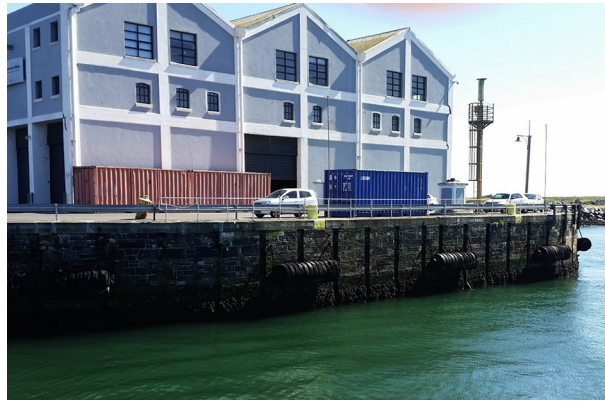


**Figure 2.1** Blockwork wall at the entrance to the Victoria Basin, Victoria & Alfred Waterfront, Cape Town. Particular care was taken with the original harbour walls and a dressed stone facing was applied to the upper precast plain concrete blocks in the tidal zone and the in-situ concrete cap. In the past, timber rubbing strakes were mounted in the vertical grooves in the wall cap.

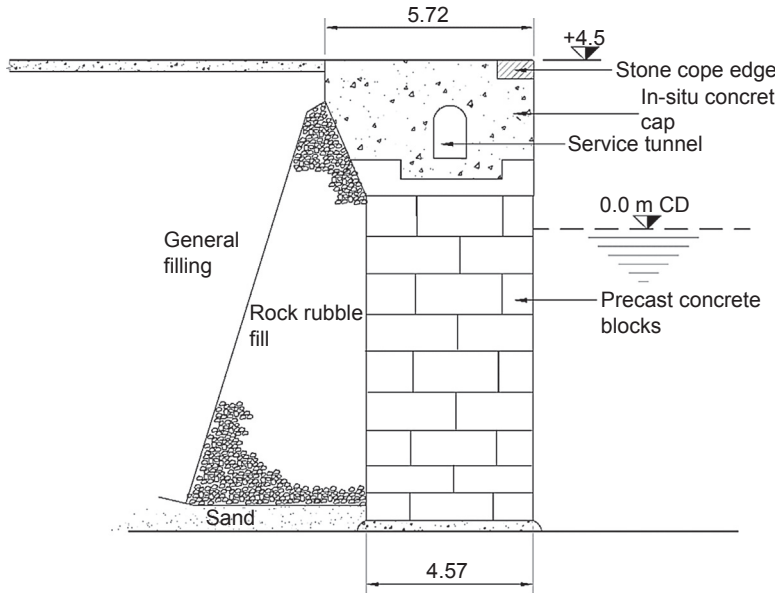



**Figure 2.2** Blockwork wall, Quay 6, Victoria Basin, Cape Town (dimensions in metres are illustrative). This second-generation wall was constructed in front of an existing quay to deepen the berth and has a plain concrete cap with a dressed stone cope edge.

Other examples of blockwork walls in Southern Africa may be found in Cape Town's Ben Schoeman Dock, Port Elizabeth, Durban (Figs 2.3 and 2.4), Richards Bay and Maputo harbours. Fig. 2.5 shows 'I' blocks from a recent (2015) blockwork wall, and it illustrates the sheer size of some of these wall elements.

The construction cost of blockwork walls is usually higher than that of other quay wall types, such as sheet pile walls, because of the greater quantity of materials that they require. However, blockwork walls for new port developments are still constructed nowadays in aggressive marine environments, such as the Middle East, where their inherent durability will provide a long service life and a lower life cycle cost than other wall types.

Blockwork walls were selected for the construction of quay walls in recent years in the ports of Richards Bay and Ngqura (South Africa) because they are durable. However, unlike the aforementioned blockwork walls, which were all designed for construction in the wet using precast blocks, the recent South African blockwork walls have been constructed in-situ, in the dry, in dig-out basins. The Ngqura harbour quay walls are described in more detail in the chapter 'Notable Southern African marine structures'.

High concrete strengths are not necessary for the precast blocks, and in fact, lower cement contents are preferred to limit the heat buildup during hydration and the subsequent shrinkage. Flexural and shear stresses during handling and in service are low, and therefore steel reinforcement is not required. As there is no steel reinforcement to

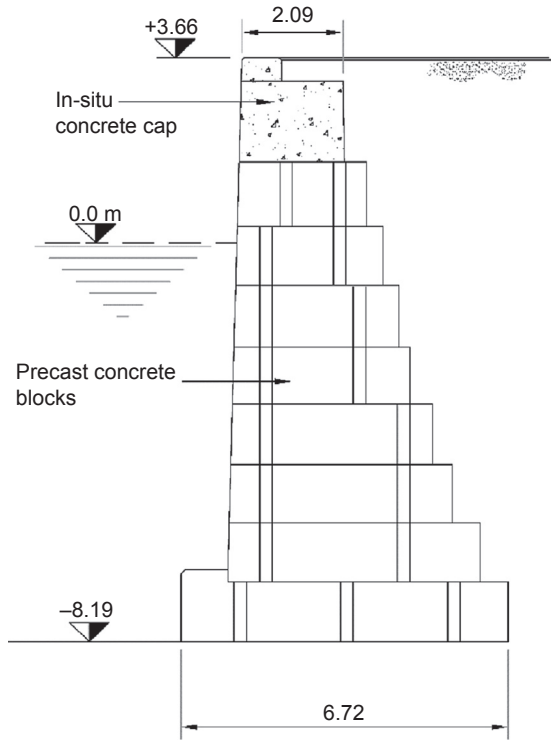



**Figure 2.3** Blockwork wall, A Berth, Durban (dimensions in metres are illustrative). This wall was constructed c. 1900 and is still in service.

resist shrinkage stresses, heat generation and shrinkage is controlled by low cementitious contents, use of cement extenders and release of the side formwork as soon as possible after casting.

### *2.1.1.2 Caisson walls*

Caisson walls are utilised in wet sites and employ a full-height, reinforced concrete caisson for the submerged substructure, as shown in Fig. 2.6. The caisson is essentially a large, precast concrete box that is constructed in a dry dock (Figs 2.7 and 2.8) or landside casting yard, and it is designed to be floated to the location and sunk into position. When cast in an onshore casting yard, it is launched by means of a slipway or lift. In common with blockwork walls, caissons are usually founded on a preplaced stone bed, and an in-situ concrete cap is used to tie the precast sections together and accommodate the substructure placing tolerances.

The caisson is reinforced, and therefore a suitable concrete mix, cover to steel and moist curing are required to ensure durability. Although the caisson transverses a range of microclimates over its height and width, it is not considered practical to vary the

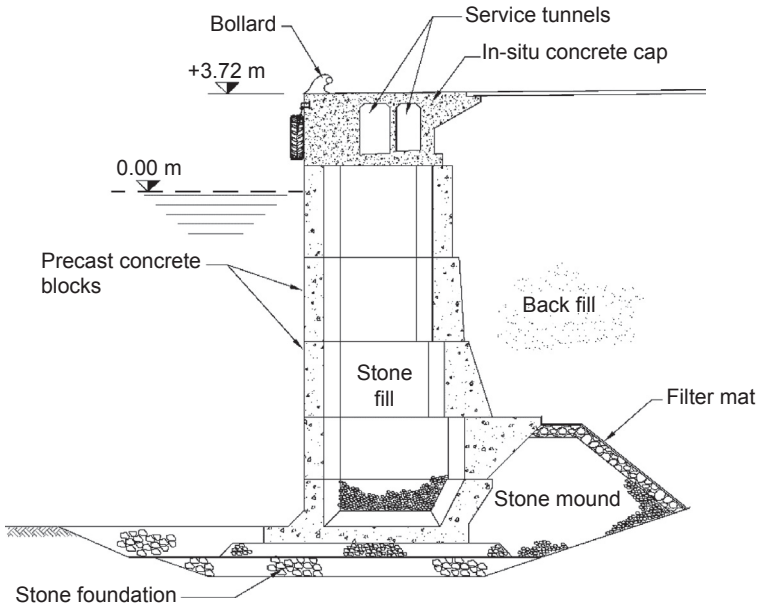



**Figure 2.4** Blockwork wall, Durban Container Terminal. This type of quay wall was constructed for the terminal developments in Durban and Cape Town in the 1970s. All of the precast blocks are plain concrete except the bottom one, which was reinforced as it was expected to experience some flexural bending. The blocks were 'I' shaped in plan and 2.95-m wide. The cap was reinforced and contains two service tunnels and a cantilever slab on the landward side to support a crane rail.



**Figure 2.5** Plain concrete 'I' blocks cast in 2015 for an extension of a blockwork wall in Saldanha Bay. Each block is 7.0 m long, 2.5 m wide and 2.3 m high with a mass of 59 tonnes. (Note: marks on left inner corner recesses are from formwork.)

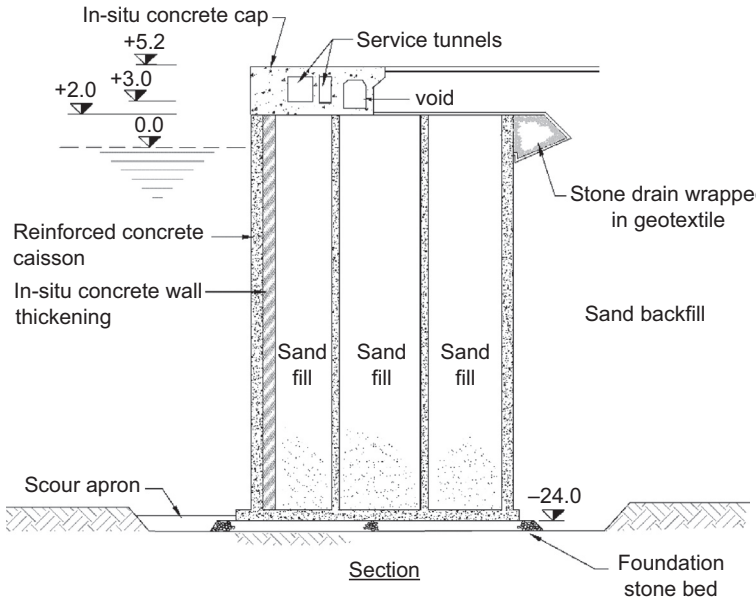



**Figure 2.6** Richards Bay Coal Terminal caisson quay wall: cross-section. The precast, reinforced caisson covers the full height of the substructure and has a constant cross-section to facilitate floating and sinking. In this case, a 1-m-thick front wall was required to resist a potential impact from a bulbous ship bow, and therefore the caisson was precast with symmetrical outer wall thicknesses so that it could float level without ballast and the thickening cast in-situ after placement.

design, and the whole caisson is designed and constructed for the worst conditions in the upper-tidal and splash zones.

Caisson quay walls have been utilised in South Africa in Saldanha Bay (Fig. 2.9), Durban (Figs 2.10 and 2.11) and Richards Bay harbours (Figs 2.6 and 2.7).

### *2.1.1.3 Counterfort walls*

Counterfort walls are usually utilised in wet sites and use full-height precast concrete substructure wall units with an in-situ cap and stone founding bed, as shown in Figs 2.12 and 2.13. For modern commercial vessel quays, the wall units are massive, and a high-capacity lifting plant is required to handle and place the units. Construction of the wall units takes place in an onshore casting yard.

The wall units make use of the counterfort support wall to reduce the span and thereby minimise the thickness of the principal wall panels and base slabs, so the precast unit is as light as possible for lifting. Despite this, the units are still very heavy. A 1981 quay wall in Botany Bay, Australia, used the 360-tonne units shown in Fig. 2.12, and a more recent development in the same harbour used units with a double counterfort that weighed 640 tonnes (Institution of Engineers Australia).

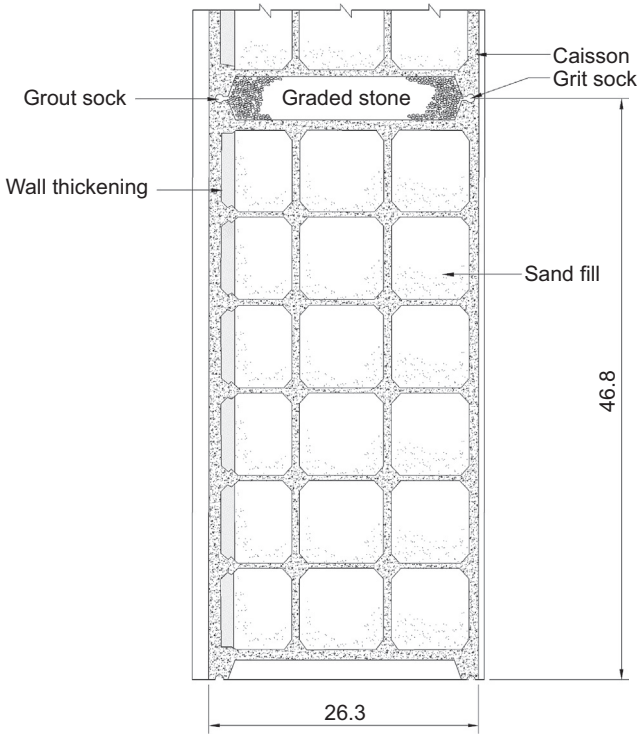



**Figure 2.7** Richards Bay Coal Terminal caisson quay wall: plan of installed caisson (dimensions in metres are illustrative). This view shows the cellular nature of a typical rectangular caisson. After the caisson was sunk into position by flooding with water, the internal thickening was cast using a tremie placing technique and the cells then filled with sand to give the required wall weight for stability. The caissons are placed with a gap between them to create a drainage path and reduce the tidal lag and hydrostatic pressure acting on the wall, and the gap is sealed with geotextile and stone to prevent wash out of the retained sand.




**Figure 2.8** Caisson construction inside a dry dock. Three caissons were cast inside the Robinson Dry Dock, in the Port of Cape Town, in 1988 for the quay wall at the Mossgas jacket fabrication site in Saldanha Bay. The caisson on the left is 22 m long, 9 m wide and 9.5 m high. The caissons were towed 120 km to Saldanha Bay, one at a time.

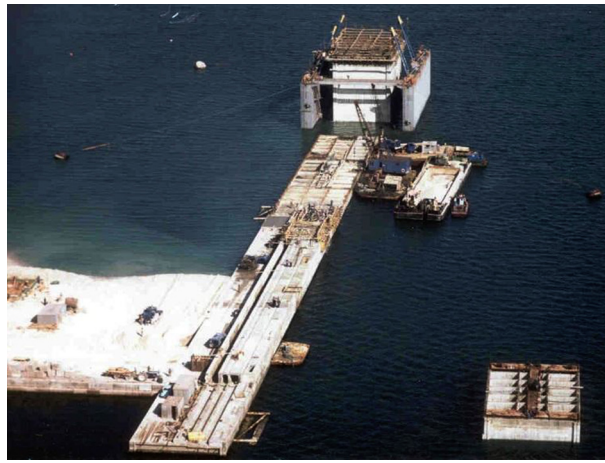


**Figure 2.9** Caisson quay wall under construction, Saldanha Bay. Visible in this view are a recently completed caisson in the floating dry dock at the top of the picture, a floating caisson awaiting installation on the lower right, sand filling into placed caissons at the top end of the quay, and construction of the superstructure cap along the central portion. Reclamation of the back of quay area has commenced.

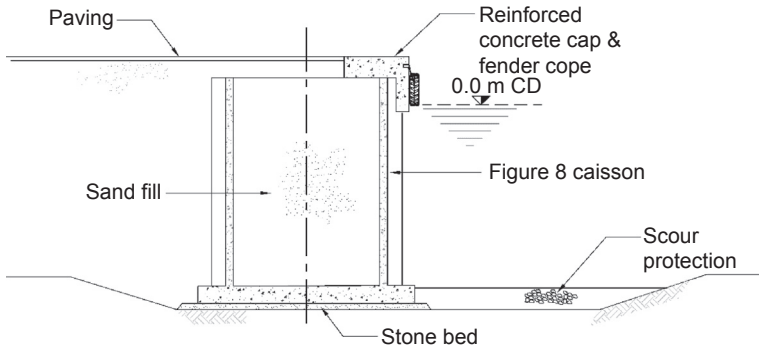



**Figure 2.10** Caisson quay wall, Durban Berths D to G. This type of caisson with a full-width cell requires a thicker base slab than the rectangular caisson shown in Fig. 2.6. This wall does not have a service tunnel, which enables a thinner cap.

Precast counterfort quay walls have been constructed in Luanda, Saldanha Bay (340 tonne units for the Multi-Purpose Terminal, Fig. 2.13) and Cape Town (Fish Quay, Victoria Basin) harbours.

The precast units are reinforced, and therefore an appropriate concrete mix, cover to reinforcement and curing regime are required.

Counterfort walls may also be cast in-situ, and this was done for the first phase of the Richards Bay coal terminal in South Africa in the mid-1970s. The wall cross-section is shown in Fig. 2.14. The wall is 30.2 m high and was cast in 30-m-long

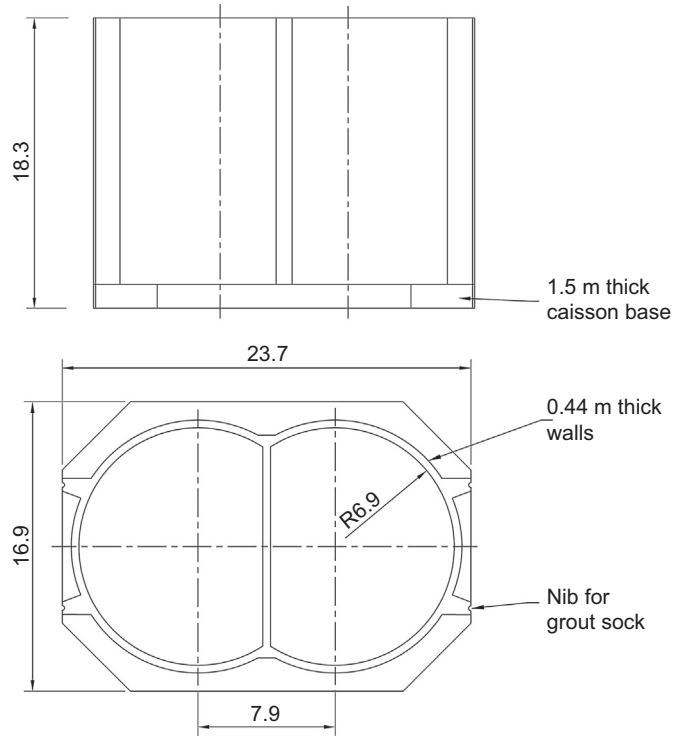



**Figure 2.11** Precast caisson, Durban Berths D to G (dimensions in metres are illustrative). This caisson type uses less concrete per metre of wall than a rectangular caisson, but more of the contained sand would be lost should a wall be breached by impact from a bulbous ship bow, which may affect wall stability. A temporary longitudinal internal wall is also required to assist floating stability during sinking of the caisson with water.

lengths inside a dewatered excavation. As weight is not a consideration for an in-situ cast counterfort wall, simpler and more robust panel thicknesses may be used, and the counterfort webs can be spaced further apart than with a precast wall.

### *2.1.1.4 Cantilever walls*

A conventional cantilever wall configuration can be used for a quay wall, but due to the thickness of the concrete sections that are required for this type of wall, they are likely to be used only in applications for small vessels or where it is possible to construct the quay wall in-situ, in the dry.

Starting in 1999, an in-situ reinforced concrete cantilever wall was constructed for a new container terminal in Antwerp, Belgium. The wall is shown in Fig. 2.15 and is 30 m high, constructed in 20-m-long panels in a dewatered excavation. As it is a cantilever design, the wall stem is appropriately sized and varies in thickness from 2.7 m at the top (underside of cap) to 5.5 m at the base, each cast taking 1600 $m^3$ of concrete.

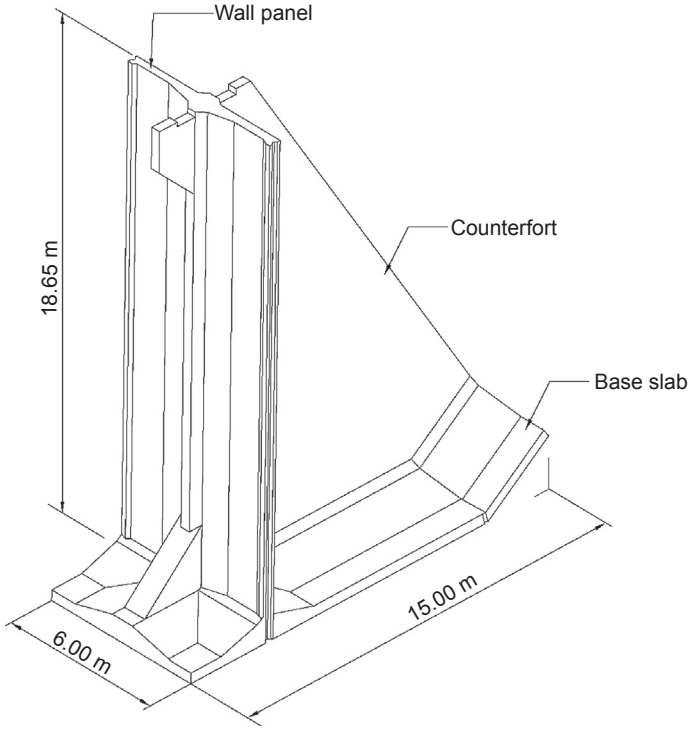



**Figure 2.12** Three-dimensional view of typical precast counterfort unit (dimensions in metres are illustrative). This unit was used for a container terminal quay wall in Botany Bay, Australia, in 1981, and weighed 360 tonnes.

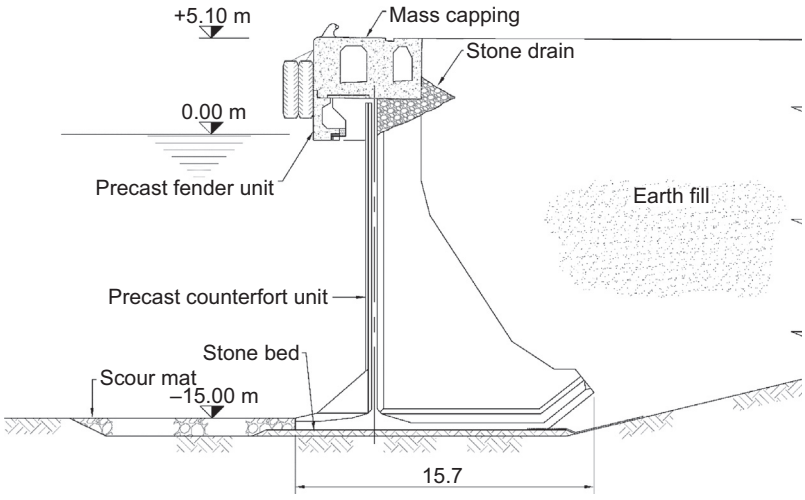



**Figure 2.13** Counterfort wall, Saldanha Bay (dimensions in metres are illustrative). This is a typical counterfort wall configuration, but the counterfort was trimmed back as far as possible to minimise the mass that had to be lifted.

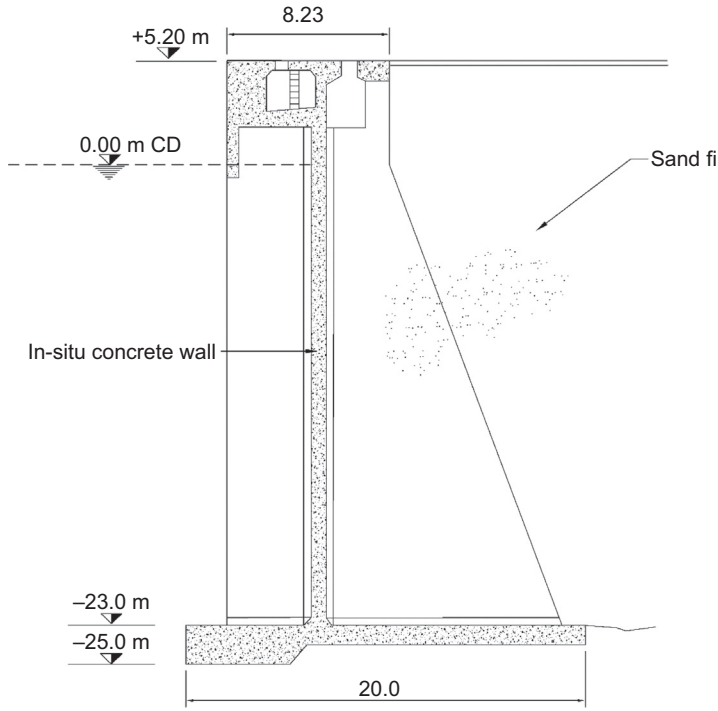



**Figure 2.14** In-situ counterfort wall, Richards Bay (dimensions in metres are illustrative). A precast wall substructure unit, such as a block or counterfort unit, requires a flat underside surface so that it can be placed on a stone bed or previously placed unit and its position adjusted if required. An in-situ cast structure, such as the counterfort wall shown in this figure, can be shaped as required to achieve an efficient structural thickness or shear key.

At the other end of the scale, much smaller cantilever wall types were used in the Victoria & Alfred Waterfront development, Cape Town, for the new Marina Basin and canal edge walls. The Waterfront walls were also constructed in the dry and are described in more detail in chapter 'Notable Southern African marine structures'.

### *2.1.1.5 Sheet pile walls*

Where ground conditions are suitable for the driving of a continuous piled wall through soil, sheet piles can form an economical wall type. The most common material used for sheet piles is steel; however, concrete piles have been used in the past. Steel sheet pile walls still require the use of concrete for some of the primary components, such as the caps and anchor walls.

#### Precast sheet piles

Sheet pile quay walls have been constructed in South Africa using both reinforced and prestressed concrete sheet piles of special cross-section. Figs 2.16—2.19 show concrete sheet pile wall examples and details of the pile cross-section and pile installation that

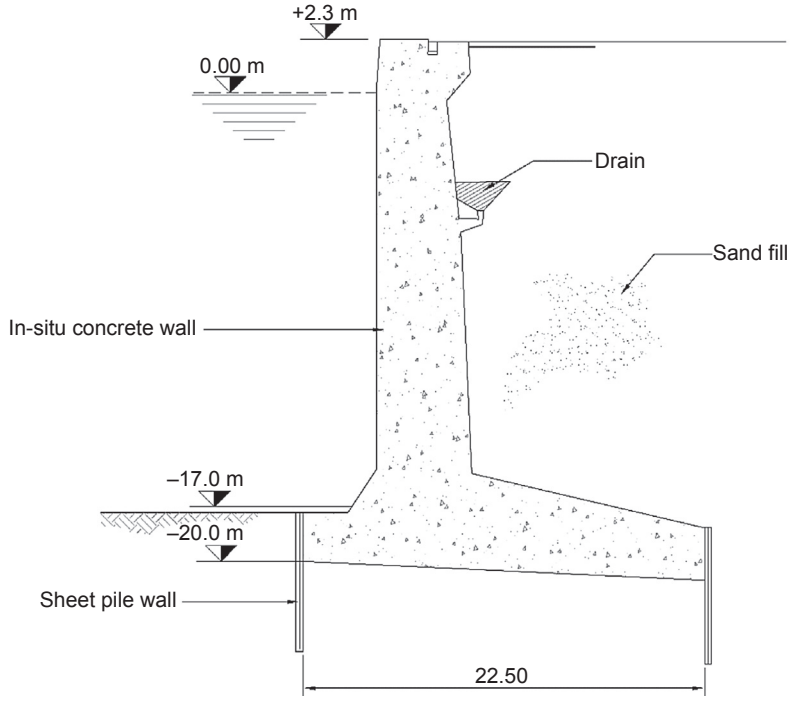



**Figure 2.15** In-situ cantilever quay wall, Antwerp, Belgium (dimensions in metres are illustrative). An in-situ construction allows use of thicker sections and more efficient use of reinforcement. The simple configuration of the wall (without counterforts) enables a quick setup of the formwork and casting of the panels.

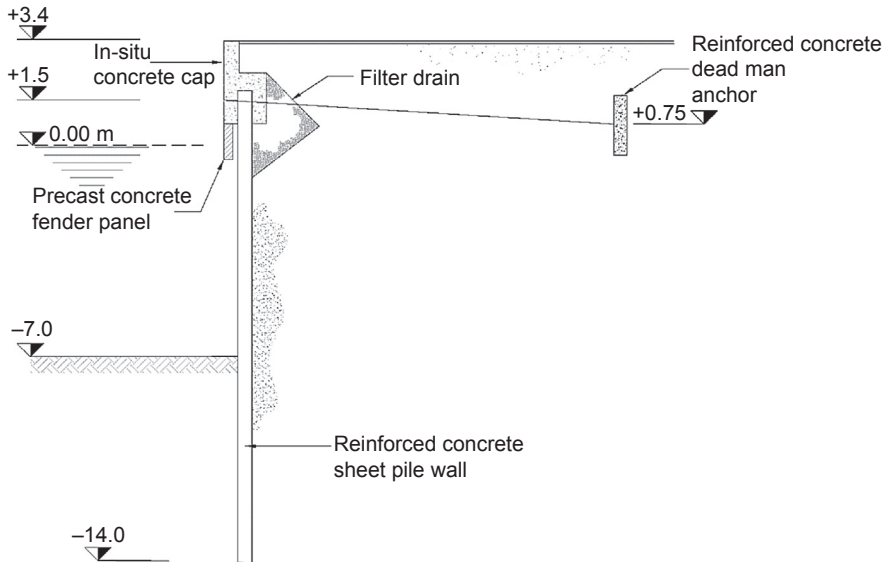



**Figure 2.16** Concrete sheet pile wall. The in-situ concrete cap acts as a waler and distributes the lateral earth loads from the sheet piles into the anchor bars, which may be at 2- to 3-m centres.

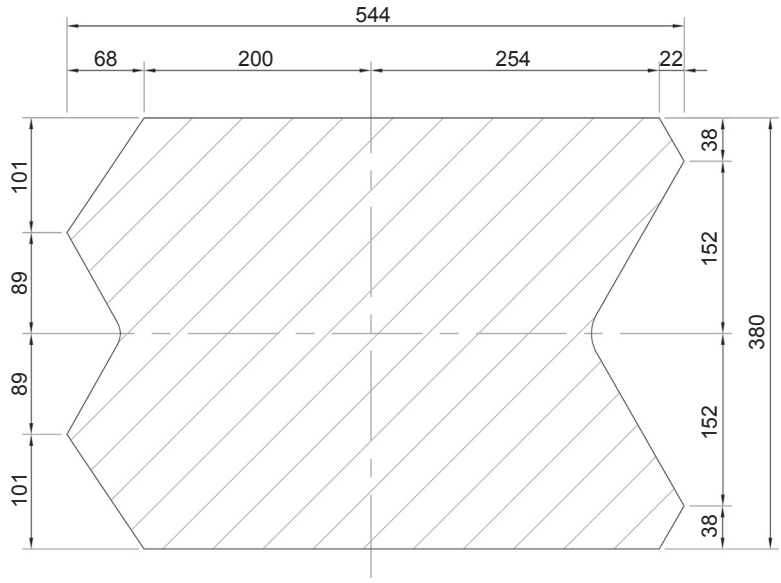



**Figure 2.17** Precast concrete sheet pile cross-section (dimensions in millimetres are illustrative). Piles of this cross-section were used in many South African structures in the 1970s and 1980s. The width transverse to the wall could be increased to give a pile with greater flexural capacity and the length could be increased to reduce the number of piles and joints to be sealed.

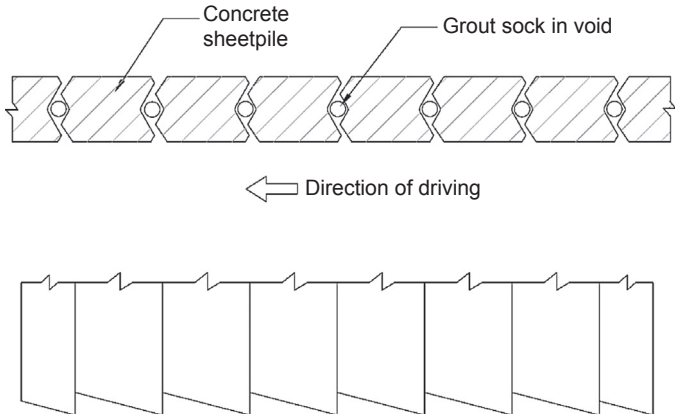



**Figure 2.18** Precast concrete sheet pile installation details. The upper view shows how the shape creates a void in between the piles into which a grout sock is installed to seal the gap. The tapered pile toe shown in the lower view acts to force the pile against the previously installed pile as it is driven.



**Figure 2.19** The retaining wall at the back of a dolphin berth in Richards Bay is constructed from concrete sheet piles with the upper section, above mid-tide, in in-situ concrete. Also of note in this photograph is the use of precast concrete for the bearing piles and longitudinal beams of the roadway. The headstock and roadway deck are in in-situ concrete.

have traditionally been used in South Africa. The piles are typically tied together by an in-situ cap at the top, which acts as a waler to distribute the tie forces to the discrete anchors. The cap creates a quay edge that is cast to normal concrete tolerances and accommodates the larger placing tolerances likely to be obtained by the driven sheet piles.

All concrete components of the wall are reinforced or prestressed, and appropriate durability measures are recommended. Pretensioned prestressing of the piles is advantageous as it enables longer pile lengths than reinforced piles and the prestress helps to close up any cracks that may occur during driving.

The chief reason for the shape of the pile cross-section is to create a void in between the piles into which is installed a grout sock to seal the gap. Unlike steel sheet piles, the concrete version does not have clutches, and therefore the grout sock between the piles is required to create the seal. The portion of sock in the tidal zone is filled with single-size stone to allow for water flow in and out of the backfill during tidal cycles.

Despite the use of the grout sock, experience has shown that the walls are vulnerable to the loss of the retained material through the gaps between the piles.

### Diaphragm walls

Cast, in-situ concrete diaphragm walls have also been used to create permanent ‘sheet pile’ quay walls; however, care must be taken with the construction to ensure the quality of the wall. Trench-cutting equipment with hydraulically driven rotary cutters is preferred to the traditional hydraulic grabs as a better quality is achieved. The rotary cutter equipment is considered to be more effective than grab equipment in constructing a vertical wall, coping with difficult ground conditions and creating less vibration during excavation. The result is a wall with a better finish and less variability in thickness and less risk of soil inclusions and loss of cover to the reinforcement.

This type of quay wall structure is only suitable for dry sites as a full height of soil or granular material is required for the diaphragm wall construction.

An in-situ concrete cap and fender cope are still required for the waler and for mounting the quay furniture if a conventional anchored sheet pile configuration is used.

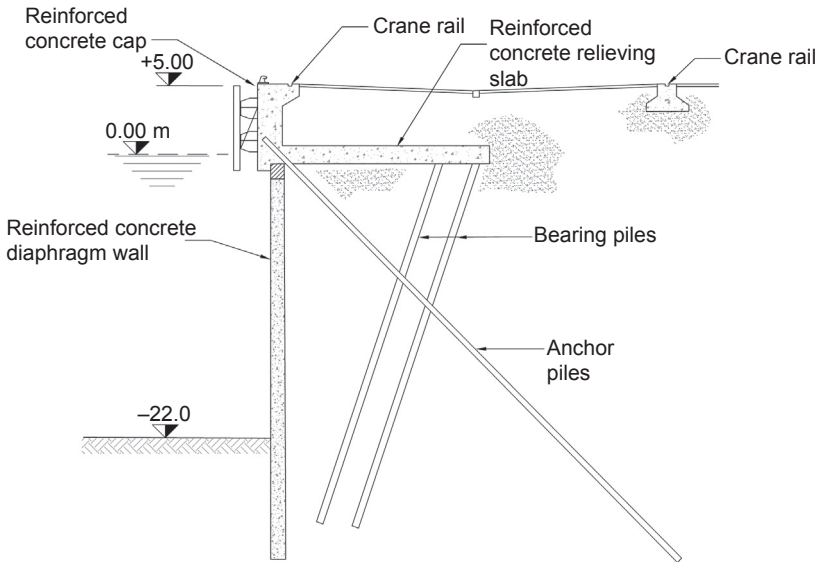



**Figure 2.20** Diaphragm sheet pile wall. The diaphragm wall, bearing piles, and anchor piles would be installed from a dry ground platform, either above high tide level or in a dewatered excavation. The top portion of a diaphragm wall cast is usually inferior concrete, and therefore the wall would be cast higher than required and cut down to level. Construction of the in-situ relieving slab and cap would be done in a dewatered excavation.

Fig. 2.20 shows a diaphragm wall utilised in a relieved sheet pile wall. The relieving slab is supported on bearing piles and carries the weight of soil above it and the vertical live loads applied on the surface, thus reducing the lateral earth loads applied to the sheet pile. The raked bearing piles serve to reduce the lateral load that has to be resisted by the anchor pile.

### Concrete components of steel sheet pile walls

Steel sheet pile quay walls utilise certain concrete components, namely the capping beam and fender cope. The cap is required to transmit lateral loads along the wall. The fender cope serves to support the fender units and, in addition, can act as a cladding for the steel piles in the tidal zone to protect them against corrosion. Steel sheet piles typically corrode fastest in the aggressive tidal zone, and therefore cladding of the piles has been adopted to ensure the desired service life. It is considered more economical and reliable to achieve the service life by cladding with concrete than other methods. Paint coatings are vulnerable to damage during driving and impractical to repair in the tidal zone. Sacrificial anodes are used to protect the steel underwater, but do not work effectively in the tidal zone.

The lower section of the fender cope traverses the tidal zone, and so it is normally precast to achieve good quality. The cope is cast into the in-situ cap, and the gap between it and the sheet piles is concreted to shield the piles.

An example of this form of quay wall is shown in Fig. 2.21.

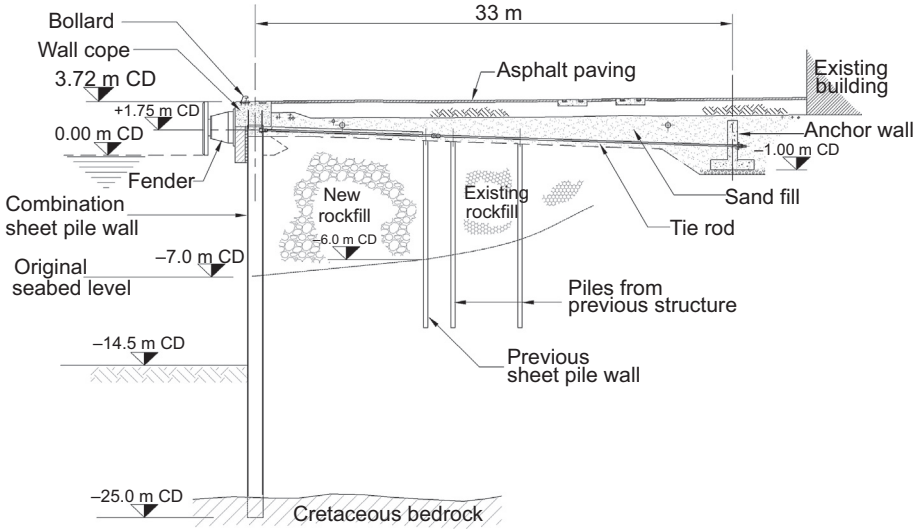



**Figure 2.21** Steel sheet pile wall with concrete cap and anchor wall (dimensions in metres are illustrative). The cap is cast in-situ with movement joints at 20- to 30-m centres, and it spreads the loads applied to it from bollards, fenders and crane rails into the sheet piles and anchor tie rods. The anchor wall is installed at a depth which provides enough passive earth resistance and is described further in section 'Anchor walls'.

## Anchor walls

Sheet pile quay walls use an anchor system to hold the top of the wall, and when a buried dead man anchor is used (as shown in Fig. 2.21), it is usually a reinforced concrete member, such as shown in Fig. 2.22, which may be a precast unit or cast in-situ.

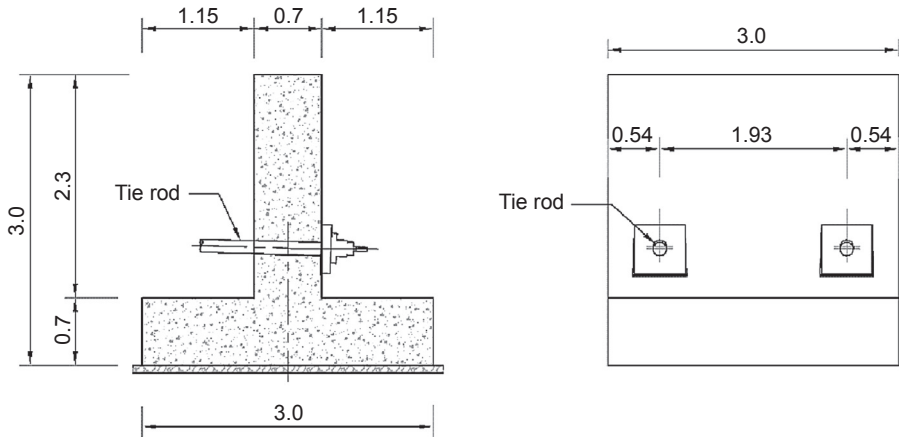



**Figure 2.22** Sheet pile wall anchor wall (dimensions in metres are illustrative). The tie rod passes through a sleeve in the wall, and the load is transferred to the wall via a square washer plate and a threaded nut.

This example has an inverted 'T' shape so that it mobilises a sufficient weight of soil above to resist the vertical component of the anchor rod force. The anchor wall is not continuous, and each unit anchors two rods.

## 2.1.2 Jetties and wharves

It is not necessary to construct a full-height quay wall with a retained back of quay area for all applications. For example, for the export or import of dry bulk or liquid products, no quay side stacking area is required as the cargo is transported between the quay side and a remote storage facility by conveyor or pipeline. Similarly for other types of vessels and operations, such as ferries, fishing, naval or recreational, no significant quay side area is necessary. In all these cases a finger pier or jetty with berths on each side is often an economical structure to construct (Fig. 2.23).

The most common jetty structure type is a suspended concrete deck supported by bearer piles, and this type is described in more detail in Section 2.1.2.1.

A deck-on-pile structure may also be constructed as an edge structure along the shoreline, as an alternative to a quay wall, and this is commonly known as a wharf. Instead of a wall the ground is retained by a rock revetment beneath the deck. Examples of wharf structures are described in Section 2.1.2.1.

In some cases, jetties and wharves are constructed without decking and comprise only a skeletal structure of beams on piles. This is usually done for dry bulk product handling facilities which use a travelling shiploader/unloader; see Section 2.1.2.2.

### 2.1.2.1 Deck on piles

Many jetties and wharves require a fully decked surface for vehicle and personnel access and handling of goods, and a deck-on-pile structure is often the most



**Figure 2.23** Jetty examples at the V&A Waterfront. The wide jetty in the centre of the photograph is the base for the Port of Cape Town's tug and pilot boat fleet and is constructed from block work walls with sand fill in between. On the left-hand side of the basin, there are jetties for small craft, each comprising a reinforced concrete deck on cast in-situ piles.

economical alternative, provided the seabed conditions are suitable for pile installation. Examples of jetty and wharf structures are shown in Figs 2.24–2.29. Reinforced concrete may be used for all or for parts of the jetty, and the deck structure is typically constructed from a mix of precast elements stitched together with in-situ cast concrete.

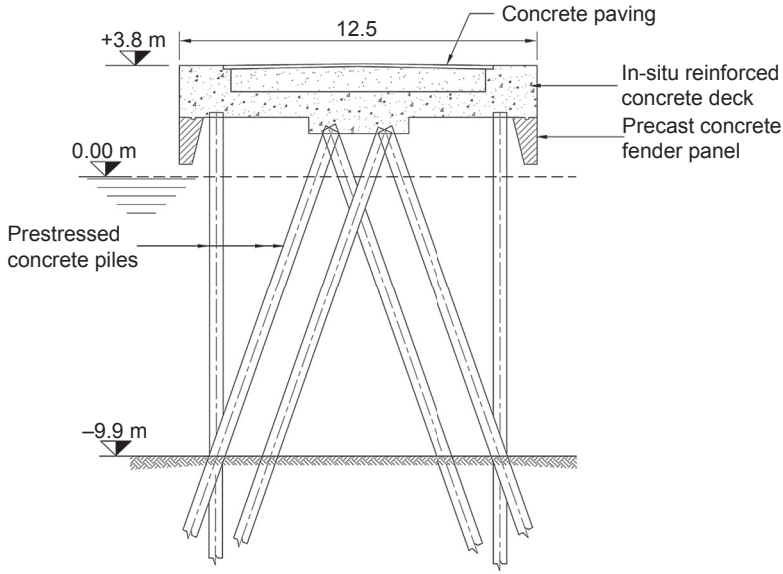



**Figure 2.24** Typical fully decked jetty (dimensions in metres are illustrative). This example would be suitable for small craft such as tugs and fishing trawlers. It has precast concrete piles and precast cope fender units and an in-situ cast deck slab. A paved sand fill layer is carried above the deck slab and adds weight to the structure, thereby reducing the tension loads in the raker piles, and in addition, it can be used to install services runs.



**Figure 2.25** The underside of a small craft jetty in Mossel Bay of similar construction technique to that shown in Fig. 2.25. The enlargements at the top of the three piles on the left were possibly done to encase damage that occurred to the pile head during driving.

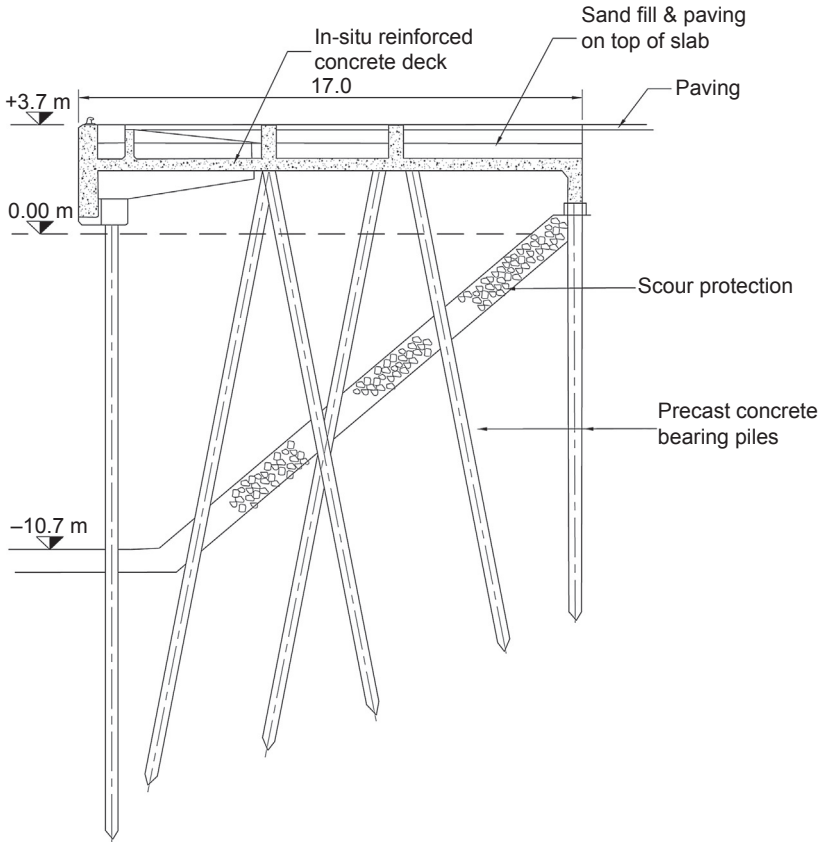



**Figure 2.26** Typical fully decked wharf (dimensions in metres are illustrative). This example has precast concrete piles and an in-situ concrete deck. The low wall at the rear reduces the width of the deck by retaining a portion of the height. This structure also has a sand fill layer above the deck to assist the raker piles and accommodate services.

Precast units are usually used for the fender copes which are located in the tidal zone. Precast units are used in the deck to enable speed of construction while minimising the over-water work that is required. It is often much simpler to place a precast unit than to erect over-water soffit formwork.

In South Africa, use has been made of precast reinforced or prestressed piles for jetties and wharves which serve smaller vessels such as fishing trawlers, such as those shown in Figs 2.24–2.29. Sizes that have been used are typically 380 × 380 mm up to 500 × 500 mm square piles. More substantial jetties serving larger vessels or carrying significant live loads require larger diameter and longer piles because of the greater loads. In North America and Asia, hollow, circular, prestressed precast concrete piles up to 1600-mm diameter have been used. Small-size precast piles, in the lengths required for a jetty structure, can be cast in a simple yard adjacent to the construction site, and transport of the long lengths to the works is straightforward. Large-diameter hollow piles



**Figure 2.27** Underside of a wharf structure in Mossel Bay. Features to note are the precast concrete raker piles, in-situ concrete deck slab and rear retaining wall, and the top of the rock revetment.



**Figure 2.28** Use of precast units in a wharf construction. This photograph shows construction in progress of a wharf structure in St. Helena Bay, South Africa. Precast reinforced concrete beams, 16.3 m long, span between a foundation at the top of the rock slope and a longitudinal piled headstock on the seaward side. The gap between the beams is closed with precast slabs, and the deck is made monolithic by an in-situ concrete slab.



**Figure 2.29** Underside of the dry bulk jetty at Richards Bay. Precast concrete units have been used for the beams, deck slabs and hanging fender panels. The piles are in-situ reinforced concrete cast inside redundant steel casings.

require more substantial casting yards and equipment, and they are usually cast in an established precast factory. Transport of the long, precast units from the casting yard to the site may then become problematic and preclude their use. For large-diameter piles, it is more likely that steel piles will be used. For a steel pile, a combination of measures is used to ensure that it has adequate service life (paint coatings, cathodic protection and provision of additional steel thickness for sacrificial corrosion). An alternative that has often been used in Southern Africa is an in-situ reinforced concrete pile cast inside a steel casing (refer the structures shown in Figs 2.29–2.31). The steel casing is driven to the required depth, and the soil inside is excavated, after which the reinforcing steel cage is inserted and the concrete cast in-situ by tremie.

Other types of substructure may be used for a jetty, particularly in conditions in which piling is not feasible. Fig. 2.32 shows a jetty configuration comprising piers constructed from caissons and a long span deck constructed from precast prestressed concrete beams with an in-situ reinforced concrete topping slab to form the deck. The iron ore export jetty in Saldanha Bay is an example of this method (Figs 2.33 and 2.34).

One advantage of using prestressed techniques in marine construction is that the member can be given a residual prestress, thereby eliminating any flexural or shrinkage cracks, hence improving resistance against chloride ingress. The concrete mix, cover and curing requirements of reinforced concrete are still necessary to ensure durability.

### *2.1.2.2 Skeletal jetties*

For the loading of dry bulk products, such as iron ore and coal, a fully decked structure is not necessary as all materials handling is done with a shiploader fed by a conveyor, and therefore vehicle access is not required. The structure is trimmed down to the minimum necessary to fulfil the specific functional requirements and is mainly influenced by the type of shiploader that is used. The structure for a travelling shiploader that traverses the length of the vessel has longitudinal beams to support the crane rails and transverse

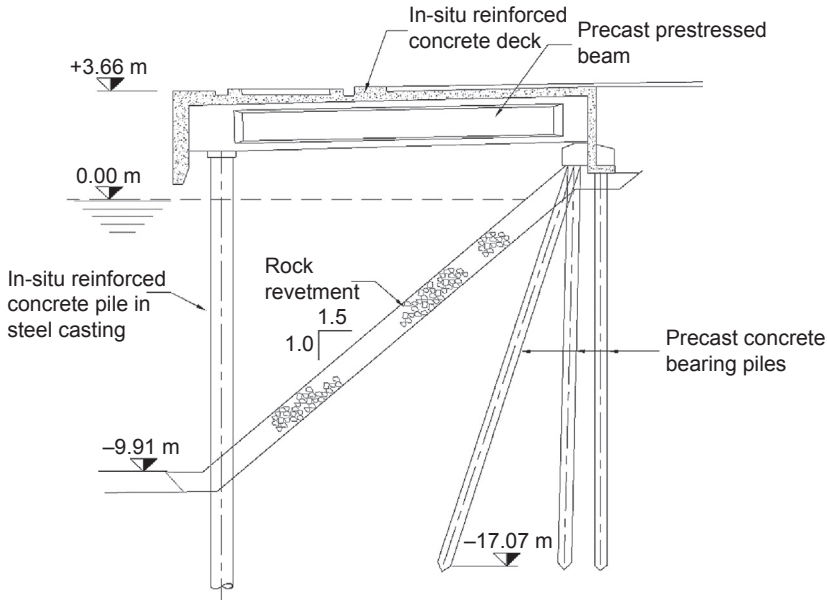



**Figure 2.30** Cargo handling wharf at Maydon Wharf, Durban, with in-situ reinforced concrete pile constructed inside a sacrificial steel casing (dimensions in metres are illustrative).



**Figure 2.31** The underside of the wharf structure shown in Fig. 2.30. The cased piles have in-situ concrete pile caps, and the transverse beams and hanging fender panels have been precast. The pile caps have different heights, which was possibly done to suit the varying top level of the driven casing.

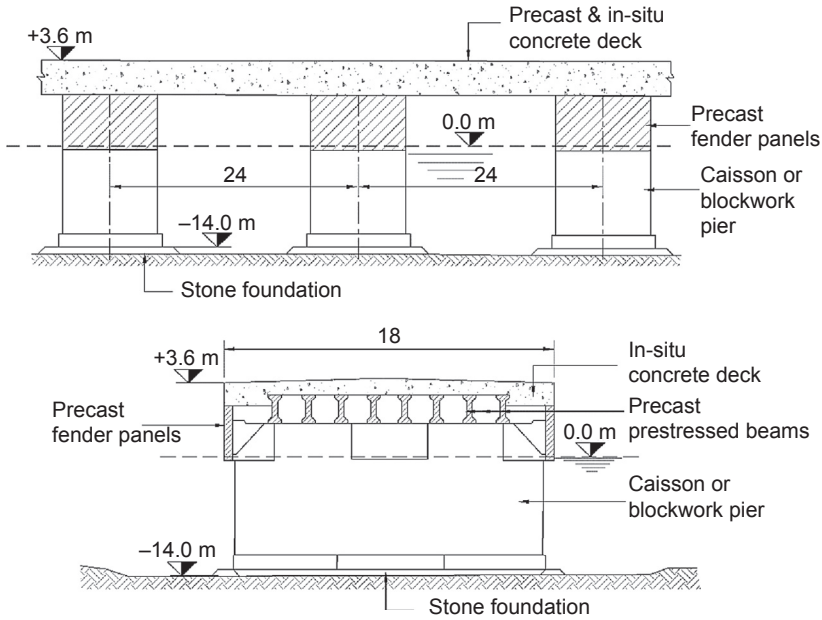



**Figure 2.32** Jetty with caisson or blockwork pier substructure (dimensions in metres are illustrative).



**Figure 2.33** Saldanha Bay iron ore export jetty. The jetty has a berth on each side, and the two ship loaders are able to load on both sides. A bulk oil berth is located beyond the right-hand ore berth. The jetty is located in a water depth of 23 m and is able to load vessels up to 350,000 dwt.

beams to maintain the rail gauge and transmit lateral loads to support points (see Fig. 2.35). A radial shiploader facility has a central platform to support the pivot of the shiploader, a curved rail beam to support the travelling seaward bogies, and individual dolphins for the berthing and mooring functions.



**Figure 2.34** Saldanha Bay iron ore export jetty. Detailed view of the jetty. Visible in this view are the 'Figure 8 shape' caissons (similar in shape to those shown in Fig. 2.11), precast pretensioned deck beams and precast fender panels. The fender panels were cast in full height 1-m widths and cantilever downward from the massive in-situ concrete cap. All components of the jetty are stained pink from iron ore dust.

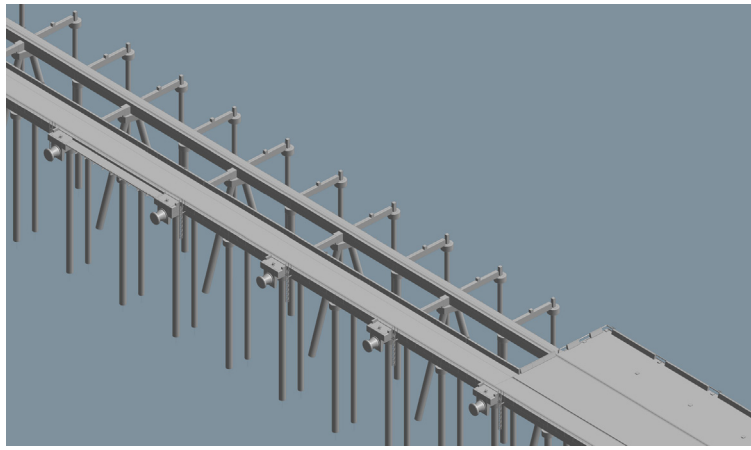


**Figure 2.35** Computer-generated model of a skeletal jetty configured for a travelling shiploader. The 300-m-long jetty is equipped with front and rear crane rails at 16.5-m gauge, a full-length roadway for access to the mooring hooks and a service deck at each end.

Vessels for the transport of bulk liquids such as oil and liquid petroleum gas require even less jetty infrastructure than dry bulk products. In addition to the requisite berthing and mooring dolphins for the vessel, there is a central decked platform for the loading arms and associated equipment (see Figs 2.36–2.38).

Typically, dry bulk and liquid bulk jetties can be located some distance off shore in water of the required depth for the vessels being loaded or unloaded. Access to the berth is then provided by an access trestle which carries the product on conveyors or in pipelines, as well as a vehicle roadway or pedestrian access.



**Figure 2.36** Liquid bulk jetty using caisson dolphins. This is the Island View No. 1 liquid bulk berth in the Port of Durban. Caisson structures are provided for the two berthing dolphins and the left-hand mooring dolphin. The central loading platform does not have any lateral loads applied to it and comprises a suspended concrete deck on vertical bearer piles. The two berthing dolphins are 70 m apart from centre to centre.



**Figure 2.37** Liquid bulk jetty using caisson dolphins. This is the Island View No. 9 liquid bulk berth in the Port of Durban. Caisson structures are provided for the three berthing dolphins, and in this case the central loading platform also functions as a berthing dolphin. Note the use of a single, prestressed, precast 'T' beam for the walkways in between the dolphins.



**Figure 2.38** LNG jetty at Quintero, Chile, with steel piles, a beam grillage structure for the platform and dolphins, and concrete decks. The overall length of the jetty measured across the outer mooring dolphins is 350 m. A typical breasting dolphin structure in shown in Fig. 2.39.



**Figure 2.39** Breasting and mooring dolphin. The steel structure resists the berthing and mooring loads, and the concrete slab is provided only as a deck for personnel.

Skeletal jetties of the types described in this section are usually constructed from a combination of steel and concrete elements, and the choice of material is influenced by local practices and costs. At one end of the scale, the jetty may have steel piles and a wholly concrete superstructure, and at the other end, the piles and structure may be steel with the only concrete used being for roadways and decking.

### 2.1.3 Dry docks and ship lifts

Dry docks and ship lifts typically use similar structural elements to those described earlier for quay walls and jetties.

Wall types that have been used in dry docks include in-situ concrete cantilever walls, caissons, and steel sheet piles with concrete superstructures. All wall types usually have a concrete superstructure equipped with a gallery/tunnel to carry the numerous services required for the dry dock operation.

Dry dock walls have to resist the lateral loads that arise from the hydrostatic pressures when the dock is dewatered. These pressures are likely to be higher than the outward hydrostatic and mooring forces that are imposed on quay walls, and the dry dock floor has to resist the hydrostatic uplift that is created when the dock is dewatered. Dry docks therefore tend to be massive, heavy structures to resist the hydrostatic forces that are present when they are dewatered. Thick concrete sections are required to resist the imposed bending moments and shears and to provide enough weight to counter the uplift.

The concrete elements of dry dock structures are typically cast in-situ because of the size of the elements required. Figs 2.40–2.42 show typical configurations of dry docks with cast in-situ concrete elements.

### 2.1.4 Boat ramps and slipways

Boat ramps are used to launch small craft using trailers and tow vehicles, and they require a sloping paved surface (typically one vertical: eight horizontal) that goes from the level of the land at the top to a point below low tide that provides sufficient depth for the boat to be floated off the submerged trailer. A typical boat ramp structure

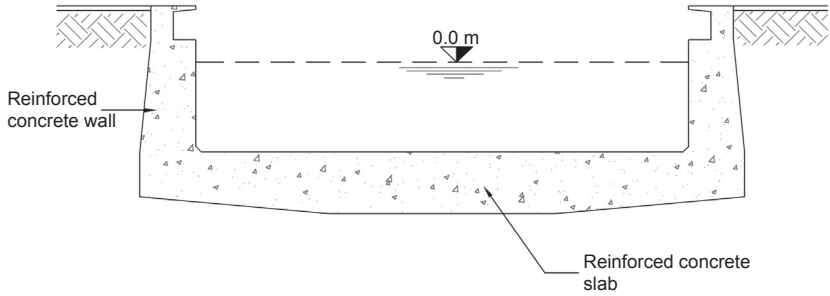



**Figure 2.40** Dry dock with in-situ concrete elements and dead weight floor. A heavy floor slab is used to counter the uplift from hydrostatic pressure when the dock is dewatered.

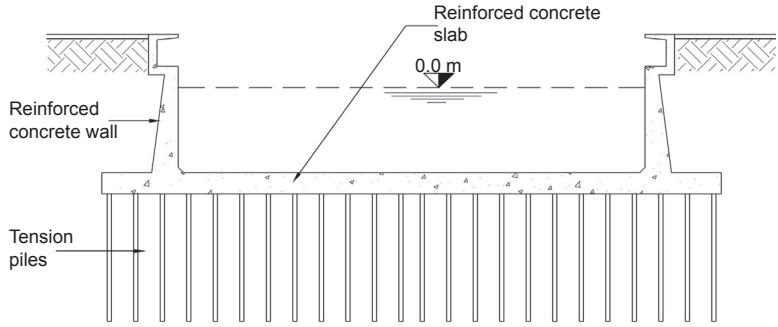



**Figure 2.41** Dry dock with in-situ concrete elements and floor anchored to the ground with anchor piles.

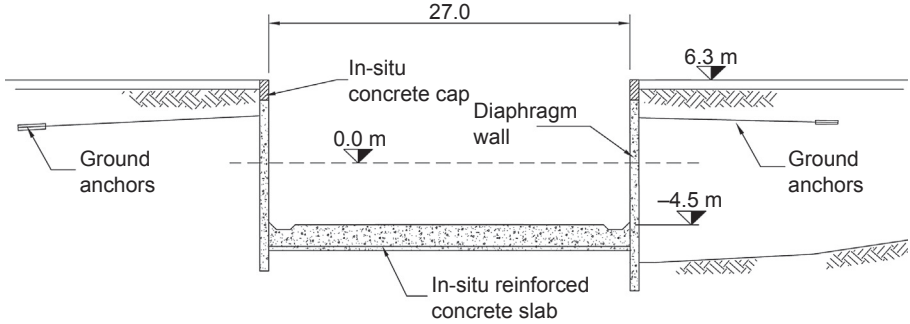



**Figure 2.42** Dry dock with anchored diaphragm walls (dimensions in metres are illustrative). This example has a heavy floor slab to resist the uplift and which also acts as a strut between the two walls to resist the lateral earth pressures.

is shown in Figs 2.43 and 2.44. A mix of concrete elements is therefore required, as in-situ concrete ground slabs are used above the tidal levels, and precast slabs are used in the wet portion. A rough finish is required to the trafficable surface to enable the tow vehicle to maintain a grip, particularly in the tidal zone and below where marine growth will be present. On the slab units in the tidal zone and below, a deep V-groove is employed, as shown in Fig. 2.45.

Slipways are used to launch vessels that are too large for vehicle trailers such as fishing trawlers. These are located in many fishing harbours around the world, and they are also used for the regular maintenance of the trawlers. Instead of trailers, a dedicated bogey is used, which is equipped with cast-iron wheels that run on steel rails. The slipway structure therefore has two or three rail beams which run the length of the structure. As with the boat ramp, the use of precast elements for the lower portion of the structure is often utilised. Figs 2.46 and 2.47 illustrate a typical South African slipway at Mossel Bay Harbour.

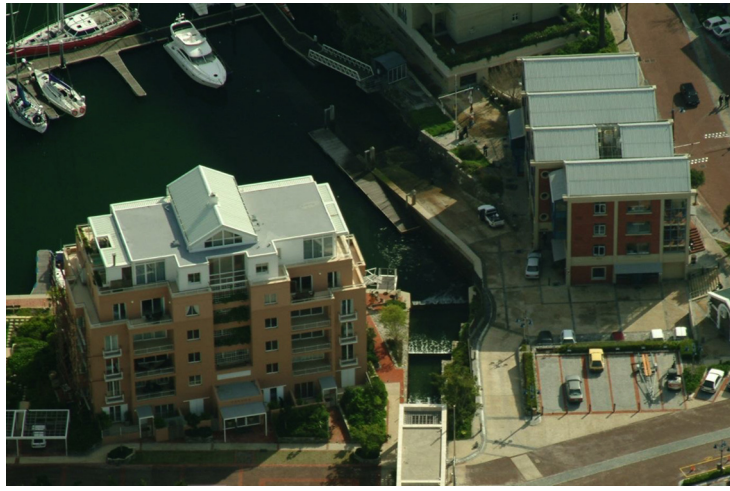


**Figure 2.43** A boat ramp for trailer launched small craft at the Victoria & Alfred Waterfront. The ramp has slope of 1:8, an exposed aggregate finish to the ground slabs above the tidal zone, and grooved finish in the tidal zone and below.

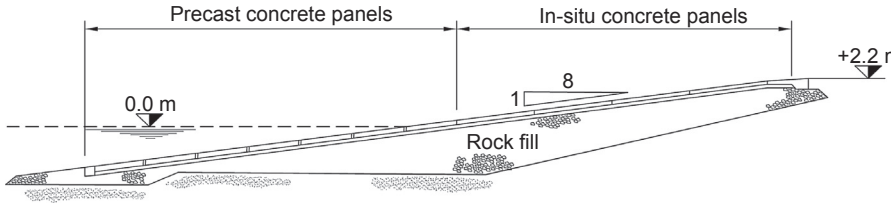



**Figure 2.44** Boat ramp longitudinal section. This view shows a typical longitudinal section through a boat ramp that is constructed in the wet. To create a good grip for the tow vehicle, the precast panels have a grooved finish, as shown in Fig. 2.45, and the in-situ panels are given a broomed or exposed aggregate surface finish. The deep grooves are used in the wet portion because of marine growth.

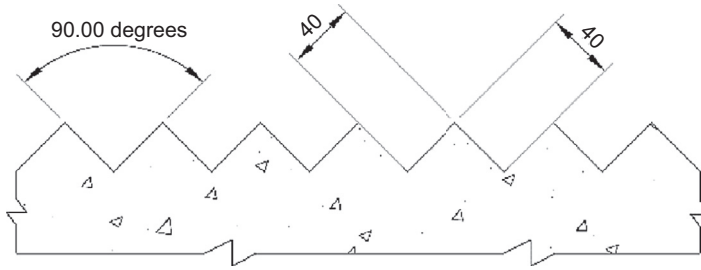



**Figure 2.45** Boat ramp surface V-grooves (dimensions in millimetres are illustrative). This surface profile is used in the lower, wet portion of the boat ramp and is formed by casting the precast panels upside-down onto a grooved casting bed.



**Figure 2.46** Mossel Bay harbour slipway. The bogey is stored in the dry on the top of the slipway on the left of the photograph and runs down the slipway to the right.

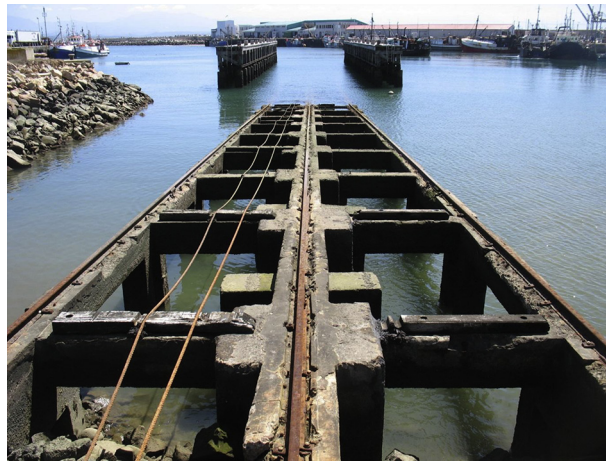


**Figure 2.47** Mossel Bay harbour slipway. A view down the slipway showing the three bogey rails and the supporting structure. The steel rope runs down to a sheave at the bottom of the slipway and is used to haul the bogey up and down. There are two lead-in jetties along the deeper portion of the slipway to assist vessels onto the submerged bogey. This upper portion of the slipway is constructed from in-situ concrete, but precast units would have been used for the lower section. Note some of the deterioration occurring in the slipway elements.

The chapter 'Concrete durability in small harbours – the Southern African experience' in this book also deals, inter alia, with boat ramps and slipways.

## 2.2 Coastal structures

Coastal structures, as their name implies, are structures situated on the coastline or in close proximity to it, and they can comprise everything from seawalls to coastal bridges or even coastal buildings. The emphasis in this section will be on civil engineering structures, not buildings. Coastal structures differ from port structures in that they have to deal with the effects of direct sea action from waves and sediment movement, as well as possible sea splash and spray. Wave action applies direct loads to seawalls and coastal jetties, and breakwater and revetment structures are required to absorb the wave energy. Sediment movement and wave action can cause abrasion of the structure.

### *2.2.1 Seawalls*

Seawalls are constructed to protect land assets from sea action. They usually have a curved shape designed to redirect the flow from a breaking wave back in a seaward direction and thereby minimise overtopping. The wall therefore has to resist the full impact force of the breaking wave and the long-term effect of erosion and abrasion from water and water-borne sediment. A typical seawall structure is shown in Fig. 2.48.

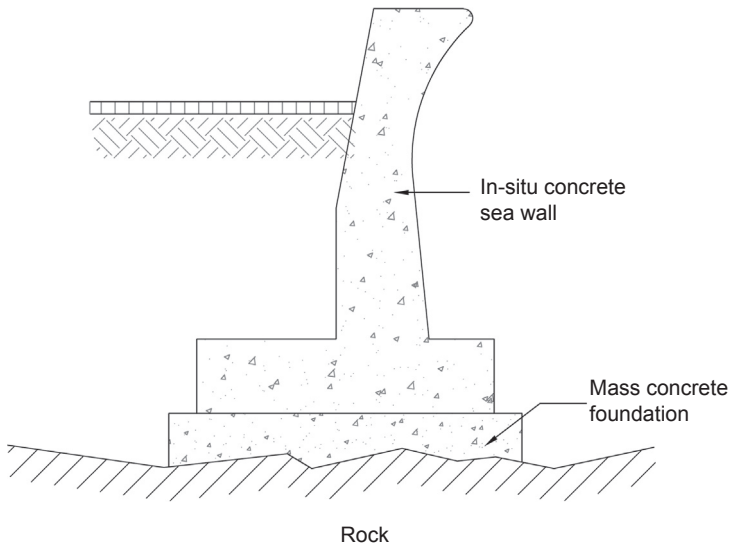



**Figure 2.48** Typical seawall cross-section. When constructing on rock, a rough foundation is usually done first, and on top of this the formed wall profile is cast.

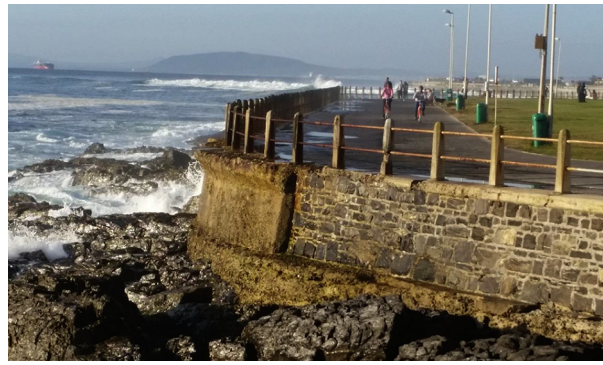


**Figure 2.49** Sea Point promenade seawall, Cape Town. The section of wall on the wall corner has a cross-section similar to that shown in Fig. 2.48. Of note are the initial concrete foundation cast onto the rock and the profiled wall cast above it. This is a harsh marine environment with abrasion and impact forces from the waves, evidenced by the damage to the wall section on the right.

Both in-situ and precast concrete elements can be used, depending on the particular configuration of the wall (Fig. 2.49).

### 2.2.2 Breakwaters and revetments

The most common form of contemporary breakwater and revetment construction consists of an armoured rock rubble mound with a concrete capping. Breakwaters are normally freestanding and form the outer protection for a harbour. Revetments are constructed along a shoreline and protect it from wave attack. Examples of breakwaters and a revetment are given in the chapter 'Notable Southern African marine structures'.

The breakwater or revetment armour may consist of large-size rock or precast concrete units depending on the design wave parameters. There are practical limits to the size and mass of armour rock that can be quarried due to the inherent geological joints, and therefore precast concrete units are used when a greater armour unit mass is required.

The concrete capping serves to reinforce the top of the mound and provide a roadway for in-service maintenance. Fig. 2.50 shows a typical rubble-mound breakwater cross-section with a cast in-situ plain concrete cap. The cap needs to be heavy enough to resist the wave loads that impact onto the splash wall on the seaward side and would typically be a minimum of 1 m thick.

Sometimes a vertical wall is used as a breakwater instead of a rubble mound. Kalk Bay harbour on the Cape Peninsula is an example of an old vertical wall breakwater that was constructed from mass concrete blocks. More common nowadays is to construct the wall from caissons, as shown in Fig. 2.51, and examples from Ngqura harbour are given in the chapter 'Notable Southern African marine structures'.

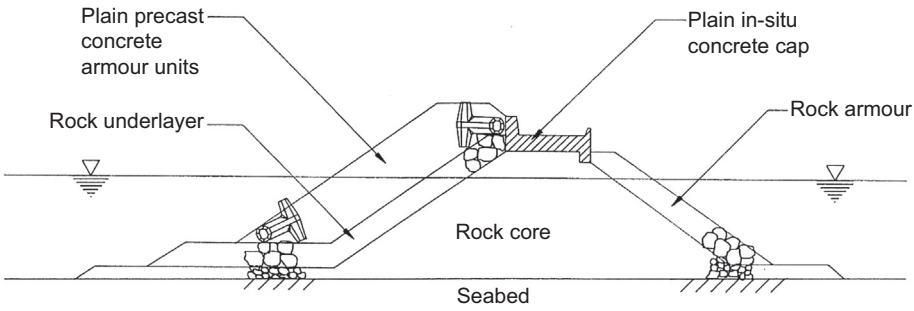



**Figure 2.50** Rubble-mound breakwater cross-section. Plain concrete is used for the armour units and the cap, although some reinforcement may be needed to strengthen the splash wall.

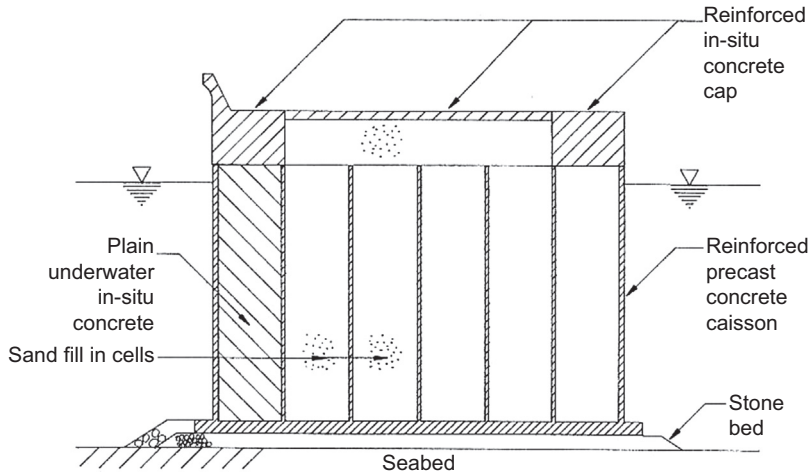



**Figure 2.51** Typical caisson breakwater. The precast caisson used for breakwaters is usually of similar form to those described in the quay wall section and is sand-filled and topped by a plain concrete cap.

### *2.2.2.1 Breakwater armour units*

A large variety of precast concrete armour units have been invented over the years, from a simple cube to complex shapes such as the cob and tetrahedron, and a selection of these are illustrated in Fig. 2.52. Breakwater armour units are typically plain, unreinforced concrete without any steel reinforcement. Some units are used in single layers, and some require two layers to pack and function correctly.

When properly packed on a breakwater, armour units move very little, and there is no need for them to be reinforced to resist the hydraulic loads from the wave impact. Attempts have been made to reinforce armour units to resist the forces that occur,

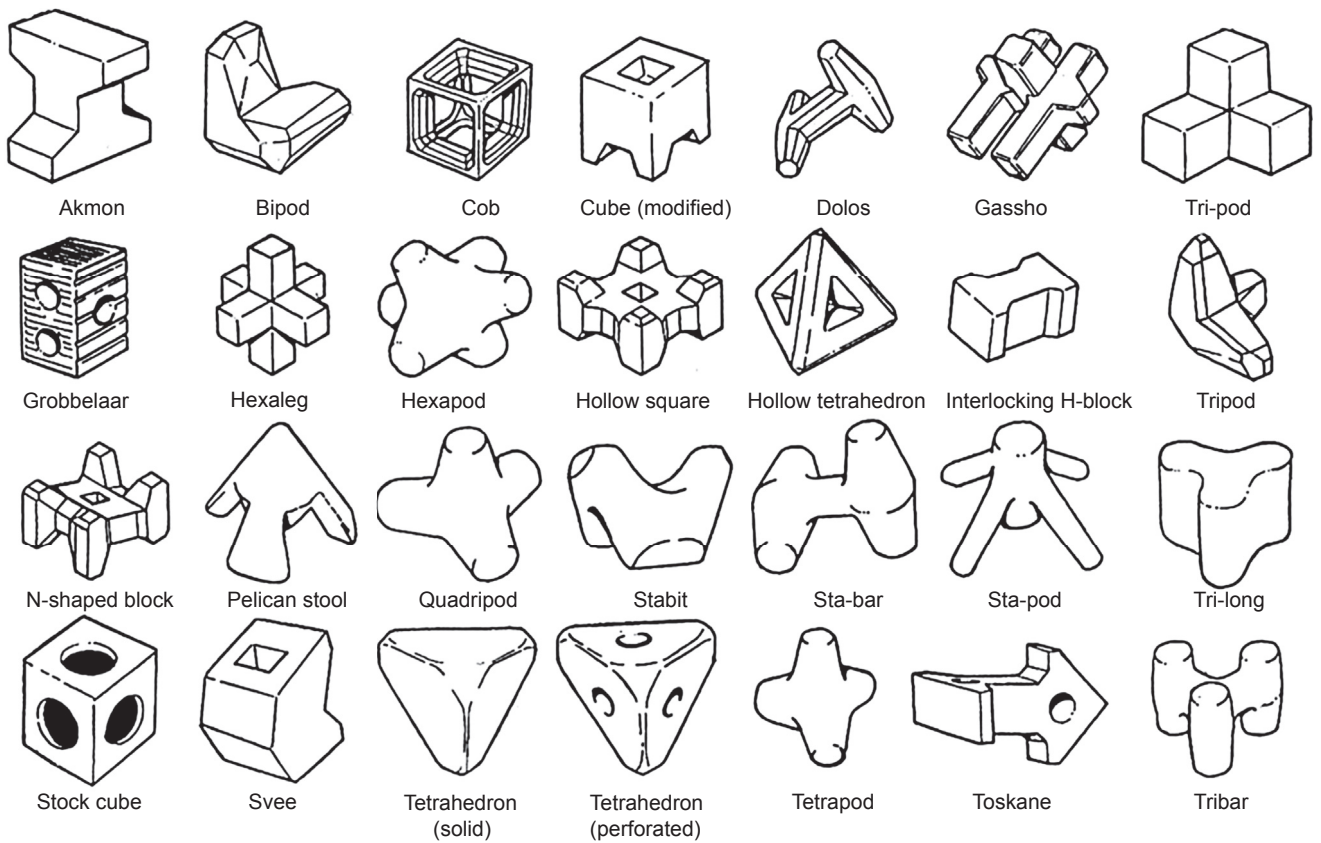



**Figure 2.52** Breakwater armour units constructed from plain concrete.

should the units move if improperly packed, but this has never been successful due to the very high impact forces that occur.

The dolos armour unit originates from South Africa and has been used extensively around the world as it is economical, requiring less concrete per square metre of breakwater surface area than most other units. It is a double-layer unit, and its shape has evolved as the design has been used and improved. The current dolos shape has a relatively thicker waist and filleted corners in comparison to the original one.

The largest dolosse that have been used in South Africa are the 30-tonne units on the Ngqura harbour breakwaters in the Eastern Cape (Fig. 2.53).

Examples of single-layer units in use are Core-loc™, Accropode™ and Cubipod (Fig. 2.54).

As armour units are unreinforced, the tensile capacity of the concrete is an important functional requirement, as is good-quality casting. Any cracks or large surface defects can have a detrimental effect on the performance of the unit. Cracks cause a reduction in the cross-sectional area of the unit, and if this is at a critical section such as the intersection of the waist and fluke of a dolos, the section can be




**Figure 2.53** 30-tonne dolos.

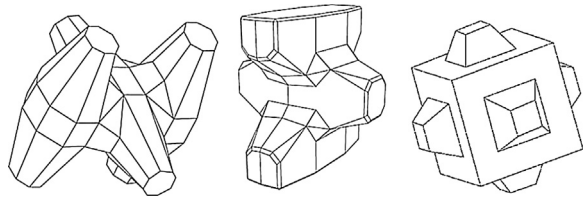


**Figure 2.54** Core-loc™, Accropode™ and Cubipod single-layer armour units.

significantly weakened. Large surface defects may also cause structural weakness or an underweight unit and hence loss of stability.

### 2.2.2.2 Breakwater cap

The main function of the breakwater cap is to protect the top of the rock mound against scour from overtopping waves and to provide a roadway for in-service maintenance. The cap frequently has a wave wall or splash wall on the seaward side, and this serves to protect personnel and vehicles on the cap from overtopping waves. The thickness of the cap and its splash wall facilitates the termination of the top of the rock mound at a lower level, thereby saving rock. Down-stands are sometimes incorporated to key into the top of the rock mound to mobilise additional weight for resistance against lateral wave loads. A typical breakwater cap is shown in Fig. 2.50, and specific South African examples are described further in the chapter 'Notable Southern African marine structures'.

It is usually advisable to cast the cap in-situ so it keys into the rock mound, but pre-cast units are sometimes incorporated to save time on site. As the top of the breakwater is narrow and access space is limited, it is conventional to cast breakwater cap panels from the roundhead end to the root. In this way, there is no need to traffic across recently cast cap panels.

### 2.2.2.3 Caisson breakwater

In deep water, it is sometimes economical and practical to construct the breakwater structure using reinforced concrete caissons instead of a rock rubble mound. The width and height of the caissons are sized to resist the hydrostatic pressures from the impact of the design wave. Wave conditions at the site have to be suitable for caisson placing, with sufficiently long periods of time when wave heights are less than 1 m, to position and sink the caisson (Fig. 2.55).



**Figure 2.55** Port of Cape Town breakwater. The end section of the breakwater is constructed from seven caissons, each with four round cells. The caisson ends just above the layer of marine growth and is topped with a solid, plain concrete cap.

The caissons are cast in the dry in a dry dock or a casting yard equipped with a lift and then floated into position and sunk by flooding. Once in place on the seabed, the caisson is flooded fully, filled with sand, and an in-situ cap is cast on top.

Caissons have been used in the end section of the main Table Bay breakwater and the Ngqura harbour breakwaters, and the latter example is described in more detail in the chapter 'Notable Southern African marine structures'. Caisson breakwaters have been used extensively in Japanese harbours due to the limited availability of rock that is suitable for breakwater construction.

### 2.2.3 Coastal jetties

Jetties are constructed in exposed coastal locations for a variety of functions, including cargo export/import, sand bypass facilities, seawater intakes, effluent outfalls and beach groynes.

Coastal jetties are designed and constructed using similar principles to jetties located within protected harbours (see Section 2.1.2), except that the design of the jetty has to take into consideration the hydrodynamic loads resulting from the waves and ocean currents at the site. Where possible the jetty superstructure is located above the maximum wave crest level to avoid the impact loads from the waves (see Fig. 2.56).

South African examples of coastal jetties include the sand bypass jetty at the Ngqura harbour (described in chapter 'Notable Southern African marine structures'), a groyne at Hobie Beach Port Elizabeth (Fig. 2.56), the seawater intake for the u'Shaka Marine World aquarium in Durban (Fig. 2.57) and the Durban beach groynes (Fig. 2.58).



**Figure 2.56** Coastal jetty wave impact. This is the groyne jetty at Hobie Beach in Port Elizabeth and is subject to depth-limited waves.



**Figure 2.57** u'Shaka Marine World intake jetty. The jetty supports a battery of intake pipes at the seaward end and made extensive use of precast concrete in its construction.



**Figure 2.58** Durban beach groynes. The groyne structure comprises two rows of square precast concrete piles supporting a precast and in-situ concrete superstructure. The space in between the piles is filled with rock to form a groyne sand barrier. https://commons.wikimedia.org/wiki/File%3ADurban_21.08.2009_12-27-33.jpg; https://upload.wikimedia.org/wikipedia/commons/3/32/Durban_21.08.2009_12-27-33.jpg; By Simisa (talk · contribs) (Own work) [CC BY-SA 3.0 (http://creativecommons.org/licenses/by-sa/3.0)], via Wikimedia Commons.

### 2.2.4 Bridges

The corrosive marine environment will affect all concrete structures located on or near the coast, and therefore it is advisable to design bridges in the coastal zone as marine structures, even though they may not have direct contact with the sea.

Different countries or regions have different requirements for coastal structures other than ports, harbours, jetties and so on, and this is outside the scope of this chapter. However, as an example, the South African National Roads Agency Limited (SANRAL) specifies a performance-based approach for bridge structures in chloride-induced corrosion environments, and this is discussed further in the chapter 'Design and specification of marine concrete structures'.

### 2.2.5 Submarine pipelines

Submarine pipelines are utilised for the transport of seawater, bulk oil and gas products, and effluent, and they are usually manufactured from steel or high-density

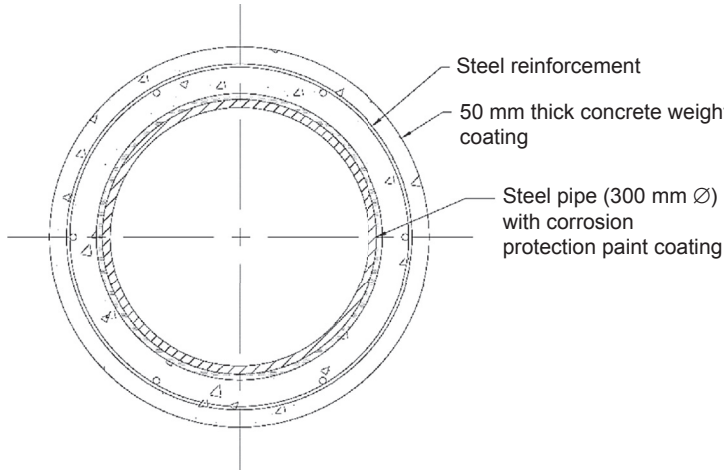



**Figure 2.59** Submarine steel pipe with concrete coating.

polyethylene (HDPE). Frequently, concrete is employed to provide weight to the pipeline to give it sufficient stability under wave loading and ocean currents.

Steel pipes usually have a continuous in-situ concrete 'coating' applied to give weight and mechanical protection to the corrosion protection coating, as shown in Fig. 2.59.

HDPE pipelines usually have discrete precast concrete weights clamped on to provide the stability, as shown in Figs 2.60 and 2.61 of a seawater intake pipeline in the Middle East. This technique has been used for a number of effluent outfalls in South Africa.

## 2.2.6 Hydraulic coastal structures

There are a number of different hydraulic control facilities in the marine environment, including ship and boat locks and surge barriers.

### 2.2.6.1 Ship and boat locks

Ship and boat locks are used to transfer vessels from one water body to another where there is a difference in level between the two. Locks have been used extensively in developed countries where ships and boats have a long history in the transport of goods, and where as a result there are significant networks of navigable waterways.

Although the majority of locks will be found inland in fresh water environments, locks do occur in the marine environment. One of the best examples is the Panama Canal locks in Central America, which is discussed in more detail in terms of construction of the new Panama Canal in the chapter 'Concrete durability of the new Panama Canal: background and aspects of testing' of this book.



**Figure 2.60** HDPE pipeline with precast concrete weights. The weights are cast in two parts and bolted together. Their size and spacing will depend on the mass required to keep the pipeline stable with the design wave loading applied.



**Figure 2.61** HDPE pipeline with precast concrete weights. Air-filled pipeline with weights being launched. Once launched, the pipeline is towed to the desired location and sunk in place by flooding with water.

Examples of locks for recreational craft at coastal marinas can be found in the United Kingdom at Chichester, Hythe and Solent, and in South Africa at the Victoria & Alfred Waterfront (V&AW) in Cape Town. The V&AW lock is shown in Fig. 2.62 and is part of the canal described in the chapter 'Notable Southern African marine structures'.



**Figure 2.62** Victoria & Alfred Waterfront boat lock. The structure has a reinforced concrete barrel and gate abutments and has sufficient weight to resist floating when dewatered.

Locks typically have an in-situ reinforced concrete lock barrel and structural steel gates. Due to the sea tidal levels and the range of water levels in the lock barrel, the walls and base slab have to be designed for differential water levels. The constant wetting and drying of the lock barrel walls will contribute to the aggressive nature of the environment.

### *2.2.6.2 Surge barriers*

Surge barriers are utilised to protect low-lying land areas adjacent to tidal rivers from inundation during extremely high water events. They usually comprise one or more steel gates with reinforced concrete abutments against which the gates seal and in which the drive equipment is located. They are usually left open and are only closed to restrict the flow of water when there is a risk of flooding.

One of the most well-known surge barriers is that across the River Thames in the United Kingdom, see Figs 2.63 and 2.64. It protects the Greater London area from the high water levels that arise from a combination of storm surge and spring tide, and it was constructed between 1974 and 1982.

There are nine piers spaced across the river with steel sector gates in between, of which the six central ones are navigable. These gates sit in a concrete sill on the river bed when open.

The reinforced concrete piers were constructed in-situ inside cofferdams, and the hollow, prestressed concrete sill units were constructed on land, floated, and then sunk into position. The sills contain two tunnels which provide access to the piers from the land.

The chapter ‘Coastal protection structures in the Netherlands’ in this book describes another major surge barrier: the Eastern Scheldt Storm Surge Barrier in The Netherlands.



**Figure 2.63** Thames River surge barrier. The six central sector gates are navigable, and of these, the four larger ones allow passage of ocean-going ships. The three sector gates on the far bank and the one on the near bank are not navigable and are raised when open. https://commons.wikimedia.org/wiki/File%3AThamesBarrierPano.jpg; https://upload.wikimedia.org/wikipedia/commons/8/82/ThamesBarrierPano.jpg; By © Bill Bertram (Pixel8) 2008 (Pixel8) [CC BY-SA 3.0 (http://creativecommons.org/licenses/by-sa/3.0)], via Wikimedia Commons.



**Figure 2.64** Thames River surge barrier. Detail of a typical pier, sill and gate. The structures are founded on the chalk bedrock, and the detail of the hollow sill and tunnels are visible in this view. The 20-m-high sector gate is shown in the raised position, and when lowered the flat surface is flush with the top of the sill.

### 2.2.7 Oil production platforms

The most common construction material that has been used for off-shore oil production platforms is steel; however in the North Sea, some 47 reinforced concrete platform bases have been utilised by the Norwegians and British. The North Sea platforms are the most well-known, but they have also been used for Brazilian, Australian and Canadian oil fields.

These are massive structures due to the water depths involved and the wave loading that has to be resisted. Due to their size and their floating draft, special dry dock facilities and deep near-shore water depths are required for their construction.

They typically have a large gravity base constructed as a cellular caisson, which provides the buoyancy for the platform, allows it to be towed to site and sunk into position and is sometimes used for storage of the oil.

Figs 2.65 and 2.66 show some examples of North Sea concrete platforms.



**Figure 2.65** Reinforced concrete oil platforms under construction. The large caisson base (100 m square × 56 m high) provides the stability for the platform, and the four 116-m-high towers support the steel topside structure.

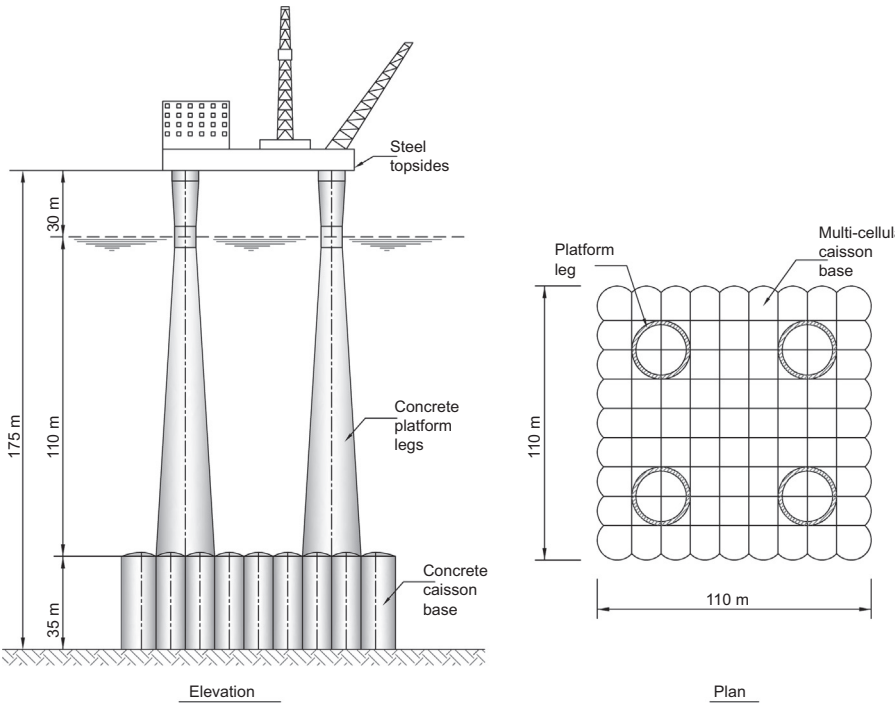



**Figure 2.66** Reinforced concrete oil platform installed on the seabed. The concrete base is towed into position without the topside modules and sunk onto the seabed, and once in place the steel topside modules are transported to site by barge and installed.

### 2.2.8 Other concrete coastal structures

Other structures in contact with the sea or located in the coastal zone are affected by the aggressive marine environment and appropriate durability measures should be taken relevant to their service life. A selection of particular marine structure types are discussed in the following sections.

#### 2.2.8.1 Lighthouses

Lighthouses are located adjacent to the sea and often in very exposed locations, and there are many marking the 3700-km-long South African coastline. The older lighthouses were constructed from masonry and cast-iron panels, whereas the more modern ones have been constructed from reinforced concrete, such as the one at Umhlanga Rocks near Durban, Fig. 2.67.

#### 2.2.8.2 Intake and outfalls

Intakes and outfalls are utilised to abstract and dispose of seawater when it is used in applications such as desalination plants, power station cooling or artificial water features. Structural elements such as breakwaters and jetties common to other port and coastal structures are frequently used.

The abstraction and disposal of cooling water for the Koeberg Nuclear Power Station near Cape Town required extensive marine works. A harbour-type structure was constructed to create a stilling basin for the water intake pump station; see Fig. 2.68. It comprises two conventional rock-rubble-mound breakwaters with mass concrete caps and armoured with dolosse.



**Figure 2.67** Umhlanga Rocks lighthouse, near Durban.



**Figure 2.68** Koeberg power station cooling water intake and pump station. The two conventional breakwater structures form a calm, protected basin for the pump station located on the shoreline.



**Figure 2.69** Koeberg power station cooling water outfall. The discharge water is piped to the head of the outfall and flows out to sea in the open channel. The main function of the outfall channel is to absorb the wave energy and to protect the channel head wall works. Visible in this photograph are the in-situ concrete caps of the concrete sheet pile channel side walls.

The power station cooling water outfall channel has a reinforced concrete headwall and side walls formed from concrete sheet piles (as described in section 'Precast sheet piles') with an in-situ concrete cap; refer Fig. 2.69.

Fig. 2.70 shows an example of an outfall for an artificial perched canal system in Dubai, comprising precast, reinforced concrete culvert units. In this type of application, the use of precast elements is the best way of achieving an immersed structure with high-quality concrete.

### *2.2.8.3 Pump stations*

Seawater is used in applications such as power stations, sand bypass systems and aquariums, and in most instances, it is necessary to pump the seawater. Although the water is

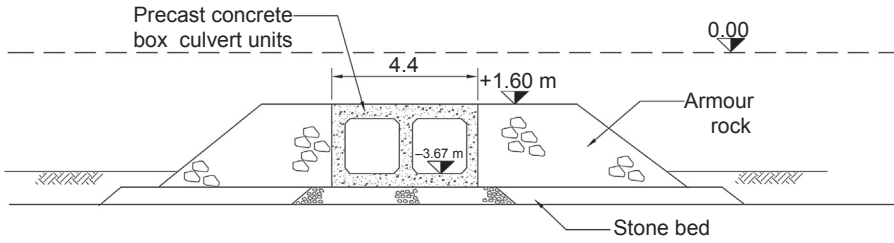



**Figure 2.70** Canal outfall, Dubai (dimensions in metres are illustrative). This outfall was constructed in benign open sea conditions, which allowed placement of a screeded stone bed and the precast units, a technique normally used in blockwork and counterfort quay walls.

generally contained in the pumps and pipes, any concrete reservoirs or chambers which come into contact with the seawater should be treated as marine structures.

## 2.3 Sea water–retaining structures

There are specialised applications in which it is necessary to contain a volume of sea water. Three of these are described as follows:

### *2.3.1 Aquarium tanks*

The displays and systems for marine aquariums contain well-oxygenated seawater and are highly aggressive environments for construction materials. Wherever possible, noncorrosive materials are used such as plastics, resins, epoxies and glass in the tanks and water reticulation systems.

However, it is usually necessary to construct the larger tank structures from reinforced concrete. Reinforced concrete tanks are usually lined, and although the concrete is not in direct contact with the seawater, it is advisable to use a marine-grade concrete with a water-retaining design in case of leaks through the lining membrane, especially in view of the consequences of premature deterioration and the very high costs associated therewith.

The tank is often contained within a building structure which is constructed from standard building grade concrete and other materials which are not intended for use in a marine environment. It is therefore essential that all seawater is contained within a watertight tank and that no leakage occurs which would be deleterious to the building structure and finishes. This is in contrast to other water-retaining structures, such as those used in water treatment and sewerage plants, where some degree of leakage is permissible, at least until self-healing takes place. The aquarium tank structure is therefore very reliant on the lining to create a watertight structure.

Aquarium tank structures have been constructed in recent years in South Africa at the u'Shaka Marine World in Durban and the Two Oceans Aquarium in Cape Town. Fig. 2.71 shows a new tank (2015) at the Two Oceans Aquarium in Cape Town and illustrates the main reinforced concrete tank structure with acrylic viewing windows and tunnel.



**Figure 2.71** Two Oceans Aquarium Predator Tank. This photograph shows the tank during construction. The water-retaining lining had not yet been applied, and the reinforced concrete tank structure is visible. Protective membranes were still applied to the acrylic windows and tunnel.

### 2.3.2 Sand bypass hoppers

Sand bypass systems are constructed to artificially maintain sediment movement along a coastline when artificial activities such as the construction of a harbour interfere with the natural functioning of the coastal system. Such systems sometimes require a sand hopper to store sand discharged from a dredger for subsequent release into the downstream side of the coast.

The sand bypass system constructed as part of the Durban harbour entrance widening, completed in 2016, includes an in-situ, reinforced concrete sand hopper (Fig. 2.72). This was designed as a conventional water-retaining structure but utilised



**Figure 2.72** Durban sand bypass system. This photograph was taken toward the end of the hopper construction, and the empty horse shoe−shaped sand hopper is visible with the gantry that carries the sand pumps on the left-hand side.



**Figure 2.73** Harmony Park tidal pool, Strand, Cape Peninsula.

a grade of concrete suitable for the marine environment and is described further in the chapter 'Notable Southern African marine structures'.

### *2.3.3 Tidal pools*

Tidal pools are popular coastal recreational facilities, and concrete walls are usually used to create the pool. They are often constructed on rocky shorelines, and since it is necessary to seal the walls onto the rock surface to create a watertight pool, cast in-situ concrete walls are preferred.

Fig. 2.73 shows a tidal pool at Harmony Park in Strand in the Cape Peninsula area where extensive use has been made of concrete to create the pool and landscaping elements.

## 2.4 Summary

A wide range of marine concrete structure types has been presented in this chapter, covering the range of techniques that have been commonly used since the start of port and coastal construction in South Africa and abroad. It is evident that concrete has become an indispensable component of marine structures, ensuring durability and robustness and facilitating techniques that could not otherwise be used.

Blockwork quay walls have already demonstrated the durability of plain concrete in the marine environment, and it is expected that the techniques and materials used in modern structures, which are described in this book, will ensure that they achieve a comparable service life.

## Sources of further information

- Accropode™, http://www.concretelayer.com/armour-solutions.
- Core-loc™, http://www.erdc.usace.army.mil/Media/FactSheets/FactSheetArticleView/tabid/9254/Article/476715/core-loc-concrete-armoring.aspx.
- Cubipod, http://www.cubipod.com/index.php/en.

- CUR, 2005. Handbook Quay Walls, Taylor and Francis, Netherlands.
- Hoberman, G., 2011. Lighthouses of South Africa, The Gerald & Marc Hoberman Collection in association with Transnet National Port Authority, South Africa.
- Horner, R.W., February 1985. Dugald Clerk Lecture: The Thames Barrier. In: Proceedings of the Institution of Civil Engineers, 78 (1).

## References

Brinkmann, B., 2005. Seehäfen, Planung und Entwurf. Springer, Germany.

Christiani & Nielsen, 60 Years of Civil Engineering 1904−1964, (Denmark).

Fairfield Energy, January 2012. Dunlin Alpha Decommissioning: Concrete Gravity Base: Stakeholder Engagement: Summary Report.

Institute of Engineers Australia, https://www.engineersaustralia.org.au/sites/default/files/shado/Divisions/Sydney%20Division/Resources/Technical%20Presentations/Combined%20JDM-SH-AKB%20-%20PBE%20Presentation%20by%20Golder,%20Hyder%20&%20Scott%20Wilson.pdf (accessed 2015.).

Mazurkiewicz, B.K., 1980. Design and Construction of Dry Docks. Trans Tech Publications, Germany.

Moss-Morris, A., Hodge, N.M., 1981. Design and construction of quay Wall for a container terminal founded on fissured clays. In: 25th International Conference of Navigation, Section II, vol. 4, Edinburgh, 1981.

Sir Robert McAlpine, http://www.sir-robert-mcalpine.com/projects/, Concrete Gravity Platforms (accessed 2015.).

TNPA (Transnet National Ports Authority), Various historical drawings.

UK Environment Agency, 2015. Thames Barrier Project Pack. https://www.gov.uk/guidance/the-thames-barrier.

Wernsen Jr., P., 2010. The Euromax Quay Wall: A Durable Construction. Ports 2010: Building on the Past, Respecting the Future, ASCE.

# Design and specification of marine concrete structures

3

*P.E. Smith*
Prestedge Retief Dresner Wijnberg (Pty) Ltd

## 3.1 Introduction to marine concrete structure design

This chapter describes the materials used in marine concrete structures, provides recommendations for the design and specification of the concrete elements in such structures and describes a selection of design aspects of some common structures and elements. The chapter only addresses the design and specification of the concrete elements and does not cover the overall design of the structures, such as general layout, stability and strength, for which other specialist sources should be consulted. This chapter is not intended to be a comprehensive design manual, but rather a guide on the recommended approaches to be taken.

The design and specification of marine structures is dominated by durability concerns, and therefore the materials selected and the way in which they are used is central to achieving the desired service life.

Plain concrete, without steel reinforcement, is generally stable and durable in the marine environment, but when steel reinforcement is added, durability becomes a major consideration because of the vulnerability of the steel to corrosion. (See also Chapter 5 of this book.) The chlorides in the seawater are the major contributor to the initiation of steel corrosion, and three different approaches can be taken to deal with this and achieve durability in the marine environment.

The most common approach is to protect the steel with a high-quality concrete cover, thus prolonging the ingress of the chlorides such that the desired service life is obtained before there is sufficient chloride concentration at the steel location to initiate corrosion, or alternatively to provide the concrete with additional means of preventing ingress of aggressive salts. A second approach is to use reinforcement materials that are corrosion resistant in a chloride-rich concrete environment, in which case the service life is less dependent on the concrete quality. The final approach is cathodic protection of the embedded steel, but as this method is infrequently used, it is only dealt with briefly at the end of the chapter.

Methods used to protect the reinforcing steel include these:

- Embedding the steel in a concrete that is resistant to chloride penetration. A combination of a concrete with low penetrability and sufficient thickness of such cover concrete provides this protection. The penetrability and thickness of the cover concrete will be the primary factors

**Marine Concrete Structures.** http://dx.doi.org/10.1016/B978-0-08-100081-6.00003-9
Copyright © 2016 Elsevier Ltd. All rights reserved.

in determining whether the service life of a structure will be, for example, 25 years or 100 years. Materials that reduce the concrete penetrability include these:
  - Cementitious extenders such as slag or fly ash added to the concrete mix.
  - A range of proprietary products that claim to fill the pores in the concrete matrix and thereby reduce the penetrability (refer Section 3.4.4.3).

  Also, it is essential that the concrete is made with a low water/binder ratio to ensure excellent impenetrability.
- Application of a coating onto the bars, such as these
  - Epoxy paint coating
  - Hot dip galvanising of the bars
- Additional protection to the concrete to limit the ingress of chlorides:
  - Chemical coatings or other chemicals such as hydrophobic sealants applied to the concrete surface
  - Nonpermeable wrapping applied to the concrete surface

Corrosion resisting reinforcement materials include these:

- Stainless steels
- Fibre-reinforced plastics (FRPs)

Section 3.4 describes these various materials in more detail.

The design and construction of all structures, including marine structures, is governed by the requirements and recommendations of codes of practice and standards issued by national institutions or standards-generating bureaus. In some countries, specific codes of practice and standards have been created for marine structures, and these provide varying degrees of guidance for the design of the concrete and reinforcement to achieve the desired service life. Section 3.3 describes the principal codes of practice in use around the world.

An important factor in the design of marine concrete structures is the variation in microenvironments in different parts of the structure. The penetration of chlorides into the concrete and the corrosion of the reinforcement are dependent on alternate wetting and drying of chloride-rich water and the presence of oxygen. The tidal zone and the splash zone above it are therefore the most aggressive zones due to the frequent wetting and the free availability of oxygen. The parts of the structure that are permanently submerged or backfilled have little oxygen present and hence are less corrosion-prone. On the other hand, the atmospheric zone, which is not wetted from splash or spray, has ample oxygen, but the chloride supply is low.

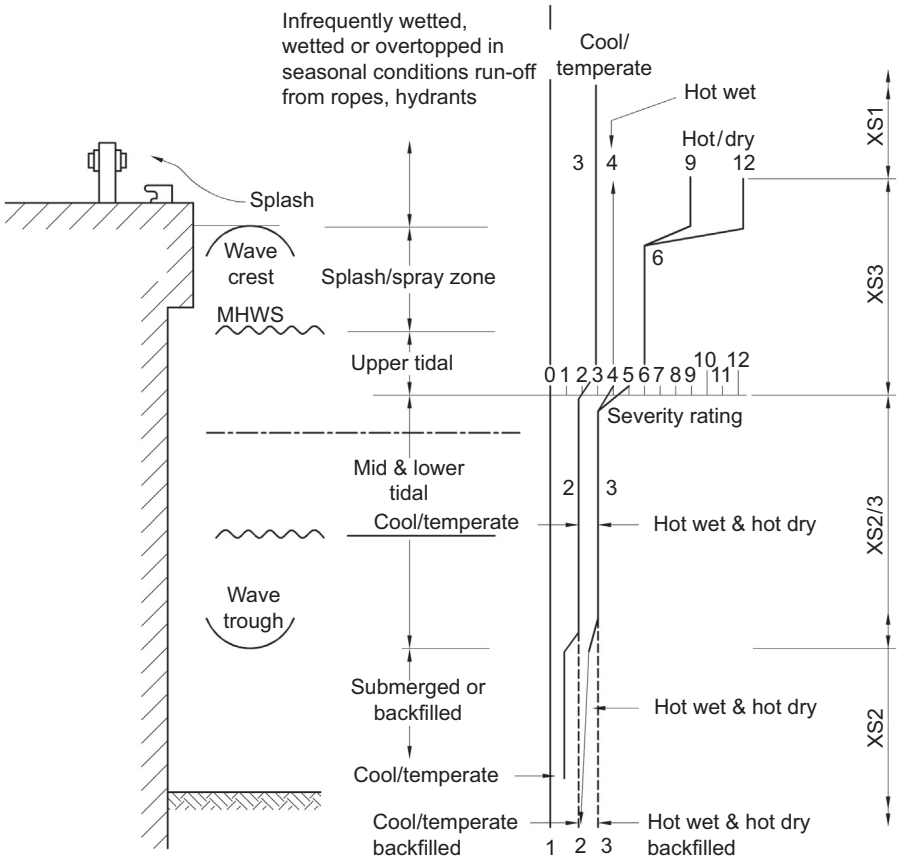
The Euro-norm classification of environments is given in BS EN 206-1:2013, which defines a series of exposure classes for the typical environments to which concrete structures are subjected. These include no corrosion risk (X0), carbonation-induced corrosion (XC), chloride-induced corrosion (XD, XS), freeze/thaw attack (XF) and chemical attack (XA). Marine structures are subject to chloride-induced corrosion from seawater, and therefore only exposure class XS is applicable, unless the possibility of freeze−thaw is also present in cold climates, in which case XF may also be a consideration. BS 6349-1-4:2013 expands on the XS classification, and this is given in Table 3.1.

Fig. 3.1 illustrates the variation in corrosivity in the different parts of a typical marine structure and the location of the XS microenvironments.

**Table 3.1 Definition of microenvironments for various exposure conditions**

| Microenvironment | Description |
|---|---|
| XS1 | Exposed to airborne salt but not in direct contact with seawater |
| XS2 | Permanently submerged |
| XS2/3 | Frequently wetted (eg, mid- and lower tidal zone and backfilled) |
| XS3 | Infrequently wetted (eg, upper tidal, splash/spray, 'dry' internal faces of submerged structures) |

Adapted from BS 6349-1-4:2013, 2013. Maritime Works-Part 1-4: General - Code of Practice for Materials. The British Standards Institution, United Kingdom, clause 4.3.3.1.




- MHWS = mean high water springs
- Upper tidal is approximately the upper quarter of the tidal range

**Figure 3.1** Microenvironments (XS1 to XS3) for various exposure conditions and suggested severity ratings for chloride-induced corrosion of reinforcement, on a scale of 1−12, for a range of climates from temperate to hot/dry. The variation in corrosion severity with climate must be considered when using European-based codes.
Adapted from Fig. 70 of BS 6349-1:2000, Part 1: Code of Practice for General Criteria.

**Table 3.2 Indicative design working life categories for maritime works**

| Design working life category | Indicative design working life (years) | Examples |
|---|---|---|
| 1 | 10 | Temporary structures[a] |
| 2 | 10 to 25 | Structural parts designed to be replaceable within a structure or facility of longer design working life |
| 3 | 15 to 30 | Structures dedicated to nonrenewable natural resources, petrochemicals or similar industrial or commercial applications (such as open-piled jetties, mooring and berthing dolphins, Ro-Ro link spans) |
| 4 | 50 | Common port infrastructure for commercial and industrial ports including reclamation, shore protection, breakwaters, quay walls |
| 5 | 100 | Common port infrastructure including breakwaters for ports of nationally significant strategic or economic value; infrastructure for regional flood defence or coastal management infrastructure |

[a]Structures or parts of structures that can be dismantled with a view to being reused should not be considered as temporary. Adapted from BS 6349-1-1:2013, 2013. Maritime Works-Part 1-1: General - Code of Practice for Planning and Design for Operations. The British Standards Institution, United Kingdom, Table 1.

The design working life of a marine structure needs to be defined from the start so that appropriate durability measures can be taken in its design. Table 1 of BS 6349-1-1:2013 provides guidance on suitable design working lives for a range of typical marine structures, and it is reproduced as Table 3.2.

The durability design for a structure, or parts thereof, should be refined based on the required design working life and the microenvironments (see, eg, Fig. 3.1).

An essential part of a project is the prior drafting and agreement of the basis of the design. This sets out the requirements of the owner/client, including project location, environmental conditions (such as tidal levels, wave size and period), function (such as vessel type and size for a port structure), imposed loads (such as shiploaders or stacked cargo), and the desired service life of the facility. It also provides the opportunity for the owner and designer to set out and agree on the type of structure, and the durability and in-service maintenance requirements. It is advisable to obtain clarity and agreement on these aspects at the start of the project to prevent any miscommunication or disagreement during the design and construction process.

## 3.2 Prescriptive versus performance-based specifications

Marine structures utilise some specific techniques, and in-service durability is always paramount, which together lead to some very particular design and specification

requirements. Unless noted otherwise, all the codes of practice and their recommendations that are covered in this section pertain to the design of concrete reinforced with plain carbon steel, the most common reinforcement in use around the world.

It is possible, given a suitable set of materials and the marine microenvironment in which a structural element is located, to design the concrete mix and cover by analysing the transport of the chlorides into the concrete to achieve the desired service life. This direct analysis of the performance of the concrete in service would enable fine-tuning of the mix parameters and cover to create the most economical, fit-for-purpose structure. This is called a performance-based approach, and to monitor and verify the quality of the concrete actually used in the structure, test methods are required that measure the relevant transport-related properties of the material. (Chapters 9, 13, 15 and 16, give interesting examples of performance-based approaches.)

The alternative approach for achieving durability is to determine by experience and testing which concrete mixes and covers will give the required performance for a required exposure and life, and then simply repeat such parameters for concrete in similar applications. This is called a prescriptive approach, where an accepted 'recipe' is followed for the particular conditions. A typical prescriptive recipe would specify minimum binder content, the type and proportions of the binder (Portland cement and extender), water/binder ratio, concrete strength and the minimum concrete cover to the reinforcement. The majority of codes of practice follow such a prescriptive approach. Quality control in this approach is limited to concrete strength tests due to the lack of test methods to verify the composition of hardened concrete.

A third approach is a 'hybrid' one with a mix of prescriptive and performance requirements (Kessy et al., 2015). In this approach, both prescriptive and performance criteria are prescribed due to the immaturity of full performance-based approaches at present. Such specifications can also contain performance criteria in the form of relevant 'durability indicators', which are measured on the actual concrete. For example, the South African National Roads Agency Limited (SANRAL) uses a hybrid type of specification for the concrete structures used in roadworks, and the section for structures located in the marine environment focuses on the performance with respect to chloride ingress. Acceptable binder mixes and minimum concrete covers are prescribed together with acceptable values for certain durability indicators. The SANRAL specification, SANRAL Table 6000/1, is described further in Section 3.6.3.4.

Some pros and cons of each approach are given in Table 3.3.

## 3.3 Codes of practice for design and specification of marine concrete structures

### *3.3.1 Introduction*

BS 6349 is considered to be the most comprehensive contemporary suite of codes for the design of maritime civil engineering works, and it represents industry best practice. The BS 6349 codes are aligned to the Eurocodes, and thus they present a harmonised

**Table 3.3 Pros and cons of prescriptive and performance-based durability specifications**

| Specification method | Pros | Cons |
|---|---|---|
| Prescriptive | Simple to use, particularly for small projects<br>The contractor does not need to have any knowledge of specialist techniques or need any specialist equipment | Specified binder contents are likely to be conservatively high to allow for the variations in exposure and materials; this may be wasteful if a more economical mix with less binder would suffice<br>High binder contents may cause excessive heats of hydration<br>No direct verification of the concrete parameters that influence service life<br>Poor construction practices may affect the durability (such as too much water added to the mix or poor compaction), but no tests available to verify the deviation |
| Performance based | Direct determination of concrete properties and service life<br>Economical use of materials<br>Tests verify properties of the concrete that are more directly applicable to durability; better control of applicable concrete properties<br>Greater awareness by the contractor of the factors affecting durability is required to implement the specification, which should lead to better concreting practices and reduction in the risk of poor concrete<br>Greater flexibility to use different materials, such as corrosion-resistant reinforcement or different binder blends | No global standardisation of suitable durability parameters and tests<br>Specialist testing equipment and personnel expertise required |
| Hybrid | Designer and/or contractor are not required to undertake theoretical calculations of the service life prediction<br>Simple to use, particularly for small projects | Specialist equipment expertise required to undertake the tests, which may not be readily available |

approach when read in conjunction with them. This chapter therefore focuses on concrete design for marine structures based on BS 6349 and the Eurocodes. A brief introduction is presented in this section, and more detail of the design requirements is given in subsequent sections on plain and reinforced concrete design. The recognised exposure classes and the recommended design lives for typical structures, according to BS 6349, have already been addressed in Section 3.1.

The approach taken to achieving concrete durability in some other national standards is also covered briefly, later in this chapter, and the differences in approach are highlighted. The terms 'binder' and 'water/binder' ratio are preferred to 'cement' and 'water/cement ratio', as currently the cementitious materials used for marine concrete are usually blends of Portland cement and an extender. However, for the sections describing these national standards, the word 'cement' has been used to match the terminology used in the standards.

### 3.3.2 BS 6349 and Eurocodes

The BS 6349 Maritime Works suite of codes provides guidance for a wide range of marine structures, including all the typical materials used in their construction. Originally published in 1984, they have been updated to complement the contemporary Eurocodes.

Guidance on the loads/actions to be used in the design of marine structures is given in BS 6349-1-2.

Annexure A of BS 6349-Part 2:2010 provides ultimate limit state (ULS) and serviceability limit state (SLS) partial factors, combination factors and combination formulas for the unique load types experienced by marine structures, as these are not given in the Eurocode EN 1990 series for structural design.

Once the design values of the actions have been determined, the ULS and SLS are analysed according to the EN 1990 suite as applicable to the material type. For concrete structures, EN 1992 is applicable.

BS 6349-1-4:2013 gives guidance on materials for marine structures, and the requirements for plain and reinforced concrete members is discussed in more detail in Sections 3.5 and 3.6.

BS 6349-1-4:2013 gives *prescriptive* recommendations for durability with reference to the exposure class and design life, and includes these:

- permissible binder types
- minimum binder contents
- maximum water/binder ratios
- minimum concrete cover to the reinforcing steel
- maximum crack widths

These recommendations provide the most comprehensive prescriptive design methodology since they provide guidance on using different cement blends. The code does also allow the usage of performance-based design methodologies, but it does not provide much guidance on this.

### 3.3.3 USA standards

Various US authorities, such as the American Concrete Institute (ACI), U.S. Army Corps of Engineers and the Naval Facilities Engineering Command, have published guidelines and specifications for marine structures, but there is no single US equivalent to BS 6349.

ACI 318-05, *Building Code Requirements for Structural Concrete*, and ACI 357R-84, *Guide for the Design and Construction of Fixed Offshore Concrete Structures*, provide prescriptive requirements for concrete durability ACI 357R-84 is more focused on marine structures and stipulates appropriate prescriptive requirements, which are described in Section 3.6.3.

### 3.3.4 Australian standards

Australian codes applicable to marine structures are AS 4997 *Guidelines for the Design of Maritime Structures*, AS 3600 *Concrete Structures* and AS 1379 *Specification and Supply of Concrete*.

The code requirements are prescriptive, and they only give requirements for a 25-year design life. For longer design lives, it is recommended that additional measures are used, such as corrosion-resistant reinforcement (refer Section 3.4.5.4) or penetrability-reduction coatings or additives.

The Australian code requirements are explained in more detail in Section 3.6.3.

### 3.3.5 Japanese guidelines

The Japan Society of Civil Engineers (JSCE) *Guidelines for Concrete, No. 15, Standard Specifications for Concrete Structures-2007, Design* and *Guidelines for Concrete, No. 16, Standard Specifications for Concrete Structures-2007, Materials and Construction* contain some prescriptive requirements based on the exposure class, but they are otherwise performance based. The guides provide the basis for a more rational durability design in which the most economical concrete mix can be determined.

More detail on the JSCE method is given in Section 3.6.3.

### 3.3.6 South African standards

The South African standards for concrete design (SANS 10100-1:2000, *The Structural Use of Concrete, Part 1: Design,* and SANS 10100-2:2014, *The Structural Use of Concrete, Part 2: Materials and Execution of Work*) provide some prescriptive requirements for marine structures.

The SANRAL constructs many road bridges in close proximity to the coast, which therefore experience marine environment conditions.

It is essential to achieve long service lives and reduce life cycle costs for bridges, and SANRAL has developed its own hybrid specification for concrete bridge design. It is based on the durability index tests developed by the Universities of Cape Town

and the Witwatersrand, and it prescribes values of the performance indicators required for the exposure classes defined by the Eurocodes, for both chloride- and carbonation-induced corrosion.

The SANS requirements and the portion of the SANRAL specification covering marine structures and chloride-induced corrosion are described in Section 3.6.3.

## 3.4 Materials

### 3.4.1 Introduction

This section describes the most common materials used in marine concrete structures. It covers the main concrete and reinforcement materials and many of the important minor constituents.

### 3.4.2 Cements and extenders

Cements used for marine structures should conform to BS EN 197-1:2011, *Cement—Part 1: Composition, specifications and conformity criteria for common cements* (or its equivalent in national codes, such as SANS 50197-1). (Clearly, in those parts of the world where the EN standards are not used, materials of equivalent type and properties can be used.)

As the durability of reinforced concrete structures benefits from blends of Portland cement and an extender, acceptable cement types include CEM II, CEM III, CEM IV and CEM V, provided these binders contain a proportion of binder or pozzolan known to resist chloride ingress into concrete, for example fly ash (FA) and ground granulated blast furnace slag (GGBS). CEM I (plain Portland cement) on its own is not recommended for use in marine concrete structures due to its poor chloride-resisting properties, but it can be used if blended at the batching plant with suitable proportions of FA or slag, or possible combinations of these materials with, for example, silica fume. More detail on the suitable cement types is given in Sections 3.5 and 3.6 in this chapter on plain and reinforced concrete design. In some codes of practice, the use of FA or GGBS is as an obligatory requirement due to their role in creating a dense, low-penetrability concrete matrix to resist chloride ion diffusion.

The extenders used in site-blended cements or in ready-mix plants should conform to the relevant standards: BS EN 450-1:2012 for FA and BS EN 15167-1:2006 for GGBS.

In the Western Cape province of South Africa, a somewhat different form of granulated slag is available, ground granulated Corex slag (GGCS), a by-product of the steel refinery in Saldanha Bay. It is an acceptable alternative to GGBS for use in marine structures, although it has a heat of hydration closer to CEM I than to GGBS (Alexander et al., 2003). When calculating the thermal shrinkage of a member, there is no benefit from using the GGCS, and the heat of hydration is taken to be the same as CEM I.

Although seawater contains sulphates, it is not necessary, indeed it is not advisable, to use sulphate-resisting cements (SRC) in marine concrete. SRC has less tricalcium aluminate (C3A) than normal cement, and as it is the C3A that reacts with the sulphates to create expansive products (gypsum and ettringite), it might be expected that lower C3A would be preferable. However, seawater also contains magnesium, and this helps to counteract the deleterious effect of the sulphates, due to the formation of a protective surface layer of $Mg(OH)_2$ or Brucite on the concrete (provided the concrete is not subjected to abrasion) (Fulton's concrete technology, 2009). Also, gypsum and ettringite, formed during sulphate attack, are more soluble in chloride solutions, giving a lower sulphate expansion. The C3A also helps to bind the chloride ions, and therefore the use of SRC would be counterproductive to durability.

### 3.4.3 Aggregates

There are no special requirements for concrete aggregates that are specific for marine structures, except in the case of structures subject to abrasion by pebbles or sand. In such cases, the coarse aggregate should be as hard as, or harder than, the material causing the abrasion.

One aggregate problem that marine structures share with onshore structures, that should always be considered, is that of alkali-silica reaction (ASR). Expansive alkali-silica gel is formed if the aggregate contains metastable forms of silica that react with the alkaline pore solution of the concrete (Fulton's concrete technology, 2009). Three factors are necessary for ASR, and they must all be present simultaneously for it to occur:

- a sufficiently high alkalinity of the pore solution (alkalinity usually caused by the cement)
- a sufficient amount of deleteriously reactive mineral or minerals in the aggregate
- environmental conditions that will promote the reaction (temperature and moisture)

If a reactive aggregate is used in the concrete, the total alkali content of the mix must be checked to verify that it is below the threshold concentration for the reaction to occur. The chief contributor to the alkalinity is the cement, but alkalis may also be introduced to the pore solution by chemical admixtures, the mix water, and seawater, and these may need be taken into consideration in the mix design. A low-alkali cement should be used if the aggregate is reactive. Cement extenders assist in minimising the risk of ASR when used in the proportions normally used for marine reinforced concrete, such as $\geq$40% GGBS or $\geq$20% FA. (Chapter 6 contains more detail on the issue of ASR in marine concrete structures.)

Aggregates that have been found to be reactive in South Africa include hornfels, greywacke and quartzite, in common with other situations around the world. For a structure to be constructed in an environment conducive to ASR, the problem can be mitigated simply by using an aggregate that is not reactive, but this may not always be possible if the source is an uneconomical distance away.

In marine structures, it has generally been found that ASR can occur in the spray zone where alternate wetting and drying occurs, but it tends not to occur in the submerged zone, or at least not in a destructive way.

The ASR check should be a standard requirement in concrete marine structure specifications.

### 3.4.4 Concrete admixtures and surface treatments

A wide range of admixtures is available to enhance and improve concrete performance, both during placing and in its hardened state.

#### 3.4.4.1 Plasticisers/superplasticisers

Plasticisers/superplasticisers (water-reducing admixtures) fulfil an essential function, as they enhance concrete workability while maintaining the low binder/cement ratios needed for marine concrete.

#### 3.4.4.2 Corrosion inhibitors

Corrosion inhibitors serve to inhibit the action of chlorides on the reinforcing steel and prolong the time until the onset of corrosion. They may be added to the concrete mix and infuse the entire element, or be applied on the surface of an existing element and penetrate in. Corrosion inhibitors are useful in cases where it is not possible to achieve full concrete cover on the reinforcement, or in repair situations.

#### 3.4.4.3 Pore filling admixtures

The hardened cement paste of concrete contains voids and capillaries that are created by the excess water in the paste, or lack of full hydration. These voids contribute to the penetrability of the concrete and allow water and chloride ions to penetrate. Admixtures are available that are claimed to fill the voids and thereby decrease the concrete penetrability. This is meant to create ‘waterproof’ concrete without the use of a surface liner or increases the service life by slowing down chloride and oxygen diffusion.

Some of the available products utilise a chemical that is intended to react to form crystals that block the voids. These products may be added to the mix or applied afterwards onto the hardened concrete surface.

#### 3.4.4.4 Coatings

A wide variety of coatings are available to seal the concrete surface and thereby inhibit the penetration of chlorides and oxygen. These are mainly used for concrete repair and rehabilitation, and their use for new structures is not recommended. Almost invariably, there are problems in marine structures with these products peeling off the concrete in time.

#### 3.4.4.5 Anti-washout admixture

It is sometimes necessary to cast concrete or grout underwater, and in such cases, the use of an anti-washout admixture is advantageous. The admixture increases the cohesion of

the cement paste without reduction of the workability and prevents washout and separation of it from the aggregate by wave or current water action or dispersion.

### 3.4.5 Reinforcement

Plain carbon steel and carbon steel with different degrees of alloying are the most commonly used reinforcement for concrete, but other materials, with higher inherent corrosion resistance, have also been developed to enhance reinforced concrete durability. The various reinforcement materials are described in this section.

#### 3.4.5.1 Carbon steel

Carbon steel and low-alloy carbon steel are used in various forms to reinforce concrete:

- Bar reinforcement is used to resist the tensile loads arising in the concrete member from flexure, shear and early age shrinkage. The principal bar reinforcement that is used is a low-alloy, high-tensile steel with a minimum characteristic yield strength of 400 MPa.
- Wire reinforcement is usually used as welded mesh and utilises a low-alloy, high-tensile steel.
- High-tensile wires are used for pretensioned, prestressed concrete members.
- High-tensile strand is used for pretensioned and posttensioned concrete members.
- High-tensile bar is used for posttensioned concrete members.

All these carbon steel types are vulnerable to corrosion, and therefore the protection given by the cover concrete is the key element in the durability of the marine structures in which they are used.

#### 3.4.5.2 Hot dip galvanised carbon steel

The corrosion resistance of carbon steel may be increased by hot dip galvanising.

The steel should be fully cut and bent prior to galvanising so that all cut ends are coated and there is no post-dip damage to the bars from the bending process. Should any modification to the bars be required after galvanising, it essential that damage is repaired by a zinc-rich coating, especially on cut ends with exposed raw steel.

Normal reinforcement detailing rules apply to hot dip galvanised steel. Because of its greater corrosion resistance than carbon steel, it is usually used in situations where reduced concrete cover is necessary.

#### 3.4.5.3 Epoxy-coated carbon steel

Epoxy-coated carbon steel reinforcement has been used extensively in North America for marine structures and bridge structures affected by de-icing salts.

The coating acts as a barrier to shield the carbon steel from chlorides and is factory applied. Care must be taken when using it to minimise damage to the coating. Cut ends have to be coated, as does damage arising from bending and placement.

Premature corrosion of the steel bar may occur due to manufacturing defects, such as low coating thickness, poor surface preparation (Griffith and Laylor, 1999),

holidays (holes) in the coating or mechanical damage to the coating during installation. Failure mechanisms that occur include under-film corrosion and de-bonding of the coating.

Epoxy-coated steel is vulnerable to manufacture and construction practices that reduce its performance, and hence its track record has been variable, quite often poor. For this reason, tougher corrosion-resistant reinforcement that is not vulnerable to damage during normal construction activities is preferred (Hartt, 2012).

### 3.4.5.4 Stainless steel

Stainless steels are typically less vulnerable to corrosion than carbon steels, and in many environments, stainless-steel structures and components perform well and are corrosion free. This corrosion resistance has led to their use as bar reinforcement in marine structures and bridges affected by de-icing salts, as a way of achieving the desired durability.

Various grades of stainless steel have been used and these are summarised in Table 3.4. (*ChrōmX* and *MMFX*$_2$ are commercial trade names).

The chemical composition of these different stainless steel types is given in Table 3.5.

- Grade 304 and 316 stainless steel: Grades 304 and 316 are commonly used austenitic stainless steels. The 304 grade steel has a lower PRE than 316 but is still very suitable as corrosion-resistant reinforcement.
- Duplex and Lean Duplex stainless steels: Duplex stainless steels have been developed as an alternative to the austenitic steels. They have higher strengths and better corrosion resistance than the austenitic steels and are cheaper as they use less nickel in their formulation.
- Grade 3CR12 stainless steel: 3CR12 is a 12% chromium ferritic stainless steel, which is a lower chrome content than the austenitic steels (316 has 18%), and it is therefore less corrosion resistant, but it is still regarded as a suitable corrosion-resistant reinforcement.
- MMFX$_2$/ChrōmX stainless steel: this steel originates from the United States and is a low-carbon, chromium alloy steel. It is manufactured using a special rolling process that produces a laminated microstructure in the steel, which minimises the formation of microgalvanic cells (the driving force behind corrosion). The ChrōmX is offered in 9000, 4000 and 2000 grades with 9%, 4% and 2% chrome contents, respectively. The 9000 grade is intended for highly corrosive environments/long-term durability, the 4000 grade for medium corrosive environments/medium term durability, and the 2000 grade for noncorrosive environments. As the three different grades have essentially the same metallurgy, they can be used in different sections of the same structure, to cater for different microclimates, without any concerns about galvanic corrosion occurring.
- Clad carbon steel: a different approach to corrosion-resistant steel is to clad carbon steel bars with a thin, metallurgically bonded, outer layer of corrosion-resistant steel, such as Grade 316. This creates a composite material with the strength and economy of carbon steel and the corrosion resistance of stainless steel. Reinforcement of this type, marketed as NUOVINOX, was available briefly in the United States and United Kingdom.

Stainless steel costs more than carbon steel, and therefore the additional cost of stainless steel is justified only if the overall life cycle cost of the structure for its full service life is more economical. Stainless steel is also useful if it is not possible

**Table 3.4 Stainless-steel reinforcement bar types**

| Alloy common name | Specification | | | Stainless steel type | Yield strength MPa |
|---|---|---|---|---|---|
| | EN | ASTM | UNS | | |
| 304 stainless steel | 1.4301 | 304 | S30400 | Austenitic | 210 |
| 316 stainless steel | 1.4401 | 316 | S31600 | Austenitic | 220 |
| 2205 Duplex stainless steel | 1.4462 | – | S31803 or S32205 | Austenite + ferritic | 460 |
| 2101 LDX Lean Duplex stainless steel | 1.4162 | ASTM A955-98 | S32101 | Austenite + ferritic | 450 |
| ChrōmX9000/MMFX$_2$ | | A1035 CS | | Microcomposite austenite-martensite | 690 or 830 |
| ChrōmX4000 | | A1035 CM | | Microcomposite austenite-martensite | 690 or 830 |
| 3CR12 stainless steel | 1.4003 | – | S41003 | Ferritic | 300 |

**Table 3.5 Stainless steel chemical composition and PRE**

| Alloy | Typical chemical composition % | | | | | | PRE[a] |
|---|---|---|---|---|---|---|---|
| | C | N | Cr | Ni | Mo | Others | |
| 304 | 0.04 | – | 18.1 | 8.1 | – | – | 18 |
| 316 | 0.04 | – | 17.2 | 10.1 | 2.1 | – | 25 |
| 2205 Duplex | 0.02 | 0.17 | 22.0 | 5.7 | 3.1 | – | 35 |
| 2101 LDX | 0.03 | 0.22 | 21.5 | 1.5 | 0.3 | 5Mn Cu | 26 |
| ChrōmX9000/MMFX$_2$ | 0.05 | – | 9.30 | 0.10 | 0.03 | – | 9 |
| ChrōmX4000 | 0.05 | – | 4.0 | 0.10 | 0.03 | – | 4 |
| 3CR12 | 0.03 | – | 11.7 | 1.5 | – | Ti | 12 |
| Carbon steel | 0.3 | – | 0.21 | 0.19 | 0.04 | – | 0 |

[a]The PRE number is the pitting resistance equivalent of the steel type and gives an indication of the corrosion resistance of the steel. It is proportional to the amount of chrome, molybdenum and nitrogen. Carbon steel is included as a bench mark for comparison.

to achieve the required service life with conventional materials (eg, a small-sized member, such as a concrete handrail post, where it is not possible to use a large concrete cover on the steel).

#### *3.4.5.5 Fibre-reinforced plastics*

FRP are composite materials comprising fibres embedded in a polymer matrix. The strength is provided by the fibres, and the polymer allows the material to be formed in a number of ways, such as moulding wrapping and pultrusion. A variety of fibres are available for the reinforcing, including glass, aramid, carbon and basalt. The FRP composites are not vulnerable to corrosion and are used in pultruded bar form as concrete reinforcement. Further information about the different FRP reinforcing bar types may be obtained from the product suppliers.

FRP reinforcement is useful for special applications, such as cases where it is not possible to obtain sufficient concrete cover or as tie bars across a movement joint.

In addition to cast-in bars, it is also used as external reinforcement, utilising carbon fibre in sheet form bonded to the surface of concrete members, for the repair or strengthening of existing structures.

### *3.4.6 Fibres in concrete*

Fibres of various types are used in concrete, and the chief benefit of using them in a marine structure is to improve the crack resistance of young concrete to reduce early age cracks, and thereby improve the durability. They may also be useful in parts of marine structures subject to impact and possible cracking damage arising therefrom.

## 3.5 Design of plain (unreinforced) concrete marine structures

### 3.5.1 Plain concrete marine structure components

The most common uses for plain concrete in marine structures are breakwater armour units, breakwater caps, and blocks in blockwork quay walls. Plain concrete is durable in the marine environment, provided it is dense and well compacted, but precautions are still required in design and construction to achieve the desired durability. Table 3.6 lays out these requirements.

Plain concrete components do not have reinforcement to resist the internal forces caused by early age shrinkage effects, and therefore care must be taken in their manufacture to minimise the factors that cause such shrinkage. One of the prime contributors to shrinkage is the temperature differential between the core temperature due to the heat of hydration and the ambient temperature of the member. High concrete strengths may therefore be disadvantageous for plain concrete as the cement contents can cause high hydration temperatures. An acceptable compressive strength for plain concrete quay wall blocks would be 25 MPa at 28 days, such as used for the blockwork quay walls in the Port of Ngqura (refer Chapter 10).

Breakwater armour units, however, are subject to loads in service that cause flexure and shear in the units, and reasonable concrete strengths are necessary. In addition to compressive strength, a minimum tensile (flexure) strength is also specified, usually in the order of 4.0 MPa at 28 days, which implies a compressive strength in the order of 40 MPa.

### 3.5.2 Grout

Grout has several applications in marine structures, such as grout socks in quay wall joints (refer examples in Chapter 2), pile/jacket joints (refer Section 3.7.5) and

**Table 3.6 Plain concrete recommendations**

| All microenvironments: XS1, XS2 and XS3 | Limiting values | |
|---|---|---|
| | Nonabrasive conditions | Abrasive conditions |
| Min. strength class cylinder/cube (MPa) | C25/30 | C40/50 |
| Max. water/binder ratio | 0.55 | 0.45 |
| Min. binder content/combination (kg/m$^3$) | 320 | 350 |
| Permitted cements and combinations | BS EN 197-1, BS EN 14216 CEM I, IIA, IIIA, IIIB, II/B-S, IIB-V, IIB-V + SR, IVB-V | |

Adapted from BS 6349-1-4:2013, 2013. Maritime Works-Part 1-4: General - Code of Practice for Materials. The British Standards Institution, United Kingdom, Table 4.

repairs (such as filling of voids caused by scour or breakage). Grout is normally pumped into a geotextile bag or former in place and an anti-washout admixture is often specified.

## 3.6 Design of reinforced concrete marine structures

### 3.6.1 Durability design

A durable reinforced concrete structure is achieved by a combination of suitable material types and the way in which they are assembled.

The control of chloride ingress into the concrete is the primary aim of durability design in marine structures, as it is the chlorides that initiate corrosion of the steel reinforcement. Thus, durability design usually governs the design of reinforced concrete elements in the marine environment, rather than designing solely for strength via ultimate load design.

Durability design covers the proportions of the concrete mix ingredients, the thickness of the concrete cover to the steel reinforcement, and the amount and layout of the steel reinforcement. The recommended materials for a durable design have been described in Section 3.4, and this section covers how those materials are used together to achieve the required durability. The recommendations of the BS EN code of practice and contemporary good practice are described.

The emphasis in this section is on the protection of carbon steel reinforcement, which is the most commonly used reinforcement worldwide, but it is recommended that similar practices should still be followed when corrosion-resistant reinforcement is used, with the possible exception of a reduction in cover.

#### 3.6.1.1 Concrete mix and cover to reinforcement

The most important component in achieving the required service life for a reinforced concrete marine structure is the layer of concrete that covers and protects the steel reinforcement, and BS 6349 provides recommendations for the quality of the cover concrete and its thickness.

BS 6349-1-4:2013 Tables 1−3 give recommendations for prescriptive concrete mixes for 30-, 50- and 100-year design working lives, respectively. The recommended cement types are given for each microenvironment, and for each of these the minimum 28-day strength, minimum binder content and maximum water/binder ratio are given for a range of nominal concrete covers.

These prescriptive recommendations provide considerable flexibility in selecting variations in the concrete cover and the cement types for the whole range of microenvironments. Although a typical marine structure may traverse a range of microenvironments, it is usually considered pragmatic to use the parameters for the most severe microenvironment, typically XS3, for all the reinforced concrete elements. If a single cover value is taken as standard for each design life and the cement types that are likely to be used locally are selected, the prescriptive recommendations then simplify to those shown in Table 3.7.

**Table 3.7 Concrete parameters for durable reinforced concrete—simplified recommendations**

| Design life years | Microenvironment | Min. Cover (mm) | Reinf. placing tolerance (mm) | Total cover (mm) | Concrete strength class (MPa) | Water/ binder ratio (max) | Min. binder content (kg/m$^3$) | Cement type |
|---|---|---|---|---|---|---|---|---|
| 30 | XS3 | 60 | 15 | 75 | C25/30 | 0.55 | 340 | IIIA<br>IIB-V |
| 50 | XS3 | 60 | 15 | 75 | C32/40 | 0.45 | 360 | IIIA<br>IIB-V |
| 100 | XS3 | 65 | 15 | 80 | C40/50 | 0.35 | 380 | IIIA<br>IIB-V |

In this table, the following should be noted:

- The placing tolerance should be increased where rough formwork is used (eg, in situ piles in the ground).
- An additional 10 mm of cover should be added for prestressing strand.
- The recommended cements are CEM IIIA containing 36–45% ground granulated blast furnace slag (GGBS) and CEM IIB-V containing 21–24% fly ash (FA). The cement and extender may be blended at the cement factory, ready-mix plant or site batch plant, depending on availability.

Extract from BS 6349-1-4:2013, 2013. Maritime Works-Part 1-4: General - Code of Practice for Materials. The British Standards Institution, United Kingdom, Tables 1–3.

However, should it be considered economically advantageous to refine the concrete design for a particular structural element that is located in a less adverse microenvironment, the tables in BS 6349-1-4:2013 should be consulted for further guidance.

### 3.6.1.2 Crack control

Concrete does not have a high tensile strength, usually in the order of 10% of its compressive strength, and therefore reinforcement is added to the tensile zones to resist the applied loads and internal stresses. Steel and concrete have different elastic moduli and tensile strengths, and as a reinforced element strains in tension, the concrete reaches its tensile capacity when the steel is still at a fraction of its yield stress. The concrete therefore cracks, and the tension is resisted only by the steel. Cracks in reinforced concrete structures are normal, and CIRIA C660 (2007), *Early age thermal crack control in concrete*, expresses this clearly:

> *It is important that clients appreciate that early thermal cracking can be consistent with good construction practice, provided that it has been dealt with properly in the design and construction process. In many cases it may be either unnecessary or uneconomical to avoid cracking entirely. Indeed, the avoidance of cracking is contrary to the concept of reinforced concrete design, which assumes that concrete has no tensile capacity and uses the reinforcement to carry the tensile stresses and to control crack widths. If concrete does not crack then the reinforcement is not being used effectively. When specific performance requirements call for cracking to be avoided, special measures are available, but these may have significant cost implications that the client should be aware of.*
>
> *The acceptability of cracking: Cracking in reinforced concrete in not a defect; indeed the very basis of reinforced concrete design is that concrete has no significant tensile strength and that sufficient reinforcement should be provided to control crack widths.*
>
> *Problems may arise however when cracks occur unpredictably, or are of sufficient magnitude to render the structure unserviceable.*

CIRIA C660 goes on to define the relationship between crack width and functionality:

> *The significance of cracking can be considered under three categories:*
>
> 1. *Cracks which lead to durability problems and consequently a reduction in structural capacity*
> 2. *Cracks which lead to a loss of serviceability of the structure (eg, leakage of water or radiation, sound transfer or damage to finishes)*
> 3. *Cracks which are aesthetically unacceptable*
>
> *The limiting crack width for durability functionality is recommended to be 0.3 mm and that for serviceability is 0.05–0.2 mm depending on the water head applied to the structure.*

Cracks in the concrete layer that protect the steel reinforcement can act as pathways for the chlorides to enter the concrete matrix, with wider cracks (eg, >0.3 mm) being more detrimental than narrower ones (Otieno et al., 2016).

There are two distinct causes of tension in concrete members that are analysed in serviceability and durability design: early age shrinkage and flexure or tension. In both cases, reinforcement is provided to control the cracking and keep it within the required limits.

## Shrinkage crack checks

Shrinkage cracking in concrete can be caused by early age thermal stresses, or by drying shrinkage, or both. The effects are much the same irrespective of the cause, and so this section treats 'shrinkage' in a generic sense.

Tensile stresses build up in concrete when it contracts due to the reduction in concrete temperature from the peak hydration temperature (from the cementitious material reaction) to the ambient temperature. The size and spacing of the cracks is dependent on a combination of factors, including the following:

- the geometry of the structural member.
- the concrete properties:
  - heat generation; dependent on the type and content of cementitious materials; FA and GGBS help to reduce the heat generation.
  - variation of strength with time.
  - thermal properties; different aggregates impart different rates of expansion and contraction to the concrete.
  - water-reducing admixtures; superplasticisers help to reduce the binder content and therefore the heat generation (subject to minimum binder content for durability).
  - placing temperature; the temperature of the concrete at the time of placing affects the maximum temperature; this may be reduced by cooling the constituents using chilled water, ice or liquid nitrogen.
  - in situ cooling; cooling pipes are effective, but expensive; surface cooling by water spray is applicable for sections less than 500-mm thick.
- Ambient temperatures. Night-time concreting is beneficial, provided the maximum temperature differential is not exacerbated by this.
- The location of construction and movement joints. Movement joints allow elements to shrink with less restraint than built in elements.
- The relative ages between adjacent casts. When the second cast of an element is cast against the first cast, it will be restrained by it and thereby increase the potential to crack. The further apart in age the two units are, the greater will be the restraint, as more shrinkage will have already taken place in the first cast.
- The quantity and arrangement of the reinforcing steel. Small-diameter bars at close spacing reduce crack widths.
- Prestressing of the elements will add a compressive stress to the elements and reduce the potential to crack, but that may not be practical or economical.
- The type of formwork. For sections <500-mm thick, steel formwork promotes dissipation of the heat and therefore a lower maximum temperature. For thicker sections a plywood or insulated form is best as the slower heat loss minimises thermal gradients across the section, which can also cause cracking.
- Treatment of the concrete after casting. Moist curing of the concrete can help reduce plastic and drying shrinkage cracking.

Some of these factors are the responsibility of the designer and some are the responsibility of the contractor. The most influential factors over which the design and construction team have some control are the reinforcement design, heat generation and its mitigation and the aggregate type.

Shrinkage reinforcement design is the responsibility of the design engineer and for this, assumptions have to be made with respect to the construction details and heat generation after casting. It is recommended that these parameters are communicated to the contractor via the project specification so that the formwork, concrete mix and sequence of construction can be formulated by the contractor to match the design. Should the contractor not be able to conform to the designer's assumptions, then the actual or expected parameters should be communicated back to the designer in order that the design can be updated to suit. The design and construction with respect to the shrinkage reinforcement should be a collaborative effort between the designer and contractor, and this should be written into the project specifications.

The member geometry, and the location and type of construction and movement joints, affect the restraint that the member experiences. If a concrete member were to be completely free to shrink without any hindrance from the ground or adjacent members, then it would shrink without restraint, and there would be no buildup of tensile stress. For example, the friction between a base and its founding can restrain the shrinkage of the concrete in the base and cause tension. When a wall panel is cast on top of a base, the base will have already undergone some shrinkage, and it will therefore restrain the fresher concrete in the wall cast. The restraint along the bottom of the members in these two examples leads to tensile stresses in a horizontal direction along the bottom of the member, and vertical cracks will form to relieve the stresses if they exceed the tensile capacity of the concrete at the time. If a member is unreinforced, then there is likely to be a small number of large-width cracks.

Depending on the configuration of the structure and the thickness of the members, external edge restraint (as described in the previous paragraph), end restraint, and internal restraint should be checked (CIRIA C660). End restraint occurs when a member, such as a slab or beam, is cast between two rigid supports at its ends. Internal restraint arises from different temperature changes within an element, and it can cause internal cracks.

During the early period, the concrete is gaining strength, and at the same time, it is first heating up due to the cement hydration reactions and then cooling down after the bulk of the hydration is complete. It is during the early age cooling period that the concrete is most vulnerable to cracking. The tensile strength of the concrete is increasing, but it is still low, and concurrently the tension in the concrete is increasing as it cools, due to restraint. At any point in time during this early stage, if the strength capacity of the concrete is not greater than the developed tension, then cracking will occur.

When a member is adequately reinforced against the tension, many narrow cracks will occur. Wider cracks (over 0.3 mm) promote chloride ingress and thereby reduce the durability of the member in service. However, current research indicates that even the smaller cracks may adversely affect its durability (Otieno et al., 2016). Minimum binder content for marine concrete is specified to lessen its penetrability, but care must be taken to not use too much binder as this may generate too much heat and lead to an

unacceptable increase in cracking or even delayed ettringite formation in extreme cases. When concrete temperatures rise above 65°C a particular type of sulphate is created that forms ettringite when water is present, after the concrete has hardened. This delayed ettringite is expansive and causes internal tension in the concrete, which manifests as cracks. Massive structure elements that generate high core temperatures during hydration and experience in-service exposure to water (such as sea spray) are the most vulnerable to this phenomenon (Godart and Divet, 2013).

Detailed recommendations for the design of reinforcement to resist the shrinkage forces are found in BS EN 1992-3:2006 and CIRIA C660.

### Flexural crack checks

When a reinforced concrete member deflects due to a flexural load, the concrete on the tension face will crack as the beam deflects and the steel is mobilised. If the load is released, the deflection reduces, and the cracks will close up.

The effect of cracks on the penetrability of the concrete to chlorides is a function of the size and spacing of the cracks, as well as the period for which they are open in response to the applied loads. For instance, a large crack width in a beam soffit caused by a travelling crane vertical live load may only be present for a short time period, and therefore have a lower deleterious effect than a smaller, but more persistent load, such as an applied dead load from a slab topping.

Generally, therefore, crack width checks for durability design are based on sustained loads that cause cracks that are open for significant periods of time. These are called quasi-permanent loads in the Eurocodes and are defined as loads that are present for long enough to influence long-term effects. Care must therefore be taken in selecting appropriate sustained load cases when calculating flexural crack widths.

Crack width calculation recommendations are given in Section 7 of BS EN 1992-1-1:2004 or Section 7 of BS EN 1992-2:2005. Annex A of BS 6349-2:2010 gives combination factors for loads applicable to marine structures.

The crack width recommendations in the Eurocode for marine exposures are given in Table 3.8.

The flexural crack width on the surface of the member is proportional to the depth of concrete cover. It can be taken that the specified maximum cracks widths are

**Table 3.8 Recommended maximum flexural crack width for marine exposure, $w_{max}$ (mm)**

| Exposure class | Reinforced members and prestressed members without bonded tendons | Prestressed members with bonded tendons |
|---|---|---|
| | Quasi-permanent load combination | Frequent load combination |
| XS1, XS2, XS3 | 0.3 | Decompression |

Extract from Table 7.101N of BS EN 1992-2:2005, 2005. Eurocode 2-Design of Concrete Structures - Part 2: Concrete Bridges - Design and Detailing Rules. The British Standards Institution, United Kingdom.

applicable to the specified nominal covers. If an increase in the thickness of the cover beyond the required minimum is selected, in order to provide an increased barrier for chloride ingress, the target crack width should be increased pro rata to the greater cover. If the target crack width is not adjusted to the increased cover, it will result in excessive steel reinforcement areas.

Generally, shrinkage cracks and flexural cracks do not occur at the same locations on a member, and therefore the cracks widths calculated for each do not have to be combined (BS 6349-1-4:2013, clause 4.4.10).

#### Minimum reinforcement

BS 6349 does not have any additional requirements for minimum reinforcement steel beyond those stipulated by BS EN 1992-1-1 and BS EN 1992-2 (ie, that reinforcement required for early age shrinkage may govern the steel area that is required), refer to section on 'Shrinkage crack checks'.

### 3.6.2 Strength design (ULS)

Normal rules for the ULS are followed for marine structures with the partial factors and combination factors given by Annex A of BS 6349-2:2010, which addresses the types of loads applicable to marine structures (including wave loading, vessel berthing and mooring loads).

Frequently, it is found that the serviceability crack width design will govern the steel reinforcement areas required, but the ULS should still be checked.

### 3.6.3 Other codes of practice

#### 3.6.3.1 USA durability design requirements (ACI 357R-84)

ACI 357R-84 defines three marine exposure zones and prescribes maximum water/cement ratio, minimum compressive strength and minimum concrete cover for each; refer to Tables 3.9 and 3.10.

**Table 3.9 ACI 357R-84 water/cement ratio and minimum compressive strength requirements**

| Zone | Maximum w/c ratio | Minimum 28-day cylinder compressive strength (MPa) |
|---|---|---|
| Submerged | 0.45 | 35 |
| Splash | 0.40 | 35 |
| Atmospheric | 0.40 | 35 |

Adapted from ACI 357R-84, 1997. Guide for the Design and Construction of Fixed Offshore Concrete Structures. American Concrete Institute, Table 2.1.

**Table 3.10 ACI 357R-84 recommended nominal concrete cover over reinforcement**

| Zone | Cover over reinforcing steel (mm) | Cover over post-tensioning ducts (mm) |
|---|---|---|
| Atmospheric zone not subject to salt spray | 50 | 75 |
| Splash and atmospheric zone subject to salt spray | 65 | 90 |
| Submerged | 50 | 75 |
| Cover of stirrups | 13 mm less than those listed above | – |

Adapted from ACI 357R-84, 1997. Guide for the Design and Construction of Fixed Offshore Concrete Structures. American Concrete Institute, Table 2.2.

To obtain high-quality concrete to protect the steel, a minimum cement content of 356 kg/m$^3$ is specified, but there is no specific requirement for the use of extenders such as FA or GGBS for durability, which is considered a deficiency in this approach.

The code does not contain any explicit crack width calculation requirements, but instead it limits the allowable tensile stress in the reinforcing steel. The in-service requirements are reproduced in Table 3.11.

ACI 357R-84 has a requirement for minimum steel in marine structures beyond the typical requirements of ACI 318-0, which is a function of the concrete cover and bar size. For further details, refer to clause 4.5.6 of ACI 357R-84.

The given durability requirements are comparable to other codes of practice with the exception of the lack of inclusion of cement extenders to improve impenetrability. The use of a limiting stress is a simpler but less flexible approach to prevention of excessive crack widths than the rigorous calculations of the Eurocode.

**Table 3.11 ACI 357R-84 allowable tensile stress for prestress and reinforcing steel to control cracking**

| Stage | Loading | Allowable stress (MPa) | |
|---|---|---|---|
| | | $\Delta_{ps}$ | $f_s$ |
| At offshore site (in service) | Dead and live loads plus monthly recurring environmental loads | 75 | 120 |
| At offshore site (in service) | Dead and live loads plus extreme environmental loads | – | 0.8 $f_y$ |

$\Delta_{ps}$, increase in tensile stress in prestressing steel with reference to the stress at zero strain in the concrete; $f_s$, stress in reinforcing bar; $f_y$, yield stress of reinforcing bars.
Extract from ACI 357R-84, 1997. Guide for the Design and Construction of Fixed Offshore Concrete Structures. American Concrete Institute, Table 4.1.

### 3.6.3.2 Australian durability design requirements (AS 4997)

Table 4.3 of AS 3600 defines the exposure classifications, and those relevant to the marine environment are amplified in AS 4997 Table 6.3, which is reproduced in Table 3.12. These definitions are similar to those in the Eurocode, but the locations are defined more precisely, and it should be noted that all exposed soffits over the sea are classified as 'splash zone'. The author has conducted many condition inspections of port structures and has observed that spalling of soffit steel due to corrosion is a frequent occurrence, which would appear to confirm the soffit classification.

Tables 6.4 and 6.5 of AS 4997 define minimum concrete covers to reinforcement for 'standard' and 'intense' compaction concretes, and these are presented combined in Table 3.13. 'Intense' compaction implies good quality control of concrete cast in rigid formwork using repetitive procedures as defined in clause 4.10.3.3 of AS 3600.

The cover requirements given in Table 3.13 are for 25 years. The code does not give explicit guidance on how to achieve a design life greater than that, and it only suggests that corrosion resistant reinforcement be used, or additives or coatings that increase durability.

Crack widths are limited in a very simple way by imposing a maximum stress in the reinforcement at SLS as given in Table 3.14.

The Australian approach to durability is very similar to the ACI one, and less rigorous than the Eurocode requirements.

### 3.6.3.3 Japanese durability design requirements (JSCE guidelines for concrete No. 15 and No. 16)

The JSCE series of guidelines covers the design and specification of all typical concrete structures and recommendations for marine structures. What sets the JSCE guidelines apart from the other codes of practice described in this section is that performance-based design and specification is recommended.

**Table 3.12 AS 4997 exposure classifications**

| Exposure environment | Exposure classification<br>Reinforced or prestressed members |
|---|---|
| Members permanently 500 mm below the seabed | A2 |
| Members permanently submerged 1 m below lowest seawater level to 500 mm below seabed level | B2 |
| Spray zone, (ie, exposed to airborne salt spray, but not in splash zone, eg, the top side of deck slabs) | C1 |
| Splash zone, from 1 m below water level up to 1 m above wave crest levels on vertical structures, and all exposed soffits over the sea | C2 |

Adapted from AS 4997-2005, 2005. Guidelines for the Design of Maritime Structures. Council of Standards, Australia, Table 6.3.

**Table 3.13 AS 4997 minimum cover to reinforcing steel for a 25-year design life**

| Exposure classification | Minimum cover-standard compaction concrete (mm) | | Minimum cover-intense compaction concrete (mm) | |
|---|---|---|---|---|
| | $f'_c = 40$ MPa | $f'_c = 50$ MPa | $f'_c = 40$ MPa | $f'_c = 50$ MPa |
| A2 | 40 | 30 | 35 | 30 |
| B2 | 50 | 40 | 40 | 30 |
| C1 | 70 | 50 | 60 | 45 |
| C2 | 75 | 65 | 65 | 60 |

Adapted from AS 4997-2005, 2005. Guidelines for the Design of Maritime Structures. Council of Standards, Australia, Tables 6.4 and 6.5.

**Table 3.14 AS 4997 maximum allowable reinforcement steel stress at SLS**

| Reinforcing bar diameter, $d_b$ (mm) | ≤12 | 16 | 20 | ≥24 |
|---|---|---|---|---|
| Steel reinforcing stress, $f_s$ MPa | 185 | 175 | 160 | 150 |

Adapted from AS 4997-2005, 2005. Guidelines for the Design of Maritime Structures. Council of Standards, Australia, Table 6.6.

There are some mandatory requirements, and JSCE No. 16 specifies minimum cement contents and maximum water/cement ratios for different exposure classes, as given in Tables 3.15 and 3.16.

JSCE No. 15 is divided into two parts: General Requirements and Standard Methods. In the first part, the formulas to be used for the verification of chloride ingress are given in Section 8.3.7 of Chapter 8. The full details of the rigorous calculations for the chloride concentration prediction are not presented here; however, the

**Table 3.15 JSCE minimum cement content of concrete for durability (kg/m$^3$) (Table C11.3.2 of *JSCE No. 16*)**

| | | Maximum coarse aggregate size (mm) | |
|---|---|---|---|
| | | 20 or 25 | 40 |
| Environmental classification | Offshore air (atmospheric) Splash zone | 330 | 300 |
| | Undersea (submerged) | 300 | 280 |

Adapted from JSCE Guidelines for Concrete No. 16, December 2010. Standard Specifications for Concrete Structures-2007, "Materials and Construction" (English version). Japan Society of Civil Engineers, Tokyo, Japan, Table C11.3.2.

**Table 3.16 JSCE maximum water/cement ratios for durability (%)**

| | | Construction conditions | |
|---|---|---|---|
| | | **Ordinary construction** | **Concrete products (Precast construction)** |
| Environmental classification | Offshore air (atmospheric) | 45 | 50 |
| | Splash zone | 45 | 45 |
| | Undersea (submerged) | 50 | 50 |

Values in Table 3.16 may be increased by 5 to 10% if substantiated by research.
Adapted from JSCE Guidelines for Concrete No. 16, December 2010. Standard Specifications for Concrete Structures-2007, "Materials and Construction" (English version). Japan Society of Civil Engineers, Tokyo, Japan, Table C11.3.1.

salient features of the method are given to illustrate a performance-based method and to give some comparison to other codes.

The central requirement of the durability check is that the predicted chloride concentration, $C_d$, at the end of the structure's service life, at the location of the reinforcement, is less than or equal to the threshold value at which the onset of corrosion occurs, $C_{lim}$. A value of 1.2 kg/m$^3$ is recommended for $C_{lim}$, which is equivalent to 0.36% of the cement for a cement content of 330 kg/m$^3$.

$C_d$ is the design value of the chloride concentration and is a function of the following:

- The concentration of chlorides at the concrete surface, $C_0$ (kg/m$^3$)
- The thickness of the concrete cover to the reinforcement, $c$ (mm)
- The length of the service life, $t$ (years)
- The design value of the chloride ion diffusion coefficient in the concrete, $D_d$ (cm$^2$/year)

$D_d$ in turn is a function of these:

- The characteristic value of the chloride ion diffusion coefficient in the concrete, $D_k$, (cm$^2$/year)
- The calculated crack width, $w$ (mm)
- The crack spacing, $l$ (mm)

The input data for the verification may be determined from measurements or previous experience with other similar structures ($C_{lim}$, $C_0$ and $D_k$), values selected by the designer ($c$ and $t$), and derived by calculation ($w$ and $l$). Ideally $D_k$ should be determined by tests on the proposed or similar concrete mix, but equations are given to calculate $D_k$ from the water/cement ratio for a mix using either plain Portland cement or a GGBS blend (Eqs. C5.2.25 and C5.2.26).

If data for $C_0$ is not available, it may be taken from a table of recommended values, reproduced in Table 3.17.

$C_0$ varies with height above sea level as well as distance from the coast, and values may be estimated from Table 3.17 by using the equivalent of 25-m distance from the shoreline for every metre of height.

**Table 3.17 JSCE chloride ion concentration, $C_0$, at concrete surface ($kg/m^3$)**

| | Splash zone | Distance from coast (km) | | | | |
|---|---|---|---|---|---|---|
| | | Near shoreline | 0.1 | 0.25 | 0.5 | 1.0 |
| Region with high airborne chloride concentration | 13.0 | 9.0 | 4.5 | 3.0 | 2.0 | 1.5 |
| Region with low airborne chloride concentration | | 4.5 | 2.5 | 2.0 | 1.5 | 1.0 |

Adapted from JSCE Guidelines for Concrete No. 15, December 2010. Standard Specifications for Concrete Structures-2007, "Design" (English version). Japan Society of Civil Engineers, Tokyo, Japan, Table C8.2.2.

**Table 3.18 JSCE limit value of crack width $w_a$ (mm)**

| Type of reinforcement | Environmental conditions for reinforcement corrosion | | |
|---|---|---|---|
| | Normal | Corrosive | Severely corrosive |
| Deformed bars and plain bars | 0.005c | 0.004c | 0.0035c |
| Prestressing steel | 0.004c | – | – |

Adapted from JSCE Guidelines for Concrete No. 15, December 2010. Standard Specifications for Concrete Structures-2007, "Design" (English version). Japan Society of Civil Engineers, Tokyo, Japan, Table 8.3.2.

The requirements for maximum allowable crack widths recognise that cracks are tapered and will increase in width with increased thickness of cover concrete. Table 8.3.2 of JSCE No. 15 gives maximum crack widths as a simple ratio of the thickness of the cover, and it is reproduced as Table 3.18.

Table 3.18 is based on the following:

- Normal environment:
  - Normal outdoor environment with ordinary conditions without any airborne salt, underground and so on
- Corrosive environment:
  - In comparison to the normal environment, there is more frequent cyclic wetting and drying and underground environment below the level of underground water containing corrosive/detrimental substances.
  - Marine structures submerged in seawater or not exposed to severe marine environment.
  - Structures located between 0.1 and 1.0 km from the shoreline.
- Severely corrosive environment:
  - Environment in which reinforcement is subjected to considerable detrimental influences
  - Marine structures subjected to tides, splash, or exposed to severe ocean winds, and so on
- The crack widths are applicable to prevention of corrosion and are not applicable to watertightness or aesthetic appearance.
- Prestressed members in corrosive and severely corrosive environments should be designed to be crack free.

- Concrete cover should not exceed 100 mm.
- Crack widths are calculated using permanent loads, except that frequently applied variable loads, which are relatively high in magnitude compared to the permanent loads, should also be taken into account.

For a typical marine structure with a cover of 65 mm, the limiting flexural crack width is therefore 0.23 mm, which is comparable to other code recommendations.

As an alternative to undertaking the calculations, the verification may be undertaken using the standard method given in Part 2 of the guideline. This is presented as a design curve and as tabulated values, reproduced in Fig. 3.2 and Table 3.19, respectively.

The input into the curve in Fig. 3.2 is the ratio of the surface chloride ion concentration, $C_0$, to the corrosion threshold concentration, $C_{lim}$, as increased by safety factors $\gamma_{cl}$ and $\gamma_i$. From the curve, a value of $\frac{c_d}{\sqrt{D_d t}}$ is obtained. The service life, $t$, should be defined initially in the project design basis, and values of $c_d$ and $D_d$ are selected to give $\frac{c_d}{\sqrt{D_d t}}$ equal or greater than the required value from the curve. A standard recommended value for the cover is likely to be used, and hence a maximum value for $D_d$ is determined.

Table 3.19 gives the required design diffusion coefficient for a range of service lives and concrete covers for the splash zone environment. Tables for other nonmarine environments are also given in the guidelines, but they are not presented here.

$D_d$ is best verified by testing the proposed concrete mix. In addition, JSCE No. 15 provides a method to predict $D_d$ based on the water/cement ratio and the crack width, which could be used to formulate a suitable mix.

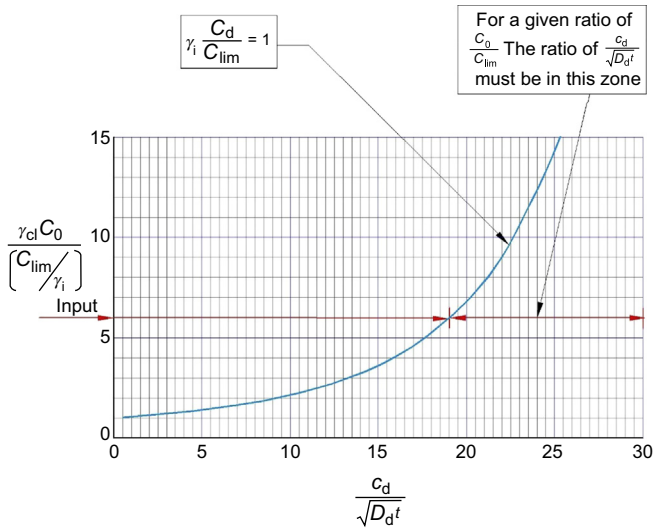



**Figure 3.2** Acceptable combinations of design concrete cover, $c_d$, and design diffusion coefficient, $D_d$.
From Figure C3.2.1 of JSCE Guidelines for Concrete No 15, December 2010. Standard Specifications for Concrete Structures - 2007, "Design" (English Version). Japan Society of Civil Engineers, Tokyo, Japan.

**Table 3.19 JSCE maximum design diffusion coefficient, $D_d$ ($cm^2$/year), for a range of concrete covers, $c_d$, and service lives, t, for the splash zone ($C_o = 13$ kg/$m^3$), (from Table C3.2.1 of *JSCE No. 15*)**

| Service life (year) | Design concrete cover, $c_d$ (mm) | | | | | | | | | |
|---|---|---|---|---|---|---|---|---|---|---|
| | 25 | 30 | 35 | 40 | 50 | 60 | 70 | 100 | 150 | 200 |
| 20 | – | – | – | 0.123 | 0.192 | 0.276 | 0.376 | 0.767 | 1.72 | 3.07 |
| 30 | – | – | – | – | 0.128 | 0.184 | 0.250 | 0.511 | 1.15 | 2.04 |
| 50 | – | – | – | – | – | 0.110 | 0.150 | 0.307 | 0.690 | 1.23 |
| 100 | – | – | – | – | – | – | – | 0.153 | 0.345 | 0.613 |

Extracted Table C3.2.1 of JSCE Guidelines for Concrete No. 15, December 2010. Standard Specifications for Concrete Structures-2007, "Design" (English version). Japan Society of Civil Engineers, Tokyo, Japan.

To undertake the durability design, the engineer is therefore required to have some knowledge of surface chloride concentrations, of diffusion coefficients and an understanding of what is achievable using local materials and construction practices. For smaller projects, the design may be based on recommended values in the guidelines, but for larger projects, it should be worthwhile to undertake testing and measurements to refine the concrete design to be the most economic.

JSCE No. 16 recommends that when the structure proceeds to construction, the performance indicators for the durability must be specified by the designer and the concrete mix formulated and tested to verify that they are met. For a marine structure, the chief durability performance indicator is the chloride ion diffusion coefficient, and indicators used for other structures are carbonation rate, freeze–thaw resistance, chemical attack resistance and fire resistance.

For testing the diffusion coefficient, three test methods are available in JSCE No. 2:

- JSCE-G571-2003: test method for effective diffusion of chloride ion in concrete by migration
- JSCE-G572-2003: test method for apparent diffusion coefficient of chloride ion in concrete by immersion in salt water
- JSCE-G573-2003: measurement method for distribution of total chloride ion in concrete structures

The JSCE approach to durability allows some flexibility to vary the materials and the concrete mix to achieve the specified requirements. For example, the use of stainless steel reinforcement could be incorporated by using an appropriate $C_{lim}$ value, or any particular binder blend could be used provided the diffusion coefficient is determined by testing.

### 3.6.3.4 South African durability design requirements (SANS 10100 and SANRAL)

SANS 10100-2:2014, *The structural use of concrete Part 2: Materials and execution of work* gives simple prescriptive durability requirements in the form of minimum concrete

**Table 3.20 Durability requirements for marine structures in *SANS 10100-2:2014***

| Condition of exposure | Description of member/surface to which the cover applies | Class of concrete (MPa) | |
|---|---|---|---|
| | | 40 | 50 |
| | | Characteristic minimum cover depth (mm) | |
| Very severe | All exposed surfaces of structures within 30 km from the sea | 60 | 50 |
| Extreme | Surfaces in contact with seawater | 65 | 65 |

The excerpt from table 3 SANS 10100-2: 2014 The structural use of concrete – Part 2: Materials and execution of work is reproduced with the permission of the South African Bureau of Standards (SABS). The South African Bureau of Standards is the owner of the copyright therein and unauthorized use thereof is prohibited.

cover and concrete strength for different conditions of exposure. The requirements for the conditions of exposure relevant to marine structures are reproduced in Table 3.20.

SANRAL Table 6000/1 specifies durability performance and some prescriptive requirements for carbonation-induced and chloride-induced corrosion. The section of the table pertaining to chloride corrosion is reproduced here and is split into two parts for ease of reference (Tables 3.21 and 3.22).

Acceptable binder blends, minimum concrete cover, and durability index values (in this case, a chloride conductivity index, SANS 3001-CO3-3 (2015)) for different microenvironments are specified in the table. The SANRAL microenvironment definitions match those of the Eurocode, and the binder blends are ones that have been commonly used in South Africa in recent years.

In a bridge application, for which the SANRAL table is intended, the piles are likely to be fully embedded in the ground. In a marine structure such as a jetty the worst environment for the piles would be in the exposed upper tidal and splash/spray zones. If the SANRAL recommendations are used for marine structure piles, the cover requirements for XS3 or XS3a should therefore govern.

With this specification approach, the contractor is able to optimise the concrete mix that achieves the prescribed performance indicator and thereby realise some economy in comparison to using a prescriptive mix.

The two main benefits of this hybrid approach are these:

- optimisation of the concrete mix before start of construction by determining a mix that provides adequate durability at least cost,
- verification that the concrete cast on site meets the required durability performance.

## 3.7 Particular considerations for the design and specification of structural components

### *3.7.1 Introduction*

This section describes a small selection of design and specification details for some of the typical structure configurations and components of marine concrete structures. It is

**Table 3.21 SANRAL microenvironment definitions**

| Microenvironment designation | Description | Conditions of exposure | Description of exposure |
|---|---|---|---|
| XS1 | Exposed to airborne salt but not in direct contact with seawater or inland saline waters | Very severe | Proven presence of chlorides; generally <1 km from sea, and coastal river valleys (where chlorides are present) and estuaries |
| XS2a | Permanently submerged in sea (or saline waters) | Severe | Permanently (or substantially) submerged in the sea (without wave action), coastal saline estuaries and rivers |
| XS2b | XS2a + exposed to abrasion | Extreme | As XS2a, but with heavy wave action |
| XS3a | Tidal, splash and spray zones | Extreme | Sea or saline estuaries and rivers, but not permanently submerged; tidal zone, and in spray or splash zone |
| XS3b | XS3a + exposed to abrasion | Extreme | As XS3a, but with heavy wave action, or where abrasion or erosion can occur |

Extracted from SANRAL Table 6000/1, August 2009. http://www.nra.co.za/, Pretoria, South Africa.

by no means an exhaustive coverage of the subject, but rather it highlights some of the more common aspects and techniques.

Marine structures fulfilling similar functions in different parts of the world may differ considerably because of local material preferences, variations in construction costs dependent on labour and material rates, the available equipment, skills and preferred methods of contractors and the location of the site. For instance, in a region with high labour costs, all-steel construction may be preferred over reinforced concrete because of the high labour content inherent in concrete structure. A structure in a remote area may be most economic when it is configured as a series of steel modules that can be fabricated in an industrial centre and then transported by sea to the site. In another area there may be abundant, cheap labour that makes locally constructed concrete the most economic. Each marine project is often unique and the items described in this section may be the seed for some appropriate techniques required for a particular concrete structure.

**Table 3.22 SANRAL durability specification requirements**

| Microenvironment designation | Recommended minimum cover (mm) | In situ durability index for various cover depths within exposure condition, 100-year life | | | | |
|---|---|---|---|---|---|---|
| | | Cover depth (mm) | Chloride conductivity (mS/cm) | | | |
| | | | Typical binder blends | | | |
| | | | 70:30 CEM I:FA | 50:50 CEM I:GGBS | 50:50 CEM I:GGCS | 90:10 CEM I:CSF |
| XS1 | 50 | 40 | 1.50 | 1.60 | 2.10 | 0.40 |
| | | 50 | 2.10 | 2.20 | 2.80 | 0.50 |
| | | 60 | 2.60 | 2.70 | 3.40 | 0.65 |
| XS2a | 50 | 40 | 1.00 | 1.10 | 1.40 | 0.30 |
| | | 60 | 1.40 | 1.60 | 2.00 | 0.40 |
| | | 60 | 1.80 | 2.10 | 2.50 | 0.50 |
| XS2b | 60* | 60 | 1.45 | 1.70 | 2.00 | 0.40 |
| XS3a | 50 | 40 | 0.65 | 0.85 | 1.00 | 0.25 |
| | | 50 | 1.10 | 1.35 | 1.45 | 0.35 |
| | | 60 | 1.45 | 1.70 | 2.00 | 0.40 |
| XS3b | 60* | 60 | 1.10 | 1.30 | 1.55 | 0.30 |

*, mandatory requirement; *CSF*, condensed silica fume; *FA*, fly ash; *GGBS*, ground granulated blast furnace slag; *GGCS*, ground granulated Corex slag (from Saldanha Steel); minimum required cover for in situ piles is 75 mm; minimum required cover for precast piles is 55 mm.
Adapted from SANRAL Table 6000/1, August 2009. http://www.nra.co.za/, Pretoria, South Africa.

### 3.7.2 Blockwork wall units

The majority of blockwork wall blocks are unreinforced, and high hydration heats should be avoided due to the lack of shrinkage crack control steel. Lower cement contents and concrete strengths are therefore specified in comparison to reinforced concrete.

The bottom block is sometimes reinforced due to the bending moments that may be induced from the bearing pressures and supporting the weight of the blocks above, for example, the wall shown in Chapter 2, Fig. 2.4, which has a slender projecting toe.

When the blockwork wall is assembled, the blocks are placed on top of each other without any grout or packing. Accurate tolerances therefore need to be specified for the bottom and top surfaces to eliminate high spots that could induce unnecessary bending or high localised stresses into the blocks.

The side formwork of an I-shaped block will restrain the unit when early age shrinkage takes place, and therefore early removal of the side forms should be specified, say within 18 h after casting.

The block handling stresses should be checked, particularly for lifting off the casting bed when the concrete will not yet be at its full strength. However, with the deep sections that are typically used, the handling stresses should be low.

### 3.7.3 Caisson units

The design of caisson units needs to take account of the full range of construction stages as well as the final in-service situation. There are a variety of differential pressures across the walls and base slab that can be experienced during the floating, sinking and sand-filling stages that need to be checked to verify the governing case. These include the following:

- differential water pressures across the outer walls and bottom slab when the caisson is floating
- differential water pressures across the internal cell walls during the sinking of the caisson onto the stone bed
- differential soil pressures across the external and internal cell walls when the cells are filled with sand; ideally sand-filling should take place evenly across the caisson, but this may not be possible due to access restrictions
- differential pressures across the base slab due to the difference between the weight of sand fill in the cells and the bearing pressures beneath the slab.

For the durability design, the different microenvironments once installed can be taken into account. The internal concrete faces are permanently buried and immersed (XS2). The outer faces on the seaward side experience the full range of microenvironments from XS1 to XS3. The installation cases are not relevant to the serviceability design as the load cases are all short term and not sustained.

### 3.7.4 Counterfort units

For the counterfort units of the size shown in Chapter 2, Figs 2.13 to 2.15, there is a strong emphasis on minimising the mass of the precast unit to keep the size and cost of

the land-based and marine lifting equipment as low and economical as possible. It is therefore usual practice to taper and refine the panel thicknesses to minimise the mass of the precast unit that has to be lifted, resulting in dense reinforcement with typically over 200 kg of steel per cubic metre of concrete.

Counterfort units are lifted off the casting bed and moved to and from storage on land, and therefore experience their full weight in air in the short term, for which ULS checks should be undertaken.

For the permanent in-service case, the slab and wall panels should be checked for ULS and SLS for the differential pressures arising from the retained and compacted soils, tidal lag, live loads and the consequent bearing pressures. The counterfort web should be checked at ULS and SLS for the tension forces arising from the same load cases.

### 3.7.5 Piles

Concrete bearing piles may be precast or cast in situ inside a casing, and sheet piles are always precast. Precast piles may be reinforced or pretensioned and prestressed, and the latter assists in closing up cracks that may form during driving.

Precast piles are cast on their sides, and the bending moments generated by their self-weight need to be checked during handling and storage in the precast yard and when the pile is pitched prior to driving. Fig. 3.3 shows the optimal position of lifting and support points for the horizontal and pitching positions such that the hogging and sagging bending moments are balanced. The first lift off the casting bed is likely to be done at an early age and the concrete strength at the time should be used for the lifting reinforcement calculation.

When piles are used on land, they are normally fully buried and terminate in a pile cap or ground beam. In marine structures the piles typically have the pile cap or headstock located above water level. There are therefore two distinct parts to the pile;

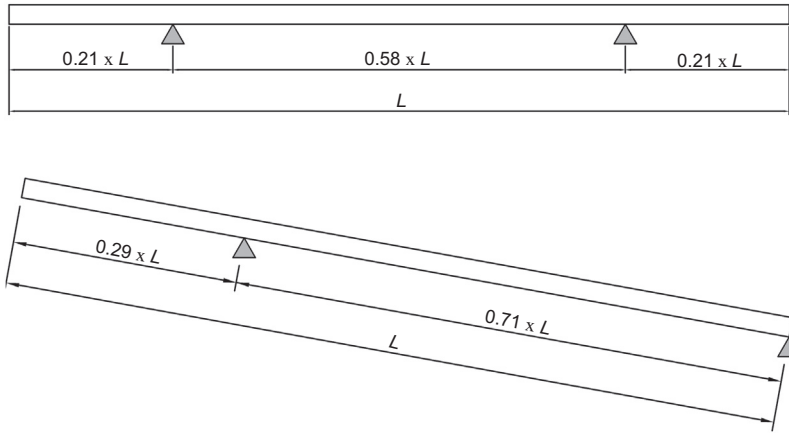



**Figure 3.3** Optimal pile lifting and support for horizontal and pitching positions.

the embedded length in which the penetration is determined by geotechnical design, and the exposed length between the seabed and superstructure, which is effectively a column. The marine pile is subject to axial and lateral loads, and the design follows normal methods and recommendations for column design subject to combined axial loads and bending moments. In a jetty or quay structure, a 2D or 3D frame analysis is undertaken to determine the pile axial loads, shears and bending moments, and a lower support point for the piles is determined or assumed at which the pile achieves 'fixity' in the soil.

The pile is subject to the full range of microenvironments from XS1 to XS3, but as it is a single element, it is pragmatic to design the whole pile for the worst exposure case. As is typical for piling, the penetration of the pile may vary from the intended design, and therefore the location of a particular microenvironment within the length of the pile is not predictable, which emphasises the need to design the whole pile for the worst exposure class.

In South African ports, a conservative approach has been taken toward piles, and in cases where it has not been possible to use a precast concrete pile, it has been preferred to cast an in situ concrete pile inside a tubular steel casing rather than have a hollow tubular steel pile. This is because concrete is viewed as more durable and requiring less maintenance than steel. In this type of pile the steel casing is taken as sacrificial without any contribution to the strength or durability of the pile.

Another approach that is used in some ports is to have steel tubular piles supporting a concrete superstructure. In this configuration the connection between the pile and the superstructure is a reinforced concrete plug in the top of the pile, which transfers the bending moments and forces via bond on the inside face of the pile. The design of this type of connection can be derived from clause 15.1, 'Grouted connections' of BS EN ISO 19902:2007. The clause covers the typical grouted connection used between offshore oil and gas jacket structures and the piles used to secure them on the seabed. Fig. 3.4 illustrates typical jetty and offshore structure pile connections.

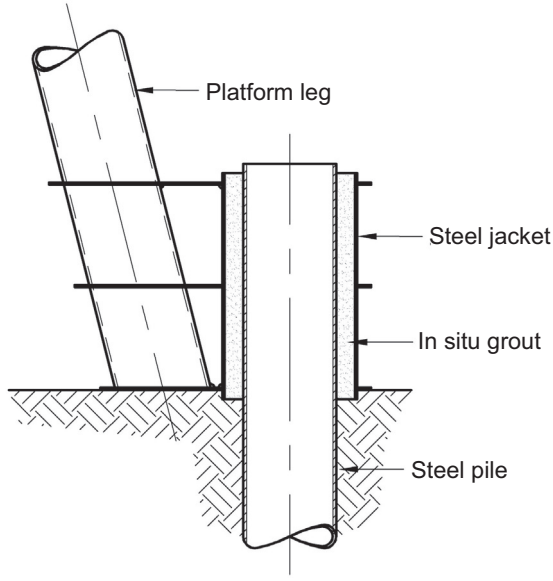
Similar design recommendations are contained in NORSOK N-004 and DNV-OS-J101. The latter standard addresses grouted connections for offshore wind turbine structures and considers the vibrations inherent in such installations.

Satisfactory durability is achieved for the steel tubular pile by using one or more methods, such as paint coating, sacrificial anodes, sacrificial steel thickness and wrapping of the pile in the tidal zone and above.

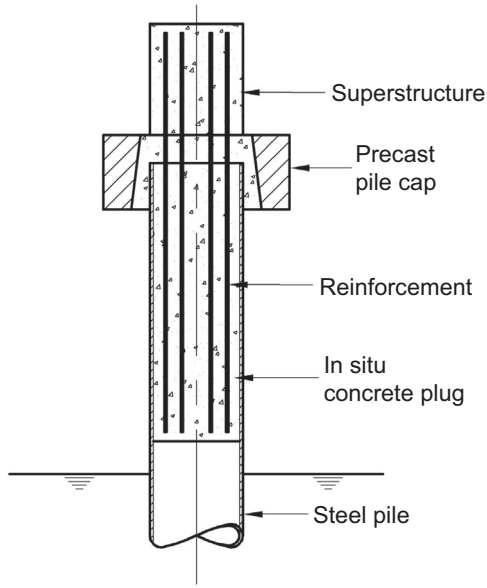
## 3.7.6 Superstructure units

### 3.7.6.1 Pile caps and headstocks

To assist the connection of precast beam elements to the supporting pile, a cap is frequently used, as shown in Fig. 3.5. The figure shows a precast pile cap that is placed on temporary supports and then connected to the pile with an in situ cast, but the whole cap could also be cast in situ. The cap is placed more accurately than the pile, provides a temporary support for the precast beam unit until it is cast in and facilitates the




Platform-pile connection




Jetty-pile connection

**Figure 3.4** Typical jetty and offshore structure pile connections.

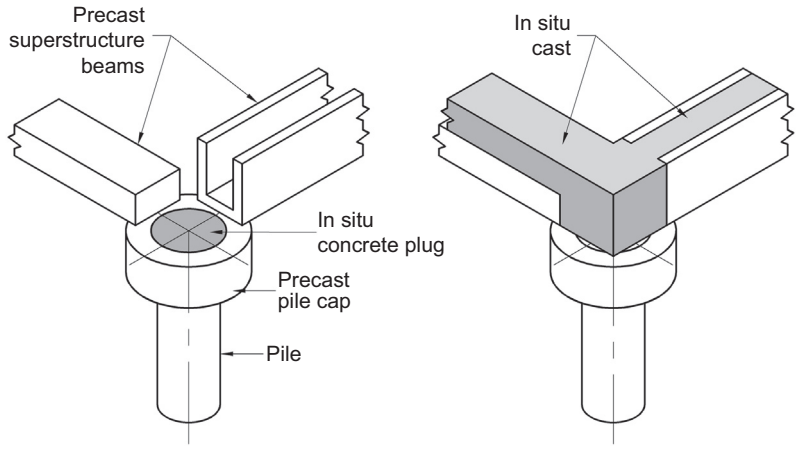



**Figure 3.5** Use of pile cap in jetty construction. Not shown in these views are the projecting reinforcing bars from the pile cap plug and the precast units that are necessary to stitch the elements together.

placement of the reinforcement used for the connection. Tighter tolerances are specified for each stage of the construction, for example:

- plan position of pile: ±75 mm
- plan position of pile cap: ±50 mm
- plan position of beam: ±20 mm

It is not practical to install a pile in the seabed to a tight tolerance, but once a pile is installed, it provides a foundation on which to construct more accurately, and therefore specified construction tolerances should take account of this.

A headstock is an enlarged pile cap supported on two or more piles and is often used in jetties or accessways to support the beams for the deck and conveyors or pipelines. Fig. 3.6 illustrates a headstock that uses a precast box that is connected to the piles with an in situ cast. The use of a precast box reduces the amount of overwater formwork that is needed, but the headstock could also be constructed as one in situ cast. The piles and headstock together form a frame, and the whole is designed as a portal to resist lateral loads, such as wave and wind actions. The supporting piles are frequently raked outward to take some of the lateral load as an axial force in the piles. The sand bypass jetty at the Port of Ngqura utilises in situ concrete headstocks and is shown in Fig. 10.49, Chapter 10.

Dolphins frequently use a large in situ pile cap, as shown in Fig. 3.7. It could be possible to design precast elements for a dolphin such as this, but because of the large size and multiple piles, it is usually considered easier to cast it in situ.

The large volume of concrete is used because its massive weight gives significant axial compressive forces in the piles. Hence the axial tension forces generated in the piles when the dolphin is loaded are reduced, which reduces the required geotechnical axial pull-out resistance of the piles. The implication of a massive cap is that it experiences low flexural stresses, and the resulting crack widths will be low.

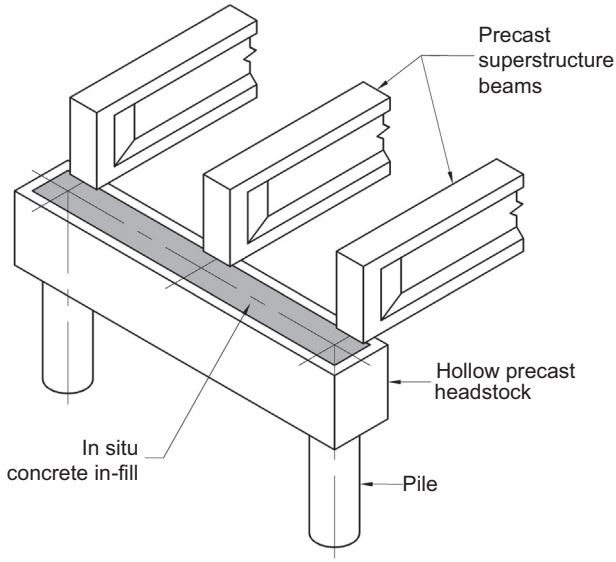



**Figure 3.6** Headstock example.



**Figure 3.7** Concrete mooring dolphin.

### *3.7.6.2 Beams*

A frequently used technique in jetty superstructures is the use of precast beam elements that are stitched together with in situ casts. Limitations in the lifting capacity of the construction crane often means that it is not possible to place the full beam section as it would be too heavy. A partial beam is therefore used, and this can be designed and

detailed as either the lower portion of the beam, including all the flexural tension reinforcement, or a hollow U-shaped box. These two approaches are illustrated in Figs 3.8 and 3.9.

The use of precast elements reduces or eliminates overwater formwork but results in a staged construction, and when flexural crack widths are calculated, care must be exercised to take into account the stresses that are built in with each stage of construction. Crack widths would be underestimated if they were to be calculated for the full sustained load applied on the complete cross-section. The self-weight of the section is increased incrementally as it is constructed, but in the early stages of the assembly, the load is resisted by the intermediate configurations of the structure, and not the full section. Flexural stresses are generated and then locked into the structure with each stage as it is built. In the early stages of the construction, the self-weight of the first components are resisted by smaller sections than the full one, and therefore the total stresses that are generated will be greater than if all self-weight was applied to the full section.

Fig. 3.8 illustrates a typical staged deck construction using half-height precast beams and deck slabs.

- Stage 1: the precast beam is placed on the pile caps, and it only supports its own weight.
- Stage 2: the beam in situ concrete is cast. The precast beam has to support its own weight and the weight of the plastic concrete in the in situ beam cast. As the second cast gains strength and hardens, the stresses are locked into the precast portion, and the new concrete has no flexural stresses.
- Stage 3: the precast deck slabs are placed onto the beam grillage, and the in situ slab topping is cast. The resisting beam now has the section properties of the combined precast and first in situ cast, and this determines the stresses generated from the weight of the precast and in situ slab. The upper part of the composite section has now started functioning and developed stresses.
- Stage 4: by the time that in-service live loads are applied, the composite section will include the in situ deck slab, and a full-depth T section is used to determine the member resistance.

The tensile stresses in the bottom of the precast beam section are cumulative and must be determined for each stage, and the effect added. It is possible that the precast beam will be uncracked for the early stages if the tensile stresses are low, and cracking will only occur as the stresses accumulate.

### *3.7.6.3 Slabs*

Use of precast slabs eliminates the need for overwater slab soffit formwork, and they are usually detailed and designed as discrete width units that span in one direction, such as illustrated in Fig. 3.10. Again, the size is usually determined by the construction crane capacity.

One implication of this configuration is that the final slab, including the topping, has a different depth in each direction. The full depth is available in the direction of the precast span, and it uses the bottom steel in the precast unit. In the orthogonal direction, however, the slab is broken up by the joints between the precast units. The units are usually given a chamfered top edge, which allows the in situ concrete to penetrate to some degree in-between the units, but it is only possible to place the slab bottom mesh across the top of the precast units. In the transverse direction, therefore, the

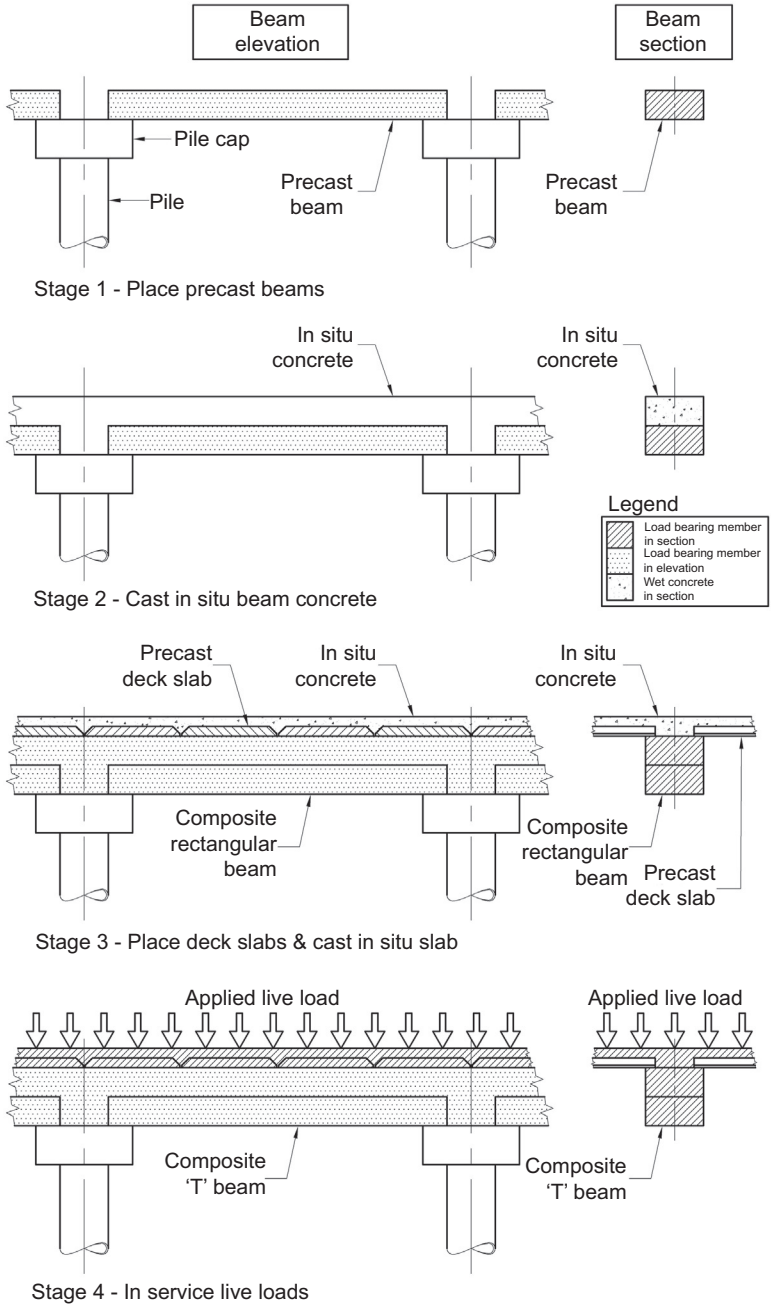



**Figure 3.8** Staged construction sequence for beams and slabs in jetty construction.

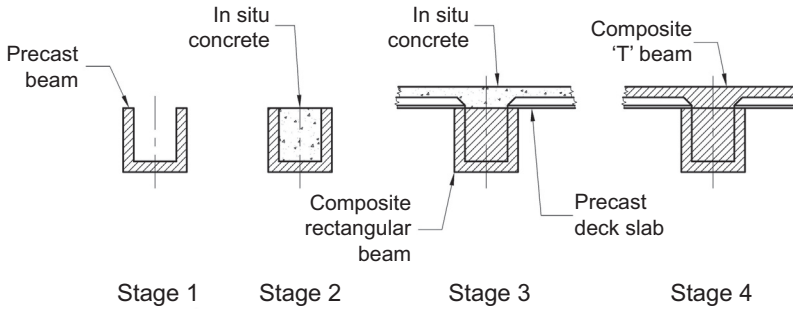



**Figure 3.9** Beam cross-sections for staged construction using hollow U precast beams. The U beam eliminates the need for side formwork for the second stage cast.

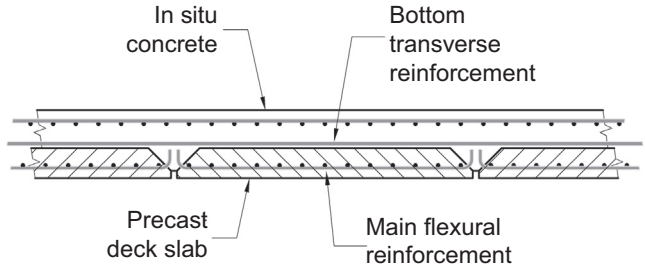



**Figure 3.10** Effect of precast deck slab configuration on transverse reinforcement.

slab depth is equal to the thickness of the in situ concrete above the precast units. This is shown in Fig. 3.10.

It is always advisable to detail gaps between precast units that are placed in a row, such as deck slab units, to allow for casting tolerances.

#### *3.7.6.4 Fender cope units*

Jetty and quay cope panels usually go down to datum or just below to provide sufficient height for the mounting of fender units and to prevent small craft from being trapped beneath at low tide. As the panels are located in the tidal zone, it is preferable to precast them; refer to Fig. 3.11. The precast units are therefore usually designed as cantilever slabs, spanning downward from the deck slab or capping, with the primary load being the reaction from the elastomeric fender.

The width of the precast cope unit limits the spread of the fender reaction load, as shown in Fig. 3.11.

Again, a gap should be detailed between the units to allow for casting tolerances.

### *3.7.7 Breakwater armour units*

Breakwater armour units are subject to loads in service that cause flexure and shear in the units, and reasonable concrete strengths are therefore necessary. In addition to

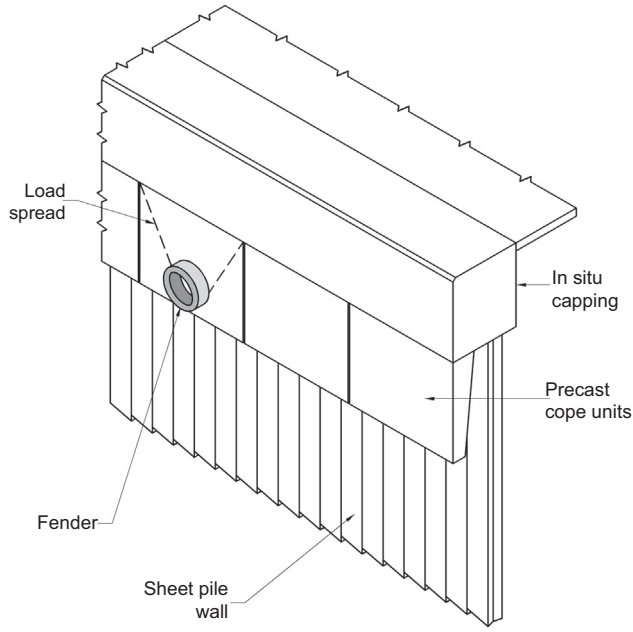



**Figure 3.11** Typical cope panel configuration.

compressive strength, for an armour unit such as a dolos or Core-loc™, a minimum tensile strength (flexural) is also specified, and it is usually in the order of 4.0 MPa at 28 days, which implies a compressive strength in the order of 40 MPa.

As the tensile strength is important for armour units, tensile tests must be specified as part of the project quality control. It is common practice to determine the relationship between tensile and compression strengths at the start of a contract and then use only the compression test thereafter.

Armour units are designed to have a certain mass for stability, which is a function of the wave conditions, breakwater geometry and the type of unit. It is therefore essential that armour units have the required mass when manufactured and that the mass is maintained for the service life of the structure. The density of the plain concrete used will determine the dimensions, and hence the volume, of the armour unit, to achieve the required mass.

Manufacturing defects that reduce the mass must be avoided in the production of the units. Armour unit specifications should therefore limit the extent of manufacturing defects that will affect the mass, such as honeycombing, grout loss at formwork joints, surface bubbles and cracks. Cracks can propagate and create a weakness that may lead to a breakage and loss of a significant portion of the unit when it is loaded in service. A crack at the junction of the waist and the fluke of a dolos may lead to the loss of the whole of the fluke. This would be a significant loss of mass and render the unit unstable under design wave conditions. The unit could then move and impact other units, causing further damage and breakage.

Repairs to surface defects and cracks in armour units are not recommended, as the repairs may not be durable in service in the harsh coastal environment, and ultimately the reduction in mass caused by the defect may not be avoided. It is preferable to accept a unit with minor defects as 'defective, but fit for service' and use it in a location on the structure where its lower mass will not be critical, or where it may be easily replaced if necessary.

## 3.7.8 General considerations

### 3.7.8.1 Chloride content

As chlorides are a major factor in the deterioration of marine reinforced concrete, it is vital to avoid their inclusion in the concrete during the construction process.

For reinforced concrete, potable water must be specified for mixing, and admixtures should be chloride-free, but for plain concrete components, without any embedded steel, seawater could possibly be used. Subsequent efflorescence may, however, be a problem. Chloride-free sand should be used, and if concrete mixing takes place on site, the aggregates should be stored in an area free from sea spray so that they do not get contaminated. Steel should also be stored in a chloride-free laydown area.

Seawater should strictly not be used for moist curing, as it will prematurely introduce chlorides to the surface of concrete.

With the possible exception of precast units cast off-site, construction takes place in the marine environment, and care must be taken to ensure that the encased reinforcement is not contaminated with chlorides from seawater spray or inundation during high tides. All steel should therefore be washed with fresh water immediately prior to the concrete pour.

### 3.7.8.2 Cover spacers

Cover spacers are used between the reinforcing steel and the casting bed or side form to ensure that the required concrete cover is achieved. It is advisable to use purpose-made concrete or mortar blocks for the spacers (Fig. 3.12) as these have equivalent or better chloride resistance than the surrounding concrete and will not create a weak point in terms of chloride penetration. However, they need to be made from the same basic mix as the main elements, and thoroughly cured prior to use. In building construction, plastic cover spacers are often used, but these are considered inappropriate for marine structures as the concrete may not bond onto the sides of the spacer and thereby create a crack and pathway to the steel for chlorides.

### 3.7.8.3 Use of stainless steels

The use of stainless steel in the marine environment is not without problems. For instance, it is advisable to apply cathodic protection to Grade 316 stainless-steel components that are fully immersed in seawater, and when it is used in anaerobic seawater conditions, pitting corrosion can occur. In concrete, corrosion of stainless steel may still occur, but at higher chloride concentrations than carbon steel. Initiation of



**Figure 3.12** Concrete mortar cover spacer in use. Note that the reinforcement in this photograph is slightly surface-rusted. This degree of rust is acceptable as it roughens the bar surface and improves the bond of the concrete.

corrosion of carbon steel commences when the chlorides reach a threshold concentration, conventionally taken as about 0.4% by mass of cement, but for stainless steels, this will occur at a much higher value. A test program conducted by the U.S. Department of Transportation, Federal Highway Administration, found that the threshold value for 3Cr12 and MMFX$_2$ steel was four times that of carbon steel, and for 2101 Lean Duplex steel, it was just under four times (Hartt et al., 2009).

The higher chloride threshold value for stainless steel has been incorporated, by a stainless steel manufacturer, into the software used for predictive modelling of reinforced concrete service life, based on the chloride diffusion into the concrete (Outokumpu). Another model, the AGEDDCA model developed by the UK Concrete Society, uses a threshold value of 3.0% chloride concentration by mass of cement for stainless-steel reinforcement, which is 3.5 times the value for carbon steel. The Life-365 model from the USA uses a chloride threshold value of 0.5% by mass of concrete for stainless steels, which at the cement contents typically used in marine concrete translates to about 3% by mass of cement.

### *3.7.8.4 Construction joints*

Most reinforced concrete structures have construction joints between casts, with reinforcement passing through these joints. The intention of the joints is to allow a monolithic structure to be broken down into a series of casts of manageable size or a logical component assembly sequence (such as connection of a precast pile to the superstructure beams and the beams to the slab). It is important for the second or subsequent casts to bond onto the previous casts to create a monolithic structure without any weaknesses that could compromise the structure's durability. As a minimum, therefore, construction joints should be specified to have an exposed aggregate finish in order to be rough enough to assist the bond. The critical part of the joint is the cover zone outside of the reinforcement, and it is essential that this is prepared correctly so that the next

cast is able to bond to the first and not compromise the durability by the formation of a crack between the two casts.

An exposed aggregate construction joint finish that is formed by application of a retarder chemical on to the construction joint surfaces immediately after casting is preferred to a surface that is roughened by mechanical means. Nonvisible cracks or loose aggregate may be caused by the mechanical roughening that could become a weak point for chloride ingress.

In precast beam construction, such as the examples in Section 3.7.6.2, it should be specified that the top and ends of the part-height precast beam or the inner surfaces, and the ends and top of the U beam, are given a construction joint finish. Similarly, the inner surfaces of precast pile caps and headstock boxes also need to be prepared.

### 3.7.8.5 Curing

The concrete used for marine structures typically has a low water/binder ratio, and therefore moist curing is specified to make water available for continued hydration of the cement at the surface. Ten days of moist curing should be specified, and experience has shown that a continuous low flow using domestic garden irrigation systems provides a low maintenance, reliable method. Manual watering of a hessian covered surface will always be unreliable and subject to dry periods due to erratic attention, especially overnight and weekends.

Liquid membrane-forming curing compounds are considered suitable for plain concrete elements, and it is essential that a pigmented product is specified so that it is easy for the applicator and quality control personnel to verify that a continuous barrier has been applied.

### 3.7.8.6 Cathodic protection

On marine structures, cathodic protection is usually used to protect steel piles or other structural elements immersed in the sea, and both sacrificial anode and impressed current systems are used.

To function, a cathodic protection system requires a cathode (usually the surface of the structure to be protected), a discrete anode, an electrical connection between the anode and cathode via the structure and an electrolyte that provides a second connection between anode and cathode to complete the electrical circuit. In a marine structure, seawater is the electrolyte, and hence only the immersed parts of the steel structure can be protected.

In a reinforced concrete superstructure, however, the concrete pore water can serve as the electrolyte, and the reinforcement is the cathode and is connected directly to the anode.

The anode has to be embedded in, or in contact with, the body of the concrete, and electrical continuity of the steel mesh is essential so that all bars are polarised and protected.

Cathodic protection is often used in the rehabilitation of chloride-contaminated structures, but it can also be applied to new-build structures as well. In a new-build

structure, provision could be made for future connection of an impressed current system by initial installation of the system electrical connections and electrical continuity of the reinforcement mesh. This would allow future activation of cathodic protection should corrosion problems arise during the service life or if the service life is to be extended.

## 3.8 Summary

This chapter has presented an overview of the design process, suitable codes to be consulted and materials to be used for marine concrete structures, with the focus on durability design. Durability is paramount and usually governs the materials used and much of the reinforcement design.

In summary the main checks to be undertaken for the durability design of a reinforced concrete marine structure are these:

- selection of a suitable concrete material specification to minimise the chloride penetrability and heat of hydration, including
  - a binder that includes one or more extenders
  - a low water/binder ratio
- selection of a suitable concrete cover to the steel reinforcement
- design of reinforcement to suit the ULS strength requirements
- design of reinforcement to suit the SLS flexural crack width requirements, using load cases and crack widths relevant to the durability design
- design of reinforcement to suit the shrinkage crack width requirements
- provision of the minimum steel area in cases where the reinforcement is not governed by the other design checks

The construction specifications should contain the following durability-based requirements:

- material type and quality, including a prescriptive, performance-based or hybrid specification for the concrete
- shrinkage design requirements (such as maximum permissible hydration temperature, aggregate type, any mandatory construction joint locations and period between successive casts)
- preparation of construction joints
- moist curing

## Sources of further information

- Marine structure design handbooks:
  - Brinkmann, B., 2005. Seehäfen, Planung und Entwurf. Springer, Germany.
  - CIRIA C674, 2010. The Use of Concrete in Maritime Engineering − A Good Practice Guide. CIRIA, London, United Kingdom.
  - CUR, 2005. Handbook Quay Walls. Taylor and Francis, Netherlands.
  - Thoresen, C.A., 2014. Port Designer's Handbook: Recommendations and Guidelines. Thomas Telford, United Kingdom.

- Design of structures in hot and dry environments:
  - Concrete Society, C136, 2002. Guide to the Construction of Concrete Structures in the Arabian Peninsula. Concrete Society, United Kingdom.
  - Concrete Society, C163, 2008. Guide to the Design of Concrete Structures in the Arabian Peninsula. Concrete Society, United Kingdom.
- Hot dip galvanising of reinforcement:
  - Hot Dip Galvanisers Association Southern Africa. http://www.hdgasa.org.za/TechnicalPapers/Reinforcement%20of%20Concrete%20Structures.pdf.
- Stainless-steel reinforcement:
  - Southern Africa Stainless Steel Development Association: 3CR12. http://www.sassda.co.za/wp-content/uploads/2013/10/3CR12INACTION.pdf.
  - International Stainless Steel Forum. http://www.worldstainless.org/architecture_building_and_construction_applications/structural_applications.
- Alkali Silica Reaction: Fulton's Concrete Technology, 2009, Chapter 10.
- Cathodic protection of steel reinforcement in concrete: ISO 12696:2012, Cathodic protection of steel in concrete, International Organization for Standardization, 2012, Switzerland.

## References

ACI 318-05, 2005. Building Code Requirements for Structural Concrete. American Concrete Institute.

ACI 357R-84, 1997. Guide for the Design and Construction of Fixed Offshore Concrete Structures. American Concrete Institute.

Alexander, M.G., Jaufeerally, H., Mackechnie, J.R., 2003. Research Monograph No. 6, Structural and Durability Properties of Concrete Made with Corex Slag. Department of Civil Engineering UCT, Cape Town, South Africa.

AS 1379-2007, 2007. Specification and Supply of Concrete. Council of Standards, Australia.

AS 3600-2009, 2009. Concrete Structures. Council of Standards, Australia.

AS 4997-2005, 2005. Guidelines for the Design of Maritime Structures. Council of Standards, Australia.

BS 6349-1-1:2013, 2013. Maritime Works-Part 1-1: General - Code of Practice for Planning and Design for Operations. The British Standards Institution, United Kingdom.

BS 6349-1-2, Maritime Works Part 1-2: General - Code of Practice for Assessment of Actions. The British Standards Institution, United Kingdom (in preparation).

BS 6349-1-4:2013, 2013. Maritime Works-Part 1-4: General - Code of Practice for Materials. The British Standards Institution, United Kingdom.

BS 6349-2:2010, 2010. Maritime Works-Part 2: Code of Practice for the Design of Quay Walls, Jetties and Dolphins. The British Standards Institution, United Kingdom.

BS EN 197-1:2011, 2011. Cement - Part 1: Composition, Specifications and Conformity Criteria for Common Cements. The British Standards Institution, United Kingdom.

BS EN 206-1:2013, 2013. Concrete − Specification, Performance, Production and Conformity. The British Standards Institution, United Kingdom.

BS EN 450-1:2012, 2012. Fly Ash for Concrete − Part 1: Definition, Specifications and Conformity Criteria. The British Standards Institution, United Kingdom.

BS EN 1992-1-1:2004, 2004. Eurocode 2-Design of Concrete Structures - Part 1-1: General Rules and Rules for Buildings. The British Standards Institution, United Kingdom.

BS EN 1992-2:2005, 2005. Eurocode 2-Design of Concrete Structures - Part 2: Concrete Bridges - Design and Detailing Rules. The British Standards Institution, United Kingdom.
BS EN 1992-3:2006, 2006. Design of Concrete Structures – Part 3: Liquid Retaining and Containment Structures. The British Standards Institution, United Kingdom.
BS EN 15167-1:2006, 2006. Ground Granulated Blast Furnace Slag for Use in Concrete, Mortar and Grout – Part 1: Definitions, Specifications and Conformity Criteria. The British Standards Institution, United Kingdom.
BS EN ISO 19902:2007, 2007. Petroleum and Natural Gas Industries – Fixed Steel Offshore Structures. The British Standards Institution, United Kingdom.
CIRIA C660, 2007. Early-Age Thermal Crack Control in Concrete. CIRIA, London, United Kingdom.
DNV-OS-J101, May 2014. Design of Offshore Wind Turbine Structures. DNV Offshore Standard, Norway.
Fulton's Concrete Technology, ninth ed., 2009. Cement & Concrete Institute, Midrand, South Africa.
Godart, B., Divet, L., 2013. Lessons learned from structures damaged by delayed ettringite formation and the French prevention strategy. In: Fifth International Conference on Forensic Engineering, Institution of Civil Engineers, April 2013, France.
Griffith, A., Laylor, H.M., June 1999. Epoxy Coated Reinforcement Study. Final Report, State research project #527. Oregon Department of Transportation, Salem, Oregon.
Hartt, W.H., Powers, R.G., Marino, F.P., Paredes, M., Simmons, R., Yu, H., Himiob, R., Virmani, Y.P., 2009. Corrosion Resistant Alloys for Reinforced Concrete. Federal Highway Administration, McLean, Virginia.
Hartt, W.H., March 2012. A Critical Review of Corrosion Performance for Epoxy-coated and Select Corrosion Resistant Reinforcements in Concrete Exposed to Chlorides. Florida Atlantic University, Florida, USA.
JSCE Guidelines for Concrete No. 2, December 2005. JSCE Standards on Test Methods for Diffusion Coefficient of Chloride Ion in Concrete (English Version). Japan Society of Civil Engineers, Tokyo, Japan.
JSCE Guidelines for Concrete No 15, December 2010. Standard Specifications for Concrete Structures - 2007, "Design" (English Version). Japan Society of Civil Engineers, Tokyo, Japan.
JSCE Guidelines for Concrete No. 16, December 2010. Standard Specifications for Concrete Structures-2007, "Materials and Construction" (English Version). Japan Society of Civil Engineers, Tokyo, Japan.
Kessy, J.G., Alexander, M.G., Beushausen, H., March 2015. Concrete durability standards: international trends and the South African context. Journal of the South African Institution of Civil Engineering 57 (1). Midrand, South Africa.
NORSOK Standard N-004, Rev. 3, February 2013. Design of Steel Structures. Standards Norway, Lysaker, Norway.
Otieno, M., Beushausen, H., Alexander, M.G., January 2016. Chloride-induced corrosion of steel in cracked concrete – part I: experimental studies under accelerated and natural marine environments. Cement and Concrete Research. http://dx.doi.org/10.1016/j.cemconres.2015.08.009.
Outokumpu Stainless, August 2009. The Use of Predictive Models in Specifying Selective Use of Stainless Steel Reinforcement. Finland.
SANRAL Table 6000/1, August 2009. http://www.nra.co.za/, Pretoria, South Africa.
SANS 10100-1:2000, 2000. The Structural Use of Concrete, Part 1: Design. South African Bureau of Standards, Pretoria, South Africa.

SANS 10100-2:2014, 2014. The Structural Use of Concrete, Part 2: Materials and Execution of Work. South African Bureau of Standards, Pretoria, South Africa.
SANS 3001-CO3-3, 2015. Civil Engineering Test Methods Part CO3-3: Concrete Durability Index Testing - Chloride Conductivity Test. South African Bureau of Standards, Pretoria, South Africa.
SANS 50197−1:2013, 2013. Composition, Specifications and Conformity Criteria for Common Cements. South African Bureau of Standards, Pretoria, South Africa.

# Construction methodologies and challenges for marine concrete structures

4

*S.N. Allen* [1], *G.A.C. Moore* [2]
[1]Former Managing Director of specialist marine construction company Stefanutti Stocks Marine (Pty) Ltd, Cape Town, South Africa; [2]Specialist Marine Civil Engineering Consultant, Cape Town, South Africa

## 4.1 Introduction

While marine construction is often viewed as a specialised area and cloaked in mystery, 'best left to the experts', there are many aspects of marine construction that fall within the ambit of general civil engineering construction practice. It is not the purpose here to describe these common aspects which are widely known and generally accepted.

The purpose of this chapter is to outline the more specialist nature of the construction of marine concrete structures and give guidelines on construction methodologies, pitfalls, and particular aspects of underwater concreting, along with comments on future challenges.

This chapter is not intended to be comprehensive, and so the projects, plant and methods featured are those within the authors' particular frame of experience and knowledge.

Only relatively recently has the advent and introduction of electronic survey equipment and software greatly eased the setting-out control (survey) of marine structures and led to accurate underwater mapping of the sea bed, both prior to and after construction or dredging, making both design and construction easier than in the past when manual 'fixed' survey methods were employed. Multi-beam surveys and their concomitant GPS systems are now accurate and definitive and give the client and contractor teams complete peace of mind in assuring marine concrete structures are accurately located, constructed and defined.

Where pertinent the authors give examples to illustrate particular methods, for construction both within and beyond the coastline of southern Africa.

In the subsequent sections, the authors will stress the importance of all stakeholders in a marine construction project. In particular, the need for all parties to have early input into both the design and construction phases is critical to maximise safety and efficiency in the project and optimise the construction methodology.

**Marine Concrete Structures.** http://dx.doi.org/10.1016/B978-0-08-100081-6.00004-0
Copyright © 2016 Elsevier Ltd. All rights reserved.

## 4.2 Marine construction methodologies: general issues

This section deals with the choice of methodology for the construction of marine concrete structures, such as those defined and discussed in Chapter 2. These choices are dependent on many things, inter alia those given below.

### 4.2.1 Location

The structure may be located in a sheltered port, harbour or natural bay, in which case the methodology adopted will take cognizance of the reduced wave conditions. This could, for instance, favour the use of a floating plant over a land-based (and therefore fixed) entry point.

Conversely, if the structure is subject to harsh open sea and wave conditions and is exposed, either a much more substantial floating plant spread (ie, the plant and equipment required to be put together to effect the project) may be required, a fixed-point entry from the land may be needed, or a temporary breakwater/wave attenuation structure may be required to construct the marine structure safely and efficiently.

When considering different locations, it is therefore essential that the conditions of waves, climate and weather be carefully assessed. This would require available data on wind and waves to be obtained. There may be direct wave data available or interpretive wind data from offshore that can be used. This data must be analysed by an expert such as an experienced coastal engineer specialising in wave dynamics, who can determine the likely downtime and risks associated with the project in the event that a floating plant is used, or alternatively if working directly into the face of the sea.

### 4.2.2 Design

The design of a marine concrete structure plays a major part in how it will be constructed. In recent years, the construction contractor has increasingly become the lead party in the entire construction process (and particularly engineer procure construct (EPC) contractors), and therefore the consulting design brief often emanates more from the contractor who will build the structure than from the client. The reasons for this are seated in the risk profile and uncertainty in the project, with the EPC contractor being able to better assess, quantify and price the risks more accurately than either the client or the design engineer and thereby being able to offer a fixed lump sum contract without variation (which is what the client is looking for in certainty of funding and obtaining a return on the project).

Regarding the design process, it is essential to engage the contractor at an early stage.

#### 4.2.2.1 Early contractor involvement and adaptive management

The project methodology can benefit significantly in terms of cost and time if an experienced marine contractor is included in the project at an early stage.

Besides having an influence on the sequencing of construction, materials and plant, a contractor can greatly assist in assessing construction risk in terms of cost and time and, most importantly, safety.

Fig. 4.1 shows some of the benefits of early contractor involvement (ECI). In terms of marine concrete construction, it is important to involve experienced construction professionals specific to the marine environment to gain benefit from expert knowledge and practical lessons learnt. Similarly, adaptive management (or adaptive resource management, ARM) is a tool that utilises iterative decision-making and monitoring to minimise risk and uncertainty in resource management. This system uses a model to set up the integration and accrual of information on resource management objectives, to improve future management, essentially as a tool for learning and influencing system changes.

### 4.2.3 Available resources

Generally, a project is most efficient in terms of time and cost when locally available resources can be utilised, in terms of materials, plant and personnel.

#### 4.2.3.1 Materials

The available material resources will often define the methodology to some degree. For instance, a breakwater design may be predicated on a certain armour rock size and weight, but the materials for this may not be economically available locally. In this case, it would be better to redesign the breakwater (if possible) to utilise rock from a local source or quarry.

Alternatively, a precast concrete armour element may be designed. This in turn leads to considerations of local availability of plant and equipment for lifting and placing, as the precast element may weigh much more than rock elements. It also must consider local expertise and ability to produce high-quality precast concrete elements. Marine plant and heavy lifting equipment can be extremely expensive to mobilise and relocate, and so a cost–benefit exercise should be undertaken at design stage to optimise the most efficient materials and plant combination to execute the project.

#### 4.2.3.2 Plant and equipment

Typical plant and equipment used on a marine construction project can include any or a combination of the following:

Floating plant spread:

- Dredgers (vessels, barges, pumps or long-reach excavators, or a combination of these)
- Barges
  - Dumb barges (ie, no equipment on board, used generally for materials handling)
  - Crane or lifting barges (with either static fixed/ringer/or tracked mobile crane setups)
  - Piling barges (generally with on-board crane(s))
- Work and service boats for personnel, survey and general servicing
- 'Land-based' equipment found on typical heavy civil engineering projects

Due to the high mobilisation costs of marine construction equipment, especially floating plant, it may be worth considering adapting a design to suit the locally available

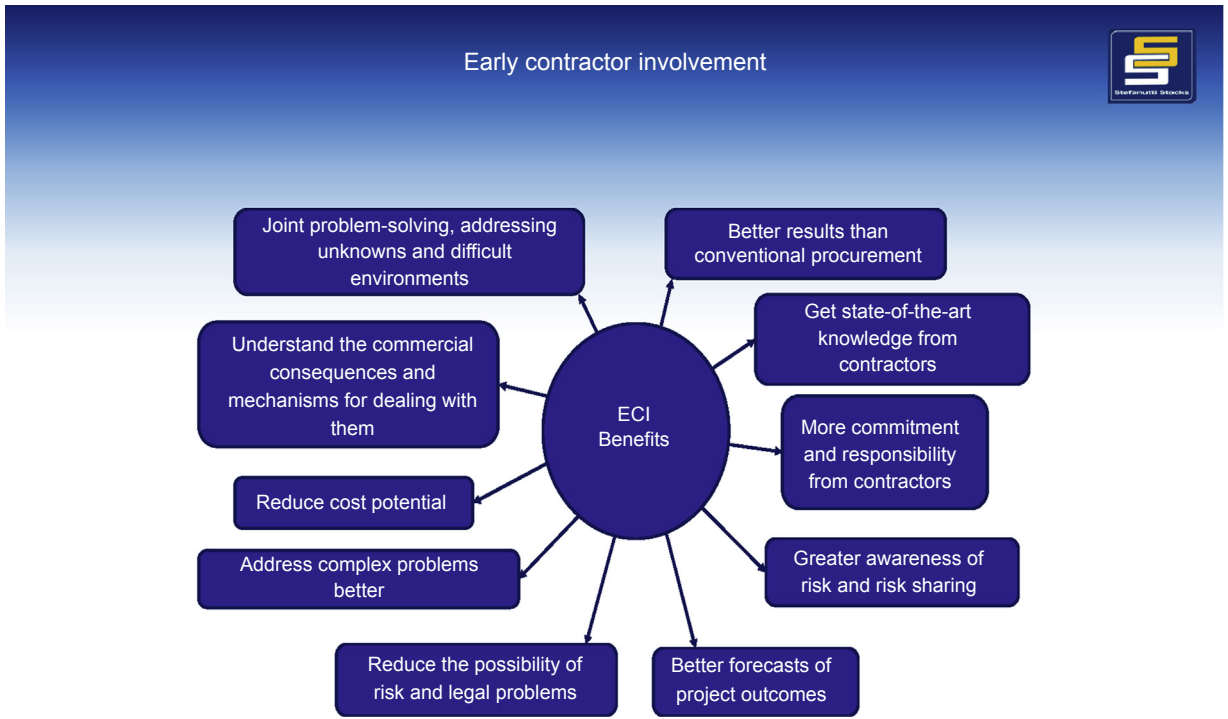



**Figure 4.1** The benefits of early contractor involvement.
Courtesy: Stefanutti Stocks Marine, South Africa.

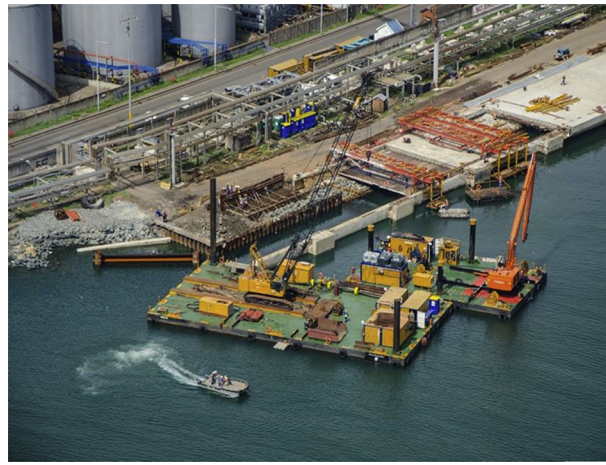


**Figure 4.2** Typical marine plant spread consisting of piling barge with crawler crane and piling rig along with dredge barge with long-reach excavator on board with 'spud' stabilising legs. Courtesy: Stefanutti Stocks Marine, South Africa.

construction equipment. For instance, if a jack-up barge (or self-elevating platform which stands on the sea bed on 'jack-able' legs taking the working platform out of the water completely) would normally be required for, say, a standard jetty construction due to high swell conditions in a particular area, the jetty could possibly be adapted to precast hand-over-hand type construction with specially modified gantries to 'lead' the construction in the open sea, effectively eliminating the use of floating plant. Fig. 4.2 illustrates the situation of using barges in construction of a marine quay wall utilising floating plant that can be stabilised with 'spud' legs which allows the barge load to be taken partially on legs that sit on the sea bed but not be 'jacked-up' out of the water.

#### *4.2.3.3 Personnel*

Marine construction is specialised, but as stated at the beginning of this chapter, there are a host of more traditional civil construction skills that can be utilised.

The more specialised skills are demanded when underwater placement of concrete is required or specialist pile driving is needed. It is pertinent therefore to try and optimise the use of locally (or nationally) available skills to minimise the need to employ expatriate experts who will come at a relatively high price to the project. This was also mentioned earlier in regard to precasting expertise.

## 4.3 Particular construction challenges for different marine concrete structures

The following section describes the construction methodologies for several structures and the particular construction methods applicable for each. General civil engineering

principles are not described, being assumed, but rather the section describes the specific marine methodologies that a marine contractor is likely to adopt and the specific challenges that may be encountered in the marine environment.

### 4.3.1 Quay walls

Of the five types of quay walls (block, caisson, counterfort, cantilever and sheet pile; see Chapter 2), the first four can be constructed 'in the dry' by conventional methods, which will not be discussed here.

Block, caisson and counterfort walls in marine construction all require some dredging to form a stable platform and the formation of a stone bed on which to place the respective units. The dredging would normally be carried out by grabbing, cutter-suction or trailer suction, and it is usually performed by a specialist subcontractor. The dredging survey must be controlled using differential GPS to tight tolerances. The platform or excavation in the sea bed would then be surveyed by multi-beam sonar to produce a set of plans and cross-sections to compare with the requirements of the construction drawings. The multi-beam survey, which is also controlled by differential GPS, should produce accuracies of $\pm 20$ mm in height and $\pm 100$ mm laterally. This is far more accurate than the older methods of depth soundings or echo soundings, and it should produce more economical construction, as the dredging can be carried out to tighter tolerances than in the past.

Similarly, modern surveying methods should help to produce more economical construction of the stone bed, as there should be less material wastage. The stone bed is usually made of 75-mm single-sized crushed stone, which would be handled by a grab crane on a barge and supplied by stone supply barges. The stone bed may initially, if the depth of stone so dictates, be carried out by rough dumping of stone from hopper barges or by grabbing off a stone barge. However, both methods require dumping to a calculated, coordinated pattern. The final stone level is achieved by using a stone spreader where compaction is not required, merely an allowance for settlement being made depending on subsoil conditions; see Fig. 4.3.

A block wall is normally constructed of precast concrete blocks laid from a crane barge, supplied by a block transport barge. The size or weight of the blocks is usually dictated by the size of equipment available, but clearly the largest size or weight of block is the most efficient. Concrete blocks are cast at a land-based precast yard, and blocks of 40 ton are usually the largest that can be handled by normal land-based plant and transport. Blocks that are much heavier can be handled by purpose-designed equipment. The crane barge for block-laying is securely anchored over the position of the block wall, and the blocks are laid to surveyed lines and levels. Where the block wall retains fill for hardstanding areas, the joints between the blocks are sealed, usually with grout socks in preformed recesses. The voids in hollow block walls are filled typically with sand or rubble. (See Chapter 2 for more details on block walls.)

A caisson wall is constructed of adjacent caissons, usually constructed in a dry dock or in an area below sea level that has been bunded off and dewatered. If the dry dock or bunded area has water depth limitations during the float-out sequence, and

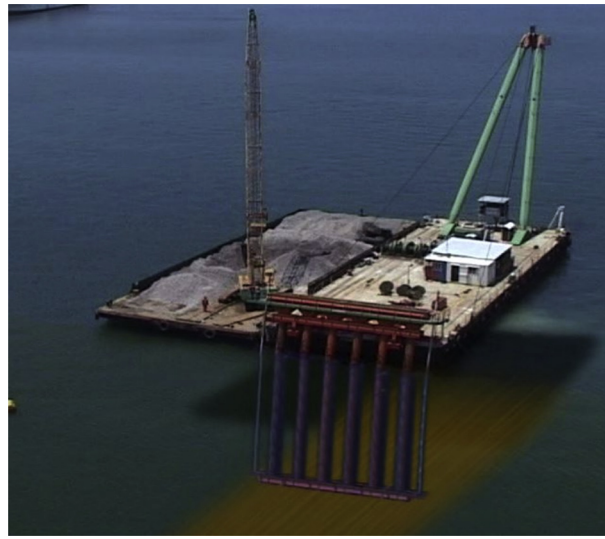


**Figure 4.3** Typical stone spreader arrangement for concrete quay wall founding. Courtesy: LTA Interbeton Bafokeng Joint Venture.

consequently the caisson cannot be constructed to full height in the dry dock or bunded area, the caisson construction can be continued with the caisson floating at a mooring. The caisson normally requires ballasting down with each vertical lift of the walls for stability. The caisson construction method depends entirely on available water depths, dry dock availability and final water depths. Caissons are floated out of the casting yard and, where water depths permit, ballasted down to a placing depth. The placing depth is the draft of the submerged structure and is a calculated depth, to clear the stone bed by an acceptable margin, at a certain state of tide. The caisson is positioned at the prescribed state of tide and then held in position on a falling tide, until it is properly grounded. The grounding is usually accelerated by water ballasting. Depending on the size of the caisson and the water conditions, the positioning of the caisson may be done by a couple of small inflatable boats in very sheltered inland waters or a fleet of large tugs in areas with large currents or heavy seas. In some conditions, it may be necessary to provide fixed points against which to push the caisson while grounding, in the form of piles. Subsequent caissons are placed against the preceding ones to form the wall, and the preformed joints between the caissons are grouted up with grout socks. The voids in the caissons are then usually filled with sand by either pumping or crane grab.

Counterfort walls are constructed from adjacent counterforts, lifted into position by heavy-lift purpose-built floating equipment, such as that shown in Fig. 4.4. The counterforts are typically constructed in the dry in a bunded area below water level. The bunded area when opened up allows the floating lifting equipment to move in and lift up the counterforts in sequential order for placing in their final position. The preformed joints between adjacent units are grouted up with grout socks. Fig. 4.5 illustrates a counterfort unit being transported by a floating gantry arrangement.




**Figure 4.4** Gantry for precast element placement.
Courtesy: Clough Murray & Roberts Marine.




**Figure 4.5** Counterfort cantilever precast unit in transit, supported by a gantry.
Courtesy: Clough Murray & Roberts Marine.

Cantilever walls are always constructed in the dry by conventional methods.

Sheet pile walls can be constructed by three possible methods. First, either the concrete (or steel) sheet pile can be driven by various means through existing or fill material, and the marine side of the fill excavated subsequently to form the wall. Second, the sheet pile wall can be driven overhand from the bank or edge of the fill. Third, the sheet pile wall can be driven from floating equipment, out in the main body of water. All methods will require a guide frame to control the alignment of the individual sheet piles. Driving can be by gravity hammer, vibrating hammer or hydraulic hammer. Fig. 4.6 shows equipment used for driving concrete sheet piling, in this case, barge-mounted.



**Figure 4.6** Specialised barge-mounted piling rig for inclined MV piles.
Courtesy: Stefanutti Stocks Marine, South Africa.

### 4.3.2 Jetties and Wharves

Jetties are typically constructed by three main methods.

The first and usually the most cost-effective is by means of 'overhand' construction, where the partially completed structure is used to support the construction equipment, usually a crawler crane, as work progresses forward and the structure is completed behind. Working from the shore, the crane drives a 'bent' (or transverse row) of piles onto which a capping beam is cast. Then, temporary support is placed from the shore to the capping beam, which allows the crane to travel forward to drive the next bent of piles and so on, the structure being completed behind the crane. See Figs 4.7 and 4.8 for a typical example of overhand construction.

The second method is construction from a temporary staging, parallel to the permanent structure. The temporary staging would normally be a timber or light steel structure designed for the loads of the construction equipment and is used solely for construction equipment and access. This method would normally be used only to cater for a specific requirement such as where the final structure would not be able to carry

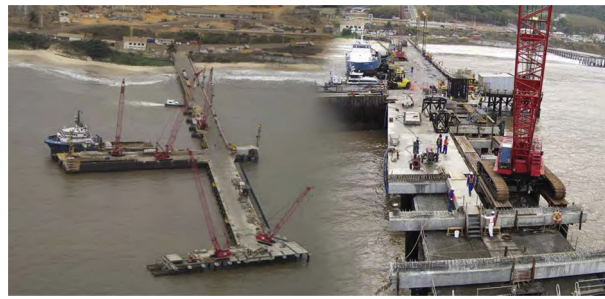


**Figure 4.7** Hand-over-hand precast and in situ jetty construction.
Courtesy: Stefanutti Stocks Marine, South Africa.



**Figure 4.8** Hand-over-hand precast and in situ jetty construction.
Courtesy: Stefanutti Stocks Marine, South Africa.

the construction equipment or where there is availability of specialised equipment or temporary works materials.

The third method involves construction from floating equipment or a jack-up barge. This is not normally the most cost-effective method, but it may be appropriate in certain circumstances, for instance, where there is limited land access.

Wharves may be constructed by any of these methods, or combinations of methods, that are used for jetties.

### 4.3.3 Breakwaters

Breakwaters generally serve to break the energy of incoming waves to an extent acceptable to vessels berthed or moored inside the shelter of the breakwater. Designs typically utilise either locally or externally sourced quarried rock, and depending on the suitability of rock, a precast option of one of the many 'off-the-shelf' precast units may be used for armour to minimise the cost of transport and manufacture of concrete. Generally, a local quarry will be sourced and the design adapted to cater for the rock that can be quarried in terms of size, shape, fracturing and density (among other factors). The outer layer of armour is the critical element when determining the construction methodology since it represent the maximum size and weight of material to be placed.

Construction methodology is therefore highly dependent on the weight and shape of the armour units utilised as primary protection on the outer faces of the breakwater. The methodology is also primarily a materials-handling exercise and therefore is very plant intensive (see, eg, Fig. 4.10). Consequently, the various criteria utilised in the design and required for construction should be made available to the contractor at an early stage so as to enable to the determination of the best construction methodology. These criteria will be based upon data on the bathymetry, hydrography, geotechnical, wave and wind conditions, and general weather.

Considering as a typical example the breakwater cross-section shown in Fig. 4.9, the general methodology would then be as follows:

- Preparation of the sea bed for the placement of the core of the breakwater
  - This can be done utilising one or a combination of the following:
    - A trailing suction hopper for removal of large volumes of soft material.
    - A floating crane with a grab system for loose, rocky materials.
    - A long-reach excavator working at the front of an advancing breakwater core (the core being placed by back-tipping from tipper trucks or placed by crane in individual skip loads).

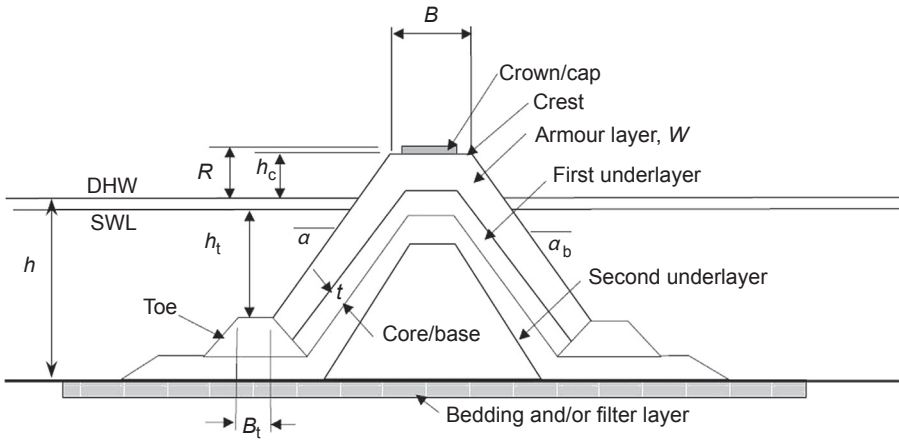



**Figure 4.9** Typical breakwater cross-section. Note: core is generally small-size, rubble-type material, underlayers being heavier, with the armour layer being the protective heaviest layer, often plain precast concrete units, for wave protection. The cap is to prevent underlayer erosion and provide a means of access for maintenance and other reasons.
Courtesy: Simon Allen.



**Figure 4.10** Illustration showing plant-intensive breakwater reconstruction utilising crawler cranes, excavators, loaders and trucks.
Courtesy: Stefanutti Stocks Marine, South Africa.




**Figure 4.11** Photo showing precast 20-ton Toskane units stacked in precast yard ready for transport and placement.
Courtesy: Stefanutti Stocks Marine, South Africa.

The preparation of the sea bed must also encompass any material removal to construct the toe of the breakwater (which in some designs can be placed with the core layer), plus the placement of any filter or bedding material as required by the design.

- The placement of further underlayers on top of the core base according to the core placement method, again realising that losses can occur during times of storm
- Placement of the armour units
  - The precast yard should be located as close to the placement site as possible to minimise transport and have sufficient stacking area; see Fig. 4.11.
  - Large precast armour units are placed by crane usually from atop the preconstructed core and underlayers.
  - Armour should be placed according to a predetermined grid system and the position of each unit noted via a GPS which is linked to the crane hook. A crane hook and ball survey will verify the placement of armour units to the drawings, taking cross-sections usually at 5-m intervals across the breakwater.
  - Special care needs to be taken when placing heavy precast armour units during high swells as the wave/water pressure can add to the weight of the armour unit suspended from the crane; see Fig. 4.12. It is extremely unwise to use the 'in water' (and hence lower) weight of the unit when it is submerged to allow further reach with the placement crane due to swell forces on the unit both near the surface and well below the surface.
- Temporary Works

  Temporary works are invariably a part of construction operations, and these also need to be carefully considered. A typical question that might arise in regard to temporary works is, 'what length of open core construction can be placed during the advancement of construction that is in an unarmoured state?' The core is subject to erosion and wash-away during times of storm or under the action of high-energy waves, and particularly during storm and spring high tide combinations. Account needs to be taken of wave conditions and an assessment of what could be lost in a storm.

  The contract program must make allowance for downtime and reinstatement of the eroded core. Such erosion will happen unless very expensive temporary protection measures (such as sheet piling or advance temporary placement of armour units that are recovered) are taken, so it is pertinent to make allowances. Fig. 4.13 shows temporary works for restoring a damaged breakwater.



**Figure 4.12** Photo showing placement of armour units by 250-ton crawler crane. Courtesy: Stefanutti Stocks Marine, South Africa.



**Figure 4.13** Photo showing temporary works for restoring damaged breakwater construction. Note in particular the temporary armouring with large rocks to allow core construction. Courtesy: Stefanutti Stocks Marine, South Africa.

### *4.3.4 Dry docks and ship lifts*

Dry-dock construction in most instances would be carried out behind a cofferdam, and the area dewatered. Construction would then proceed using normal concrete construction methods, similar to constructing a deep basement for a large building. The floor may require permanent tension piles to prevent uplift from high external water pressure, when the dry-dock is pumped dry to work on vessels.

Ship lifts are purpose-designed mechanical structures, supported off either piled concrete structures or concrete walls or a combination of piles and concrete walls. Construction is carried out by the types of construction described earlier for jetties or concrete block walls.




**Figure 4.14** Typical slipway in Saldanha Bay, West Coast, South Africa. Courtesy: Stefanutti Stocks Marine, South Africa.

### 4.3.5 Boat ramps and slipways

Boat ramps can be one of the most difficult marine concrete structures to construct as, except in very sheltered waters, the effects of waves together with tidal variations must be dealt with. Where conditions permit, it may be possible to construct the boat ramp behind a cofferdam, but it is usual that construction takes place in the wet. It is normal to make as much use of precast concrete sections for the ramp as possible, stitching the sections together with small in situ-joints, which are relatively easy to protect from wash-out of the wet concrete.

Slipways usually consist of a boat cradle on rails, which is pulled out of the water by a winch at the top of the slipway; see Fig. 4.14. Slipways above water level are usually constructed in a similar method to boat ramps, with wide paved working areas. Below water level, it is only the rail that has to be supported and tied together. It is normal to support the rail on precast rail beams, which are then supported in turn on piles or concrete footings, depending on the underwater ground profile. The precast beams are then stitched together with small in-situ joints as mentioned earlier. (Chapter 14 also deals with marine structures such as boat ramps and slipways).

## 4.4 Particular aspects of underwater concrete construction

Casting concrete underwater is often approached nervously by inexperienced persons, but concreting underwater is actually the perfect medium in which to cast concrete. Probably the single biggest risk in casting concrete on land is proper curing of the concrete. Underwater, the concrete cures perfectly, with no loss of water.

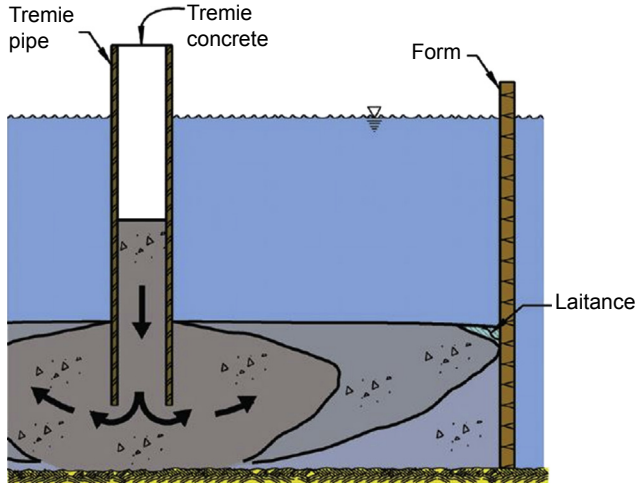



**Figure 4.15** Typical depiction of tremie concrete.
Courtesy: unsigned Internet.

There are two fundamental principles for casting in situ concrete underwater: the first is that the delivery end of the tremie pipe or pipe from the concrete pump is always kept submerged in the plastic concrete, keeping the shaft full of concrete and ensuring as uniform a flow as possible (see Fig. 4.15), and the second is that wash-out of fine material in the concrete must be prevented.

Keeping the end of the delivery pipe submerged in the concrete is a relatively easy task; conversely, it can just as easily be executed incorrectly due to factors such as lack of attention, low visibility underwater, heavy seas, etc. The tremie pipe is usually marked in metre increments from the toe, and the level of the concrete is dipped from water level with a weighted tape. It is then simple arithmetic to calculate the depth of the tremie in the concrete, but during a long concrete pour, attention has been known to wander!

Preventing wash-out of fine material is only necessary where working in the surf zone or where there are strong currents. To prevent wash-out, the shutter must be water-tight, and the top of the concrete must be covered with a water-tight cover, after concreting, or a sacrificial layer of concrete can be used, where applicable.

There are several proprietary concrete admixtures for preventing wash-out in concrete, but in the authors' experience, these tend to extend the setting time of the concrete, leaving the concrete at risk of wash-out for a longer period, thus to some degree defeating the purpose of the admixture! Therefore, an effective way of preventing wash-out is to use a concrete accelerating admixture and make the shutter water-tight.

It is not common to use any compaction equipment on underwater concrete as the flowability and slump required for tremie concrete or pumped concrete should be sufficient for self-compaction, generally around 130-mm slump or more depending on temperature, discharge length and time. However, the concrete mix should be carefully

designed and assessed prior to its use in the underwater construction, and constant checks need to be made during the operation that the concrete is of the correct consistency.

## 4.5 Marine construction specifications

Chapter 3 deals with the subject of specifications for marine concrete, but a note here on the particular aspects of specification from the construction perspective is appropriate. Most contract documentation for marine projects in South Africa is bespoke (or project-based) specification, and it includes specifications from general practice (such as SABS, British Standards, Eurocodes, ASTM, ACI standards, etc.), along with custom-written specifications for particular aspects, such as materials, most notably concrete mixes, breakwater materials, corrosion protection of steelwork and the like.

While there is a good deal of commonality between marine construction and general construction specifications, some of the factors to be aware of with particular reference to marine construction specifications are outlined next.

Generally, specifications must not preclude any specific methodology that a contractor may wish to use in the tender, barring the obvious limitations of and possible effects on safety, quality, efficiency and price. Consequently, performance-based specifications are generally favoured. Specific aspects to be considered are given next.

### *4.5.1 Tolerances*

In a dynamic environment, such as the sea, it is impractical to apply tolerances that are generally acceptable in other types of construction. Enforcing 'tight' tolerances will only result in the contractor inflating the price to achieve these tolerances which could be unnecessary.

For instance, consider the following examples:

- Dredging tolerances are generally zero in upper height limit and up to 500 mm lower tolerance.
- Stone beds for supporting concrete structures have to allow for settlement and are generally therefore very specific to the particular project.
- Placement of core and armour layers of breakwaters is very difficult to position within strict tolerances due to the shape of these elements, and so a 'general' profile has to be adopted with relevant tolerances.
- Construction of piles can be fairly generous if the concrete (precast or in situ) has sufficient built-in tolerance to allow for pile deviations (caused by obstructions etc.).

### *4.5.2 Materials*

It is always best to design with the locally available materials. However, in some instances, this may not be possible; in fact, one of the authors is witness to a contract in Angola where concrete stone was imported from Canada, thousands of kilometres across the Atlantic!

## 4.6 Future challenges and opportunities

While the general and practical on-site traditions in constructing marine concrete structures have not changed very much over the last, say, 50 years or so, in the future, environmental challenges will to some extent dictate how we develop and deliver our structures. 'Green' renewable energy can be obtained from, for example, quay walls and breakwaters, using subsidiary arrangements to convert the wave energy. Energy from offshore wind farms is already well established, but it is worth noting that these require significant founding in aggressive environments. See further in the next section.

Although there is advanced technology and modelling available to predict, say, longshore transport, there will be increasing pressure from the environmental lobbying groups to reduce and even restrict development adjacent to the oceans.

As engineers, it is our responsibility to ensure that we deliver an increasingly environmentally friendly product, and herein lies the possibilities and challenges for today's marine civil engineering community.

### *4.6.1 Renewable energy*

Renewable energy using the sea has not been particularly successful in the past due to the high capital cost of installing wind vanes or wave generators in the sea. These installations require large massive underwater structures to secure them, and hence the plant required to produce these foundations is expensive to both mobilise and run.

Oscillating water columns inside breakwaters that are especially designed and constructed to incorporate these 'pipes', can take advantage of the rising and falling column of water with every wave.

### *4.6.2 Monitoring technology*

Marine structures are regularly exposed to corrosive sea salts in an aggressive environment, where tidal wetting and drying cycles lead to accelerated chloride ingress and the corrosion of the reinforcing steel. (These aspects are well covered elsewhere in this book; see Chapters 5 and 6 in particular.) The visible damage caused by chloride-induced corrosion is in the form of rusting and spalling, which can affect the lifespan and durability of the structure.

Traditionally, visual inspections have been relied on to identify such deterioration, and in some cases, diver surveys (often with video reporting) have also been used to monitor the 'health' of a marine concrete structure. However, this technology is undergoing rapid change, with specialised companies that can offer initial structural assessment and testing to establish the level of corrosion protection required to increase durability and service life. Ultimately, bespoke corrosion protection solutions are offered which may incorporate embedded sacrificial galvanic anodes or impressed current systems that can be remotely monitored.



**Figure 4.16** Typical 3D model extract.
Courtesy: Stefanutti Stocks Marine, South Africa.

### 4.6.3 Computer modelling and software

Increasingly, potential clients are looking for not just 'one-stop-shop' solutions from contractors, but also for assistance in providing nontechnical team members a means of understanding the technology and methodologies used to ensure full understanding of a project.

Newer technology in this area involves 3D models (which can now be fairly easily printed), and 3D animation (where a library is built up and can be used to simulate a project build). It also includes building information management which uses up to 5D technology that integrates modelling, design, construction, program scheduling and cost in one simulation; this enables efficient evaluation of changes to any one facet of the project. Although relatively new, it is believed that this technology will rapidly become the standard for not only reporting on projects, but also for assessing any major changes to a project. See Fig. 4.16.

## Sources of further information and advice

In this age of information technology overload, the Internet presents an ever-increasing library of information on any subject, and marine construction is no different. Thus, the interested reader can undertake searchable international online content.

However, first-hand practical advice should also be sought, and for this people with the requisite experience should be sought out.

Two sources that can be mentioned for more general and international information on concrete and marine structures are:

- Dupray, S., Knights, J., Robertshaw, G., Simm, J., Wimpenny, D., Ballard, B.W., 2010. The Use of Concrete in Maritime Engineering – A Guide to Good Practice. CIRIA, London.
- PIANC, 2015. The World Association for Waterborne Transport Infrastructure. Available from: http://www.pianc.org/.

For early contractor involvement (ECI), see:

- https://www.porttechnology.org/technical_papers/early_contractor_involvement_in_infrastructure_projects/ or https://www.gov.uk/…/Early_contractor_involvement__ECI__guidance__… www.hs2.org.uk

In South Africa, as in other parts of the world, there are very few dedicated marine construction contractors as the work load is sporadic at best. Generally, contractors have to market themselves as multidisciplinary companies to sustain order books.

That said, in Southern Africa, the following sources are useful:

- The South African Institution of Civil Engineering (SAICE) has a good library where books can be sourced; see http://saice.org.za/services/saice-topical-publications
- The Engineering Council of South Africa (ECSA) can be approached to find professionals with experience and expertise in marine construction, and one could also look for a mentor in this field; see https://www.ecsa.co.za/SitePages/Mentor%20Search.aspx
- The South African Federation of Civil Engineering Contractors (SAFCEC) is the organisational body representing civil engineering contractors, and a search via nature of work would reveal current contractors in the field: http://www.safcec.org.za/search/custom.asp?id=2363
- The Concrete Society of Southern Africa has an annual source book that lists various categories of services; see http://www.concretesociety.co.za/source-book-online

There are also various publications where articles on marine construction projects and methodology can be found such as:

- The Construction World magazine at http://crown.co.za/construction-world
- The Civil Engineering Contractor Magazine at http://brookepattrick.co.za/products/the-civil-engineering-contractor
- The SAICE magazine at http://saice.org.za/services/civil-engineering-magazine

# Deterioration of concrete in the marine environment

5

*M. Santhanam* [1], *M. Otieno* [2]
[1]Indian Institute of Technology Madras, Chennai, India; [2]University of the Witwatersrand, Johannesburg, South Africa

## 5.1 Introduction

The marine exposure condition presents a challenging environment for concrete as a material. The long-term performance of concrete in such an environment is dependent on a complex interplay of physical and chemical mechanisms which are mainly aggressive to concrete. Regarding reinforced concrete in particular, chloride ingress by diffusion is probably the most important mechanism of deterioration, leading to corrosion of the embedded reinforcing steel. However, the overall situation is complicated by concomitant deterioration of the material itself by sulphate attack and physical effects such as salt crystallisation and mechanical action of the waves. It is imperative to understand the mechanisms to suitably design concrete structures for such environments.

It is well known that the durability of concrete in any service environment is primarily controlled by the permeability characteristics of concrete, or more generally the penetrability of the concrete. The ingress of aggressive chemicals from the external environment also occurs through the interconnected pores of concrete. The key to obtaining a durable concrete system is therefore to use a low w/c, along with the use of supplementary cementitious materials, particularly slag and silica fume, which have been shown to perform in an excellent manner in marine conditions.

This chapter first considers the different kinds of exposure in the marine environment. This is followed by a description of the chemical reactions possible in cementitious systems in a marine environment. Additionally, the mechanisms of physical deterioration are presented. The performance of different types of cementitious binders in marine environments is reviewed briefly, and steel corrosion characteristics are also presented. The chapter closes with a discussion of future challenges.

## 5.2 The marine environment

### *5.2.1 Transport processes in the marine environment*

The major transport processes in the marine environment are captured in the schematic diagram based on BS 6349-1 (Fig. 5.1). Presented subsequently is a brief description of the prevailing transport phenomena. While the mathematical expressions for these mechanisms are well established, they tend to describe ‘ideal’ situations, which typically

**Marine Concrete Structures.** http://dx.doi.org/10.1016/B978-0-08-100081-6.00005-2
Copyright © 2016 Elsevier Ltd. All rights reserved.

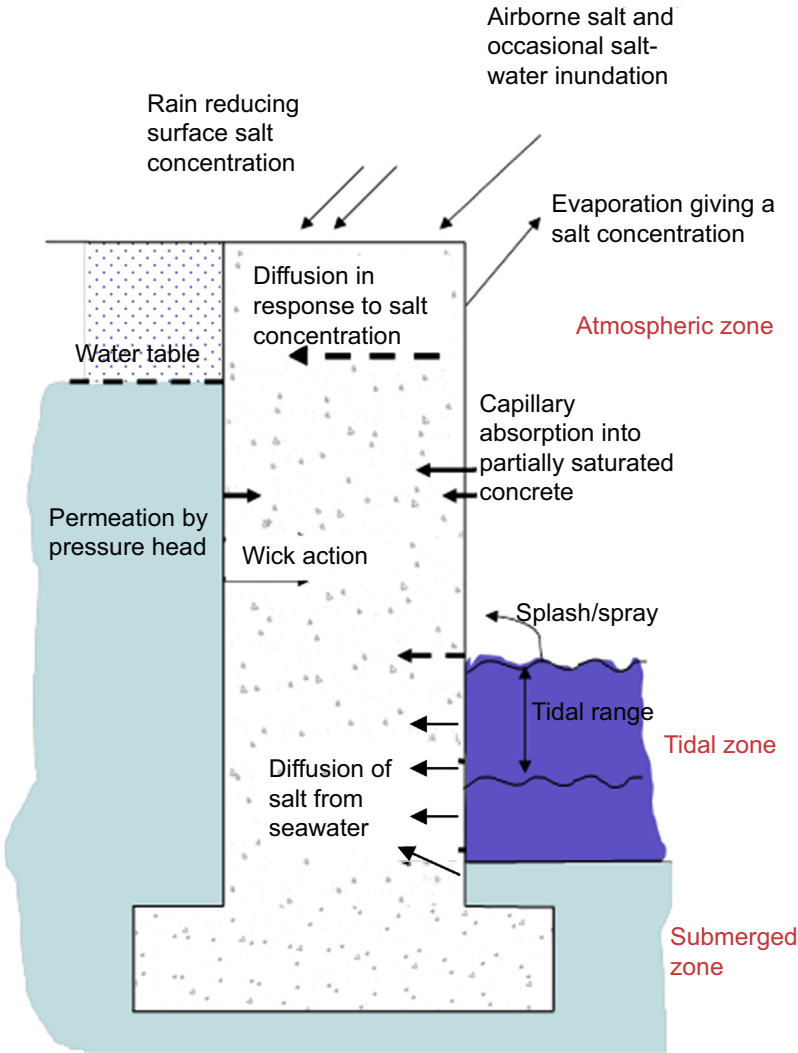



**Figure 5.1** Different exposure conditions in the marine environment.
Based on BS 6349-1, 2000. Maritime Structures – Part 1: Code of Practice for General Criteria. British Standards, London.

do not occur in practice. Thus, it is difficult to predict the actual behaviour in a real situation, and a measure of local experience or empiricism is usually needed.

- Absorption: This refers to the bulk uptake of water into a porous material such as concrete. It generally occurs in unsaturated or partially saturated concrete subjected to complete or partial immersion. This parameter is easy to measure but not accurate in the sense that it is difficult to penetrate all pores of concrete, and therefore a 'true' measure of porosity cannot be obtained (vacuum saturation can be attempted to get a better result). In any case, since the

bulk of the available capillary porosity is penetrated, the measured absorption does actually give a good indication of the durability.

- Capillary suction (sorption): This refers to the intake of water due to capillary action, typically unidirectionally. This represents situations where the concrete is in contact with water on only one surface (such as a slab on grade in contact with ground water below, or a marine quay wall in contact with water on one face only). The sorptivity test is a good representation of capillary uptake of water, and it is also reproducible.
- Permeation: This mechanism operates in the classic permeability situation, where saturated liquid transfer controlled by a pressure gradient occurs across the concrete. After the attainment of steady-state conditions, Darcy's law may be applied:

$$Q = \frac{KA\Delta P}{L} \qquad [5.1]$$

where $Q$ is the volume of liquid flowing ($m^3$); $K$ is the coefficient of permeability ($m^2$); $A$ is the permeated area ($m^2$); $\Delta P$ is the pressure differential across the specimen ($N/m^2$) and $L$ is the thickness of penetrated section (m).

Intrinsic permeability can also be derived as shown:

$$D = \frac{\eta K}{\rho g} \qquad [5.2]$$

where $D$ is the intrinsic permeability ($m^2$); $\eta$ is the viscosity of the permeating liquid ($Ns/m^2$); $\rho$ is the density of water (or the permeating solution) and $g$ is the acceleration due to gravity ($m/s^2$).

Ionic species dissolved in water also can move by permeation of water. Permeation is higher when cracks and defects are present in the concrete.

- Ionic diffusion: This is the movement of ionic species dissolved in water, driven by a concentration gradient, that is, movement of ionic species from higher concentration zones to lower concentration zones. As it governs the transport of chlorides, it is possibly the most important transport phenomenon.
- Migration: This refers to ionic (specifically chloride) transport driven by difference in electrical potential, typically during accelerated testing of chloride transport; chlorides tend to move toward the zones with more positive electrical potential. However, in real service conditions, migration may not occur in most cases.
- Convection: This describes the transport of a solute (eg, chloride or sulphate ions in water) as a result of bulk moving water (Boddy et al., 1999). It thus results typically in ionic transport driven by a difference in moisture content, such as in drying fronts, or in repeated wetting and drying conditions. Together with diffusion, it is the main transport mechanism for chloride ingress in cracked concrete (Paulsson and Johan, 2002).

### 5.2.2 Marine exposure zones

After the understanding of transport mechanisms, it is very important to establish a proper understanding of what constitutes the marine environment. While a direct interpretation of the term would apply to structures that are directly in contact with marine

conditions, there are also other possibilities such as structures that are sufficiently close to the marine conditions as to be affected by seawater spray or airborne aerosols. In the latter case, this could imply 'marine conditions' occurring a considerable distance inland from the direct marine zone.

There are three main possible exposure conditions for a reinforced concrete structure in a marine environment. They are (1) the atmospheric zone, (2) the tidal zone or splash zone and (3) the submerged zone (Fig. 5.1).

In the case of the atmospheric zone, the structure is exposed to airborne chlorides. Thus, chloride-induced corrosion of steel can be a deterioration mechanism in this zone. Further, the structure can be subjected to carbonation-induced corrosion depending on other factors such as relative humidity or temperature. However, compared to carbonation-induced corrosion, chloride-induced corrosion will be the major deterioration mechanism. With regard to the transport mechanisms, both gaseous as well as water vapour diffusion can take place in this exposure condition. In addition to diffusion, sorption is another prevailing transport mechanism as alternate wetting and drying can occur due to rain. Further, physical degradation of the structure can occur due to salt crystallisation.

Concrete exposed to the splash or tidal zone is usually regarded as being in the worst deterioration condition of all the exposure categories. All the mechanisms such as diffusion, sorption, wick action and permeation perform significant roles in the transport of aggressive species in this zone. Moreover, mechanical action of waves can lead to physical deterioration such as abrasion and erosion, and drying cycles can lead to salt crystallisation.

Regarding concrete fully immersed in the sea, there is no effect of sorption, but on the other hand, effect of permeation will be more. In addition, diffusion will also play a major role. Thus, impermeability will be more crucial than strength. Concrete can deteriorate because of chemical deterioration processes such as sulphate attack or leaching and due to chloride-induced corrosion.

While there is unanimity among practitioners the world over with respect to the dangers to concrete structures posed by the marine environment, the international guidelines on exposure classifications for concrete in such conditions have significant differences. A comparison of the different classification systems from some of the international codes is presented in Appendix 1. A major point of difference is the definition of the coastal environment. While most codes seem to give a general description, the Australian code AS3600 (2009) gives very clear guidelines regarding the distance from the coast that needs to be considered to apply the prescriptions for coastal environment. Further, the AS3600 is the only code that gives a detailed description of the splash/tidal zone. There are also other differences in terms of permissible chloride contents in the concrete and in the specification of the cover.

## 5.3 Chemical mechanisms of concrete deterioration

While it is clear that the performance of concrete in seawater depends on an interplay of physical and chemical mechanisms, it is important to understand each of these

**Table 5.1 Composition of seawater from around the world**

| Major ions | Concentration (g/l) | | | | | |
|---|---|---|---|---|---|---|
| | Mediterranean Sea | North Sea | Atlantic Ocean | Baltic Sea | Arabian Gulf | Red Sea |
| $Na^+$ | 12.400 | 12.200 | 11.100 | 2.190 | 20.700 | 11.350 |
| $Mg^{2+}$ | 1.500 | 1.110 | 1.210 | 0.260 | 2.300 | 1.867 |
| $Cl^-$ | 21.270 | 16.550 | 20.000 | 3.960 | 36.900 | 22.660 |
| $SO_3^-$ | 2.596 | 2.220 | 2.180 | 0.580 | 5.120 | 3.050 |
| TDS[a] | 38.795 | 33.060 | 35.370 | 7.110 | 66.650 | 40.960 |

[a]Total dissolved solids.
Based on Biczok, I., 1967. Concrete Corrosion Concrete Protection. Chemical Publishing Company Inc., NY; and Mehta, P.K., 1999. Sulfate attack in marine environment. In: Marchand, J., Skalny, J. (Ed.), Materials Science of Concrete Special Volume: Sulfate Attack Mechanisms. The American Ceramic Society, Westerville, OH, pp. 295–300.

separately. In this section, the chemical mechanisms are discussed, while the physical mechanisms are described in the subsequent section.

On an average, seawater contains about 35 g/l of dissolved salts. However, this is variable, and it depends on specific geographic locations. Table 5.1 presents a range of compositions for seawater from different sources (Biczok, 1967; Mehta, 1999). It is clear from the data that the chloride ions are predominant. The sulphates are typically contributed by $MgSO_4$. The severity of deterioration ultimately depends upon the combination of various effects in an environment. Although the chloride and sulphate concentrations are both highest in the case of the Arabian Gulf, the Northern Atlantic marine environment is affected by the freezing conditions in this region.

The chemical reactions with concrete that are brought about by seawater can lead to the creation of several altered phases, as shown in Table 5.2. The first stage of the attack is the reaction of seawater with calcium hydroxide, which can lead to the formation of a double layer of gypsum and brucite. Further, the dissolved $CO_2$ concentration of the seawater can also cause a stable layer of aragonite to be deposited on the top

**Table 5.2 Original and altered phases in cementitious composites exposed to seawater**

| Original phases | Altered phases |
|---|---|
| Calcium hydroxide | Gypsum; brucite; aragonite |
| Calcium silicate hydrate (CSH) | Decalcified CSH; in some cases, magnesium silicate hydrate (MSH); thaumasite |
| Calcium aluminate hydrate and AFm | Friedel's salt; ettringite |

surface of the concrete. The formation of a surface layer of aragonite and brucite is reported by several researchers (De Weerdt et al., 2014). Sometimes, the surface layers can act as temporary barriers that can prevent further easy ingress of the seawater. However, in due course, due to other reactions taking place in the system as well as the mechanical action (erosion) of the seawater, the protective layer degrades, and the reaction front can further penetrate the concrete layers underneath.

Gypsum formed in this reaction can combine with the calcium (sulfo-) aluminates in the system and lead to the formation of ettringite. However, the ettringite formed in chloride-rich conditions may not be expansive (Mehta, 1991), which is an ameliorating factor in seawater attack of concrete. Further, the reduced availability of calcium aluminates, as a result of chloride binding to produce Friedel's salt or similar compounds (Verbeck, 1975), is expected to further reduce the extent of ettringite formation. While compounds like Friedel's salt are known to be nonexpansive, there is a danger of forming hydroxychlorides at very high chloride concentrations (such as in desalination outfall tunnels), which may lead to cracking in the concrete (Galan et al., 2015).

Several researchers have confirmed the microstructural alterations in cementitious phases attacked by solutions of combined chloride and sulphates (Brown and Badger, 2000; Brown and Doerr, 2000; Santhanam et al., 2006; De Weerdt et al., 2014). The relative distribution of the different phases in the concrete varies. While ettringite and gypsum are found closer to the top surfaces of concrete, Friedel's salt exists more in the interior zones (Brown and Badger, 2000). Another common feature that is noticed in the advanced stages of attack is the decalcification of calcium silicate hydrate (CSH) and conversion to noncementitious M-S-H (Santhanam et al., 2006). Kurdowski (2004) studied the attack of a simulated seawater solution on C-S-H paste, and determined that the diffusion of $Cl^-$ was much faster than for $Mg^{2+}$. C-S-H was seen to become quickly decalcified in strong chloride solutions (such as seawater), and formation of M-S-H was also observed. The formation of a surface layer of brucite and basic magnesium chloride was reported. Under the surface skin, the paste contained phases such as Friedel's salt.

Additionally, when limestone-ordinary Portland cement (OPC) binders are used, there are possibilities of thaumasite formation (Sibbick et al., 2003). At this stage, the integrity of the matrix is compromised, and a major loss in strength is registered.

Lea (1970) opines that the solubility of calcium hydroxide is high in seawater compared to plain water. This is another reason for the predominant brucite and aragonite deposits on the concrete surface in such conditions (Thomas et al., 1999). This insoluble layer of aragonite serves as an additional barrier (it also has a hardness greater than brucite). The major gap that exists in the understanding is the quantification of time required for these layers to get removed from the surface leading to rapid rates of attack.

While permeation and sorption are very likely transport processes in a marine environment, the transport of chlorides into the concrete by diffusion needs to be given special consideration because of the resultant corrosion of the reinforcing steel, which is the most debilitating feature for the reinforced concrete (RC) structures. The severity of chemical attack from sulphates and carbon dioxide further exacerbate the conditions leading to quicker depassivation of steel and subsequent corrosion.

The diffusion of chlorides into concrete is generally modelled as a nonsteady-state phenomenon, using Fick's second law. While the chloride profiles, or the change in chloride concentration with the depth of concrete, are well defined in the case of simulated exposures in laboratory conditions, the chemical alterations of the surface zone of concrete brought about by the action of sulphate and carbon dioxide lead to errors in deriving solutions to the chloride profile using the error function. Further, there may be a buildup of the chloride concentration at the surface because of other effects in the splash/tidal zones. An example of the differences in the chloride profiles in the different zones of a concrete column is presented in Fig. 5.2.

Sulphate-resisting cements (low $C_3A$ type) could be less beneficial than expected in protecting the concrete, as $C_3A$ has the capability of binding the chlorides into nonexpansive products such as Friedel's salt.

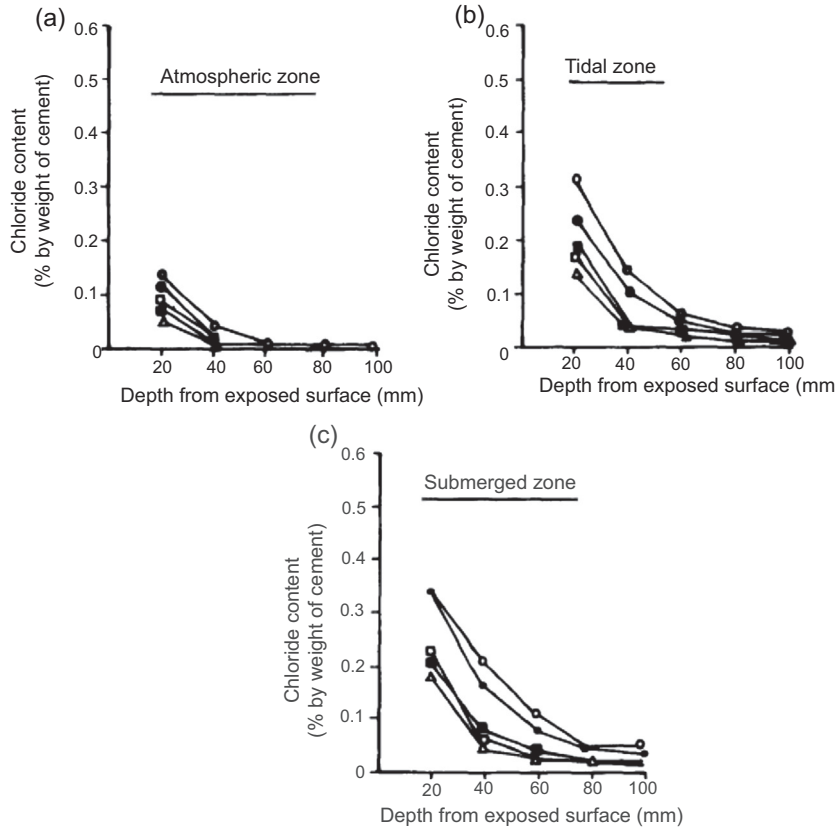



**Figure 5.2** Differences in the chloride profiles obtained for the different zones.
From Roy, S.K., Chye, L.K., Northwood, D.O., 1993. Chloride ingress in concrete as measured by field exposure depths in the atmospheric, tidal and submerged zones of a tropical marine environment. Cement and Concrete Research 23, 1289−1306.

## 5.4 Physical mechanisms of deterioration

The formation of phases such as gypsum and ettringite lead to a lowering of the quality of the concrete surface zone. The overall effect of the chemical attack is a progressive reduction in the integrity of the concrete. In other words, the surface concrete gets weaker and more prone to erosion by the splashing action of the waves. In this manner, the chemical and physical mechanisms act together to cause deterioration.

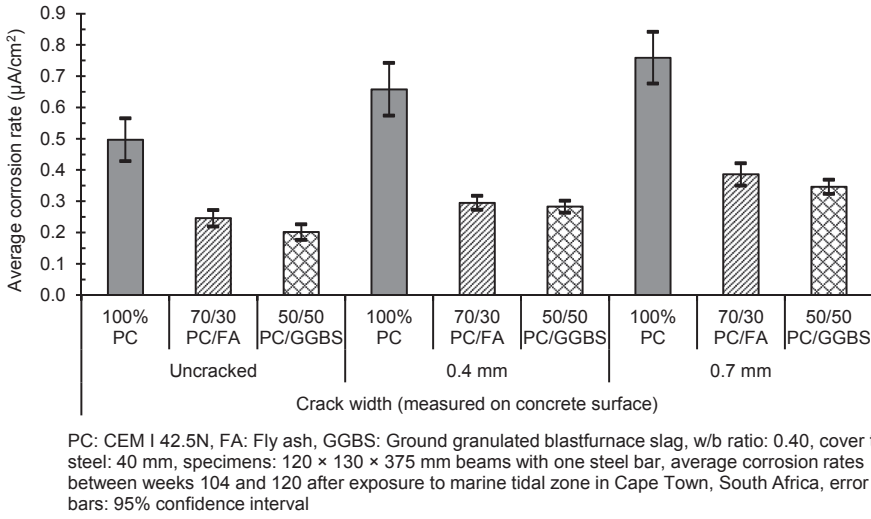
As shown in Fig. 5.1, the wick action created by drying, in addition to the drying and wetting phenomena caused by the tidal action, creates abnormally high chemical concentrations at the concrete surface in this zone. After the salt is deposited on the concrete, there is subsequent evaporation of the water, and the resultant nucleation and growth of the salt crystals can lead to expansive pressures in the surface pores of the concrete (Scherer, 2004). The extent of damage created on the surface depends on the available porosity, the supersaturation of the salt and the existence of repulsive force between the salt and the pore surface (Scherer, 2004).

Salt weathering is greater in horizontal or inclined surfaces (Neville, 2013), as well as in conditions where there are prolonged drying spells. Neville (2013) also suggests that the dissolution by dew of airborne salts that get deposited on the concrete, and subsequent evaporation, can also cause salt weathering damage.

## 5.5 Steel corrosion in the marine environment

As already mentioned in previous sections, chloride-induced steel corrosion is the major form of deterioration in reinforced and prestressed RC structures. It is caused by ingress of chlorides into concrete mainly by diffusion, although convection and permeation can also occur. Before chloride-induced corrosion of steel can initiate, a critical concentration of chlorides, commonly referred to as chloride threshold, is required at the steel level to destroy the passive thin protective film coating on the steel surface. Chloride threshold can be presented as either free (water soluble) chlorides, total (acid soluble) chlorides or $[Cl^-]/[OH^-]$ ratio. However, presentation as total chlorides is the most commonly used approach, and it is generally taken to be 0.4% by mass of cement, although recent studies have shown that it varies from cement to cement and is affected by various factors including temperature (Angst et al., 2009).

Penetrability of concrete is considered the most important concrete parameter that affects both the time to corrosion initiation and its propagation, although other factors such as cover depth are equally important. Consequently, any factors that affect concrete penetrability such as w/b ratio, binder type, curing and compaction have an indirect influence on steel corrosion. Furthermore, phenomena that affect the condition of the concrete prior to or after corrosion initiation will have an effect on corrosion. One such phenomenon is cracking of the concrete cover, which has been shown to have a significant effect on the penetrability of concrete and, consequently, both corrosion initiation and its propagation (Miyagawa, 1985; Suzuki et al., 1990; Pettersson and Jorgensen, 1996; Raupach, 1996; Scott and Alexander, 2007; Otieno et al., 2010). Some results obtained by Otieno (2014) are shown in Fig. 5.3. For marine




PC: CEM I 42.5N, FA: Fly ash, GGBS: Ground granulated blastfurnace slag, w/b ratio: 0.40, cover to steel: 40 mm, specimens: 120 × 130 × 375 mm beams with one steel bar, average corrosion rates between weeks 104 and 120 after exposure to marine tidal zone in Cape Town, South Africa, error bars: 95% confidence interval

**Figure 5.3** Effect of cover cracking on corrosion rate.
From Otieno, M., 2014. The Development of Empirical Chloride-Induced Corrosion Rate Prediction Models for Cracked and Uncracked Steel Reinforced Concrete Structures in the Marine Tidal Zone (Ph.D. thesis). Department of Civil Engineering, University of Cape Town.

RC structures, cracking of the concrete cover can be caused by a variety of chemical deterioration mechanisms including salt crystallisation, freeze−thaw cycles, ettringite formation and sulphate attack (see Table 5.2).

Corrosion of steel has been reported to progress at different rates in the tidal, splash/spray and airborne marine environments, with very little corrosion activity being reported in the submerged zone. Furthermore, the tidal zone is usually considered to be the most aggressive due to the wetting and drying cycles by the seawater. However, as will be seen in Chapter 'Marine exposure environments and marine exposure sites', the aggressiveness of a marine exposure zone should be characterised taking into account other factors including climatic conditions, spatial variability and frequency of the high and low tides.

## 5.6 Future challenges

The prediction of deterioration in marine concrete structures is a major challenge that will still require much research input. A typical example is the prediction of combined transport and deterioration mechanisms in both cracked and uncracked concretes. With respect to cracked concrete, much more effort will be needed to first understand the fundamental transport processes in these concretes. A further challenge that both engineers and researchers will continue to face is the need to constantly assess the suitability of new cements to meeting the increasingly demanding durability requirements

## Appendix 1 Comparison of major durability requirements from different codes pertaining to the marine environment

| | IS 456-2000 | ACI 318 M-08 | EN 206-1 2000 | BS 8500-2006 (50 years design life) | BS 8500-2006 (100 years design life) | AS 3600 2009 |
|---|---|---|---|---|---|---|
| Environmental classifications | Mild, moderate, severe, very severe and extreme | Corrosion protection of reinforcement: C0, C1 and C2 | No risk of corrosion or attack: X0<br>Corrosion induced by chlorides from seawater: XS1, XS2 and XS3 | No risk of corrosion or attack: X0<br>Corrosion induced by chlorides from seawater: XS1, XS2 and XS3 | No risk of corrosion or attack: X0<br>Corrosion induced by chlorides from seawater: XS1, XS2 and XS3 | A1, A2, B1, B2, C1, C2 and U |
| Design/ anticipated life (in years) | Not specified | Not specified | 50 years | 50 years | 100 years | 50 years $\pm$ 20% (40−60 years) |
| Definition of coastal zones | Not specified | Not specified | Not specified | Not specified | Not specified | Distance from coast defined in three categories: (1) up to 1 km; (2) beyond 1 km and up to 50 km; (3) beyond 50 km with different exposure classifications |
| Definition of tidal and spray zones | Not specified | Not specified | Not specified | Not specified | Not specified | Tidal/splash zone is the zone 1 m below lowest astronomical tide and up to 1 m above highest astronomical tide on vertical structures and all exposed soffits of horizontal structures over the sea; spray zone is the zone from 1 m above wave crest level |

| | | | | | | |
|---|---|---|---|---|---|---|
| Chlorides in concrete | Based on type/use of concrete maximum total acid soluble chloride content specified varying from 0.4 to 3.0 kg/m$^3$ | Chloride limits for new construction specified varying from 0.06 to 0.2% by mass | Maximum chloride content by mass of cement specified for different classifications ranging from 1 to 0.2% | | | |
| Requirement of concrete cover | Nominal cover to meet durability requirements specified varying from 20 to 75 mm for different exposure conditions; minimum cover of footings to be 50 mm | Cover to meet durability requirements separately proposed for concrete exposed to or protected from earth/weather, separately for precast and cast-in situ concrete | Concrete cover as per EN 1992; cover decided by the structural class (strength grade) of concrete | Concept of $\Delta c$ introduced which is defined as allowance in design for deviation; different compressive strength specified for different exposures with various values of $\Delta c$ | Concept of $\Delta c$ introduced which is defined as allowance in design for deviation; different compressive strength specified for different exposures with various values of $\Delta c$ | Covers specified from 20 to 60 mm based on environmental classification and characteristic strength of concrete |

including extended maintenance-free service life. These challenges will without doubt demand the development of robust tests and flexible testing and design standards to meet these challenges.

## References

Angst, U., Elsener, B., Larsen, C.K., Vennesland, Ø., 2009. Critical chloride content in reinforced concrete − a review. Cement and Concrete Research 39 (12), 1122−1138.

BS 6349-1, 2000. Maritime Structures − Part 1: Code of Practice for General Criteria. British Standards, London.

Biczok, I., 1967. Concrete Corrosion Concrete Protection. Chemical Publishing Company Inc., NY.

Boddy, A., Bentz, E., Thomas, M.D.A., Hooton, R.D., 1999. An overview and sensitivity study of a multi-mechanistic chloride transport model. Cement and Concrete Research 29 (6), 827−837.

Brown, P.W., Badger, S., 2000. The distributions of bound sulfates and chlorides subjected to mixed NaCl, $MgSO_4$, $Na_2SO_4$ attack. Cement and Concrete Research 30, 1535−1542.

Brown, P.W., Doerr, A., 2000. Chemical changes in concrete due to the ingress of aggressive species. Cement and Concrete Research 30, 411−418.

De Weerdt, K., Justnes, H., Geiker, M.R., 2014. Changes in the phase assemblage of concrete exposed to sea water. Cem Concr Compos 47, 53−63.

Galan, I., Perron, L., Glasser, F.P., 2015. Impact of chloride-rich environments on cement paste mineralogy. Cement and Concrete Research 68, 147−183.

Kurdowski, W., 2004. The protective layer and decalcification of C-S-H in the mechanism of chloride corrosion of cement paste. Cement and Concrete Research 34, 1555−1559.

Lea, F.M., 1970. Chemistry of Cement and Concrete. John Wiley & Sons, New York.

Mehta, P.K., 1991. Concrete in the Marine Environment. Elsevier Applied Science, London.

Mehta, P.K., 1999. Sulfate attack in marine environment. In: Marchand, J., Skalny, J. (Eds.), Materials Science of Concrete Special Volume: Sulfate Attack Mechanisms. The American Ceramic Society, Westerville, OH, pp. 295−300.

Miyagawa, T., 1985. Early Chloride Corrosion of Reinforcing Steel in Concrete (Ph.D. thesis). Department of Civil Engineering, University of Kyoto.

Neville, A.M., 2013. Properties of Concrete, 5th Edition. Pearson.

Otieno, M., 2014. The Development of Empirical Chloride-Induced Corrosion Rate Prediction Models for Cracked and Uncracked Steel Reinforced Concrete Structures in the Marine Tidal Zone (Ph.D. thesis). Department of Civil Engineering, University of Cape Town.

Otieno, M.B., Alexander, M.G., Beushausen, H.-D., 2010. Corrosion in cracked and uncracked concrete − influence of crack width, concrete quality and crack re-opening. Magazine of Concrete Research 62 (6), 393−404.

Paulsson, J.T., Johan, S., 2002. Estimation of chloride ingress in uncracked and cracked concrete using measured surface concentrations. ACI Materials Journal 99 (1), 27−36.

Pettersson, K., Jorgensen, O., 1996. The effect of cracks on reinforcement corrosion in high-performance concrete in a marine environment. In: Third ACI/CANMET International Conference on the Performance of Concrete in Marine Environment. St. Andrews, Canada, pp. 185−200.

Raupach, M., 1996. Chloride-induced macrocell corrosion of steel in concrete − theoretical background and practical consequences. Construction and Building Materials 10 (5), 329−338.

Roy, S.K., Chye, L.K., Northwood, D.O., 1993. Chloride ingress in concrete as measured by field exposure depths in the atmospheric, tidal and submerged zones of a tropical marine environment. Cement and Concrete Research 23, 1289−1306.

Santhanam, M., Cohen, M.D., Olek, J., 2006. Differentiating Seawater and Groundwater Sulfate Attack on Portland Cement Mortars. Cement and Concrete Research 36 (12), 2132−2137.

Scherer, G.W., 2004. Stress from crystallization of salt. Cement and Concrete Research 34, 1613−1624.

Sibbick, T., Fenn, D., Crammond, N., 2003. The occurrence of thaumasite as a product of seawater attack. Cem Concr Compos 25 (8), 1059−66.

Scott, A.N., Alexander, M.G., 2007. The influence of binder type, cracking and cover on corrosion rates of steel in chloride-contaminated concrete. Magazine of Concrete Research 59 (7), 495−505.

Suzuki, K., Ohno, Y., Praparntanatorn, S., Tamura, H., 1990. Mechanism of Steel Corrosion in Cracked Concrete. In: Page, C., Treadaway, K., Bramforth, P. (Eds.), Corrosion of Reinforcement in Concrete. Society of Chemical Industry, London, pp. 19−28.

Thomas, M.D.A., Bleszynski, R.F., Scott, C.E., 1999. Sulfate attack in a marine environment. In: Skalny, J., Marchand, J. (Eds.), Material Science of Concrete—Sulfate Attack Mechanisms. American Ceramic Society, Westerville, OH, pp. 301−314.

Verbeck, G.J., 1975. Mechanisms of corrosion of steel in concrete, corrosion of metals in concrete. ACI Publication SP-49, 21−38.

# The durability of concrete for marine construction: materials and properties

6

*M. Thomas*
University of New Brunswick, Fredericton, Canada

## 6.1 Introduction

Marine environments represent some of the most aggressive environments for concrete structures as the conditions can promote a variety of deterioration processes. These include corrosion of embedded steel reinforcement, freeze–thaw and salt scaling damage, abrasion (due to ice and suspended particulate matter) and chemical alteration sometimes leading to softening of the paste due to the action of $Mg^{2+}$, $CO_3^{2-}$ and $SO_4^{2-}$ ions present in the seawater. These processes are discussed in Chapter 5. The severity of the exposure depends on, among other things, the composition of the seawater (eg, salinity), climatic conditions (eg, temperature and number of freeze–thaw cycles), the action of waves and ice, and the marine zone (eg, immersion, tidal, splash or spray zones) to which the concrete is exposed (see Chapter 7).

Concrete can be produced to be durable in even the most aggressive of marine environments, but consideration must be given to the precise conditions of exposure. In other words, the materials and proportions selected for one marine exposure condition may not be the best choice for a different exposure condition. For example, high levels of fly ash and slag produce concrete with a high resistance to chlorides making it suitable for use in tidal and splash zones; however, in sheltered elevated areas of a structure, such as the top of a pier underneath a bridge deck, the high levels of these materials may render the concrete more susceptible to carbonation.

## 6.2 Desirable properties for marine concrete

Marine concretes can be made durable. However, they require certain properties, which are closely related to the exposure conditions and microenvironment of the concrete structure. This section considers desirable properties for marine concrete in terms of some of the important deterioration mechanisms to which the concrete can be subjected.

**Marine Concrete Structures.** http://dx.doi.org/10.1016/B978-0-08-100081-6.00006-4
Copyright © 2016 Elsevier Ltd. All rights reserved.

### 6.2.1 Exposure class and type of structure

Correctly characterising the exposure condition is the first step in determining the appropriate concrete properties required to provide an adequate service life. Most specifications have exposure-classification systems to aid in the design process. For example, EN206:2013 has exposure-class designations to cover environments that are conducive to corrosion induced by carbonation (XC), corrosion (of steel) induced by chlorides from seawater (XS) and freeze/thaw attack (XF) that may be relevant in a marine environment. It is also possible that all three environments may exist for a single structure. In addition, seawater is typically considered to represent a moderate sulphate-exposure condition. If more than one exposure class is relevant, the concrete must be designed to meet the most onerous requirements in terms of materials, proportions and properties.

Seawater typically has a salinity of 3.5% (35 g/L dissolved salt) primarily due to sodium chloride and magnesium sulphate; the concentrations of the major ions are approximately 20,000 mg/L chloride ($Cl^-$); 11,000 mg/L sodium ($Na^+$); 2700 mg/L sulphate ($SO_4^{2-}$) and 1400 mg/L magnesium ($Mg^{2+}$). (Note that salinities can vary in different oceans: see Table 5.1, Chapter 5 in this book.) Small quantities of carbonate ions ($CO_3^{2-}$) are also present, and depending on the $CO_3^{2-}$ concentration, the pH ranges from 7.0 to 8.4. The salinity is obviously lower in estuaries where the seawater mixes with river water, but lower concentrations are also found in some 'open' bodies of seawater such as the Baltic Sea (1.0%). Much higher salt concentrations (>20 or 30%) can be found in salt lakes such as the Dead Sea in the Middle East and the Great Salt Lake in Utah.

The temperature of the seawater also has a significant impact on the severity of exposure. Cold climates introduce the threat of frost attack; however, the risk of damage is not so much related to the temperature extremes as the number of freeze−thaw cycles that are experienced by the concrete. On the other hand, warm climates promote more rapid chloride penetration and corrosion of reinforcement as the rate of both processes increases with temperature.

The nature of the deterioration is not only dependent on the environmental exposure conditions but also on the type of structure and the location of the element within the structure. For example, in massive concrete structures with little or no steel reinforcement, there is no risk of reinforcement corrosion, and the principal deterioration mechanisms will be chemical attack and, in some locations, freeze−thaw deterioration. Steel-reinforced concrete structures have the additional threat of chloride-induced corrosion of the embedded steel. Prestressed concrete, whether pre- or posttensioned, will generally be less prone to steel corrosion due to better crack control compared with conventionally reinforced concrete; however, the consequences of corrosion are usually more catastrophic for prestressed concrete. Even within a single concrete element, the deterioration processes at work may be different. For example, consider a column in the sea carrying a bridge, where four main exposure conditions can be identified:

| | |
|---|---|
| Submerged | Chemical attack (by $Mg^{2+}$, $SO_4^{2-}$ and/or $CO_3^{2-}$) is the main deterioration process as there is typically no risk of freezing and limited oxygen available to support corrosion of the steel. |
| Tidal zone | One of the most aggressive zones, as the conditions can promote corrosion (chlorides and oxygen present), the number of freeze–thaw cycles is at a maximum, and abrasion by waves and ice occur in this zone. |
| Splash zone | The region at or just above the high-tide level represents one of the worst conditions for corrosion risk as chlorides and oxygen are present and chloride penetration may be accelerated due to wetting and drying. |
| Spray zone | As the height above sea level increases, the exposure becomes less aggressive as chloride loading decreases and the concrete becomes less saturated, which reduces the impact of freeze–thaw cycles. However, in dry, sheltered areas (eg, under the bridge deck), it is possible that carbonation-induced corrosion may occur. |

Other microclimate effects within the same structure (or element) may occur due to orientation with regard to the sun, prevailing wind and current (ice flows).

### 6.2.2 Chloride resistance

The role of chloride ions in the breakdown of the passive layer on reinforcing steel and subsequent initiation of corrosion is discussed in Chapter 5. If steel-reinforced concrete is exposed to a marine environment, it is essential that measures are taken to protect the steel from chloride-induced corrosion. There are many corrosion-protection strategies, but one of the main lines of defence is to provide a concrete with high resistance to chloride-ion penetration; of course, it is also essential to ensure that the depth of the concrete cover over the steel is sufficient and that cracking of the cover concrete is minimised.

Chlorides may penetrate concrete as a result of various transport mechanisms; these include the following:

- *Diffusion* describes the mass transfer of chloride (or other) ions from areas of high concentration (eg, the surface exposed to seawater) to regions of low concentration (eg, the location of the steel). The diffusion coefficient, $D$, of the concrete is the material property that affects the rate of chloride ingress due to a concentration gradient, the magnitude of the gradient being the driving force.
- *Convection* describes the mass transfer of salt-laden water into concrete due to a moisture gradient (salt water is 'sucked' into relatively dry concrete). Terms like 'capillary suction' and 'absorption' are often used to describe movement of salt water due to moisture gradients, and various coefficients have been derived for concrete (eg, rate of absorption, $I$, determined by ASTM C1585).
- *Permeation* describes the penetration of salt water due to a hydraulic gradient (salt water is 'driven' into concrete under pressure). The hydraulic conductivity (or water permeability), $k$, of concrete is the material property that affects the flow rate due to a hydraulic gradient, the magnitude of the gradient being the driving force.

- *Migration* describes the movement of ions under an electrical gradient (negatively charged chloride cations are 'driven' in the direction of the positively charged anode). The migration rate depends on the diffusion coefficient, *D*, of the concrete and the potential gradient. Electrical migration tests have been used to measure the diffusion coefficient, *D*.

More than one mass transport mechanism may be at work in marine-exposed concrete. For example, in a tunnel submerged under the sea, chlorides will diffuse into the concrete liner due to the concentration gradient, permeate as a result of hydraulic gradient, and be sucked in due to 'wicking' from the saturated external surface to the drier interior surface.

In the tidal zone, it is likely that diffusion is the dominant mass transport process as the bulk of the concrete will remain saturated or close to saturation due to the twice-daily submersion with water. In the splash zone, it is expected that absorption plays a role in the build-up of chloride at the surface due to cyclic wetting and drying, with diffusion governing the rate of penetration below the surface. Generally, there is a good correlation between mass transport properties, and concrete with low hydraulic conductivity (water permeability) tends to have a low diffusion coefficient.

The chloride resistance of concrete is dependent on both the physical structure of the pore system and the chemical composition of the binder. A well-refined pore structure characterised by small and disconnected pores will have a high *physical* resistance to chloride penetration. This is usually achieved by proportioning the concrete to have a low water/binder ratio (w/b) and by selection of an appropriate binder. The selection of the binder is also an important consideration with regard to *chemical* resistance to chloride penetration, as some cementitious binders are able to bind a significant quantity of the penetrating chloride ions, thereby preventing further ingress of the bound chlorides.

The use of supplementary cementing materials (SCM) such as fly ash, slag, silica fume, metakaolin and other pozzolans can have a profound effect on the chloride resistance of concrete, as their proper use can result in a much refined pore structure and concomitantly reduced permeability, compared to Portland cement (PC) concrete without SCM. Furthermore, many SCMs contain significant amounts of alumina ($Al_2O_3$) which can increase the chloride-binding capacity of the concrete (Zibara, 2001), thereby further increasing chloride resistance. The role of SCMs is discussed in Section 6.3 of this chapter.

### 6.2.3 Freeze–thaw resistance

Concrete exposed to cycles of repetitive freezing and thawing can suffer deterioration if the concrete is in a saturated condition; the presence of salt solution (eg, seawater or deicing salts) at the surface tends to exacerbate the action of freeze–thaw cycles often promoting surface scaling. The critical degree of saturation is often reported to be 91.7% as water undergoes 9% expansion on freezing to form ice, and if more than 91.7% of the volume of the pores is filled with water, there is no space to accommodate the ice that forms. This is a gross oversimplification of the physics of ice formation in a porous body containing a complex pore solution, and readers are referred to Scherer

and Valenza (2005) for a more comprehensive treatise. The tidal zone and the splash zone immediately above the high-tide level are the most aggressive zones with regard to the action of freezing and thawing as there are more freeze–thaw cycles in this zone, and the concrete will likely be above critical saturation. Below low-tide level, there are either no or very few cycles of freeze–thaw, and above the splash zone the concrete is less likely to be saturated, and the number of freeze–thaw cycles is also less.

Saturated concrete will generally have satisfactory resistance to freeze–thaw action provided the following four conditions are met:

- The concrete has a satisfactory entrained air-void system. The amount of air required increases as the paste volume of the concrete increases; typically concrete with nominal maximum aggregate size of 20 mm requires somewhere in the region of 5–8% air by volume. It is also important that the air-void system is composed of relatively small bubbles that are closely spaced rather than large bubbles that are spaced far apart. The spacing factor, L-bar, defines the maximum distance between any point in the paste and the nearest bubble. Although specifications vary, it is generally considered that the spacing factor L-bar should be no greater than about 230–250 μm.
- The concrete should achieve a sufficient amount of strength prior to the freezing. If concrete freezes while still plastic, the large volume of freezable water in the system creates irreparable damage (eg, formation of ice lenses) from which the concrete will never recover even with extended curing after the first freeze. In the United States, it is recommended that the concrete be prevented from freezing until the compressive strength reaches at least 3.5 MPa.
- Concrete also needs to achieve a sufficient compressive strength to resist the stresses generated by multiple cycles of freezing and thawing. In Canada, the minimum 28-day strength requirement for concrete exposed to freezing and thawing while saturated (F2 exposure class) is 30 MPa (CSA A23.1); there is a similar requirement in the ACI Building Code (ACI 318).
- Finally, for concrete to have adequate freeze–thaw resistance, the aggregate needs to have acceptable frost resistance. Certain coarse aggregates undergo deterioration when exposed to freeze–thaw cycles in a saturated condition; the damage is related to the pore structure of the aggregates. Air-entraining concrete only protects the paste portion of the concrete, and frost-susceptible aggregates should be avoided in concrete that will be exposed to freezing and thawing in a saturated condition.

### 6.2.4 Resistance to sulphates and other chemical attacks

The typical sulphate concentration of seawater is in the region of 2700 ppm $SO_4^{2-}$. This concentration is relatively high and would represent a severe sulphate-exposure class in most specifications. However, many investigators have shown that seawater is not as destructive as its sulphate content would indicate, and they ascribe this to the interaction of the chlorides which prevents the expansive formation of ettringite (Thomas and Skalny, 2006).

Magnesium ions dissolved in the seawater combine with $Ca(OH)_2$ to form brucite, $Mg(OH)_2$, which is highly insoluble and serves to provide a protective layer on the concrete surface in many cases. However, if the concrete is highly permeable (eg, high w/b), the combined action of magnesium and carbonate ions can result in

decalcification of the C−S−H to form aragonite (a calcium carbonate phase) and a magnesium silicate hydrate phase with little strength.

As a consequence of the combined chemical reactions that occur in seawater, the chemical attack is characterised generally by erosion and loss of coherence of the cementing phase (eg, because of decalcification of the C−S−H), and the composition of the cement appears to play only a minor role (Thomas and Skalny, 2006). The best line of defence against chemical attack in a seawater environment is to provide low-permeability concrete with a low w/b; consideration should also be given to using SCMs to further reduce the permeability (see Section 6.3.2).

### 6.2.5 Abrasion resistance

Marine structures are exposed to abrasion and erosion due to wave action, sea currents and ice. The abrasive action is increased significantly as the amount of solid material (eg, silt and sand) suspended in or associated with the water or ice increases. The abrasion resistance of concrete is a function of the strength of the concrete and abrasion resistance of the aggregate. The use of a hard siliceous aggregate together with a low-w/b paste will generally produce an abrasion-resistant concrete. A comprehensive description of ice-abrasion mechanisms has been presented by Jacobsen et al. (2015).

### 6.2.6 Alkali−aggregate reaction

Alkali−aggregate reaction (AAR) is a reaction between the alkali hydroxides in the pore solution of the concrete (supplied predominantly by the PC) and certain aggregates; alkali−silica reaction (ASR) involves certain silica minerals in the aggregate, whereas the much less widespread alkali−carbonate reaction (ACR) involves certain argillaceous dolomites with a specific texture. AAR is an expansive-type reaction in which the concrete is usually severely cracked and damaged. Damage due to AAR occurs in all types of structures. One requirement of deleterious AAR is that the concrete is exposed to sufficient levels of moisture in service. This requirement is clearly met in marine structures, and hence, measures to minimise the risk of AAR damage have to be considered when selecting materials and proportions for marine concrete.

There is a good deal of controversy surrounding the sodium present in seawater and whether this potentially provides an external source of alkali which can penetrate the concrete and augment the alkali hydroxide concentration of the pore solution, thereby increasing the risk of AAR. A comprehensive review of the literature on the effects of NaCl in seawater and deicing salts, and of other compounds used as anti-icing or deicing chemicals, was published by Folliard and coworkers (Folliard et al., 2008). At high levels of concentration, NaCl can exacerbate ASR expansion; however, at seawater concentrations, the impact of NaCl is minimal and restricted to the surface.

## 6.3 Appropriate binders and cements

### 6.3.1 Types of Portland cement

It is well established that the use of sulphate-resisting PCs (SRPC, Type V or Type HS in North America) increases the resistance of concrete to normal sulphate-exposure conditions. However, as discussed in Section 6.2.4, the interaction between sulphates and concrete in seawater is different from normal aqueous environments, and the type of PC does not seem to play a significant role. It has been established that the chloride-binding capacity of PC increases significantly as the aluminate content ($C_3A$) in the cement increases; this has been demonstrated for both admixed chlorides (Rasheeduzzafar et al., 1992) and chlorides introduced after hydration (Zibara, 2001). Increased chloride binding is beneficial as it will both slow down the rate of penetration of chlorides into concrete and increase the chloride threshold concentration required to initiate corrosion. Consequently, some specifications prohibit the use of SRPC or low-$C_3A$ cements in a marine environment. However, as discussed in Section 6.3.2, when PC is combined with at least moderate amounts of SCM, the impact of the PC composition on chloride ingress is minimal.

### 6.3.2 Supplementary cementing materials

SCMs have a very significant impact on the performance of marine concrete. Perhaps the greatest benefit is that SCMs reduce the permeability of concrete, making it more resistant to the penetration of chloride and other ions. Other advantages are that most SCMs also reduce the risk of damage due to ASR and delayed-ettringite formation. A comprehensive text on the impact of SCMs on the durability of concrete has recently been published by the author of this chapter (Thomas, 2013).

The impact of SCMs on chloride ingress in a marine environment is demonstrated in Figs 6.1–6.3 (Thomas and Bremner, 2012; Alexander and Thomas, 2015). The figures show chloride profiles for large concrete blocks ($0.305 \times 0.305 \times 0.914$ m) after 25 years of exposure in the tidal zone of a marine exposure site on Treat Island, which is near Eastport, Maine, in the United States. In all but one case, the concrete mixes have w/b = 0.40, the exception being the concrete with 7% silica fume (w/b = 0.34). In all cases, there is substantial chloride penetration in the control blocks without SCM (0%), with 0.2–0.3% Cl by mass of concrete at a depth of 80 mm, considerably in excess of typically used corrosion-threshold values (eg, 0.05–0.10%). Also in all cases, the partial replacement of PC with fly ash, slag, silica fume or combinations thereof leads to much reduced penetration, with little additional chloride above background being found at depths of 50–60 mm.

There are literally hundreds of publications that confirm the effectiveness of SCMs in providing increased resistance to chloride-ion penetration in laboratory and field-exposure tests, as well as in real structures exposed to a marine environment. The increased resistance is mainly attributed to a refinement in the pore structure when SCMs are used; however, as mentioned earlier, alumina-bearing SCMs also increase

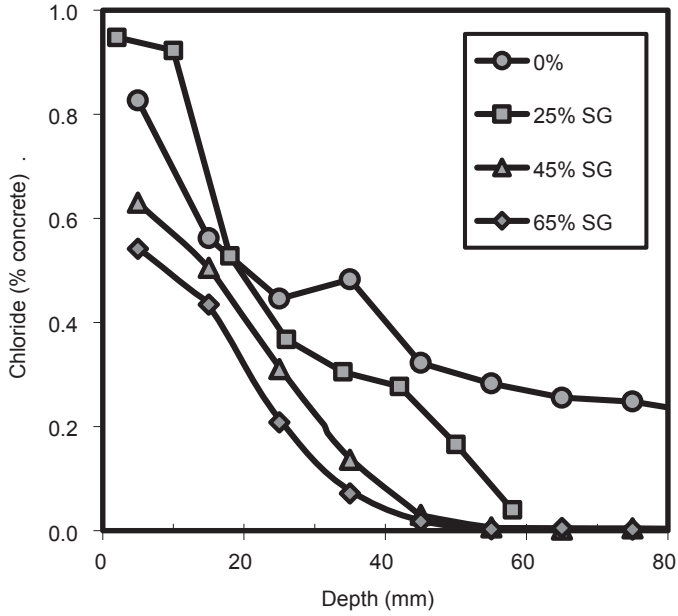



**Figure 6.1** Chloride profiles for concrete containing slag (SG) after 25 years in a marine tidal zone (Thomas and Bremner, 2012).

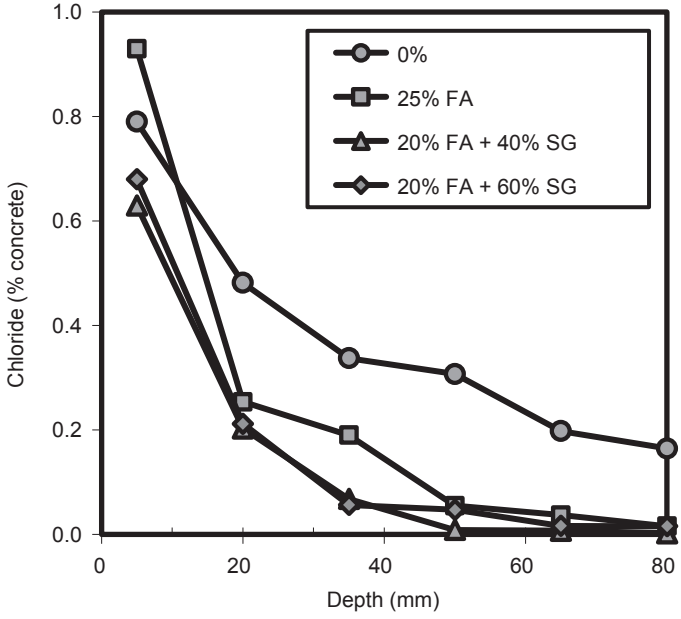



**Figure 6.2** Chloride profiles for concrete containing combinations of fly ash (FA) and slag (SG) after 25 years in a marine tidal zone (Alexander and Thomas, 2015).

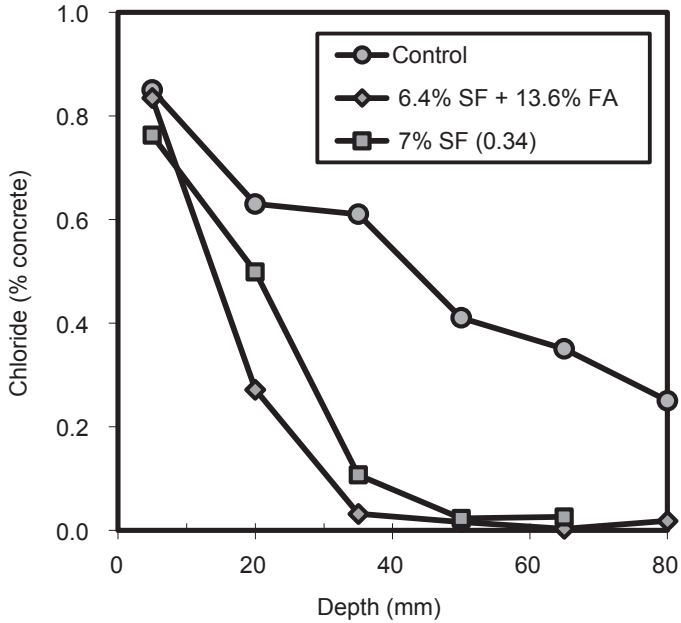



**Figure 6.3** Chloride profiles for concrete containing combinations of fly ash (FA) and silica fume (SF) after 25 years in a marine tidal zone (Alexander and Thomas, 2015).

the chloride-binding capacity of the hydrates which further impedes the penetration of chlorides (Zibara, 2001; Thomas et al., 2012a).

As a note of precaution, the full impact of SCMs on increasing resistance to chloride penetration may not be fully realised by testing such concretes at early ages (eg, up to 28 days). With slowly reacting pozzolans such as fly ash and latent hydraulic materials like slag, reductions in chloride transport properties such as diffusion occur over years. The diffusion coefficient of slag and fly ash concretes has been found to decrease by one or two orders of magnitude between early age tests (eg, 28 days) and after many decades (Bamforth, 1999; Thomas and Bamforth, 1999).

The time-dependence of mass transport properties, such as the diffusion coefficient, has been modelled using power−law relationships such as that shown in Eq. [6.1] (Bamforth, 1999; Thomas and Bamforth, 1999):

$$D_t = D_{28} \cdot \left(\frac{28}{t}\right)^m \qquad [6.1]$$

where $D_t$ and $D_{28}$ are, respectively, the diffusion coefficient at time $t$ and 28 days, and $m$ is a coefficient that varies with the type of cementing material. Typical $m$ values may be 0.2 for concrete without SCM and 0.6 for concrete containing moderate to high levels of fly ash or slag (Bamforth, 1999; Thomas and Bamforth, 1999).

Most SCMs are also effective at reducing the risk of damaging expansion when alkali−silica reactive aggregates are used in concrete. The amount of SCM required

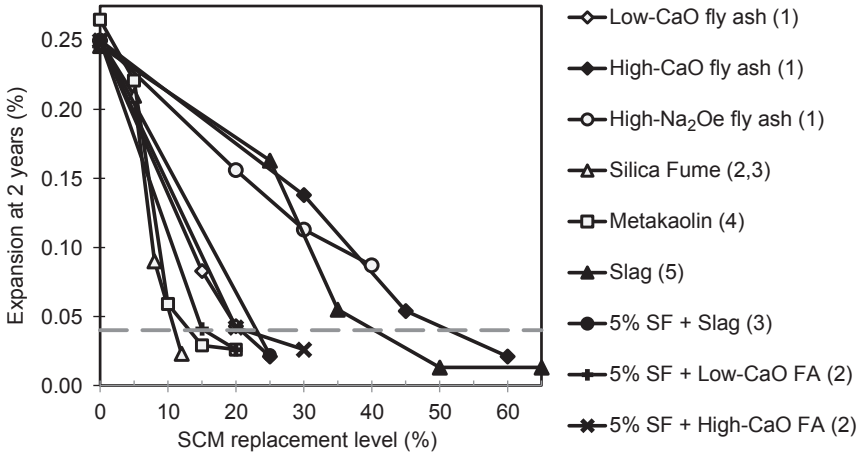



**Figure 6.4** Effect of type and amount of SCM on the (two-year) expansion in the concrete prism test (Thomas, 2011).

is a function of the type and composition of the SCM, the reactivity of the aggregate, the available alkalis in the system, and the exposure conditions of the concrete. A comprehensive review on the effect of SCMs on ASR has been published by Thomas (2011). Fig. 6.4 shows the impact of various SCMs on the 2-year expansion of concrete prisms stored over water in sealed containers at 38°C (test method ASTM C1293). Generally, the efficacy of the SCM in this role increases with the amount of reactive silica it contains.

### *6.3.3 Non-Portland cements*

There are limited data on the performance of non-Portland cements exposed to marine environments. Earlier reports for concrete produced with calcium-aluminate cement (CAC) indicated a very high resistance to chloride-ion penetration in seawater (Aitcin et al., 1995; Dunster et al., 1990); however, more recent studies have indicated the resistance to be inferior to that of PC, especially when the CAC is converted prior to exposure (Yi and Thomas, 2014). Further studies are required to evaluate the marine performance of alternative cements.

## 6.4 Aggregates and admixtures

All concretes contain fine and coarse aggregates. Usually, these are of hard rock, either natural gravels or crushed from sound rock, and therefore are not likely to be susceptible to the effects of chlorides or sulphates. Also, virtually all modern concretes

contain admixtures. Therefore, it is important to consider briefly these materials in terms of marine concrete durability.

### 6.4.1 Role of aggregates

Generally, there are no specific properties or performance requirements for aggregates exposed to marine environments. Aggregates should be well-graded, have suitable physical properties, be frost-resistant (if exposed to freeze−thaw in service), and meet the normal requirements for aggregates for concrete construction given in standard specifications. If the aggregates are alkali−silica reactive, then appropriate measures should be taken to minimise the risk of deleterious reaction. The exception to the aforementioned is areas of structures that are exposed to severe abrasion, such as ice abrasion. In these cases, the aggregate should be selected to produce a high degree of abrasion resistance; generally, siliceous aggregates are more resistant than carbonate aggregates. In general, it is preferable to maximise the aggregate content in the concrete mix to enhance durability, subject to other concrete requirements such as adequate workability, cohesiveness and so on.

### 6.4.2 Chemical admixtures

Many types of chemical admixtures are likely to be used in marine concrete for much the same reasons they are used in nonmarine applications. This section focuses on admixtures used to enhance corrosion resistance and prevent washout in concrete placed underwater.

#### 6.4.2.1 Corrosion inhibitors

Corrosion inhibitors are frequently used in steel-reinforced concrete as part of the overall corrosion-protection strategy when the concrete is exposed to chlorides. There are many types of corrosion inhibitors used in concrete, the most common being calcium-nitrite inhibitor (CNI). The nitrite ions in CNI help to stabilise the passive layer on the steel surface, which increases the chloride threshold concentration required to initiate corrosion, thereby increasing the time to corrosion initiation and, thus, the service life of the concrete. The impact of increasing the chloride threshold is particularly marked in concrete that has a high resistance to chloride-ion penetration.

#### 6.4.2.2 Anti-washout admixtures

Anti-washout admixtures increase the viscosity and cohesiveness of the concrete, thereby increasing the resistance of the concrete to segregation and allowing the concrete to be placed underwater, sometimes even without the use of tremies. These admixtures usually consist of water-soluble cellulose or acrylic polymers. (However, a caution is that if these admixtures substantially retard the setting time of concrete, they may cause problems due to washout if the sea conditions are rough.)

## 6.5 Alternative reinforcement

Steel-reinforced concrete normally contains plain 'black' steel, even in marine conditions, largely due to cost considerations. As indicated earlier, it is possible to produce durable reinforced concrete in marine environments by proper attention to the chloride-resistant nature of the concrete matrix, and by adequate cover to the steel, as well as by excellent concreting practices such as thorough compaction and good curing. However, occasionally it is necessary to use alternative types of reinforcement to give greater assurance of corrosion-free performance of the structure.

### 6.5.1 Epoxy-coated steels

The problem of premature deterioration of steel-reinforced concrete structures due to corrosion initiated by chlorides was first realised in the early 1960s. Epoxy-coated reinforcement (ECR) was developed as a potential solution to this problem about 10 years later, and the market expanded rapidly to the extent that ECR became the preferred corrosion-protection strategy in highway structures in North America. The first problems with corrosion of ECR in marine structures were encountered in the Florida Keys in the mid- to late 1980s and attributed to debondment of the epoxy from the steel (Zayed et al., 1989). Since then, a number of studies have indicated poor performance of ECR in highway structures, and these have been comprehensively documented by Manning (1996). However, the vast majority of structures constructed with ECR and exposed to either deicing salts or seawater are performing well. It is unclear at this time what the impact of ECR is on the service life of reinforced concrete structures in marine exposures.

### 6.5.2 Corrosion-resistant steel

Stainless steel reinforcement (SSR) for concrete is available in many parts of the world. The superior corrosion resistance of stainless steel is widely accepted, and there have been a number of projects that have used such reinforcement. Stainless steel is generally defined as an iron-based steel alloy with a minimum of 12% by weight of chromium (Hartt et al., 2004). As such, the composition of stainless steel can vary widely, and since the corrosion resistance of SSR is dependent on its alloying composition, the performance of the steel in a corrosive environment also varies widely. High-grade stainless steels such as 316LN (containing chromium, nickel, molybdenum and nitrogen as alloying compounds) have proved to be extremely effective in reducing the risk of corrosion in reinforced concrete structure (Hansson et al., 2009). Unfortunately, cheaper compositions with lower amounts of alloy (and without molybdenum and/or nitrogen) show inferior performance, especially with regard to pitting corrosion. There are a number of tests for determining the performance of stainless steel. For example, ASTM A955 includes an annex for evaluating the corrosion resistance of SSR; there are two tests (rapid microcell test and cracked beam test)

with performance limits. New compositions proposed for use as reinforcement for concrete should be tested using performance tests like these, and the results should be compared with 316LN.

### 6.5.3 Nonferrous reinforcement

Nonferrous reinforcement is available commercially, the most common types being fibre-reinforced polymers (FRP) with either glass or carbon fibres. These materials are obviously not prone to normal corrosion, although the long-term stability of the material in the high-pH environment that exists in concrete has not been established. Because FRP has mechanical properties different from steel, different procedures have to be used for designing reinforced concrete (eg, see ACI 440.1R-15 Guide for the Design and Construction of Structural Concrete Reinforced with Fiber-Reinforced Polymer Bars).

## 6.6 Mix design and proportioning

### 6.6.1 Prescriptive approach

There are numerous prescriptive specifications for marine concrete; such specifications may include some or all of the following requirements:

- maximum w/b
- minimum cement content
- type of cement
- minimum depth of cover
- minimum air content (and possible other air-void parameters)
- minimum concrete strength grade (it could be argued that, technically, the strength is a performance requirement)

A simple example of such a specification is the ACI 318 Building Code. Reinforced concrete exposed to seawater is a C2 exposure class, but it also has to meet the requirements for class S1 (moderate sulphate resistance) and the requirements for F2 if exposed to freezing and thawing in service. The combinations of these requirements are as follows:

- w/b $\leq$ 0.40 (for C2)
- minimum cement content (NOT required in ACI 318)
- cement: type MS (moderate sulphate-resistant cement) or equivalent (for S1)
- cover $\geq$50 mm
- target air = 6% (for 20-mm aggregate)
- concrete strength $\geq$5000 psi (34.5 MPa)

There is no requirement in ACI 318 to use SCMs despite the substantial reduction in chloride penetration that is achievable through their use.

**Table 6.1 BS 8500-1 durability recommendations for reinforced or prestressed elements with an intended working life of at least 100 years in a marine tidal zone (XS3 exposure class)**

| | | Strength class, maximum w/b and minimum cement content (kg/m$^3$) for specified cover (mm) and 20-mm aggregate | | | | |
|---|---|---|---|---|---|---|
| **Cover depth (mm) →** | | **45** | **50** | **55** | **60** | **65** |
| Cement type | CEM 1, IIA, IIB-S, SRPC | | | | C45/55<br>0.33, 380 | C40/50<br>0.40, 380 |
| | IIB-V, IIIA | C40/50<br>0.35, 380 | C35/45<br>0.40, 380 | C32/40<br>0.45, 360 | C28/35<br>0.50, 340 | C25/30<br>0.55, 320 |
| | IIIB, IVB-V | C32/40<br>0.40, 380 | C28/35<br>0.45, 360 | C25/30<br>0.50, 340 | C25/30<br>0.50, 340 | C25/30<br>0.50, 340 |

The Canadian Standard (CSA A23.1-2014) has similar requirements, although there is a performance requirement to achieve a 'rapid chloride permeability test, RCPT' value of less than 1500 Coulombs within 91 days for a C1 exposure class (note that the value is 1000 Coulombs for a C-XL exposure class) (see Section 6.7 in this chapter for a discussion of this test). It is extremely difficult to meet this limit without using one or a combination of SCMs.

EN206:2013 requires a maximum w/b $\leq$ 0.45, a minimum cement content of 340 kg/m$^3$, a minimum air content of 4% (if freeze−thaw resistance required), and a minimum strength class of C34/45. However, the complementary British Standard (BS 8500-1) provides multiple options by allowing various combinations of cover depth, cement type, w/b, strength class and minimum cement content. Table 6.1 shows an example of the options for exposure class XS3 (marine tidal zone). For example, if a CEM I cement is used with 65-mm cover, the remaining requirements are for a strength class of C35/45, w/b $\leq$0.45, and cement content $\geq$380 kg/m$^3$. Reducing the cover depth to 55 mm results in higher strength class (C45/55), lower w/b ($\leq$0.35) and more cement content ($\geq$380 kg/m$^3$). If a CEM IIIB cement (with 66−80% slag) is used with 55-mm cover, the strength class required is only C25/30, w/b $\leq$ 0.50 and cement content $\geq$340 kg/m$^3$ to take advantage of the low permeability and high resistance to chloride-ion penetration offered by the high slag content.

### 6.6.2 *Performance approach (eg, design of mixes to meet performance parameters)*

In a performance-based approach, relevant performance tests need to be conducted and the concrete is required to meet various limits depending on the exposure class. The concrete producer can then select materials and mixture proportions without

restrictions, provided it is demonstrated that the concrete meets the performance requirements. For example, for reinforced concrete exposed to the tidal or splash zone where chloride-induced corrosion of embedded reinforcement is the main durability concern, the principal performance test would be some measure of chloride-ion resistance. The bulk-diffusion test (ASTM C1556 and Nordtest Method NT BUILD 443) has been used for a number of structures (eg, Hart et al., 1997). Service-life models such as Life-365 (Ehlen et al., 2009) and ConcreteWorks (Riding et al., 2013) can be used to determine the value of the diffusion coefficient required for a specific structure based on its depth of cover and the exposure conditions. Due to the duration of the test, it is more suitable for prequalification of concrete mixtures, rather than quality control (QC) or quality assurance (QA). There are more rapid 'index' tests that can be used as a surrogate for the chloride diffusion test for the purposes of QC and QA; such are discussed in Section 6.7 of this chapter.

Other relevant performance tests for marine exposure include, but are not limited to, freeze−thaw resistance, air-void parameters (total volume plus either spacing factor and/or specific surface), abrasion resistance, alkali-silica reactivity and drying shrinkage (to control cracking).

## 6.7 Testing of marine concretes

There are a wide variety of tests for concrete to determine properties that are relevant to the performance in a marine environment. These are mentioned in the preceding section, and details can be found in text books. For the purpose of this chapter, only tests relevant to chloride ingress will be discussed.

### 6.7.1 Traditional (long-term) durability tests

For concrete in a marine tidal zone, diffusion is the predominant mechanism of chloride transport, and the chloride diffusion coefficient is an appropriate performance indicator; this can be measured using the bulk-diffusion test (ASTM C1556 and Nordtest Method NT BUILD 443). In these tests, saturated concrete samples, sealed on all but one face, are exposed to chloride solutions for a given period of time, $t$, after which the samples are profile-ground and the chloride concentration, $C_x$, is determined as a function of the depth, $x$, from the exposed surface. The apparent diffusion coefficient, $D_a$, and the surface concentration, $C_0$, are determined by fitting the following numerical solution to Fick's second law to the concentration profile ($C_x$ vs $x$):

$$C_x = C_0\left(1 - \operatorname{erf}\frac{x}{2\sqrt{D_a t}}\right) \qquad [6.2]$$

There are other chloride penetration tests such as the '90-day salt ponding test' (AASHTO T259), but with this test it is difficult to determine mass transport coefficients and select performance requirements (eg, limits).

### 6.7.2 Rapid index tests

A number of rapid indexes such as the accelerated migration test (NT BUILD 492), the RCPT (ASTM C1202), and various measures of electrical resistivity (or conductivity) have been found to correlate reasonably well with the results of the bulk-diffusion test (Stanish et al., 2001). Such tests may offer a satisfactory surrogate to diffusion tests for QA or QC purposes. For example, Fig. 6.5 shows the relationship between the bulk-diffusion coefficient (ASTM C1556) and the 'rapid chloride permeability' (ASTM C1202) for concrete samples cut from the same cylinder and tested at the same age. The results represent 88 different concrete mixtures produced during various research studies at the University of Toronto and the University of New Brunswick. Variables for the laboratory-exposed concretes included w/b, binder type (fly ash, slag, silica fume and metakaolin used in binary and ternary mixes) and age (from 1 month to 5 years); a few mixes incorporated calcium-nitrite or lithium-nitrate admixtures, and one mix was classed as an ultra-high performance concrete, UHPC (Thomas et al., 2012b).

It can be seen from Fig. 6.5 that the rapid chloride permeability test (RCPT) correlates reasonably well with the diffusion coefficient determined on the same concrete at a similar age; however, there does not exist a single relationship that can reliably be used to predict the diffusion coefficient from the RCPT.

The RCPT is essentially a measure of electrical conductivity, and as such, a similar relationship might be expected between the bulk-diffusion coefficient and the results of other methods for measuring electrical resistivity or conductivity, and this has been confirmed by Stanish and coworkers (Stanish et al., 2001).

It should be recognised that the electrical resistivity of concrete and the rate of diffusion of chlorides both depend on the pore structure (size, connectivity and tortuosity of pores) to some extent, and this explains why there is a reasonable correlation. However, the resistivity also depends on the composition (ie, electrical conductivity) of the

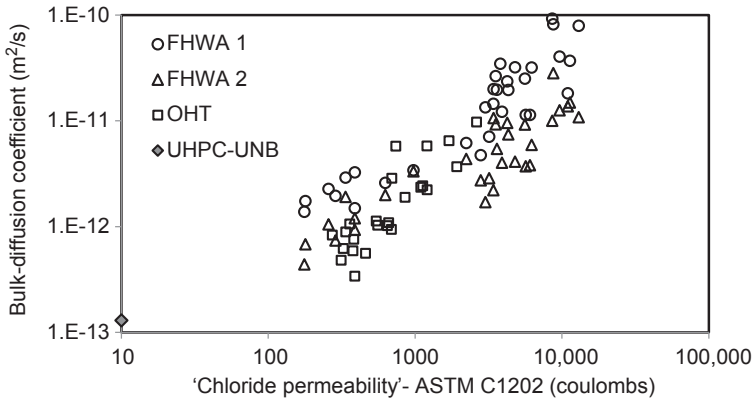



**Figure 6.5** Relationship between bulk-diffusion coefficient (ASTM C1556) and 'Rapid Chloride Permeability' (ASTM C1202) (log scales).



**Figure 6.6** Use of a four-point (Wenner-type) probe to measure surface resistivity on a field-exposure block.

pore solution, whereas the rate of chloride ingress depends on the composition of the hydrates and the ability of the hydrates to bind chlorides. For this reason, caution is advised when predicting transport properties from electrical properties for mixes outside of the range where a reasonable correlation has been established.

### 6.7.3 In situ tests (for QC/QA)

Electrical resistance can be measured on structures using a variety of devices. Fig. 6.6 shows a four-point (Wenner-type) probe being used to measure the surface resistivity on a concrete block on a field-exposure site.

## 6.8 Future trends

### 6.8.1 Extending service life (beyond 100 years)

Theoretically, it is possible to achieve a 100-year service life for reinforced concrete exposed to a marine environment, even in tidal and splash zones, by using traditional concrete-making materials (including SCMs and, possibly, corrosion inhibitors) with adequate cover and proper practices to minimise cracking. In addition to preventing chloride-induced corrosion, the concrete may also have to be proportioned to prevent deleterious ASR, freeze−thaw and ice abrasion.

Extending the life beyond 100 years may require additional measures or combined strategies (such as SCM plus corrosion inhibitors). However, it is inevitable that chlorides will eventually reach the steel whether it takes 100 years or longer. Consequently,

the only viable options for providing corrosion-protection indefinitely are to use corrosion-resistant reinforcement such as high-grade stainless steel (eg, 316LN) or nonferrous reinforcement (eg, FRP bars).

### 6.8.2 Reducing environmental footprint

From a material perspective the carbon footprint of concrete is determined to a large extent by the quantity of PC clinker that it contains, as the production of clinker results in the release of substantial amounts of $CO_2$ (average worldwide is approximately 0.85 tonnes of $CO_2$ for every tonne of clinker). The clinker content of concrete can be greatly reduced through the use of SCMs, which also serves to increase the durability of the concrete. Another option is to increase the use of Portland-limestone cements (PLC). Recent research has shown that up to 15% limestone can be interground with clinker without adversely affecting durability performance, although this requires the PLC to be ground finer than a PC (without limestone) produced from the same clinker (Tennis et al., 2011).

## Sources of further information and advice

- Gjorv, O.E., 2014. Durability Design of Concrete Structures in Severe Environments. CRC Press, 270 p.
- Mehta, P.K., Concrete in a Marine Environment. Taylor and Francis, London, 224 p.

## References

AASHTO T259, 2012. Standard Method of Test for Resistance of Concrete to Chloride Ion Penetration. AASHTO, Washington.

ACI 318, 2008. Building Code Requirements for Structural Concrete and Commentary. American Concrete Institute, Farmington Hills, Michigan.

Aitcin, P.C., Blais, F., George, C.M., 1995. Durability of calcium aluminate cement concrete: assessment of concrete from a 60-year-old marine structure at Halifax, NS, Canada. In: Malhotra, V.M. (Ed.), Proceedings of the Second CANMET/ACI International Symposium on Advances in Concrete Technology. ACI SP-154, American Concrete Institute, Detroit, pp. 145−167.

Alexander, M., Thomas, M., 2015. Service life prediction and performance testing − current developments and practical applications. Cement and Concrete Research 78 (2015), 155−164.

ASTM A955/A955M-15, 2015. Standard Specification for Deformed and Plain Stainless-steel Bars for Concrete Reinforcement. ASTM International, West Conshohocken, PA. www.astm.org.

ASTM C1202-12, 2012. Standard Test Method for Electrical Indication of Concrete's Ability to Resist Chloride Ion Penetration. ASTM International, West Conshohocken, PA. www.astm.org.

ASTM C1293-05, 2005. Standard Test Method for Determination of Length Change of Concrete due to Alkali-Silica Reaction. ASTM International, West Conshohocken, PA. www.astm.org.

ASTM C1556-04, 2004. Standard Test Method for Determining the Apparent Chloride Diffusion Coefficient of Cementitious Mixtures by Bulk Diffusion. ASTM International, West Conshohocken, PA. www.astm.org.

ASTM C1585-13, 2013. Standard Test Method for Measurement of Rate of Absorption of Water by Hydraulic-cement Concretes. ASTM International, West Conshohocken, PA. www.astm.org.

Bamforth, P.B., 1999. The derivation of input data for modelling chloride ingress from eight-year U.K. coastal exposure trials. Magazine of Concrete Research 51 (2), 87–96.

BS-EN-206, 2013. Concrete - Part 1: Specification, Performance, Production and Conformity. European Standard.

BS 8500–1, 2015. Concrete. Complementary British Standard to BS EN 206. Method of Specifying and Guidance for the Specifier. British Standards Institution, London.

CSA A23.1-14/A23.2-14, 2014. Concrete Materials and Methods of Concrete Construction/Test Methods and Standard Practices for Concrete. Canadian Standards Association, Toronto.

Dunster, A.M., Crammond, N.J., Pettifer, K., Rayment, D.L., 1990. An assessment of ageing calcium aluminate cement concrete from marine structures. In: Mangabhai, R.J. (Ed.), Calcium Aluminate Cement. E & FN Spon, London, pp. 264–271.

Ehlen, M.A., Thomas, M.D.A., Bentz, E.C., May 2009. Life-365 Service Life Prediction Model™ Version 2.0. Concrete International, pp. 41–46.

Folliard, K.J., Thomas, M.D.A., Fournier, B., 2008. The Effects of Potassium Acetate De-icing Chemicals on the Performance of Concrete Containing Fly Ash: A Literature Review. EPRI, Palo Alto, CA, 1018167.

Hansson, C.M., Anders, K.A., Bergsma, B.P., 2009. The Influence of Surface Condition and Loading on the Corrosion Behaviour of Stainless Steel Reinforcing Bars. University of Waterloo, Department of Mechanical and Mechatronics Engineering. Highway Infrastructure Innovation Funding Program.

Hart, A.J.R., Ryell, J., Thomas, M.D.A., October 1997. High performance concrete in precast concrete tunnel linings, meeting chloride diffusion and permeability requirements. In: Proceedings of the PCI/FHWA International Symposium on High Performance Concrete, pp. 294–307.

Hartt, W., Powers, R., Leroux, V., Lysogorski, D., 2004. A Critical Literature Review of High-performance Corrosion Reinforcements in Concrete Bridge Applications. U.S. Department of Transportation, Office of Infrastructure and Development, Federal Highway Administration.

Jacobsen, J., Scherer, G.W., Schulson, E.M., 2015. Concrete/ice abrasion mechanics. Cement and Concrete Research 73, 79–95.

Manning, D.G., 1996. Corrosion performance of epoxy-coated reinforcing steel: North American experience. Construction and Building Materials 10, 349–365.

NT BUILD 443, 2014. Concrete, Hardened: Accelerated Chloride Penetration. Nordtest, Denmark.

NT BUILD 492, 1999. Chloride Migration Coefficient from Non-steady-state Migration Experiments. Nordtest, Denmark.

Rasheeduzzafar, Ehtesham Hussain, S., Al-Saddoun, S.S., 1992. Effect of tricalcium aluminate content on chloride binding and corrosion of reinforcing steel. ACI Materials Journal 89, 3–12.

Riding, K., Thomas, M.D.A., Folliard, K.J., November–December 2013. Apparent diffusivity model for concrete containing supplementary cementitious materials. ACI Materials Journal 110 (6), 705–714.

Scherer, G.W., Valenza II, J.J., 2005. Mechanisms of frost damage. In: Skalny, J., Young, F. (Eds.), Materials Science of Concrete, vol. VII. American Ceramic Society, pp. 209–246.

Stanish, K.D., Hooton, R.D., Thomas, M.D.A., 2001. Prediction of Chloride Penetration in Concrete. US Department of Transportation, Federal Highway Administration, Publication No. FHWA-RD-00−142.

Tennis, P.D., Thomas, M.D.A., Weiss, J.W., 2011. State-of-the-Art Report on Use of Limestone in Cements at Levels of up to 15%. PCA R&D Serial No. SN3148. Portland Cement Association, Skokie, IL, 74 pages.

Thomas, M.D.A., 2011. The effect of supplementary cementing materials on alkali-silica reaction: a review. Cement and Concrete Research 41, 1224−1231.

Thomas, M.D.A., 2013. Supplementary Cementing Materials in Concrete. CRC Press, Boca Raton, FL, 210 p.

Thomas, M.D.A., Bamforth, P.B., 1999. Modelling chloride diffusion in concrete: effect of fly ash and slag. Cement and Concrete Research 29, 487−495.

Thomas, M.D.A., Skalny, J., 2006. Chemical resistance of concrete. In: Lamond, J.F., Pielert, J.H. (Eds.), Significance of Tests and Properties of Concrete and Concrete Making Materials. ASTM STP 169D, American Society for Testing and Materials, West Conshohocken, PA, pp. 253−273.

Thomas, M.D.A., Bremner, T., 2012. Performance of lightweight aggregate concrete containing slag after 25 years in a harsh marine environment. Cement and Concrete Research 42, 358−364.

Thomas, M.D.A., Hooton, R.D., Scott, A., Zibara, H., 2012a. The effect of supplementary cementitious materials on chloride binding in hardened cement paste. Cement and Concrete Research 42, 1−7.

Thomas, M.D.A., Green, B., O'Neal, E., Perry, V., Hayman, S., Hossack, A., 2012b. Marine performance of UHPC at treat island. In: Schmidt, M., et al. (Eds.), Proceedings of Hipermat 2012, 3rd International Symposium on UHPC and Nanotechnology for High Performance Construction Materials, Kassel, March 7−9, pp. 365−370.

Yi, H., Thomas, M.D.A., 2014. The performance of CAC concrete in an aggressive marine environment. In: Calcium Aluminates: The International Conference. France, Avignon, pp. 556−569.

Zayed, A., Sagues, A., Powers, R., 1989. Corrosion of epoxy-coated reinforcing steel in concrete. In: Corrosion 89, Paper No. 379, National Association of Corrosion Engineers, Houston, TX.

Zibara, H., 2001. Binding of External Chlorides by Cement Pastes (Ph.D. thesis). University of Toronto, Canada, 320 p.

# Marine exposure environments and marine exposure sites

7

*M. Otieno* [1], *M. Thomas* [2]
[1]University of the Witwatersrand, Johannesburg, South Africa; [2]University of New Brunswick, Fredericton, Canada

## 7.1 Introduction

The useful life of a concrete structure is highly dependent on the interaction between the structure and severity of its environmental exposure. Furthermore, concrete in a marine environment (coastal and offshore) may deteriorate as a result of the combined effects of chemical action of seawater constituents on the cement hydration products, alkali-silica reaction, crystallisation of salts in the pores, frost action in cold climates, corrosion of embedded steel in reinforced and prestressed members, physical erosion due to wave action or a combination thereof. Some of these physical and chemical deterioration mechanisms including sulphate attack, lime leaching, salt crystallisation, reinforcement corrosion, erosion and abrasion were covered in Chapter 5. Among these deterioration mechanisms, chloride-induced corrosion of the embedded steel reinforcement is generally cited as the most pernicious mode of deterioration in marine reinforced concrete structures. Consequently, most studies on concrete structures in marine environments have focused on chloride-induced corrosion. A large stock of marine concrete structures including harbours and docks, wharves, jetties, bridges, breakwaters and retaining walls is affected directly or indirectly by these modes of deterioration, considering that oceans make up to 80% of Earth's surface (Mehta and Monteiro, 2006). Also, in most cases, the risk associated with failure in these structures is usually high both from social and economic viewpoints. As a result, stringent guidelines are usually provided in concrete design codes, which reflect both prescriptive and performance-based approaches. However, these are seldom adequate and should therefore be complemented with past experiences from in situ structures and long-term laboratory and field studies to make informed decisions regarding aspects such as type of binder and aggregate, maintenance and repair strategies and so on, to minimise the inherent risk.

Even though concrete design codes provide general guidelines to achieve a concrete that is potentially resistant to deterioration in a given marine environment, in some cases such guidelines may not adequately suffice, mainly because of differences in factors affecting aggressivity of these environments including temperature, concentration of aggressive ions in the sea water, wind intensity and direction, and duration of wetting and drying cycles due to high and low tides. These factors should be taken into account if a successful durability design for marine reinforced concrete structures

**Marine Concrete Structures.** http://dx.doi.org/10.1016/B978-0-08-100081-6.00007-6
Copyright © 2016 Elsevier Ltd. All rights reserved.

is to be adopted and successfully implemented. This chapter collates these factors mainly from past studies and experiences, and it presents a general overview with the objective of drawing salient lessons that can aid practicing engineers in making informed decisions during design of new structures and in the development of maintenance and repair strategies for existing ones. More importantly, the lessons can also be used in the development of more practical and effective performance-based design guidelines for concrete structures in various marine exposure environments.

## 7.2 Variability of marine exposure environments in terms of severity

The characterisation of a marine exposure environment for either investigative or actual design purposes is an important step toward understanding and simulating the modes and rates of deterioration of concrete structures exposed to such environments. As already mentioned in Chapter 5, marine environments, with respect to deterioration of concrete structures, are conventionally categorised into exposure zones such as submerged, tidal, splash and spray zones. This classification scheme has been adopted in various concrete design codes such as the European Standard EN 206 (BS-EN 206, 2013). Based on this classification, it is usually assumed that, for example, in the case of reinforcement corrosion, the tidal zone is the most aggressive. In reality, such a decision should be based on a careful assessment of a combination of various factors, some of which have already been mentioned in the introduction of this chapter. Therefore, in addition to the conventional classification, it should be appreciated that a diversity of microclimates will exist in a given marine environment, even within a given exposure zone, and these will vary from one marine exposure environment or zone to another. All these factors need accurate characterisation to facilitate the quantification of aggressivity of a marine environment. (The reader should also refer to Chapter 14 of this book, which has further useful information on the characteristics and features of marine environments.)

An appropriate combination of the following factors should be considered when characterising a marine exposure environment in a performance-based, service-life design approach.

### *7.2.1 pH and concentration of aggressive species in the seawater*

Even though most seawaters are assumed to be fairly uniform in ionic composition and are characterised by a typical salinity of about 3.5%, variations in salinity (see Table 5.1, Chapter 5) depend on the balance between evaporation and precipitation, or freshwater inflow, and the extent of mixing between surface and deeper waters. In addition, the extent of artificial pollution, for example, from processing industries, can also have a significant influence on the ionic composition of seawater. The pH of seawater usually varies between 7.5 and 8.4, but values lower than 7.5 may be

encountered due to high concentration of dissolved carbon dioxide, which would make the seawater more aggressive to certain concretes (Mehta and Monteiro, 2006).

### 7.2.2 Temperature and relative humidity

Most deterioration processes in the marine environment involve chemical reactions that are exacerbated by an increase in temperature. Both the temperature of the water and that of the surrounding environment are important and should be considered. For example, the surrounding air temperature may determine the duration of wetness of the concrete during low tides and also the chloride threshold level for reinforcement corrosion initiation (Rincón et al., 2007). Furthermore, temperature can also increase the salinity and hence aggressiveness of the seawater by causing evaporation. Relative humidity of the surrounding marine environment can also have an influence on sustaining of various chemical deterioration processes. High relative humidity coupled with increased temperatures can accelerate damage due to various deterioration processes and also aggravate ongoing ones. In addition, both the rate of diffusion of chloride (and other) ions and the rate of steel corrosion increase with increasing temperature.

### 7.2.3 Precipitation and inflow of fresh water

The salinity of the seawater is affected by the amount of rainfall and inflow of freshwater (or polluted water) from, for example, rivers and processing industries. Rainwater can also act to wash away chlorides from the surface of the concrete, thereby diminishing the extent of chloride penetration into concrete.

### 7.2.4 Duration of wetting–drying cycles and time of wetting due to tides

These are important factors to consider especially in the tidal exposure zone. Depending on the expected mechanism of deterioration, the frequency of wetting and duration of low and high tides can significantly affect the rate of deterioration by affecting the degree of saturation of the concrete. This can affect the time to initiation and rate of progress of some deterioration mechanisms. For example, in the case of steel reinforcement corrosion, an increased degree of concrete saturation due to longer duration of wetting cycles can act to either shorten the time to attainment of the chloride threshold, and hence time to corrosion initiation, or stifle the rate of corrosion. A practical example was reported by Costa and Appleton (2002) where evidence from the docks of a shipyard located in the estuary of River Sado on the west coast of Portugal showed that the steel reinforcement was de-passivated after the first few cycles of dock filling in the upper zone that was exposed to long dry periods. These zones later showed extensive spalling in comparison to the lower zones of the dock wall, which were subject to frequent wetting cycles of about 48 h twice a month.



**Figure 7.1** Wet candle device stationed at a marine exposure environment in Cape Town. Courtesy of Alao, O.O., 2015. Refinement of Air-borne Chloride Exposure Classes for Reinforced Concrete Structures in the Cape Peninsula (M.Sc. (Eng) Dissertation). Department of Civil Engineering, University of Cape Town.

### 7.2.5 Wind intensity and direction

Wind intensity mainly affects the extent to which structures that are not in close proximity to the sea can be affected by airborne deleterious substances such as chlorides. The distance to which airborne marine species can be transported can be estimated using the well-known wet candle test (Fig.7.1) (ASTM-G-140, 2008). The direction of the wind has an effect on the spatial variability of the airborne species. Consequently, the orientation of the structure must also be borne in mind when assessing the effect of wind intensity and direction on the aggressivity of a marine environment. Further, wind intensity can cause more turbulent seas and drive spray onto structures to a greater extent than in windless conditions.

### 7.2.6 Type and amount of suspended solid particles in seawater

The type and amount of suspended solid particles in seawater affects mainly physical deterioration processes such as attrition, abrasion and erosion, and it may be a problem for structures or structural members in the tidal and splash zones, which experience frequent movement of seawater due to wave action, swells and surges. An increased amount of suspended solid particles in seawater in these zones increases the extent

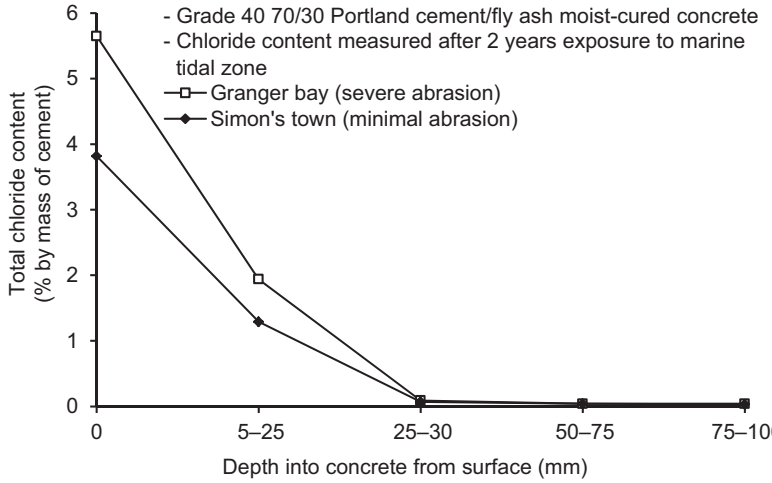



**Figure 7.2** Effect of abrasion on chloride penetration.
Based on data from Mackechnie, J.R., 1996. Predictions of Reinforced Concrete Durability in the Marine Environment (Ph.D. thesis). Department of Civil Engineering, University of Cape Town.

of deterioration of concrete as a result of removal by abrasion of insoluble salts such as brucite and aragonite, which are usually deposited on the concrete surface and hence slow down chloride ingress by blocking the surface concrete pores. The surface barrier is usually relatively thin and may be broken down by attrition from wave action and thermal effects of cracking (Buenfeld and Newman, 1986; Liam et al., 1992). Consequently, concrete that is not sheltered from physical agents causing surface damage may lose this protection, resulting in easier penetration by chlorides compared to protected concrete. Furthermore, concretes exposed to rough seas or hot climates experience more rapid ingress of chlorides in the tidal zone than lower down in the submerged zone (Liam et al., 1992). Typical results from a study by Mackechnie (1996) in different coastal areas in Cape Town are shown in Fig. 7.2, where the rate of chloride ingress was found to be higher in tidal zones with increased abrasion damage than in otherwise similar zones.

### 7.2.7 Freeze–thaw cycles

Frost action is a problem in cold climates and can contribute substantially to the severity of a marine environment. Damage due to frost action results in increased penetrability, making concrete susceptible to other forms of attack such as corrosion of the reinforcing steel. It should therefore be taken into account when assessing the severity of a marine environment. Further, the direct action of sea-ice by way of impact and abrasion on a marine structure can further damage it and needs to be accounted for in design and construction. (See Chapter 2, on *design and specification of marine*

*concrete structures.*) (See also Chapter 8 on the case study on the Confederation Bridge in Canada for examples of ice damage to marine concrete.)

### 7.2.8 Other factors

In addition to the factors already discussed, other salient factors such as structural form, distance from the sea, height of the structure and seasonal and geographical variations of parameters such as temperature, precipitation, wind intensity and duration of wetting−drying cycles affect the aggressivity of a marine environment and should therefore also be taken into account. Orientation of the structure with regard to the sea and sun can play a role in defining the severity of the microclimate. For example, parts of the structure that are exposed to frequent sunlight (eg, south-facing elements in northern latitudes, vice versa in southern latitudes) will dry more quickly and be at an elevated temperature, which will tend to increase chloride ingress during wetting periods and accelerate the onset and subsequent rate of corrosion due to increased temperature and oxygen availability.

### 7.2.9 Summary

From the previous discussion, it should be obvious that the aggressivity of a given marine environment will be influenced by a combination of interrelated factors that may have additive, synergistic or opposing effects depending on the type of deterioration under consideration. A holistic approach taking into account all the relevant factors should therefore be adopted when characterising the severity of marine exposure environments. Studies that support such an approach are available in the literature. For example, a study by Rincón et al. (2007) concluded that a holistic analysis should be carried out to establish the potential aggressivity of a marine exposure environment. Another study by Song et al. (2008) compared chloride transport in concretes from three different latitudes (the United Kingdom, Japan and Venezuela), and they found that concrete structures exposed to a tropical marine environment are more susceptible to chloride attack; they concluded that the tropical climate is a worse condition for chloride ion penetration due to the high level of relative humidity, temperature and chloride concentration.

It is therefore clear that the broad and necessarily simplistic guidelines given in concrete design codes such as EN 206 (BS-EN 206, 2013) may not be adequate in characterising and quantifying the aggressiveness of a given marine exposure environment. They can, nevertheless, give rough guidance on materials selection for given marine exposure zones. In a more rigorous and holistic approach, a combination of the various factors already discussed should be considered. These factors must also be taken into consideration when assessing and comparing the performance of concrete structures in a given marine environment or different marine environments as they can strongly influence the expected time to initiation of corrosion, rate and degree of deterioration and so on. These factors will also influence the choice of concrete-making materials, repair materials and methods, and maintenance strategies to be

adopted. In short, durability requirements for different marine microclimates should be differentiated in performance-based design approaches.

## 7.3 Categorisation of marine exposure environments

On the one hand, compared to other structural materials, concrete generally has a satisfactory record of performance in seawater (Mehta and Monteiro, 2006). On the other hand, the variability in performance of concretes in various exposure environments poses a major challenge to researchers and engineers. Melchers and Li (2009) state that '…specialist treatments and new materials may not be the solution to the problem since already some 50 years ago, Wakeman et al. (1958) posed the question "*Why do some concrete structures seem to last indefinitely in seawater while others deteriorate within a comparatively short time*?"' Similarly, some 30 years later, Burkowsky and Englot (1988) noted that for New York and New Jersey road bridges, a wide variation in durability performance was observed, even for major bridges that were essentially similar in design and construction. While some have required extensive maintenance, others are '…standing up well – even after 60 years of service. The question that begs to be answered is…why the difference?' The answer to this question lies at least in part in the variability in the characteristics of different marine exposure environments – even those conventionally perceived to be similar in aggressivity.

Numerous studies have been carried out in different marine environments around the world to assess the performance (resistance, time to corrosion initiation, rate and degree of deterioration) of concrete structures. These studies have shown that, for a given concrete, its performance is dependent not only on the concrete mix composition and quality of construction (eg, degree of compaction, adequacy of curing, etc.) but also on the various environmental or exposure factors discussed in previous sections, which cause one marine environment to differ from another.

Marine environments can be grouped into four main categories, based on marine concrete performance in different regions (Fookes et al., 1986): cool/cold, temperate, hot and dry, and hot and wet. This categorisation, which is based on the climatic region within which a marine environment exists, should not be confused with that presented in Chapters 3 and 5, which is based on the location within a given marine environment.

### *7.3.1 Cold marine environments*

Cold marine environments are characterised by near-freezing temperatures and lie mostly in far northerly or southerly latitudes where the climate usually has a marked temperature difference between summer and winter, with annual average temperatures below 10°C and summer temperatures below 20°C. Rainfall generally is moderate. In these marine environments, concretes made without entrained air are subject to cracking damage due to freeze–thaw cycles, which then results in increased concrete penetrability. Increased penetrability makes the concrete susceptible to other forms of deterioration, such as corrosion of the reinforcing steel. Therefore, the freeze–thaw

resistance of concrete is an important durability requirement for concretes in such marine environments. A good guide to concrete practice for these conditions is ACI 318 (2011). Typical examples of cool marine environments include Canada, Denmark, Norway, northeast United Kingdom, Portugal, Scotland, Sweden and areas of eastern Europe, Asia and Russia, and New Zealand and parts of South America. (See Chapters 8 and 11 for case studies in this environment.)

### 7.3.2 Temperate marine environments

These marine environments have annual average temperature ranges between 10 and 20°C, infrequent freezing temperatures and moderate rainfall. As freezing and thawing is not present in these regions, the principal causes of physical and chemical deterioration of the concrete itself are wetting and drying cycles, and salt crystallisation in the evaporation zone. Reinforcement corrosion is a principal cause of deterioration of reinforced concrete in these marine environments. Wick action of reinforced concrete in the concrete may cause the area affected to be above the actual area of contact with sea water. Typical examples of temperate marine environments include Barcelona, San Diego, San Francisco, temperate parts of Europe, for example, The Netherlands and Cape Town and others further "east". (See Chapters 10, 12 and 14 for case studies in this environment.)

### 7.3.3 Hot and dry marine environments

These environments have summer temperatures exceeding 45°C and little rainfall, which can allow the surface zone to dry significantly due to evaporation. The dry surface zone exhibits increased sorptivity potential that can lead to rapid chloride penetration on even occasional contact with seawater; this can cause deterioration in concrete well above the usual splash zone. In the case of steel corrosion, once the steel has been de-passivated by the chlorides, the rate of corrosion will also be high due to the increased availability of oxygen through the partly dry capillaries in the cover concrete. In hot-dry marine environments, aerosol deposition rates are low (BS 7527-2-3, 2014), and the presence of wind-borne salty dust particles is a more common source of chlorides than aerosol deposits even near the shore, as heavy night-time dew on cooled surfaces provides a transport medium for chlorides to penetrate the concrete. Typical examples of hot and dry marine environments include coastal regions in the Middle East (eg, Saudi Arabia, Turkey, UAE, Yemen, Iran and Oman).

Some of the countries mentioned fall within the Persian Gulf region. This is a particularly interesting hot and dry marine environment that is worth discussing in a little more detail based on past experiences. The Persian Gulf region is characterised by high ambient temperatures with salt-laden humidity and large fluctuation in the diurnal and seasonal temperature and humidity. Diurnal temperature ranges from 3 to 50°C and can vary by as much as 30°C. The relative humidity may range from 40% to 95% in a typical summer day but can be as high as 95% or as low as 5%. Tides

in the Persian Gulf have a tidal range of 2−4 m at the northern Persian Gulf and 1−2 m at the rest (Zwarts, 1991−92). It is also characterised by high salinity. A comparison of the ionic concentration of the gulf and other seas shows the higher salinity of the Gulf seawater, with chloride ion concentration of about 3.6% (see Table 5.1, Chapter 5). This has been attributed to the semi-isolation of the Arabian sea, type of ocean current system, high level of evaporation and little rainfall and freshwater inflow of rivers (Shekarchi et al., 2009). These exposure conditions can cause concrete temperatures to rise up to 60°C and higher (Fookes, 1993) resulting, on the one hand, in temperature-induced strains that cause microcracking of the concrete in cases where movements are restrained, and on the other hand, in an increased rate and depth of chloride penetration. The cracks increase the penetrability of concrete to ingress by deleterious substances such as chlorides.

In recent decades, the Persian Gulf region has experienced significant development in marine construction, but many reinforced concrete structures are showing signs of deterioration, mainly due to the chloride-induced corrosion of reinforcement (Safehian and Ramezanianpour, 2013). As a result, most structures in this region have been characterised by shorter service life spans than their counterparts elsewhere (Shekarchi and Moradi, 2007; Tamimi et al., 2008; Ramezanianpour et al., 2011). In many cases, even structures that meet the requirements of concrete codes have been observed to show corrosion problems in the early years of their service life (Ghods et al., 2007). These observations are clearly as a result of the severe marine exposure conditions, which pose a major challenge to reinforced concrete construction. The experience gained from existing deteriorating reinforced concrete structures in this region has led to researchers and engineers adopting customised approaches in an attempt to mitigate against the rapid deterioration process (Ramezanianpour et al., 2012). (See Chapter 9 for a case study in this environment.)

### 7.3.4 Hot and wet or moist marine environments

These environments are typical in tropical regions where the annual average temperature ranges from 24 to 35°C. The average annual rainfall and relative humidity ranges from 1000 to over 1500 mm and from 60% to 96%, respectively, while the salinity of the seawater ranges between 26% and 32%. There are two main seasons: the wet season and the dry season, with trade winds which blow year round, being moist as they have passed over warm seas (Liam et al., 1992; London and Senior, 1992; Wilson, 2005). However, these marine environments can have high variations of humidity, temperature, wind speed and direction, and amount of chlorides that could be deposited on the structures (Castro et al., 2001). With respect to chloride ingress into concrete in these marine environments, studies have shown that the environmental conditions of a tropical climate promote the formation of two zones in a member: one internal that is always damp (in near-saturated condition) and one external that is exposed to wetting and drying cycles (Castro et al., 2001). Typical examples of hot and moist marine environments include Bangkok, Calcutta, Hong Kong,

Singapore, Gulf of Mexico, coastal areas of Cuba, Yucatán, México, and Shenyang and Wanning cities in China. (See Chapters 13, 15 and 16 for case studies in this environment.)

In summary, the rate of deterioration is usually higher in the hot-dry and hot-wet marine exposure environments when compared to the other zones. It should therefore be appreciated that marine exposure environments around the world are not the same and must be treated as such. Furthermore, because sea temperatures and ocean currents close to the shore have a major influence on the coastal climate, emphasis should be placed on the localised coastal climate rather than the predominant inland weather conditions.

## 7.4 Holistic approach to quantification of severity of marine exposure environments

It is now clear that in addition to the conventional marine exposure classification of tidal, splash, spray and submerged zones (see Chapter 5), a holistic approach that takes into consideration the climatic zone (cool, temperate, hot and wet, and hot and dry) of a given marine environment in quantifying the severity of each of these exposure zones should be adopted. Such an approach acknowledges that marine environments around the world are far more varied than any concrete code of practice has recognised, and it will demand that we go beyond the recommendations of these codes if a performance-based, service-life approach is to be realistic. For this to be achieved, much research attention is still needed to quantify and incorporate the effects of different marine exposure conditions in prediction models. In doing this, attention should be given to differences in the severity of marine exposure categories discussed in the previous sections.

In short, it is not sufficient to specify only the exposure zone (tidal, splash, spray or submerged) of a concrete structure in a marine environment; the corresponding climatic conditions should also be specified and allowed for when assessing the severity of a marine environment. A typical example of an attempt to apply such an approach in the case of chloride-induced corrosion of steel was suggested by Slater and Sharp (1998). In their approach, the severity of a marine exposure zone is arbitrarily rated (from 1 to 12) not only based on the exposure zone (submerged, tidal, splash/spray) but also on the climatic zone of the marine environment (cool, temperate, hot-wet, hot-dry). However, for such an approach to be useful in durability design, the severity rating should represent a quantifiable deterioration parameter such as chloride concentration, duration of wetting−drying cycles, ambient temperature and so on, or a combination thereof. Another example where the severity of marine environment has been characterised was presented by Alexander and Beushausen (2007). In their case, modifications were made to some of the BS EN 206 (BS EN 206, 2013) exposure classes to accommodate severe abrasion from sea water that is experienced in some coastal environments in South Africa (see Table 7.1).

**Table 7.1 Marine exposure classes adopted in South Africa**

| EN 206-1 class | Description of the exposure environment |
|---|---|
| XS1 | Exposed to airborne salt but not in direct contact with sea water |
| XS2a | Permanently submerged |
| XS2b[a] | XS2a + exposed to abrasion |
| XS3a | Tidal, splash and spray zones |
| XS3b[a] | XS3a + exposed to abrasion |

[a]Subclasses added for South African coastal conditions.
Alexander, M.G., Beushausen, H., 2007. Performance-based durability design and specification in South Africa. In: Proceedings of the International Concrete Conference and Exhibition (ICCX - Concrete Awareness), 14–16 February, 2007, Cape Town, South Africa; based on BS-EN-206, 2013. Concrete - Part 1: Specification, Performance, Production and Conformity. European Standard.

## 7.5 Examples of marine sites around the world: field testing of marine concrete

One of the main reasons for limited data on deterioration of marine concrete structures is the relatively slow nature of the deterioration processes. This has led to adoption of accelerated and simulated laboratory tests that provide data within a short duration depending on the testing technique used. However, even though deterioration of concrete in real marine exposure conditions may take many years to reach a meaningful extent, it allows for deterioration mechanisms to be accurately assessed under normal exposure conditions, which is not possible with accelerated laboratory tests. Results from field investigations are also essential for determining the long-term performance of concrete, validating findings from early age durability tests and ultimately refining specifications, test procedures and management strategies.

Even though attempts have been made to simulate marine exposure environments in the laboratory, the complex physicochemical interactions between sea water and the constituents of concrete make it very difficult. Simulated marine exposure environments also have a number of limitations. For example, the multivariate effect of a marine environment is diminished by considering one variable in isolation. In most cases, the variable perceived to be most dominant in a given mechanism of deterioration is isolated and studied while ignoring the synergistic effect of other variables. In some cases, even though concrete is exposed to real marine environments, this is done under controlled conditions in tanks, estuaries or cages and barriers; see Fig. 7.3 (Cook et al., 1989; Gjørv et al., 1994). This, contrary to observations in in-service marine concretes (Buenfeld and Newman, 1986; Liam et al., 1992), assumes that effects such as wave action, abrasion, tidal action and surface drying are insignificant and do not accelerate the deterioration process. Such exposure conditions can be considered close to reality but may be relatively mild in comparison to real marine exposure conditions. Even

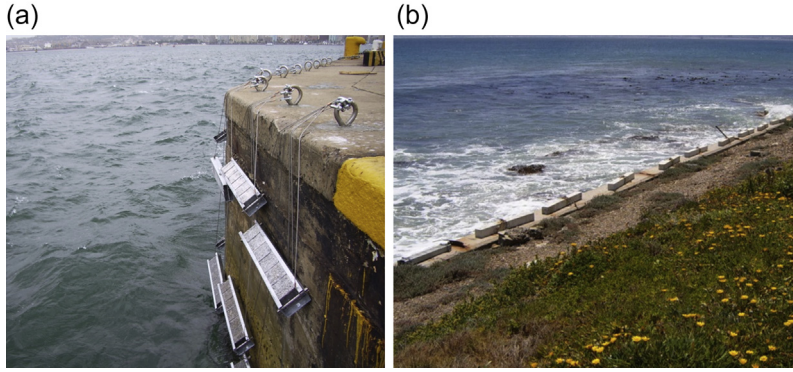



**Figure 7.3** Caged concrete specimens exposed to (a) tidal zone in Durban, and (b) splash zone in Cape Town, to monitor chloride ingress.
Courtesy of R. Heiyantuduwa.

though conflicting evidence has been reported in some marine environments, the reduction in severity of the marine environment in such exposure conditions is attributed to concrete being sheltered from wave action, but conflicting evidence has been found in other environments (Liam et al., 1992).

Various exposure sites around the world have been used to study concrete deterioration in marine environments. Typical examples include the Building Research Establishment's (BRE) marine exposure site (established in the late 1970s) at Shoeburyness on the Thames estuary in Essex, United Kingdom, which uses a series of steel racks and tanks to contain concrete specimens in the tidal zone samples (Osborne, 1994), and the Dundee marine exposure site on the Tay estuary, a sheltered site with small concrete specimens being stacked in steel cages suspended in the sea (Dhir et al., 1993). Mackechnie (1996) asserts that these conditions do not represent the extreme conditions experienced by in situ concrete such as cracking from thermal and shrinkage effects. These differences should be taken into account in durability design of marine concrete. One way to overcome these challenges is to use large concrete specimens or in-service structures as opposed to small-sized or medium-sized RC members (eg, Fig. 7.4 and Fig. 7.5). For example, Malhotra et al. (1987) used fairly large free-standing reinforced concrete specimens for marine exposure testing in the tidal zone of the Bay of Fundy to simulate realistic marine conditions.

Table 7.2 presents a summary of field exposure studies in various marine sites around the world, including the key findings thereof.

## 7.6 Lessons learnt from past experience and studies

Valuable lessons from monitoring the performance of concrete structures in various marine environments around the world are important and can help in streamlining the design, maintenance and repair criteria for new and existing structures. With

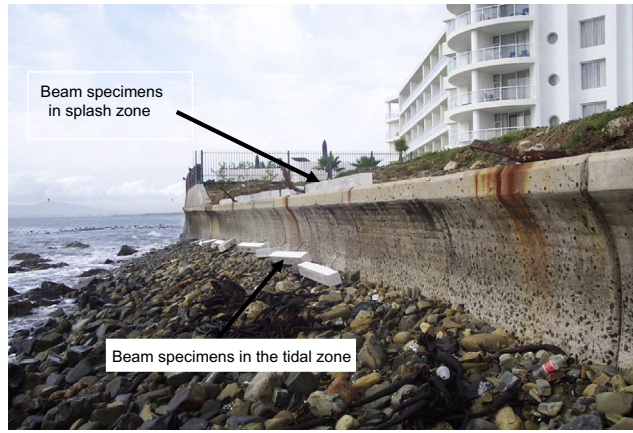



**Figure 7.4** Medium-sized (150 × 150 × 1500 mm) beam specimens in the tidal and splash zones in Granger Bay, Cape Town, to monitor corrosion.

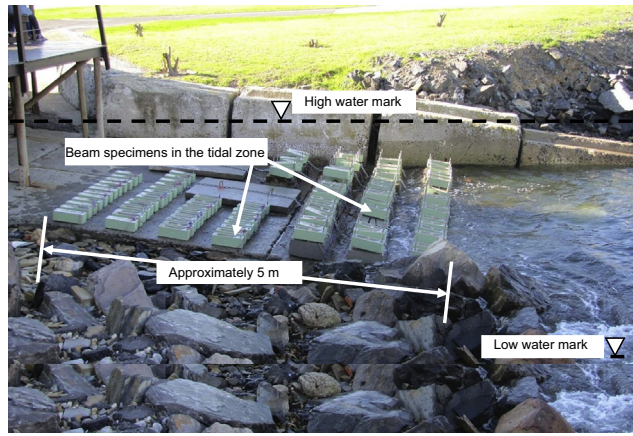



**Figure 7.5** Small-sized (120 × 130 × 375 mm) beam specimens in the tidal zone in Table Bay, Cape Town.

respect to design of new structures, lessons from past experience can aid in identifying the salient factors to be incorporated in future designs and in the development of service-life prediction models to ensure they are as close a representation of reality as possible. Furthermore, the lessons from real-life situations can be used to update concrete design codes. Some of these lessons are summarised in the following sections.

### *7.6.1 Dominant mechanism of deterioration*

Various forms of deterioration can occur in marine concrete structures; these are covered in Chapter 5. In reinforced and prestressed marine concrete structures, there is a general consensus that chloride-induced corrosion of steel reinforcement is the

**Table 7.2 Summary of some marine exposure sites around the world**

| Exposure site | Exposure zone and duration | Other details | Key findings |
|---|---|---|---|
| Tay estuary<br>Air temperature: 20°C<br>Sea water temperature: 4−14°C<br>Relative humidity: 95%<br>Sea water chloride content: 14%<br>Dhir et al. (1993) | • Splash zone<br>• 5 years | • Full-scale reinforced concrete specimens:<br>  • Beams: 5 × 425 × 325 mm<br>  • Columns: 500 × 375 × 340 mm<br>  • Slabs: 675 × 425 × 250 mm<br>• Concrete grades: 20−60 N/mm$^2$<br>• Binder: plain PC, PC/PFA<br>• w/b ratio: variable (0.35−0.82) | • Good correlation between laboratory and field specimens with respect to relationship between half-cell potential and corrosion rate |
| West coast of Malaysia (Port Dickson)<br>Annual average RH: 84%<br>Annual mean temperature: 27 ± 1.7°C<br>Mustafa and Yusof (1994) | • Spray zone<br>• 1 year | • 100-mm cube specimens<br>• Binder: plain PC (365 kg/m$^3$)<br>• w/b ratio: 0.50<br>• Specimens placed at distances:<br>  • 30 m from seashore and 5 m above sea level<br>  • 30 m from seashore and 15 m above sea level<br>  • 400 m from seashore and 5 m above sea level<br>  • 400 m from seashore, 5 m above sea level and protected from directly facing the sea | • Chloride content at any given depth in concrete not only increased with proximity to seashore but also depended on the exposure conditions of the specimens; even when the specimens were at the same location, the specimens at higher altitude of those protected from direct wind had less chloride content<br>• It is necessary to examine the chloride content distribution in different parts of a concrete structure |

| | | | |
|---|---|---|---|
| Mediterranean sea<br>Annual average temperature: 17°C (Range: 11.2−25.9°C)<br>Annual rainfall: 575 mm/m$^2$<br>Wind: east-northeast at 6.5 km/h<br>Moreno et al. (2015) | • 20 m from edge of sea (16 m from water line)<br>• 45 years | • Building in Cullera (Spain) is 10 m above sea level<br>• Building composed of reinforced concrete frames with floor slabs<br>• Tests carried out on beams, joists and columns<br>• Sea water temperature is between 12°C in winter to 24−25°C in August and September | • Chloride contents in the concrete were high (average of 0.7%)<br>• Concrete cover was completely carbonated<br>• Deep pitting in the reinforcement, which in some cases was accompanied by salt sediments in and around the corroded areas, even after being treated with $HNO_3$ |
| Table Bay, Cape Town (see Fig. 7.5)<br>Otieno et al. (2015) | • Tidal zone<br>• Ongoing (since 2010) | • Cracked and uncracked 120 × 130 × 375 mm beams with a single steel bar (20- and 40-mm cover) exposed to marine tidal zone<br>• Single surface flexural crack widths of 0.4 and 0.7 mm were used; some specimens were also cracked but unloaded to assess the effect of incipient cracks<br>• Concretes made using two w/b ratios (0.40 and 0.55), and three binders (100% CEM I 42.5N plain Portland cement (PC), 50/50 PC/GGBS, and 70/30 PC/FA) | • The severity of corrosion propagation in the tidal zone is not only dependent on the wetting and during cycles but also on the frequency or duration of the cycles<br>• Corrosion rates in the fly ash- and slag-blended concretes have been found to be significantly lower than those in Portland cement concretes of the same cover depth, crack width and w/b ratio<br>• Total chloride contents at the steel level as high as 3% by mass of binder have been measured in the cracked specimens; however, these do not correspond to high corrosion rates in the specimens<br>• Effects of abrasion are also being observed on the specimens (see Fig. 7.6) |

*Continued*

**Table 7.2 Continued**

| Exposure site | Exposure zone and duration | Other details | Key findings |
|---|---|---|---|
| Norwegian coastline, eg, Trondheim and Oslo harbours Gjorv (1994) | • Variable marine exposure conditions | • Harbour structures (up to 80 years old)<br>• Coastal bridges (less than 25 years old)<br>• Offshore concrete structures (50−60 years old) | • Most of the effects of corrosion appeared after 5 years of exposure<br>• The harbour structures still showed remarkable serviceability; these structures had a minimum cement content of 400 kg/m$^3$ and a cover thickness of 100 mm; strength requirement was 35 MPa; the deck slabs performed better than deck beams in terms of steel corrosion<br>• The coastal bridges performed poorly due to premature corrosion; those parts of the bridges that have been exposed to prevailing winds and salt spray showed the least chloride penetration compared to that of the more protected parts; older bridges performed better than those built after 1970; this was attributed to improved concrete technology, which required very strict quality assurance and control<br>• No corrosion problems reported on the offshore structures<br>• Corrosion of embedded steel poses the greatest threat to the long-term performance of concrete structures in this environment<br>• Proper selection of concrete quality and cover thickness, in addition to proper quality assurance and quality control can ensure that reinforced and prestressed concrete remains serviceable with little or no maintenance for a long period of time in this marine environment |

| | | | |
|---|---|---|---|
| Thames estuary in Essex (BRE exposure site)<br>Average annual temperature: 10.1°C<br>Average annual rainfall: 552 mm<br>Chloride concentration: 18.2 g/L (total salinity 32.5 g/L) | • Submerged, tidal and splash zone (see Fig. 7.7) | Site was abandoned around 2000 as there were insufficient funds for maintenance<br>Reinforced and unreinforced concrete specimens | • No corrosion of embedded steel for fully submerged samples (lack of oxygen)<br>• Corrosion of embedded steel in tidal zone and splash zone<br>• Chloride profiles show benefits of using fly ash (Thomas and Matthews, 2004) and slag (Osborne, 1999) |
| Treat Island, near Eastport, Maine, USA<br>Average annual temperature: 6.6°C<br>Average annual rainfall: 1139 mm<br>Chloride concentration: 19.3 g/L (total salinity 35.2 g/L) | • Submerged, tidal and splash zone (see Fig. 7.8)<br>• Highest tides in the world (up to 6.7 m)<br>• 100 to 160 freeze−thaw cycles per year | Site established in 1936 and owned by U.S. Army Corps of Engineers<br>Multiple research studies on concrete have been conducted at this site over the past 8 decades | • No corrosion of embedded steel for fully submerged specimens (lack of oxygen) or specimens on mid-tide wharf<br>• Corrosion of embedded steel exposed just at high tide level<br>• Chloride profiles show benefits of using fly ash (Thomas et al., 2011)<br>• Data have been used to validate service-life model, Life-365 (Thomas et al., 2011) |

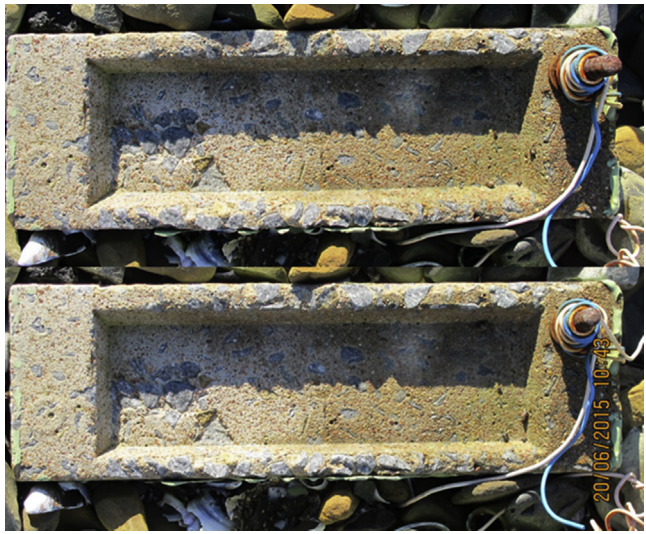



**Figure 7.6** Abraded concrete specimens after 4 years of exposure in the tidal zone in Table Bay, Cape Town.



**Figure 7.7** Specimens in the tidal zone in the BRE exposure site, Thames estuary in Essex.

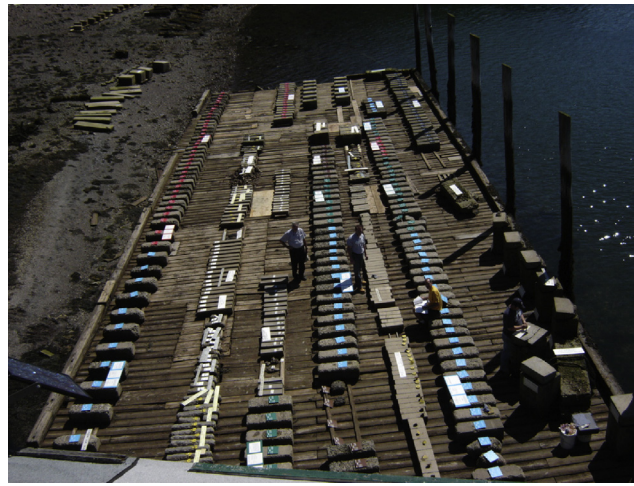


**Figure 7.8** Specimens in the tidal and splash exposure zones in Treat Island, near Eastport, Maine, USA.

main cause of durability failure. This mechanism is very severe in marine environments in hot-dry and hot-wet/humid climates such as the Persian Gulf and tropical zones, respectively. With respect to corrosion initiation, researchers have made various observations. For example, Melchers and Li (2009) reviewed a number of long-term studies on the performance of reinforced concrete structures in various natural marine environments around the world including South Africa, United States, United Kingdom, Austria and The Netherlands, and they observed that the time to corrosion initiation did not depend strongly on the concentration of chlorides at the reinforcement. Similar results have also been reported in accelerated laboratory and natural field studies where high chloride concentrations are measured at the steel level, but corrosion initiation is not observed or very low corrosion rates between 0.1 and 0.5 $\mu A/cm^2$ (Broomfield et al., 1993) are observed (Castel et al., 2003; Otieno, 2014). The time to corrosion initiation is mainly dependent on the availability of oxygen to support the cathodic reaction. This is governed largely by the duration of the drying period, which for structures or structural members in the tidal zone depends on the duration of wetting due to the high and low tides. This also affects the rate of corrosion after its initiation.

### 7.6.2 Effect of concrete mix composition and quality on durability performance

Other chapters have stressed the importance of materials selection and design for the durability of concrete structures in marine environments. The use of blended cement concretes is certainly preferred, if not essential, to using plain Portland cement concretes due to the superior durability performance of the former. A number of short-term and long-term accelerated and natural (field) studies that have been carried out in the past have motivated the adoption of blended cement concretes mainly due to

decreased penetrability and chloride binding capacity (Leng et al., 2000; Tarek et al., 2002; Luoa et al., 2003; Scott and Alexander, 2007; Thomas et al., 2008, 2011).

For example, some studies have focused on the utilisation of fly ash in concrete to protect reinforced concrete within marine sites in hot and humid climate zones, for example, the Gulf of Thailand (Chalee and Jaturapitakkul, 2009; Chalee et al., 2010). Results from these studies indicate that in addition to just using fly ash, increasing its fineness and the level of Portland cement replacement results in a significant increase in resistance of the concrete to chloride penetration and hence increased time to steel corrosion initiation and decreased corrosion rates. Additionally, where the climate varies greatly from warm summers to cool winters (eg, in Essex, United Kingdom, marine site), Thomas and Matthews (2004) also found that chloride concentration at a given depth in the concrete as well as steel corrosion were reduced significantly in fly ash concretes compared to concrete without fly ash.

In another case, Castel et al. (2003) reported that even though, for many marine structures, the time to corrosion initiation was less than 5 years, it was considerably greater for reinforced concrete structures constructed using limestone or (nonreactive) dolomite aggregates, or with blast furnace slag cement. For these cases, the time to corrosion initiation was at least 10 years and in most cases greater than 15 years or even greater. For most of the structures studied, it was less than about 20 years, consistent with anecdotal observations for many modern marine reinforced concrete structures.

Mehta and Monteiro (2006) reported that in the mild climates of southern France and southern California, *unreinforced* mortar and concrete specimens remained in excellent condition after more than 60 years of seawater exposure, except when the penetrability of concrete was high. Concretes with high penetrability showed considerable loss of mass due to magnesium ion attack, carbon dioxide attack and calcium leaching. In spite of the use of high $C_3A$ Portland cements, expansion and cracking of concrete due to ettringite was not observed in low-permeability concretes. It was therefore concluded that, in this case, the effect of cement composition on durability to seawater was apparently less significant than the effect of the penetrability of concrete. However, this may not be the case in other deterioration mechanisms such as steel corrosion due to chloride ingress where, in addition to concrete penetrability, binder type also plays a significant role in its mitigation by, for example, helping to bind chloride ions.

In general, a proactive approach to selection of concrete mix constituents taking into account both the anticipated mechanism of deterioration and a carefully characterised marine environment with respect to its severity is imperative if service-life design for marine concrete structures is to be adequate.

### 7.6.3 Effect of cracking

The presence of cracks in marine concrete structures, if not taken into account, can significantly diminish the positive gains of good concrete durability design. Many studies have shown that cracks significantly increase the penetrability of concrete (Malhotra, 1987) and consequently shorten or eliminate the time to corrosion initiation

and increase the rate of corrosion propagation (Miyagawa, 1985; Suzuki et al., 1990; Pettersson and Jorgensen, 1996; Raupach, 1996; Scott and Alexander, 2007; Otieno et al., 2010). Therefore, in addition to characterisation and quantification of the severity of a marine environment, service-life prediction models should take into account the effect of cracking on the rate of deterioration. For example, Mehta and Monteiro (2006) reported that piers of the San Francisco Ferry Building in California, in spite of having a low-permeability concrete, experienced corrosion-induced cracking in the reinforced concrete members after 46 years of service that was attributed to poor consolidation of concrete and structural microcracking, which increased the penetrability of the concrete. It is therefore important that the inevitable presence of cracking is taken into account when carrying our durability design of marine reinforced and prestressed concrete structures. This can be done by using relevant service-life models that take into account the transport mechanisms of various species in cracked concrete.

### 7.6.4 Spatial variability of deterioration

The fluctuation of different environmental and concrete-related (intrinsic and extrinsic) factors influencing the deterioration of marine concrete structures affects both the time to initiation and degree of a given form of deterioration in different locations in the structure. Some of these factors including temperature, structural form and orientation, concrete penetrability and distance from the sea have been discussed in this chapter and in other chapters of this book. As a result, deterioration in a concrete structure in a marine environment may not be uniform throughout the structure. The effect of spatial variability has been acknowledged by some researchers (eg, Liu and Weyers, 1998; Melchers and Li, 2006; Yuan et al., 2010) but is yet to be successfully quantified and incorporated in prediction models and design codes mainly because of the complexity involved in choosing the most suitable durability design for each micro-exposure condition of the structure. The current conservative approach, in most cases, is to adopt one exposure condition deemed to be most severe with respect to a given mechanism of deterioration and design for that. In many cases, this is probably the most practical route, but it is conceivable that in other cases this may be unduly conservative.

In summary, this chapter has presented a strong case for a more stringent characterisation of marine exposure environments in addition to the commonly used criterion that uses four main zones (submerged, tidal, splash/spray and airborne). This should then be incorporated into service-life prediction models to facilitate a successful implementation of performance-based design approaches and development of effective maintenance repair strategies for marine concrete structures.

## 7.7 Future trends

The adoption of an approach of characterising marine environments that takes into account the climatic zone is bound to be faced with the challenge of climate change,

more specifically, global warming. This will require that concrete specialists make design codes easily adaptable to change in climatic conditions. The deterioration of marine concrete will also need a better understanding of transport mechanisms in cracked concrete so that these can be incorporated into service-life prediction models. Much research is still needed in this area. It is also imperative for more research to better understand certain deterioration mechanisms such as sulphate attack and soft water attack to improve on the characterisation of severity of a marine environment (Neville, 2006).

## Sources of further information and advice

### *Further reading*


- Alexander, M., Thomas, M., 2015. Service life prediction and performance testing − current and practical developments. Cement and Concrete Research 78, 155−164.
- Ballim, Y., Alexander, M.G., Beushausen, H.-D., Moyo, P., 2008. Reflections on future needs in concrete durability research and development. Proceedings of the 2nd International Conference on Concrete Repair, Rehabilitation and Retrofitting, 24−26th November, Cape Town, South Africa, 73−80.
- Gjørv, O.E., 2009. Durability Design of Concrete Structures in Severe Environments. Taylor & Francis, ISBN:9780415414081.
- Mehta, P.K., Bremner, T.W., 1996. Concrete in the marine environment − some lessons for the future. In: Mehta, P.K. (Ed.), Proceedings of the 3rd International Conference on Performance of Concrete in the Marine Environment, St Andrews by the Sea, New Brunswick, Canada, pp. 175−190.
- Mehta, P.K., Monteiro, P.J.M., 2006. Concrete − Microstructure, Properties and Materials, third ed. McGraw Hill, New York.
- Mehta, P.K., 2003. Concrete in the Marine Environment. Taylor & Francis, ISBN:978-0-203-49825-5.
- Moreno, J.D., Bonilla, M., Adam, J.M., Borrachero, M.V., Soriano, L., 2015. Determining corrosion levels in the reinforcement rebars of buildings in coastal areas − a case study in the Mediterranean coastline. Construction and Building Materials 100, 11−21.
- Slater, D., Sharp, B.N., 1998. Chapter 6 − Concrete in Coastal Structures, Allen, R.T.L. (Ed.), Thomas Telford.
- SP-65, 1980. Performance of Concrete in Marine Environment. American Concrete Institute, ISBN:9780870317019.


### *Concrete codes*


- BS EN 206, 2013. Concrete − Part 1: Specification, performance, production and conformity. European Standard.
- BS 6349-1, 2000. Maritime structures − Part 1: Code of Practice for General Criteria. British Standards, London.
- BS 7527:2-3, 2014. Classification of Environmental Conditions − Part 2−3: Environmental Conditions Appearing in Nature − Air Pressure. British Standards Institution.
- Fib Model Code, 2010. 3rd FIP/CEB Model Code for Concrete Structures. Comite Euro-International du Beton and Federation International de Precontrainte.

## References

ACI-318-11, 2011. Building Code Requirements for Structural Concrete. American Concrete Institute, Farmington Hills, MI, ACI.

Alao, O.O., 2015. Refinement of Air-borne Chloride Exposure Classes for Reinforced Concrete Structures in the Cape Peninsula (M.Sc. (Eng) Dissertation). Department of Civil Engineering, University of Cape Town.

Alexander, M.G., Beushausen, H., 2007. Performance-based durability design and specification in South Africa. In: Proceedings of the International Concrete Conference and Exhibition (ICCX - Concrete Awareness), 14−16 February, 2007, Cape Town, South Africa.

ASTM-G-140, 2008. Standard Test Method for Determining Atmospheric Chloride Deposition Rate by Wet Candle Method. Annual Book of ASTM Standards, Philadelphia, USA.

Broomfield, J.P., Rodriguez, J., Ortega, L.M., Garcia, A.M., 1993. Corrosion rate measurements in reinforced concrete structures by a linear polarization device. In: Proceedings of the International Symposium on Condition Assessment, Protection, Repair, and Rehabilitation of Concrete Bridges Exposed to Aggressive Environments, ACI Fall Convention, 9th−10th November, Minneapolis, MN, pp. 644−651.

BS-7527-2-3, 2014. Classification of Environmental Conditions − Part 2-3: Environmental Conditions Appearing in Nature - Air Pressure. British Standards Institution.

BS-EN-206, 2013. Concrete − Part 1: Specification, Performance, Production and Conformity. European Standard.

Buenfeld, N.R., Newman, J.B., 1986. The development and stability of surface layers on concrete exposed to sea-water. Cement and Concrete Research 16 (5), 721−732.

Burkowsky, B., Englot, J., 1988. Analyzing good deck performance on port authority bridges. Concrete International 10 (11), 25−33.

Castel, A., Vidal, T., Francois, R., Arliguie, G., 2003. Influence of steel-concrete interface quality on reinforcement corrosion induced by chlorides. Magazine of Concrete Research 55 (2), 151−160.

Castro, P., Rincón, O.T., Pazini, E.J., 2001. Interpretation of chloride profiles from concrete exposed to tropical marine environments. Cement and Concrete Research 31 (4), 529−537.

Chalee, W., Jaturapitakkul, C., 2009. Effect of w/b ratios and fly ash finenesses on chloride diffusion coefficient of concrete in marine environment. Materials and Structures 42 (4), 505−515.

Chalee, W., Ausapanit, P., Jaturapitakkul, C., 2010. Utilization of fly ash concrete in marine environment for long term design life analysis. Materials and Design 31 (3), 1242−1249.

Cook, D.J., Hinczak, I., Jedy, M., Cao, H.T., 1989. The behaviour of slag cement concretes in marine environment - chloride penetration. In: ACI SP-114-3rd International Conference on Fly Ash, Silica Fume, Slag and Natural Pozzolans in Concrete, Detroit, USA, pp. 1467−1483.

Costa, A., Appeleton, J., 2002. Case studies of concrete deterioration in a marine environment in Portugal. Cement and Concrete Composites 24 (1), 169−179.

Dhir, R.K., Jones, M.R., McCarthy, M.J., 1993. Quantifying chloride-induced corrosion from half-cell potential. Cement and Concrete Research 23 (6), 1443−1454.

Fookes, P.G., Simm, J.D., Barr, J.M., 1986. Marine concrete performance in different climatic environments. In: Proceedings of the International Conference on Concrete in the Marine Environment. The Concrete Society, London, pp. 115−130.

Fookes, P.G., 1993. Concrete in the Middle East: past, present and future − a brief review. Concrete (July/August), 14−20.

Ghods, P., Alizadeh, R., Chini, M., Hosseini, M., Ghalibafian, M., Shekarchi, M., 2007. Durability-based design in the Persian Gulf. Concrete International (December), 50–55.

Gjørv, O.E., Tan, K., Zhang, M.H., 1994. Diffusivity of chlorides from sea water into high strength lightweight concrete. ACI Materials Journal 91 (5), 447–452.

Gjørv, O.E., 1994. Steel corrosion in concrete structures exposed to Norwegian marine environment. Concrete International 16 (4), 35–39.

Leng, F., Feng, N., Lu, X., 2000. An experimental study on the properties of resistance to diffusion of chloride ions of fly ash and blast furnace slag concrete. Cement and Concrete Research 30 (6), 989–992.

Liam, K.C., Roy, S.K., Northwood, D.O., 1992. Chloride ingress measurements and corrosion potential mapping study of a 24-year-old reinforced concrete jetty structure in a tropical marine environment. Magazine of Concrete Research 44 (160), 205–215.

Liu, T., Weyers, R.W., 1998. Modelling the dynamic corrosion process in chloride contaminated concrete structures. Cement and Concrete Research 28 (3), 365–379.

London, N.A., Senior, M., 1992. Principles of Geography for Caribbean Examinations Council, second ed. Longman. ISBN-13:978-0582039896.

Luoa, R., Caib, Y., Wang, C., Huanga, X., 2003. Study of chloride binding and diffusion in GGBS concrete. Cement and Concrete Research 33 (1), 1–7.

Mackechnie, J.R., 1996. Predictions of Reinforced Concrete Durability in the Marine Environment (Ph.D. thesis). Department of Civil Engineering, University of Cape Town.

Malhotra, V.M., Carette, G., Bremner, T., 1987. Durability of concrete containing supplementary cementing materials in marine environment. In: ACI SP-100-Katherine and Bryant Mather International Conference on Concrete Durability, Detroit, USA, pp. 1227–1258.

Malhotra, V.M., 1987. Properties of fresh and hardened concrete incorporating ground granulated blast furnace slag. In: Malhotra, V.M. (Ed.), Supplementary Cementing Materials for Concrete. Minister of Supply and Services, Canada, pp. 291–336.

Mehta, P.K., Monteiro, P.J.M., 2006. Concrete – Microstructure, Properties and Materials, third ed. McGraw Hill, New York.

Melchers, R.E., Li, C.Q., 2006. Phenomenological modeling of reinforcement corrosion in marine environments. ACI Materials Journal 103 (1), 25–32.

Melchers, R.E., Li, C.Q., 2009. Reinforcement corrosion initiation and activation times in concrete structures exposed to severe marine environments. Cement and Concrete Research 39 (11), 1068–1076.

Miyagawa, T., 1985. Early Chloride Corrosion of Reinforcing Steel in Concrete (Ph.D. thesis). Department of Civil Engineering, University of Kyoto.

Moreno, J.D., Bonilla, M., Adam, J.M., Borrachero, M.V., Soriano, L., 2015. Determining corrosion levels in the reinforcement rebars of buildings in coastal areas – a case study in the Mediterranean coastline. Construction and Building Materials 100, 11–21.

Mustafa, M.A., Yusof, K.M., 1994. Atmospheric chloride penetration into concrete in semi-tropical marine environment. Cement and Concrete Research 24 (4), 661–670.

Neville, A.M., 2006. Neville's Insights and Issues. Thomas Telford, London, 314 pp.

Osborne, G.J., 1994. The durability of gasifier slag and fly ash cement concretes in aggressive environments. In: 2nd International Conference: Ash – A Valuable Resource, South African Coal Ash Association, Midrand, South Africa, pp. 535–558.

Osborne, G.J., 1999. Durability of Portland blast-furnace slag cement concrete. Cement and Concrete Composites 21 (1), 11–21.

Otieno, M.B., Alexander, M.G., Beushausen, H.-D., 2010. Corrosion in cracked and uncracked concrete – influence of crack width, concrete quality and crack re-opening. Magazine of Concrete Research 62 (6), 393–404.

Otieno, M., Beushausen, H., Alexander, M., 2015. Chloride-induced corrosion of steel in cracked concrete − Part I: Experimental studies under accelerated and natural marine environments. Cement and Concrete Research 79, 373−385.

Otieno, M., 2014. The Development of Empirical Chloride-induced Corrosion Rate Prediction Models for Cracked and Uncracked Steel Reinforced Concrete Structures in the Marine Tidal Zone (Ph.D. thesis). Department of Civil Engineering, University of Cape Town.

Pettersson, K., Jorgensen, O., 1996. The effect of cracks on reinforcement corrosion in high-performance concrete in a marine environment. In: Third ACI/CANMET Int. Conference on the Performance of Concrete in Marine Environment, St. Andrews, Canada, pp. 185−200.

Ramezanianpour, A.A., Pilvar, A., Mahdikhani, M., Moodi, F., 2011. Practical evaluation of relationship between concrete resistivity, water penetration, rapid chloride penetration and compressive strength. Construction and Building Materials 25 (1), 2472−2479.

Ramezanianpour, A.A., Jahangiri, E., Ahmadi, B., Moodi, F., 2012. Evaluation and modification of the fib service-life design model for the Persian Gulf region. In: Proceedings of the Fib Symposium on Concrete Structures for Sustainable Community, June 11−14, Stockholm, Sweden.

Raupach, M., 1996. Chloride-induced macrocell corrosion of steel in concrete - theoretical background and practical consequences. Construction and Building Materials 10 (5), 329−338.

Rincón, O.T., Sánchez, M., Millano, V., Fernández, R., Partidas, E.A., Andrade, C., Martínez, I., Castellote, M., Barboza, M., Irassar, F., Montenegro, J.C., Vera, R., Carvajal, A.M., Gutiérrez, R.M., Maldonado, J., Guerrero, C., Saborio-Leiva, E., Villalobos, A.C., Tres-Calvo, G., Torres-Acosta, A., Pérez-Quiroz, J., Martínez-Madrid, M., Almeraya-Calderón, F., Castro-Borges, P., Moreno, E.I., Pérez-López, T., Salta, M., Melo, A.P., Rodríguez, G., Pedrón, M., Derrégibus, M., 2007. Effect of the marine environment on reinforced concrete durability in Iberoamerican countries: DURACON project/CYTED. Corrosion Science 49, 2832−2843.

Safehian, A., Ramezanianpour, A.A., 2013. Assessment of service life models for determination of chloride penetration into silica fume concrete in the severe marine environmental condition. Construction and Building Materials 48, 287−294.

Scott, A.N., Alexander, M.G., 2007. The influence of binder type, cracking and cover on corrosion rates of steel in chloride-contaminated concrete. Magazine of Concrete Research 59 (7), 495−505.

Shekarchi, M., Moradi, F., 2007. Concrete durability issues in the Persian Gulf. In: Proceedings of the Cement Based Materials and Civil Infrastructure (CBM-CI) International Workshop, Karachi, Pakistan, ISBN 978-969-8620-06-6, pp. 357−370.

Shekarchi, M., Moradi, F., Pargar, F., 2009. Corrosion damage of a reinforced concrete jetty structure in the Persian Gulf − a case study. Journal of Structure and Infrastructure Engineering 7 (9), 701−713.

Slater, D., Sharp, B.N., 1998. In: Allen, R.T.L. (Ed.), Chapter 6-Concrete in Coastal Structures. Thomas Telford.

Song, H.W., Lee, C.H., Ann, K.Y., 2008. Factors influencing chloride transport in concrete structures exposed to marine environment. Cement and Concrete Research 30 (1), 113−121.

Suzuki, K., Ohno, Y., Praparntanatorn, S., Tamura, H., 1990. Mechanism of steel corrosion in cracked concrete. In: Page, C., Treadaway, K., Bramforth, P. (Eds.), Corrosion of Reinforcement in Concrete. Society of Chemical Industry, London, pp. 19−28.

Tamimi, A.K., Abdella, J.A., Sakka, Z.I., 2008. Prediction of long term chloride diffusion of concrete in harsh environment. Construction and Building Materials 22 (1), 829–836.

Tarek, U.M., Yamaji, T., Hamada, H., 2002. Chloride diffusion, microstructure and mineralogy of concrete after 15 years of exposure in tidal environment. ACI Materials Journal 99 (3), 256–263.

Thomas, M.D.A., Matthews, J.D., 2004. Performance of PFA concrete in a marine environment – 10 year results. Cement and Concrete Composites 26 (1), 5–20.

Thomas, M.D.A., Scott, A., Bremner, T.W., Bilodeau, A., Day, D., 2008. Performance of slag concrete in a marine environment. ACI Materials Journal 5 (6), 628–634.

Thomas, M.D.A., Bremner, T., Scott, A.C.N., 2011. Actual and modeled performance in a tidal zone. Concrete International (November), 23–28.

Wakeman, C.M., Dockweiler, E.V., Stover, H.E., Whiteneck, L.L., 1958. Use of concrete in marine environments. ACI Proceedings 54 (4), 841–856.

Wilson, M., 2005. The Caribbean Environment. Oxford University Press. ISBN-13: 978–0198338512.

Yuan, Y., Jiang, J., Peng, T., 2010. Corrosion process of steel bar in concrete in full lifetime. ACI Materials Journal 107 (6), 562–567.

Zwarts, L., 1991-92. Wadden en wadvogels in de Golf. Waddenbulletin, pp. 65–68, cited by Shekarchi, M. and Moradi, F. (2007) Concrete durability issues in the Persian Gulf. In: Proceedings of the Cement Based Materials and Civil Infrastructure (CBM-CI) International Workshop, Karachi, Pakistan, ISBN 978-969-8620-06-6, pp. 357–370.

# The Confederation Bridge

8

*P.-C. Aïtcin* [1], *S. Mindess* [2], *W.S. Langley* [3]
[1]Université de Sherbrooke, Quebec, Canada; [2]University of British Columbia, Vancouver, British Columbia, Canada; [3]Concrete & Materials Technology, Inc, Lower Sackville, Nova Scotia, Canada

## 8.1 Introduction

One of the most severe environments that concrete structures can experience is that of marine exposure in northern, temperate regions. The concrete will be subjected not only to chemical attack by seawater, but also to freeze–thaw cycles, wave action, cycles of wetting and drying and abrasion by ice. For the structure to have an extended service life (in the case of the Confederation Bridge, at least 100 years), careful attention must be paid to all phases of the construction project, from the proper structural design, choice of materials, concrete mix design, the mixing, placing and curing of the concrete and appropriate post-construction monitoring. The Confederation Bridge provides an excellent case in point as to how this can be achieved.

The Confederation Bridge is a two-lane toll bridge. It links the Canadian province of Prince Edward Island to the province of New Brunswick on the mainland, across the Abegweit Passage of the Northumberland Strait (Fig. 8.1). The curved, 12.9-km bridge (Fig. 8.2) is the longest in the world crossing ice-covered water. It was constructed over a 4-year period, at a cost of about 1.3 billion Canadian dollars, and it was opened on 31 May, 1997. Over 5000 workers were involved in the construction.

Interestingly, the construction of this bridge required a Canadian constitutional amendment! As part of the negotiations leading to the admission of Prince Edward Island into the Dominion of Canada in 1873, the Canadian government agreed to provide

> *efficient steam service for the conveyance of mails and passengers to be established and maintained between the Island and the mainland of the Dominion, winter and summer, thus placing the Island in continuous communication with the Intercolonial Railway and the railway system of the Dominion….*

This was provided by steamship services across the Northumberland Strait. However, steamship service was not entirely satisfactory for a number of reasons, particularly in winter, and discussions about constructing a bridge date back to the late 19th century. Eventually, in the 1980s, serious discussions about providing a fixed link to replace the ferry service began again. This generated a highly divisive debate on the island, between those trying to preserve the ecology and lifestyle of the island,

**Marine Concrete Structures.** http://dx.doi.org/10.1016/B978-0-08-100081-6.00008-8
Copyright © 2016 Elsevier Ltd. All rights reserved.

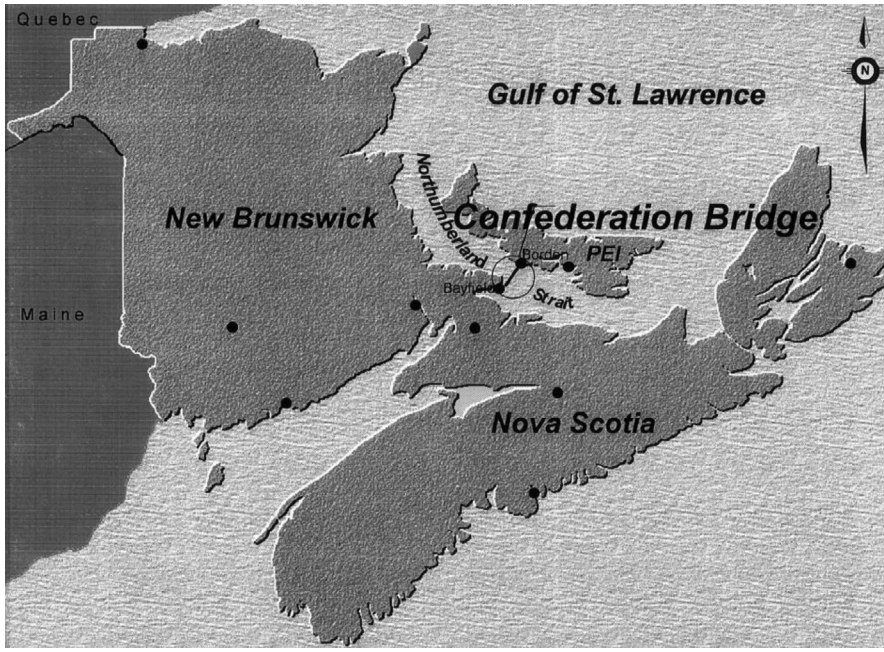



**Figure 8.1** Location of the Confederation Bridge, linking Prince Edward Island (PEI) and New Brunswick, Canada.
Prepared by Strait Crossing.



**Figure 8.2** The Confederation Bridge linking the Canadian provinces of Prince Edward Island and New Brunswick.
Photograph by Alain Boily. Strait Crossing has purchased rights to this photo.

and those who wanted a fixed link to improve commerce and tourism. Eventually, a plebiscite was held in 1988, with 59.4% in favour of a fixed link. This required a constitutional amendment:

> *That a fixed crossing joining the Island to the mainland may be substituted for the steam service referred to in this Schedule……*

The toll rates for the bridge were a great concern, and it was finally decided that the tolls would be the same as the fares on the ferries, and they would not increase beyond the projected increases in ferry fares over time. The tolls are adjusted annually based on the rate of inflation; they are currently (2015) C$45.50 per round trip for an automobile.

The Abegweit Passage is the most direct route across the Northumberland Strait. However, it is covered by ice for 3−4 months each year. The ice which forms is typically about 300 mm in thickness. In April of each year, this ice cover starts to break up into large pieces, some of them up to several kilometres in size. Drift ice from the north causes ridging and rafting in the ice floes, and ice in the order of 1.5 m in thickness is common. Grounding of the ice along the shoreline of the Northumberland Strait picks up sand and gravel, which is very abrasive to the ice shields (Fig. 8.3) as the ice moves around the piers due to changing wind, tide and currents. As discussed subsequently, this was one of the major issues to be resolved in the design and subsequent monitoring of the bridge.



**Figure 8.3** Ice shield in winter, with ice impacting and impinging on a bridge pier. Photography by Donald J. McGinn on behalf of Strait Crossing.

## 8.2 Financial considerations

Although three quite different proposals were put forward for the construction of a fixed link (a tunnel, a bridge and a combined tunnel-causeway-bridge), the single bridge proposal was finally accepted. The developer of this proposal, Strait Crossing Development Inc. (SCDI), was required to finance the construction privately. The bridge was conceived as a BOOT project (build, own, operate, transfer). The bridge was to be designed, constructed, operated and maintained by SCDI for a period of 35 years, after which the ownership of the bridge would pass to the Canadian government. For a 33-year period, The Canadian government is to pay annually to SCDI the amount of the subsidy it had been providing for the ferry service (about C$44 million) and to increase it according to the rate of inflation.

## 8.3 Design considerations

### *8.3.1 Weight limitations*

The HLV *Svanen* is a huge catamaran (Fig. 8.4) that had been used previously in the construction of the 1.8-km-long Great Belt (Storebælt) Bridge linking the Danish islands of Zealand and Funen (see chapter: Danish strait crossings: Lillebælt, Storebælt, Øresund and Femern Bælt for details of this case study). The Northumberland Strait is sufficiently deep that the *Svanen* could be used in the Confederation Bridge construction. The *Svanen* has a lift capacity of 8000 tonnes (including a 500-tonne handling system), and so the maximum weight of the prefabricated cantilever beams could not exceed 7500 tonnes. (To put this in perspective, this is about 300 tonnes




**Figure 8.4** The HLV *Svanen* catamaran, lifting a 7500-tonne prefabricated cantilever beam. Photograph by Alain Boily. Strait Crossing has purchased rights to this photo.

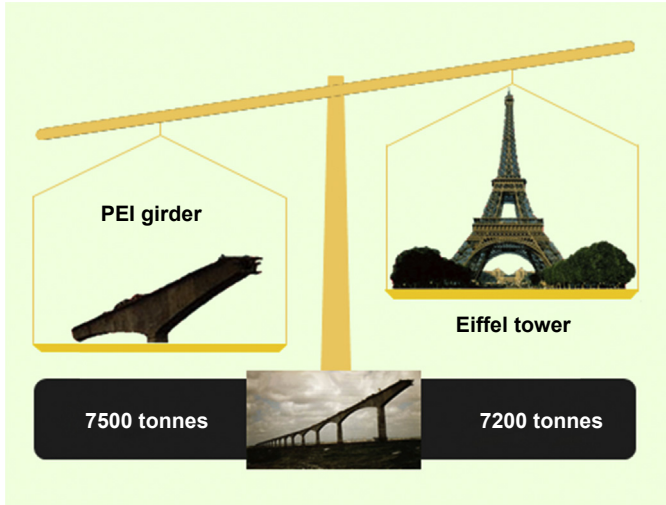



**Figure 8.5** Comparison between weights of the Confederation Bridge double cantilever beams and the Eiffel Tower.
Prepared by Jacques Combault on behalf of Strait Crossing.

heavier than the cast iron structure of the Eiffel Tower, Fig. 8.5.) Only two short sections at both ends of the bridge had to be built more conventionally, because the *Svanen* could not operate in such shallow waters.

### 8.3.2 Prefabrication

The construction of the bridge was carried out by a consortium of Ballast Nedam, GTMI (Canada), Inc., Northern Construction Co. Ltd. and Straight Crossing, Inc. The main prefabrication site was located near the shoreline on Prince Edward Island (Fig. 8.6), where the main girders, pier shafts, integral ice shields and pier footings were constructed. These elements were moved to the bridge locations by the *Svanen*. The approach spans of the bridge (constructed in shallow water) were cast-in-place concrete, in cofferdams on the Prince Edward Island side and on piled foundations on the New Brunswick approach. The superstructure on the approach spans was segmentally precast units placed with a launching truss. These units were precast in a small fabrication yard on the New Brunswick side. Fig. 8.7 shows the fabrication area for the footing components. A schematic of the various precast elements is shown in Fig. 8.8. All of these precast elements were then erected using the *Svanen*. Fig. 8.9 shows the *Svanen* lifting a prefabricated beam, and Fig. 8.10 shows the *Svanen* placing one of the ice shields.

Since the construction of the bridge piers was estimated to represent almost one-third of the construction costs, it was decided to locate the piers at an average distance from each other of 250 m, though this spacing had to be reduced at both ends of the bridge. This limited the number of piers to 45. As the lifting capacity of the *Svanen* was 7500 tonnes, and the design compressive strength of the concrete was limited to 55 MPa, the maximum length of the prefabricated double cantilever beams was limited to about 190 m. It was thus necessary to join adjacent cantilever beams using drop-in spans about 60 m in length (see Fig. 8.8).




**Figure 8.6** General view of the precasting site.
Photograph by Alain Boily. Strait Crossing has purchased rights to this photo.




**Figure 8.7** Portion of the site for fabrication of the footing components.
Photograph by Alain Boily. Strait Crossing has purchased rights to this photo.

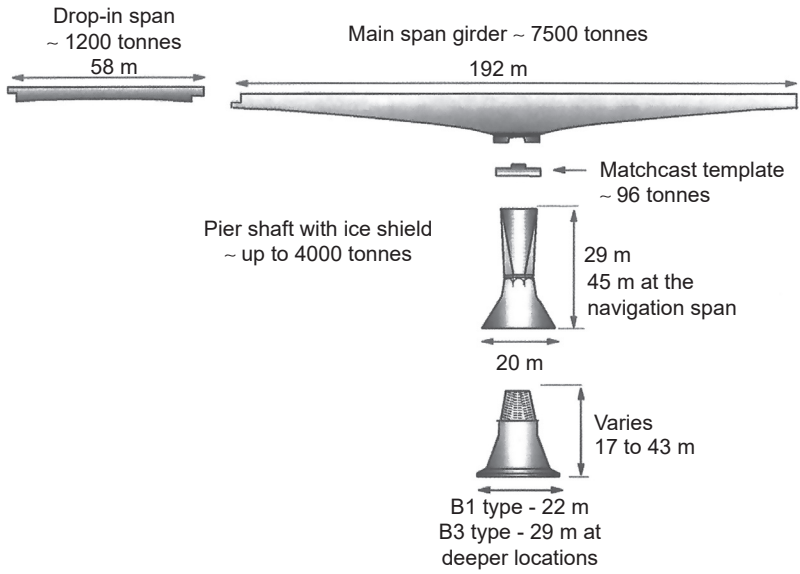



**Figure 8.8** Schematic of the various precast elements, all put in place using the *Svanen*. Prepared by Strait Crossing.



**Figure 8.9** The *Svanen* lifting a precast beam.
Photograph by Alain Boily. Strait Crossing has purchased rights to this photo.



**Figure 8.10** The *Svanen* being used to transport an ice shield.
Photograph by Alain Boily. Strait Crossing has purchased rights to this photo.

### 8.3.3 Design compressive strength of concrete

To build the longest and lightest cantilever beams possible, it was necessary to use a high-performance concrete (HPC). However, in 1995 the maximum compressive strength ($f'_c$) permissible in Canada was 70 MPa. It was finally decided to build the precast elements with an air-entrained HPC with a design strength of 55 MPa.

The durability of the concrete was also an important design factor. The design target for the chloride diffusion coefficient was $3.5 \times 10^{-13}$ m$^2$/s. It was considered that HPC containing both silica fume and fly ash would be required to meet this requirement, without leading to excessive temperatures in the massive concrete sections. The Canadian government specified a 100-year design life for the structure. This was considered to be a very strict requirement, since the concrete in the tidal zone would be exposed to 5 or 6 months in winter of freeze–thaw cycles in seawater, and 2 months of severe ice abrasion conditions in the spring.

### 8.3.4 Freeze–thaw resistance

Given the severe environmental exposure, the concrete was required to be freeze–thaw resistant according to CSA A23.1. At that time (1992), this standard required a bubble spacing factor less than 230 μm, with a maximum spacing of 260 μm. There

was no minimum air content requirement in the hardened concrete. If this value could not be achieved, the concrete had to pass the requirements of Procedure A of ASTM C666. In this test, the concrete is subjected to repeated cycles of freezing and thawing, between temperatures of 4°C and −18°C, while the specimen is kept continuously in fresh water. Each cycle is to last between 2 and 5 h. (This does lead to cooling rates of up to 11°C/h, which is unrealistically high, since cooling rates higher than about 3°C/h are rare. The test is therefore a very severe one.) The test is continued for 300 cycles, until the dynamic modulus of elasticity has fallen to 60% of its initial value. However, the engineer in charge of concrete quality control for the Confederation Bridge project (W.S. Langley) required that the concrete delivered at the end of the pumping line be able to sustain 500 freeze−thaw cycles. This was considered prudent, given the design service life of 100 years.

Since it turned out not to be possible to meet the 230-μm spacing factor after pumping, a laboratory study was carried out to find the maximum spacing factor that would provide adequate freeze−thaw resistance after 500 freeze−thaw cycles, using Procedure A of ASTM C666 described earlier. Five batches of concrete were prepared at the Université de Sherbrooke using increasing dosages of an air-entraining admixture, to obtain spacing factors of 450, 350, 300, 230 and 180 μm. Two specimens of each type of concrete were then exposed to 500 freeze−thaw cycles at the Lafarge Research Centre in Montreal. It was found that the two specimens with 450-μm spacing factors failed after 400 cycles; all of the other samples passed the 500 cycle requirement.

It was therefore decided that the concrete produced on site should have a maximum spacing factor of 350 μm, corresponding to an air content of at least 5% after pumping. Field experience showed that to ensure the concrete contained at least 5% air after pumping, a concrete containing at least 6% air had to be produced at the batching plant. The spacing factor of this pumped concrete was measured, and it was found to meet the 350-μm limit.

Interestingly, since there was some space available at the Lafarge freeze−thaw apparatus, it was decided that one specimen each from the four batches that passed the 500-cycle requirement would continue to be exposed to further freeze−thaw cycles. It was found that these specimens failed in the same order as the decreasing value of the spacing factor. The last specimen to fail was the one with a spacing factor of 180 μm; it failed after 1950 cycles!

### 8.3.5 Materials

The specifications for the bridge required that the aggregates pose absolutely no risk of alkali−aggregate reaction. Approximately 15 quarries in Atlantic Canada and Quebec were evaluated as a source of stone and sand for the concrete construction. The closest quarries on both sides of the Northumberland Strait were not able to provide such coarse aggregates. Finally, a quarry producing a strong granite/granodiorite coarse aggregate from Folly Lake, Nova Scotia, was chosen for the stone (a distance of about 300 km). This quarry had a good historical record of usage and was proven to be nonreactive with cement alkalis. These aggregates were loaded and unloaded directly

in ships, which was both economical and ecologically sound. Since there was not enough clean concrete sand in Prince Edward Island to build the entire bridge, a natural nonreactive quartz sand was imported from Sept-Iles, Quebec. This was also transported by ship (a distance of over 800 km).

The cement specified and developed by Lafarge specifically for the Confederation Bridge was a low-alkali, silica-fume blended cement. It was produced in Brookfield, Nova Scotia. Class F fly ash (low calcium) was used in various bridge components and ranged from 10 to 15% in the footings and piers, and up to 30% in the more massive elements such as the main pier hammerheads. The fly ash originated from the Lingan, Nova Scotia, power generating plant.

## 8.4 Bridge design

The Confederation Bridge is a complex multi-span concrete box girder structure, 12.9 km in length (Langley and Leaman, 1998). It consists of multiple rigid frames and simply supported drop-in spans. The spans are separated by expansion joints and bearings to accommodate the movements associated with loading, creep, shrinkage and thermal effects. Each span consists of a variable-depth box girder, with a depth of 14.5 m at the pier location and decreasing parabolically to 4.5 m at the end of the span. The width of the box girders varies from 5.0 m at the bottom to 7.0 m at the top. The piers for the main girders are founded in upward of 35 m of water and in current velocities approaching 2 m/s. The bridge has a typical clearance of 40 m above sea level, with the exception of a navigation span which is 60 m above water. The deck width of the bridge is 11 m, providing one traffic lane and one wide shoulder in each direction.

The approach section on Prince Edward Island consists of six spans of 93 m each, supported on foundations founded on bedrock with shear keys to resist the lateral loads of wind, waves and ice. The 14 approach spans on the New Brunswick side of 93 m each are founded on battered, concrete-filled pipe piles. The support piers for the approach sections were constructed of match cast segments which were posttensioned vertically in place.

The main bridge consists of forty four spans of 250 m each. The main span girders were constructed as 192.5-m-long double cantilever beams (Figs 8.4 and 8.8). They were match cast and posttensioned at the staging facility and then transported to the site. Each unit is made of 18 line-cast segments built at 10 fixed locations in the assembly yard (Fig. 8.6). The pier segments were always cast at the same location and then transported to the first casting line and fixed to the first two forms. These two first segments were cast one on each side, cured and posttensioned. This assembled part was then moved to the next casting line, and so on all the way to the sixth casting line, where the double cantilever beam was completed. At each location of the casting lines the work crews were always prefabricating the same element. The final weight of the cantilever beam was 7500 tonnes, the maximum load that could be handled by the *Svanen* (Fig. 8.4). Drop-in spans of 52 m or 60 m were built either to connect two cantilevers to create a frame or to close the gap between two frames.



**Figure 8.11** Ice shield with a 93-MPA protective concrete cover, showing only minor abrasion after 10 years of service.
Photography by Donald J. McGinn on behalf of Strait Crossing.

The support piers for the marine spans consist of an 8-m-diameter, hollow, hexagonal concrete shaft, ranging in height up to 45.8 m. The piers for the main spans were cast on land, moved to a jetty by an innovative hydraulic slider, and then transported to the site using the *Svanen*. The top of the shaft is joined rigidly to the superstructure. To protect the piers against ice forces, a conical ice shield is placed within the tidal zone, extending 4 m below and 3.5 m above the mean sea level. The ice shields were designed with a slope of 52 so as to fracture the ice in flexure as it rides up on the shield and thus lessens the horizontal ice loading on the piers. The ice shields are protected against ice abrasion using either a 10-mm-thick steel plate or a 100-mm-thick cover of a 93 MPa HPC (Fig. 8.11).

The footings on which the pier shafts are seated are 22−26 m in diameter. The footings are seated on previously installed concrete positioning pads, and further supported by tremie concrete placed between the pier base and the bedrock.

## 8.5 Concrete mix design

Once all of the design parameters were fixed, the mixture compositions of the concretes to be used for the different parts of the bridge were established. Because of the freeze−thaw exposure, an air-entrained concrete was required. As stated earlier, a low-alkali blended silica-fume cement (7.5% silica fume) designed and manufactured by Lafarge specifically for the Confederation Bridge was used, along with a

**Table 8.1 Average composition of three of the concretes used during the construction of the Confederation Bridge**

| | Marine girders | Ice shield | Thick sections |
|---|---|---|---|
| w/b | 0.30 | 0.25 | 0.36 |
| Water (kg/m$^3$) | 145 | 142 | 159 |
| Blended silica-fume cement (kg/m$^3$) | 430 | 520 | 307 |
| Fly ash, Class F (kg/m$^3$) | 45 | 60 | 133 |
| Aggregate (kg/m$^3$): Coarse, $\Phi_{max} = 20$ mm | 1030 | 1100 | 1055 |
| Fine | 705 | 562 | 745 |
| Air-entraining agent (L/m$^3$) | 0.18 | 0.35 | 0.09 |
| Water reducer (L/m$^3$) | 1.80 | 1.60 | – |
| Set retarder (L/m$^3$) | – | 0.58 | – |
| Superplasticizer (L/m$^3$) | 3.20 | 6.00 | 1.10 |

Courtesy of W. Langley, after Aïtcin P.-C., 1996. High-Performance Concrete, E & FN Spon, London and New York, 591 pp.

polynaphthalene-based superplasticizer. Fly ash was also incorporated into the concrete mix. It was then relatively straightforward to design a concrete mix containing 5–6% air, with an average strength of 72 MPa. This required a w/b ratio of 0.30. The compositions of some of the concretes used to build the bridge are given in Table 8.1. The total volume of concrete placed (including the dock and yard development) was 440,000 m$^3$; of this total, 280,000 m$^3$ was HPC.

Because of the relatively high cement contents and the large size of some of the elements, temperature modelling and on-site monitoring were carried out. It was determined that post-cooling was not required. The mass concrete sections of the bridge used 29% fly ash to reduce heat generation as well as chipped ice as part of the mixing water. Generally, the maximum temperature was less than 60°C (with a specified maximum of 70°C). On occasion, temperatures were found to exceed the maximum specified; in these cases, microstructural analysis indicated the absence of significant cracking. The concrete mixture was not prone to delayed ettringite formation.

## 8.6 Ice shields

The abrasion resistance of a concrete depends on the relative resistance of its mortar and its coarse aggregate. They constitute almost equal masses of the concrete: 1000–1100 kg/m$^3$ of coarse aggregate compared to 1300–1400 kg/m$^3$ of mortar. As shown by Laplante et al. (1991), when studying the abrasion resistance of concrete, it is necessary to consider three different cases:

- The mortar is not as strong as the coarse aggregates. In this case, it is the mortar that is the 'weakest link'; it will preferentially be abraded away until the coarse aggregate particles become detached.
- The mortar is stronger than the coarse aggregates. In this case, it is the coarse aggregate that will preferentially abrade. The surrounding paste will then wear away until more coarse aggregate particles reappear at the surface of the concrete.
- The mortar and the coarse aggregates have the same abrasion resistance. In this case, they wear out at the same rate, so that the concrete surface rapidly becomes polished. (This is the worst case for pavements, because the polished wear surface leads to hydroplaning conditions for automobiles when it is raining.)

In the case of the Confederation Bridge, the coarse aggregates were very strong; it was therefore decided to increase compressive strength as much as possible to improve the resistance of the concrete to ice abrasion. To reduce the w/b ratio as much as possible, a clean Class F fly ash was selected. Using a fly ash dosage of about 10%, it was possible to produce a 150-mm slump concrete at a w/b ratio of 0.25 and to achieve an average compressive strength of 93 MPa, which is excellent for an air-entrained concrete!

## 8.7 Field performance of the Confederation Bridge concretes

Originally, it was proposed to construct the piers with steel ice shields over the 60-MPa concrete. The 10-mm-thick steel ice shields were used as the formwork for the concrete as well. However, after construction of a number of these shields, concerns were raised about the concrete vibration below the 52 haunch. Investigations revealed that there were voids present in these regions, which were then filled with an ultrafine cement slurry. Subsequently, to assure adequate consolidation of the concrete, it was decided to use a 93-MPa concrete and to dispense with the steel cladding. Fig. 8.12 shows a close-up of the surface of such an ice shield after it had been in service for about 13 years. It may be seen that the type of abrasion that had developed corresponds to the first case described earlier: the coarse aggregates are much stronger than the mortar that surrounds them. The 93-MPa compressive strength of the concrete was essentially that of the mortar. That is, the mortar was the weakest link in the concrete when the test cylinders were broken.

The steel cladding that was used on some of the piers was cathodically protected. However, it was not clear if and to what extent the steel cladding was electrically connected to the reinforcing steel; thus, a proper amperage was not applied to the cathodic system. In some cases, the corrosion of the steel cladding was accelerated and corrosion commenced from the interior of the steel. As the steel corroded and became thinner, tearing of the steel cladding became common, and so to protect the concrete surface from gouging by torn plates, the protection was removed from the ice shield. This is currently being performed as required.

Extensive abrasion testing was performed on samples of the 60-MPa concrete (now at 70+ MPa) and compared with that of the 93+MPa concrete, which as

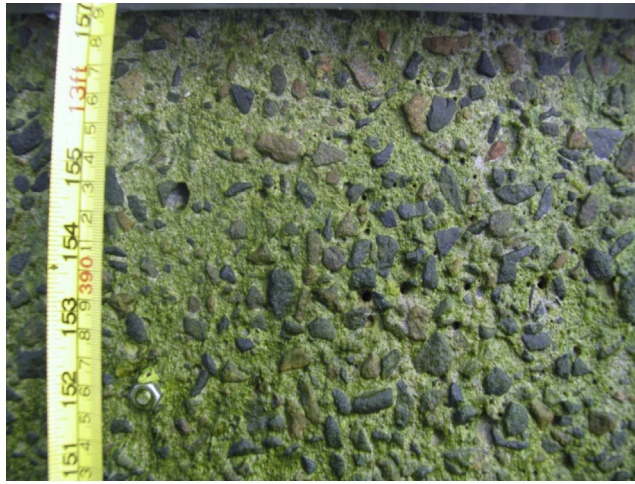



**Figure 8.12** Abraded surface of an ice shield after about 13 years of service.
The small screw in the lower left part of the photograph is used to help measure the depth of abrasion.
Photography by Donald J. McGinn on behalf of Strait Crossing.

stated earlier has performed well. It was determined that, for the quality of the paste and coarse aggregate, there was no significant difference in the abrasion resistance of the two concretes. It would appear that a minimum strength of about 55 MPa will ensure adequate bond strength to keep the coarse aggregate in place, so that the wear due to abrasion will affect mainly the coarse aggregate.

The depth of cover over the reinforcing steel in the area of the ice shields was 100 mm. This value was chosen because, from a review of the literature (Huovinen, 1993; Nawwar and Malhotra, 1988) and a review of the performance of other structures, it was estimated that the abrasion rate would be in the range of 0.17−0.35 mm/year, which would be well within the limit of allowable wear over the 100-year design life of the structure. Currently, the average rate of abrasion as measured on the structure itself is less than 0.4 mm/year (Campbell, 2013), which is consistent with the design assumptions, and which should ensure the 100-year life of the structure. It should be noted that in several instances the concrete cover was found to be low, and in such cases the concrete cover was reinstated using an acrylic-based coating. In general, the joint venture team had quality control integrated into the work force, and steel placement (due to the extended life) was a priority for careful scrutiny.

The concrete elements of the bridge are inspected every two years, and specific elements are tested at 5-year intervals. Some experimental blocks made with the concrete used for the cantilever frames have been exposed to tides and to freezing and thawing cycles at the foot of the bridge near the Prince Edward Island end (Fig. 8.13). These blocks are examined visually every year, and till now they do not exhibit any signs of distress. As well, chloride diffusion testing has been performed and compares favourably with the prediction model established for construction. In fact, the measurements performed in 2012 were significantly less than predicted.



**Figure 8.13** Experimental concrete blocks at the foot of the Confederation Bridge, Prince Edward Island side.

## 8.8 Conclusions

The ice shields that protect the piles of the Confederation Bridge are exposed to particularly severe exposure conditions: cycles of wetting and drying in the marine tidal zone; freeze−thaw cycles for 4−6 months per year and ice abrasion for about 2 months per year. Nonetheless, the HPC used to build these ice shields appears to be behaving satisfactorily, with a projected life well beyond the specified 100 years. This was achieved by the careful, step-by-step procedures used to design the concrete mix so that it would satisfy all of the requirements and specifications, which included:

- ease of placement
- meeting the specified strength
- resistance to freezing and thawing
- protection of the reinforcing steel
- high resistance to corrosion

## References

Aïtcin, P.-C., 1996. High-Performance Concrete. E & FN Spon, London and New York, 591 pp.

Campbell, D., 2013. Effects of ice loads on the Confederation Bridge. Journal of Undergraduate Engineering Research and Scholarship, Vol. 1. PT-13. Faculty of Engineering and Applied Science, Memorial University, St. John's, Newfoundland, Canada, March 13.

Huovinen, S., 1993. Abrasion of concrete structures by ice. Cement and Concrete Research 23 (1), 69−82.

Langley, W.S., Leaman, G.H., 1998. Practical uses for high-volume fly ash concrete utilizing a low calcium fly ash. In: Malhotra, V.M. (Ed.), ACI SP-178, Fly Ash, Silica Fume, Slag & Natural Pozzolans in Concrete, Proceedings of Sixth CANMET/ACI International Conference, Bangkok, Thailand, pp. 545−574.

Laplante, P., Aïtcin, P.-C., Vezina, D., 1991. Abrasion resistance of concrete. Journal of Materials in Civil Engineering 3 (1), 19−28.

Nawwar, A.M., Malhotra, V.M., 1988. Development of a Test Method to Determine the Resistance of Concrete to Ice Abrasion and/or Impact. American Concrete Institute SP 109, pp. 401−426.

# Marinas in the Arabian Gulf region

9

*K. Heath*
Clough Murray & Roberts, Cape Town, South Africa

This chapter addresses the subject of marine concrete structures with reference to marinas in the Arabian Gulf region. The emphasis is on the durability and long-term performance of these structures. The first part of this chapter provides the reader with information on the development of marine concrete structures in the Arabian Gulf, including the historical background, the challenges of executing the construction in this environment, and the types of marine structures used for marinas in the Arabian Gulf region.

In the second part of the chapter, a case study of a significant marina is presented in which the measures implemented to ensure the long-term durability of the reinforced concrete elements are presented with regard to the durability specification, concrete mixture, service-life predictions and quality assurance procedures adopted on site. The monitoring and results of the durability testing conducted on site are presented and discussed.

## 9.1 The development of marine concrete structures in the Arabian Gulf

### *9.1.1 Historical background*

Prior to the 1980s, local materials available in the Arabian Gulf were used to make concrete without fully understanding the properties of the resulting concrete mix, their limitations and potential long-term durability. Very few tests were carried out to determine the durability of the concrete mix, and contractors, engineers, technicians and labourers were not familiar with the local materials or environmental conditions. There were also very few construction standards and specifications applicable to the use of local materials.

During the construction boom, starting in the early 1970s, many designs were accompanied by poorly planned construction, executed with unskilled supervision, and low quality was accepted in return for quick profits. Ready-mixed concrete was widely used without proper quality control. Inexperienced contractors, together with the entry of foreign design and construction teams, joined the industry in the Arabian Gulf. Over time, the experience of engineers and contractors and their technical expertise regarding local materials and specifications improved. A variety of specifications, guidelines and technologies from Europe, the United States and Asia were used on local construction projects. Toward the end of the 1970s, the construction industry

**Marine Concrete Structures.** http://dx.doi.org/10.1016/B978-0-08-100081-6.00009-X
Copyright © 2016 Elsevier Ltd. All rights reserved.

began to realise the consequences of using foreign specifications that had failed to address the properties of local materials and the harsh environmental conditions encountered in the Arabian Gulf.

Since the early 1980s, deterioration of concrete structures on the Arabian Gulf coast caused by reinforcement corrosion, due to a combination of the extremely hot weather and aggressive chloride and sulphate attack, became a major issue. Specifications, guidelines, and knowledge of local materials and the effect of the local environmental conditions improved but were still not at the required standard. Although construction expertise improved, especially on large projects, reported cases of concrete deterioration and remedial repair increased.

#### *9.1.1.1 Case study: Dubai Dry Docks*

An example of the lack of knowledge with regard to local materials used in concrete structures exposed to the harsh environmental conditions in the Arabian Gulf is the Dubai Dry Docks.

The Dubai Dry Docks is one of the leading ship repair yards in the world. Construction was performed over the period 1977 to 1979. The facilities are located within a private port on the Arabian Gulf coast protected by 4 km of breakwater. The docking facilities include three conventional dry docks ($521 \times 100$ m, $411 \times 80$ m and $366 \times 66$ m), a floating dry dock ($205 \times 32$ m), over 2000 m of wet berths and a separate tank-cleaning berth.

The dry dock piers and berths were formed by reinforced concrete caissons that were slip-formed on land, floated and sunk into position, filled with dredged material, and then topped with facilities that were constructed in situ (eg, mechanical and electrical service galleries and trenches, hauling-in beams, crane rail beams, bollard bases, capstan pits, fenders, road surfaces, etc.).

Widespread reinforcement corrosion problems became evident in the late 1990s in the concrete caissons forming this ship repair facility. As a result, hydro-demolition and subsequent high-quality concrete repairs to the berths and the pump house structures were carried out between 2000 and 2004 amid a fully operational ship repair yard.

Due to the deterioration of reinforced concrete structures built during the 1970s and 1980s in the Arabian Gulf, such as the Dubai Dry Docks, focus in the past few decades has been placed on the specification, construction and quality control of reinforced concrete construction in the Arabian Gulf.

### *9.1.2 Challenges of designing and constructing marine concrete structures in the Arabian Gulf*

Many contracts in the Arabian Gulf are executed using the design-and-construct model where the contractor is responsible for both the design and construction elements of the project.

There are many challenges facing the contractor when designing and constructing reinforced concrete structures in the Arabian Gulf, including the harsh climatic and environmental conditions, the nature of the locally available construction materials,

and the construction execution, where there may be many different nationalities that make up the labour force who have different cultures, educational backgrounds and languages, making communication at times difficult.

Most of the materials required for a marine-grade reinforced concrete mix are either imported or sourced locally in the Arabian Gulf region. Ordinary Portland cement and other cements are produced locally, while cement extenders such as fly ash, slag and microsilica are largely imported. Consideration should be made with regard to the availability of the required cement extenders, especially during times of economic boom. For example, severe shortages of fly ash (pulverised fuel ash) were encountered on a specific marina project, and the required supply of concrete could not be met during the peak production stages of the project, which led to the omission of the fly ash in the mix during that time, with consequences for concrete durability. Locally available desalinated water is used in the concrete mix. The coarse aggregates are sourced locally in the UAE, for example from Ras Al Kaimah (typically limestone), and the fine aggregates are usually locally available natural dune sands (typically limestone and quartz).

Ensuring quality control on site during concrete manufacture, transport, placement and curing can also be a challenge due to the high ambient temperatures experienced in the region. The temperature requirements (ambient and concrete) are usually specified in the project specifications. In general, the deeper or larger the section is, the lower the concrete temperature is that is required at time of placing. The target temperature for a 45 MPa characteristic strength mix is approximately 30°C and goes up to around 34°C for smaller elements. The concrete temperature can be controlled by adding chilled water at the ready-mix plant or on site. During the very hot summer months, when daytime ambient temperatures can easily reach 40°C, flaked ice needs to be added. A typical flaked ice plant can produce around 36 tons in a 24-h period and typically has storage capacity for 50 tons. Approximately 25% of the chilled water is replaced by flaked ice during these extremely hot periods. This, in turn, limits the daily concrete output from a batching plant to approximately 750 $m^3$ (ie, an average discharge capacity of between 70 and 80 $m^3$ of concrete per hour). Due to the high temperatures prevailing during the day, it is common to carry out the concreting operation during the night shift.

The specifications usually require concrete mix verification tests to be carried out every 10,000 to 30,000 $m^3$ of concrete. Usually a 1-$m^3$ block of concrete is cast and the following data recorded: slump loss over 60 min, strength of laboratory cured cubes (7 and 28 day) in a controlled environment with a temperature of $20 \pm 3$°C, field-cured cubes (7 and 28 day), maximum temperature rise and differential between core/surface and ambient temperatures. Thermocouples cast into the block are used to measure the temperature differential over a 48- to 60-h period. For marine concrete in the severe exposure zone (tidal zone), controlled permeability liners (CPF) are specified for the formwork to control water loss and temperature differential between core/surface and ambient.

The correct curing method/material used in high ambient temperature environments is of utmost importance to ensure durable concrete due to the high evaporation rates when using water and hessian.

The marine environment presents many challenges due to the harsh environmental conditions under which structures must be built and survive. Chloride ingress is one of the most common environmental attacks that leads to the corrosion of reinforcing steel and the deterioration of concrete structures, especially in the marine environment where structures are exposed to saltwater and wetting and drying cycles. The measured chloride ion concentration in the Arabian Gulf waters is roughly 1.5 times that of the open oceans in most parts of the world (eg, average chloride ion content of seawater in Abu Dhabi was measured at 26,765 mg/L compared to 'normal' salinity levels of 16,450 mg/L measured from seawater in the Indian Ocean along the South African coast). Seawater temperature also has a significant effect on the concrete diffusion coefficients, making the rate of chloride ingress higher as the average temperature of the Arabian Gulf waters is approximately 30°C. This can be compared with seawater temperatures of 10−19° C off the coast of Cape Town, South Africa.

As a result, it has become normal practice to specify concrete durability tests, and these include among others a combination of capillary index monitoring tests carried out on concrete sections cut from cubes, permeable void tests, rapid chloride permeability testing, water absorption, water permeability and initial surface absorption.

### 9.1.3 Types of marine concrete structures constructed in the Arabian Gulf

Concrete construction in the Arabian Gulf region has exploded in recent decades, with high-rise buildings and significant waterfront developments including extensive marinas being developed over a very short period of time.

The concrete structures being developed in waterfront developments in the Arabian Gulf consist mainly of precast and cast in situ unreinforced and reinforced concrete. The majority of waterfront seawalls used in marina projects are constructed using precast concrete with the exception of diaphragm walls, which are cast in situ.

#### 9.1.3.1 Unreinforced precast concrete

Due to the experience of the deterioration of reinforced concrete structures built during the 1970s and 1980s, unreinforced concrete construction is the preferred method of construction for waterfront structures exposed to seawater along the coastline in the Arabian Gulf.

The most common form of unreinforced concrete construction used in seawalls for waterfront developments are precast concrete blockwork walls of which there are many examples (Fig. 9.1).

#### 9.1.3.2 Reinforced in situ and precast concrete

Reinforced concrete infrastructure construction in the Arabian Gulf region has seen massive growth since 2000, including many high-rise office and apartment complexes as well as recreational and industrial waterfront marina-type developments.

The rapid deterioration of reinforced concrete structures constructed along the Arabian Gulf coastline during the 1970s and 1980s, as experienced in the Dubai



**Figure 9.1** Unreinforced blockwalls, Port HIDD, Bahrain.

Dry Dock, provided a humbling and expensive lesson forcing a reevaluation of requirements to ensure long-term concrete durability.

In the Arabian Gulf, the use of reinforcing bars in concrete has generated concern relating to the corrosion of steel reinforcement in the marine environment. There are solutions to this problem that include the use of sophisticated marine concrete mixes with conventional steel reinforcement, or BFRP (Basalt Fibre Reinforced Polymer) or GFRP (Glass Fibre Reinforced Polymer), which provide a zero corrosion option. Concrete mixtures that are able to resist the ingress of chlorides and can therefore be used with normal steel reinforcing generally contain extenders (or supplementary cementitious materials [SCMs]). The range of reinforced concrete seawall structures being constructed for recreational and industrial waterfront developments in the Arabian Gulf today includes, among others, in situ concrete diaphragm walls and precast concrete gravity-type retaining walls.

### *9.1.3.3 Diaphragm walls*

Diaphragm wall construction is a proven form of construction technology accepted throughout the world for creating both quay walls and retaining walls (Fig 9.2). Providing an efficient and economic design, these walls also use construction plant, which is readily available worldwide. This solution provides a structure that is significantly quicker and more economical to build than an unreinforced blockwork type wall, a type of construction that is heavy, difficult to place quickly, and requires working at and below seawater level. Diaphragm walls are especially effective in reclaimed areas. Precast concrete fascia panels are manufactured in high-quality factory conditions and applied to the diaphragm walls to create the required architectural appearance Fig. 9.3.

Some examples of the use of diaphragm walls in the Arabian Gulf are the Al Sowwah Quay Wall and the Al Raha, Eastern Precinct, Marina Walls in Abu Dhabi.

The Al Sowwah Quay Wall is a 2-km-long diaphragm quay wall around the new prestigious Al Sowwah commercial district island development in Abu Dhabi. The original design for the quay wall was a traditional blockwork-type wall construction using heavy, unreinforced mass concrete blocks.

The Al Raha Beach development project, located on the beach side of the main highway leading into Abu Dhabi from Dubai, consists of eight precincts incorporating

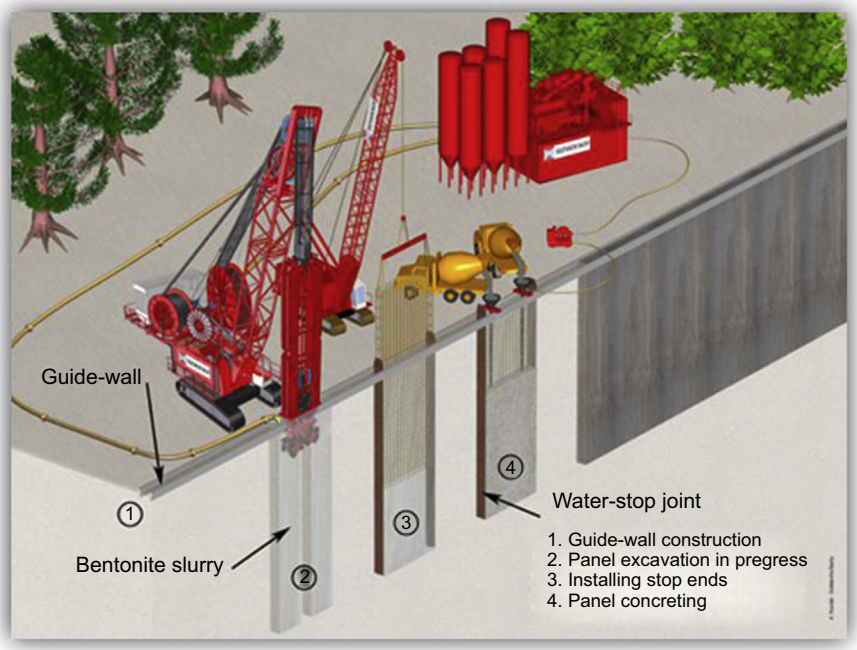



**Figure 9.2** Diaphragm wall construction sequence.
http://www.bacsol.co.uk/technique/diaphragm-walls/. Bachy Solentache Flyer.



**Figure 9.3** Diaphragm walls precast fascia panel installation (R. Secco/Image'In).
Bachy Solentache.

hotels, marinas, parks, business facilities and restaurants linked together by a network of canals, bridges and water transportation, on an area of 520 Ha. When completed, the development will accommodate over 120,000 residents and feature around 70 high-rise towers.

The Al Raha development consists of both types of quay wall construction. The Eastern precinct is constructed using reinforced concrete diaphragm wall construction, and the Western precinct is constructed using reinforced concrete gravity-type retaining walls.

The Al Raha Eastern Precinct island walls consist of 20 km of cantilever diaphragm walls with 20 km of precast fascia panels. The diaphragm quay walls were designed to resist 100-year return period waves and mooring forces from large yachts. Because of the extremely aggressive environment, a detailed assessment and prediction of the lifespan of the reinforced concrete quay walls was made. The client's requirements for a design life of 100 years were demonstrated to be met by an analysis of potential chloride permeability, measurements of the resistance of the concrete to chloride penetration, and appropriate mix design and specification of minimum concrete cover and quality control. Concrete with a 28-day characteristic cube strength of 45 MPa was used for the diaphragm walls, which are 1- to 1.2-m thick, at a depth from 14 to 19 m.

The diaphragm walls have architectural facing panels on the front face of the quay wall and provide an aesthetic finish to the exposed portion. The precast facing panel is integrated with the diaphragm wall capping beam (Fig. 9.3).

The diaphragm walls in the Eastern precinct were followed by an alternative solution for the Western precinct marina walls at Al Raha, which consisted of reinforced concrete L-shaped gravity-type retaining walls that were significantly more economical to build than the diaphragm wall option adopted in the Eastern precinct.

However, as a result of the poor track record of reinforced concrete built in the early 1970s and subsequent resistance to the use of reinforced concrete in waterfront structures in the Arabian Gulf, great emphasis was placed on the durability of the concrete used in these seawalls. The long-term durability of these reinforced concrete L-shaped wall structures required the incorporation of appropriate construction materials and methods followed by an appropriate program of monitoring and measuring actual performance on site. This forms the subject of the following case study section of this chapter.

## 9.2 Case study: construction and quality control of a reinforced concrete marina seawall (Heath and Alexander, 2012)

The approach to the in situ quality control taken to ensure the long-term durability of reinforced concrete, with reference to the Al Raha, Western precinct L-walls, is discussed.

### *9.2.1 Unreinforced block wall versus reinforced concrete L-wall*

The client's requirements were for a 5- to 6-m high sea wall with a 100-year design life. The postulated design was an unreinforced precast mass concrete block wall

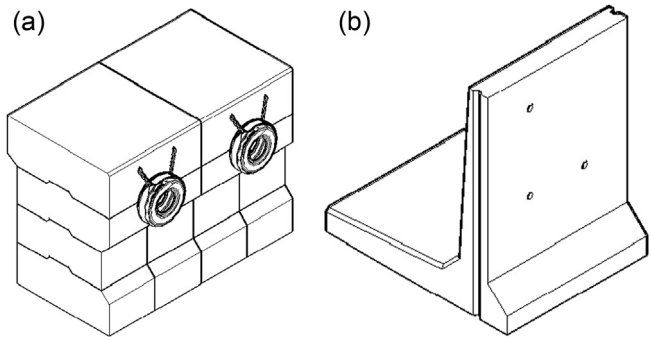



**Figure 9.4** (a) Postulated unreinforced precast concrete block wall and (b) alternative precast reinforced concrete L-wall.

(Fig. 9.4 (a)). However, the client found that the initial block wall proposals would be too costly and too slow to implement. The contractor value-engineered an alternative precast concrete L-wall solution that was more economical and quicker to construct than the initial block wall design (Fig. 9.4 (b)).

Several factors contributed positively to the feasibility of the reinforced concrete L-wall solution:

- Compared to the block wall solution, a much smaller volume of concrete per linear metre of wall was required to ensure the stability of the sea wall.
- Due to the reduced mass of the wall, the stone column foundation would need to support less load.
- An equivalent block wall would comprise up to four concrete blocks. The time required to place one such block would be similar to that required to install a single L-wall precast unit. The installation time for the L-wall would therefore be at least four times quicker than that required for the block wall.

### 9.2.2 Alternative reinforcement and other corrosion protection systems considered for the L-wall

The major drawback of the L-wall solution was the need for steel reinforcement, especially along the landward face of the precast units, where the loads imposed by the retained backfill would induce hogging moments, placing the concrete face in contact with the backfill in tension.

The use of an imposed current system (cathodic protection) was investigated, but this was not economically viable or practical. An alternative option for reinforcing the concrete units that was investigated was the use of GFRP bars. At the time of tendering, the price of steel and that of GFRP were comparable. Unfortunately, the client's engineer was not convinced that there was sufficient certainty on the implications – both structural and durability related – of using GFRP, so conventional steel reinforcement was settled upon.

Due to the use of steel reinforcement in the wall units, strict concrete quality control was required. The long-term durability of the concrete was deemed to be one of the

most important technical aspects of this project. Therefore, various measures were implemented to ensure the durability of the precast concrete, which included a durability specification, the use of appropriate concrete materials, strict quality control and the implementation of an appropriate program of monitoring and measuring actual performance on site.

By considering these measures, the contractor was able to reduce the period until the first major maintenance, and the client was prepared to compromise the maintenance-free life of an equivalent unreinforced block wall for the economy and speed of installation of the reinforced concrete L-wall.

### 9.2.3 Construction methodology

The Al Raha, Western precinct, island consists of 6340 50-ton precast reinforced concrete L-shaped wall units, which are placed side by side forming the 19-km-long perimeter of the artificial islands (130,000 $m^3$ concrete in total) (Fig. 9.5).

The 6340 units were cast in the precast yard. At peak production, the precast yard was required to manufacture 18 units per day, with a monthly requirement of 100 units.

The manufacture and delivery of concrete required for the precast units was supplied using a ready-mix subcontractor. The batching plant was established in the precast yard, which had a capacity of 120 $m^3$/h. The plant had separate cement, fly ash, microsilica and admixture silos. Water was stored in cooled tanks, and an ice plant was used to lower the temperature of concrete during the hot summer months. The units were cast on their sides such that they were rotated 90 degree from their position, enabling the entire unit to be cast at once and thus avoiding different stages of concreting and cold joints (Fig. 9.6).

Concrete production was a 24-h operation, with the day shift carrying out the preparation of moulds, placing the prefabricated steel reinforcing cages into the moulds, and closing the moulds ready for concreting. The primary task of the night shift was to cast the units prepared during the day and finish off and prepare units not completed during the day shift. Prior to casting, the moulds were cleaned and treated with approved mould release agent to facilitate easy removal of the precast element from the mould.

The actual concrete used in the work had a slump in the order of 180 $\pm$ 25 mm. The placement and vibration of the concrete were carefully carried out to ensure good

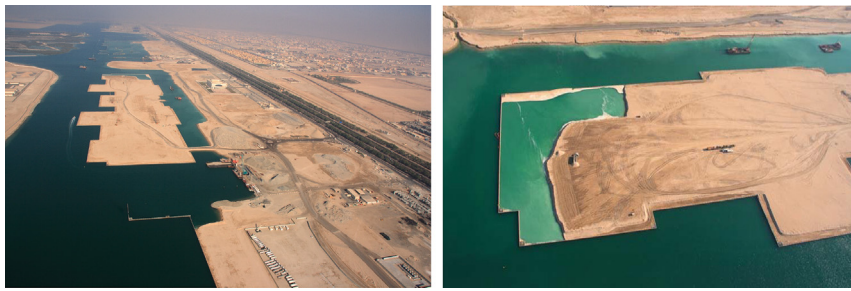


**Figure 9.5** Al Raha, Western precinct, islands.



**Figure 9.6** Concrete batching plant in the precast yard and casting beds.

compaction and prevent honeycombing. Compaction was by 4-inch poker vibrators, and care was taken during the casting and vibration of the concrete to avoid displacement of the reinforcement. The concrete volume cast at peak production was 450 $m^3$ per day.

Pumping of the concrete was required as all the moulds were higher than the discharge chute of the trucks, and making ramps for each unit was impractical. Placing the concrete using a crane was an option, but the rate of placing would have been too slow to allow completion of an average of 18 units per shift. Carrying out the concreting operation during the night shift allowed for units cast during the early hours of the shift to be ready for stripping after 16 h and the formwork to be cleaned and prepared for the next pour.

The precast units were lifted off their casting beds once the field-cured cubes had achieved a compressive strength of 16 MPa. The strength was usually achieved after 12−16 h, and daily checks of the cubes cast specifically for this reason were carried out. The walls were lifted using a three-point lift, with four prestressing strands of 15-mm diameter provided in the three lifting point positions (Fig. 9.7).



**Figure 9.7** Precast units lifted from casting beds and placed in storage. Note the plastic sheets secured around the elements to aid in curing.

As soon as the precast unit was stripped, curing was undertaken, using a water-based curing compound. Application of the compound was undertaken using a manual sprayer to evenly apply the curing compound to all the faces of the precast unit before they were placed in the storage yard, where they were further wrapped in plastic sheets to assist in curing (Fig. 9.7).

When the units reached the desired strength after 28 days, they were tilted in an upright position, the lifting strands were cut off, and the remaining recess grouted.

The transportation of the units was carried out by two low-bed trucks able to carry the 50-ton units (Fig. 9.8). The trucks parked under the gantry crane, loaded with one unit, which was then transported to the load-out quay located a distance of 600 m away, and offloaded by a 250-ton capacity crawler crane. Specially designed and fabricated lifting frames were used to lift the precast units onto the transport barges (Fig. 9.9).

The L-units were placed on a preprepared screeded stone foundation bed on the sea floor. Below the stone foundation bed, stone columns were constructed to improve the



**Figure 9.8** Precast units lifted from storage and placed on low-bed trucks.



**Figure 9.9** Units being lifted onto barges using lifting frame and 250-ton crawler crane.

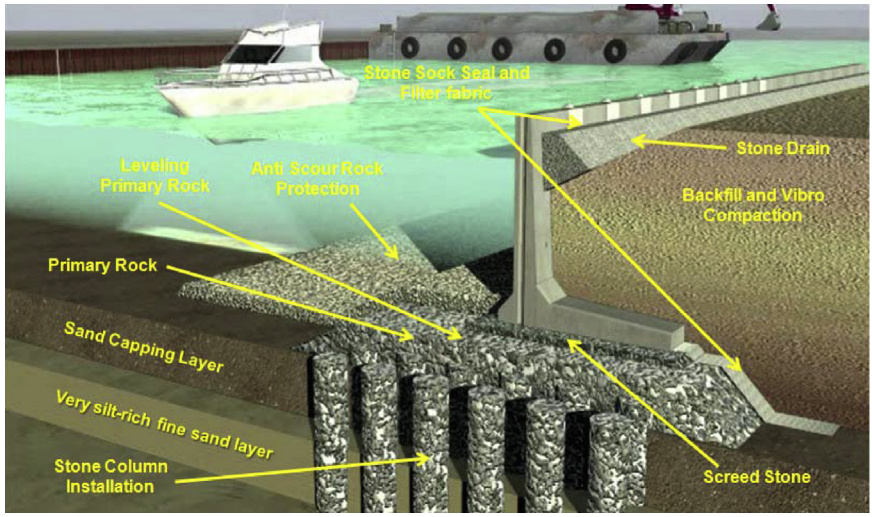



**Figure 9.10** Graphic of stone foundation bed.

bearing capacity and stability of the foundation. The foundation material comprised up to a 3-m-thick layer of very silt-rich fine sand that was unsuitable for the wall unit foundations (Fig. 9.10).

Placing of the wall units was undertaken off a moored barge (55 × 18 m) with a 2500-ton winch. A 250-ton crawler crane was mounted on the deck, and the barge was water-ballasted to ensure an even trim. An open deck in the centre of the barge enabled a number of units to be stored in case the supply barges were in transit. Unit placing was a daylight operation, but extended hours were worked with the use of floodlights. Under good conditions and consistent supply of units, an average of 20 units placed per day was achievable. The L-units were lifted off the barge with a purpose-designed lifting frame that was attached onto the unit in the dry and disconnected underwater by divers (Fig. 9.11).

Once the units had been placed side by side, the recessed gap between the units was filled with a geofabric stone sock filled with 13-mm stone chips. This allows the



**Figure 9.11** Placement of L-walls on screeded stone foundation bed.

equalisation of water level behind the wall with the sea level. This process is assisted by a horizontal stone drain placed at the back of the wall. All joints between units were sealed with an additional layer of geofabric to ensure there would not be a gradual loss of backfill material through the wall.

The backfilling works for the islands and the mainland were done by others and managed by the client's engineer. Close coordination was required to ensure backfilling, and that the subsequent activity of vibro-compaction of the placed backfill was done in the required sequence. Special care was required with the backfilling to prevent the fill from coming between the seawall and the 1-m-wide, vertical, geo-textile strip. It was also an environmental requirement that backfilling was done in such a way as to avoid trapping large bodies of water, as this would kill any marine life.

### 9.2.4 Measures implemented to ensure long-term durability of reinforced concrete

The harsh marine environment posed obvious challenges for ensuring the durability of the steel-reinforced concrete sea walls. Furthermore, the client's initial requirements for a maintenance-free design life of 100 years would be near-impossible to achieve. The contractor therefore implemented a series of measures to mitigate the risk of reinforcement corrosion damage to the sea walls. These included the following aspects.

#### 9.2.4.1 Concrete mixture design

A ternary concrete mixture was designed that included Portland cement, fly ash and microsilica in the ratio of 70:25:5. The cement extenders would greatly reduce the rate of chloride ion ingress into the concrete and hence increase the time before the start of reinforcement corrosion. The concrete mixture design, based on the client's requirements, was developed and tested using trial mixes at the University of Cape Town, South Africa, and is indicated in Table 9.1.

#### 9.2.4.2 Risk assessments, service-life predictions and concrete cover

The contractor carried out a service-life prediction assessment of the proposed concrete mixture to verify that the concrete mixture design would provide the necessary protection to the reinforcement for the design life of the sea wall.

Concrete cover is one of the most critical determinants of service life and concrete durability. An increased cover-to-reinforcement would also provide a substantial barrier against the ingress of the harmful chloride ions found in high concentrations in the marine environment. Therefore, a service-life prediction exercise was carried out to determine the expected service life to first corrosion for various depths of concrete cover.

Two existing service-life prediction models were used to investigate the expected service life of the proposed concrete mixture. These were the UCT (University of Cape Town) Model (Mackechnie, 2001) and the Life-365 Model (Thomas and Bentz, 2000). Calculations using both these models produced similar results, so the UCT

**Table 9.1 Concrete mixture design**

| Mixture proportions for 1 $m^3$ of ready-mix concrete | | | | |
|---|---|---|---|---|
| **Material** | **Type** | **Source** | | **Max (kg)** |
| | | ***Ras-Al Khaimah (RAK), UAE*** | ***% Cem*** | |
| Cementitious | Portland cement[a] | RAK cement factory | 70 | 287 |
| | Fly ash | Trace. Ex. RAK cement factory | 25 | 102.5 |
| | Microsilica | Elkem. Ex. RAK cement factory | 5 | 20.5 |
| | | Subtotal | 100 | 410 |
| Water | Drinking water | Abu Dhabi Distribution Company | | 151.7[b] |
| Admixture | SP2000 superplasticiser | Fosroc | | 10.6l |
| | | | ***% Agg.*** | |
| Aggregates | 20-mm Crushed | Stevin Rock, RAK limestone | 33 | 619.7 |
| | 10-mm Crushed | Stevin Rock, RAK limestone | 22 | 412.4 |
| | 5-mm Crushed | Stevin Rock, RAK limestone | 32 | 600.8 |
| | Dune sand natural | Al Ain UAE (limestone and quartz) | 13 | 243.3 |
| | | Subtotal | 100 | 1876 |
| | | Total | | 2448 |

[a]BS EN 197 2000 CEM I.
[b]Includes 10 L for absorption by aggregates.
Twelfth International Conference on Recent Advances in Concrete Technology and Sustainability Issues - Supplementary Paper No. 4 Rapid Chloride Permeability Testing: Is it Appropriate for Concrete Durability Quality Control Testing?

model was adopted. The UCT model for determining the chloride surface concentration ($C_S$), 50-year diffusion coefficient ($D_C$) and time to onset of corrosion (ie, when 0.4% chloride concentration by mass of binder is achieved at the reinforcement) for various cover depths is described next.

The chloride conductivity value of the concrete mixture at 28 days was determined by the UCT model to be 0.42 mS/cm. Chloride conductivity is measured on concrete specimens generally at 28 days, and it is a measure of the resistance of the material to chloride ingress (Streicher and Alexander, 1995). It is correlated to the associated

chloride diffusion coefficient of the concrete (Mackechnie and Alexander, 2002). The chloride conduction test is used in South Africa in preference to the RCP test.

$C_S$ in the tidal/splash zone along the coast of South Africa is between 4.5 and 5% chlorides by mass of binder (Mackechnie, 2001). However, the measured $Cl^-$ ion concentration in the Gulf waters is roughly 1.5 times that of South African waters (average $Cl^-$ ion content of seawater in Abu Dhabi was measured at 26,765 mg/L compared to 'normal' salinity levels of 16,450 mg/L measured from seawater along the South African coast). The $C_S$ value of 4.5−5% normally used in the UCT model was multiplied by 1.5 to obtain a more realistic estimate of the $C_S$ of concrete exposed to Arabian Gulf seawater (ie, a $C_S$ value of 6−7.5% was used). It was, however, deemed prudent to carry out the service-life analysis for an upper $C_S$ value of 10%.

Long-term diffusion coefficients were determined by using the correlation of the 28-day chloride conductivity and the 28-day diffusion coefficient, adjusted for long-term using the following equation:

$$D(t) = D_{\text{ref}} \left( \frac{t_{\text{ref}}}{t} \right)^m \qquad [9.1]$$

where $D(t)$ = diffusion coefficient at time $t$; $D_{\text{ref}}$ = diffusion coefficient reference time $t_{\text{ref}}$ (28 days); $m$ = constant (depending on binder type and mix proportions); $t$ = the age of the concrete for when the diffusion coefficient is required.

The value of $m$ in Eq. [9.1] was taken as 0.62, based on data from previous results with this type of binder. Using Eq. [9.1], a 50-year diffusion coefficient ($D_C$) value of $1.1 \times 10^{-12}$ m$^2$/s was determined using the UCT model under South African conditions. The value of $D_C$ was doubled, as temperature is known to have a significant effect on diffusion coefficients, and the temperature of the Arabian Gulf waters was measured as 30°C compared to 15−19°C of Cape Town seawater (Thomas and Bentz, 2000; Silica fume association, 2001). Therefore a diffusion coefficient ($D_C$) of $2.2 \times 10^{-12}$ m$^2$/s was used as an upper bound under Arabian Gulf conditions. This resulted in four scenarios:

Scenario 1 ($C_S = 6\%$ $D_C = 1.1 \times 10^{-12}$ m$^2$/s),

Scenario 2 ($C_S = 6\%$ $D_C = 2.2 \times 10^{-12}$ m$^2$/s),

Scenario 3 ($C_S = 10\%$ $D_C = 1.1 \times 10^{-12}$ m$^2$/s),

Scenario 4 ($C_S = 10\%$ $D_C = 2.2 \times 10^{-12}$ m$^2$/s).

These four scenarios were used to determine the service life of the concrete in the walls using a chloride conductivity of 0.42 mS/cm and a chloride threshold of 0.4% by mass of binder for various depths of concrete cover. The results obtained are presented in Fig. 9.12.

The results indicated that for a concrete cover of 75 mm, a corrosion-free life was likely to vary from about 100 years under the most adverse conditions (Scenario 4) to

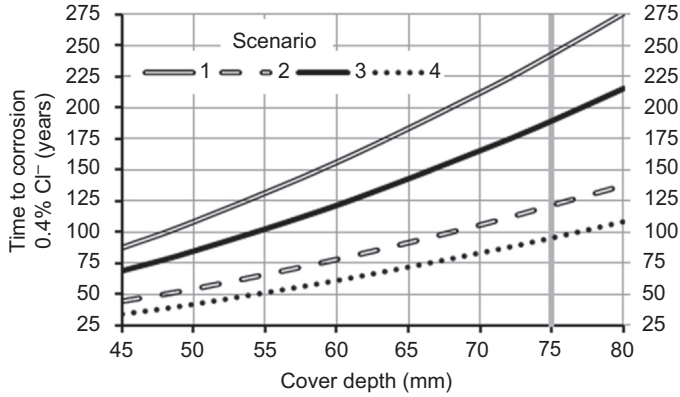



**Figure 9.12** Service-life predictions.

greater than 200 years under the most favourable conditions (Scenario 1).[1] It was concluded from this analysis that the proposed concrete mixture should be adequate for 100-year service life if the cover provided was 75 mm.

### 9.2.4.3 Allowable crack widths

Strict specifications on the allowable crack widths were observed during structural design to prevent accelerated pathways for chloride ions to access the steel reinforcement.

Once the unit was delivered to the load-out quay, it was coated with an approved bituminous material to a thickness of 300 μm on the landward face to seal the expected design crack widths and increase the durability against chloride ingress (Fig. 9.13). The area to be coated corresponded to the section of the unit that would be exposed to crack widths of greater than 0.1 mm.

### 9.2.4.4 Quality assurance procedure

A comprehensive concrete durability specification, quality assurance procedure and quality controls, which included several durability tests, were implemented during construction. The durability tests included rapid chloride permeability (RCP[2]) tests of cubes and in situ cores, water absorption tests, water permeability tests, reinforcement cover surveys (using a cover metre) and compressive strength cube tests. An approved independent testing laboratory was used for the testing carried out on site.

The durability specification indicated which elements of the site concrete would be tested and what the acceptable limits and frequencies for the tests were to check compliance of the concrete during construction.

[1] This is a deterministic evaluation. Clearly, a probabilistic evaluation would be preferable, but the key parameter variabilities were unavailable at the time.

[2] The RCPT is widely used in the Gulf area for rapid testing for quality control purposes – its main use here.



**Figure 9.13** Bituminous coating applied to L-walls.

## Concrete testing program

A durability test was required that would be simple to conduct and could be performed in a short time by local testing agencies. Various tests have been developed around the world for concrete durability quality control testing. However, not all of these tests can be carried out by testing agencies throughout the world. The most common and widely used test in Abu Dhabi was the RCP test. It is a quick test to carry out compared with other durability tests. The RCP test is relatively easy to conduct and has been adopted as a standard (ASTM C1202, 2005). Most testing agencies throughout the world have the standard test equipment for the RCP test.

The concrete quality was therefore monitored using concrete strength tests as well as a number of durability tests that included RCP (ASTM C1202, 2005), water absorption (BS 1881-122, 1983), water permeability (DIN 1048-5, 1991) and initial surface absorption tests (BS 1881-208, 1996).

The concrete testing program specified during construction is indicated in Table 9.2.

**Table 9.2 Summary of concrete testing program**

| Test | Standard | Age | Frequency |
|---|---|---|---|
| Strength test (cubes) | BS 1881-116 (1983) | 28 days | 3 cubes every 20 $m^3$ |
| RCPT (cores from standard cubes) | ASTM C1202 (2005) | 28 days | 3 cubes every 7th unit |
| RCPT (cores from as-built units) | ASTM C1202 (2005) | 28 days | 3 cores every 15th unit |
| Water absorption | BS 1881-122 (1983) | 28 days | At monthly intervals |
| Water permeability | DIN 1048 Part 5 (1991) | 28 days | At monthly intervals |
| Initial surface absorption | BS 1881-208 (1996) | 28 days | At monthly intervals |

## Acceptance limits for concrete tests

Trial mixture test results were used to determine the as-built (structure) and acceptable material potential (standard laboratory cured cube) limits for the RCP testing, as indicated in Table 9.3.

The difference between the as-built (structure) and material potential (standard laboratory cured cube) values given was deemed to be too small taking into account the reported variability of RCP test results carried out on cores extracted from in situ concrete. The accepted RCP test limit from literature in the Middle East for standard cured cubes was 2000 Coulombs (Pocock and Corrans, 2007). This was deemed too high for standard cured cubes, and some engineering judgement was used in setting the acceptable limits based on the trial mix results. The acceptable limit for the $RCP_{As\text{-}built}$ (structure) was set at 2000 Coulombs, and the acceptable limit for the $RCP_{Char\ Mat'l}$ (standard laboratory cured cube test) was set at 1020 Coulombs.

The acceptance limits for the concrete tests specified are indicated in Table 9.4.

The acceptance limits for concrete tests other than RCP tests were based on available literature. Concrete cover surveys were specified on 10% of the as-built units until there was sufficient data available to establish confidence that the acceptable limits were being achieved.

**Table 9.3 Summary of RCP test limits based on trial mix results**

| Parameter | RCP test (Coulombs) |
|---|---|
| $RCP_{Char\ As\text{-}built}$ | 1050 or **1020**[a] |
| $RCP_{Char\ Mat'l\ potential}$ | 955 or **925**[a] |
| $RCP_{target}$ (average of three cubes from trial mixture) | 850 |

[a]The more stringent of these two values pertains in each case, ie, the **bold** value.
Twelfth International Conference on Recent Advances in Concrete Technology and Sustainability Issues - Supplementary Paper No. 4 Rapid Chloride Permeability Testing: Is it Appropriate for Concrete Durability Quality Control Testing?

**Table 9.4 Acceptance limits for concrete quality tests**

| Test | Acceptance limit at 28 days |
|---|---|
| Compressive test | <5% of test results < the characteristic strength (45 MPa) |
| RCPT (cores from unit) | <10% of test results > the characteristic value (2000 Coulombs) |
| RCPT (standard cubes) | <10% of test results > the characteristic value (1020 Coulombs) |
| Water absorption | <2% (Pocock and Corrans, 2007) |
| Water permeability | <10 mm (Pocock and Corrans, 2007) |
| ISAT (10 min) | <0.25 mL/m$^2$/s (Neville, 1995) |
| Cover | Nominal = 75 mm with −5 mm/+10 mm, ie, 70−85 mm |

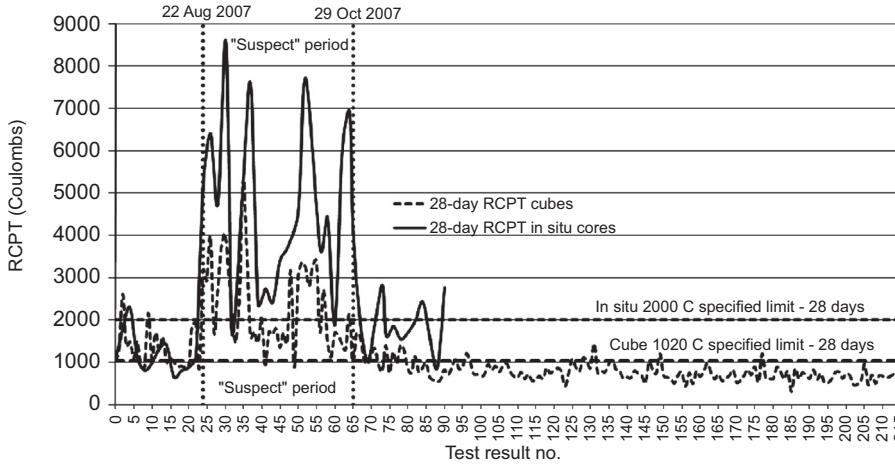
### 9.2.4.5 *Monitoring of concrete quality during construction: results and discussion*

The tests based on the concrete testing program were conducted on samples of the concrete from standard laboratory cured cubes and cores extracted from the wall elements (ie, the structure). The results over the duration of the project are summarised.

#### Rapid chloride permeability test results

The RCP test results are summarised in Fig. 9.14.

Regular monitoring of the durability testing was carried out on site in accordance with the durability specification. From the first cast in July 2007 until the end of August 2007, the RCP test values recorded were consistently lower than the required acceptance limits. However, the results deteriorated and varied to a far larger degree over a period of two months, between the August 22, 2007 and October 29, 2007, when unusually high RCP test results (above 5000 Coulombs compared to the acceptance limit of 2000) were noted, as can be seen in Fig. 9.14. As a result of the close monitoring of the durability test results, this 'suspect period' of high RCP test values was identified. An investigation into the cause was undertaken. No definitive answer could be agreed upon as to the root cause of the high RCP tests. However, once the problem had been made known to all affected parties, the RCP test values showed a




| | Standard laboratory cubes | | Cores from as-built units (in situ) | |
|---|---|---|---|---|
| | All results | Excl. | All results | Excl. |
| Number of results | 215 | 161 | 46 | 23 |
| Mean (Coulomb) | 1151 | 792 | 2992 | 1363 |
| Maximum (Coulomb) | 5345 | 1293 | 8604 | 1981 |
| Minimum (Coulomb) | 316 | 316 | 651 | 651 |
| Standard deviation (Coulomb) | 787 | 191 | 2148 | 433 |
| Characteristic value (Coulomb)* | 2174 | 1040 | 5784 | 1926 |
| Coefficient of variation (%) | 68% | 24% | 72% | 32% |

* Mean + 1.3 standard deviation

**Figure 9.14** RCP test results (28 day).

marked improvement and in fact returned to well below the acceptance limits set in the durability specification, as can be seen in Fig. 9.14.

From all the available test data, the most probable cause for the high RCP test values during the suspect period was as a result of the fly ash being omitted from some of the concrete delivered over that period of time.

### Other testing carried out

Petrographic tests were also carried out on various concrete samples extracted from the concrete units. These petrographic tests indicated the lack of fly ash in some of the concrete.

In situ testing in the form of chloride penetration measurements of actual samples obtained from placed 'suspect' units were conducted and indicated higher than normal chloride penetration for the units cast during the suspect period. Chloride penetration testing done on units cast outside the suspect period confirmed that chloride penetration was at acceptable (low) levels.

Based on these high RCP test values, the decision was made that all the c.1000 units cast during the suspect period should be retrofitted with sacrificial anodes. This was done toward the end of the contract period.

The question was also raised as to the possible prudence of fitting all the precast units with sacrificial anodes to protect every unit against unforeseen occurrences during casting, handling and placing or during the unit's design life that could compromise its integrity and durability. It was ultimately decided that the additional expense was not warranted as all correct procedures had been followed, and there was no indication from the custom-built monitoring units or the on-going durability testing that any unexpected chloride ingress had taken place. It was, however, agreed that on-going monitoring of the units by the client or his engineer would be prudent to detect any unexpected chloride ingress or durability issues.

Further testing was carried out, during July 2011, on cores recovered from the front face of units that had been exposed to the marine seawater environment for between 961 and 1226 days at the time of testing.

The testing carried out by the University of Cape Town included chloride ingress testing and petrographic testing to determine the constituents of the concrete samples.

The service-life predictions were calculated using the chloride ingress concentrations obtained from the cores and the findings were as follows:

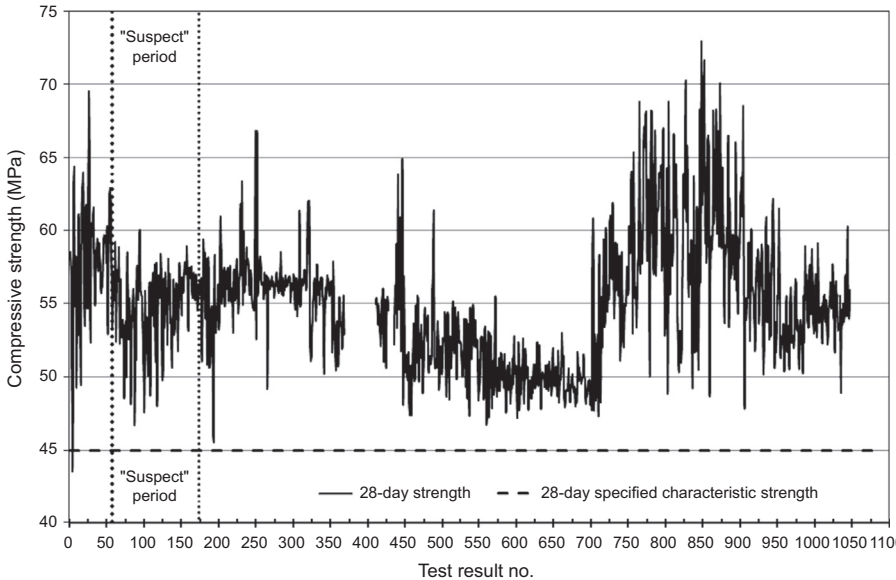
- Units that were cast during the suspect period had high chloride ingress values, and the time to onset of corrosion (0.4% chlorides by mass of binder) for 75-mm cover varied from 4 to 9 years.
- In contrast, units that were cast outside the suspect period had lower chloride ingress values, and the time to onset of corrosion (0.4% by mass of binder) for 75-mm cover varied from 18 to 27 years. (It can be noted that these predicted times to corrosion are considerably lower than the predictions given previously in this chapter, indicating that, models derived for actual conditions are needed rather than those derived for seawaters that are very different from the waters of the Gulf.)

Further petrographic testing of the samples confirmed the absence of fly ash in the units from the suspect period and fly ash in the units cast outside the suspect period.

In conclusion, quality control testing using the RCP test was considered an effective test in bringing to the contractor's attention any durability problems within 28 days of its occurring. The reason for the spike in the RCP test results (ie, suspect period) was in all likelihood as a result of the fly ash being omitted intermittently from the concrete over that period.

## Compressive strength test results

The compressive strength test results according to BS 1881 are summarised in Fig. 9.15.




| | |
|---|---|
| Number of results | 998 |
| Mean (MPa) | 55.0 |
| Maximum (MPa) | 72.9 |
| Minimum (MPa) | 44.1 |
| Standard deviation (MPa) | 4.4 |
| Characteristic value (MPa)* | 47.8 |
| Coefficient of variation (%) | 8% |

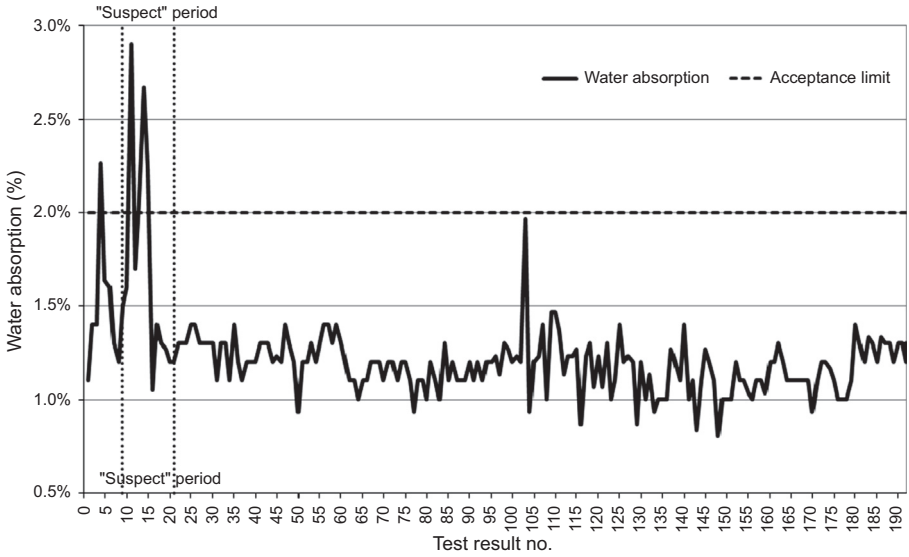
*Mean + 1.64 standard deviation

**Figure 9.15** Compressive strength results (28 day).
Twelfth International Conference on Recent Advances in Concrete Technology and Sustainability Issues - Supplementary Paper No. 4 Rapid Chloride Permeability Testing: Is it Appropriate for Concrete Durability Quality Control Testing?

Fig. 9.15 shows that the strengths varied overall from about 45 to 70 MPa, with most results clustered in the range of 50−60 MPa in the earlier stages and 55−65 MPa in the later stages. During the suspect period (roughly test results 55−175), strengths were not unduly adversely affected, while the durability results (RCP tests) were seriously affected, indicating again the inadequacy of relying on strength results alone to check in situ durability.

## Water absorption test results

The water absorption test results, according to BS 1881-122 (1983), are summarised in Fig. 9.16. As shown, 2.6% of the results were above the acceptance limit of 2%, and these tests coincided with the same time period as the suspect RCP test values shown in Fig. 9.14.




| | |
|---|---|
| Number of results | 193 |
| Mean (%) | 1.23 |
| Maximum (%) | 2.90 |
| Minimum (%) | 0.80 |
| Standard deviation (%) | 0.25 |
| Characteristic value (%)* | 1.65 |
| Coefficient of variation (%) | 21% |

* Mean + 1.64 standard deviation

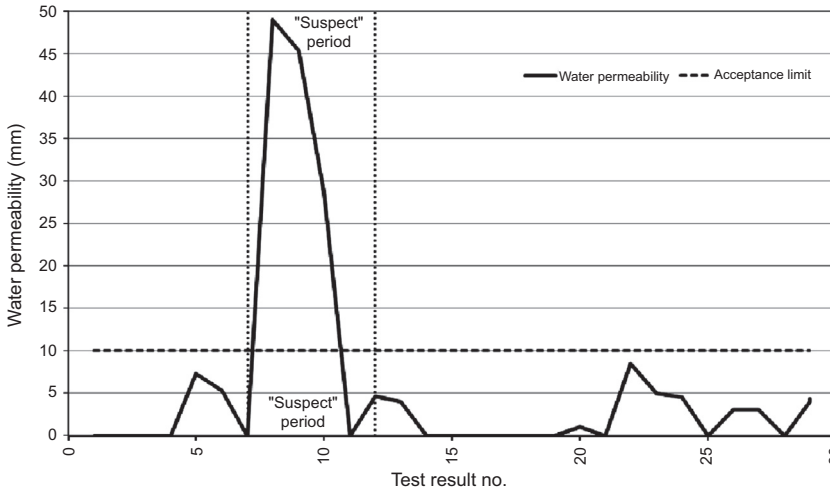
**Figure 9.16** Water absorption test results (28 day).
Twelfth International Conference on Recent Advances in Concrete Technology and Sustainability Issues - Supplementary Paper No. 4 Rapid Chloride Permeability Testing: Is it Appropriate for Concrete Durability Quality Control Testing?

## Water permeability test results

The water permeability test results according to DIN 1048-5 (1991) are summarised in Fig. 9.17 (this is actually a water penetration test, not a true water permeability test); 10% of the results were above the acceptance limit of 10 mm, and these tests also coincided with the same time period as the suspect RCP test values were shown in Figs 9.14.

## Initial surface absorption test results

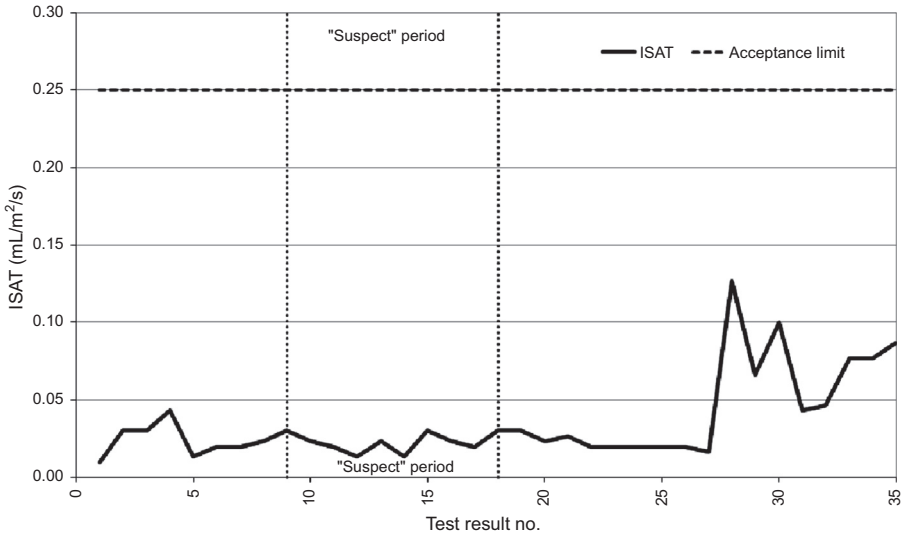
The initial surface absorption test results according to BS 1881-208 (1996) are summarised in Fig. 9.18. All results obtained were below the acceptance limit of 0.25 mL/m$^2$/s.




| | |
|---|---|
| Number of results | 30 |
| Mean (mm) | 5.9 |
| Maximum (mm) | 49.0 |
| Minimum (mm) | 0.0 |
| Standard deviation (mm) | 12.5 |
| Characteristic value (mm)* | 26.4 |
| Coefficient of variation (%) | 211% |

*Mean + 1.64 standard deviation

**Figure 9.17** Water permeability test results (28 day).
Twelfth International Conference on Recent Advances in Concrete Technology and Sustainability Issues - Supplementary Paper No. 4 Rapid Chloride Permeability Testing: Is it Appropriate for Concrete Durability Quality Control Testing?




| | |
|---|---|
| Number of results | 35 |
| Mean (mL/m$^2$/s) | 0.04 |
| Maximum (mL/m$^2$/s) | 0.13 |
| Minimum (mL/m$^2$/s) | 0.01 |
| Standard deviation (mL/m$^2$/s) | 0.03 |
| Characteristic value (mL/m$^2$/s)* | 0.08 |
| Coefficient of variation (%) | 77% |

* Mean + 1.64 standard deviation

**Figure 9.18** Initial surface absorption test results (28 days).
Twelfth International Conference on Recent Advances in Concrete Technology and Sustainability Issues - Supplementary Paper No. 4 Rapid Chloride Permeability Testing: Is it Appropriate for Concrete Durability Quality Control Testing?

## 9.3 Conclusions

The first part of this chapter covered the development of marine concrete structures in the Arabian Gulf, including the historical background, the challenges of executing the construction in this extremely harsh environment and the types of marine structures used for marinas in the Arabian Gulf region.

There are many challenges facing the contractor when designing and constructing reinforced concrete structures in the Arabian Gulf, including the harsh climatic and environmental conditions, the nature of the locally available construction materials and the construction execution. Ensuring quality control on site during concrete

manufacture, transport, placement and curing can also be a challenge due to the high ambient temperatures experienced in the region.

Chloride ingress is the most common environmental attack that leads to the corrosion of reinforcing steel and the deterioration of concrete structures, especially in the marine environment where structures are exposed to saltwater and wetting and drying cycles. As a result, it has become normal practice to specify concrete durability tests. These include, among others, a combination of capillary index monitoring tests carried out on concrete sections cut from cubes, permeable voids tests, rapid chloride permeability testing, water absorption, water permeability and initial surface absorption.

Due to the experience of deterioration of reinforced concrete structures built during the 1970s and 1980s, unreinforced concrete construction is the preferred method of construction for waterfront structures exposed to seawater along the coastline in the Arabian Gulf. The most common form of unreinforced concrete construction used in seawalls for waterfront developments are precast concrete blockwork walls of which there are many examples.

Reinforced concrete infrastructure construction in the Arabian Gulf region has seen massive growth in the past two decades, including many high-rise office and apartment complexes as well as recreational and industrial waterfront marina-type developments. The range of reinforced concrete seawall structures being constructed for recreational and industrial waterfront developments in the Arabian Gulf today includes, among others, in situ concrete diaphragm walls and precast concrete gravity-type retaining walls. However, as a result of the poor track record of reinforced concrete built in the early 1970s and subsequent resistance to the use of reinforced concrete in waterfront structures in the Arabian Gulf, great emphasis is now placed on the durability of the concrete used in these seawalls. The long-term durability of these reinforced concrete structures requires the incorporation of appropriate construction materials such as cement extenders, suitable construction methods, followed by an appropriate program of monitoring and measuring actual performance on site.

The second part of this chapter gives a case study that confirms quality control testing using the RCP test can be considered effective in bringing to the contractor's attention any concrete durability problem within a short time (typically 28 days) of it occurring. The RCP test therefore seems to be an appropriate test for concrete durability specifications and quality control. The RCP test highlighted that the units cast within the 'suspect' period did not comply with the durability specification, and the contractor was able to intervene and improve the durability of the suspect units by fitting them with sacrificial anodes to account for the apparent lack of fly ash in the concrete mix. The author has sourced another project in the United States where RCP testing was also used for quality control, and the results also highlighted the absence of fly ash in the concrete (Bognacki et al., 2010).

A lesson learnt on this project is that due consideration should be made concerning the availability of the required cement extenders, especially during times of economic boom. The project used a ternary concrete mix, and severe shortages of fly ash were encountered. The required supply of concrete could not be met during peak production stages of the project. This may well have been a factor in the fly ash being omitted from the concrete during the 'suspect' period.

The results of the durability tests conducted on the concrete outside the suspect period indicated that the wall units complied with the concrete durability specification.

## References

ASTM C1202, 2005. Electrical Indication of Concrete's Ability to Resist Chloride Ion Penetration. American Society for Testing and Materials (ASTM).

Bognacki, C.J., Pirozzi, M., Marsano, J., Baumann, W.C., 2010. Rapid chloride permeability testing's suitability for use in performance-based specifications. Concrete International 32 (5), 47−52.

BS 1881-116, 1983. Testing Concrete. Method for Determination of Compressive Strength of Concrete Cubes. British Standards Institution, London.

BS 1881-122, 1983. Testing Concrete, Method for Determination of Water Absorption. British Standards Institution, London.

BS 1881-208, 1996. Testing Concrete, Recommendations for the Determination of the Initial Surface Absorption of Concrete. British Standards Institution, London.

DIN 1048-5, Section 3.6, 1991. Testing Concrete. Water Permeability. German Standard.

Heath, K., Alexander, M.G., 2012. Rapid chloride permeability testing: is it appropriate for concrete durability quality control testing? Supplementary paper no. 47. In: 12th Int. Conf. On Recent Advances in Concrete Technology and Sustainability Issues, Prague, Oct 2012. American Concrete Institute, Farmington Hills, pp. 47−63. ACI SP-289.

Mackechnie, J.R., 2001. Predictions of Reinforced Concrete Durability in the Marine Environment. Research Monograph. University of Cape Town.

Mackechnie, J.R., Alexander, M.G., 2002. Durability predictions using early-age durability index testing. In: Proceedings, 9th Durability and Building Materials Conference, Australian Corrosion Association, Brisbane, 11 p.

Neville, A.M., 1995. Properties of Concrete, fourth ed. Addison Wesley Longman Ltd.

Pocock, D., Corrans, J., 2007. Concrete durability testing in Middle East construction. Concrete Engineering International 11 (2), 52−54.

Silica Fume Association, 2001. Life-cycle Costs of Reinforced Concrete Exposed to Chlorides.

Streicher, P., Alexander, M.G., 1995. A chloride conduction test for concrete. Cement and Concrete Research 25 (6), 1284−1294.

Thomas, M.D.A., Bentz, E.C., 2000. Life 365, Computer Program for Predicting the Service Life and Life Cycle Costs of Reinforced Concrete Exposed to Chlorides. Concrete Corrosion Inhibitors Association, Potomac, MD.

# Notable Southern African marine structures

10

*P.E. Smith*
Prestedge Retief Dresner Wijnberg (Pty) Ltd

## 10.1 Introduction

This chapter concentrates on Southern African marine structures of notable size and function. Other marine structures in Southern Africa, smaller but not less notable, are covered in chapter 'Concrete durability in small harbours – the Southern African experience' of this book. Five projects from Southern Africa, with which the author has had direct involvement, are described, some of which include multiple structure types. They range from the major commercial port projects in Durban and Ngqura to the marine infrastructure for the Victoria & Alfred Waterfront development in Cape Town. As will be seen, all these projects make extensive use of concrete as the major structural material.

## 10.2 Victoria and Alfred Waterfront development

Development of the Victoria and Alfred Waterfront (V&AW), from a run-down and underutilised area of the Cape Town harbour to a vibrant and popular waterfront, began in 1988. The development site comprised the existing Victoria and Alfred harbour basins dating from the late 1800s, a dry dock and Syncrolift, and a land area that hosted a number of uses. The docks primarily served the fishing industry, as well as ship maintenance facilities and berthing of the port authority service boats.

An aerial photograph is given in Fig. 10.1 showing the V&AW precinct and the location of the developments described in this section.

The first basin to be constructed was the Alfred Basin, which was dug out of the bedrock immediately behind the original shoreline, and the second basin was the Victoria Basin, which was constructed in the sea.

On the west side of the Alfred Basin, a further basin was quarried out in the 1880s. The rock from this was used to create the two arms of the Victoria Basin, and it was intended to act as a third basin. However, by the time that the Victoria Basin was completed, the newly excavated basin was deemed too small for the latest generation of ships calling at the Cape, and it was never finished as a basin and flooded. Instead, the old quarry and the surrounding area were utilised by oil companies as an oil storage facility until the late 1980s.

The quarry and surrounding land were a valuable development opportunity for the newly formed Victoria & Alfred Waterfront Company, and development of this area

**Marine Concrete Structures.** http://dx.doi.org/10.1016/B978-0-08-100081-6.00010-6
Copyright © 2016 Elsevier Ltd. All rights reserved.




**Figure 10.1** Cape Town: Victoria and Alfred Waterfront aerial view.
Adapted from project drawings by Victoria & Alfred Waterfront (Pty) Ltd/Prestedge Retief Dresner Wijnberg (Pty) Ltd and Google Earth.

was one of the first actions arising from the waterfront master plan. This work commenced in 1993.

The Granger Bay precinct between the northwest side of the Victoria Basin and the Granger Bay shoreline was underutilised and also became a prime focus of the early waterfront development.

### *10.2.1 Granger Bay shoreline protection*

The V&A Waterfront master plan earmarked the Granger Bay precinct for a shopping mall and hotel development, and since these faced onto the Victoria Basin, road access and parking was required on the Granger Bay side. The Granger Bay shoreline experiences aggressive wave attack during winter storms, and the planning study determined that there was insufficient setback from the shoreline for the proposed road system. The existing Granger Bay land reclamation was at a level that suited the Victoria Basin quayside, and when combined with the existing informal shoreline protection, it was very vulnerable to wave overtopping and flooding.

A section of properly engineered shoreline protection was therefore required to safeguard the new precinct infrastructure. A dolosse-armoured revetment was designed

in a position and alignment that would suit the layout of the future marina that was planned for Granger Bay.

The 240-m-long revetment was constructed in the summer of 1993/1994 offshore of the existing shoreline and is armoured with 20- and 25-tonne dolosse, the larger units being used for the roundhead on the eastern end; see left-hand portion in Fig. 10.2. Fig. 10.3 shows a typical cross section through the revetment.

A total of 1090 No. 20 tonne dolosse and 335 No. 25 tonne dolosse were cast on site in a precast yard specifically set up for the project. Fig. 10.4 shows the precast yard, Fig. 10.5 shows a 25-tonne dolos being lifted for placement on the revetment slope, and Fig. 10.6 shows the seaward face of a section of completed revetment.




**Figure 10.2** V&AW Granger Bay shoreline protection revetment. The dolosse-armoured revetment is shown in the foreground. The wider portion of the section armoured with 25-tonne dolosse is visible at the left end.
Photograph: Victoria & Alfred Waterfront (Pty) Ltd.

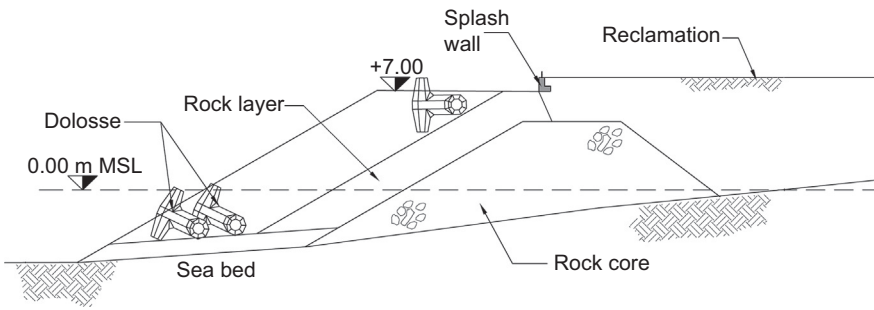



**Figure 10.3** V&AW Granger Bay shoreline protection. Revetment cross section.
Adapted from project drawings by Victoria & Alfred Waterfront (Pty) Ltd/Prestedge Retief Dresner Wijnberg (Pty) Ltd.



**Figure 10.4** V&AW Granger Bay shoreline protection. Casting yard. Photograph: Prestedge Retief Dresner Wijnberg (Pty) Ltd.



**Figure 10.5** V&AW Granger Bay shoreline protection. Placing a 25-tonne dolos. Photograph: Prestedge Retief Dresner Wijnberg (Pty) Ltd.

The revetment was designed to have minimal overtopping and was therefore given a high crest level. This enabled it to have a small reinforced concrete retaining wall on the crest rather than a heavy, plain concrete cap. The revetment has now been in service for over 20 years and has not required any maintenance in that time.

### *10.2.2 New Marina Basin*

Construction of the new Marina Basin in the old quarry referred to earlier commenced in 1993, and a number of marine structures were required for the basin as described next (see Fig. 10.7). The majority of the new basin's infrastructure was undertaken



**Figure 10.6** V&AW Granger Bay shoreline protection. Typical dolosse packing on the revetment.
Photograph: Prestedge Retief Dresner Wijnberg (Pty) Ltd.



**Figure 10.7** V&AW Marina Basin. The Marina Basin is in the centre of the photograph, the Alfred Basin is on the left, and top right is the canal, which was still under construction at the time of the photograph.
Photograph: Victoria & Alfred Waterfront (Pty) Ltd.

in the dry before the cut through to the Alfred Basin was blasted out and the basin flooded (see Fig. 10.8).

### *10.2.2.1 Residential edge wall*

Residential apartments have been developed along the western and southern sides of the Marina Basin. Each apartment block has an underground parking garage, and to minimise groundwater emanating from the Marina Basin entering the garages, a water-tight basin edge wall was required to retain the high tide water levels. The edge wall is



**Figure 10.8** V&AW Marina Basin. Construction of the basin in the dry. The concrete structures visible in this view are the Residential Edge Wall on the right-hand side, the North Wharf on the left-hand side, the jetty is centre-top, and to the left of it some edge lining. Photograph: Victoria & Alfred Waterfront (Pty) Ltd.

shown in Figs 10.9−10.11. The wall is founded on rock, and the plain concrete foundation provides the seal onto the bed rock. As the wall is a highly visible and prominent edge to the residential precinct, care was taken with its aesthetical appearance to ensure that it matched the landscape theme of the Waterfront and the adjacent historic port structures.

The Alfred Basin was originally carved out of the greywacke bed rock, and the visible quay edges comprise stonework lining to the excavated rock face or gravity stone walls. The quay faces have a random stonework finish, and this theme was carried over to the new basin edge walls. The structural water-retaining wall was given a stonework facing from the local rock and a concrete cap. A 19-mm, brown sandstone aggregate was used for the cap, and the surface was roughened to give an 'aged' aesthetic to the wall.

The wall was cast in 8-m-long panels, and the contraction joints between them were sealed with conventional and swelling hydrophilic rubber waterstops.

The design life of the edge wall is nominally 100 years, but at the time of its design, in 1994, the durability research and service life prediction models were not as advanced as at present, and a simple prescriptive-based approach was adopted in the hope of achieving the required durability. The prescribed concrete mix requirements are given in Table 10.1. The contractor elected to use the fly ash (FA) option, but due to the slow strength gain that was experienced with the 30% FA content, the proportion of the extender was reduced to 25%.

Subsequent contemporary investigation was undertaken by Hargey (2015) on the concrete mixes used in the waterfront marine structures, by assessing the current state of ingress of chlorides into the concrete elements. The assessment gives a predicted life of at least 125 years to initiation of corrosion in the structural concrete, which used greywacke aggregate. Many of the upper structure elements, such as the caps, were

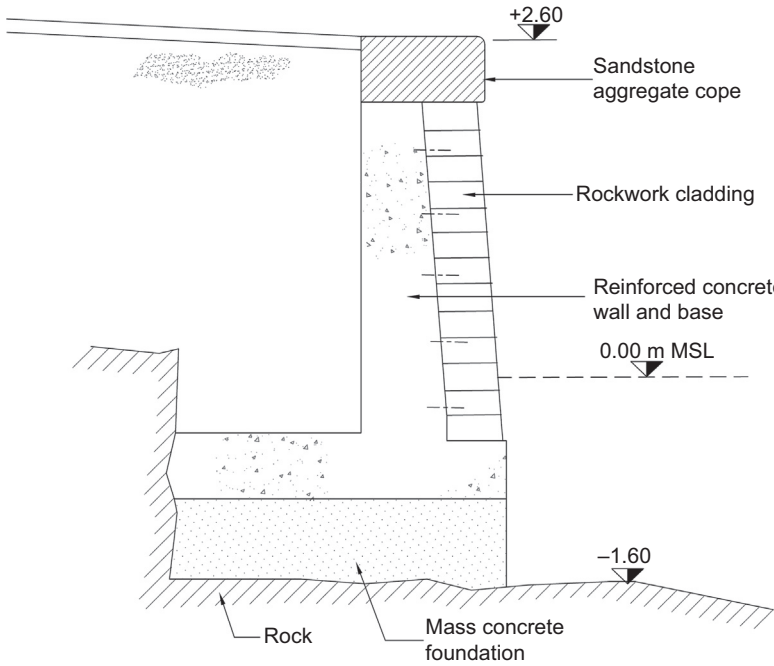



**Figure 10.9** V&AW Residential Edge Wall cross section.
Adapted from project drawings by Victoria & Alfred Waterfront (Pty) Ltd/Prestedge Retief Dresner Wijnberg (Pty) Ltd.



**Figure 10.10** V&AW Residential Edge Wall under construction. Visible is this view are the plain concrete foundation, reinforced concrete cantilever wall with a waterstop in the joint, and the rock cladding.
Photograph: Prestedge Retief Dresner Wijnberg (Pty) Ltd.



**Figure 10.11** V&AW Residential Edge Wall. Completed section of wall. Photograph: Prestedge Retief Dresner Wijnberg (Pty) Ltd.

**Table 10.1 V&AW new basin concrete durability requirements**

| Concrete grade (28-day characteristic strength (MPa)/stone size (mm)) | Cement type | Cement extender type and percent content | Minimum cement content ($kg/m^3$) | Maximum water/ binder ratio |
|---|---|---|---|---|
| 45/19 | PC | GGBS (45−55%) or FA (30−35%) | 420 | 0.40 |

*PC*, plain Portland cement, *GGBS*, ground granulated blast furnace slag, *FA*, fly ash.
Minimum cement content is the sum of the mass of cement and extender, ie, total binder content.

made using sandstone aggregates and roughened after curing to give the desired architectural finish. At the time of construction, it was realised that the roughening of the cap concrete combined with the sandstone aggregate would lower the expected durable life of the element, and this has been confirmed by Hargey, who predicted a variable time to initiation of corrosion of 30−100 years for these elements.

### *10.2.2.2 Cut edge lining*

The basin edges through the cut to the Alfred Basin comprised a concrete panel lining to the excavated rock face with the same stone cladding and top cap as the residential wall. The lining was anchored to the rock face with 3-m-long drilled and grouted steel dowels. See Figs 10.12 and 10.13.

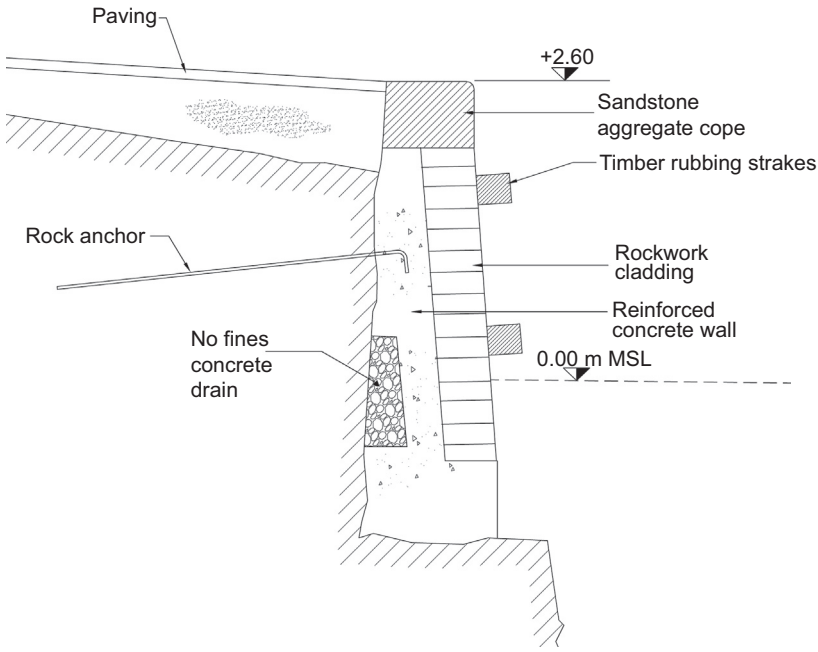



**Figure 10.12** V&AW edge lining cross section.
Adapted from project drawings by Victoria & Alfred Waterfront (Pty) Ltd/Prestedge Retief Dresner Wijnberg (Pty) Ltd.



**Figure 10.13** V&AW edge lining. Edge lining in the cut to the Alfred Basin under construction. Visible in the view are the lining base cast, wall panel and rock cladding. The lining was only constructed over the upper, visible part of the edge, and the permanently submerged lower section was given a coating of shotcrete or left as natural rock.
Photograph: Prestedge Retief Dresner Wijnberg (Pty) Ltd.

The cut lining also incorporated the underground foundations for a bascule bridge and manholes, as well as a bank of ducts for an underwater services crossing. Unlike the residential wall, the lining was not required to be water-retaining, and in fact the opposite was needed so that a water head did not build up behind the panels. The lining therefore included a no-fines concrete drain and cast in drain holes.

### 10.2.2.3 North Wharf

The Waterfront planned to construct a multistory building on the northern side of the basin, but due to the restricted space available between the water's edge and the adjacent Robinson dry dock, the building footprint was required to project out over the water. A reinforced concrete wharf structure was therefore designed to act as a foundation for the seaward portion of the building.

The wharf columns and beam grillage were constructed in situ in the dry from reinforced concrete and precast slab units with an in situ topping were used for the wharf deck slab. The columns were founded on the basin bed rock so that there would be no differential settlement between the front and rear of the building. As it was intended that small craft would berth against the wharf, precast fender panels and bollards were incorporated in the structure. The fender units were cast off site at the contractor's precast yard. The use of precast units reduced the work required on site and thereby saved time on the construction program.

The wharf structure is shown in Figs 10.14 and 10.15.

### 10.2.2.4 East jetty

Unlike the North Wharf, the east jetty was founded on fill material above the basin bedrock. The jetty was designed to berth small craft on each side and is shown in Fig. 10.16.

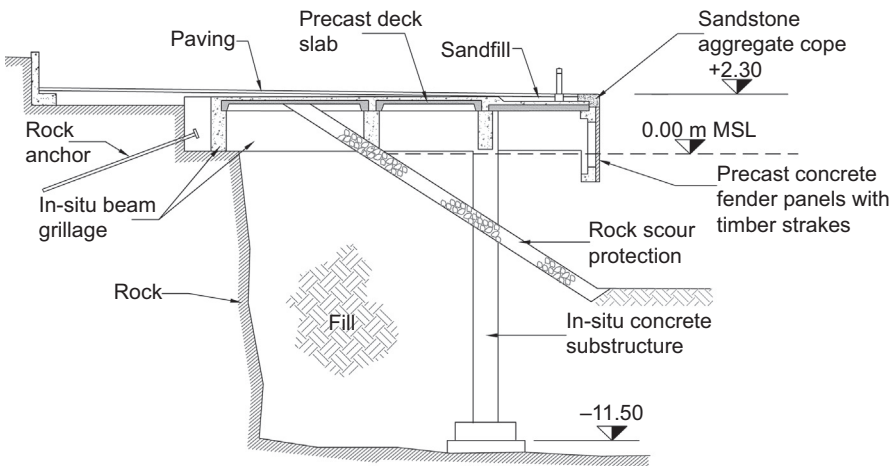



**Figure 10.14** V&AW North Wharf cross section.
Adapted from project drawings by Victoria & Alfred Waterfront (Pty) Ltd/Prestedge Retief Dresner Wijnberg (Pty) Ltd.



**Figure 10.15** V&AW North Wharf under construction. This view shows in situ construction of the beam grillage on the left on top of fill and placement of precast deck slabs in the centre. Photograph: Victoria & Alfred Waterfront (Pty) Ltd.

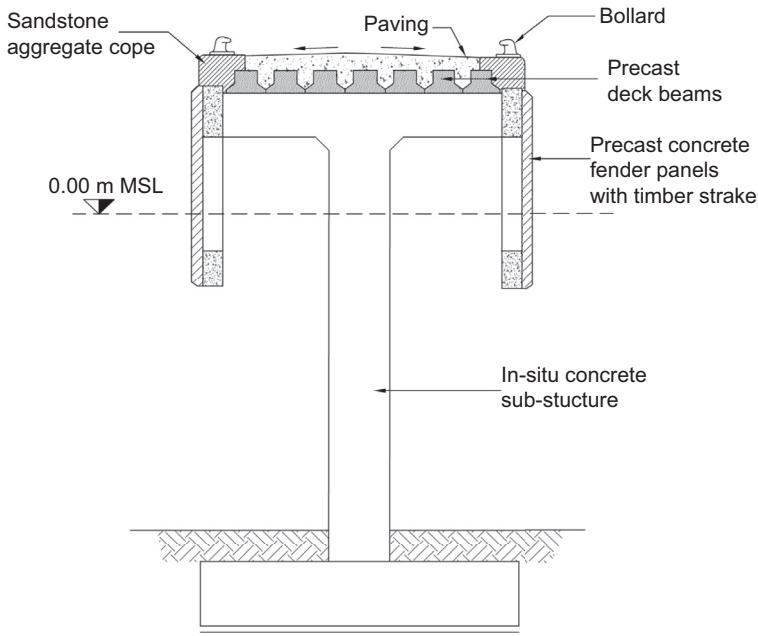



**Figure 10.16** V&AW east jetty cross section.
Adapted from project drawings by Victoria & Alfred Waterfront (Pty) Ltd/Prestedge Retief Dresner Wijnberg (Pty) Ltd.



**Figure 10.17** V&AW east jetty construction. Visible in these views are the in situ concrete substructure, placed precast deck beams and erection of the precast fender panels in progress. Photograph: Prestedge Retief Dresner Wijnberg (Pty) Ltd.

The structure was constructed in the dry primarily from in situ reinforced concrete except for the precast deck units and fender panels (refer Fig. 10.17). The jetty could have been constructed entirely in situ, but use was made of precast units to speed up the construction.

#### *10.2.2.5 Aquarium deck*

The aquarium deck is a timber walkway on the north side of the basin in front of the Two Oceans Aquarium. To reduce the volume of expensive hardwood and to create a durable structure, the walkway substructure was constructed from reinforced concrete. This included the columns and primary crossbeams. All the bearers, deck planks, and vertical fender planks were of hardwood.

A typical walkway cross section is shown in Fig. 10.18, while Fig. 10.19 shows the deck during construction.

### *10.2.3 Canal*

The canal has a water level perched at 3.5 m above mean sea level and runs from the Cape Town International Convention Centre (CTICC) at the end of Long Street, which traverses the city, through to the northern end of the Waterfront residential development. The layout of the 1.5-km long canal is shown in Fig. 10.20. Figs 10.21 and 10.22 show views of the portion of the canal in the Waterfront residential area.

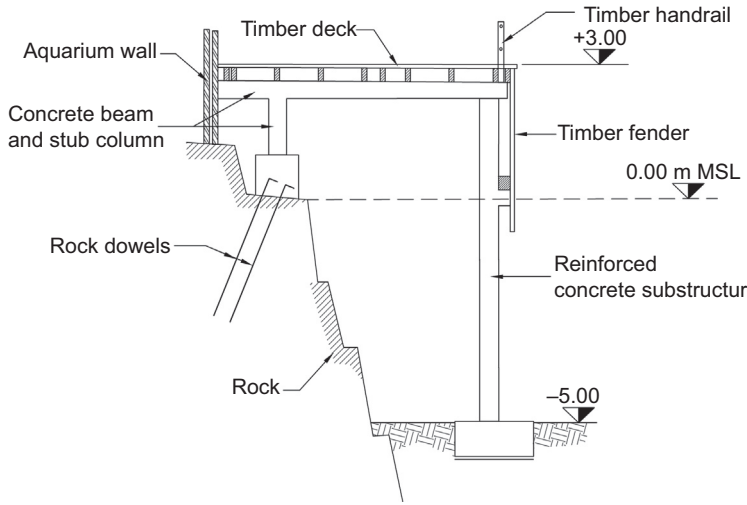



**Figure 10.18** V&AW aquarium deck cross section.
Adapted from project drawings by Victoria & Alfred Waterfront (Pty) Ltd/Prestedge Retief Dresner Wijnberg (Pty) Ltd.



**Figure 10.19** V&AW aquarium deck under construction showing the concrete column and beam substructure and commencement of the timber deck construction.
Photograph: Prestedge Retief Dresner Wijnberg (Pty) Ltd.




**Figure 10.20** V&AW Canal layout. The canal runs from the convention centre at the bottom right-hand corner of the photograph to a boat lock in the Marina Basin.
Adapted from project drawings by Victoria & Alfred Waterfront (Pty) Ltd/Prestedge Retief Dresner Wijnberg (Pty) Ltd and Google Earth.



**Figure 10.21** V&AW canal. Portion of the canal in the residential area.
Photograph: Victoria & Alfred Waterfront (Pty) Ltd.



**Figure 10.22** V&AW canal. Typical canal view. The view illustrates the successful integration of civil engineering infrastructure with the landscape architecture that was achieved with this development.
Photograph: Prestedge Retief Dresner Wijnberg (Pty) Ltd.

The canal was created to enhance the environment for the residential and commercial precincts through which it passes, and it also serves as a transport route between the Waterfront and the CTICC.

The canal is an artificial perched water body, and the bed and edges were required to be water-retaining. All canal edges are, in situ, reinforced concrete, cantilever retaining walls, typically cast in 8-m-long panels. The joints between the panels are simple contraction joints, which are sealed with hydrophilic swelling waterstops. A typical canal wall cross section is shown in Fig. 10.23.

The top of the wall, above the water-retaining panel, has precast concrete cope units. A family of cope units was designed, including typical plain units, lighting units, mooring hook units and service point units. They were developed in collaboration with the project architectural advisors, and several trial units were cast with varying aggregates and surface finishes to achieve a suitable aesthetic that fitted in with the Waterfront theme. Several of the old quay walls in the Waterfront basins are topped with a dressed stone cope, and the aim was to create an edge with contemporary materials that would have a similar worn appearance. The chosen finish utilised a brown sandstone aggregate and a light sand blast of the exposed faces to remove the smooth laitance on the surface. The cope units are unreinforced, and therefore there is no possibility of reinforcing corrosion damage. Any minor damage to the surface caused by the sand blast is not likely to affect their durability.

The canal depth and the wall heights vary along its length. In the residential precinct, in the downstream half of the canal, the 3-m water depth was designed to accommodate yachts up to 15 m in length. It is not possible for yachts to travel upstream, and therefore the upstream canal depth was reduced to 2.0 m and 1.5 m, which is suitable for motor boats. Fig. 10.24 shows construction of the canal walls for the residential precinct.

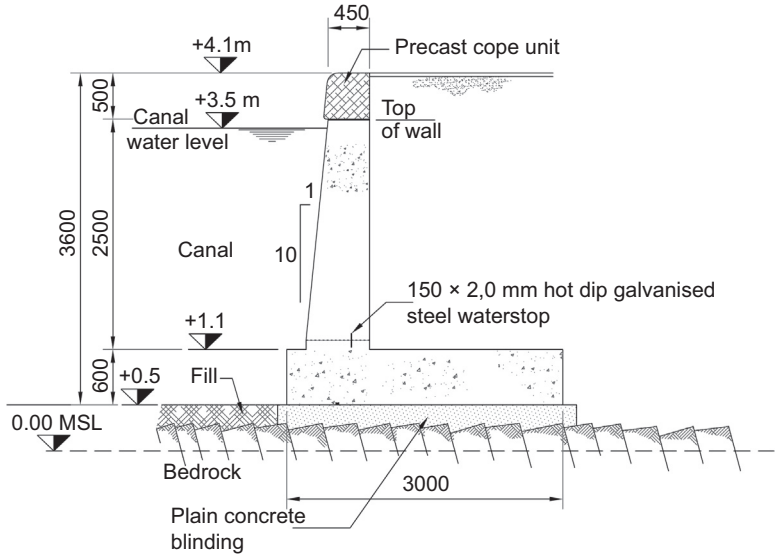



**Figure 10.23** V&AW canal. Typical canal wall cross section.
Adapted from project drawings by Victoria & Alfred Waterfront (Pty) Ltd/Prestedge Retief Dresner Wijnberg (Pty) Ltd.



**Figure 10.24** V&AW canal. Canal wall under construction. Visible in this view are the plain concrete blinding onto the bed rock, the reinforced concrete wall base and panel, and stacked behind the wall on the left are precast wall cope units. This section of canal is 3.0-m deep.
Photograph: Prestedge Retief Dresner Wijnberg (Pty) Ltd.

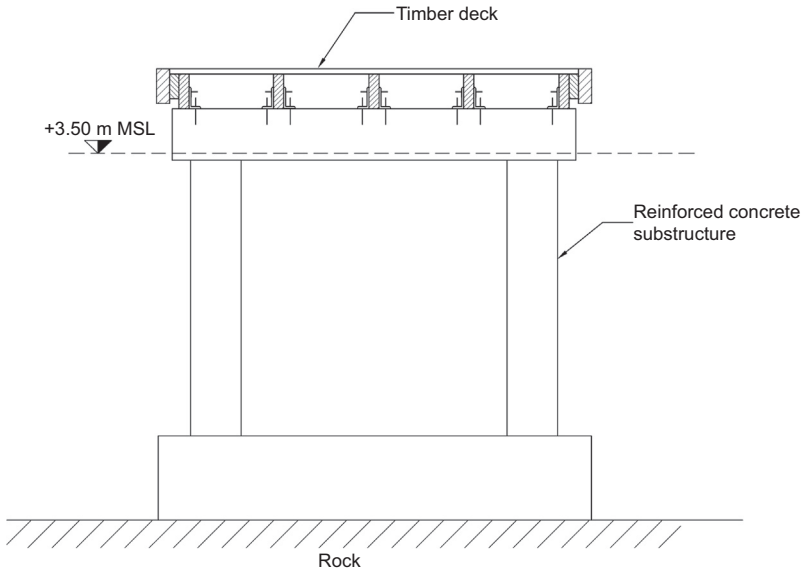



**Figure 10.25** V&AW canal. Canal jetty cross section.
Adapted from project drawings by Victoria & Alfred Waterfront (Pty) Ltd/Prestedge Retief Dresner Wijnberg (Pty) Ltd.

Approximately 60% of the canal is founded on rock, and the bed between the walls was grouted to seal the rock joints for water tightness. The remainder of the canal was founded on reclaimed sand, and the bed was sealed with a plastic membrane.

In addition to the edge walls, other canal structures were constructed from reinforced concrete, including an outfall spillway, outfall culvert, wave absorbers, lifting bridge foundations, and jetty substructures. As with the Marina Basin walkway, the canal jetties have reinforced concrete columns and crossbeams with hardwood bearers and decking, as shown in Fig. 10.25.

## 10.3 New Port of Ngqura Harbour, Eastern Cape, South Africa

### *10.3.1 Ngqura Harbour*

Ngqura is a green−fields, deep water port developed for the trans-shipment of bulk commodities for the 15,000-ha Coega Industrial Development Zone and hinterland, and to act as a regional container hub for sub-Saharan Africa. It is located in Algoa Bay, Eastern Cape, 20 km from Port Elizabeth and midway between the ports of Cape Town and Durban.

The construction of the harbour commenced in 2002 and took three years to build. The port layout is shown in Fig. 10.26.

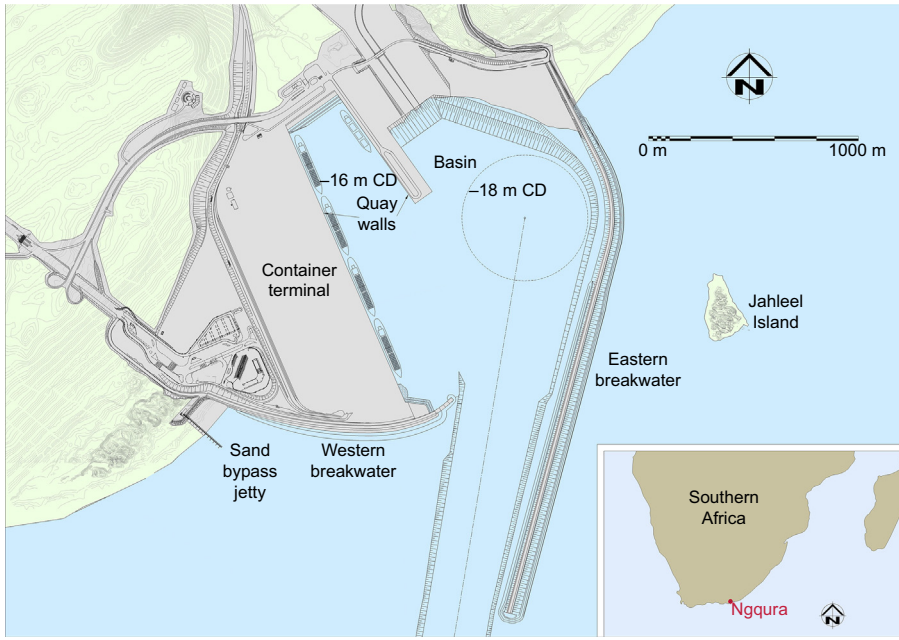



**Figure 10.26** Ngqura Harbour layout.
Adapted from project drawings by Transnet National Ports Authority/Prestedge Retief Dresner Wijnberg (Pty) Ltd.

The marine works for the port included main and secondary breakwaters, quay walls, dredging of the port entrance channel and outer basin, dry excavation of the inner basin and a sand bypass system. The breakwaters, quay walls and sand bypass system all had concrete elements, and these are described next.

## *10.3.2 Breakwaters*

### *10.3.2.1 Rubble mound breakwaters*

The 2610-m-long main breakwater and the 1090-m-long secondary breakwater both have rock-rubble trunk structures with a plain concrete cap and dolosse armour. Typical cross sections of the two breakwaters are shown in Figs 10.27 and 10.28.

Dolosse were considered the most suitable armour unit for the exposed conditions, and a total of 25,000 of the 30-tonne units was used, all cast in a dedicated on-site casting yard (Figs 10.29 and 10.30). The yard was equipped with two rows of soffit forms and half the number of side forms. This enabled freshly cast dolosse to remain supported on the soffits for their concrete to gain strength while the next batch was cast. A membrane curing compound was used for curing the dolosse.

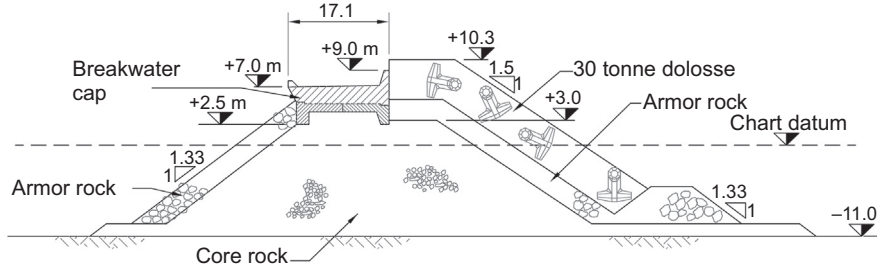



**Figure 10.27** Ngqura main breakwater cross section (dimensions in metres). Of particular note is the two-stage cap.
Adapted from project drawings by Transnet National Ports Authority/Prestedge Retief Dresner Wijnberg (Pty) Ltd.

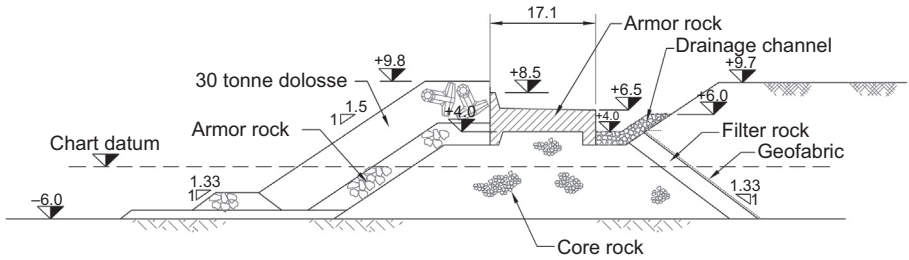



**Figure 10.28** Ngqura secondary breakwater cross section (dimensions in metres).
Adapted from project drawings by Transnet National Ports Authority/Prestedge Retief Dresner Wijnberg (Pty) Ltd.

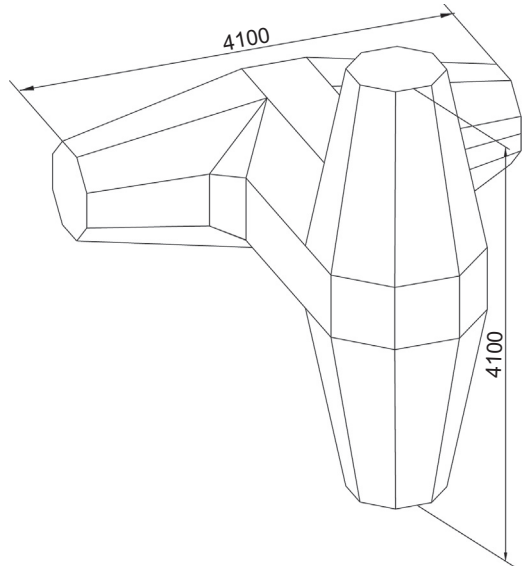



**Figure 10.29** Thirty-tonne dolos isometric view, Ngqura breakwaters (dimensions in millimetres).
Adapted from project drawings by Transnet National Ports Authority/Prestedge Retief Dresner Wijnberg (Pty) Ltd.



**Figure 10.30** Ngqura dolosse casting yard. The casting area with two rows of casting positions is in the centre-left portion of the yard. Immediately adjacent to it, on the seaward side, is a small storage area for freshly cast dolosse, while further away and to the right are the main long-term storage areas.
Photograph: Transnet National Ports Authority.

The cap for the secondary breakwater was constructed in the conventional way. After the rock-rubble structure was constructed full length and the caissons placed at the end, the cap was cast in 8.0-m-long panels from the head back to the root. The cap included a service duct for the sand bypass system and a wave wall. Plain concrete was used for the main part of the cap, and reinforced concrete was used for the wave wall and duct edge wall. For these reinforced components, a prescriptive concrete specification was used, similar to that described in Table 10.1.

For most of the length of the main breakwater, a two-part cap was used. This comprised a lower cast that was constructed as the breakwater progressed and an upper cast that was constructed from the roundhead back toward the root. The first stage cap was constructed to secure the top of the mound against sea action during the long construction period. It was cast in two halves, one on the seaward side and one on the harbour side, so that truck access to the core construction face could be maintained when the first half was cast. The cap was constructed from plain concrete except for the wave wall, which was reinforced, and again a marine grade of concrete was used for the wall.

### *10.3.2.2 Caissons*

A large caisson forms the roundhead of the main breakwater, and four caissons form the last 107 m of the secondary breakwater. It was considered impracticable to construct a conventional dolosse armoured roundhead for the main breakwater,

as either a dolos unit larger than 30 tonnes or a flatter armoured slope would have been required, both of which would have demanded a larger and more expensive crane than planned for the trunk construction. In addition, dolosse larger than 30 tonnes were considered to have too great a risk of breakage in service. It is anticipated that in future the port may be expanded to the southwest, which would entail extension of the main breakwater and a new secondary breakwater. The caissons for both breakwaters could then be refloated and reused in the new locations.

The main breakwater caisson is shown in Figs 10.31–10.36. It is 66 × 23 × 20 m (length × width × height) and utilised 5100 $m^3$ of reinforced concrete.

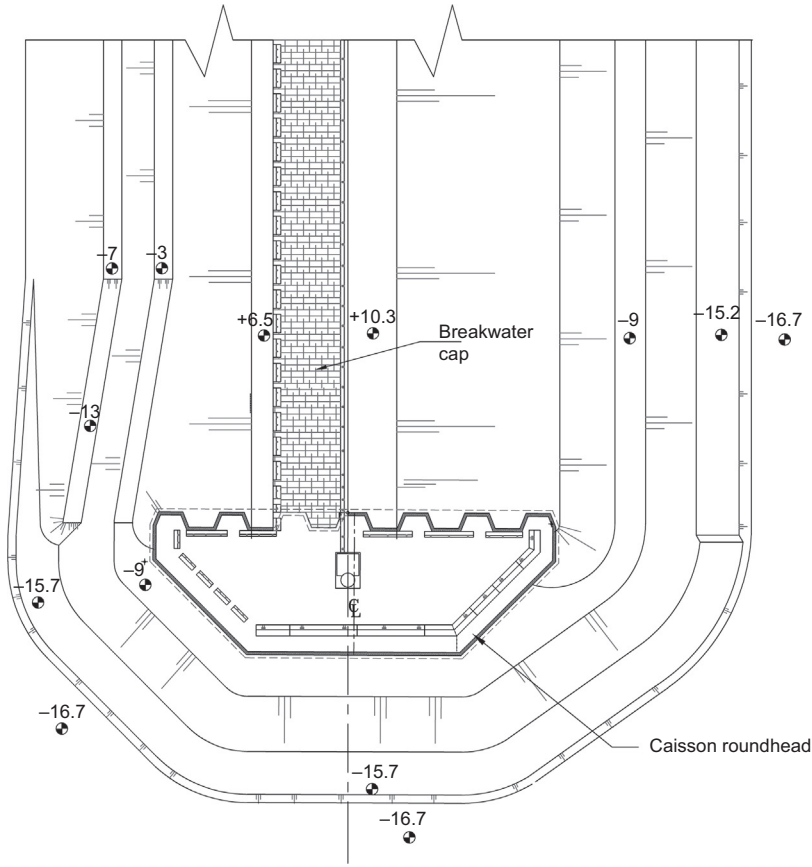



**Figure 10.31** Ngqura main breakwater caisson roundhead: plan view.
Adapted from project drawings by Transnet National Ports Authority/Prestedge Retief Dresner Wijnberg (Pty) Ltd.

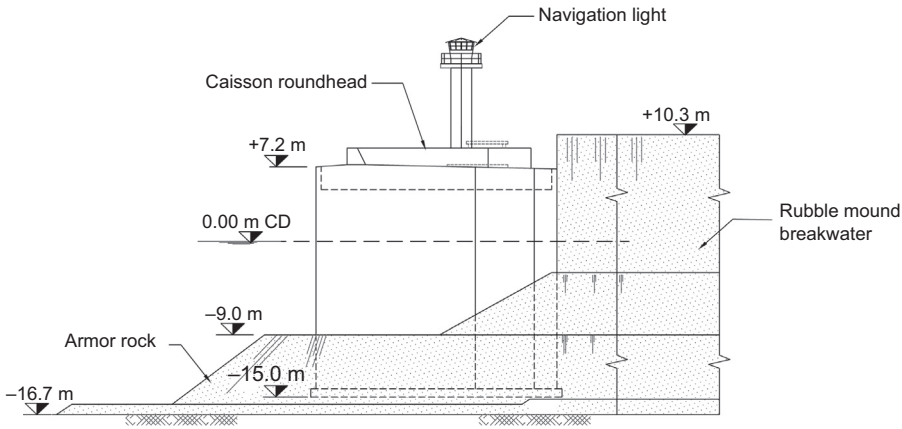



**Figure 10.32** Ngqura main breakwater caisson roundhead: elevation.
Adapted from project drawings by Transnet National Ports Authority/Prestedge Retief Dresner Wijnberg (Pty) Ltd.

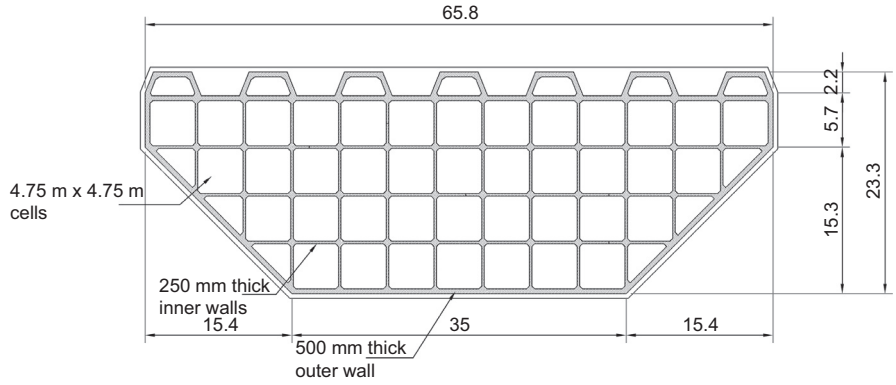



**Figure 10.33** Ngqura main breakwater caisson roundhead: caisson plan dimensions (in metres).
Adapted from project drawings by Transnet National Ports Authority/Prestedge Retief Dresner Wijnberg (Pty) Ltd.

The secondary breakwater caissons are shown in Figs 10.37–10.41. Each one was $26 \times 17 \times 16$ m and utilised 1600 $m^3$ of reinforced concrete; a further 950 $m^3$ of plain concrete was cast in the cap after placing.

The main basin of the harbour was dug out of the shoreline in the dry and was used as a dry dock for the caisson construction. The secondary caisson bases were each cast in one pour, but the main caisson base was done in three pours due to its size. The caisson walls were all cast continuously using the sliding technique, and the main caisson was done in four sections. Moist curing was used for the caisson concrete and for the walls; this was applied as a fine spray beneath the sliding formwork.



**Figure 10.34** Ngqura main breakwater caisson roundhead during construction. At this stage, the full extent of the base slab had been cast, and the first of four wall lifts had been slid. The sliding formwork for the second slide was in the process of being assembled on the left-hand side at the time of the photograph.
Photograph: Transnet National Ports Authority.



**Figure 10.35** Ngqura main breakwater caisson roundhead. Completed caissons floating in the flooded harbour basin prior to placing in the breakwaters.
Photograph: Transnet National Ports Authority.

All the caissons were floated when the basin was flooded, and then moored alongside the quays until they were installed. After sinking into position at the breakwater, each caisson was filled with water to give it some stability against wave loading during the construction period. The breakwater rock mound was then extended up to the caisson, the cells filled with sand, and the in situ plain concrete cap cast on top to give the final design weight and stability.



**Figure 10.36** Ngqura main breakwater caisson roundhead. At the time of this photograph, the roundhead caisson had been placed and the core rock dumped up against it, shortly to be followed by the armour layers. The caisson was capped with 2500 $m^3$ of plain concrete. Photograph: Transnet National Ports Authority.

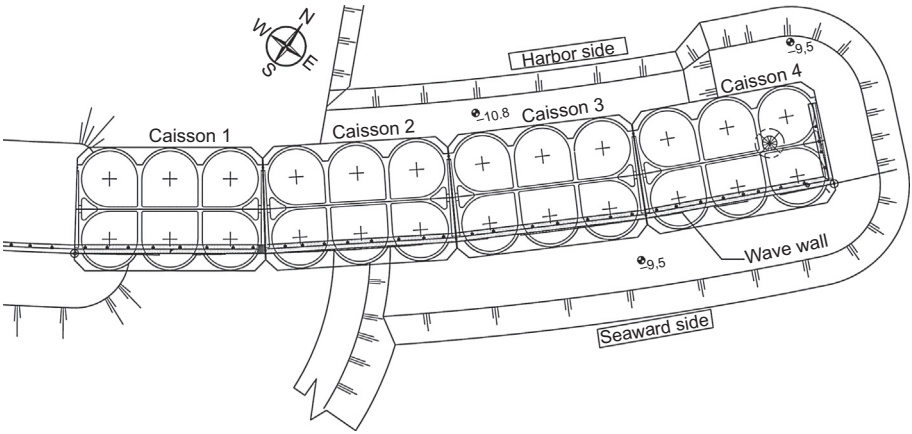



**Figure 10.37** Ngqura secondary breakwater caissons. The last 107 m of the secondary breakwater comprises four caissons placed in a gentle curve.
Adapted from project drawings by Transnet National Ports Authority/Prestedge Retief Dresner Wijnberg (Pty) Ltd.

### *10.3.3 Quay walls*

As the port basin is located behind the shoreline, it was possible to excavate the basin and construct the quay walls in the dry, founded directly onto the bedrock. Advantage was taken of the dry excavation, and an in situ concrete blockwork gravity quay wall

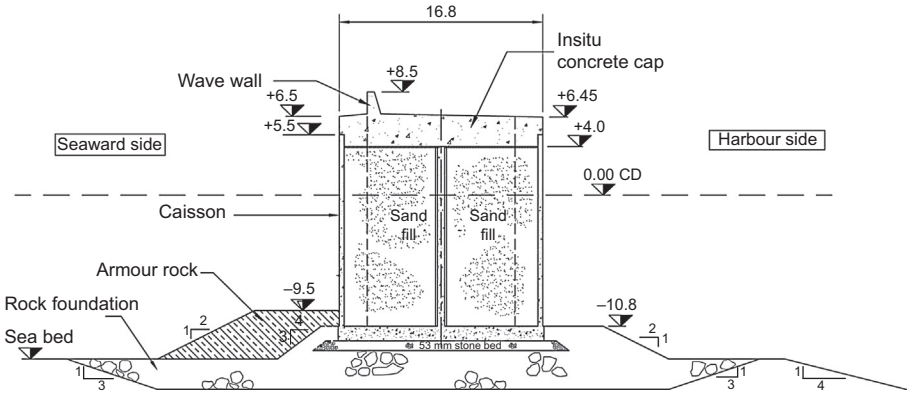



**Figure 10.38** Ngqura secondary breakwater caisson: cross section (dimensions in metres). Adapted from project drawings by Transnet National Ports Authority/Prestedge Retief Dresner Wijnberg (Pty) Ltd.

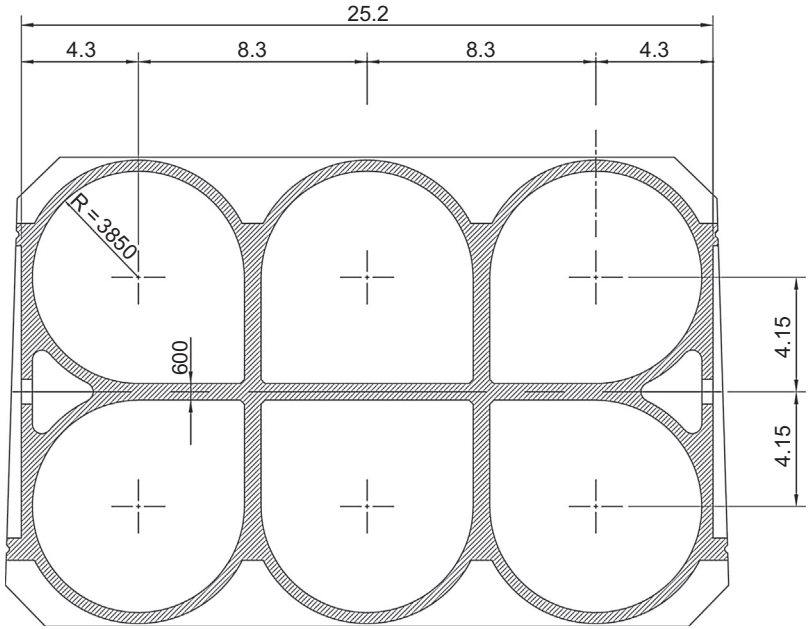



**Figure 10.39** Ngqura secondary breakwater caissons: plan dimensions (in metres). Adapted from project drawings by Transnet National Ports Authority/Prestedge Retief Dresner Wijnberg (Pty) Ltd.



**Figure 10.40** Ngqura secondary breakwater caissons under construction. Two of the four caissons have been completed in this view.
Photograph: Transnet National Ports Authority.



**Figure 10.41** Ngqura secondary breakwater caissons. All four of the caissons have been placed in this view, and sand filling of the cells is in progress.
Photograph: Transnet National Ports Authority.

design was utilised. The quay wall layout is shown in Fig. 10.42, and the cross section in Fig. 10.43. Figs 10.44 and 10.45 give other details. The total length of quay wall constructed in the dry is 1800 m, and the walls are 21.5-m high from sea bed level to top of cope.

The wall blocks are all of plain concrete to create a durable, low-maintenance structure, but use was made of reinforced concrete soffit slabs to span over the rear of the



**Figure 10.42** Ngqura quay walls. The photograph shows the quay walls at the end of the construction in the dry. The main basin had been excavated and was flooded soon afterwards. Photograph: Transnet National Ports Authority.

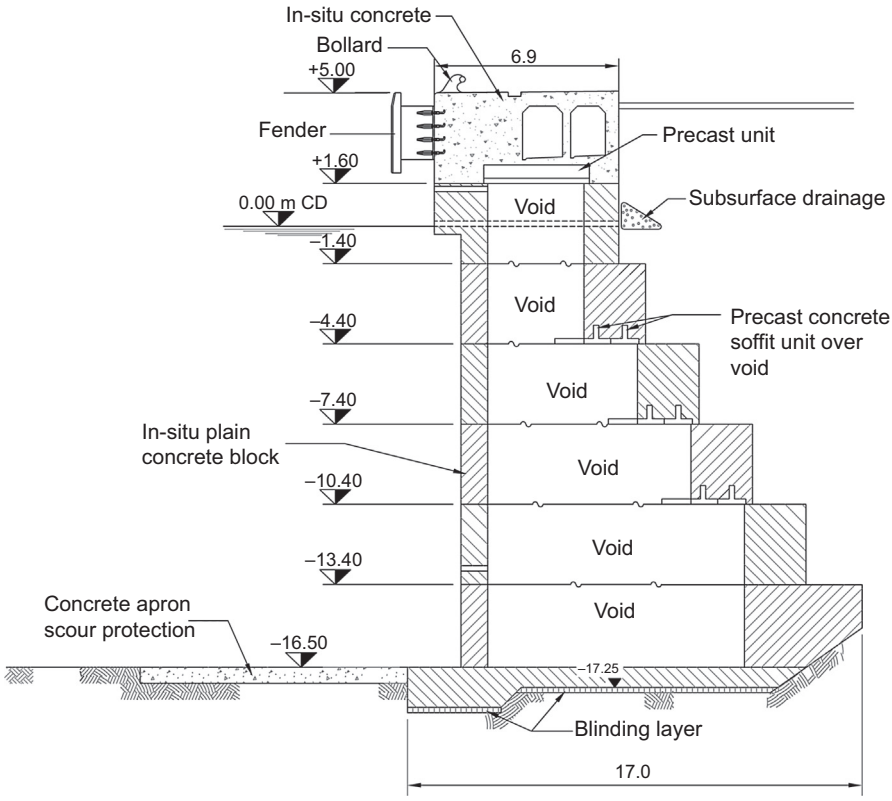



**Figure 10.43** Ngqura quay walls: typical quay wall cross section (Dimensions in metres). The wall has six plain concrete blocks, and each was cast as a single pour. Reinforced concrete soffit slabs were used to span over the rear of the voids to support the wet concrete of the block above when it was cast.
Adapted from project drawings by Transnet National Ports Authority.

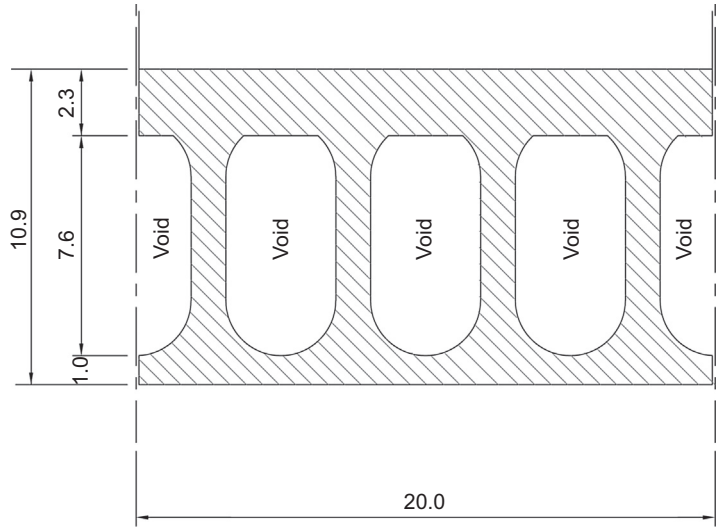



**Figure 10.44** Ngqura quay walls: typical plan view of quay wall block cast in 20-m-long in situ sections (Dimensions in metres).
Adapted from project drawings by Transnet National Ports Authority.



**Figure 10.45** Ngqura quay walls: a section of quay wall nearing completion. The length of wall adjacent to the caissons has had all the blocks cast and awaits the cap. The end wall and opposite wall are still in progress, and precast soffit units for the remaining blocks are laid out on the bank behind. Backfilling of the wall closely followed its construction.
Photograph: Transnet National Ports Authority.

wall voids where block casts were smaller than the preceding one. The only major reinforced concrete elements are the 20-m-long cap casts, which distribute the applied bollard and fender loads into the wall.

### 10.3.4 Sand bypass jetty

The port requires a sand bypass system to maintain sediment transport along the coastline that would otherwise be interrupted. This comprises a 225-m-long jetty on the southern side of the port on which are mounted six jet pumps that extract 200,000 $m^3$ per year of sand from the beach and hydraulically pump it via booster pump stations to the opposite side of the port. As the jetty is located on the exposed coast, it was designed to resist wave loading as well as the normal self-weight and deck live loads. See Figs 10.46–10.49. The height of the deck was selected to be above the maximum wave crest level of an extreme storm event so that the wave loading on the jetty will be limited to that only on the piles, with no wave impact loads on the deck.

The jetty structure comprised a reinforced concrete deck and pipe support beams founded on reinforced concrete piles. The vertical and raked in situ piles were cast inside steel casings and were socketed into the bed rock. The deck soffit and pipe support beams were originally configured as precast units but were ultimately built as in situ elements. A working platform was built into the surf zone by the contractor for the jetty construction in order to facilitate the use of land-based construction methods. It was considered easier by the contractor to construct the superstructure using standard falsework with soffit forms, rather than using precast elements.



**Figure 10.46** Ngqura sand bypass jetty. The jetty is located on the western side of the secondary breakwater root.
Photograph: Transnet National Ports Authority.

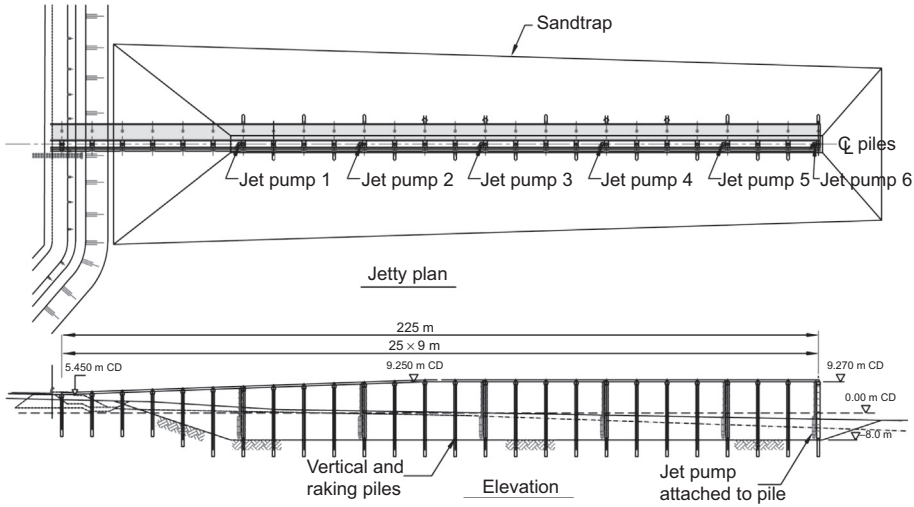



**Figure 10.47** Ngqura sand bypass jetty: plan and elevation of the jetty.
Adapted from project drawings by Transnet National Ports Authority/Prestedge Retief Dresner Wijnberg (Pty) Ltd.

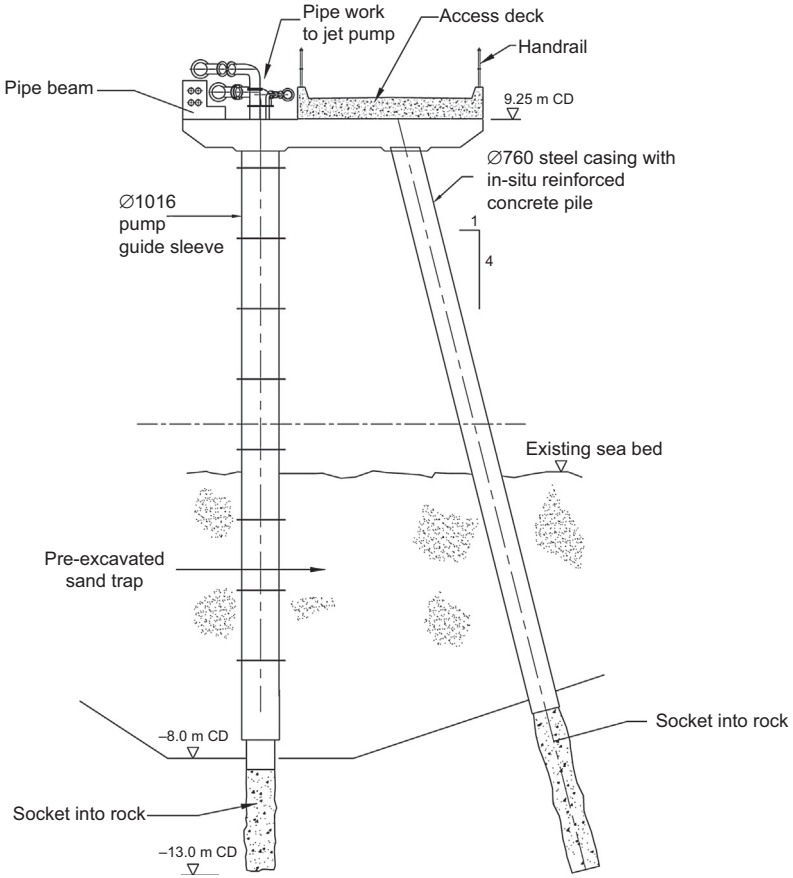



**Figure 10.48** Ngqura sand bypass jetty: typical jetty cross section. The raker piles are provided to resist lateral wave loads.
Adapted from project drawings by Transnet National Ports Authority/Prestedge Retief Dresner Wijnberg (Pty) Ltd.



**Figure 10.49** Ngqura sand bypass jetty: underside of the completed jetty. Photograph: Transnet National Ports Authority.

## 10.4 Durban Harbour entrance, Kwazulu-Natal, South Africa

### *10.4.1 Durban Harbour entrance widening and deepening*

Durban is South Africa's busiest multi-cargo port, handling 60% of the country's exports and imports, which amounts to over 80 million tons of cargo per annum. The port handles containers, bulk liquids (petroleum products), dry bulk products (eg, coal, chrome ore), agricultural products (eg, sugar, citrus, grains), new vehicles and a variety of break-bulk cargos, and it is also home to ship building and repair facilities.

Durban harbour's entrance was widened and deepened in the early 2000s to create safe access for larger vessels than were previously using the port. The design vessel for the reconfigured entrance is a 6600 TEU (100,000 dwt) container ship or equivalent (overall length = 347 m, beam = 42.8 m, and loaded draft = 14.0 m) and access is intended under most weather conditions.

In addition to the excavation and dredging that was required to enlarge the entrance, upgrading and strengthening of the south breakwater and construction of a new north groyne were required, and both of these structures contained significant concrete elements.

Construction of the upgrade started in 2007 and took three years. The layout is shown in Fig. 10.50.

### *10.4.2 South breakwater*

The alignment and length of the existing south breakwater was satisfactory for the new entrance configuration, but it was necessary to strengthen it to provide the required

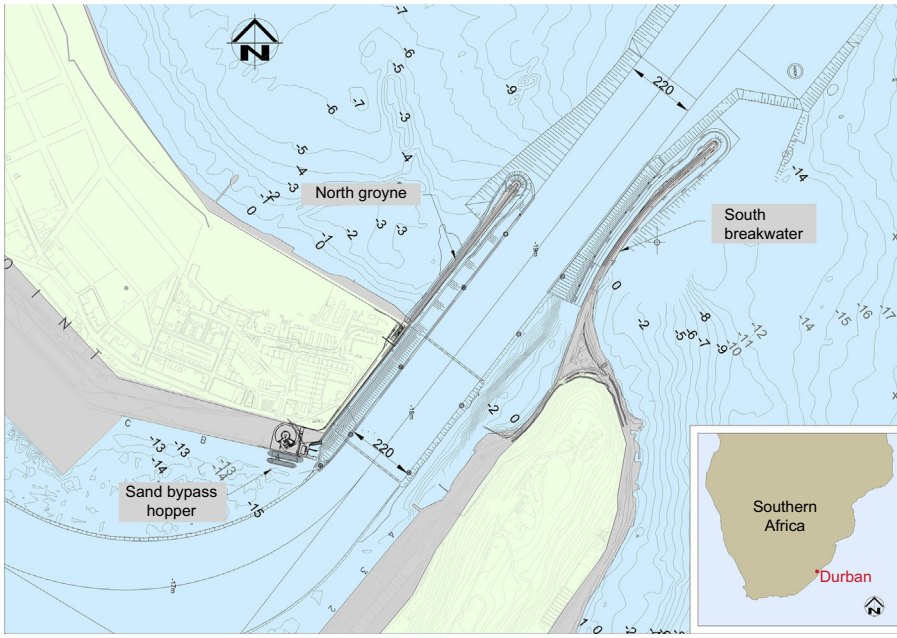



**Figure 10.50** Durban harbour entrance widening and deepening layout.
Adapted from project drawings by Transnet National Ports Authority/Prestedge Retief Dresner Wijnberg (Pty) Ltd.

level of serviceability. The breakwater is the primary protection against waves for the entrance.

Strengthening of the breakwater comprised raising the concrete cap, and the addition of new 45-tonne antifer cube armour units to the seaward face of the existing mound and 30-tonne antifer units to the new dredged slope on the entrance side, as shown in Fig. 10.51. The robust antifer unit was used because of the anticipated risk of settlement arising from constructing on top of an existing structure. An armour unit such as a dolos would not have been able to tolerate significant settlements without breakage of some of the units.

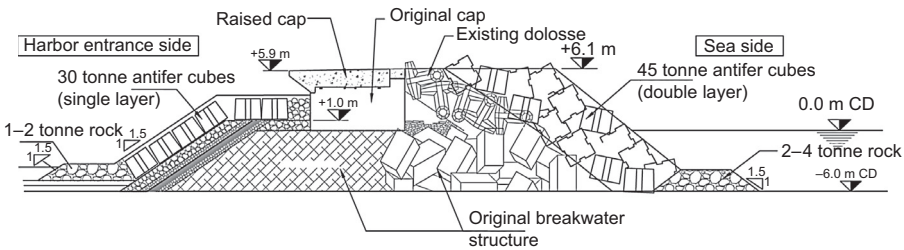



**Figure 10.51** Durban south breakwater: typical cross section.
Adapted from project drawings by Transnet National Ports Authority/Prestedge Retief Dresner Wijnberg (Pty) Ltd.

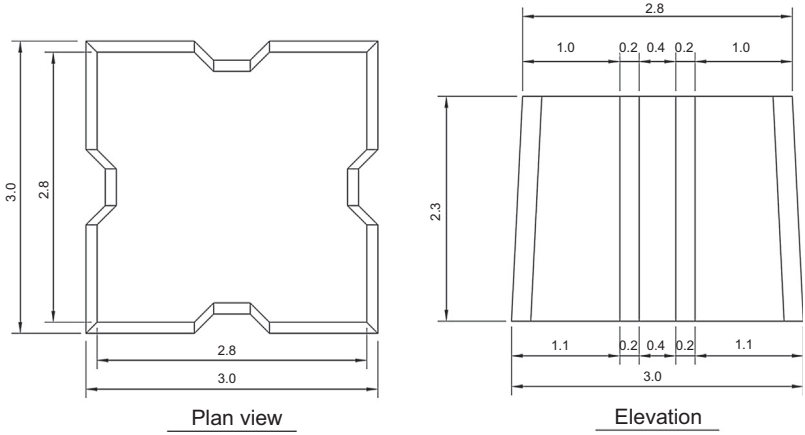



**Figure 10.52** Durban south breakwater: 45-tonne antifer cube armour unit (dimensions in metres).
Adapted from project drawings by Transnet National Ports Authority/Prestedge Retief Dresner Wijnberg (Pty) Ltd.

### 10.4.3 North groyne

To widen the channel, it was necessary to demolish the existing north groyne and construct a new one further to the north. The groyne functions to retain the adjacent beach along the edge of the deep channel.

The reconstructed groyne is a traditional rock-rubble structure with a plain concrete cap, and 20-tonne dolosse and 10- and 5-tonne antifer cube armour units (see Fig. 10.53). The antifer units were placed along the groyne trunk, and the dolosse were utilised on the roundhead.

One unusual application of concrete in this structure was the recycling of concrete from the original groyne and entrance edge walls. The old concrete was crushed into a suitable grading, and about 50,000 tonnes were used in the groyne core and filter layers, replacing some of the imported rock.

### 10.4.4 Sand bypass hopper

The littoral drift of sand along the coast at Durban is from south to north, and a sand trap has been dredged adjacent to the harbour entrance to catch the sand coming from

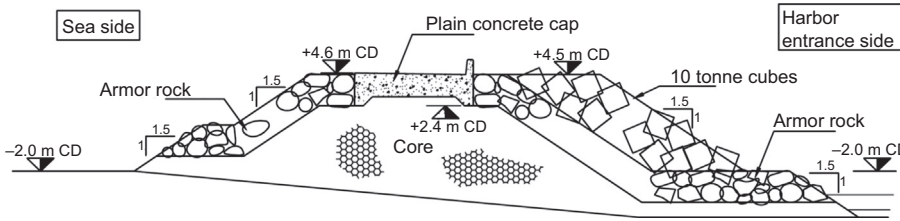



**Figure 10.53** Durban north groyne: typical cross section.
Adapted from project drawings by Transnet National Ports Authority/Prestedge Retief Dresner Wijnberg (Pty) Ltd.



**Figure 10.54** Durban sand bypass: hopper aerial view.
Photograph: Transnet National Ports Authority/Pete van der Spek of SkyPics.

the south so that it does not silt up the harbour entrance channel. The sand trap has to be emptied by a dredger to maintain its function, and most of the trapped sand is disposed of offshore, but some has to be transferred to the city's beaches to the north so that they are not denuded by the interrupted littoral drift.

The sand bypass system utilised in Durban comprises a sand hopper that is fed by the dredger and in turn feeds the beaches via a pipeline and booster pump stations. The original sand bypass facility had to be demolished when the harbour entrance was widened, and a new one was constructed behind A berth, just inside the harbour.

The sand bypass hopper is an onshore marine structure and is shown in Figs 10.54 and 10.55. The sand hopper includes the main hopper itself for the sand storage, and

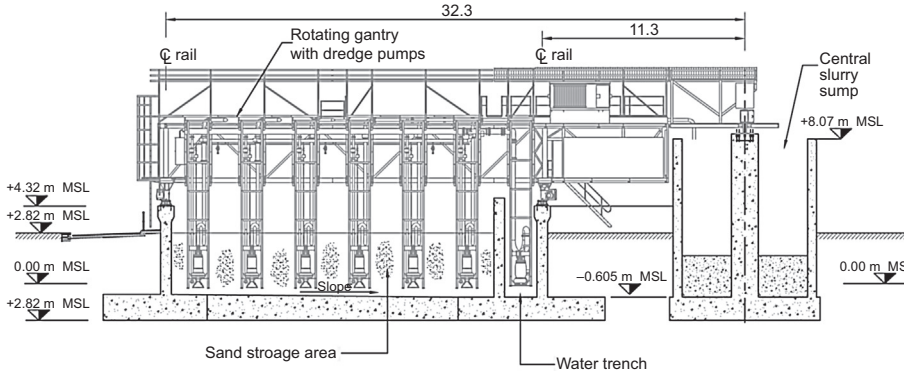



**Figure 10.55** Durban sand bypass: cross section (dimensions in metres).
Adapted from project drawings by Transnet National Ports Authority/Prestedge Retief Dresner Wijnberg (Pty) Ltd.

ancillary chambers for sand discharge, fresh seawater, discharge water and a filter system. It is equipped with a travelling gantry onto which are mounted the pumps that recover the sand from the hopper for onward pumping to the beaches.

The horseshoe-shaped hopper has a diameter of 65 m and a depth of 5 m. To minimise the visual impact of the hopper, it is sunk into the ground with only the top metre of the walls projecting above. It is constructed from in situ reinforced concrete, for which a prescriptive mix was specified similar to that given in Table 10.1, together with 10 days of moist curing. The base slab and walls were cast in discrete panels to minimise shrinkage cracking. All joints were sealed with a dual waterstop system, and an off-shutter finish was used for all formed surfaces.

Stainless-steel dowels are used at every slab and wall joint to prevent any differential movement of the panels. This was done to prevent disruption of the waterstops and differential settlements that would affect the wall-mounted gantry crane rail.

Although the hopper structure is not located in the sea and subject to the tide, it will experience many filling and emptying cycles during its service. The bottom zone of the hopper will always contain a layer of saturated sand, except during major maintenance when it is cleaned out. When sand is pumped into the hopper from the dredger, the slurry flows along its full length. The hopper is therefore subject to frequent wetting and drying cycles and sand abrasion, which together create a typical aggressive marine environment for the concrete. The project concrete specification for reinforced members called for a minimum cementitious content of 420 kg/m$^3$ with either 25−30% FA or 40−50% GGBS extender. The contractor wished to use a local CEM II A-M(V-L) pre-blended cement containing 12% of FA, and they made up the extender content to the required level of 45% using GGBS, the most economical extender available. The ternary blend was considered to be acceptable for the durability function. A concrete cover of 75 mm to the reinforcement was specified and moist curing for 10 days was undertaken.

## 10.5 Durban Maydon Wharf 12, Kwazulu-Natal

### *10.5.1 Maydon Wharf upgrade*

Maydon Wharf in Durban harbour consists of a series of 14 berths that handle a variety of cargo including agricultural products (sugar, grains, animal feeds, timber and wood chips), heavy minerals, steel products and various break-bulk cargos. The quay structures are of varying ages and types of construction, including steel sheet pile quay walls and concrete wharves. The steel sheet pile walls were constructed over 60 years ago and are all beyond their service life. A program is therefore in place to reconstruct the old sheet pile quays to rejuvenate the terminal and allow accommodation of larger vessels.

The first berth that was reconstructed was Number 12; work on the site started in August 2011 and took 15 months to complete.

The 268-m-long quay wall comprises an 18.2-m-high steel combi-sheet pile wall with a reinforced concrete cap and anchor wall. See Figs 10.56−10.58.

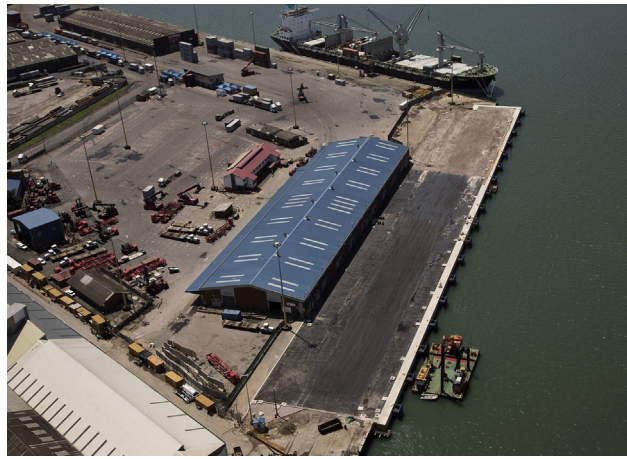


**Figure 10.56** Durban Maydon Wharf 12: aerial view of the completed quay wall with the contractor's work barge still berthed alongside at bottom right.
Photograph: Transnet National Ports Authority Pete van der Spek of/SkyPics.

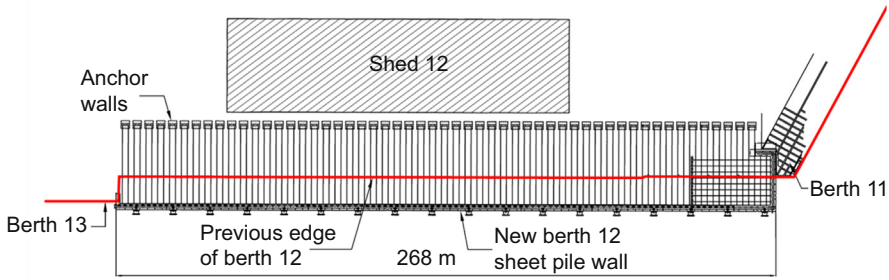



**Figure 10.57** Durban Maydon Wharf 12: plan view.
Adapted from project drawings by Transnet National Ports Authority/Prestedge Retief Dresner Wijnberg (Pty) Ltd.

### *10.5.2 Concrete components*

The main structural component of the quay wall is the steel sheet pile, but reinforced concrete still has an important role to play in the structure. The cap serves to spread the concentrated bollard and crane rail loads to the anchors and piles. Below the main cap are the hanging cope panels that support the elastomeric fenders and safety ladders. In addition to supporting the quay furniture, the cope acts as a cladding to protect the steel sheet piles in the tidal zone. The cope face is a reinforced, precast concrete unit that cantilevers down from the in situ cap cast. The gap between the cope unit and the sheet piles is filled with plain in situ concrete that seals the face of the steel within the tidal zone and prevents free access of salt water and oxygen, thereby minimising corrosion of the bare steel. Sacrificial anodes protect the steel surface of the fully immersed pile, but in the tidal zone, cathodic protection is less effective, and therefore it is preferred to clad and shield the pile. See Fig. 10.59.

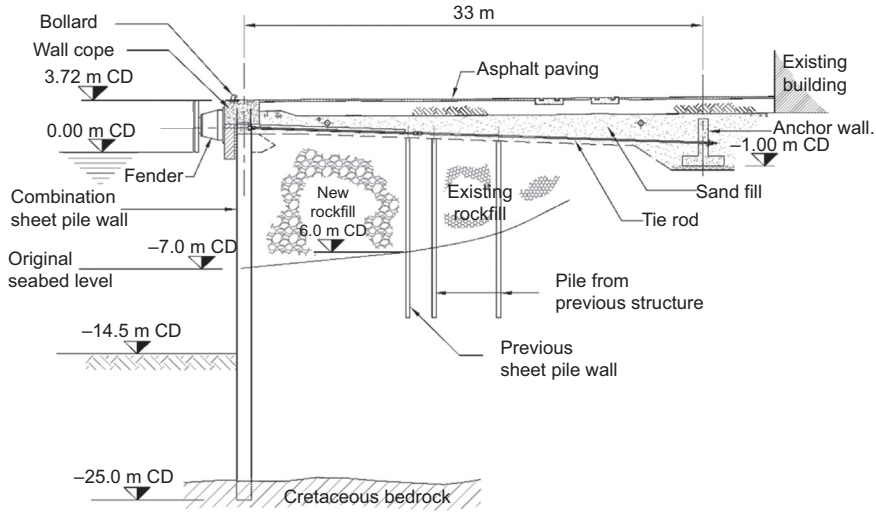



**Figure 10.58** Durban Maydon Wharf 12: typical cross section.
Adapted from project drawings by Transnet National Ports Authority/Prestedge Retief Dresner Wijnberg (Pty) Ltd.

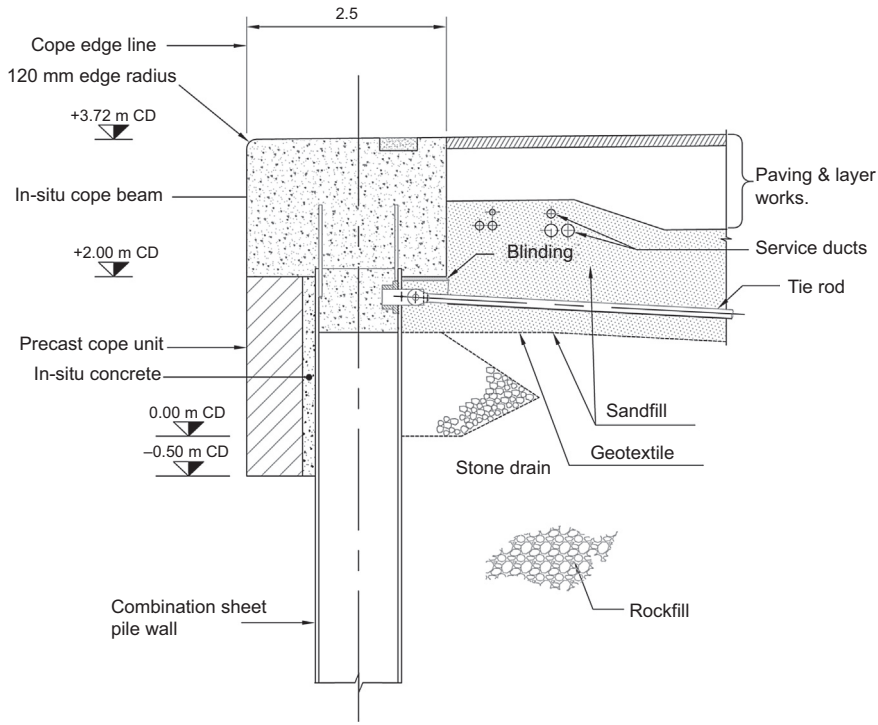



**Figure 10.59** Durban Maydon Wharf 12: cope cross section.
Adapted from project drawings by Transnet National Ports Authority/Prestedge Retief Dresner Wijnberg (Pty) Ltd.

A reinforced concrete, inverted T, deadman anchor block was used for the quay wall. It is connected to the sheet pile wall by steel anchor rods. Anchor walls such as this may be precast or cast in situ, and in this case the contractor elected to use in situ. Although it is fully buried and subject to little oxygen exchange in service, the full requirements for reinforced concrete in the tidal zone were applied, as once buried, there will be no possibility of access for maintenance.

## 10.6 Rupert's Bay Wharf, St Helena Island, South Atlantic Ocean

### *10.6.1 St Helena Island development*

The island of St Helena is located about 2000 km due west of Luanda in the South Atlantic, and it is of volcanic origin. It was discovered by the Portuguese in the 16th Century, briefly claimed by the Dutch until they had established their Cape colony, and then occupied by the British in 1659. Initially used as a base for the English East India Company, it became a formal British Crown Colony in 1834. Most famous for the detention of Napoleon Bonaparte, the island was also used to imprison Zulu king Dinuzulu kaCetshwayo and over 6000 Boer prisoners during the Anglo-Boer war.

Access to this remote island has always been by sea, but this has now changed with the construction of a new airport funded by the UK Department for International Development. The airport will open up the island for tourism, thereby boosting the local economy. In addition to the airport itself, the project includes a new wharf and boat ramp in Rupert's Bay. The island has never had a formal harbour, and ship-to-shore transfers have always been undertaken by small craft. The new wharf provides an improved and safer facility for cargo handling and passenger transfer.

The harbour works consist of a single 183-m-long arm comprising a 120-m-long quay wall on the landward side and protected by a breakwater on the seaward face. The layout of the harbour is shown in Fig. 10.60.

### *10.6.2 Quay wall*

The harbour works were constructed by the airport contractor, who had limited marine experience and little marine equipment available, and this influenced the design and method of construction of the quay wall. In particular, the contractor wished to use a land-based construction method as far as practical and to avoid piling due to the shallow rock level present on the site.

There are no significant construction resources on the island, except rock for the aggregate, and all materials, plant, and fuel had to be imported from Namibia and South Africa. The main item of plant available for the wharf construction was a 200-ton crawler crane.

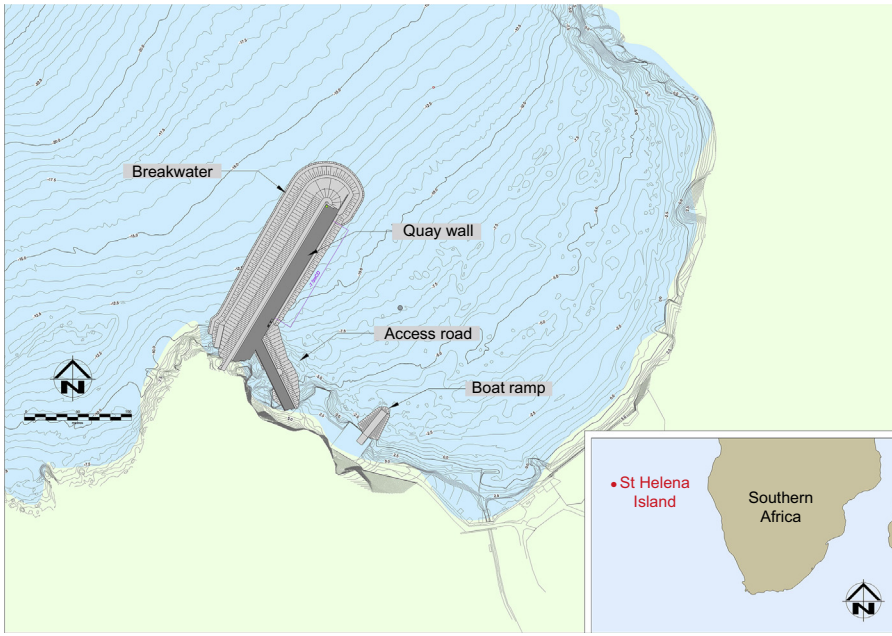



**Figure 10.60** Rupert's Bay Wharf. General Arrangement of the quay wall and breakwater. Adapted from project drawings by Government of St Helena/Basil Read Holdings Limited/ Prestedge Retief Dresner Wijnberg (Pty) Ltd.

Fig. 10.61 shows the quay and breakwater cross section, and a detail of the wall and breakwater crown wall is shown in Fig. 10.62. The wall is made up of 37 stacks of blocks, each of which has one foundation block and 9 hollow wall blocks. The voids in the blocks are filled with stone to key them together and provide the mass for the gravity wall stability. A further six block stacks are used to retain a portion of the breakwater roundhead.

A hollow wall block, rather than a heavier solid block, was selected for the quay wall to suit the lifting capacity of contractor's construction crane. Details of the hollow

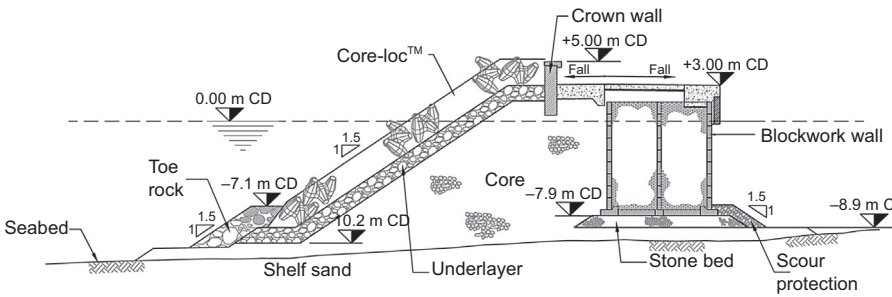



**Figure 10.61** Rupert's Bay Wharf: typical cross section of the quay wall and breakwater. Adapted from project drawings by Government of St Helena/Basil Read Holdings Limited/ Prestedge Retief Dresner Wijnberg (Pty) Ltd.

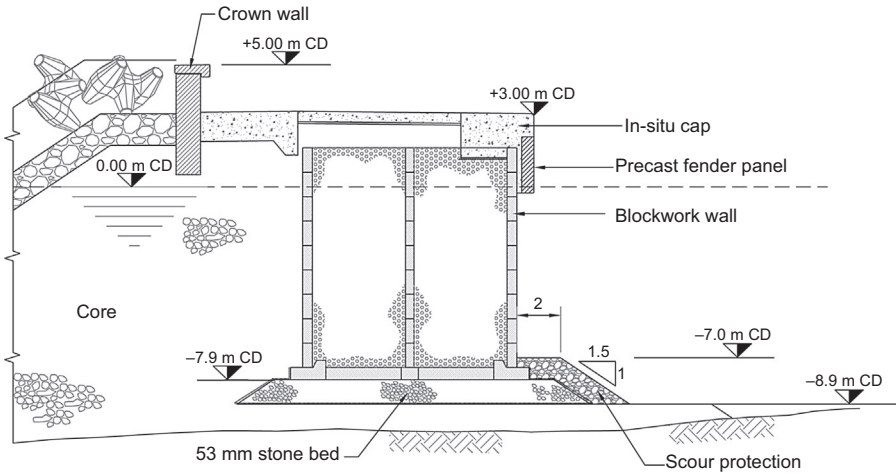



**Figure 10.62** Rupert's Bay Wharf: detail of quay wall and breakwater crown wall.
Adapted from project drawings by Government of St Helena/Basil Read Holdings Limited/ Prestedge Retief Dresner Wijnberg (Pty) Ltd.

wall blocks are shown in Figs 10.63−10.68. The mass of the foundation and wall blocks are 27 and 23 tons, respectively.

A single 8.8-m-long block size was used for the full height of the wall so that the crawler crane could run on the completed stacks to advance the wall construction. This approach was different to normal blockwork wall practice in which the block size narrows from bottom to top to create the most efficient design.

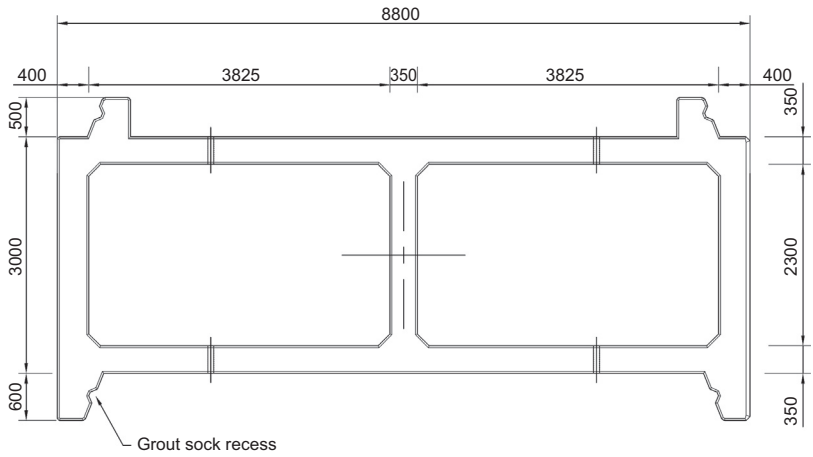



**Figure 10.63** Rupert's Bay Wharf: plan view of a precast wall block unit. Each unit is 1.0-m high (dimensions in millimetres).
Adapted from project drawings by Government of St Helena/Basil Read Holdings Limited/ Prestedge Retief Dresner Wijnberg (Pty) Ltd.



**Figure 10.64** Rupert's Bay Wharf: view of the wall block precast yard.
Photograph: Prestedge Retief Dresner Wijnberg (Pty) Ltd.

An in situ concrete cap is cast along the top of the wall and used to spread the bollard loads into the wall stacks. A precast cope panel cantilevers down from the cap in front of the block stacks and supports the elastomeric fender units.

### *10.6.3 Breakwater*

The breakwater structure that backs onto the quay is a rock rubble structure armoured with 7.2-ton Core-loc units, see Figs 10.69–10.71.



**Figure 10.65** Rupert's Bay Wharf: lifting of wall base block.
Photograph: Basil Read Holdings Limited.



**Figure 10.66** Rupert's Bay Wharf: lifting of typical wall block.
Photograph: Basil Read Holdings Limited.

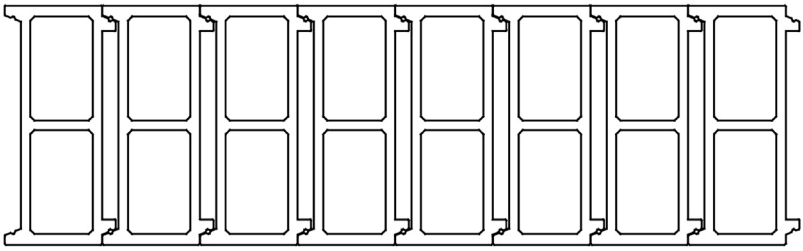


**Figure 10.67** Rupert's Bay Wharf: quay wall block interlock.
Adapted from project drawings by Government of St Helena/Basil Read Holdings Limited/ Prestedge Retief Dresner Wijnberg (Pty) Ltd.

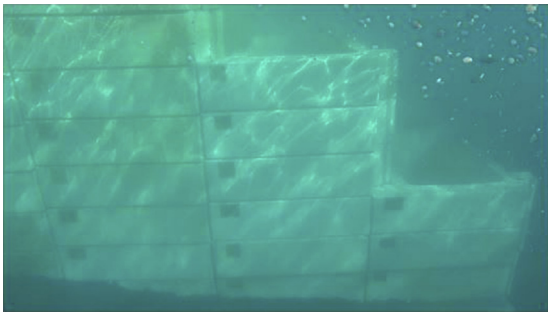


**Figure 10.68** Rupert's Bay Wharf: quay wall block assembly, underwater view.
Photograph: Basil Read Holdings Limited.



**Figure 10.69** Rupert's Bay Wharf: Core-loc casting yard.
Photograph: Prestedge Retief Dresner Wijnberg (Pty) Ltd.



**Figure 10.70** Rupert's Bay Wharf: 7.2-ton Core-loc in storage before placing in the breakwater.
Photograph: Basil Read Holdings Limited.

A crown wall is located on top of the mound, and its height was selected to limit the amount of overtopping onto the back of quay. To reduce the construction time, the stem of the wall was precast in 2.7-m-long sections, and the in situ cast was limited to the wall base and cap; see Figs 10.72 and 10.73.

## 10.7 Other notable marine structures

There are numerous other notable marine structures in the Southern African region, but space has precluded their inclusion in detail, and therefore only brief descriptions of certain examples are given as follows.




**Figure 10.71** Rupert's Bay Wharf: start of Core-loc placing.
Photograph: Basil Read Holdings Limited.

### *10.7.1 Commercial ports*

The South African commercial ports are vital links for the functioning of the country's trade and industry. TNPA (Transnet National Ports Authority) is responsible for their development, operation and maintenance. The ports for which TNPA are responsible are Richards Bay, Durban, East London, Ngqura, Port Elizabeth, Mossel Bay, Cape Town and Saldanha Bay, and between them there is a wide variety of significant port structures. South African ports have many of the port structure types




**Figure 10.72** Rupert's Bay Wharf: breakwater crown wall. Placing of precast wall panels.
Photograph: Basil Read Holdings Limited.



**Figure 10.73** Rupert's Bay Wharf: breakwater crown wall. First wall base cast. Photograph: Basil Read Holdings Limited.

described in the chapter 'Types of marine concrete structures', including blockwork, caisson, and counterfort quay walls, and piled jetties and wharves. The port structures are typically large engineering undertakings, and each quay wall is a significant project by itself.

Blockwork quay walls have been used extensively, and there are examples in most of the ports. Typically, they are constructed from precast blocks, but in situ blockwork walls have been used in Richards Bay and Ngqura, as described in Section 10.3.3. They have proved to be durable in service and only become obsolete when a greater berth depth is required for modern vessels with a deeper draft than the original ones.

There are caisson quay walls in Richards Bay and Saldanha Bay harbours. In addition, the 1-km-long iron ore export jetty in Saldanha Bay uses individual caisson piers with precast, prestressed beams spanning in between to form the deck.

Precast counterfort units have been used for the multipurpose terminal in Saldanha Bay and a trawler quay in Cape Town. The first phase of the Richards Bay coal terminal quay wall was constructed as an in situ counterfort wall, as described in the chapter 'Types of marine concrete structures'.

All the ports have breakwaters, and dolosse are the most common armoured unit, but other units have also been used such as plain rectangular blocks (typically 20-ton mass) and antifer cubes. (Chapter: Concrete durability in small harbours – the Southern African experience has details of some of these harbours.)

### *10.7.2 Shark Rock Pier*

Shark Rock Pier is located on the city sea front in Port Elizabeth, and its primary purpose is as a groyne to retain a section of recreational beach (refer to Fig. 2.57 in chapter: Types of marine concrete structures). A series of concrete panels located between the pier columns retain the beach sand, and it is equipped with a full-length concrete deck to provide crane access for installation or adjustment of the panel configuration. The deck is open to the public and is a popular amenity.

### 10.7.3 Durban seafront groynes

The beaches along the Durban city seafront have been subject to variations in the sand levels that have affected their function as an important tourist amenity. To stabilise the beaches, a series of groynes have been constructed along the seafront (refer to Fig. 2.59 in chapter: Types of marine concrete structures). The groyne structure was designed to be constructed incrementally out from the shore and comprises two rows of closely spaced, square, precast concrete piles with a precast deck unit spanning between the rows. The volume between the piles is filled with rock and provides the barrier for the groyne action.

## Sources of further information

- Birkby, R., 1998. The Making of Cape Town's Victoria & Alfred Waterfront, Victoria & Alfred Waterfront (Pty) Ltd.
- Coega Development Corporation, http://www.coega.co.za/.
- Saint Helena Airport project, http://www.sainthelenaaccess.com/news/about/.
- Saint Helena general information, http://sthelenatourism.com/.
- Transnet National Ports Authority, http://www.transnetnationalportsauthority.net/OurPorts.
- Transnet Port Terminals, http://www.transnet-tpt.net/.
- Victoria & Alfred Waterfront, http://www.waterfront.co.za/.

## Reference

Hargey, Y., September 2015. Reinforced Concrete Service Life Prediction of Marine Structures in Service. Master of Engineering Minor Dissertation. University of Cape Town.

# Danish strait crossings: Lillebælt, Storebælt, Øresund and Femern Bælt[1]

11

*M.W. Braestrup*
Ramboll, Denmark

## 11.1 Introduction

Denmark is a country of less than six million people, located in northern Europe, between the continent and the Scandinavian Peninsula. Apart from the Jutland Peninsula, which borders Germany, the country consists of a multitude of islands, the major ones being identified in Fig. 11.1. No location is more than 50 km from the sea; consequently, the movement of goods and people has traditionally been by ship. During the last century, however, a growing number of ferries have been replaced by fixed traffic links, culminating with the Storebælt Link, completed in 1998, and the Øresund Link, opened in 2000. These bridges and tunnels represent a sizable societal investment (exceeding EUR 10,000 million in today's prices), and 100 years has been specified as the design life, that is, the time period in which the structure can be in service without major repair or rehabilitation works. For the planned Femern Bælt Tunnel, the lifetime is specified at 120 years.

Concrete is the predominant construction material for Danish infrastructure, and consequently, structural concrete durability is the major factor determining the design life. The subsequent sections outline the development of concrete durability design in Denmark, from the time when concrete was generally considered to be maintenance free, to the present use of sophisticated mix designs, coupled with extensive performance testing, monitoring and maintenance.

## 11.2 Concrete durability issues

The principal construction material for the Danish strait crossings is structural concrete, which is used for all bridge substructures, including anchor blocks and pylons of suspension and cable-stayed bridges, for all submerged tube tunnels and for bored tunnel linings. Thus, a total exceeding 1,000,000 $m^3$ of concrete went into the Storebælt Link, and a similar amount was used for the Øresund Link, with 700,000 $m^3$ in the Øresund Tunnel alone. For the planned Femern Bælt Tunnel the

[1] More information and pictures can be found on the websites: www.sundogbaelt.dk, www.storebaelt.dk, and www.femern.com

**Marine Concrete Structures.** http://dx.doi.org/10.1016/B978-0-08-100081-6.00011-8
Copyright © 2016 Elsevier Ltd. All rights reserved.




**Figure 11.1** Location map with major islands and straits.

concrete consumption will be 2,600,000 $m^3$. Even though a substantially larger amount of concrete is poured in Denmark each year, it is the spectacular civil works that capture the public's attention, and concrete durability is the primary concern in the management and preservation of the infrastructure assets.

Satisfactory performance of the structure can be ensured by focussing on the following:

- structural design
- material selection
- placing and curing
- inspection and maintenance

### 11.2.1 Principal deterioration mechanisms

For concrete structures in a marine environment, the principal deterioration mechanisms are mutually self-enhancing. **Alkali–silica reactions** are prevented by the specification of nonreactive aggregates and low-alkali cement. **Frost damage** is avoided by the specification of air entrainment and by design ensuring the drainage of water from concrete surfaces. **Chloride-induced corrosion** is mitigated by the specification of a dense, crack-free concrete cover of sufficient depth to the reinforcement. This is achieved by adopting a three-powder binder mix, including low-alkali Portland cement (PC), pulverised fly ash (PFA) and microsilica (MS), and a low water/binder ratio, calculated by applying efficiency factors to the contents of PFA and MS (k-factors, see EN 206, 2013, Clause 5.2.5.2). To ensure good dispersion the MS is normally added as slurry, the water being included in the water content of the concrete mix.

Repairs due to reinforcement corrosion can be substantially reduced by preparing the structure for cathodic protection during the construction phase, ensuring electrical connection between the reinforcing bars, and by installing corrosion monitors in all the relevant structural parts, enabling the cathodic protection to be activated, if necessary. Alternatively, corrosion-resistant reinforcement may be specified in the most exposed locations.

In the period prior to World War II, the durability of concrete was not addressed as a separate issue. The concrete was produced using the best available materials and workmanship, which included compaction by hand. For the Lillebælt Bridge, which is owned by the Danish State Railways, discarded rails were used as reinforcement in caissons and piers.

Through the 1950 and 1960s, it was conventional wisdom that concrete as a material was almost maintenance free (in contrast with structural steel, which needs regular painting). The fallacy of this view was brought home around 1970 when serious deterioration was experienced in post-war industrially produced concrete. The problems were mainly confined to building projects, but unsatisfactory performance was observed also for civil works, and significant research was instigated to improve the concrete quality, including the use of PFA and later MS to reduce chloride ingress. The preoccupation with concrete durability peaked for the Storebælt Link and matured with the Øresund Link, to the extent that we now with some confidence can specify a 120-year design life for the Femern Bælt Tunnel.

## 11.3 The Lillebælt Bridges

### *11.3.1 Description*

Lillebælt is the westernmost of the three Danish straits connecting the Baltic Sea to the North Sea (Fig. 11.1), and it is also the narrowest, with the shore-to-shore distance between Funen and Jutland being approximately 1 km. The 1.2-km road and railway **Lillebælt Bridge** (Fig. 11.2) was completed in 1935.

The Lillebælt Bridge was basically conceived as a railway bridge, with a narrow roadway added almost as an afterthought. This became a major bottleneck as vehicular traffic increased in the 1950 and 1960s, and in 1970 a dedicated motorway bridge was finally completed. The **New Lillebælt Bridge** (Fig. 11.3) incorporates a 600-m steel box girder suspension span, being the first Danish suspension bridge.



**Figure 11.2** https://en.wikipedia.org/wiki/File:The_Little_Belt_Bridge_(1935)_(close).jpeg.



**Figure 11.3** The New Lillebælt Bridge with the Lillebælt Bridge in the background (Munch-Petersen, C (Ed.), 2003).

### 11.3.2 Design

For both Lillebælt bridges, the client commissioned a detailed design, which was submitted to international tender. The successful contractor consortium then executed the works under the supervision of the client and his consultant.

The **Lillebælt Bridge** between the concrete arch approach bridges is an 825-m-long steel truss (Fig. 11.4). It appears to be a continuous girder, but it has hidden articulations, to cater for uneven pier settlements in the plastic clay (see Section 11.3.5).

The 1700-m-long **New Lillebælt Bridge** includes a 600-m main suspension span and two 240-m side spans (Fig. 11.5). The 118-m-high pylons are founded on caissons, each resting on 210 No. high-strength concrete piles driven 30 m into the plastic Lillebælt clay. The structural concrete anchor blocks are buried on shore, the weight, including the earth overburden, being 70,000 t. A total of 61 prefabricated 69-mm bridge strands, manufactured from 4.6-mm hot dip galvanised wire, make up the 580-mm main cables. Locked coil strands were used for the dual suspender cables.

### 11.3.3 Materials

The concrete of the 1935 **Lillebælt Bridge** was specified as a 1:2:3 mix with a PC content of 355 kg/m$^3$ and a cube strength of 200 kg/cm$^2$ (ca. 19.6 MPa). The mixing took place in a tower, from which the concrete was sent down a chute to the structure and compacted by hand. Recent investigations have shown that the strength is 30−35 MPa, that there are unhydrated cement particles, and that the paste porosity generally corresponds to a water/cement ratio of less than 0.40. The air entrainment is low, but in the splash zone the piers were provided with a 220-mm granite facing (primarily as protection against ice), which has prevented the freeze−thaw cycles from reaching the concrete and thereby contributed to the durability.

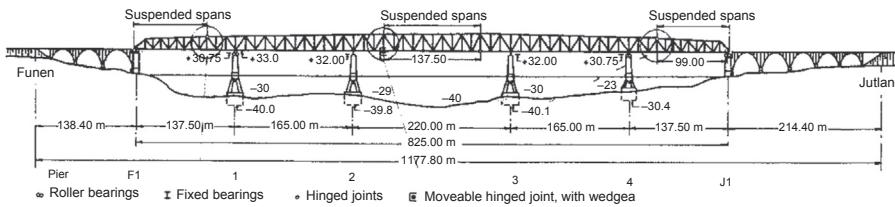



**Figure 11.4** The Lillebælt Bridge, elevation (Braestrup, 2005).

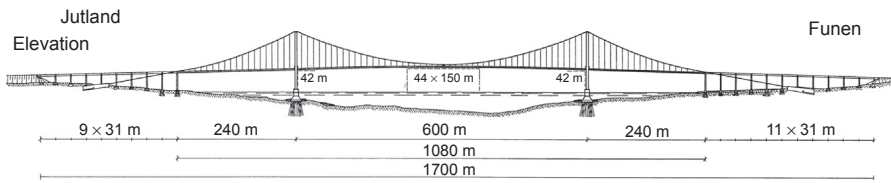



**Figure 11.5** The New Lillebælt Bridge, elevation (Braestrup, 2005).

For the **New Lillebælt Bridge**, the concrete was supplied from onshore mixing plants, using a cement with a low-alkali content (0.3−0.4% $Na_2O_{eq.}$). Class I concrete, used for the most important components such as the pylons, had a cement content of 300 kg/m$^3$, a specified water/cement ratio of 0.55, and crushed granite aggregates were used.

### 11.3.4 Execution

The four concrete foundation caissons for the offshore piers of the **Lillebælt Bridge** (Fig. 11.4) were launched from shore upside down as floating vessels, sliding down a ramp, and then turned around and placed on the seabed. The piers were cast in stages, eventually being moved to the final position where they were sunk into the tertiary clay (Lillebælt clay) by excavation inside the caissons. The steel truss was erected member by member, cantilevering out from the piers.

The pylon caissons for the **New Lillebælt Bridge** (Fig. 11.5) were constructed in a dry dock and towed to their final positions on the pile foundations, at water depths of approximately 20 m. The pylons were cast in situ using climbing formwork.

The hollow box stiffening girder was welded in Nakskov, Denmark, in 12-m sections, which were joined into 24-m units at the bridge site and hoisted onto the main cables. A dehumidification plant is installed in the girder, obviating the need for internal painting, a feature adopted on all later Danish hollow box steel bridges.

### 11.3.5 Inspection and maintenance

The Lillebælt Bridge and the New Lillebælt Bridge are integral parts of the Danish rail and road networks, and inspection and maintenance are carried out in accordance with the normal procedures of the railway and road authorities.

For the steel superstructure of the **Lillebælt Bridge** a rigorous painting maintenance program has been carried out throughout the life of the bridge, the average paint lifetime being 20−30 years. The opening of the Storebælt Link railway in 1997 necessitated an assessment of the Lillebælt Bridge to take account of the increase in number, weight and speed of future trains. Statically the structure was found capable of supporting the loads, and new fatigue calculations documented a remaining lifetime exceeding 100 years.

Regular inspection of the concrete substructure has detected no serious damage or deterioration. The movements of the four piers are monitored once a year. Due to the plasticity of the tertiary clay in which the caissons are founded, the cumulative settlements in the period 1935−2002 amounted to 125, 270, 425 and 365 mm, respectively, and the pier tops had drifted 20−180 mm toward the north and 10−80 mm toward the east. As a result of the differential pier movements, the superstructure has had to be adjusted several times by insertion of wedges in the movable, hinged joints. To avoid additional compressive stresses in the superstructure in the summer, a program was initiated in 1992 to bring Pier 2 (see Fig. 11.4) back into position, using a combination of jacking against the superstructure and tie-bar pull-back toward the Funen abutment, and currently a pull-back force of 1.4 MN is applied.

A characteristic feature of the plastic clay is that the settlements continue linearly with time, no decay being observed. As recent research has shown that the clay is susceptible to strain softening, this has led to a concern that a failure might eventually develop. As a mitigation measure in 2014, 125,000 $m^3$ of rock was placed as a 6.5-m-thick layer between the most critical piers, to act as counter fill, preventing overturning failure.

For the **New Lillebælt Bridge**, the routine inspection program has detected no significant damage or deterioration of the concrete pylons.

## 11.4 The Storebælt Link 1997 (rail), 1998 (road)

### *11.4.1 Description*

The 18-km Storebælt Link joins Funen and Zealand via the intermediate islet Sprogø (Fig. 11.6). Construction started in 1989, and the project comprises the following main components:

- The **West Bridge**, a 6.6-km combined road and railway bridge. With a navigational height of 18 m, it crosses the western channel between Funen and Sprogø.
- The **New Sprogø**, a 1.2-$km^2$ land reclamation, increases the area of Sprogø fourfold, to accommodate bridge abutments and tunnel ramp.
- The **East Tunnel**, an 8-km twin tube bored railway tunnel under the eastern channel between Sprogø and Zealand. It is the second longest underwater tunnel in Europe, after the Channel Tunnel.
- The **East Bridge**, a 6.7-km motorway high-level bridge over the international shipping lane in the eastern channel. It includes the world's second longest suspension bridge span of 1624 m, with a navigational height of 65 m.

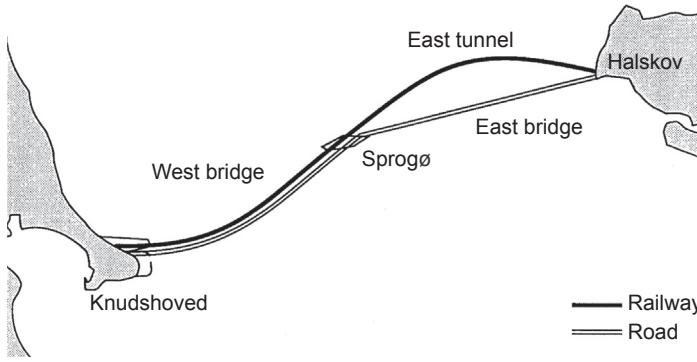



**Figure 11.6** The Storebælt Link between Funen (left side) and Zealand (right side) (www.storebaelt.dk).

The division of the traffic over the eastern channel is due to the following considerations:

- the preference of motorists for crossing on a bridge rather than through a tunnel
- the difficulty in carrying heavy freight trains on the large bridge span needed for navigational safety
- a political desire to complete the railway link three years ahead of the motorway link

In the event, technical difficulties with the tunnel boring operation resulted in a delay of four years in the tunnel construction. The rail link, via the West Bridge and the East Tunnel, became operational in June 1997, whereas the opening of the motorway link, via the West Bridge and the East Bridge, took place in June 1998. The construction costs constituted approximately EUR 4000 million, which were financed by government-guaranteed loans, the payback period of the toll-funded link being estimated at 28 years.

### 11.4.2 Design

For contractual purposes, the Storebælt project was split into five main components:

- West Bridge
- New Sprogø land reclamation
- East Tunnel
- East Bridge substructure
- East Bridge superstructure

For each component, the owner (see Section 11.7) retained a consultant, who prepared a detailed design, which was tendered for construction. The successful contractor then executed the works under the supervision of the owner and the consultant. An exception was the West Bridge, where the adopted solution was an alternative proposed by the winning contractor, who then assumed responsibility for the detailed structural design.

The 6.6-km-long **West Bridge** comprises two structural concrete hollow box girders, one for the dual-track railway, and another – lower and wider – for the four-lane motorway. The girders are supported by individual pier shafts, resting on a common foundation caisson, placed on a gravel bed (Fig. 11.7). The maximum caisson height is 29 m, and the maximum navigational clearance under the bridge is 18 m. The bridge consists of 51 spans of length 110 m and 12 spans of 82 m. Each of the longer spans corresponds to a single, precast concrete element, centred on the pier and cantilevered out to mid-span. The shorter spans occur at the abutments and at the other five expansion joint locations, where a shorter girder is provided over the pier. The expansion joints divide the bridge into six continuous sections, which are longitudinally restrained by fixed bearings. All other bearings have Teflon sliding surfaces, allowing longitudinal movements relative to the pier shafts. The expansion joints between the continuous sections must accommodate movements exceeding 1 m.

The 8-km-long **East Tunnel** comprises two railway tubes, the bored length being approximately 7.4 km, with cut-and-cover tunnels and portal buildings constructed in

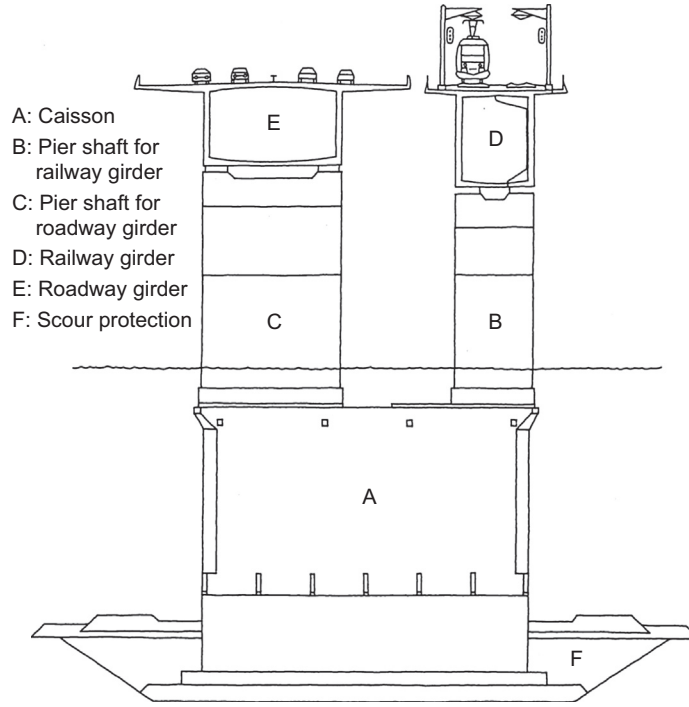



**Figure 11.7** Storebælt West Bridge cross-section (www.storebaelt.dk).

open pits at either end. The internal tunnel diameter is 7.7 m, and the lining of the bored tunnel is made from precast concrete segments with a thickness of 0.4 m. The centre-to-centre distance between the bored tubes is 25 m, and 4.5-m-diameter cross-passages are provided at 250-m spacing (Fig. 11.8). The cross-passages house installations and serve as emergency exits.

The 6.7-km-long motorway **East Bridge** includes a main suspension bridge, with two side spans of 535 m and a 1624-m central span with a navigational clearance of 65 m (Fig. 11.9). The approach bridges of 1528 m west and 2530 m east, respectively, have spans of 193 m. The superstructure is a steel box girder, and the substructure

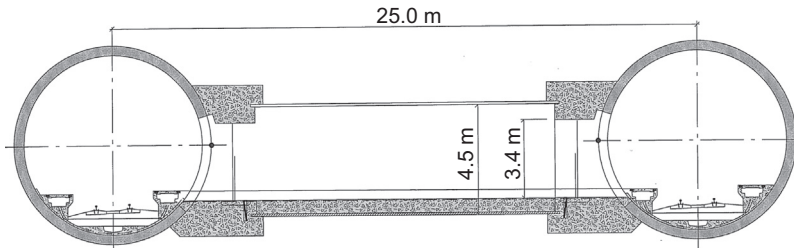



**Figure 11.8** Storebælt East Tunnel cross-section (Gimsing, 1998b).



**Figure 11.9** Storebælt East Bridge (www.storebaelt.dk).

comprises 19 piers, two anchor blocks and two pylons. The foundation levels of the approach bridge piers range from −5.5 m to −12.0 m, and the levels of the bearings for the superstructure are between 7.6 and 46.0 m. The foundation caissons for the 325,000 t anchor blocks measure 121.5 m by 54.5 m, with a height of 16.0 m, and are placed at −12 m. The dimensions of the pylon caissons are 78.3 m by 35.2 m by 20.3 m, and the foundation level is at −23.8 m.

### 11.4.3 Materials

The concrete specification imposed strict requirements, especially aimed at ensuring adequate resistance to chloride penetration. This topic was in focus in 1988, when the requirements were formulated. The requirements can be summarised as follows:

- minimum PC content: 300 kg/m$^3$
- minimum PFA content: 10% of binder
- limits on MS content: between 5% and 8% of binder
- maximum addition (PFA + MS) content: 25% of binder
- maximum water content: 135 l/m$^3$ (Type A), 140 l/m$^3$ (Type B)
- maximum water/binder ratio: 0.35 (Type A), 0.40 (Type B)
- minimum compressive strength: 45 MPa

The bulk of the concrete was Type B, Type A concrete being for particularly exposed areas (splash zones, edge beams, tunnel lining, etc.). The water/binder ratio was calculated with efficiency factors of 0.5 and 2.0 on the contents of PFA and MS, respectively (see Section 11.2.1). The specified concrete strength is understood as the characteristic cylinder strength at 28 days of maturity (ie, equivalent days at 20°C). Typical real strengths were approximately 80 MPa.

Some typical mix designs are given in Table 11.1. All numbers (except air content) are in kg/m$^3$ (dry weight), and the amounts of admixtures (air entrainer, plasticiser, superplasticiser) are omitted. Concrete Type B* was a modification introduced to improve workability, see Section 11.4.4. Different compositions were used for ballast concrete, tremie concrete, in situ concrete for tunnel cross-passages, injection grout behind tunnel linings, etc.

**Table 11.1 Typical concrete compositions for the Storebælt Link**

| Concrete type | West Bridge | | | East Tunnel | | East Bridge | |
|---|---|---|---|---|---|---|---|
| | A | B | B* | A | B | A | B |
| PC | 328 | 335 | 340 | 335 | 315 | 320 | 310 |
| PFA | 40 | 40 | 75 | 41 | 40 | 47 | 47 |
| MS | 20 | 20 | 20 | 21 | 15 | 20 | 19 |
| Water | 131 | 133 | 155 | 131 | 161 | 133 | 138 |
| Sand 0–2 mm | 294 | 287 | 231 | 537 | 685 | 618 | 612 |
| Sand 0–8 mm | 431 | 431 | 540 | – | – | – | – |
| Stone 2–8 mm | – | – | – | – | 128 | 396 | 397 |
| Stone 8–16 mm | 448 | 448 | 366 | 1420 | 961 | 476 | 477 |
| Stone 16–25 mm | – | – | – | – | – | 336 | 337 |
| Stone 16–32 mm | 630 | 630 | 552 | – | – | – | – |
| Air (vol %) | 6 | 6 | 6 | 0.8 | 5 | – | – |

Apart from prestressing steel, ordinary black reinforcement was used throughout, except for the tunnel lining segments, where entire rebar cages were epoxy coated by immersion in a fluidised bed.

### 11.4.4 Execution

The elements for the **West Bridge** (girders, pier shafts, caissons), weighing up to 6500 t, were prefabricated at Lindholm, close to the Knudshoved abutment on Funen (Fig. 11.10). The first concrete works were the slipforming of the foundation caissons, which turned out to be virtually impossible with the highly engineered, high-performance concrete previously described. Modification of the concrete mix (Type B* in Table 11.1) solved the casting problems, but even so, subsequent microscopic analyses revealed surface microcracking. This might be due to the stickiness of the slow-setting concrete, but later investigations have revealed similar microcracks in older slipformed structures. This is not likely to have much impact on durability, but as an extra precaution, cathodic protection of the reinforcement is provided by sacrificial zinc anodes. Slipforms were replaced by climbing formwork for the remainder of the Storebælt project (as well as for the Øresund Link), and slipforming has generally gone out of favour in Denmark.

For each element type a production line was established, where the element was cast in stages. Between casting sequences the element was moved by hydraulic jacks, pushing the element forward along skid beams, provided with Teflon slides. At the end of the line, the element was picked up by the heavy-lift vessel *Svanen* (Fig. 11.10) and placed in the bridge line. Before load-out, a temporary steel cofferdam was fixed to the

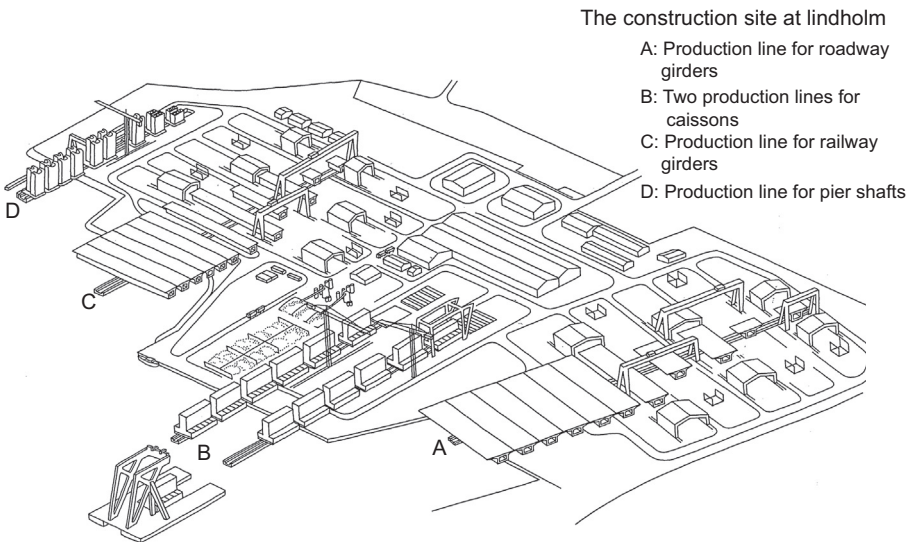



**Figure 11.10** Storebælt West Bridge prefabrication yard at Lindholm (Frandsen and Gimsing, 1998).

top of the caisson, allowing the grouting of the pier shaft to be performed in the dry. Each 110-m-long girder element consists of five segments, which were cast in three positions in fixed steel shuttering.

The **East Tunnel** tubes (Fig. 11.8) were bored by four full-face tunnel boring machines, deployed at either end of the two tubes. Attached to the rail-mounted tunnel boring machine was an approximately 200-m-long train, accommodating the controls, the conveyer belt for excavated material, and the equipment for mounting the tunnel lining, one ring at a time. A total of seven segments, including a smaller key segment, constitute a lining ring of width 1.65 m. The tunnel lining segments are joined by semi-circular stainless-steel bolts, water tightness being ensured by rubber gaskets, and the annulus between the lining and the soil is injected with cement grout containing a large amount of PFA, to bind chlorides and sulfates from the environment.

The main durability concern for the tunnel lining is the penetration of salty ground water, and the fact that evaporation at the internal surface will lead to concentration of chloride in the concrete. The defence against reinforcement corrosion is threefold: (1) the grouting around the lining exterior, (2) the low permeability of the concrete and (3) the epoxy coating of the reinforcement. As a last resort, cathodic protection can be installed, in which case each reinforcement cage would have to be connected to an external power source.

The segments were prefabricated at a temporary factory located at the Halskov abutment. Due to the strict dimensional tolerances, the segments were cast in steel forms, and the long vibration time for the stiff (no-slump) concrete did cause occasional equipment break-down. The delay in the tunnel boring operation resulted in

the need for long-term storage for most of the approximately 62,000 lining segments and 15,000 railway base bottom elements.

All but the smallest **East Bridge** piers were prefabricated in three segments, viz foundation caisson, lower shaft and upper shaft. The prefabrication yard was located approximately 56 km from the bridge, and a floating crane placed the pier segments. The four caissons for anchor blocks and pylons were prefabricated at the same site, towed to the bridge line and lowered onto prepared gravel beds in the seabed. The remainder of the 53-m high anchor blocks and the 254-m-high pylons (Fig. 11.9) were then cast in situ, using climbing formwork.

The poor workability of the concrete combined with closely spaced reinforcement resulted in cases of honeycombing in large castings of the pylons, which were repaired by water jetting of the damaged concrete (Fig. 11.11), followed by trowelling in of repair concrete. Some concern was also caused by cracking and damage on one of the anchor blocks, which turned out to be thermal surface cracks due to inadequate curing and frost spalling caused by cooling pipes which had inadvertently been left open. Both places were repaired, and they are subject to close monitoring.

A novel feature of the Storebælt project was the systematic application of pull-out testing to document the concrete compressive strength, using the LOK-Test and the CAPO-Test (Fig. 11.12). The former is used where it is possible to place a steel disc in the fresh concrete, mounting the device on the formwork; the latter is used for hardened concrete, a steel ring being inserted and expanded to fit a specially drilled hole and reamed recess. The 25-mm-diameter steel disc or ring, embedded at 25 mm from the surface, is pulled out against a 55-mm-diameter counter-pressure ring. The relationship between pull-out force and concrete strength is very nearly linear, and it is established by compression testing of standard 150-mm by 300-mm cylinders and pull-out testing on 200-mm cubes from identical batches of concrete, cast,

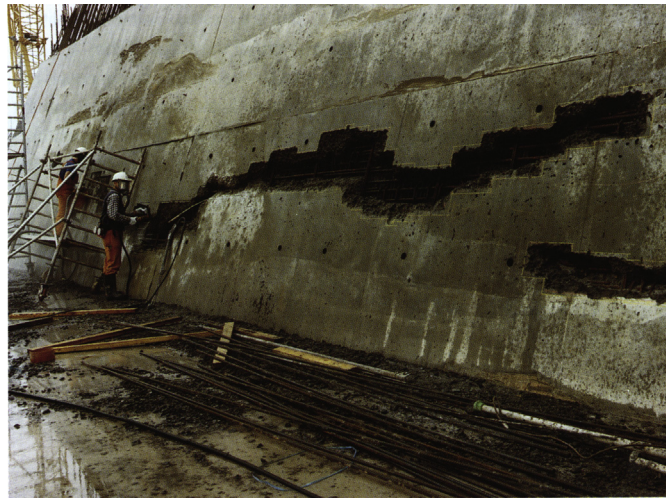


**Figure 11.11** Storebælt East Bridge pylon: water jetting of damaged concrete (Gimsing, 1999).

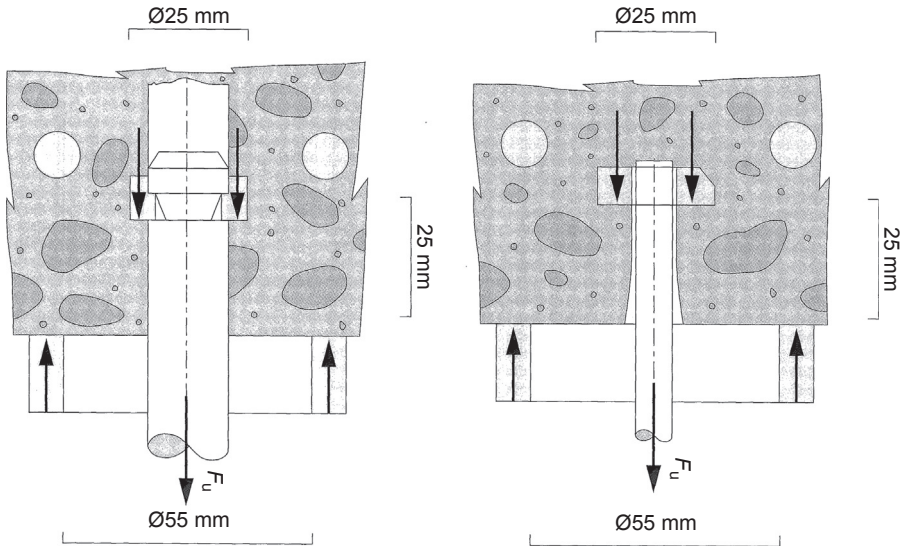



**Figure 11.12** Principle of CAPO (left) and LOK (right) strength testing (Gimsing, 1999).

vibrated, and cured in the same way. During production, approximately 40 LOK or CAPO tests were carried out per 1000 $m^3$ of concrete. The results showed a high variability, probably due to the use of nonskilled operators, and the owner concluded that the method is unsuitable for production testing, but it is recommended for further investigation if the cylinder strength testing fails in an inspection section.

A comprehensive quality management system, complying with ISO 9001, was implemented on the Storebælt project. This included the requirement for the contractors to document suitable qualifications and experience of their personnel, and consequently, project-oriented concrete technology courses were held before major work was started. A computer-based quality information system (known by the Danish acronym KIS) was established to manage the flow of quality-related documents (more than 64,000 generated for the East Bridge substructure alone). KIS only became fully operational for the East Bridge works, but data from the West Bridge and the East Tunnel have subsequently been entered into the system, which now constitutes a comprehensive database, providing full traceability from the material specification through concrete production, testing, placing and curing to testing of the hardened concrete.

### 11.4.5 Inspection and maintenance

The technical operation and maintenance of the Storebælt Link is primarily based upon the guidelines that are part of the owner's integrated management system for quality, environment and safety. The owner's organisation is fairly lean, the majority of the work being outsourced to contractors, suppliers and consultants. Already by year-end 1995, the owner tendered consultancy services for the entire operation and



**Figure 11.13** Storebælt East Bridge inspection vehicle (www.storebaelt.dk).

maintenance, comprising concrete structures, steel structures, installations and pavements. Since basically only one tenderer — a joint venture of the major players — was capable of performing the assignment, the owner decided to instigate competition by splitting the work into several packages. Thus in 2000, services for operation and maintenance of concrete structures and of steel structures were awarded to different consultants, similar packages being awarded for the other services.

Principal inspections are planned for 6-yearly intervals, with routine inspections every two years, approximately. (For description of the inspection types and their actual frequency, see Section 11.8). In addition to the normal access facilities (stairs, ladders, lifts) a mobile platform vehicle was designed for inspecting the outer surfaces of the West Bridge girders and the upper parts of the East Bridge piers and anchor blocks (Fig. 11.13). For the West Bridge roadway girder, an improved version has been commissioned, and a similar platform has been in operation on the East Bridge. Sky climbers are used to inspect the pylons and the piers.

In most cases, the two types of visual inspections (routine and principal) suffice to identify the minor repair and maintenance works to be carried out. A special inspection is performed in those situations where visual inspections are insufficient to decide remedial actions. A special inspection includes activities such as setting up a damage hypothesis, planning of inspection extent, the use of nondestructive testing and sampling of structural materials for laboratory analysis. Based on the collected information, several rehabilitation alternatives are evaluated — taking into account direct and indirect costs — often combined with a structural safety evaluation. The result of the special inspection is a recommendation regarding which remedial action is to be carried out and when.

The Storebælt inspection program envisages the monitoring of reinforcement corrosion by means of embedded corrosion monitors. The sensors consist of six steel probes placed at different levels in the concrete cover (Fig. 11.14). As chlorides penetrate into the concrete, the threshold level will be exceeded, and the probe will start to corrode. A total of 450 corrosion monitors were installed on the Storebælt Link concrete structures, but the data collection and interpretation have met with technical difficulties.

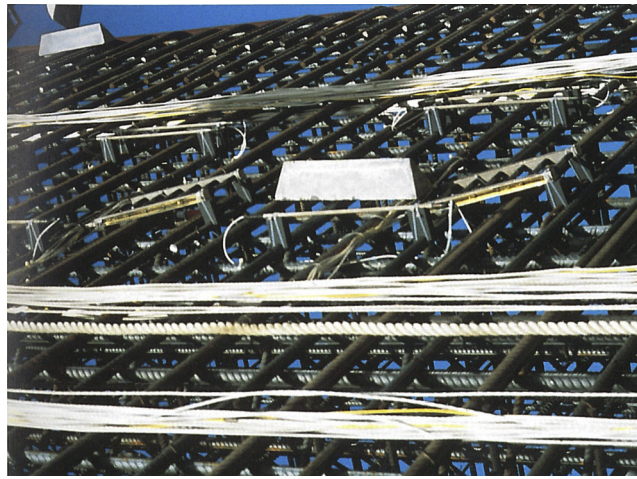


**Figure 11.14** Corrosion monitoring sensors installed in concrete cover (Frandsen and Gimsing, 1998).

## 11.5 The Øresund Link

### *11.5.1 Description*

The 16-km **Øresund Link** connects the Danish capital of Copenhagen on Zealand with the city of Malmö in southern Sweden by a four-lane motorway and a dual-track railway (Fig. 11.15). In 1995, construction started on the coast−coast section, which consists of the following parts:

- A 0.9-km$^2$ reclaimed peninsula near the Copenhagen airport at Kastrup.
- A 3.8-km immersed **Øresund Tunnel** under the main navigational channel between Kastrup and the islet Saltholm, the world's largest immersed tunnel in terms of volume.
- A 4.0-km-long artificial island, Peberholm, south of Saltholm, which is a protected wildlife sanctuary.
- A 7.8-km-long bridge between Peberholm and Lernacken in Sweden, Europe's longest combined road and railway bridge. The **Øresund Bridge** crosses a relocated shipping lane by a 490-m cable-stayed span with a navigational height of 57 m, the largest cable-stayed bridge span in the world in terms of length combined with traffic load.

The tunnel option was motivated by the proximity of the Copenhagen airport at Kastrup, which precludes a high bridge over the Drogden shipping lane. Associated structures include portal buildings for the tunnel and a viaduct at the eastern end of the island, bringing the parallel road and railway at ground level to a position with the motorway placed above the railway on the bridge.

The link was opened to traffic in July 2000. The construction cost for the coast−coast section amounted to approximately EUR 2000 million, which is increased by some 50% due the extensive land works, including an underground railway station

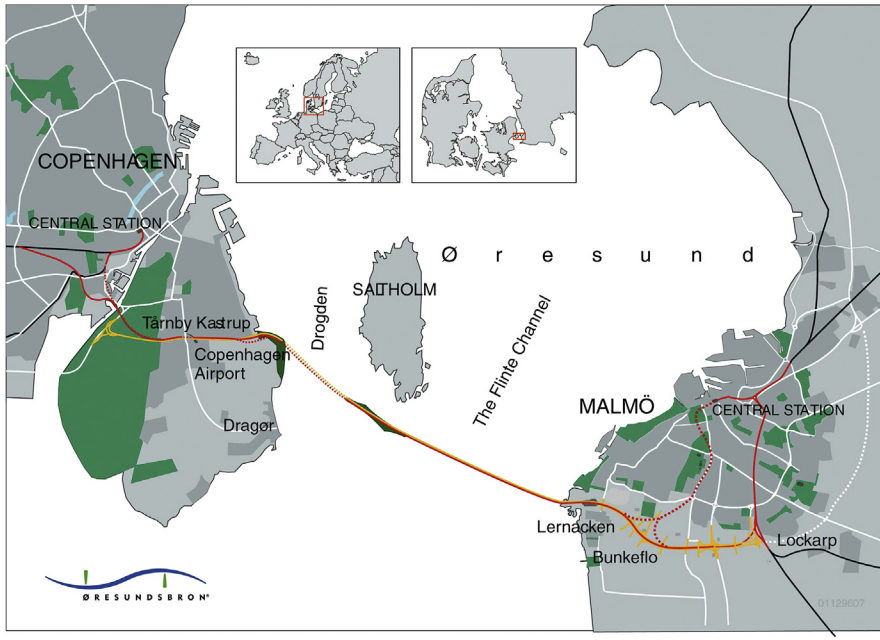



**Figure 11.15** The Øresund Link between Denmark and Sweden (www.sundogbaelt.dk).

at the Kastrup airport. The entire link is toll-funded, with the payback period for the government-guaranteed loans estimated at 25−30 years.

### *11.5.2 Design*

The Øresund Link project was divided into three main components, tendered and awarded as 'design and construct' contracts:

- tunnel
- dredging and reclamation
- bridge

The design and construct concept implies that the detailed design is carried out by the contractors, based upon conceptual designs included in the contract documents, where the concepts in turn are based on defined functional criteria. The contract documents were prepared by the owner (see Section 11.7) assisted by house consultants, forming an integrated project organisation.

The 3.8-km **Øresund Tunnel** accommodates two tubes for the four-lane motorway, two tubes for the dual-track railway, and a service gallery between the two motorway tubes, which doubles as a smoke-free escape route in case of major accidents (Fig. 11.16). The cross-section is 38.8 m by 8.6 m, the height being governed by the railway clearance profile. The tracks are fastened directly to the bottom slab, the omission of ballast reducing the required tunnel height. No membrane is

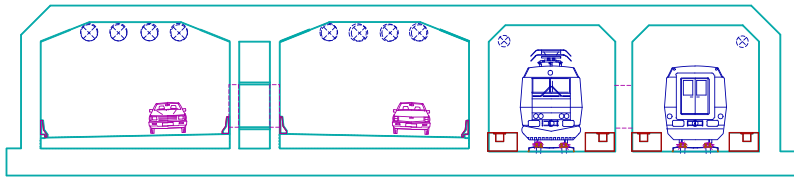


**Figure 11.16** Øresund Tunnel cross-section (www.sundogbaelt.dk).

specified, the rationale being that any leaks are next to impossible to locate and repair, and once the membrane is penetrated, water will migrate to the weakest point in the concrete. It is therefore a wiser allocation of resources to ensure a crack-free concrete in the first place, and omit the membrane. The immersed part of the tunnel consists of 20 elements, each approximately 175-m long, resulting in a total immersed tunnel length of 3510 m. The elements were placed in a pre-dredged trench, and founded on a gravel bed. The first 15 elements were installed from the Kastrup end, the last five being installed from Peberholm. Thus, the closure joint was located between elements No 15 and 16. The final tunnel profile is in general below seabed level, and at the Drogden navigation channel the top of the cover is 10 m below water level.

The 7.8-km Øresund Bridge includes a cable-stayed high bridge having a central 490-m navigation span with minimum headroom of 57 m, and two side spans 160 and 141 m on each side (Fig. 11.17). The western approach bridge from Peberholm consists of 22 spans ($4 \times 120$ m $+ 18 \times 140$ m) and the eastern approach bridge from Lernacken of 27 spans ($3 \times 120$ m $+ 24 \times 140$ m). Along the bridge alignment, the Øresund is very shallow, the shipping lane being dredged to 7 m. The bridge superstructure is in two levels with a four-lane motorway at the top deck and a dual-track railway at the bottom deck. The two levels are separated by two parallel Warren-type steel trusses, in composite action with the transversely prestressed concrete top flange.

On the approach spans, the ballasted railway is carried in a concrete trough section supported on transverse steel girders spanning 20 m between the lower transverse members and in composite action with these members. The troughs also act as containment barriers to protect the truss diagonals in case of train derailment.

In the cable-stayed spans, the concrete troughs are substituted by a shallow steel box between the lower chords, the containment being provided by steel parapets. The bridge deck is continuous between expansion joints at a maximum distance of 1470 m, giving a maximum expansion of 1200 mm (±600 mm), as stipulated by the railway authorities. The cable planes are vertical, and each cable plane is supported

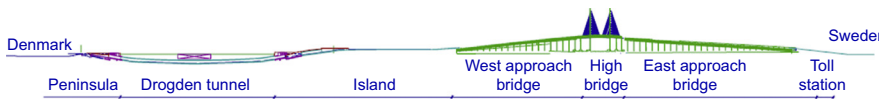



**Figure 11.17** Øresund Link elevation (www.sundogbaelt.dk).

by towers unconnected above deck level. This requires the cable plane to coincide with the centroid axis of the tower leg. The cables are thus placed at a distance from the carriageway edge, making maintenance easier and reducing the risk of accidental loads on the cables.

### 11.5.3 Materials

The concrete specifications, like those for Storebælt, contained detailed requirements for the component materials, but the requirements for the concrete composition were formulated more loosely, to enable the contractor to adapt the concrete to the chosen method of execution. The requirements can be summarised as follows:

- minimum total binder content: 340 kg/m$^3$
- minimum PC content: 275 kg/m$^3$ (tunnel), 325 kg/m$^3$ (bridge)
- maximum PFA content: 15% (tunnel), 0% (bridge)
- maximum MS content: 5.0%
- maximum water/binder ratio: 0.40 (Type A), 0.45 (Type B)

The efficiency factors on the PFA and MS were 0.3 and 2.0, respectively (see Section 11.2.1). For the tunnel, the total binder content could alternatively be blast furnace slag cement. The master specification was developed by a joint Swedish-Danish working party, and the restrictions on the use of fly ash reflect a Swedish reluctance toward this type of mineral addition. Concrete Type A was to be used on the bridge structures from the lower limit of the splash zone (level −3 m) to a level 6.0 m above the deck. On the tunnel, concrete Type A was to be used for the outer walls, roof and floor and for the New Jersey roadway crash barriers (with PC only). Concrete Type B with blast furnace slag cement was not to be used for the structural parts of ramps and portal buildings exposed to frost and marine environment. Blast furnace slag cement has been used successfully on several immersed tunnels in the Netherlands, and the restrictions on the application to the Øresund Link project are due to doubts about the resistance to frost action. In the event, the tunnel contractor chose to use PC exclusively, because the tunnel element production schedule did not permit the slower strength development of blast furnace slag cement.

Some typical mix designs are given in Table 11.2. All numbers (except water/binder ratio) are in kg/m$^3$ (dry weight), and the amounts of admixtures (air entrainer, retarder, plasticiser, superplasticiser, stabiliser) are omitted. The self-compacting concrete (SCC) mix, used for the underwater closure joint of the tunnel, is characterised by a high binder content, a carefully developed aggregate grading curve, a high amount of plasticiser and the use of stabiliser. The concrete Type A* was a special mix used in Cadiz (see Section 11.5.4).

### 11.5.4 Execution

No early age cracking was accepted for structures in the splash zone (bridge) or water-retaining structures (tunnel). For all other structures, the maximum allowable early age crack width was 0.2 mm. The temperatures and stresses were simulated by computer

**Table 11.2 Typical concrete compositions for the Øresund Link**

| Concrete type | Øresund Tunnel | | | Øresund Bridge | | |
|---|---|---|---|---|---|---|
| | A | B | SCC | A | A* | B |
| PC | 324 | 295 | 380 | 375 | 380 | 341 |
| PFA | 52 | 50 | 70 | – | – | – |
| MS | 12 | 15 | 22.5 | 12.5 | 19 | 12.5 |
| Water | 143 | 143 | 174 | 145 | 134 | 154 |
| Sand 0–2 mm | 633 | 509 | 750 | 647 | 561 | 677 |
| Stone 2–8 mm | 404 | 422 | 290 | 288 | 141 | 156 |
| Stone 8–16 mm | 476 | 501 | 710 | 439 | 447 | 607 |
| Stone 16–25 mm | 374 | 357 | – | 466 | 621 | 494 |
| Water/binder ratio | 0.39 | 0.42 | 0.39 | 0.36 | 0.32 | 0.42 |

Only ordinary black steel reinforcement was used, in addition to prestressing steel.

programs for early age crack control. The specified minimum cover to the reinforcement ranged from 30 mm (internal faces in box girders and portal buildings, New Jersey barriers), 50 mm (structures below the splash zone, external faces under waterproofing, internal faces in general) to 75 mm (external faces in general). For prestressing steel the concrete cover was specified as 5 mm greater than these values, however, not less than the diameter of the bar, tendon or posttensioning duct in question. During all phases of production, concreting and curing, strong emphasis was placed upon pretesting and production testing and upon the contractors' quality management systems, including inspection plans and quality documentation. Furthermore, the installation of corrosion monitors was specified (see Section 11.4.5).

The quality management approach adopted on the Øresund Link was based on the principle that the contractors approved their own work, and they were required to carry out quality system audits on their subcontractors and suppliers, as well as internally. The owner's staff also conducted audits, on a regular basis and in accordance with a program, on predefined areas of each contractor's activities. It soon became obvious that unnecessary duplication of work could be avoided by coordinating the two audit programs, and as cooperation evolved, the contractors invited the owner and his consultants to attend their audits as observers. The aim of the audits was to check whether the contractor's actual execution of the various activities complied with his Quality Plans.

All 20 elements for the immersed part of the **Øresund Tunnel** were fabricated in a purpose-built casting yard at the Nordhavn area of the Copenhagen Harbour (Fig. 11.18). Each element is made from eight segments, joined together by temporary prestressing. The precasting facility applied production techniques developed and tested in the construction of bridges over the last 20 years, but it was the first time these

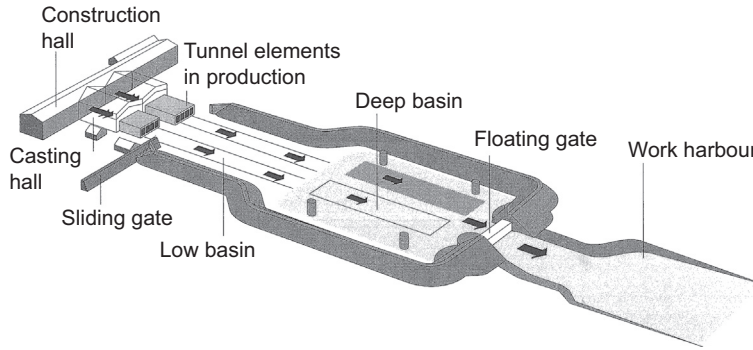



**Figure 11.18** Øresund Tunnel element fabrication yard, Nordhavn, Copenhagen Harbour (www.sundogbaelt.dk).

techniques were applied to immersed tunnel construction. This involved casting and incrementally launching segments weighing up to 7000 t and elements of 56,000 t.

Factory conditions were achieved by the erection of sheds where the reinforcement was assembled and prefabricated. A central shed covered two production lines, where two segments were made simultaneously per week to meet the time schedule. Each 22-m segment was constructed on specially prepared formwork, being cast in one single pour of 2800 $m^3$ of concrete over a 30-h period. By casting an entire section in a single operation, production was speeded up, and thermal cracking of the concrete was minimised. The joints between segments were provided with a continuous waterstop in each face, containing groutable tubes to ensure watertightness. The temporary prestressing cables holding the segments together were cut when the element had been placed in the trench and backfilled.

When the last segment was ready and joined with the previous seven segments, the entire element was jacked to the end of the skidding beams, out of the factory shed and into a diked enclosure, including a deep basin with access to the sea. Both ends of the tunnel element were equipped with a steel frame for the immersion joint, including a GINA Rubber profile for initial watertightness and a temporary end bulkhead. The sliding gate to the production facility and the floating gate to the sea were then closed, and water was pumped into the basin to a height of 9.9 m above sea level. The two elements, resting on the skidding beams, were ballasted in such a way that they floated in a level position. Once afloat, the elements were pulled toward the deeper end of the basin and moored at two dolphins. The water in the basin was then lowered back to sea level, the floating gate opened, and one by one, the elements were towed out by tugs to a temporary mooring location, where they were outfitted with equipment for immersion and towed the 18 km to the tunnel site. The production rate was two tunnel elements every two months.

When all 20 elements had been placed in the pre-dredged trench, construction of the closure joint took place inside a watertight steel structure, installed along the entire circumference of the tunnel tube. Whereas casting of the bottom slab and wall sections was possible with standard casting techniques and normal concrete, the closure joint



**Figure 11.19** Øresund Bridge, approach span erection using the heavy-lift vessel *Svanen* (www.sundogbaelt.dk).

roof slab required that the entire concrete volume of approximately 80 $m^3$ be pumped into a cavity closed on all sides. The casting included many obstacles (reinforcement, waterstops, cooling pipes, etc.), whereby compaction (eg, by vibration) was not possible, and it was necessary to develop a fully SCC for this single casting, as described earlier.

A high degree of prefabrication was also used for the **Øresund Bridge** (Fig. 11.19), the concrete caissons, pier shafts, and troughs for the railway deck of the approach bridges being produced in a construction yard at Malmö North Harbour. Reinforcement was prefabricated as cages, caissons and pier shafts up to 52-m high were cast using climbing formwork and launched by jacking. There were two production lines for the caissons and 10 fixed positions for casting the pier shafts, each area working in a slightly different way. For the caissons, cast to 4 m above water level, construction started at one end of the line, proceeding through five stages, the caissons being moved by jacking on skidding beams. The pier shafts, between 9- and 52-m high and weighing up to 750 t, were built from start to finish in the same position and moved by a heavy lifting system. Altogether 51 caissons and piers were produced: 26 for the eastern approach bridge, 4 for the high bridge, and 21 for the western approach bridge, as well as a total of 672 railway deck troughs.

Approach span steel trusses, including the concrete road deck, were prefabricated in Cadiz in southern Spain, using concrete type A* (Table 11.2). The concrete road deck weighing 3300 t was cast inside an air-conditioned plant cooled to a temperature of 20°C. The concrete strength was 50 MPa, and the concrete was air-entrained since it needed to be frost resistant. The requirement was a minimum of 3% air in hardened concrete unless the specified pretesting had shown that higher air content was necessary to comply with the requirements for frost resistance (salt scaling max 0.5 $kg/m^2$ after 56 cycles), according to the Swedish Standard SS 137244 (the Swedish Borås method). Approximately halfway through the program, it was found that the limit in salt scaling was exceeded. By then several more girders had been cast, and subsequent investigations revealed that 12 out of the 49 girders in total failed the

test. The cause was found to be increased dust content in the crushed aggregate. This required increased dosage of superplasticiser to keep the required workability, but this in turn had the effect of increasing the air content of fresh concrete, wherefore the dosage of air entraining admixture was reduced. The contractual result was an extended warranty period of 15 years for the 12 decks in question. The performance is monitored on the edge beams since the deck itself is fairly protected under the waterproofing membrane.

The 140-m-long girders were produced with a cycle time of two weeks, and they were loaded onto two seagoing barges. The average transport time was 14 days to sail from Cadiz around Denmark to the Malmö North Harbour construction yard, where the railway deck troughs were inserted. On average, one approach bridge span was produced and erected every fortnight. Steel sections for the eight girder elements for the cable-stayed high bridge were prefabricated in Karlskrona in Sweden. Some steel sections were also prefabricated at the Malmö construction yard, where the girders were assembled and the road decks were concreted.

The only components constructed in situ were the bridge towers. The two pylon caissons were prefabricated in Malmö Central Harbour in an abandoned dry dock, and towed to site using a purpose-built catamaran. A floating concrete production plant was grounded using ballast alongside, and the 204-m-high tower legs were cast using climbing formwork in lifts of 4 m, the concrete being lifted by buckets. The cycle time was 5−8 days in two shifts. On the western pylon, some cracking was observed on early pours, and on parts of the northern leg the concrete did not meet required standards. The cracks were repaired, but two lifts on the northern leg were demolished and recast.

The heavy-lift vessel *Svanen* was used for installation of the prefabricated parts (caissons, pier shafts, approach spans, high bridge superstructure). Since having worked on the Storebælt West Bridge, the vessel had been rebuilt to carry 8700 t and increased in height by some 30 m (Fig. 11.19). As relocation of the navigation channel took place after completion of the high bridge, the cable-stayed spans were placed by *Svanen* on temporary support towers resting on the seabed, allowing the cables to be installed subsequently.

### 11.5.5 Inspection and maintenance

To ensure low maintenance costs during the operational phase, a detailed inspection plan for the concrete structures was prepared, specifying inspection periods, test procedures and systematic recording of observations. The inspection plan also specified the types of monitoring to be installed on the structure, and they included an overview of actions to be taken after inspection, such as modified inspection frequencies, initiation of cathodic protection and repair or replacement of elements. The inspection requirements for the principal structures are briefly summarized next (for a description of the inspection types and their actual frequency, see Section 11.8).

The **immersed tunnel** is mainly exposed to chlorides, which may lead to high chloride contents at both faces of the exposed elements. The tunnel entrances are also subjected to freezing and de-icing salting. The potential for chloride induced

corrosion must be monitored to permit timely activation of the cathodic protection so that extensive damage can be avoided. Cores cannot be taken from the tunnel faces exposed to external water pressure, but other samples may be taken where possible and be used to verify the chloride transportation and lifetime models.

The **tunnel ramps** are exposed to chlorides, freezing and de-icing. The structures are prepared for cathodic protection and equipped with corrosion monitors for activation of the cathodic protection before the onset of extensive damage. Cores and other samples may be taken where possible for model verification.

The **roadway bridge deck** and the **railway containment troughs** are exposed to freezing and, to some extent, to chlorides from de-icing salts. The drainage of water from all concrete surfaces is to be monitored. The waterproofing of the bridge deck will reduce the aggressiveness of the environment, but the edge beams will be highly exposed and therefore are subjected to detailed inspection. Minor repairs of edge beams may be envisaged, with replacement being considered as an alternative to larger repairs.

The **bridge piers** and **pylons** are exposed to chlorides, to freezing up to some distance above the bridge deck, and also to de-icing salts at the deck level. The exposed parts of the pylons are prepared for cathodic protection and equipped with corrosion monitors for timely activation of the cathodic protection. Cores and samples may be taken where possible, particularly at the splash zone, for verification of the chloride transportation model.

The **bridge abutments** and **viaduct** are in some areas exposed to chlorides, freezing and de-icing salts. Where possible, they are prepared for cathodic protection and equipped with corrosion monitors for activation of the cathodic protection in due time. Cores and other samples may be taken to verify the chloride transportation model. The viaduct beam elements are less exposed, and repairs may be envisaged of edge beams only. Replacement of severely damaged beam elements shall, however, be considered as an alternative to more extensive repairs.

## 11.6 The Femern Bælt Tunnel

### *11.6.1 Description*

The 19-km Femern Bælt Tunnel will connect the town Rødbyhavn on the Danish island Lolland with Puttgarten on the German island Fehmarn by a four-lane motorway and a dual-track railway (Fig. 11.20). With an immersed tube length of 17.6 km, it will by far be the longest immersed tube tunnel in the world.

The tunnel will supplement or replace the car and railway ferry, which has operated between the two towns since 1963. The inception of the project dates back to the 1991 intergovernmental treaty between Denmark and Sweden, instigating the construction of the Øresund Link, in which the Danish government committed itself to work for a fixed traffic connection to Germany to facilitate Sweden's access to the continent. Such a traffic corridor was subsequently prioritised in the Trans-European Network

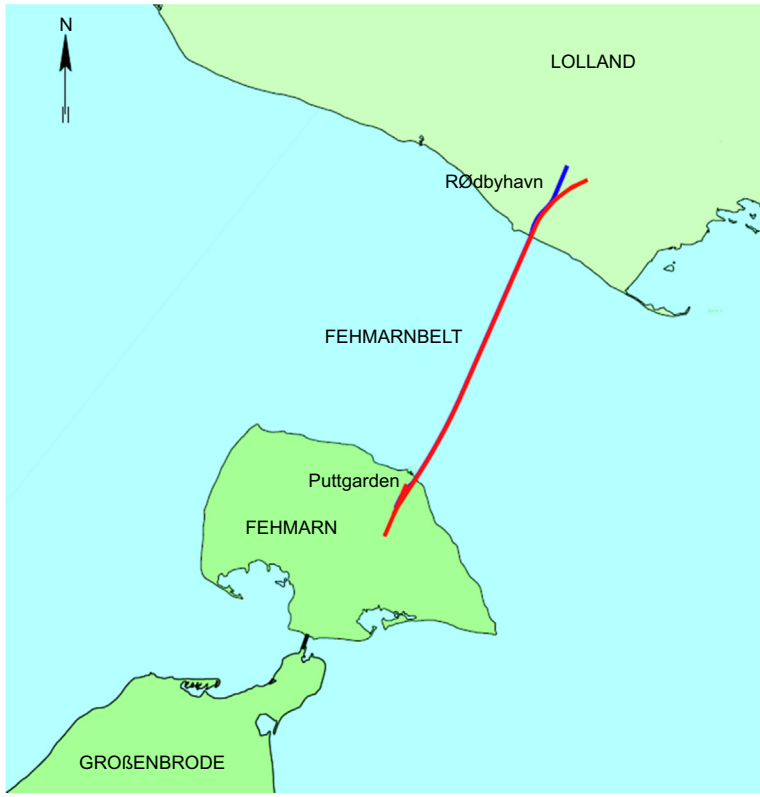



**Figure 11.20** The Femern Bælt Tunnel between Denmark and Germany (www.femern.com).

scheme of the European Union, and the EU will contribute significantly toward the construction costs, estimated at EUR 7400 million for the coast−coast section. To this should be added onshore upgrading of motorway sections from two lanes to four lanes and of railway sections from single to dual track, as well as electrification. The estimated costs of these significant land works, which include replacements or widening of some major bridges, are EUR 1300 million in Denmark and EUR 1500 million in Germany (all at 2015 prices). Like at Storebælt and Øresund, the fixed link will be toll-funded, the construction being financed by loans taken on the international finance markets.

Feasibility studies were carried out, and negotiations started with the German government, eventually resulting in an intergovernmental treaty in 2008. The feasibility studies, completed at the turn of the current century, considered the following alternatives:

- cable-stayed bridge
- suspension bridge
- immersed tube tunnel
- bored tunnel

The studies identified the cable-stayed bridge as the preferred solution, the immersed tunnel being the preferred alternative. However, after the signature of the 2008 treaty, the newly established owner's organisation commissioned two independent design teams to reconsider and optimise the two alternatives, and at the same time address some concerns that had been raised, particularly to the bridge solution. The rather surprising result of this endeavour was that the immersed tunnel came out as the most feasible, and in 2011, this was adopted as the preferred solution. Decisive factors were that the bridge piers close to the German coast would be founded on the same plastic clay as the Lillebælt Bridge (see Section 11.3.5) and that the tunnel could be operated using longitudinal ventilation only, without compromising the requirements for air quality.

The major construction contracts have been tendered, and contract negotiations are ongoing. The current project schedule envisaged construction to start mid 2015, with completion in 2021. However, the environmental approval procedure in Germany is dragging on, which – along with other concerns, see Section 11.7 – has resulted in a delay. No revised schedule has been announced, but a postponement of at least three years is likely.

### 11.6.2 Design

Like the Øresund Tunnel, the 19-km **Femern Bælt Tunnel** accommodates two tubes for the four-lane motorway, two tubes for the dual-track railway and a central service gallery (Fig. 11.21). Due to the length of the tunnel, the central gallery will not be used as an escape route; rather, in case of an accident, people will be evacuated (escape doors at 110-m spacing) into an adjacent traffic tube, which will be closed for traffic (the same solution has also been adopted for Øresund, due to experience from realistic

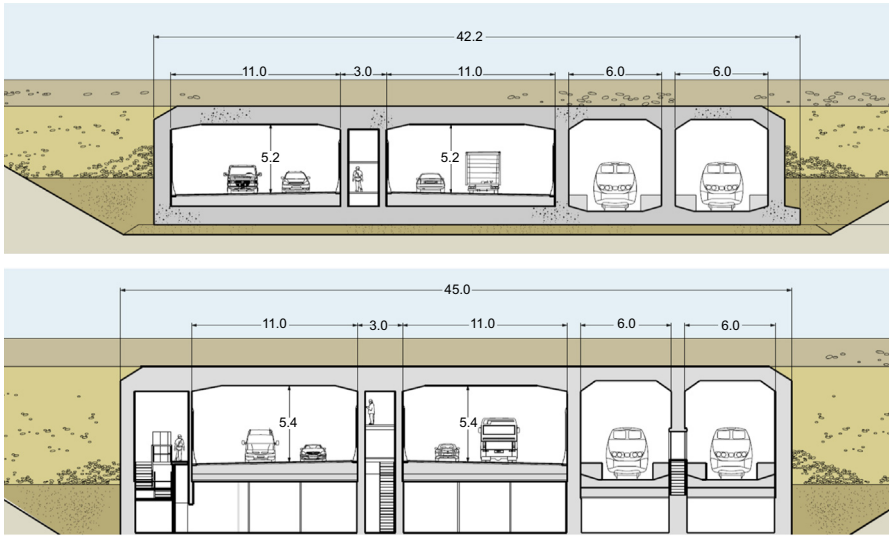



**Figure 11.21** Femern Bælt Tunnel cross-section, standard (top) and special (bottom) elements (www.femern.com).

fire drills). Note that in contrast to the Øresund tunnel, the motorway tubes include an emergency lane through the entire length.

The 17.6-km immersed tube part of the tunnel consists of 89 elements, of which 79 are standard (Fig. 11.21, top) and 10 are special (Fig. 11.21, bottom). The 217-m-long standard elements are 42.2 m by 8.9 m. The special elements are shorter (46 m) but wider (45 m) and deeper (13 m) to accommodate a lay-by for maintenance staff parking and underground rooms for transformers and other equipment, which for such a long tunnel could not be housed in the standard elements.

### 11.6.3 Materials

The concrete specification will be based upon the experience from Storebælt and Øresund, the design lifetime being 120 years (against 100 for the previous projects). Basis for the requirements are the EN 206 (2013) and EN 1370 (2009), the latter supplemented by a dedicated project application document. A quality control program supported by conformity procedures is envisaged, as is a comprehensive program of pretesting and trial castings.

To that end, 15 concrete blocks cast with different binder systems were installed in 2010 to monitor the performance in the seawater on site (Fig. 11.22). Seven blocks are provided with sensors and electrodes, and the following testing program is being carried out at the following times: at casting in 2010, after 28 days, 6 months, 2 years, 5 years, and at completion of the tunnel. The testing, carried out by the Danish Technological Institute (DTI), comprises documentation of the following:

- workability, density and air content
- setting time and bleeding




**Figure 11.22** Femern Bælt Tunnel field exposure site in Rødbyhavn (DTI).

- strength development (compressive and split tensile)
- frost resistance and air void structure
- chloride ingress resistance
- microstructure (petrographic)

### 11.6.4 Execution

The construction of the **Femern Bælt Tunnel** will apply the methods tried and tested at the Øresund tunnel, albeit at a somewhat larger scale, the weight of the standard elements being 76,600 t. All tunnel elements will be fabricated in a casting yard close to the Rødbyhavn Harbour (Fig. 11.23). There will be one production line for the 10 special elements and eight production lines for the 79 standard elements. Each bay of two production lines is a replica of the Øresund tunnel element yard (Fig. 11.17), and the four bays will be operating in pairs, each pair sharing a sliding and a floating gate. The fabrication, outfitting and tow-out of the elements will be as described for the Øresund tunnel; see Section 11.5.4.

### 11.6.5 Inspection and maintenance

The operation of the Femern Bælt Tunnel will be integrated with the Storebælt and Øresund fixed links, and similar operation and maintenance systems will be adopted.

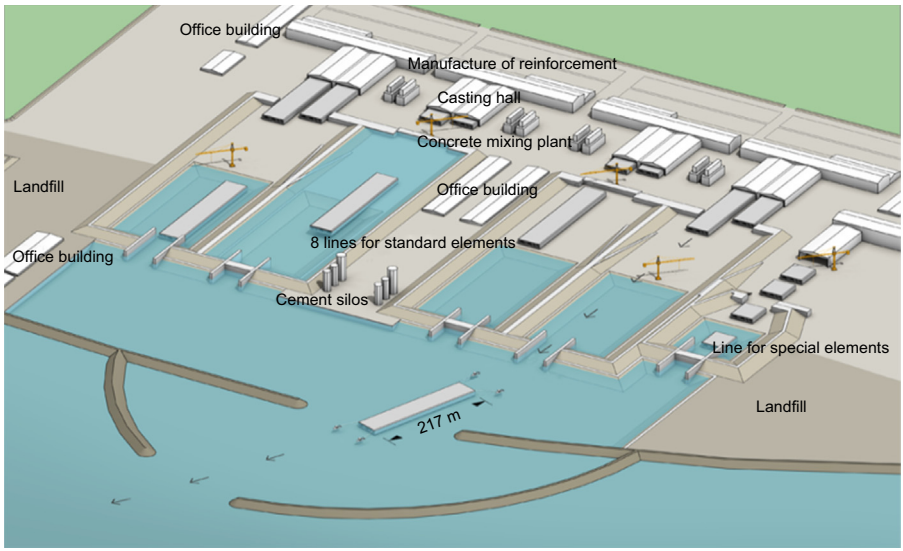



**Figure 11.23** Femern Bælt Tunnel element fabrication yard (www.femern.com).

## 11.7 Ownership and financing

Traditionally, all fixed (ie, ferry lines excluded) Danish traffic infrastructure has been owned by public bodies, toll-free and financed from the national budget. Thus, the Lillebælt Bridge is owned and operated by the National Railways and the New Lillebælt Bridge by the Danish Road Directorate. However, the political decision to let the **Storebælt Fixed Link** be user-funded necessitated the formation of a private company, A/S Storebælt, later incorporated into Sund & Bælt Holding A/S (Fig. 11.24). The sole shareholder is the Danish government, represented by the current minister of transport, who appoints the board of directors, which in turn retains the management team. The share capital is modest, the funds for construction being raised on the international finance markets where the state guarantee of the loads ensures a favourable credit rating.

A similar model was adopted for the **Øresund Link**, but the owner, Øresundskonsortiet, in charge of the coast−coast construction was in this case a Swedish-Danish joint venture, the name being changed to Øresundsbro Konsortiet in the operational phase. The land works on the two shores were the responsibility of the partners, Øresundsforbindelsen and SVEDAB, which were owned by the respective governments jointly and severally guaranteeing the loans financing the entire construction. Currently, the fixed link is managed by A/S Øresund as a subsidiary of Sund & Bælt Holding A/S (Fig. 11.24).

This business model has also been adapted for the **Femern Bælt Tunnel**, except that in this case the German government has declined to accept responsibility for the financing of the coast−coast section, hence the loans will be guaranteed by the Danish government alone. This means that the cost of the German land works will be borne by the German infrastructure budget, whereas the Danish land works as well as the coast−coast section will be financed by the toll revenue. The construction is the responsibility of Femern A/S, incorporated under Sund & Bælt Holding A/S (Fig. 11.24).

The advantage of this financial model is that whereas a private investor would demand a rate of return of 10−13%, state-guaranteed loans can be obtained at much

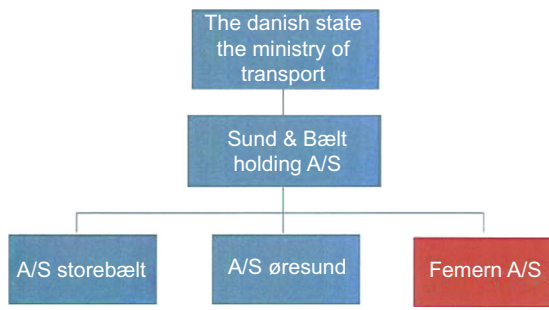



**Figure 11.24** Ownership of the Danish strait crossings (www.sundogbaelt.dk).

lower interest rates. The construction budgets and the estimated payback periods are based upon a 3% real interest rate, with refinancing typical at five year intervals, but in the event, substantially lower rates have been obtained for the Storebælt and the Øresund Links.

Ultimately, the financial viability of the fixed links depends upon the road traffic (the railway companies pay a fixed, annual fee). For the **Storebælt Link** the budget assumed an average annual daily traffic (AADT) of 14,500 vehicles (representing almost a doubling of the previous ferry traffic), increasing at an annual rate of 2%. In the event, the traffic has exceeded expectations, the AADT being 16,000 vehicles during the first six months of operation, increasing to almost 30,000 in 2014. As a result, the payback period could have been reduced to approximately 25 years, but the government has chosen to siphon the surplus off to fund other traffic investments. Likewise, it is not likely that the fees will be substantially reduced, let alone abolished, in 2030 when the loans are scheduled to have been paid back, not least because it would compromise the business model of the planned Femern Bælt Tunnel.

The success of the Storebælt Link resulted in the opening AADT of the **Øresund Link** to be optimistically estimated at 11,000 vehicles, later prudently reduced to 10,000. The actual traffic, however, was a disappointing AADT of 8700 vehicles during the first full year (2001) of operation. Subsequently, usage picked up substantially, increasing by much more than that the budgeted 2% per year, the AADT reaching 15,700 in 2006. In recent years, however, in the wake of the financial crisis, traffic has stagnated at approximately 17,000 vehicles, and as a result, the estimated payback period has been pushed back to 34 years.

For the **Femern Bælt Tunnel**, the budget envisages an AADT of 11,000 vehicles, increasing at an annual rate of 1.4%, provided that the upgrade of the adjoining infrastructure is completed. This assumption is, however, cast into doubt by the fact that despite the 2008 treaty obligation to complete the German land works by 2021, the corresponding construction works have not yet been budgeted. The traffic predictions have also been criticised for not adequately accounting for competition from continued ferry services and from the Storebælt Link. Furthermore, recently received bids for the major construction contracts have pushed up the construction cost estimate, and the contribution from the EU has turned out to be less than expected. Consequently, the payback period, envisaged at 32 years, might exceed the 50 years, implying that the project is not financially viable. Ongoing negotiations with contractors aim to bring down the construction cost by delaying completion until 2024, increasing the likelihood of a timely completion of the German land works.

## 11.8 Asset management

Integrated asset management systems have been implemented on the Storebælt and the Øresund Links since they went into operation in 1998 and 2000, respectively, and they will be adapted to the Femern Bælt Tunnel. The purpose of an asset management system is to save money by extending the lifetime of existing structures, to facilitate

prioritising of limited operation and maintenance budgets, and to avoid unforeseen costs. The management systems are characterised by these:

- frequent visual inspections and/or continuous monitoring of the structures for timely detection of significant damage
- prioritisation of inspections and remedial works based on the condition of the structures and knowledge of the exposure conditions
- use of state-of-the-art nondestructive testing technologies to investigate damage mechanisms observed during the visual inspections

Three levels of inspections are normally identified:

**Routine Inspections** are performed every day/week/month/year to form the basis for routine maintenance and cleaning and to identify any irregular situations.
**Principal Inspections** are performed every 3−6 years to identify needs for rehabilitation or special inspections and to allocate medium-term (5−10 years) budgets.
**Special inspections** comprise detailed inspection, combined with nondestructive and laboratory testing and assessment, performed when required to determine cause and extent of damage and to propose a rehabilitation strategy.

Another important justification of an integrated management system for major infrastructure assets is the need for overview of the huge amount of data generated during the operational phase. The management system must be able to archive as-built drawings, inspection reports, repair documentation, photos, laboratory reports, etc. Typically, the management system is hosted on a central server so that all relevant personnel are able to access the material whether on site on in the office.

The implementation of the management systems on Storebælt and Øresund are described in Sections 11.4.5 and 11.5.5, respectively. Both management systems are Internet-based, enabling consultants and service contractors to report directly through the system. The systems have facilities for handling documents so that notes, reports, videos, photos and drawings can be stored. Via the job control, the systems provide an overview of the requested, planned, ongoing and performed activities.

## 11.9 Conclusions

Experience with the Lillebælt bridges shows that by careful maintenance and attention to structural behaviour, it is possible to preserve the serviceability of major bridges for 80 and 45 years, respectively.

For the most recent Storebælt and the Øresund projects, it is instructive to compare a number of key issues having an impact on the expected structural lifetime performance.

Storebælt adopted the traditional **contract philosophy** with a detailed tender design prepared by the owner's consultants and executed by the contractors as best they could. Only the West Bridge contractor was in charge of the detailed design, which, however, implied that the owner had less control of the appearance, the resulting structure being aesthetically less satisfactory. The 'design and construct' approach adopted

at Øresund meant that the contractors could adapt the detailed structural design to their most competitive execution methods. At the same time, the owner was firmly in control of aesthetics and environmental impact through a conceptual tender design, including rigorous definition drawings, accompanied by an illustrative design, demonstrating to the contractors one way of fulfilling the requirements.

At Storebælt the **concrete specification** was fairly comprehensive, including limits on binder content, water content, water/binder ratio, as well as compressive strength, leaving the contractor little room for adaptation to his production methods. The prescriptions for Øresund were less detailed, specifying neither maximum water content nor compressive strength, giving the contractor considerable freedom in the mix design. In comparison with Storebælt the maximum water/binder ratio was relaxed, the reason being that ratios below 0.40 often lead to internal microcracking, which can hardly be considered beneficial. Very low water/binder ratios also result in the mixes that are difficult to cast without a large dosage of plasticiser, which again entails long setting times. In the event, however, the water/binder ratios on the two projects were fairly similar, the main difference being that on Øresund more emphasis was placed on functionality, documented by trial casting, than on detailed specifications.

The **high degree of prefabrication** adopted in both projects implied that the majority of the structural components were produced under factory conditions or at construction yards, where the environmental conditions could be controlled. Due to the repetition of operations, the procedures were improved and problems were solved along the way. Thus, the only major setbacks occurred in in situ construction of pylons and anchor blocks, resulting in extensive repair or demolition at an early stage and before the bridges were put into operation.

The use of **corrosion monitoring** by means of embedded sensors was pioneered at Storebælt and further developed at Øresund, where the provision of corrosion sensors was written into the contract documents from the start.

The rigorous **management** system adopted at Storebælt generated a unique documentation of the works, but the implementation was marred by a lack of commitment from the contractors' side. The approach at Øresund to a large extent relied upon the contractors' self-control. The quality system audits, conducted jointly by owner, consultants and contractors, fostered a spirit of cooperation which was largely responsible for the remarkable fact that this major infrastructure project was completed before time, within budget and without any litigation (Russel, 2000).

For both strait crossings, the planning and reporting of **inspection and maintenance** works are based upon an asset management system, improving the overview and ensuring timely follow-up on all activities.

## Bibliography

Braestrup, M.W., 2005. Principal lessons and innovations from the construction of the Danish strait crossings. In: Analytical Methods and New Concepts in Concrete and Masonry Structures. 5th International Scientific Conference, Gliwice−Ustron, pp. 12−14. June 2005, Proc & CD, 12 pp.

DSB & Vejdirektoratet, 1986. At Slå Bro – På dansk ("Bridging – the Danish way", in Danish), Copenhagen, 128 pp.

EN 206, 2013. Concrete – Part 1: Specification, Performance, Production and Conformity. CEN. December, 93 pp.

EN 1370, 2009. Execution of Concrete Structures. CEN. December, 66 pp.

Frandsen, A.G., Gimsing, N.J. (Eds.), 1998. West Bridge. Storebæltsforbindelsen, Copenhagen, 179 pp.

Gimsing, N.J. (Ed.), 1998a. East Bridge. Storebæltsforbindelsen, Copenhagen, 390 pp.

Gimsing, N.J. (Ed.), 1998b. East Tunnel. Storebæltsforbindelsen, Copenhagen, 199 pp.

Gimsing, N.J. (Ed.), 1999. Concrete Technology. Storebæltsforbindelsen, Copenhagen, 271 pp.

Gimsing, N.J. (Ed.), 2000. The Bridge. Øresundsbron, Copenhagen, 288 pp.

Johannesen, E., 1994. Danmarks Broer (Danish Bridges, in Danish). Borgen, Copenhagen, 113 pp.

Munch-Petersen, C. (Ed.), 2003. Danske bygningsingeniørers virke/Danish Civil and Structural Engineering (in Danish and English). Danish Society for Structural Science and Engineering, Copenhagen, 223 pp.

Russel, H., 2000. Partnership Pays: Project Management the Øresund Way. Øresundsbro Konsortiet, Route One Publishing Ltd, 110 pp.

# Coastal protection structures in the Netherlands

12

*J. Gulikers*
Ministry of Infrastructure and the Environment, Rijkswaterstaat-GPO, Utrecht, the Netherlands

## 12.1 Introduction

The Netherlands, located on the North Sea coast of Europe, has many important concrete structures built in or near seawater. One of the first major projects in the marine environment was the sea locks near IJmuiden built in 1876 (Kleine Sluis or Small Lock; see Fig. 12.1) to allow ships to sail to the harbour of Amsterdam through the Noordzeekanaal. Since then, many marine concrete structures have been built along the Dutch coast, encompassing discharge sluices, sea locks, quay walls and importantly, the sea defence structures built as part of the Delta Project. The most prominent and impressive example of the latter is the Eastern Scheldt Storm Surge Barrier, having a design service life of 200 years (see later).

Marine environments are known to be very hostile to construction materials. In practice, numerous examples can be given of premature damage confronting the asset owner with consequent costly maintenance and repair. Since the construction of the Noordersluis built in 1921−29, the use of blast furnace cement has become common for use in concrete in marine structures in the Netherlands. Previous experience obtained with the use of plain Portland cement, eg, in the Kleine Sluis (Small Lock) and Middensluis (Middle Lock) near IJmuiden, and the discharge sluices and lift-locks in the Afsluitdijk (built in 1921−29), revealed that these structures were severely prone to both sulphate attack and alkali−silica reaction (ASR). Experience over a period of nearly 100 years has clearly demonstrated the benefits of blast furnace slag cement in achieving reinforced concrete structures with outstanding performance (Bijen, 1996). This is one of the major reasons for the Dutch Ministry of Infrastructure to explicitly require the use of cements with a minimum slag content of 50%, including provisions for proper curing (ROK, 2015).

This chapter will focus mainly on experience with the long-term performance of the major structural elements of the Eastern Scheldt Storm Surge Barrier, the most important and impressive coastal defence structure in the Delta Project in the Netherlands.

**Marine Concrete Structures.** http://dx.doi.org/10.1016/B978-0-08-100081-6.00012-X
Copyright © 2016 Elsevier Ltd. All rights reserved.



**Figure 12.1** Kleine Sluis (Small Lock) near IJmuiden built in 1876; the combination of concrete and masonry suffered from sulphate attack and alkali−silica reaction; completely renovated 1997−99.
Courtesy of https://beeldbank.rws.nl, Rijkswaterstaat/Rens Jacobs

## 12.2 Historical background to the Delta Project

In February 1953, the southwestern part of the Netherlands suffered from the largest flooding disaster in several centuries. A northwester had raged for many hours, producing a surge 4 to 5 m higher than AOD (Amsterdam Ordnance Datum, mean sea level as defined for Amsterdam). During this event, the sea engulfed 200,000 ha of fertile land as well as many towns and villages in the southwestern Netherlands. Eventually, 1835 people and 200,000 head of cattle drowned, approximately 72,000 people had to be evacuated, and more than 47,000 homes, factories, and offices were either damaged or destroyed.

In view of these disastrous consequences, shortly thereafter it was readily agreed that such a catastrophe had to be prevented in the future. In the same year (1953), the so-called Delta Committee recommended the strengthening of the existing flood defences and dikes, and in addition, to cut the shoreline by 700 km. The latter involved closing off all tidal inlets in the delta area of the southwestern part of the Netherlands and raising all existing flood defences to so-called delta level (ie, 5 m above AOD). The major aim of these measures was to reduce the risk of flooding to a 1:4000-year flood in the delta area and the northern part of the Netherlands, and to a 1:10,000-year flood in the Randstad area (ie, the central area of the Netherlands with Amsterdam, Rotterdam, and The Hague as the major cities).

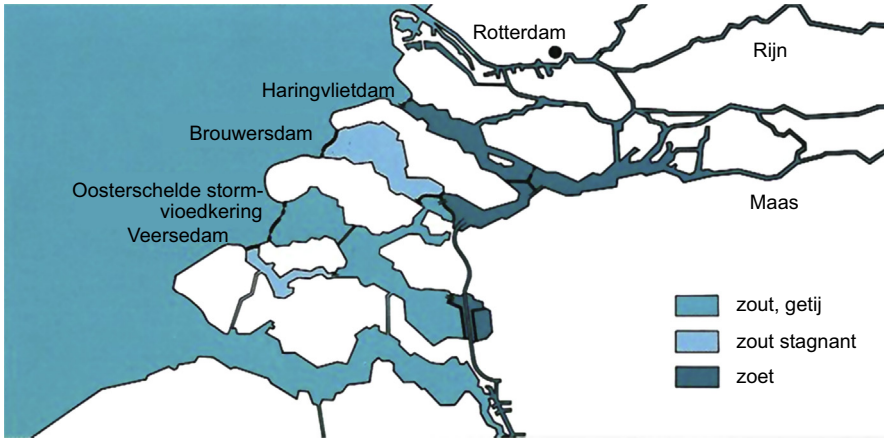



**Figure 12.2** Major sea defence structures in the Delta Project (descriptions of waters: zout, getij means salt, tidal; zout stagnant means salt stagnant; zoet means fresh).

The Delta Project comprises a number of major sea defence structures, the most important being the Haringvliet dam (1960−62), the Eastern Scheldt Storm Surge Barrier (1978−86) and the Maeslant Storm Surge Barrier located near Rotterdam (1996−98); see Fig. 12.2.

## 12.3 Eastern Scheldt Storm Surge Barrier

### *12.3.1 General description of the barrier structure*

The original proposal was to close off the Eastern Scheldt by a dam. However, this area was regarded as a unique natural habitat, and consequently, at an early stage, studies were performed to assess the feasibility of developing either an open dam or a storm surge barrier equipped with sliding gates to allow for sufficient tidal movements. To limit the construction risks, it was decided to prefabricate as many elements of the barrier structure as possible on land. Thereafter, the prefabricated units would be transported to the construction site to be assembled.

The storm surge barrier encompasses three tidal channels (ie, Hammen, Schaar and Roompot) and covers a total distance of approximately 2800 m. The barrier structure comprises 65 concrete piers connected by threshold beams placed on the seabed and upper beams placed 1.5 m above AOD. Together with the steel sliding gates, these three concrete elements form the essential barrier elements, with the piers acting as the backbone; see Fig. 12.3. On top of the piers, box girder bridge elements with a span of 45 m are provided to allow for traffic. The construction of the barrier started in 1978, and on October 4, 1986, it was officially taken into service.

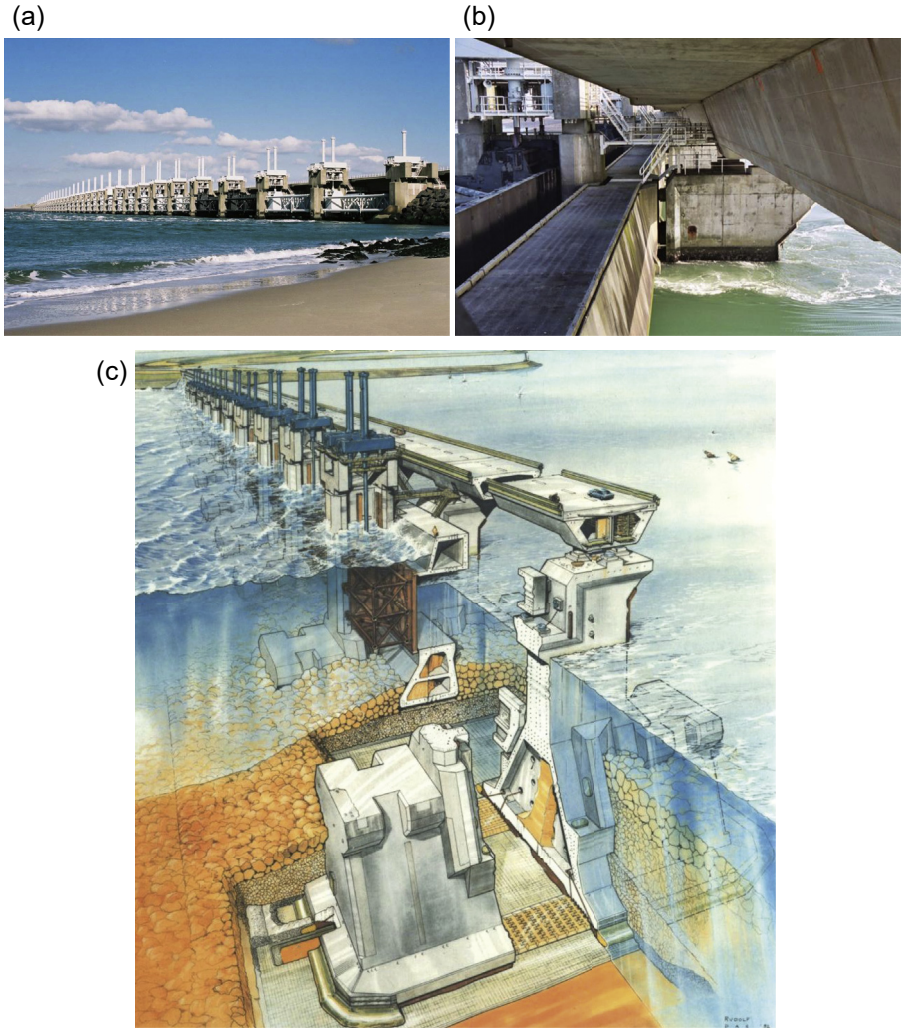



**Figure 12.3** Eastern Scheldt Storm Surge Barrier. Photo (a) shows the North Sea view of the barrier in the Roompot tidal channel; photo (b) shows three of the four major structural elements comprising the barrier, ie, steel sliding gate, upper beam and pier (threshold beam being submerged); view (c) is an isometric schematic view showing the main barrier elements.

### *12.3.2 Durability design*

For the concrete elements comprising the Eastern Scheldt Storm Surge Barrier (ie, the piers, upper beams and threshold beams), a design service life of 200 years was imposed by the Delta Committee. However, this was not accompanied by any clear performance requirements for the structure in terms of amount of damage (cracking, spalling, percentage of corroding steel, etc.). For the bridge elements,

no clear value for the design service life was specified in the project documents; however, based on the then-prevailing national standards (VB'74, 1974), it is assumed that at least 50 years was aimed at. Given the marine exposure environment, it was obvious that the decisive mode of deterioration relevant to durability design would be reinforcement corrosion resulting from chloride ingress into the reinforced concrete structures.

In view of the extremely long (200-year) design service life required for the essential elements constituting the storm surge barrier, an extensive literature research was undertaken. The result was that, probably for the first time, a mathematical model describing chloride ingress over time (Collepardi et al., 1970) was employed for the design of a new structure to predict the long-term performance (Hageman, 1982).

#### 12.3.2.1 Exposure conditions

The Eastern Scheldt barrier is constructed on the North Sea coastline of the southwestern part of the Netherlands, which means that the barrier is subjected to a typical temperate marine environment (see Chapter 7). The chloride concentration of the seawater in the North Sea and Eastern Scheldt bay amounts to approximately 18 g/L, and the temperature of the seawater varies during a yearly cycle between 5 and 20°C. The tidal variation at the location of the Eastern Scheldt barrier is approximately 3 m between high and low tide (ie, AOD $\pm$ 1.5 m). The prevailing wind-direction is from the southwest. (The latter information could be relevant for the interpretation of chloride profiles retrieved at a later stage from the structure, so as to distinguish between the leeward and the windward side of the barrier.)

#### 12.3.2.2 Design considerations

At that time (1976) until 1986, an imposed design life of 200 years for the storm surge barrier was considered a stringent requirement for a concrete structure, especially when taking into account the prevailing aggressive marine exposure conditions. In addition, there was a lack of experience with regard to designing for durability for such a long design life. This was compounded by the fact that inspection and maintenance were considered to be virtually impossible especially for the piers and threshold beams, as large parts were permanently located in the submerged zone.

Traditionally, design for durability meant application of simple deemed-to-satisfy provisions using limits for maximum water/cement ratio ($w/c$), minimum crack width, minimum cement content and minimum cover depth, as prescribed by the prevailing standards at that time. However, most if not all limiting values were largely based on short-term national experience obtained for significantly less severe exposure conditions, considering a reference design life of 50 years. Acknowledging this lack of experience in durability design, a serious attempt was made in the project to achieve the desired service life by analysing the processes involved in reinforcement corrosion, ie, both chloride transport over time into the concrete cover as well as the corrosion process following onset of corrosion.

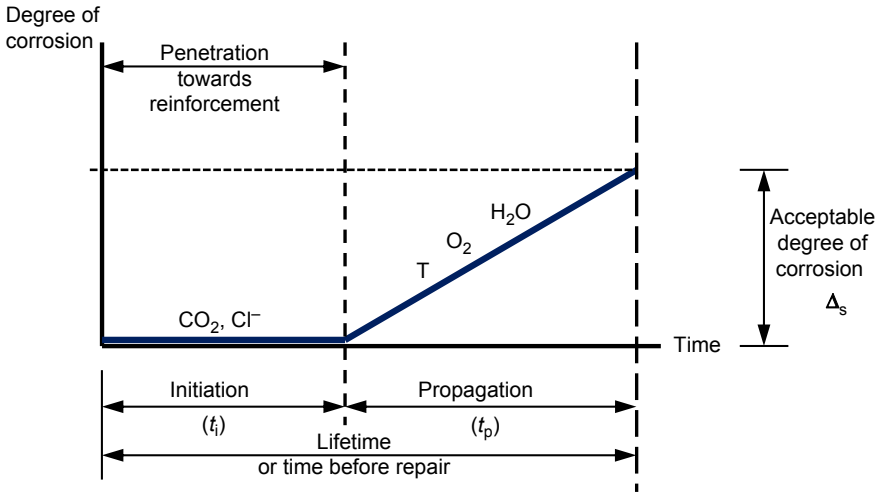



**Figure 12.4** Conceptual two-stage model (following Tuutti, 1982).

Already at the start of the design in 1976, it was acknowledged that corrosion of the embedded reinforcing steel and long-term durability of the elements would be closely linked to cracking of the concrete cover (Hageman, 1982). Therefore, the design provisions were aimed at achieving concrete elements 'that will be as crack-free as possible', in particular the concrete surface/near-surface zone.

As a starting point, Hageman adopted the concept that the lifetime of the barrier elements with respect to reinforcement corrosion, $t_{sl}$, equalled the sum of the initiation time, $t_i$, and the propagation time, $t_p$ (see Fig. 12.4):

$$t_{sl} = t_i + t_p \qquad [12.1]$$

This conceptual approach characterised by a clear distinction in the two stages of the corrosion process was originally introduced by Beeby (1978) and later graphically visualised by Tuutti (1982). Somewhat surprisingly for that time, Hageman's analysis placed significant emphasis on the inclusion of the propagation stage of reinforcement corrosion, and hence the attempts to control or eliminate cracking as far as possible.

With respect to the cause of depassivation, a distinction was made between carbonation and chloride ingress. It was anticipated that for all barrier concrete elements, carbonation would not be decisive for durability. The deterministic calculations clearly demonstrated that for an anticipated cover thickness of 70 mm and taking into account a high-quality and largely crack-free concrete, the carbonation front would not reach the level of the reinforcing steel within the design service life of 200 years. This conclusion was also supported by findings on the carbonation depths measured on existing marine concrete structures.

Regarding the development of reinforcement corrosion resulting from the ingress of chlorides, three stages in time were distinguished:

1. the corrosion initiation stage, ie, the time until depassivation of the steel occurs
2. the first stage of corrosion propagation with an intact concrete cover, ie, the time period starting from the onset of corrosion until longitudinal cracks appear parallel to (and above) the outer steel bars, or the concrete cover spalls off
3. the second stage of corrosion propagation with a damaged concrete cover, ie, the time period in which the exposed bare reinforcement steel freely corrodes under the influence of weather, wind and water

This is actually an elaboration of the simple Tuutti model shown in Fig. 12.4, indicating the advanced thinking at that time.

With respect to the exposure conditions, three zones were distinguished:

- splash zone
- submerged zone
- tidal zone

For the initiation stage (ie, the ingress of chloride into the concrete cover prior to the onset of active corrosion), the common analytical solution to Fick's second law of diffusion was applied. The corrosion propagation stage was modelled taking into account the supply of oxygen through the concrete cover to sustain the corrosion process following depassivation. This approach applied to the piers in particular; however for the upper and threshold beams, similar considerations were considered to be valid.

Data retrieved from several international publications as well as measurements of chloride profiles from existing Dutch marine structures were used as input values for the model parameters. For the initiation stage, a deterministic approach was adopted with a constant value for the apparent chloride diffusion coefficient, $D_a$. For the splash and tidal zones, $D_a$ was taken as 0.2 $cm^2$/year (equal to $0.63 \times 10^{-12}$ $m^2$/s), and for the submerged zone $D_a$ was taken as 0.5 $cm^2$/year (equal to $1.59 \times 10^{-12}$ $m^2$/s). Independent of the exposure zone, a chloride content at the exposed concrete surface $C_s = 2.4\%$, an initial chloride content $C_i = 0.02\%$, and a critical chloride content $C_{crit} = 0.5\%$ were assumed. (All chloride contents are expressed in % by mass of cement.)

Fig. 12.5 shows the corresponding predicted development over time of the chloride content at a depth $x = 70$ mm for concrete based on blast furnace slag cement, as well as for concrete made with Portland cement using $D_a = 3$ $cm^2$/year and 5 $cm^2$/year for the splash/tidal and the submerged zones, respectively. This deterministic approach resulted in predicted corrosion initiation times $t_i$ of 3 and 5 years for concrete made with Portland cement, whereas for concrete with blast furnace slag cement, the corresponding $t_i$ were 30 and 75 years.

Regarding the type of cement, Hageman (1982) remarked: 'The considerably more favourable behaviour of blast furnace slag cement, with respect to Portland cement is pointed out; this is a familiar phenomenon in maritime structures. It is assumed that this is caused by the ability to form chemical compounds with the chlorides and

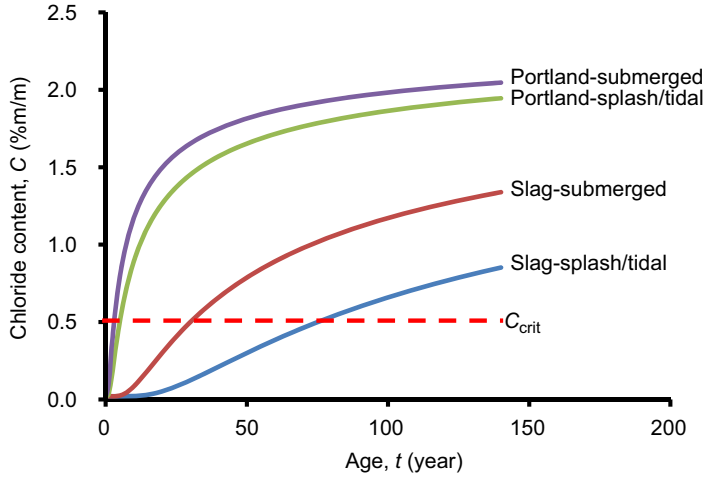



**Figure 12.5** Predicted development of the chloride content over time at a depth $x = 70$ mm (deterministic approach) for the Eastern Scheldt concrete structures.

thus making a part of the ions harmless. Other investigators are of the opinion that this effect can also be attributed to the finer pore structure of the blast furnace slag cement paste.'

On the other hand, it is well known that concrete made with blast furnace slag cement is more vulnerable to curing conditions, and consequently longer curing is required to fully achieve its advantageous durability properties. Interestingly, the impact of cracks on chloride ingress and the corrosion process, and thus on the eventual durability of the concrete elements, was treated very seriously. Based on engineering judgement, it was postulated that near a crack, the initiation time may locally be reduced to 20−40% of the value that would be found for uncracked concrete.

In view of this serious effect of cracking, Hageman noted: 'This unfavourable influence of cracks on the initiation time leads up to the practical conclusion, that in those zones where lifetime is determined by the initiation time, design, construction and maintenance must be such that:

- the probability of cracking remains within acceptable limits (design)
- any initial cracks and other imperfections are repaired (construction phase)
- any cracks and remaining imperfections which will be repaired afterwards will also be repaired in time (maintenance)'

Regarding the propagation time, $t_p$, the influence of oxygen transport through the concrete cover on the corrosion rate was explicitly taken into account. Based on available literature, in particular Schiessl (1976) and Tödt (1955), a modified diffusion equation for oxygen transport was derived. For the submerged zone, the oxygen concentration at the concrete surface was taken as $C_o = 0.13 \times 10^{-4}$ g/cm$^3$, and the oxygen diffusion coefficient as $D_b = 100$ cm$^2$/year (equal to $0.32 \times 10^{-9}$ m$^2$/s); for both the tidal and the splash zones, $C_o = 3 \times 10^{-4}$ g/cm$^3$ and $D_b = 3000$ cm$^2$/year

(equal to $9.5 \times 10^{-9}$ m$^2$/s) were used as input values. Eventually, for an anticipated cover depth of 70 mm, this calculation exercise resulted in a predicted corrosion rate $k_s \approx 91.7$ μm/year for the splash zone, $k_s \approx 18.5$ μm/year for the tidal zone, and $k_s \approx 0.8$ μm/year for the submerged zone; see Fig. 12.6.

Finally, for both the splash and tidal zone, $k_s = 100$ μm/year, and for the submerged zone, $k_s = 1$ μm/year was adopted.

The loss of strength of a corroded reinforcing bar is expressed − also in the case of pitting corrosion − in terms of a mean (fictitious) reduction $\Delta_s$ of the bar radius at which disintegration of the concrete cover is assumed to occur. Based on data provided by Tuutti (1982) for loss of steel by corrosion as a function of the ratio between cover depth and rebar diameter, $c/Ø$, the acceptable degree of reinforcement corrosion in the piers of the storm surge barrier with $c/Ø$ in the range 3−4, was in a more-or-less arbitrary way fixed at $\Delta_s = 200-300$ μm. However, it was also noted that quite often in practice, situations have been observed without visible damage of the concrete cover for $\Delta_s$ exceeding 200−300 μm.

In Fig. 12.7, the results of this 'arithmetical approach' are presented according to the conceptual model by Tuutti for the splash/tidal and submerged zone with a distinction between cracked and uncracked concrete.

According to the predictions, the propagation stage is very short (approximately 2 years; see Fig. 12.7) for both the splash and tidal zones, and consequently the lifetime will, to a great extent, be determined by the initiation time. In contrast, for the submerged zone the length of the initiation stage is limited, and thus the predicted propagation time, which is very extended, will provide the largest contribution, eventually resulting in a lifetime in excess of 200 years. However, it should be noted that

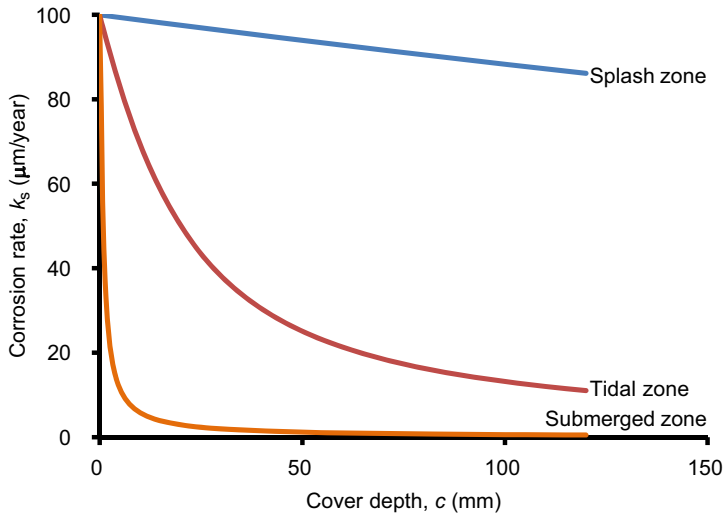



**Figure 12.6** Predicted corrosion rates (after depassivation) as a function of cover depth (deterministic approach) for the Eastern Scheldt concrete structures with a distinction between submerged, tidal, and splash zone.

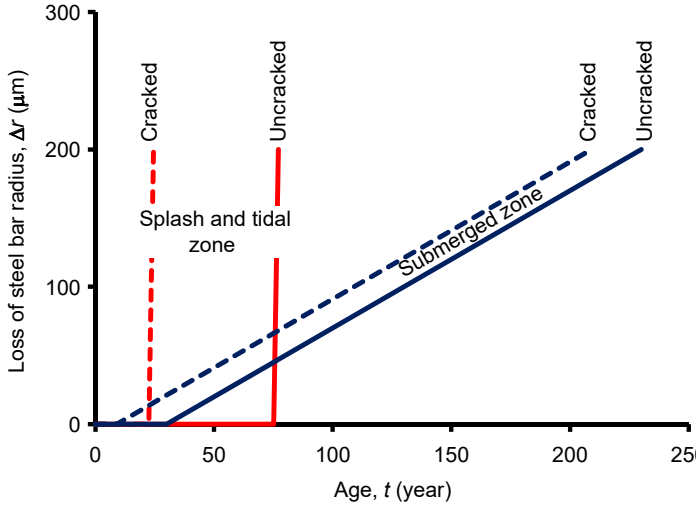



**Figure 12.7** Initiation and propagation stage of reinforcement corrosion according to the arithmetical approach adopted for the Eastern Scheldt Storm Surge Barrier (Hageman, 1982).

for the durability design of the Eastern Scheldt Storm Surge Barrier, neither short- nor long-term experimental investigations into transport properties of concrete were performed to validate the input values used in the model or to optimise mix proportions and cover depth.

With respect to management and maintenance of the barrier, it was recommended that in the splash and to a lesser extent in the tidal zones, once damage was observed, action should be taken very quickly, in view of the predicted high corrosion rate and consequently the rapid development of damage. This would be advantageous in order to consider and apply 'simple' repair options. Therefore the limiting value of $\Delta_s$ could also be considered as a 'warning limit', which is of importance to plan proper maintenance. As already remarked, the structure would not always give visible 'warnings'.

Sixty-five very large piers form the backbone of the Eastern Scheldt Storm Surge Barrier; see Fig. 12.8. The height of these piers varies from 30 to 40 m, and the overall weight amounts to approximately 18,000 tons. The actual height depends on the position of a pier in the tidal channel, with the largest height for the deepest parts of the channel. A special production unit was developed for the concrete, and it took nearly 1.5 years to produce a single pier. In view of the necessity to prevent premature cracking, all piers were prestressed, and the concrete was actively cooled with cooling tubes during casting. In addition, the risk of cracking was further minimised by the use of concrete with blast furnace slag cement, resulting in slower hydration and thus a lower rate of hydration heat. Each pier was cast in several phases (or lifts). The concrete composition of each phase contained 350 kg/m$^3$ CEM III/B, and $w/c = 0.45$.

The precast upper beams were also prestressed, and they employed gravel aggregate concrete (325 kg/m$^3$ CEM III/B, $w/c = 0.45$). For the bridge elements located on top of the barrier, gravel aggregate concrete was also used, with 325 kg/m$^3$ CEM



**Figure 12.8** View showing the piers under construction.

III/B and $w/c = 0.44$, except for the sections at the abutments where low-density concrete was used with expanded clay as lightweight aggregate (400 kg/m$^3$ CEM III/B, $w/c = 0.38$). Low-density concrete was chosen in view of the very high span of about 75 m at the abutments, as well as for practical reasons regarding transport and assemblage of the precast bridge elements on site.

### 12.3.3 Condition assessment and survey

In practice, it is common that in-depth investigations are executed only when visible damage has been observed. In line with this approach, it is rather unusual to determine chloride profiles and even more unusual to perform potential mapping when there is no evidence of emerging problems regarding reinforcement corrosion.

In view of the function of the Eastern Scheldt barrier, the owner of the barrier structure considered that having advanced reliable information on the development of the actual performance over time was of vital importance to plan for timely and adequate maintenance activities. For structures exposed to a marine environment, reinforcement corrosion induced by penetrating chloride is considered the major threat, and thus the availability of reliable quantitative information on chloride ingress was considered

essential for assessment of its current condition, as well as for predicting the onset of reinforcement corrosion. Since the barrier came into operation in 1986, chloride profiles have been obtained within the monitoring program in 1989 and again in 1994. However, the number of chloride profiles obtained in these early condition assessments was very limited; moreover, the exposure period was too short to draw reliable conclusions on future developments.

In 2002 (ie, 16 years after the official opening), large-scale investigations were performed on site by retrieving a large number of concrete cores from a selected pier and upper beam, and from 17 bridge elements (de Rooij and Polder, 2002). Since nowhere on the concrete surface was there any visual evidence of reinforcement corrosion or any other deterioration mechanism observed, the locations for drilling were rather based on geometrical and practical considerations, in particular easy accessibility. Also, concrete cover measurements were performed at the test areas since no information on the achieved cover depths was available. For a reliable assessment of the current condition and prediction of onset of corrosion, as-built information is preferred rather than to rely on information provided on design drawings.

On site, each test area of about 1 $m^2$ of concrete surface was investigated in more detail through the following:

- visual examination and description of the test area
- measurement of rebar position and depth
- determination of carbonation depth
- measurement of concrete resistivity (Wenner Probe)
- measurement of rebar potential

Also, per test area, various core samples were taken for further investigation in the laboratory, involving chloride profiling, microscopy, rapid chloride migration testing, resistivity measurements, splitting tensile tests, and compressive strength tests.

### *12.3.3.1 Evaluation of measured chloride profiles*

To obtain quantitative information on chloride ingress resulting from exposure to the marine environment, concrete cores of 50-mm diameter were drilled from a test area on one of the piers and one of the upper beams. All chloride profiles were determined in depth increments of 10 mm, by cutting each concrete core into six slices, each having a net thickness of 8 mm. The chloride content was expressed as a percentage (%) by mass of cement. It should be noted that all material in a concrete sample that was soluble in nitric acid was considered to be cement. This includes the entire cement content including the blast furnace slag component. This is a fair assumption since the aggregate used for the concrete elements of the storm surge barrier was a river gravel that was known to be chemically inert.

Fig. 12.9 shows the chloride profiles obtained from a test area on the front face of the upper beam, predominantly exposed to splashing, comprising a concrete surface of $0.5 \times 1.5$ m. After an exposure period of 18 years (taking into account that the concrete elements were placed in the service environment approximately 2 years prior to the official opening in 1986), the overall chloride penetration depth amounts to

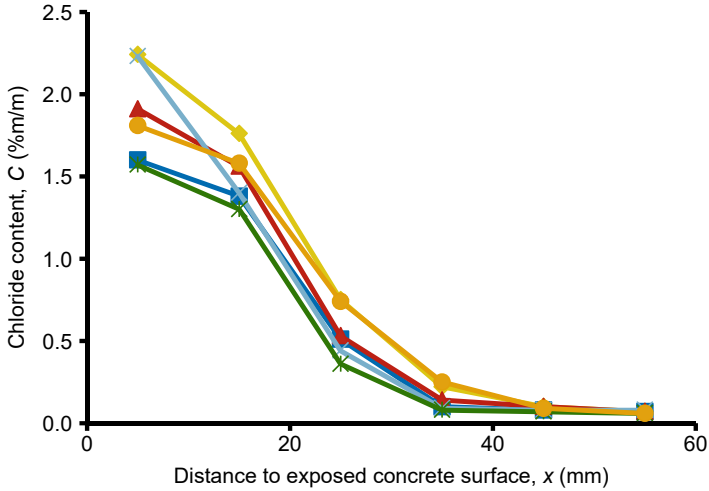



**Figure 12.9** Measured total chloride profiles obtained for upper beam Hammen 8 after an exposure period of 18 years (splash zone).

approximately 40 mm. Moreover, from the chloride content measured at a depth >40 mm, it is clear that the initial chloride content, $C_i$, is negligible, which is according to expectations.

The six chloride profiles demonstrate relatively small differences in chloride ingress. As the achieved cover depth in the test area of upper beam Hammen 8 ranges from 48 to 68 mm, it is concluded that the reinforcing steel is still in a passive condition.

In contrast, the chloride profiles determined for the tidal zone of pier Hammen 8 demonstrate significantly higher scatter; see Fig. 12.10. In addition, the chloride contents in the near-surface zone in the pier are much lower than those measured in upper beam Hammen 8, and the chloride contents appear to remain roughly constant up to a depth of approximately 15 mm. As the achieved cover depth in the test area of pier Hammen 8 ranges from 52 to 60 mm, it is concluded that the reinforcing steel is still in a passive condition. However, the achieved cover depth appears to be significantly less than the deterministic value used in the arithmetical approach.

Although the concrete quality of the Eastern Scheldt bridge elements is considered to be quite homogeneous (precast concrete) and the test locations are geometrically similar (at approximately halfway up the height of the wall) and thus experience similar exposure conditions (spray zone), the measured chloride profiles show a considerable scatter in Fig. 12.10. This is not only reflected in the level of the surface chloride content, $C_s$, but also in the magnitude of the apparent diffusion coefficient, $D_a$.

As a comparison, in Fig. 12.11 a number of chloride profiles are given for concrete exposed in the tidal zone during 42 years in Pier 11 of the Haringvliet dam. A distinct difference to the chloride profiles obtained for pier Hammen 8 (18 years of exposure) is observed, although the exposure conditions are similar, and both concretes are based

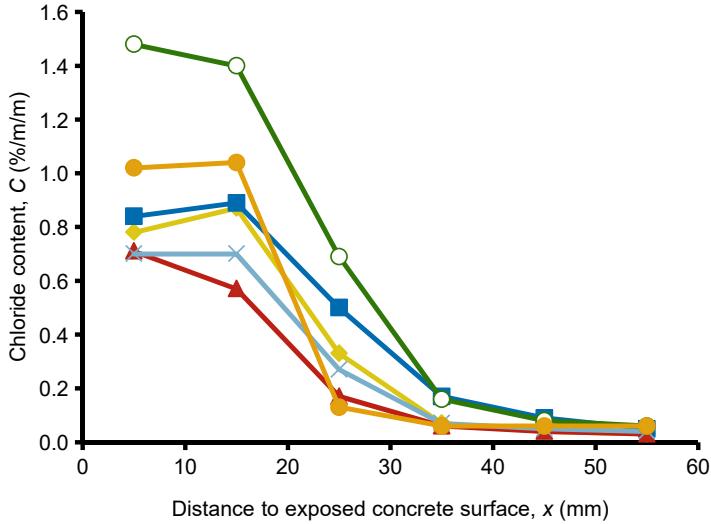



**Figure 12.10** Measured chloride profiles obtained for pier Hammen 8 after an exposure period of 18 years (tidal zone).

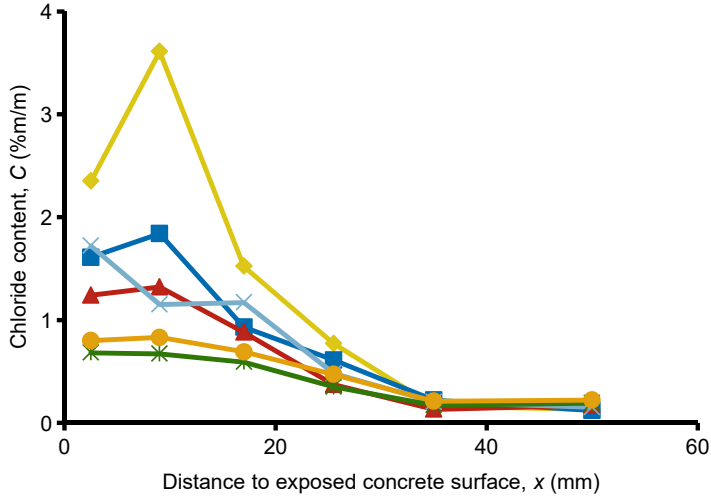



**Figure 12.11** Measured chloride profiles obtained for pier 11 in the Haringvliet dam after an exposure period of 42 years (tidal zone).

on slag cement. It has been argued that for the piers of the Haringvliet a less-reactive slag cement was used due to coarser grains, resulting in a slower but still continuing hydration even after several decades. The Haringvliet dam was built in 1960–62 (ie, approximately 20 years before construction of the Eastern Scheldt Storm Surge Barrier started). Based on records made available by the producer of the blast furnace

slag cement, a comparison could be made between the characteristics of the cement used for the Haringvliet dam and the cement for the Eastern Scheldt barrier. This comparison highlighted a significant increase of fineness in the course of time. The slower reactivity demonstrated by the cement at the Haringvliet dam is considered to have a beneficial effect on the development of resistance against chloride ingress over time.

With respect to the exposure conditions, the cantilever of the Eastern Scheldt box girder bridge effectively results in concrete surfaces being sheltered from direct contact with rain; see Fig. 12.12. Moreover, the steel sliding gates in front of the bridge elements will prevent the concrete surfaces from being directly exposed to rain or splash. These exposure conditions will promote the occurrence of long drying periods. Only on rare occasions when the steel sliding gates are lowered, will the concrete surfaces of the bridge elements be exposed to severe splashing, but then only for short periods of time. On average, this exposure to splashing will occur only a few days each year. According to this reasoning, it is likely that during the short splashing period capillary suction will be the prevalent mode of chloride transport, followed in the long period thereafter by redistribution of the absorbed seawater including the dissolved chlorides to deeper levels in the cover zone.

The occurrence of long dry periods would also suggest that carbonation would have advanced more deeply, particularly taking into account the use of blast furnace

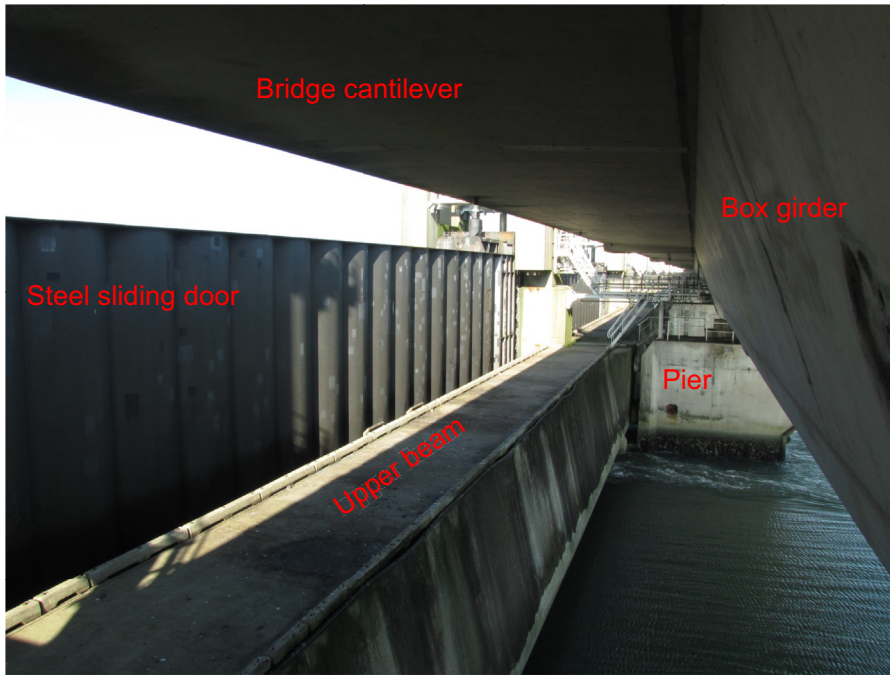



**Figure 12.12** Exposure conditions prevailing at the bridge sections: concrete surfaces are sheltered from direct rain through the cantilever and from direct splash through the sliding gate.

slag cement. However, the carbonation depths measured after 18 years of exposure were less than 12 mm. Thus, carbonation is not considered a major threat to the structures.

Overall, after 18 years of exposure, chlorides have locally penetrated to the level of the reinforcing steel at such levels that initiation of reinforcement corrosion is considered probable. On the positive side, in all samples the measured concrete resistivity exceeds 350 Ω m (35 kΩ cm), even under water-saturated conditions. According to (Broomfield. 1997), this corresponds to low corrosion rates, provided the steel has become depassivated.

## 12.4 Conclusions

From the case study of the Eastern Scheldt Storm Surge Barrier in the Netherlands presented in this chapter, a number of interesting facts emerge – indicating the great value in post-construction investigations of structures to draw lessons from their performance.

1. Among other aspects, chloride ingress into concrete exposed to a marine environment exhibits a wide variability, both on micro and macro scales of observation. This implies that for a sound and reliable condition assessment and service life prediction, a significant number of concrete samples should be retrieved preferably at three subsequent points in time, the first investigation at an age between 10 and 15 years, and using a time interval of 10–20 years. Unfortunately, many asset owners seem not to be aware of this, or to consider the costs involved in such investigations to be unreasonable.
2. The field investigations performed on the marine structures in the Delta Project have shown that for these structures, chloride ingress remains limited even after a reasonable period of time, predominantly due to the consistent use of blast furnace slag cement, adequate measures to limit surface cracking, proper quality control during construction, and adequate curing.

For the Eastern Scheldt Storm Surge Barrier, the next condition assessment will be performed in 2016, and for the Haringvliet dam, investigations are scheduled for 2017. At this stage, it is not anticipated that the Dutch sea defence structures will be in need of repairs within a time period of the next 40 years.

## References

Beeby, A.W., 1978. Cracking and Corrosion, Concrete in the Oceans. Technical Report No. 1. CIRIA/UEG, Cement and Concrete Association, Department of Energy.

Bijen, J., 1996. Blast Furnace Slag Cement for Durable Marine Structures. Stichting Betonprisma, 's-Hertogenbosch, ISBN 90-71806-24-3.

Broomfield, J.P., 1997. Corrosion of Steel in Concrete – Understanding, Investigation and Repair, first ed. E & FN Spon, ISBN 0-419-19630-7.

Collepardi, M., Marcialis, A., Turriziani, R., 1970. The kinetics of penetration of chloride ions into the concrete. Il Cemento 67 (4), 157–164.

Hageman, J.G., June 1982. The Lifetime of the Eastern Scheldt Barrier − an Arithmetical Approach of the Corrosion Process in Reinforced Concrete. Report No 1337-1-0.

ROK, 2015. Richtlijnen Ontwerp Kunstwerken (Guidelines for the Design of Infrastructure Facilities). Rijkswaterstaat, Utrecht (in Dutch).

de Rooij, M., Polder, R.B., 2002. Appendices − investigation of the influence of different marine exposure zones on concrete parts of the Eastern Scheldt Storm Surge Barrier. In: TNO Report 2002-CI-R2118-1A, Delft, 30 July, 2002.

Schiessl, P., 1976. Zur Frage der zulässigen Rissbreite und der erforderlichen Betondeckung im Stahlbetonbau unter besonderer Berücksichtigung der Karbonatisierung des Betons. Deutscher Ausschuss für Stahlbeton, Berlin. Heft 255.

Tödt, F., 1955. Korrosion und Korrosionsschutz. Walter de Gruyter u. Co. Verlag.

Tuutti, 1982. Corrosion of Steel in Concrete. Swedish Cement and Concrete Research Institute, Royal Institute of Technology, Stockholm. ISSN: 0346−6906, Department of Building Materials.

VB'74, 1974. Voorschriften Beton (Code for Concrete Structures). Nederlands Normalisatie Instituut, Delft (in Dutch).

# Hong Kong–Zhuhai–Macau sea link project, China

13

*K. Li* [1], *Q. Li* [1], *Z. Fan* [2]
[1]Tsinghua University, Beijing, China; [2]CCCC 4th Harbor Research Institute, Guangzhou, China

This chapter introduces the mega-project on the southeastern coast of China, the Hong Kong–Zhuhai–Macau (HZM) sea link project. The first part of chapter details the general layout of the project, the main technical requirements, as well as the service conditions, highlighting the technical challenges in the project. Then, to meet the design working life of 120 years, the durability design of the concrete structures is described in terms of the overall philosophy, procedure and methods. Thereafter, the chapter provides the quality control procedures for durability in the construction phase, and a comprehensive model-based durability assessment is performed for the concrete structures on the basis of the data collected during the construction phase. Finally, the strategy of life-cycle management is elaborated for concrete structures through durability inspection/monitoring, maintenance planning, and durability assessment and redesigning.

## 13.1 Introduction to HZM project

The HZM project links the cities of Zhuhai and Macau on the southeastern coast of the China mainland with the city of Hong Kong across the water region of Ling'ding Ocean. The total length of the project is close to 36 km, consisting of sea bridges of 28.8 km, two offshore artificial islands, and an immersed tube tunnel of 6.8 km, with a total investment over 12 billion US dollars. The traffic capacity is dual three lanes with a design speed of 100 km/h. The design working life of the whole project is 120 years (HZMBA, 2010). The preliminary study of the project occurred from 2008 to 2010, the detailed study phase started from 2010, and the construction works are expected to end in 2017. The general view of the HZM project is given in Fig. 13.1.

The sea bridges consist of four navigable spans (Jiuzhou span 298 m, Jianghai express span 258 m, Qingzhou span 458 m and Hong Kong side span 150 m) and non-navigable spans of 28.8 km. The structures for the three navigable spans of Jiuzhou, Jianghai express and Qingzhou are cable-stayed bridges, while the Hong Kong side span adopts a continuous beam structure. These spans are connected by 110-m non-navigable spans of continuous steel box girders, cf. Fig. 13.2. Except for the pylons and auxiliary piers in the navigable spans, all the piers and the bearing

**Marine Concrete Structures.** http://dx.doi.org/10.1016/B978-0-08-100081-6.00013-1
Copyright © 2016 Elsevier Ltd. All rights reserved.

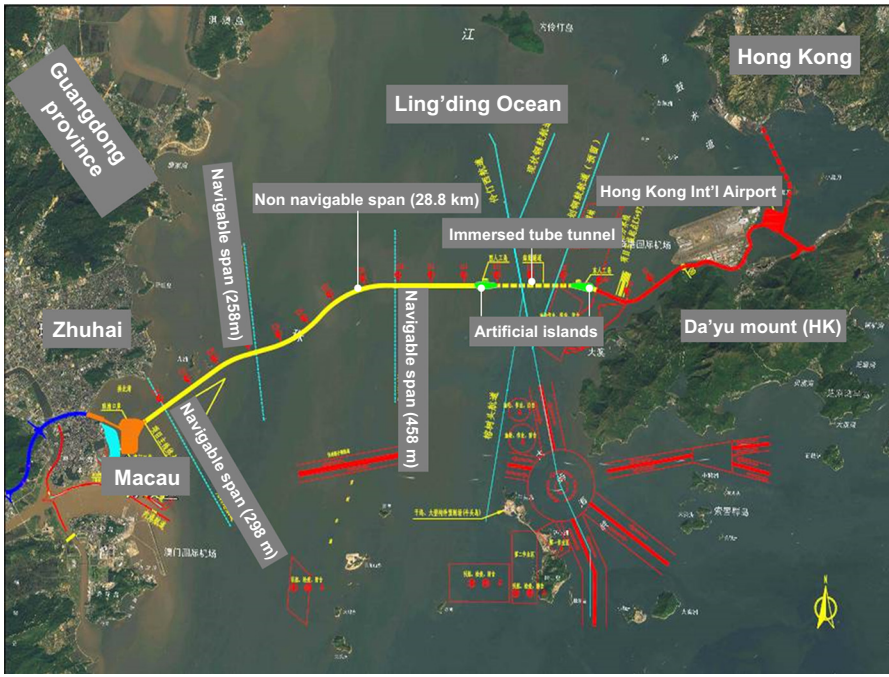



**Figure 13.1** General overview of Hong Kong−Zhuhai−Macau sea link project. Courtesy of HZM Bridge Administration.



**Figure 13.2** Non-navigable bridge spans during construction. Courtesy of the HZM Bridge Administration.



**Figure 13.3** Segments of immersed tunnel tube in prefabrication and in floating transport sequence.
Courtesy of the HZM Bridge Administration.

platforms of the sea bridges are prefabricated in segments and assembled in place. The immersed tube tunnel is made of concrete, constructed on the sea bed with a water depth of 40 m, and consists of four in-place segments (112.5 m each) and 27 prefabricated segments (180 m each). The cross-sectional dimension of the tunnel tube is $38 \times 11.4$ m with wall thickness of 1.5 m, accommodating two traffic directions with three lanes in each direction. The prefabricated segments of the immersed tunnel are made in a factory near the project site and transported to their final position site by the floating −sinking method, cf. Fig. 13.3. Once positioned on the sea bed, the tunnel segments are connected by flexible waterproof joints. Two offshore artificial islands are constructed serving as the connections between the sea bridges and the immersed tunnel. The area of artificial islands is nearly 200,000 $m^2$, constructed with the help of cofferdams made from sand-filled steel tubes; see Fig. 13.4. The structural elements of the HZM project are given in Table 13.1 together with the constituent materials and related construction methods.

The HZM project is exposed to a subtropical marine monsoon climate. The annual average temperature is 22.3−23.1°C with the highest and lowest recorded temperatures as 38.9°C and −1.8°C. The annual average humidity is 77−80% with large seasonal variation. The predominant wind directions are east and southeast, with recorded annual average wind speeds of 3.1 m/s (Zhuhai site), 3.6 m/s (Macau site) and 6.6 m/s (HK site). The highest values of the seawater salinity (TDS) are 32.9 g/L for the eastern part and 25.4 g/L for the western part on the bottom of sea bed; the lowest values of salinity are 8.1 g/L and 10.4 g/L for the eastern and western regions on the surface of seawater. The concentration of chloride ions ($Cl^-$) in the seawater is between 10,700 and 17,020 mg/L and the sulphate ions $\left(SO_4^{2-}\right)$ between 1140 and



**Figure 13.4** Artificial island under construction.
Courtesy of the HZM Bridge Administration.

2260 mg/L. The pH of the seawater is between 6.65 and 8.63. The highest astronomic tide is retained as 3.52 m and lowest astronomic tide is −1.32 m; the effective wave amplitude $H_{1/3}$ is retained as 3.92 m for a return period of 100 years. On the basis of these data, the exposure zones are evaluated for unsheltered conditions as atmospheric zone (>+6.26 m), splash zone (+6.26 to −0.40 m), tidal zone (−0.40 to −2.10 m) and immersed zone (<−2.10 m).

There exist multiple technical challenges in this mega-project, including the control of the foundation sediment for the immersed tube tunnel during construction, anti-seismic design of the long immersed tube tunnel, high-performance and water-tightness requirements for the segment joints for a 120-year service life, massive production of the prefabricated steel/concrete elements and their assembly in marine conditions, the connection of piles and prefabricated bearing platforms in a seawater environment, durability design for a 120-year service life for the concrete and steel structures, and life-cycle and cost-efficient management of the project during its service life. A major Chinese national scientific and technology research program (No. 2011BAG07B04) was set up in 2011 to respond to these challenges and to provide the scientific and technical support for the project. One of these technical challenges was to ensure the service life of 120 years for the concrete structures in an aggressive marine environment. The following parts of this chapter focus on the approaches and measures taken to ensure the service life of 120 years for the concrete structures, covering the durability design, quality control in construction, durability assessment and life-cycle management of concrete structures.

**Table 13.1 Constitutive elements of concrete structures in the HZM project**

| Structure | Element | Material | Function | Construction |
|---|---|---|---|---|
| Cable-stayed bridges (navigable spans) | Integral pylon | RC (base)/steel (upper part) | Principal | Cast in place (RC)/prefabricated (steel) |
| | Cable | High-strength steel | Principal | Prefabricated |
| | Box girder | RC (deck)/steel (box girder) | Principal | Cast in place (RC)/prefabricated (steel) |
| | Pier (auxiliary) | RC | Principal | Cast in place |
| | Bearing platform | RC | Principal | Cast in place |
| | Pile | Steel tube/concrete | Principal | Cast in place (concrete)/driven pile (steel tube) |
| Steel box girder bridges (non-navigable) | Box girder | Steel (in sea) | Principal | Prefabricated |
| | | PC (approach to artificial islands) | Principal | Cast in place (PC) |
| | Pier | RC | Principal | Cast in place (upper)/prefabrication (base) |
| | Bearing platform | RC | Principal | Prefabrication (with base part of pier) |
| | Pile | Steel tube/concrete | Principal | Cast in place (concrete)/driven pile (steel tube) |
| Immersed tube tunnel | Tube segment | RC (in sea) | Principal | Prefabricated |
| | | RC (approach to artificial islands) | Principal | Cast in place |
| | Anti-shock pier | RC | Secondary | Prefabricated |
| | Segment joint | Rubber | Principal | Prefabricated |
| | Pile | Compacted sand | Principal | Bored hole, cast in place |
| Artificial islands | Retaining wall | Concrete | Principal | Cast in place |
| | Breakwater | Concrete | Principal | Prefabrication |
| | Facilities | RC/steel | Secondary | Cast in place (RC)/prefabrication (steel) |

*RC*, reinforced concrete; *PC*, prestressed concrete.
Li, K.F., Li, Q.W., Zhou, X.G., Fan, Z.H., 2015a. Durability design of Hong Kong–Zhuhai–Macau sea-link project: principle and procedure. Journal of Bridge Engineering, ASCE, 1–11, 04015001, Table 1, Reproduced by permission of ASCE.

## 13.2 Durability design: philosophy and procedure

### 13.2.1 Design philosophy

For the concrete structures exposed to the marine environments of the project site, the possible deterioration mechanisms include the carbonation-induced corrosion of reinforcing steel by $CO_2$ in the atmosphere, chloride-induced corrosion of reinforcing steel by chloride in the seawater, and physical and chemical attack on concrete by salts $\left(SO_4^{2-}, Mg^{2+}\right)$ in seawater and soils. Moreover, internal expansive reactions in structural concrete, such as alkali−aggregate reaction and delayed ettringite formation (DEF), should be avoided given the crucial function of the concrete elements.

The global philosophy of durability design with respect to these deterioration processes was to formulate the requirements at both the material and structural levels, combining the material design with the structural design to achieve a working life of 120 years. Table 13.2 gives the requirements, divided into material and structural levels. For the raw materials of the structural concretes, the mass ratio of calcium aluminates ($C_3A$) in cement was controlled to 5−8%; the $SO_3$ content was controlled to below 4% of binder; the aggregates were required to be non-alkali-reactive, and the alkali content of the concrete was controlled to below 3 kg/m$^3$. By these specifications, the risks of chemical salt attack and internal expansive reactions were regarded as being sufficiently low to be exempted from direct durability design. Accordingly, the carbonation-induced corrosion and chloride-induced corrosion remain as the most critical processes for durability design.

The design working life of the whole project is 120 years. Aiming at this target, the durability design at the structural level was to first determine the working lives for structural elements on the basis of their structural importance and technical feasibility. The principal elements adopted the same working life as the whole project, 120 years, and the secondary or replaceable elements could adopt shorter lives. For these elements, the maintenance and replacement schemes were to be specified in the design phase. Durability limits states (DLS) are needed for quantitative durability design (ISO, 2008). These states are specified as the minimum acceptable performance levels for different durability processes (Li et al., 2008). For carbonation-induced and chloride-induced corrosion processes, two DLS can be defined: (a) corrosion initiation and (b) corrosion to an acceptable extent. In the project, PC elements, principal RC elements, and RC elements with high maintenance difficulty adopted the DLS (a) while secondary RC elements adopted the DLS (b).

### 13.2.2 Design for durability

The model-based method was used to determine the design parameters in Table 13.2 for chloride-induced corrosion and carbonation-induced corrosion, including the concrete cover quality (diffusivity, carbonation resistance), concrete cover thickness and the allowable crack opening. The concrete cover quality and thickness were designed using the durability models with the target service lives and DLS. In this phase, the concrete elements were assumed to be exposed directly to aggressive agents

**Table 13.2 Requirements for durability of concrete structures in the HZM project**

| Requirements | | Carbonation-induced corrosion | Chloride-induced corrosion | Salt attack | | Internal expansion reaction | |
|---|---|---|---|---|---|---|---|
| | | | | Physical | Chemical | AAR | DEF |
| Material level | *w/b* ratio | √ | √ | √ | √ | √ | √ |
| | Binder type | | √ | | √ | √ | √ |
| | Binder content | √ | √ | √ | √ | √ | √ |
| | $Cl^-$ content | | √ | | | | |
| | $C_3A$ content | | | | √ | | √ |
| | $SO_3$ content | | | | √ | | √ |
| | Alkali content | | | | | √ | |
| | Alkali reactivity | | | | | √ | |
| Structural level | Cover quality | √ | √ | √ | √ | | |
| | Cover thickness | √ | √ | √ | √ | | |
| | Crack control | √ | √ | √ | √ | | |

Li, K.F., Li, Q.W., Zhou, X.G., Fan, Z.H., 2015a. Durability design of Hong Kong−Zhuhai−Macau sea-link project: principle and procedure. Journal of Bridge Engineering, ASCE, 1−11, 04015001, Table 4, Reproduced by permission of ASCE.

($CO_2$, $Cl^-$) and the surface protection measures were to be taken into account later. The design procedure follows a partial factor format with a target reliability index $\beta = 1.3$ (fib, 2006) to constitute a first basic requirement for concrete cover quality.

### 13.2.2.1 Chloride ingress

The design model for chloride-induced corrosion was adapted from the widely used analytical model of Fick's second law (DuraCrete, 1998; fib, 2006). With the DLS specified as the corrosion initiation (ie, DLS (a)), the design equation in partial factor format is written as follows:

$$G_1 = \frac{C_{cr}}{\gamma_c} - \gamma_s C_s \left[ 1 - \mathrm{erf}\left( \frac{x_d^{nom} - \Delta x_d}{2\sqrt{(\gamma_D D_{Cl}^0)\cdot(\gamma_\eta \eta)\cdot t_{SL}}} \right) \right] \geq 0 \qquad [13.1]$$

where $C_{cr,s}$ = threshold chloride concentration for steel corrosion and concrete surface chloride concentration (% binder), respectively; $x_d^{nom}$ and $\Delta x_d$ = concrete cover nominal thickness and its construction error (m); $D_{Cl}^0$ = chloride diffusivity of concrete at a given age ($m^2/s$); $\eta$ = ageing factor of concrete chloride diffusivity (−); $t_{SL}$ = design service life of structural elements; erf = mathematical error function. The terms $\gamma_{c,s,D,\eta}$ are the partial factors for the corresponding parameters. The ageing factor $\eta$ describes the gradual decrease of concrete chloride diffusivity with time:

$$\eta(t_0, t) = D_{Cl}(t)/D_{Cl}^0 = \left(\frac{t_0}{t}\right)^n \quad \text{with } \eta(t_0, t > 30 \text{ years}) = \eta(t_0, t = 30 \text{ years}) \qquad [13.2]$$

where $n$ = exponential coefficient for the ageing law, and $D_{Cl}^0$ = concrete diffusivity at age $t_0$. The mechanisms for this decrease can be concrete densification due to long-term hydration of binders (Andrade et al., 2011) and/or the interaction between the chloride ions and the solid matrix of concrete. Since it is not rational to assume these processes can develop indefinitely, this decrease law was truncated at $t = 30$ years to ensure a conservative design.

To apply this design model, the characteristic values for the parameters and their corresponding partial factors should be determined for the concrete structures. For this purpose, the statistical properties were regressed for the design parameters, $C_{cr}$, $C_s$, $x_d$, $D_{Cl}^0$ and $n$, from long-term exposure tests on a similar exposure site (Zhanjiang Exposure Station) and structural inspections during the last 30 years in the same region of project. The statistical properties and the regression details were reported in Li et al. (2015a,b). On the basis of the obtained statistical properties, the partial factors and characteristic values for the design parameters were calibrated using a fully probabilistic scheme for a target reliability index of $\beta = 1.3$

**Table 13.3 Design parameters for chloride ingress of concrete elements in the HZM project (design life $t_{SL} = 50$, 120 years, $\beta = 1.3$)**

| Parameter | | Immersed zone | Tidal zone | Splash zone | Atmospheric zone |
|---|---|---|---|---|---|
| $C_{cr}$ (%binder) | Characteristic value | 2.0 | 0.75 | 0.75 | 0.85 |
| | Partial factor $\gamma_c$ | 2.0 | 1.7 | 1.7 | 1.1 |
| $C_s$ (%binder) | Characteristic value | 4.50 | 3.82 | 5.44 | 1.98 |
| | Partial factor $\gamma_s$ | 1.05 | 1.05 | 1.05 | 1.1 |
| $D_{Cl}$ ($10^{-12}$ m$^2$/s) | Characteristic value | 3.0 | 3.0 | 3.0 | 3.0 |
| | Partial factor $\gamma_D$ | 1.05 | 1.1 | 1.1 | 1.1 |
| Ageing coefficient $\eta$ (−) | Characteristic value | 0.074 | 0.067 | 0.061 | 0.047 |
| | Partial factor $\gamma_\eta$ | 1.05 | 1.05 | 1.05 | 1.35 |
| Cover $x_d$ (mm) | Nominal value $x_d^{nom}$ | 60 | 80 | 80 | 50 |
| | Construction error $\Delta x_d$ | 10 | 10 | 10 | 10 |

Li, K.F., Li, Q.W., Zhou, X.G., Fan, Z.H., 2015a. Durability design of Hong Kong−Zhuhai−Macau sea-link project: principle and procedure. Journal of Bridge Engineering, ASCE, 1−11, 04015001, Table 6, Reproduced by permission of ASCE.

(Li et al., 2015b); see Table 13.3. Following the custom of structural design, the cover thickness was not calibrated as a characteristic value with its partial factor, but specified as its minimum requirement $x_d^{min}$ and its nominal value $x_d^{nom}$, with the difference $\Delta x_d$ as the construction error.

The design procedure takes the characteristic value of chloride diffusion coefficient $D_{Cl}^0$ and nominal value of concrete cover $x_d^{nom}$ as design parameters. Using Eq. [13.1], the characteristic values of these two parameters are calculated for the concrete elements in the immersed, tidal, splash and atmospheric zones. For the quality control purpose, the diffusion coefficients are calculated for both 28-days values ($t_0 = 28$ days) and 56-days values ($t_0 = 56$ days) in Fig. 13.5: for cover thickness range of 75−85 mm, the design ranges for $D_{Cl}^0$ are, respectively, $2.5{-}3.3 \times 10^{-12}$ m$^2$/s (28 days) and $1.8{-}2.4 \times 10^{-12}$ m$^2$/s (56 days) for RC elements in splash zones for 120 years.

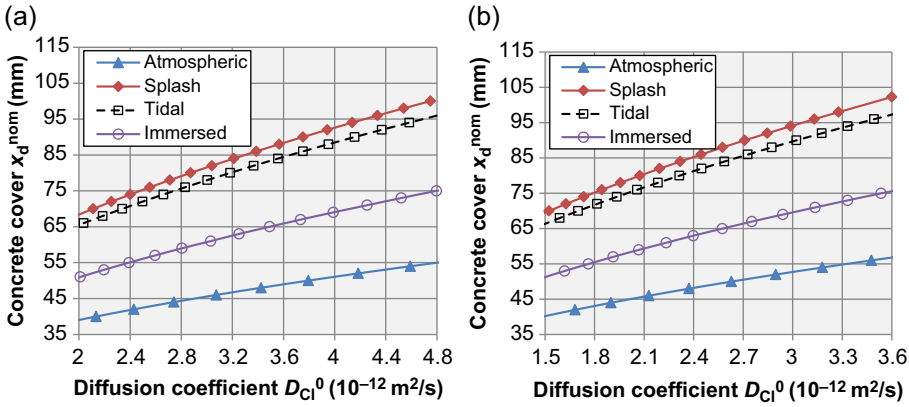



**Figure 13.5** Design results for chloride diffusivity and concrete cover thickness in terms of (a) 28-days values and (b) 56-days values for $\beta = 1.3$ and $t_{SL} = 120$ years.
Li, K.F., Li, Q.W., Zhou, X.G., Fan, Z.H., 2015a. Durability design of Hong Kong−Zhuhai−Macau sea-link project: principle and procedure. Journal of Bridge Engineering, ASCE, 1−11, 04015001, Figure 3, Reproduced by permission of ASCE.

### *13.2.2.2 Carbonation*

The carbonation model is an extended form of the widely used square root of time law for carbonation depth $x_c$ (DuraCrete, 1998; fib, 2006), and the design equation is expressed in partial factor format as follows:

$$G_2 = x_d - x_c(t_{SL}) = x_d - W_t\sqrt{2k_e\left(\frac{h}{\gamma_{RH}}\right)k_c\left(k_t R_{ACC,0}^{-1}\gamma_R + \varepsilon_t\right)\cdot C_{CO_2}\cdot t_{SL}} \geq 0 \quad [13.3]$$

where $W_t$ = weather function expressing the influence of atmospheric precipitation on concrete carbonation process (−); $k_e$ = environmental factor of humidity with detailed expression in (fib, 2006) (−); $k_c$ = curing factor defining the influence of curing time during concrete hardening (−); $\left(k_t R_{ACC,0}^{-1} + \varepsilon_t\right)$ = carbonation resistance of concrete in natural environment; $R_{ACC,0}^{-1}$ = concrete carbonation resistance in accelerated test conditions (20°C, RH = 65%), in (mm²/year)/(kg/m³); $k_t$ = regression parameter between the two resistances; $\varepsilon_t$ = error term; $C_{Co_2}$ = $CO_2$ concentration in atmosphere (kg/m³) and $t_{SL}$ = design life (year). The terms $\gamma_{RH,R}$ are partial factors for relative humidity and concrete carbonation resistance. Eq. [13.3] takes the corrosion initiation as DLS. The calibration of these partial factors followed a fully probabilistic approach, and the calibrated factors in (fib, 2006) were directly used in the design.

The design value of cover thickness $x_d$ refers to $x_d^{nom} - \Delta x_d$. The statistical properties for the parameters needed for partial factor calibration can be found in (fib, 2006).

**Table 13.4 Design parameters for carbonation of concrete elements in the HZM project**

| Parameter | | $t_{SL}$ = 50 years | | $t_{SL}$ = 120 years | |
|---|---|---|---|---|---|
| | | Interior | Exterior | Interior | Exterior |
| Humidity $h$ (−) | Characteristic value | 77% | 85% | 77% | 85% |
| | Partial factor | 1.3 | 1.3 | 1.3 | 1.3 |
| Carbonation resistance $R_{ACC,0}^{-1}$ $(mm^2/a)/(kg/m^3)$ | Characteristic value | Design | Design | Design | Design |
| | Partial factor | 1.5 | 1.5 | 1.5 | 1.5 |
| Concrete cover $x_d$ (mm) | Nominal value $x_d^{nom}$ | Design | Design | Design | Design |
| | Construction error $\Delta x_d$ | 10 | 10 | 10 | 10 |
| Environmental factor $k_e$ (−) | Design value | 1.10 | 0.99 | 1.10 | 0.99 |
| Curing factor $k_c$ (−) | Design value (14 days) | 1.0 | 1.0 | 1.0 | 1.0 |
| Regression parameter $k_t$ (−) | Design value | 1.25 | 1.25 | 1.25 | 1.25 |
| Error term $\varepsilon_t$ $(mm^2/year)/(kg/m^3)$ | Design value | 315.5 | 315.5 | 315.5 | 315.5 |
| $CO_2$ concentration $C_{Co_2}$ $(10^{-4}\ kg/m^3)$ | Design value | 8.2 | 8.2 | 8.2, 32.8 | 8.2 |
| Weather function $W_t$ (−) | Design value | 1.0 | 0.523 | 1.0 | 0.479 |

Li, K.F., Li, Q.W., Zhou, X.G., Fan, Z.H., 2015a. Durability design of Hong Kong−Zhuhai−Macau sea-link project: principle and procedure. Journal of Bridge Engineering, ASCE, 1−11, 04015001, Table 7, Reproduced by permission of ASCE.

The calibrated partial factors and the retained model parameters are given in Table 13.4. Four representative cases are considered: interior surface and exterior surface of concrete elements for service lives of 50 years and 120 years. Compared to interior surfaces, exterior surfaces have elevated humidity and lower weather function due to rain exposure conditions. For $CO_2$ concentration, a high concentration of $32.8 \times 10^{-4}$ (ie, four times design value) is also retained to consider the possible $CO_2$ accumulation in the tunnel from automobile exhaust gases. The characteristic values of concrete cover thickness $x_d^{nom}$ and the carbonation resistance $R_{ACC,0}^{-1}$ are retained as design parameters, and the design results are presented in Fig. 13.6.

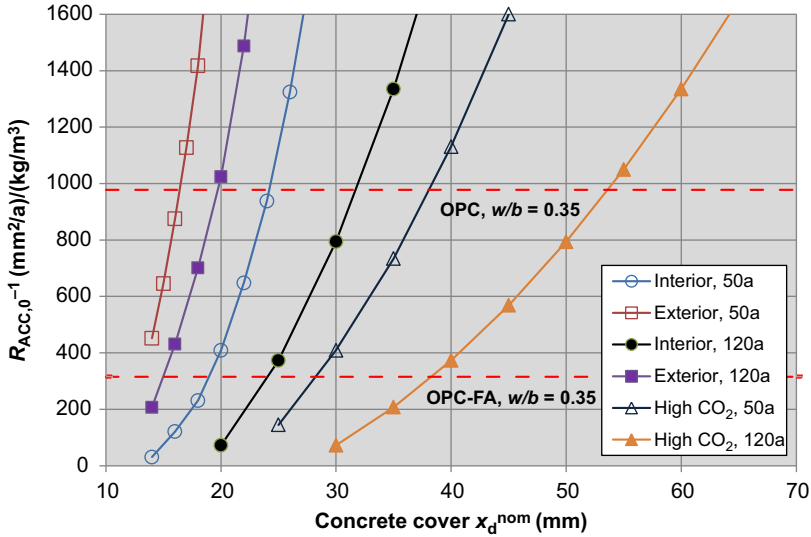



**Figure 13.6** Design results of concrete carbonation resistance and cover thickness for $\beta = 1.3$ and $t_{SL} = 50$, 120 years.
Li, K.F., Li, Q.W., Zhou, X.G., Fan, Z.H., 2015a. Durability design of Hong Kong−Zhuhai−Macau sea-link project: principle and procedure. Journal of Bridge Engineering, ASCE, 1−11, 04015001, Figure 4, Reproduced by permission of ASCE.

### *13.2.2.3 Durability requirements*

The preliminary concrete proportioning sets the water to binder ratio ($w/b$) at around 0.35 for structural concretes in the HZM project, and both fly ash and slag are used in the binder. In Fig. 13.6, two horizontal lines represent, respectively, OPC binder concrete and OPC-FA (ordinary Portland cement incorporating 20% fly ash) binder concrete with $w/b = 0.35$. Using the OPC line for structural concretes for bridge elements, the required cover thicknesses are 24 mm (interior, 50 years), 17 mm (exterior, 50 years), 32 mm (interior, 120 years) and 20 mm (exterior, 120 years). Knowing that the achievable $D_{Cl}^0$ values for structural concretes cannot be lower than $2 \times 10^{-12}$ m$^2$/s (28 days), the corresponding requirement for cover thickness for all exposure zones must be larger than 30 mm ($t_{SL} = 50$ years) and 40 mm ($t_{SL} = 120$ years) according to Fig. 13.5. The same conclusion can be reached using the OPC-FA line for concrete cover thickness requirements for the immersed tube tunnel. Thus, the design values of cover thickness from carbonation requirement in Fig. 13.6 do not control the design.

On the basis of the design results for chloride ingress, the values of required cover thickness and chloride diffusion coefficient are obtained, and they are given in Table 13.5 for the main concrete elements. These results provide the basis of durability requirements for RC elements in the HZM project. The rapid chloride migration (RCM) test, conforming to NT Build 492 (Nordtest, 1999), was used to measure the chloride diffusivity during the construction phase. However, the design values from

**Table 13.5 Model-based durability design results for concrete structures in the HZM project (design life $t_{SL} = 50$, 120 years, $\beta = 1.3$)**

| Element | Exposure | $t_{SL}$ (year) | DLS | $x_d^{nom}$ (mm) | Design value $D_{nssd}$ ($10^{-12}$ m$^2$/s) | | Control value $D_{nssm}$ ($10^{-12}$ m$^2$/s) | |
|---|---|---|---|---|---|---|---|---|
| | | | | | 28 days | 56 days | 28 days | 56 days |
| Box girder (exterior) | Salt fog | 120 | (a) | 45 | 3.0 | 2.0 | 6.0 | 4.0 |
| | Splash | 120 | (a) | 80 | 3.0 | 2.0 | 6.0 | 4.0 |
| Box girder (interior) | $CO_2$ | 120 | (a) | 35 | – | – | – | – |
| | Salt fog | 120 | (a) | 45 | 3.0 | 2.0 | 6.0 | 4.0 |
| Pier, pylon (exterior) | Salt fog | 120 | (a) | 50 | 3.5 | 2.2 | 7.0 | 4.5 |
| | Splash | 120 | (a) | 85 | 3.5 | 2.2 | 7.0 | 4.5 |
| Pier (interior) | $CO_2$ | 120 | (a) | 35 | – | – | – | – |
| | Salt fog | 120 | (a) | 50 | 3.5 | 2.2 | 7.0 | 4.5 |
| Bearing platform | Splash | 120 | (a) | 85 | 3.5 | 2.2 | 7.0 | 4.5 |
| | Immersed | 120 | (a) | 65 | 3.5 | 2.2 | 7.0 | 4.5 |
| Bored hole pile | Immersed | 120 | (a) | 65 | 3.5 | 2.2 | 7.0 | 4.5 |
| RC facilities (artificial islands) | Splash | 50 | (a) | 60 | 3.5 | 2.2 | 7.0 | 4.5 |
| | $CO_2$ | 50 | (a) | 20 | – | – | – | – |
| Tunnel tube (exterior) | Splash | 120 | (a) | 80 | 3.5 | 2.2 | 7.0 | 4.5 |
| Tunnel tube (interior) | Salt fog | 120 | (a) | 50 | 3.5 | 2.2 | 7.0 | 4.5 |
| | $CO_2$ | 120 | (a) | 30 | – | – | – | – |

*DLS*, durability limits states.

Li, K.F., Li, Q.W., Zhou, X.G., Fan, Z.H., 2015a. Durability design of Hong Kong–Zhuhai–Macau sea-link project: principle and procedure. Journal of Bridge Engineering, ASCE, 1–11, 04015001, Table 8, Reproduced from permission of ASCE.

Eq. [13.1] cannot be used directly for quality control by the RCM method because the $D_{Cl}^{0}$ in Eq. [13.1] is the apparent chloride diffusion coefficient regressed from in situ exposure tests at a given concrete age, while the RCM measures a short-term migration coefficient under an electrical field. The former is a non-steady-state diffusion (NSSD) coefficient, while the latter is a non-steady-state migration (NSSM) coefficient. Theoretical analysis on the difference between the two coefficients can be found in (Tang, 1999). Thus it is necessary to establish a relationship between the NSSD design value and the NSSM quality control value. To achieve this aim, concrete materials in the Zhanjiang Exposure Station were reconstituted in the laboratory, and the NSSM coefficients were measured by the RCM method at 28 and 56 days. Using the correlation between these two groups of coefficients, the design values were converted to the corresponding RCM values for quality control in Table 13.5.

## 13.3 Quality control in construction

During the construction phase, on-site laboratories were set up to control the quality of structural concrete both for the concrete raw materials and for the properties of the hardened concrete. The target properties of concrete in the laboratory were compressive strength and chloride diffusion coefficient by the RCM method. Meanwhile, in situ nondestructive tests (NDT) were also performed on the prefabricated tunnel segments. This section reports the data collected on the compressive strength and the chloride diffusivity as well as the NDT results, providing a basis for evaluating the concrete quality achieved in construction.

### 13.3.1 Quality controls for durability

The acceptance criteria were set up for the compressive strength and the chloride diffusivity, respectively (HZMBA, 2012). For the compressive strength, both the average and the minimum values for a given specimen group are controlled. For a group containing five or more specimens, the acceptance criterion is expressed as shown:

$$m_{fcu} - s_{fcu} \geq f_{cu,k}, f_{cu,min} \geq f_{cu,k} - C\sigma_0 \quad [13.4]$$

where $m_{fcu}$ and $s_{fcu}$ = the average value and standard deviation of compressive strength of specimens, respectively, $f_{cu,k}$ and $f_{cu,min}$ = the characteristic value for required compressive strength (strength grade) and the minimum strength of specimens, respectively, and $\sigma_0$ = assumed standard deviation of compressive strength. The coefficient $C$ depends on the number of specimens: $C = 0.7$ (5−9), 0.9 (10−19), 1.0 (>19). For specimen groups containing two to four specimens, the following criteria apply:

$$m_{fcu} \geq f_{cu,k} + \sigma_0, f_{cu,min} \geq f_{cu,k} - 0.5\sigma_0 \quad [13.5]$$

The acceptance criteria for chloride diffusivity from the RCM method were formulated on a similar basis. According to the technical specification document (HZMBA, 2012), the following requirements apply to specimen groups containing five or more specimens:

$$m_{Cl} + s_{Cl} \leq D_{nssm,k}, D_{Cl,max} \leq D_{nssm,k} + C\sigma_{Cl} \quad [13.6]$$

where $m_{Cl}$ and $s_{Cl}$ = the average value and standard deviation of chloride diffusivity of specimens, respectively, $D_{nssm,k}$ and $D_{Cl,max}$ = the characteristic values for required RCM chloride diffusivity and the maximum value of diffusivity, respectively, and $\sigma_{Cl}$ = the standard deviation of chloride diffusivity regressed from laboratory specimens with sufficient number. The coefficient $C$ takes the same value as for Eq. [13.4] in terms of specimen number. For specimen groups containing two to four specimens, the following criteria apply:

$$m_{Cl} \leq D_{nssm,k} - \sigma_{Cl}, D_{Cl,max} \leq D_{nssm,k} + 0.5\sigma_{Cl} \quad [13.7]$$

Note that the design results $D_{nssm}$ in Table 13.6 should be used as the characteristic value $D_{nssm,k}$ in Eqs. [13.6] and [13.7].

### 13.3.2 Chloride diffusivity

The chloride diffusivity data of the structural concretes were collected from the on-site laboratories for different concrete elements in the different contract bids. The chloride diffusion coefficients were measured on concrete specimens under standard curing conditions (20°C and RH >95%) for given ages, 28 and 56 days, by the RCM method. These data are presented in Table 13.6 for the tunnel tube segments, the prefabricated concrete elements, and the cast-in-place elements of bridge structures, respectively.

For tunnel segments, the target mean values for $D_{nssm}$ were, respectively, $6.5 \times 10^{-12}$ and $4.5 \times 10^{-12}$ $m^2/s$ for 28 and 56 days. The mean values of measured $D_{nssm}$ are $4.68 \times 10^{-12}$ $m^2/s$ (28 days) and $2.95 \times 10^{-12}$ $m^2/s$ (56 days), much lower than the required values. The coefficient of variation of this $D_{nssm}$ is 9.9% (28 days) and 8.7% (56 days), smaller than the expected level of 20% in the design phase, especially for 56 days age. This decrease of data dispersion will help to reduce the uncertainty associated with the chloride diffusivity. For concretes in the bridge structures, much lower mean values, compared to the required values, were obtained for both the prefabricated and cast-in-place elements. The $D_{nssm}$ dispersion of prefabricated bridge elements was very near 20% for both 28- and 56-days ages, but the variance ranges from 4 to 44% for cast-in-place elements. Note that there is much less data from cast-in-place elements than from the prefabricated elements, and only five sets of data were collected for box girder elements, so the regressed statistical properties should be treated with caution.

**Table 13.6 Collected data on chloride diffusivity of structural concretes and statistical properties**

| Element | Age (days) | Specimen number | Average ($10^{-12}$ m$^2$/s) | Standard deviation ($10^{-12}$ m$^2$/s) | Variation coefficient (−) (%) |
|---|---|---|---|---|---|
| Tunnel segment (C45), prefabricated | 28 | 148 | 4.71 | 0.47 | 10.0 |
| | 56 | 148 | 2.96 | 0.26 | 8.8 |
| Bearing platform (C45), prefabricated | 28 | 39 | 4.37 | 0.88 | 20.1 |
| | 56 | 27 | 2.99 | 0.56 | 18.9 |
| Pier (C50), prefabricated | 28 | 30 | 4.27 | 0.76 | 17.8 |
| | 56 | 27 | 2.89 | 0.56 | 19.4 |
| Bridge deck (C60), prefabricated | 28 | 48 | 4.48 | 0.92 | 20.5 |
| | 56 | 42 | 3.48 | 0.78 | 22.5 |
| Box girder (C55), cast-in-place | 56 | 5 | 2.80 | 0.10 | 3.57 |
| Pier (C50), cast-in-place | 56 | 8 | 3.25 | 0.82 | 25.1 |
| Bearing platform (C45), cast-in-place | 56 | 9 | 2.43 | 1.08 | 44.3 |
| Bore-hole pile (C35), cast-in-place | 56 | 22 | 3.12 | 0.55 | 17.8 |

### 13.3.3 Concrete cover thickness

The measurements of concrete cover thickness are presented in Table 13.7 for tunnel segments and cast-in-place concrete elements. The concrete cover was measured through the common midpoint (CMP) method. The CMP method detects the depth of reinforcing bars through transmitting an electromagnetic wave pulse and receiving the reflected waves from the steel bars by two adjacent antennas. The measurement error of the device used in the HZM project was evaluated as around 3 mm through comparison with measurements on extracted cores from test segments of the tunnel.

For the prefabricated tunnel segments, the required values for thickness were respectively 50 mm (intrados) and 70 mm (extrados). The measurements showed

**Table 13.7 Collected data on concrete cover thickness of RC elements and statistical properties**

| Element | Measurement number | Average (mm) | Standard deviation (mm) | Coefficient of variation (%) |
|---|---|---|---|---|
| Tunnel segment (intrados) | 6386 | 53.5 | 3.46 | 4.71 |
| Tunnel segment (extrados) | 6571 | 73.4 | 3.90 | 4.17 |
| Bridge deck (cast-in-place) | 220 | 50.5 | 1.11 | 2.2 |
| Piers (cast-in-place) | 501 | 80.0 | 6.74 | 8.43 |
| Bearing platform, splash zone (cast-in-place) | 70 | 95.5 | 4.22 | 4.42 |
| Bearing platform, immersed zone (cast-in-place) | 200 | 71.0 | 6.85 | 9.65 |

that the mean values are 53.5 mm (intrados) and 73.4 mm (extrados); the construction error, corresponding to the distance between the fifth percentile value and the mean value, is 5.8 mm (intrados) and 6.4 mm (extrados), slightly larger than the expected construction tolerance, 5.0 mm, for prefabricated elements. For the cast-in-place concrete elements in bridge structures, the design value for concrete cover thickness for bridge decks was 45 mm, and the measured mean value attained 50.5 mm with only 1.11 mm as the standard deviation (SD); the design thickness for piers, in the splash zones, was 70 mm and the measured values were 80.0 mm as mean value and 6.74 mm as the SD value. The design values for bearing platforms in the immersed and splash zones were, respectively, 60 mm and 80 mm, and their measured values were mean of 71.0 and 95.5 mm, respectively, and SD values of 6.85 and 4.22 mm, respectively. Globally, the measured values of concrete cover thickness, including the mean values and their SD values, conform to the expected values with a certain safety margin.

### *13.3.4 NDT measurements*

The NDT measurements included air permeability measurements using the Torrent Permeability Tester (TPT), and electrical resistance measurements using a Wenner probe, on the extrados of prefabricated tunnel segments at different hardening ages. The principle of the TPT is to create a vacuum above the concrete surface and measure the steady flow of air permeating through the concrete surface (Torrent, 1992). The principle of electrical resistivity measurements is to obtain the electrical current under a certain electrical potential. During the NDT measurement, both TPT and Wenner probe measurements were performed at the same point, with the ambient temperature and water content of concrete surface (measured by a Tramex water content metre) also recorded. The results are given in Fig. 13.7 for 28- and 56-days ages.

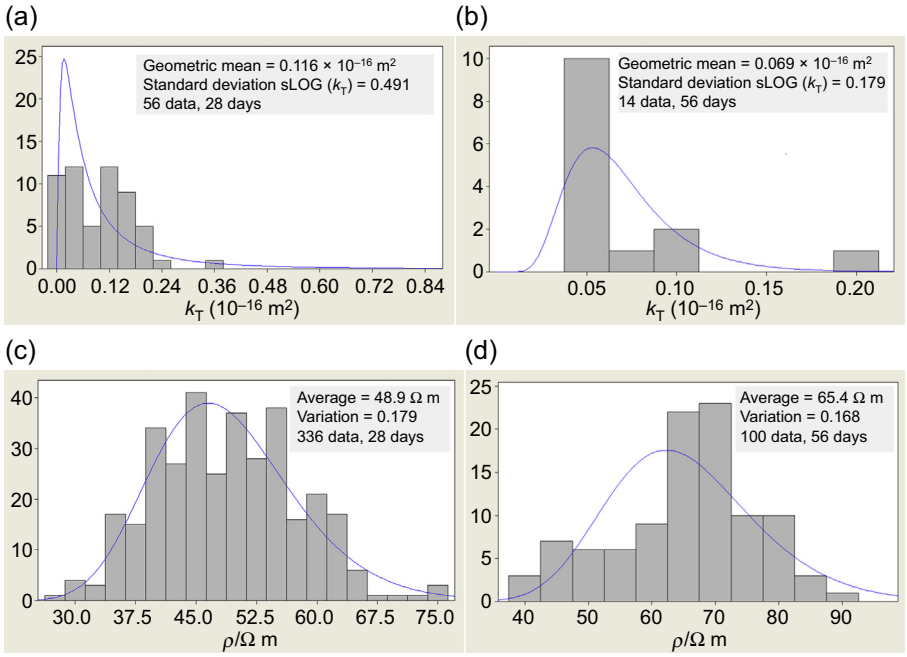



**Figure 13.7** Histograms of air permeability measurement (a, b), and electrical resistivity measurement (c, d) on the extrados of prefabricated tunnel segments.

For the air permeability, the $k_T$ values were relatively low for the structural concrete, on the order of $10^{-18}$ m$^2$, and the 56-days values were systematically lower than the 28-days values. The variability of $k_T$ values for 56-days measurements was also quite low (sLOG below 0.2), according to Swiss experience (Jacobs et al., 2009). Note that both the geometric mean $k_{Tgm}$ and deviation sLOG compare well with results obtained on segments of the Port of Miami Tunnel ($k_{Tgm} = 0.57 \times 10^{-16}$ m$^2$ and sLOG = 0.24 at 120-days age), made with high-quality concrete (Torrent et al., 2013). For the electrical resistance, the 56-days values are systematically higher than the 28-days values, due to both the densification of the concrete pore structure during hardening and drying on the concrete surface. Thereafter, the electrical resistivity values were relatively stable with the coefficient of variation being around 15%.

## 13.4 Durability assessment

During the construction, it is necessary to quantify the durability actually achieved through the construction process. In the design phase, the statistical properties of durability parameters were obtained though the exposure data; see Table 13.3. On the basis of the data discussed earlier, the statistical properties of these parameters for the concrete elements were updated, and a durability assessment was performed using the full

probabilistic method, considering the real construction options for the achieved durability in the construction processes. The assessment results would also provide the basis for maintenance planning and life-cycle management.

### 13.4.1 Assessment model

The assessment model for chloride-induced corrosion is also adapted from the analytical model of Fick's second law, similar to the design model in Eq. [13.1]. With the corrosion initiation specified as DLS, the assessment equation can be written as follows:

$$G = (C_{cr} - C_0) - (C_s - C_0)\left[1 - \mathrm{erf}\left(\frac{x_d}{2\sqrt{D_{Cl}^0 \eta(t_0, t)t}}\right)\right] \geq 0 \qquad [13.8]$$

where $C_0$ = initial chloride concentration in concrete (% binder). This assessment equation differs from Eq. [13.1] in two aspects: (1) the parameters in this model, except the time $t$, are all statistical variables; (2) the initial chloride content $C_0$ is considered. Hereafter, this model can be used through the full probabilistic approach to evaluate the failure probability of durability:

$$p_f(t_{SL}) = \mathrm{prob}[G(t_{SL}) < 0] \qquad [13.9]$$

The service life is judged to be satisfied or not satisfied, by comparing the failure probability at $t = t_{SL}$ with the target failure probability $p_{target}$. Note that in reliability theory, the target failure probability is also expressed by the reliability index $\beta$ through the relation $\beta = \Phi^{-1}(1 - p_f)$, where $\Phi^{-1}(\bullet)$ is the inverse cumulative density function of the standard normal distribution.

Thus, the assessment model contains six parameters: $C_{cr}$, $C_s$, $C_0$, $x_d$, $D_{Cl}^0$ and $n$ (or $\eta$). The statistical properties of the parameters $C_{cr,s}$ and ageing exponent $n$ were investigated in depth on the basis of the long-term exposure tests in the design phase (Li et al., 2015b), and the same statistical properties are retained in the durability assessment. For the initial concentration $C_0$, a uniform distribution is calibrated for the structural concretes from the chemical analysis of raw materials. For the chloride diffusivity $D_{Cl}^0$, and concrete cover thickness, the collected data in Tables 13.6 and 13.7, respectively, are used to update the statistical properties. As before, the chloride diffusivity in Table 13.6 refers to $D_{nssm}$, and it should be converted to $D_{nssd}$ value. Since the data in Tables 13.6 and 13.7 are not exhaustive for all concrete elements, the elements not covered by the collected data still retain the statistical properties from the design phase. The updated statistical properties of the model parameters are summarised in Table 13.8.

### 13.4.2 Construction options for durability

In the construction phase, different protective measures were adopted for the concrete elements in the HZM project. Without attempting to be exhaustive, this section

**Table 13.8 Updated statistical properties of parameters for durability assessment for RC/PC elements in the HZM project**

| Parameter (distribution) | Statistical properties | Immersed zone | Tidal zone | Splash zone | Atmospheric zone |
|---|---|---|---|---|---|
| Surface concentration $C_s$ (lognormal) | Average (%) | 4.78 | 4.05 | 5.76 | 2.10 |
| | Deviation (%) | 0.71 | 0.62 | 0.86 | 0.32 |
| Initial concentration $C_0$ (rectangle) | Lower bound $L$ (%) | 0.02 | | | |
| | Upper bound $U$ (%) | 0.04 | | | |
| Critical concentration $C_{cr}$ (beta) | Lower bound $L$ (%) | 1.0 | 0.45 | 0.45 | – |
| | Upper bound $U$ (%) | 3.5 | 1.25 | 1.25 | – |
| | Coefficient $a$ (–) | 0.30 | 0.22 | 0.22 | – |
| | Coefficient $b$ (–) | 0.45 | 0.36 | 0.36 | – |
| Critical concentration $C_{cr}$ (lognormal) | Average (%) | – | – | – | 0.85 |
| | Deviation (%) | – | – | – | 0.13 |
| Diffusion coefficient $D_{Cl}^0$ (lognormal) | Average ($10^{-12}$ m$^2$/s) | Table 13.6/design value[a] | | | |
| | Coefficient of variance | Table 13.6/0.2 × design value[a] | | | |
| Exponent coefficient $n$ (normal) | Average (–) | 0.44 | 0.46 | 0.47 | 0.53 |
| | Deviation (–) | 0.028 | 0.029 | 0.029 | 0.079 |
| Concrete cover $x_d$ (normal) | Average (mm) | Table 13.7/Design value[b] | | | |
| | Deviation (mm) | Table 13.7/5.3 (cast-in-place), 3.5 (prefabricated)[b] | | | |

[a]For the elements that Table 13.6 does not cover, chloride diffusivity takes the design value with the standard deviation as 20% of the design value.
[b]For the elements that Table 13.7 does not cover, concrete cover thickness takes the design value with the standard deviation as 5.3 mm (cast-in-place) or 3.5 mm (prefabricated).

provides the construction options of the protective measures for the concrete elements for one bridge bid, for the prefabricated tunnel segments and for the artificial islands. These protective measures include silane impregnation on the concrete surface, epoxy-coating on steel rebars, stainless-steel rebars, coating on the steel pile surface and cathodic protection of steel rebars. These measures were adopted to increase the durability safety margin and/or to compensate for possible adverse effects from construction defects. The construction options for different concrete elements are given in Table 13.9.

These protective measures should be taken into account in the durability assessment since some measures, such as stainless-steel rebars, can significantly increase the durability safety margin for concrete elements. On the basis of state-of-the-art knowledge and practice of these measures, the following assumptions are retained in the durability assessment modelling:

1. *Silane impregnation*. The treatment of concrete by silane impregnation renders the concrete surface hydrophobic, reduces substantially the seawater penetration and thus retards the chloride ingress into concrete (Aguiar et al., 2008). The valid duration of protection depends on its own ageing process, and Chinese experience in marine harbours indicates that the valid duration of silane impregnation is usually more than 10 years. Accordingly, silane impregnation is assumed to delay the accumulation of chloride on concrete surface to its stabilised value by 10 years in the assessment.
2. *Epoxy-coated rebars*. The corrosion resistance of coated rebars is reported to increase substantially as the surface damage of coating is strictly controlled (Basham, 1999). Since no special measures were undertaken against the mechanical damage of epoxy-resin coatings on steel bars, it is conservatively assumed that these coatings have no impact on the corrosion initiation of reinforcing steel bars in the durability assessment.
3. *Stainless-steel rebars*. These bars are used in the RC/PC elements in the splash zones. The critical chloride concentration, $C_{cr}$, for stainless steel is reported to be 10−20 times higher than for carbon steel bars (Kouril et al., 2010). The investigation of the corrosion resistance of the stainless-steel rebars used in the HZM projects confirmed this estimation of magnitude for $C_{cr}$. In the assessment, the $C_{cr}$ of stainless bars is conservatively taken as 5 times the value of conventional carbon steel rebars.
4. *Cathodic protection*. Cathodic protection imposes an electrical current or sacrificial anode on the steel bars to eliminate the anodic reaction on the steel surface (Kumar, 1998). The cathodic protection in the HZM project refers to the imposed current method for the steel rebars in the tunnel tube segments. In the assessment, the protection is assumed to passivate completely the reinforcing steel once it is put into function, keeping the steel in passivation during its active duration.

### 13.4.3 Durability assessment through the full probabilistic method

The fully probabilistic analysis for the durability assessment of the RC/PC elements is accomplished using Monte-Carlo simulations. A computer-based program was developed especially to perform the probabilistic assessment. In the simulation, six parameters are considered as joint occurrence random variables: $C_{cr}$, $C_s$, $C_0$, $x_d$, $D_{Cl}^0$ and $n$.

**Table 13.9 Protection measures used for concrete elements in the HZM project**

| Element (structure) | Position | Exposure | Concrete | Protection measures | $\beta_{SL}$ |
|---|---|---|---|---|---|
| Bridge deck, prefabricated (NV, NVV spans) | – | Salt fog | C60 | Epoxy-coated bars | 3.50 |
| Bridge deck, cast-in-place (NV, NVV spans) | – | Salt fog | C60 | Epoxy-coated bars | 3.67 |
| Box girder, cast-in-place (artificial islands) | Exterior | Salt fog | C50 | Epoxy-coated bars/silane impregnation | 3.85 |
| | Interior | Salt fog | C50 | – | 3.67 |
| Pylon, cast-in-place (NV spans) | – | Salt fog | C60 | Stainless bars<br>Silane impregnation | > 5.0 |
| Pier, cast-in-place (NV spans) | Exterior | Salt fog | C50 | Silane impregnation | > 5.0 |
| | | Splash | C50 | Stainless bars<br>Silane impregnation | > 5.0 |
| | Interior | Salt fog | C50 | – | > 5.0 |
| | | Splash | C50 | | 2.37 |
| Pier, prefabricated (NNV spans) | Exterior | Salt fog | C50 | Silane impregnation | > 5.0 |
| | | Splash | C50 | Epoxy-coated bars<br>Silane impregnation | 2.32 |
| | Interior | Salt fog | C50 | – (>+8.00 m)<br>Silane impregnation (<+8.00 m) | >5.0 |
| | | Splash | C50 | | 1.55 |

| | | | | | |
|---|---|---|---|---|---|
| Bearing platform, cast-in-place (NV spans) | – | Splash | C45 | Stainless bars<br>Silane impregnation | >5.0 |
| | | Immersed | C45 | Stainless bars<br>Silane impregnation | > 5.0 |
| Bearing platform, prefabricated (NNV spans) | – | Immersed | C45 | Silane impregnation | 2.81 |
| Tunnel segment, prefabricated (immersed tunnel) | Exterior | Splash | C45 | Cathodic protection | 2.13 |
| | Interior | Salt fog | C45 | – | 2.81 |
| Bored hole pile, cast-in-place (NNV span) | – | Immersed | C35 | – | 2.73 |
| Steel composite pile, cast-in-place (NV, NVV spans) | – | Immersed | C35 | Steel coating/cathodic protection | 2.39 |

*NV*, navigable spans; *NNV*, non-navigable spans; $\beta_{SL}$, reliability index at $t = 120$ years "-", no protection measures.

The statistical properties are presented in Table 13.8, and the construction options for protection measures are taken into account following Table 13.9 with the assumptions taken in the previous section. For a given exposure age $t$, the Monte-Carlo simulations are performed to calculate the failure probability of Eq. [13.9], and 1,000,000 samplings are used to ensure the solution of 'real' probability. Accordingly, the failure probability is solved with time from $t = 0$ to $t = 120$ years. The assessment results are presented from Fig. 13.8 in terms of the failure probability for the different RC/PC elements in the HZM project. Note that the failure probability through this chapter, without mention otherwise, refers to the failure probability with respect to the corrosion initiation of rebars in Eq. [13.9].

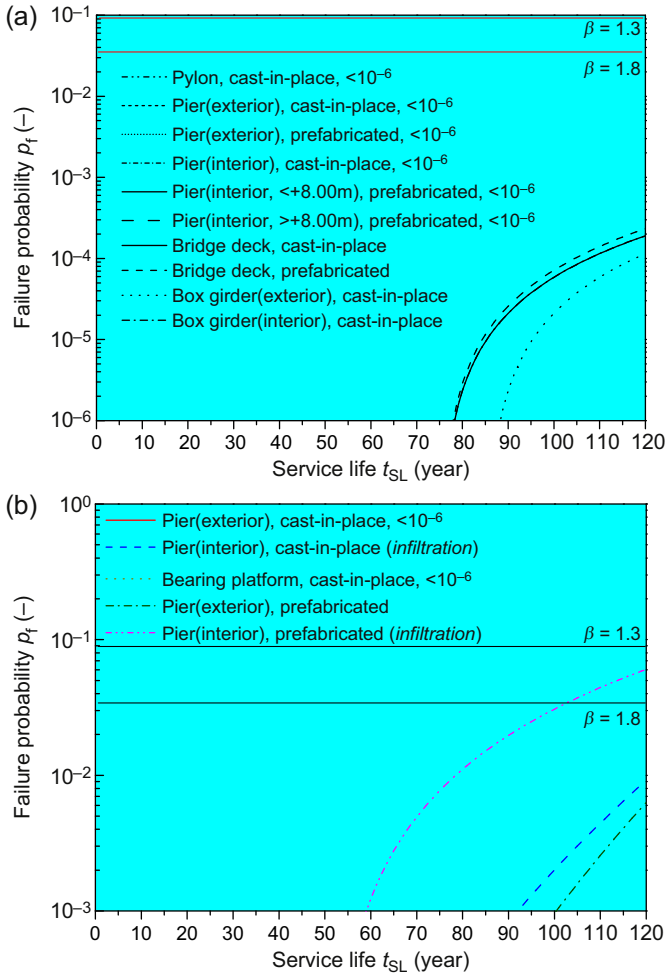



**Figure 13.8** Failure probability of concrete elements in the HZM project through Monte-Carlo simulation for (a) bridge elements in atmospheric zone, (b) bridge elements in splash and tidal zones, (c) bridge elements in immersed zone and (d) immersed tube tunnel segments.

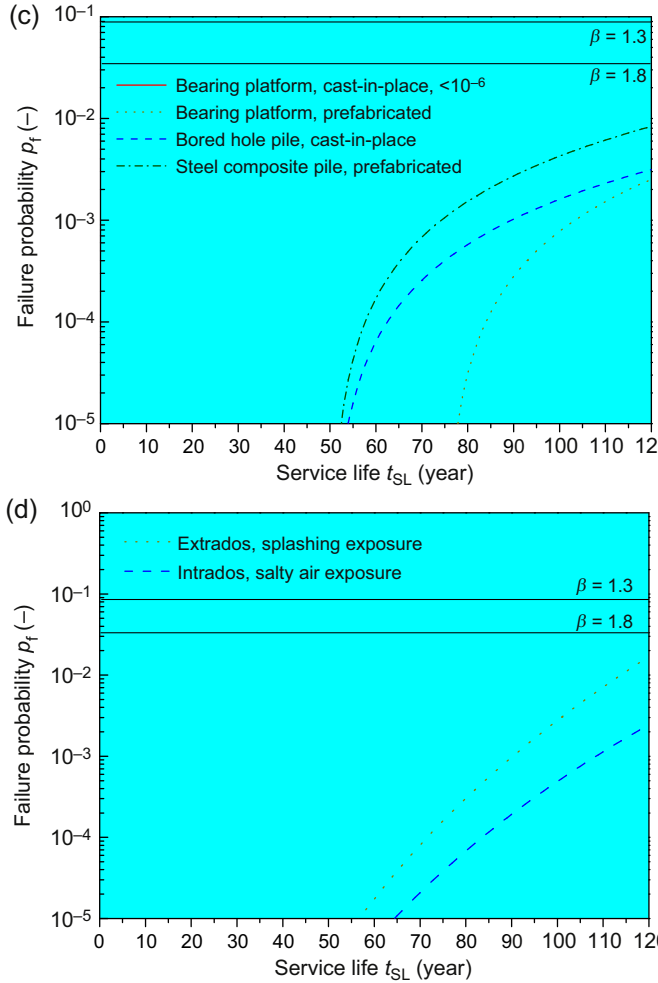



**Figure 13.8** Continued.

### *13.4.3.1 Bridge elements in atmospheric zone*

These bridge elements include pylons, bridge decks, box girders and piers. The pylons are situated in the navigable spans and cast in place using C60 concrete. The stainless-steel rebars were used in the first layer of reinforcement, and the silane impregnation was applied to the element surface. By these two measures, the failure probability of pylon elements is rather low, ie, lower than $10^{-6}$ and the reliability index $\beta > 5.0$ at 120 years.

The bridge decks are used on the steel (composite) box girders, either prefabricated or cast in place using C60 concrete. Epoxy-coated rebars were used, and the failure probability of bridge decks is 0.019% ($\beta = 3.67$) (prefabricated) and 0.0232%

($\beta = 3.50$). The concrete box girders are used in the non-navigable spans approaching the artificial islands, cast in place using C50 concrete. At the exterior of girders, the epoxy-coated steel rebars were used in the first layer of reinforcement, and the silane impregnation was applied. The failure probability at 120 years is 0.011% and $\beta = 3.85$ for the exterior, and 0.019% and $\beta = 3.67$ for the interior.

The piers are either prefabricated, in non-navigable spans, or cast in place in navigable spans. Note that the piers have a void structure, and the pier interior is assumed to be exposed to the marine atmosphere (aerosol) in design. For the cast-in-place piers, silane impregnation was applied to the exterior, and no additional measure is taken for the interior. The failure probability is less than $10^{-6}$ (exterior, interior) at 120 years, and the corresponding reliability index is $\beta > 5.0$. For the prefabricated piers, the exterior adopted silane impregnation, and the internal side adopted also silane impregnation for the latitude <8.00 m (the upper limit of splash zone at +6.26 m latitude). With these measures, the obtained failure probability is less than $10^{-6}$ at 120 years for both interior (>+8.00 mm, <+8.00 mm) and exterior.

### 13.4.3.2 Bridge elements in splash and tidal zones

These bridge elements are the piers and the bearing platforms. The tidal zone is conservatively merged into the splash zone in this assessment. The pier exterior is subject to splash/tidal actions, and the interior is exposed to the marine atmosphere. The piers are prefabricated for non-navigable spans using C50 concrete, and the epoxy-coated rebars were used for the first layer of steel bars with the silane impregnation on the external surface. The piers are cast in place in navigable spans using C50 concrete with stainless bars (first reinforcing layer) and surface silane impregnation as durability measures, in addition to 70-mm concrete cover. The assessment gives $p_f < 10^{-6}$ and $\beta > 5.0$ for the cast-in-place piers (exterior), and $p_f = 1.02\%$ and $\beta = 2.32$ for the prefabricated piers (exterior) at 120 years.

The bearing platforms in the navigable spans are exposed to splash/tidal actions. These platforms are cast in place with C45 concrete, using stainless-steel rebars and surface silane impregnation as additional measures in addition to 80-mm concrete cover. The failure probability is calculated as $p_f < 10^{-6}$ and $\beta > 5.0$ at 120 years. Here an accidental case is considered for seawater infiltration into the pier voids, making the pier interior susceptible to direct seawater contact. This water infiltration can be induced by seawater penetration through working joints between prefabricated pier segments. Under this scenario, the exposure condition of the pier interior, in the worst case, can be equal to the splash zone. Fig. 13.8(b) shows that the $p_f$ rises to 0.89% (cast in place) and 6.03% (prefabricated) at 120 years, the corresponding reliability index $\beta$ decreases to 3.11 (cast in place) and 1.55 (prefabricated). This observation highlights the importance of the water-tightness of pier joints and the corresponding inspection/monitoring.

### 13.4.3.3 Bridge elements in immersed zones

These elements include bearing platforms, bore-hole piles and steel composite piles. The bearing platforms are cast in place for navigable spans with C45 concrete using

stainless-steel bars and surface silane impregnation; the prefabricated platforms are used for non-navigable spans with surface silane impregnation. The assessment gives $p_f < 10^{-6}$ and $\beta > 5.0$ for cast-in-place bearing platforms, and $p_f = 0.25\%$ and $\beta = 2.81$ for prefabricated bearing platforms, cf. Fig. 13.8(c).

The bore-hole piles use C35 concretes and concrete cover of 65 mm is prescribed without other additional measures. The assessment gives $p_f = 0.32\%$ and $\beta = 2.42$ at 120 years. The steel composite piles have C35 concrete poured into steel tubes, and the steel tubes were protected by coating and cathodic protection. The result for steel composite piles, $p_f = 0.83\%$ at 120 years, is just nominal since the coating is supposed to protect the steel for 60 years and the cathodic protection is to start up to assure another 60 years for the steel tubes.

#### 13.4.3.4 Immersed tube tunnel

The segments of the immersed tube tunnel are made of C45 concrete, and the segments are mostly prefabricated but cast in place for the connection part (approach) of the tunnel to the artificial islands. The assessment covers only the prefabricated segments of tunnel. The extrados of the segment is physically immersed and exposed directly to seawater, and the intrados of the segment is exposed to traffic and marine (salty) atmosphere in the tunnel. Considering the possible availability of seawater and atmosphere on the steel bars, the extrados is considered to be subjected to splash actions. The assessment gives $p_f = 1.7\%$ and $\beta = 2.13$ for extrados, and $p_f = 0.25\%$ and $\beta = 2.81$ for intrados at 120 years.

### 13.4.4 Summarising remarks

Globally, the concrete elements all achieve reliability indexes above 2.0 at 120 years, and these quantitative results on the durability safety margin provide a first basis for maintenance planning during the service life of these elements. The bridge elements in the atmospheric zones have very low failure probability (ie, $p_f < 10^{-3}$ at 120 years and the corresponding reliability index $\beta > 3.0$). The silane impregnation was generally adopted as a protective measure for the concrete elements, the stainless-steel rebars were adopted for pylons, and the epoxy-coated rebars were used for decks and box girders. The bridge elements in the splash/tidal zone, ie, piers and bearing platforms, have a satisfactory margin for durability: the cast-in-place piers and bearing platforms, using both stainless-steel rebars in the first reinforcing layer and surface silane impregnation, have quite high reliability index, $\beta > 5.0$; the prefabricated piers adopted epoxy-coated bars in the first reinforcing layer and surface saline impregnation, achieving $\beta = 2.32$ at 120 years. The bridge elements in the immersed zone also have a satisfactory durability margin: the cast-in-place platforms used stainless-steel rebars and surface silane impregnation, and the failure probability is very low; the prefabricated platforms used epoxy-coated steel rebars, and thus have a reliability index $\beta = 2.81$ at 120 years; the bored-hole piles achieve $\beta = 2.42$ at 120 years without special protection. For the prefabricated tunnel segments, the reliability index is evaluated, respectively, as $\beta = 2.81$ (interior) and $\beta = 2.13$ (exterior) at 120 years.

## 13.5 Life-cycle management

As indicated, the concrete elements in the HZM project have undergone a comprehensive model-based durability design, quality control in construction and durability assessment using the collected data during the construction phase. However, uncertainty still remains for the durability performance during the actual service life due to the representivity of the collected data, and/or the limitation of the models used and current knowledge on deterioration processes. To ensure the service life of 120 years for the concrete structures, life-cycle management should be established. The essential elements for life-cycle management include planning the maintenance activities, mastering the real durability performance of concrete elements through inspection and monitoring, and adjusting the maintenance activities on the basis of the correct interpretation of the inspection/monitoring data.

### *13.5.1 Inspection and monitoring for durability*

The inspection and monitoring of the durability performance of the concrete elements are crucial to understand and establish their real durability states. For concrete elements in the HZM project, inspection schemes have been set up, including acceptance inspection (after the construction works), daily inspection (period of 1−7 days), regular inspection (period of 1−5 years), special inspection (after accidental events) and ultimate inspection (upon demolition). The daily inspection involves only the surface quality check of concrete elements, while other inspections would include the quality and thickness of concrete cover, the cracking extent of concrete elements, the state of the steel rebars and the contents of aggressive agents such as chlorides.

The durability monitoring of concrete elements consists of two basic aspects: (1) monitoring the electrochemical stability of steel rebars and the ingress of aggressive agents, using embedded sensors, and (2) monitoring the long-term ingress of chlorides via the long-term exposure station built on the project site. The embedded sensors used in the concrete elements can record the corrosion potential and the corrosion rate of steel rebars, the chloride concentration, and the pH value in the concrete. These sensors were installed in concrete elements in different exposure conditions, including the pylons (atmospheric and splash), piers (atmospheric and splash), concrete box girders (atmospheric and splash) and tunnel segments (intrados and extrados). These sensors are connected to data loggers, accessible to external data transfer. The long-term exposure station was built on the west artificial island with exposure platforms for atmospheric, splash, tidal, and immersed zones. This exposure station is a permanent part of the HZM project, and it will function during the entire service life of the concrete structures. Plain concrete and reinforced structural concrete specimens were exposed to different exposure conditions after hardening in the laboratory. On a regular basis, the specimens are to be taken to the laboratory to investigate: (1) the surface chloride accumulation, (2) the chloride diffusivity and its ageing with time, (3) critical chloride concentration of corrosion, (4) the protective effect of surface silane impregnation, and (5) the stability of stainless-steel and epoxy-coated rebars. The first concrete specimens were cast and placed in the exposure station in 2014, cf. Fig. 13.9.



**Figure 13.9** Long-term exposure station for concrete structures in the HZM project. Courtesy of the HZM Bridge Administration.

### 13.5.2 Strategy for life-cycle management

With the help of the inspection program and the long-term durability monitoring, it is possible to establish a strategy for life-cycle management for the concrete structures in the HZM project. The global strategy is illustrated in Fig. 13.10, combining the durability assessment, the durability redesign, the inspection/monitoring schemes, and the maintenance scheme during service life. The durability assessment at the acceptance stage quantifies the durability margin for concrete elements, as shown in Fig. 13.8. This quantification also provides the basis for the maintenance planning and inspection scheme for the concrete elements. For the elements with a low or relatively low safety margin at this stage, the durability redesign is to be performed to implement the protective measures and/or the inspection and maintenance planning. Then, during the service life, the collected data from inspection and monitoring will serve to update the durability safety margin via a durability assessment, which, in turn, will update the inspection/maintenance schemes for the concrete elements with safety margins lower than the expected level.

The basic maintenance planning is established on the basis of the durability assessment in the previous section. A preventive maintenance strategy is adopted, intervening to slow or arrest the deterioration of concrete elements at an early stage. The basic maintenance planning considers mainly two aspects: the durability performance level of elements denoted by a failure probability $p_f$ or reliability index $\beta_{SL}$ at 120 years with respect to the corrosion initiation of rebars, and the structural importance of elements. The maintenance techniques consist of surface chloride extraction

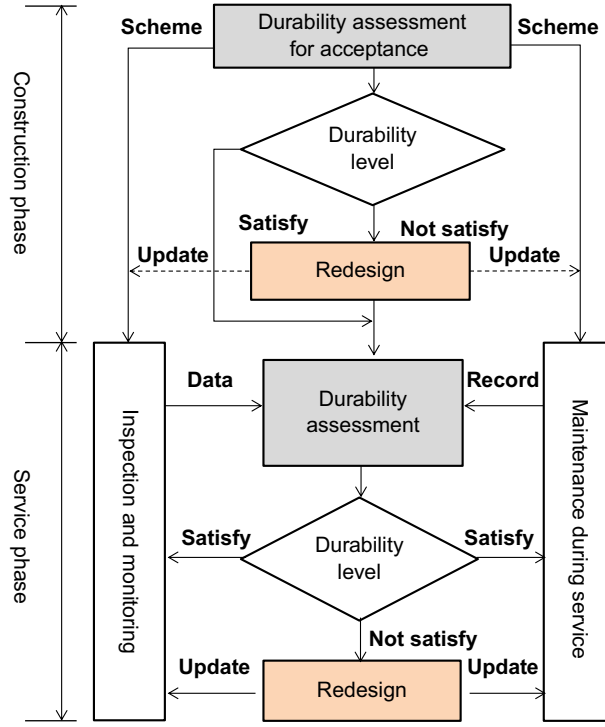



**Figure 13.10** Life-cycle management strategy for concrete structures in the HZM project.

by an electrochemical method, and applying silane impregnation on the surface of elements periodically. The maintenance period is recommended to be 20−40 years: the intervention period of 20 years is recommended for the elements without stainless-steel rebars, and the period of 40 years is attributed to the elements using stainless-steel rebars due to their much lower failure probability ($<10^{-6}$). For tunnel segments, a cathodic protection system has been installed, but not yet activated, to protect the steel bars against unexpected durability failure. The activation time is preliminarily set at 100 years, corresponding to the failure probability $p_f = 1\%$. It should be noted that this basic maintenance scheme is required to interact with, and respond to, the durability inspection/monitoring data and the real-time durability assessment during the service life.

## 13.6 Conclusions

This chapter has introduced the HZM sea link project, covering the durability design, quality control, durability assessment during construction and the life-cycle management of concrete structures in the project. The durability design established first a general philosophy, dividing the requirements into material and structural levels,

prioritising different deterioration processes and employing model-based methods to determine the quantitative design parameters for durability. On the basis of the quantitative requirements, quality control was performed on concrete compressive strength and chloride diffusivity as control parameters. The on-site data were collected for chloride diffusivity and concrete cover thickness, and using NDT measurements, for air permeability and electrical resistivity. Using these data, the statistical properties for parameters in the chloride ingress model were updated, and a comprehensive durability assessment was achieved through a full probabilistic method. The assessment shows that the safety margins for durability performance are satisfactory, with $\beta_{SL}$ above 2.0 at 120 years. The life-cycle management of concrete structures in the HZM project consists of implementing a global strategy to combine the inspection/monitoring scheme, maintenance planning and the real-time durability assessment during the service life.

## Acknowledgement

The work is supported by the China National Science and Technology Support Planning Project No. 2011BAG07B04. The collaboration of the HZM Bridge Administration (Zhuhai, China) is acknowledged. Mr Wang Pianpian (Master's student) in Tsinghua University and Mr Shengnian Wang (chief engineer) of CCCC 4th Harbor Research Institute are also acknowledged for their participation in the research work.

## References

Aguiar, J.B., Camoes, A., Morira, P.M., 2008. Coatings for concrete protection against aggressive environments. Journal of Advanced Concrete Technology 6 (1), 243−250.

Andrade, C., Castellote, M., Andrea, R., 2011. Measurement of ageing effect on chloride diffusion coefficients in cementitious materials. Journal of Nuclear Materials 412 (1), 209−216.

Basham, K., 1999. Choices in corrosion-resistant bars. Concrete International 1−4. C99J027.

DuraCrete, 1998. Probabilistic Performance Based Durability Design of Concrete Structures, Modelling of Degradation. Document BE95-1347/R4-5, The Netherlands.

fib, 2006. Model Code for Service Life Design. fib Bulletin 34. Federation Internationale des Bétons, Lausanne.

HZMBA, 2010. Bidding Documents for General Contracting of Design and Construction of HZM Project Main Works in Artificial Islands and Tunnel. Hong Kong-Zhuhai-Macau Bridge Administration, Zhuhai, China.

HZMBA, 2012. Technical Specifications for Quality and Durability of Structural Concrete in HZM Project. Hong Kong-Zhuhai-Macau Bridge Administration, Zhuhai, China.

ISO, 2008. General Principles on the Design of Structure for Durability (ISO13823:2008(E)). International Organization for Standardization, Genève, Switzerland.

Jacobs, F., Leemann, A., Denarié, E., Teruzzi, T., 2009. Recommendations for Quality Control of Concrete With Air-permeability Measurements. VSS Report 641. Office Fédéral des Routes, Bern.

Kouril, M., Novak, P., Bojko, M., 2010. Threshold chloride concentration for stainless steels activation in concrete pore solutions. Cement Concrete Research 40, 431−436.

Kumar, V., 1998. Protection of steel reinforcement for concrete—a review. Corrosion Review 16 (4), 317−358.

Li, K.F., Chen, Z.Y., Lian, H.Z., 2008. Concepts and requirements of durability design for concrete structures: an extensive review of CCES01. Materials and Structures 41, 717−731.

Li, K.F., Li, Q.W., Zhou, X.G., Fan, Z.H., 2015a. Durability design of Hong Kong−Zhuhai−Macau sea-link project: principle and procedure. Journal of Bridge Engineering, ASCE 1−11, 04015001.

Li, Q.W., Li, K.F., Zhou, X.G., Zhang, Q.M., Fan, Z.H., 2015b. Model-based durability design of concrete structures in Hong Kong−Zhuhai−Macau sea link project. Structural Safety 53, 1−12.

Nordtest, 1999. Concrete, Mortar and Cement-based Repair Materials: Chloride Migration Coefficient From Non-steady Migration Experiments (NT Build 492). Nordtest Method, Nordtest, Espoo, Finland.

Tang, L.P., 1999. Concentration dependence of diffusion and migration of chloride ions. Part 1, Theoretical considerations. Cement and Concrete Research 29, 1463−1468.

Torrent, R., 1992. Torrent—a two chamber vacuum cell for measuring the coefficient of permeability to air of the concrete cover on site. Materials and Structures 25, 358−365.

Torrent, R., Armaghani, J., Taibi, Y., May 2013. Evaluation of Port of Miami Tunnel Segments: carbonation and service life assessment made using on-site air permeability tests. Concrete International 39−46.

# Concrete durability in small harbours: the Southern African experience

14

*K.P. Mackie*
Keith Mackie Consulting Coastal & Harbour Engineer, South Africa

## 14.1 Background to small harbours

In this context, 'small' harbours generally refer to facilities for small craft, harbours that are physically small, harbours of whatever size dedicated to accommodating small vessels, and areas in large commercial harbours set aside for small craft. All instances imply relatively small structures. Coastlines around the world vary enormously, in climate, in the shape of the coast, and in exposure to oceanic tides and waves. For example, the coastline of Southern Africa (see Fig 14.1) is arguably the straightest in the world with the shortest coastline relative, that is, to the area of land it serves. It has the least amount of headlands and embayments and hence of naturally protected




**Figure 14.1** Southern African coastline.

**Marine Concrete Structures.** http://dx.doi.org/10.1016/B978-0-08-100081-6.00014-3
Copyright © 2016 Elsevier Ltd. All rights reserved.

water. The straightness of a coast can be measured by its fractal index. The value for the South African coast is 1.048, compared to the West Coast of Britain of 1.22 and Australia of 1.13 (Mackie, 1993). The fractal index of a coast is measured as the rate of change '$m$' of the measured length versus the gauge distance used to 'step off' the coast. Since this is a negative amount, the index is expressed as '$1 - m$'. The significant measure, the fractional component, '$m$', is measured on a log−log scale and significantly understates the differences in the coastlines mentioned (Gliek, 1987).

This chapter will focus largely on structures on the Southern African coastline. The climate on the coasts of Southern Africa can be described as 'arid' on the West Coast, varying from meagre rainfall in the south to full, dry desert in the north with no significant rainfall. Temperature regimes are generally mild with winter minima on the order of 10°C to summer maxima of 30°C. Humidity is usually low but can be surprisingly high, particularly in the north where the coast is regularly fog-bound. East of Cape Town, the coast is well watered, with rainfall increasing to the north. North of Port Elizabeth, the climate becomes subtropical with significantly more rainfall increasing to the north. The temperature range is not significantly different from the West Coast, but the median is significantly higher, so too is the ambient humidity.

There is a strict water temperature divide between West and East Coast. On the West Coast, the prevailing southeast wind induces a strong upwelling of cold bottom water. Water temperatures generally vary between 9 and 15°C. The upwelling is absent on the East coast, and water temperatures vary between 18 and 27°C: warmer in the north, cooler in the south.

## 14.2 The seashore

Strictly, seashore refers to the region landward of the sea, foreshore to seaward of the shore. However, in the following discussion 'seashore' has been loosely used to cover both.

The seashore is perhaps the most common region where concrete structures experience a very severe and adverse environment. It is also a region of great misunderstanding and technical mythology even among professional engineers. To understand the environmental impacts on concrete structures, a clear picture of the seashore region is essential. The following is a brief summary of the salient features of this region.

Notionally, the seashore is the region between the upper and lower limits of the reach of the waters of the sea, although depending on the relevant issues, it could extend well outside this zone. For this purpose, the limits are those commonly experienced and exclude extreme and rare occurrences, for example, tsunami. While these extreme events are relevant to the survival of coastal structures, the impacts are inevitably matters of hydraulic forces and structural strength, not concrete durability.

The region of the seashore with respect to any explicit aspect such as, for instance, the shoreline, is always a fuzzy zone. Not only are the traces of these aspects fractal in space, they are fractal in time as well. Any attempt to delimit a Euclidean boundary of an aspect of the seashore will always be an approximation, in many cases unacceptably approximate, and it can easily lead to apparent anomalies in concrete durability in the

seashore. Hence a good understanding of the seashore processes is needed when attributing zonation with respect to concrete durability.

The following is a brief listing of the various aspects of the seashore with particular reference to Southern Africa (Mackie, 2012).

### 14.2.1 Tides

The tides on earth are caused by the tidal forces of the sun and the moon, the first derivative of gravitational forces with respect to distance. They are proportional to the inverse cube of the distance. Despite the very small mass of the moon relative to the sun, its relative proximity to the earth means that its gravitational effect is about twice that of the sun. The situation is shown in Fig. 14.2.

Under the attractor, the effect of tidal forces is to draw up the closer fluid waters of the oceans under the sun and the moon into a bulge away from the more distant rigid body of the earth and, on the opposite side, to draw the rigid body away from the more distant fluid sea leaving another bulge on that side. This can be seen in Fig. 14.2.

In principle, the same effects occur within the substance of the earth, exacerbated at the shoreline by the fluctuating weight of the superimposed tide water, but for tidal purposes, the effect is trivial. It is worth keeping in mind, however, when doing precise levelling at the seashore as, for instance, in measuring settlements or in setting very precise heavy crane rails. Taking check readings a few hours apart to an accuracy of 10 μm (0.01 mm) is quite sufficient to detect this effect, which could confuse the readings if not understood.

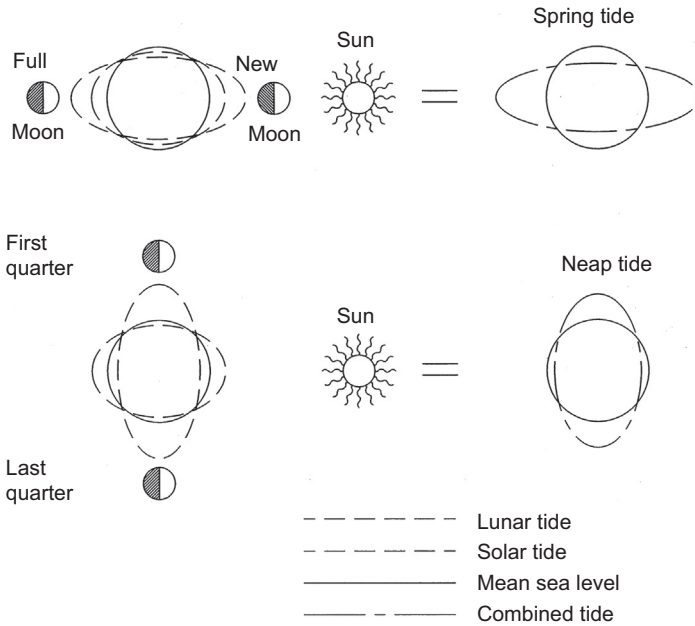



**Figure 14.2** The genesis of the tides.

The tidal periodicity follows the lunar day of approximately 24.8 h. As a result of the double bulge, the tidal period is a nominal 12.4 h from high tide to high tide. The spring−neap tide cycle follows the lunar month of approximately 29.6 days for a periodicity of a nominal 14.8 days from spring tide to spring tide.

Aside from this simplistic picture, there are a number of other, lesser astronomical, orbital parameters to take into account that complicate the tidal effects. While the primary effect remains dominant, the signal does appear to be very noisy, but as an astronomic artifact, it remains deterministic, and the whole pattern repeats with a periodicity of the approximately 18.6 year 'synodic' cycle.

In practice, the oceanic basins of the world contain the tidal bulges and force the waters of the sea to oscillate to the combination of the forcing of the tides and the natural periods of the basins. This has two prominent effects. First, it can bias the two tides of the day making one larger than the other. In some cases, the one tide can be completely suppressed so that in those parts of the ocean, such as the far Northern Pacific, there is only one tide each day. Second, it can distort the range of the tides. Generally, on open oceanic shores, the tide range is on the order of 1-m neaps to 2-m springs, but on some shores, notably the waters around the British Isles or in the Mozambique Channel, the tides can be extreme. Where the tide has been amplified by the restriction of a deep estuary, it can range up to 10-m springs and more as it does in the Severn Estuary at the head of the Bristol Channel.

The net effect of the tides is to impart an apparent instability to the level of the sea surface, the position of the waterline on the shore, and the concomitant degree of immersion/emergence of concrete structures on the seashore or the variability in their distance from the water. Fig. 14.3 gives an indication of the percentage of time a particular stage of tide or level is immersed or reciprocally emerged.

Published tide tables usually quote the stage of the tide as a height above 'chart datum'. This in turn is conventionally fixed at the level of the lowest astronomic tide (LAT) (see Fig. 14.4). LAT is the lowest tide at any particular site predicted by astronomic theory alone. Its use for tide prediction is the standard practice in Southern Africa and is used in this chapter.

Fig. 14.4 illustrates and defines the tidal parameters in standard use in Southern Africa. The reference to 'high water mark' in Fig. 14.4 needs some comment (Mackie, 2014). Strictly, it is a legal definition of property boundaries. On the Southern African coasts, it is intended to mark the maximum excursion of the swash during normal storms on a sloping shore. By implication, it applies to the storm swash occurring during mean spring high tide. This concept is not a tidal characteristic. It is a characteristic of the storm wave swash. It is relevant to corrosion as an indicator of the maximum reach of inundation of a structure by the sea.

### 14.2.2 Waves

The waves of concern on the seashore are the oceanic wind waves, but of the type known as gravity waves. Simplistically, the wind blows the water up into heaps and gravity pulls it back down again, and so the waves progress in the direction of the generating wind.

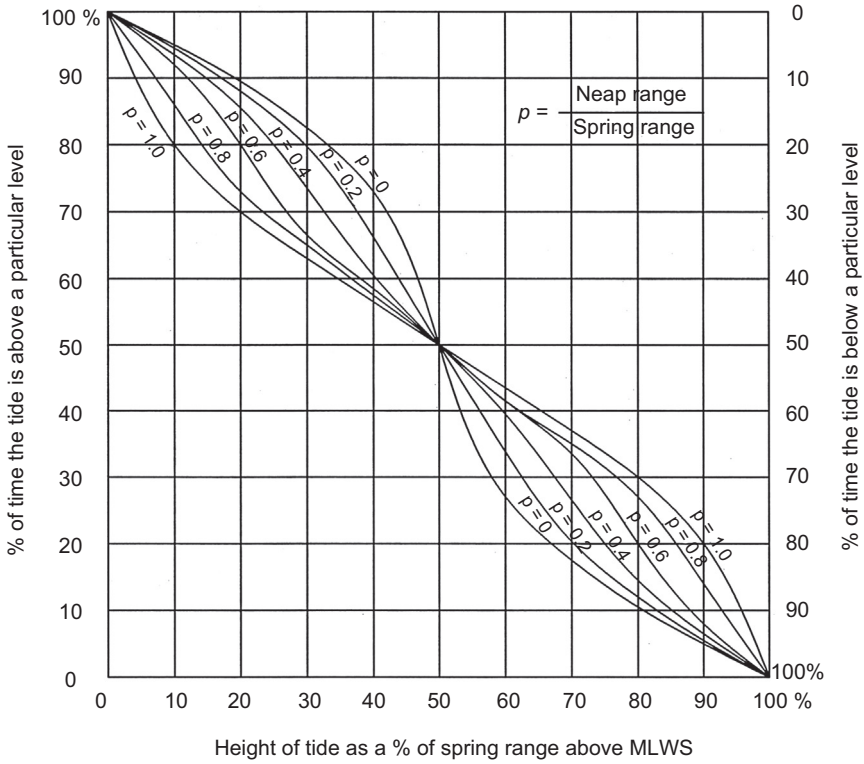



**Figure 14.3** Percentage of time a structural element in the tidal zone is immersed/emerged.

The simplest theoretical description of waves is a sine wave, a field of 'corrugations'. See Fig. 14.5. In practice, this sine wave description of oceanic waves is adequate for most purposes, except that a real sea is not just a single sine wave field. It is inevitably a complex of many such fields of differing wave period and often of different directions.

The wave length shown in Fig. 14.5 is generally represented as '*L*' and the wave height as '*H*'.

Unlike riverine and channel flow that is 'steady flow', wave motion is 'unsteady flow'. The water particles oscillate back and forth in orbits about a mean position, and in principle, there is no mean displacement of water.

In deep water, the wave motions dissipate at a depth of about half the wave length (see Fig. 14.6). The water depth has no effect on the wave celerity, the translational velocity of the wave crests. This is a function of only the wave period. As the wave shoals to a depth less than half the wave length, friction with the bottom slows down the wave motions at the bottom locally and, more generally, the celerity of the wave as a whole. At a depth of about one-twentieth of the wavelength, the celerity of the wave becomes a function of only the square root of the depth.

Note that the wave height (*H*) has no effect on the celerity of the waves. It is, however, a direct indicator of wave energy, which is directly proportional to the square of the wave height.

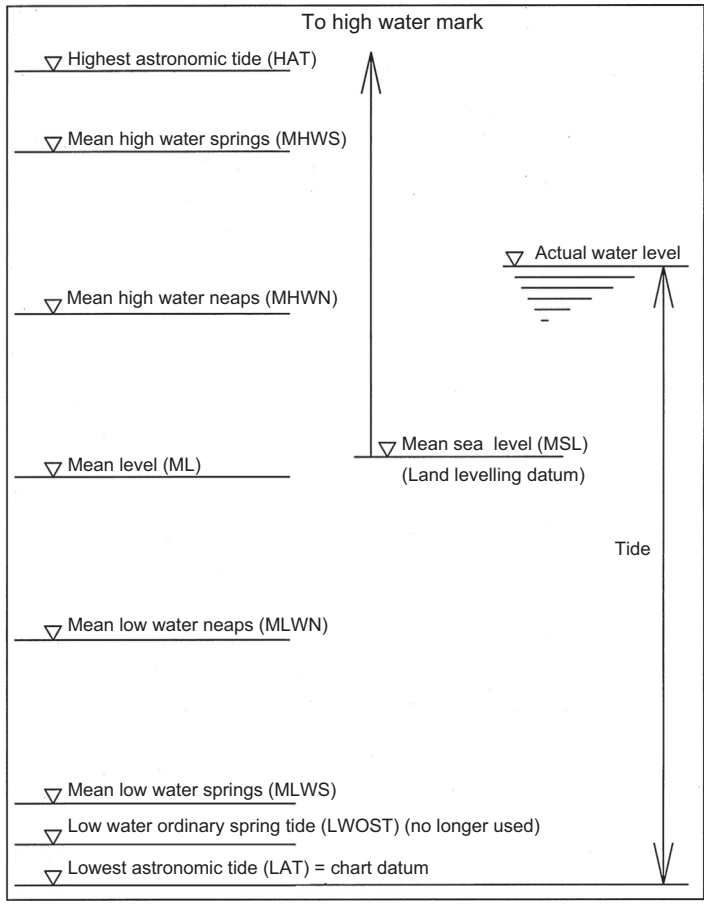



**Figure 14.4** The tidal parameters in standard use in Southern Africa.

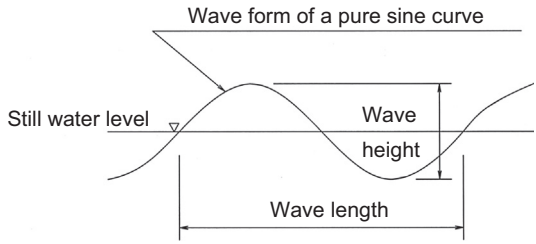



**Figure 14.5** Generic wave form.

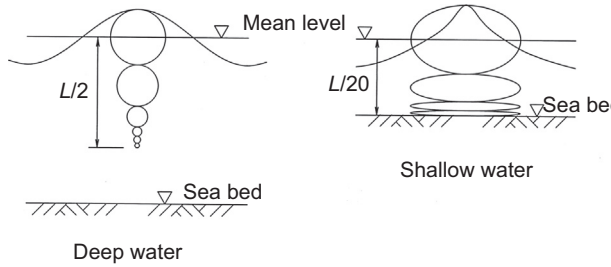



**Figure 14.6** Effect of water depth on water particle orbital velocities under a wave.

### 14.2.3 Wave shoaling: the process of moving into shallower water

Formally, waves break when the forward orbital velocities of the water particles exceed the celerity of the wave. This can occur in deep water as 'white horses' when the wave steepness (the wave height to wave length ratio) exceeds 0.142. In shoaling water, the equivalent occurs when the depth of the bed below still water level is less than 1.28*H*.

Overall, the shoaling process can be described by three zones:

- the wave: the unbroken shoaling wave
- the surf: the broken wave, effectively a moving hydraulic jump
- the swash: the run up of a thin film of sheet flow at first up the beach, and then back down again

There are two transitions:

- the breaker: between wave and surf
- the collapse: between surf and swash

The breaker region can vary from an extensive field of 'spilling' breakers where the breaker starts as a minor surf at the crest of the wave, gradually growing larger as the wave shoals, until it consumes the whole wave and becomes fully formed surf. Boundaries of this zone are not clearly defined. However, in the extreme, as the bed slope relative to the wave steepness increases, the whole process can be compressed onto a point on the wave trajectory where it becomes a 'plunging' breaker transitioning directly from a wave to surf.

The whole shoaling process is mediated by two parameters: beach slope, *m*, the tan of the angle of the beach slope to the horizontal, and wave steepness, the ratio of the wave height to the wave length, *H*/*L*.

In general, a flat seabed (low *m*) and steep waves (high *H*/*L*) lead to spilling breakers (Fig 14.7). As the seabed steepens (high *m*) and the wave steepness decreases (low *H*/*L*), the field of spilling breakers shortens, and the break moves toward plunging.

The surf, the hydraulic jump, moves forward over an underlying layer of water on the sea bed. The process of shoaling eventually exhausts this underlayer, and the surf runs onto the beach. At this point, it immediately senses the bed and collapses into a swash. It is as swash that the waters of the sea reach their maximum excursion onto dry land.



**Figure 14.7** Spilling breakers.

On some steep beaches, the break and the collapse can be concatenated. The wave can progress directly to this point, break as a plunging breaker directly onto the beach, and immediately collapse to a swash (Fig. 14.8).

On very steep beaches, generally with slopes in excess of around 1 in 3, the wave collapses directly to swash without any break, effectively a 'collapsing' breaker. The limiting condition is where there is a vertical sea wall in water deeper than the breaker depth of 1.28 of the wave height, when the interaction becomes a 'clapotis', complete reflection of the wave. The water level will rise up smoothly, without turbulence to a level somewhat exceeding twice the wave height, $H$. If the crest of the wall is below this level, it will overtop, and the sea will flood the areas behind the wall.

Note the ramp in the centre of Fig. 14.9 that has received the wave as a collapsing breaker with a significantly greater run up than the clapotis.



**Figure 14.8** Plunging breaker and surf.

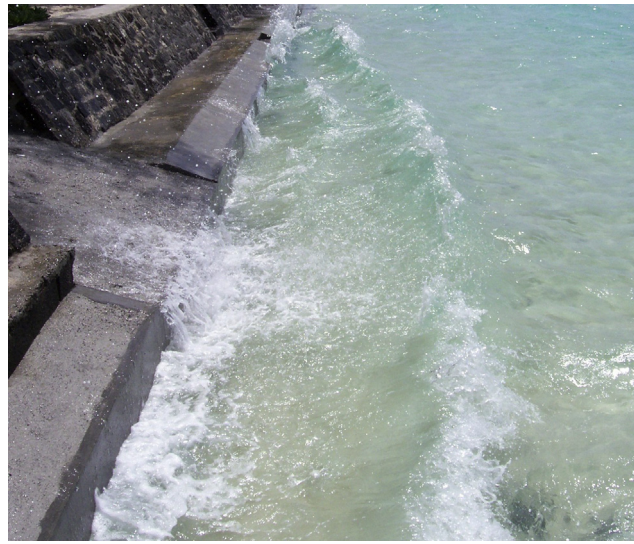


**Figure 14.9** Clapotis reflection.



**Figure 14.10** Bagnold explosion, Gansbaai breakwater.

In some cases of seawalls, the approaching wave can break directly onto the vertical face of the wall as a plunging breaker. The air trapped inside the 'tube' between the water and the wall is highly compressed. When the wave energy is dissipated, the air explodes violently sending up a plume of water, often in storm conditions, in excess of 30-m high, drenching everything around. This phenomenon is called a Bagnold explosion; see Fig. 14.10.

Ultimately, when the wind that creates the waves gets up in strength, it is capable of whipping spume off the sea onto downwind structures. This is particularly true for an



**Figure 14.11** Wind-whipped spray.

onshore wind blowing over the turbulence of the surf, particularly off the crest of a plunging breaker (Fig. 14.11).

### 14.2.4 Sea level

At the seashore, in addition to the tidal effects, the sea level is not constant. It varies with atmospheric pressure, generally a lowering of sea level of about 300 mm under extreme high pressure or a rise of about 300 mm under extreme low pressure, respectively. Storm surge – the effect of wind shear on the water – approaching a coast can also raise the water level. Common storms are usually associated with low pressure systems, so the combined effects can raise the sea level by the order of 1 m.

Wave set-up is perhaps the most significant factor in transient sea level change. The energy of the waves is dissipated in breaking, but the dissipation of the momentum of the waves requires a force acting seaward, against the forward momentum of the waves. This is supplied by the hydraulic gradient of the elevation of sea level on the shore. It commonly amounts to the order of 20% of the deep water wave height (see Fig. 14.12). For common storms with wave heights of 5–10 m, the wave set-up will be on the order of 1–2 m. In practice, the waves inevitably reach the shore in sets of higher and lower waves with a periodicity on the Southern African shores of around 2.5 min. The set-up of the waves can often be observed in small basins

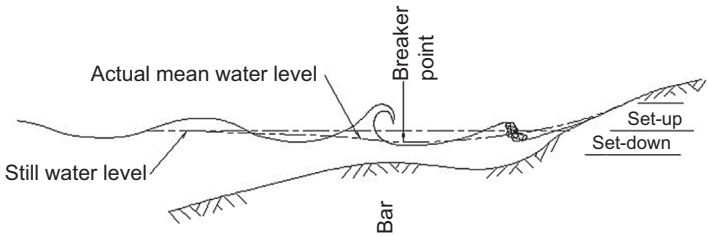



**Figure 14.12** Wave set-up.

on the shores of open, exposed coasts as a rise and fall of water level in the basin of about 2 m at this periodicity.

The excursion of the swash up the beach for normal swells and minor storms can be taken to be, very roughly, an altitude equal to the wave height above the sea level at the shore line due to set-up. The swash rides on top of the set-up.

### 14.2.5 Shoreline stability

Much of the seashore is formed of sandy beaches, and these only exist in equilibrium with the ambient wave field. The turbulence in the break, the surf and the swash are able to lift the sand grains into suspension as each wave passes and then redeposit them when it has passed, a process of saltation. Any particular wave field will keep moving sand around by this means until it reaches an equilibrium. At equilibrium, at each spot, a like amount of sand is deposited to the amount that was lifted. Considerable reshaping of a beach can take place this way.

One of the commonest features is the annual summer−winter beach. In winter, the storm waves erode the upper beach and redeposit the sand as a bar just seaward of the break to force the break. This reduces the impact on the shore until equilibrium is reached. In summer, the smaller swell waves weld the bar back against the beach by accretion. The net effect is to bring any structures built on the beach into direct contact with the seawater. This is illustrated in Figs 14.13 and 14.14.

Another effect is 'littoral' drift. Inevitably, the waves are not precisely aligned to the orientation of the shoreline. There will be a residual, shore-parallel component of the momentum of the incoming waves driving a very weak longshore current or 'littoral drift' in the surf zone. It has the effect of biasing the saltation of the grains of sand and causing the sand to drift downcoast in the direction of the shore-parallel



**Figure 14.13** Summer beach.



**Figure 14.14** Winter beach.



**Figure 14.15** Groin showing accretion and erosion.

component of the waves. (Note: the littoral drift is inevitably too weak to move sand itself. It merely biases the fall of sand grains lifted by the wave break.)

Any interference with this process will cause the sand to dam up, to accrete on the updrift side and erode on the downdrift side to keep supplying sediment to sustain the drift; see Fig. 14.15.

Where this occurs at natural headlands, often the wind will pick up the surplus sand on the updrift side and march it across the headland in a bypass dune field. On the downdrift side, it will resupply the beach. In many cases, these bypass

dune fields have been artificially stifled, resulting in the erosion of the downdrift beaches. A good example is the great dune of Hout Bay in the Cape Peninsula. It has been stifled of sand on the updrift side by urban development. It is now starved of sand and deflating.

### 14.2.6 Zonation

Issues of corrosion and durability of construction materials such as concrete are very dependent on the location of the elements or structures relative to the seashore. In some cases, the behaviour of different materials with respect to their position relative to the water may also vary according to the material. Durability issues are commonly at their worst where the elements are partially or intermittently immersed in sea water, the severity falling off with distance from the water and from the seashore. In this marine zone, the patterns of variation of aggressivity to concrete structures become extremely complex.

It is not uncommon to see texts dealing with marine corrosion or durability drawing contours of intensity at fixed offsets from the coast, all without attempting to define the zero point. These commonly give horizontal offsets of say 100 m, 500 m, 1 km, 5 km, etc. As described in the foregoing sections, any physical zonation will be a 'fuzzy' zone, any boundary will be fractal, and they only make sense in this context. Attempts to interpret these in terms of Euclidean geometry as, for instance, the high water mark, will always be strictly invalid and can result in significant error.

Corrosion intensity can vary by orders of magnitude within a metre, particularly around corners. At times, it can remain virtually constant at peak intensity for a long way inland. The town of Walvis Bay (Namibia) is built on fine grained, wind-blown marine sediments with a salt content of around 10% and perpetual, heavy night fogs from the sea. The corrosion intensity remains at substantially seashore intensity throughout the town for over a kilometre inland.

Marine organisms that populate the seashore seem to respond to the same water level changes that affect concrete durability. As residents, their behaviour integrates the overall effect of the water level changes and makes an excellent indicator (Stephenson and Stephenson, 1949; Griffiths, 2015).

Two particular cases stand out:

- The upper balanoid zone. This is the zone of closely packed, small star barnacles (*Chthamalus dentatus*), white to grey in colour, that terminate on a clear line at the neap high water level.
- The littorina zone. This is the zone populated by small periwinkle snails (*Littorina*). It lies above the upper balanoid between neap high water level and the limit of splash wetting above the spring high water level as indicated by the limit of periwinkles. In practice, the density of the periwinkles toward and above the spring high water level falls off until there are no periwinkles left. Hence, the upper boundary of this zone tends to be poorly defined.

Although these two zones are biologically determined, they seem to be very consistent, easily observed in the field, and consistent with the hydrography of the tides (see Fig. 14.16). It remains, however, to confirm formally that they are relevant to concrete durability.

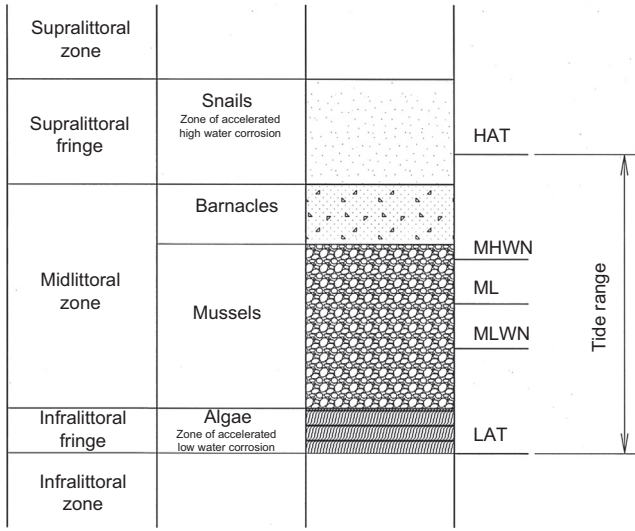



**Figure 14.16** Biological tide level zones.
After Stephenson and Stephenson, 1949.

The structure in Fig. 14.17 was built in the mid-1970s and, at the time of the photo, about 40 years later, is free of signs of visible corrosion. It is notable, however, that there are no snails in the littorina zone anywhere in this harbours. The snails are completely absent. Although the underwater portion around LAT is not clear, it seems to indicate the algal growth of the *infralittoral fringe*.

The permanently immersed portions of steel structures have recently been found to exhibit 'accelerated low water corrosion' (ALWC) (PIANC, 2005).

ALWC occurs in the infralittoral fringe region close to the LAT position (see Fig. 14.16). This region is almost permanently immersed in water with a high dissolved oxygen content leading to a narrow band of intense growth of algae and sessile organisms. The intensity is sufficient to create an anaerobic condition underneath the growth at the contact with the steel that supports anaerobic sulphate reducing bacteria that attack steel (see Fig. 14.18.)

By contrast, reinforced concrete structures, either permanently immersed in seawater or surface-piercing, are generally free of corrosion damage in the permanently submerged zone and unaffected by biological activity. However, above the balanoid zone, they experience elevated levels of corrosion intensity starting in the supralittoral fringe and extending into the supralittoral zone (see Fig. 14.19). This has been described as 'accelerated high water corrosion' (AHWC) (Mackie, 2008a). It generally falls off quite rapidly higher into the supralittoral zone to more ambient levels of corrosion intensity.

On sloping concrete ramps, a different regime seems to apply. Here, green algae seems to be the only growth extending through the midlittoral zone on the sloping surfaces, but see Fig. 14.20.

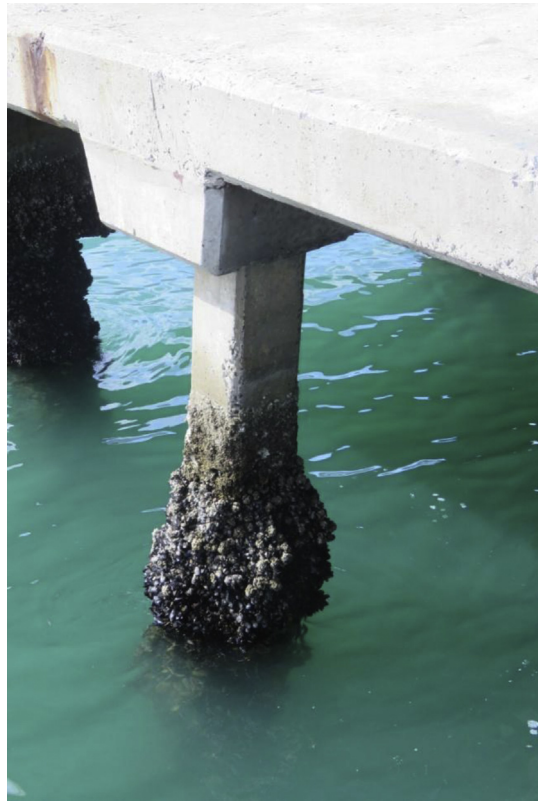


**Figure 14.17** Marine growth on a concrete pile in Hout Bay. Photo taken at spring low tide, 2015.



**Figure 14.18** Steel exhibiting 'accelerated low water corrosion'.



**Figure 14.19** Typical AHWC to jetty cope wall and pile cap ends.



**Figure 14.20** Slipway, Hout Bay harbor.

Common usage for the regions above high spring tide is the 'splash zone'. The best that can be said of it is that it seems to concatenate the idea of physical splash, which corresponds to the upper reaches of the supralittoral zone, and the saline aerosols, which are windborne well above and well inland beyond this zone. The splash zone is a concept that is undefined and is best abandoned.

Corrosion due to wind-born saline aerosols in the supralittoral zone that can reach quite some distance from the seashore is very real (see Fig. 14.11). However, the expression of this effect is very erratic and locality dependent.

In principle, plant communities can act as indicators of saline aerosol distributions onshore. Botanical research on this is ongoing, but it seems that the factors are not just salt but also the organic and mineral content of the aerosols, the soil types, the geology,

and possibly other factors. While zonation of plant communities does occur with respect to the proximity to the sea, for the present, this does not seem to be a usable method of zonation for assessing concrete durability (Verboom, 2015).

## 14.3 Case studies of selected small harbour structures, or constructions of limited size

Concrete structures in small harbours or other structures of limited scale built on the coast represent a wide variety of ages, types, exposures and competence in their design and construction. Some represent best practice at the time of their construction, while others have been constructed by a local artisan, in some cases using sea water to mix the concrete. The samples given next, of the population of these structures on the coasts of Southern Africa, illustrate a wide variety of strategies used in their construction.

### *14.3.1 Reinforced concrete 'marina' floating moorings at Durban Point Yacht Club*

This system of floating moorings or 'marina' was built between 1988 and 1990 in the waters of the Port of Durban in the mooring area allocated to the Durban Point Yacht Club (DPYC) on the esplanade. The walkways were constructed of reinforced concrete. The design consisted of 6 × 2-m walkways and 7 × 1-m yacht 'finger' moorings and a number of specials. Each was formed by 156 × 76 channel iron frames, flanges pointing outward, with reinforcement spanning the interior at mid-height and welded to the containing frames, the whole hot-dip galvanised. The frames were then filled with 40 MPa concrete (Gowans, 1990) (although no information is available on details of the concrete mix, particularly with respect to its ability to form a durable structure).

The project was thoroughly engineered, and the structure was very successful and lasted until recently. A publication on the project at the time of construction stated:

> *The marina has provided an affordable enhancement to the leisure facilities in Durban and should act as a catalyst for similar developments elsewhere in the Republic.*

The project was well publicised and was soon copied in other harbours, albeit with varying quality of engineering and varying methods of anticorrosion protection for the steel components including the concrete reinforcement. One of these was a large marina built for a syndicate under the aegis of the Atlantic Boat Club in Hout Bay in the Cape Peninsula.

None of these other reinforced concrete marinas gave the same life expectancy; deterioration by corrosion of the reinforcement and the steel frame at the contact with the concrete occurred within less than 5 years. The installation in Hout Bay began to fail before the project was even completed. All of these marinas have now been replaced.



**Figure 14.21** Durban concrete marina (ca. 1989).



**Figure 14.22** Hout Bay concrete marina (ca. 1991).

The overriding impression is that, unlike the Durban marina, these others were not subject to proper marine engineering design. In the case of the Hout Bay marina, the only anticorrosion protection to the steel frames and reinforcement was provided by an inadequate paint coating.

In general, corrosion was not treated seriously in these other cases, presumably due to the default attitude that 'if it worked in Durban, it must work anywhere else', an attitude fostered by the comment, in 1984, in the context of the same site,

> *Durban is notorious for having one of the worst corrosive climates in the world.*
> *Anon (1984).*

This misconception was exacerbated by the publication in 1988 of the results of BG Callaghan's 20-year corrosion exposure trials at various sites around Southern Africa. It was an exemplary study in all respects except for explicit information on the locality of the various sites. He had one site in the middle of Durban Harbour and another labelled 'Durban Bluff' without further emendation. It was this latter that gave exceptionally high corrosion rates supporting the 1984 comment (Callaghan, 1988).

Further enquiry disclosed that the 'Durban Bluff' site was on the outer, oceanic side of the bluff at the edge of a rocky shore and exposed to the prevailing onshore wind and to splash from breaking waves, a very corrosive environment. The attribution of the 'Durban Bluff' corrosion exposure to the DPYC marina site where the corrosion exposure was, in fact, mild was completely inappropriate. Ultimately, this misconception was a significant factor in the cause of the failure of the other marinas that were installed at sites where the ambient corrosion intensity was much more severe than the DPYC site, particularly the Hout Bay site.

## 14.3.2 Sea Point Seawall, Cape Town

### 14.3.2.1 History

Although some construction started on the Sea Point Seawall on the Atlantic seaboard of Cape Town, close to the city centre, prior to 1924, the greater part of the wall was built between 1924 and 1940. It has an unusually severe marine exposure. Although some stretches are relatively protected, notably a stretch in the mid-regions at the head of a beach, much of it is exposed to the full fury of the South Atlantic with storm waves breaking directly onto the wall (Gates, 2015); see Fig. 14.23.

In general, the wall has a mass concrete core founded on exposed bed rock close to low tide elevations, in the case of gullies, below low water. The area behind the wall



**Figure 14.23** Sea Point Seawall under storm attack.
Courtesy Ingerop.

was reclaimed initially as a landfill, then topped with earth fill, and finished with lawns and walkways. The sea front of the wall was faced with stone masonry to protect the concrete. The stone was quarried on site and reflects the three rock types along the wall: greywacke, sandstone of the Table Mountain series and Cape granite, although this last at the northern end of the wall may have been imported from roadworks elsewhere. It was capped with a reinforced concrete cope. The total length of the wall is about 5 km.

A comprehensive visual survey of the wall was made in 1995, largely limited to the condition of the stone facings. Two primary issues were identified:

1. The mortar pointing was the underlying weakness in the stone facing, allowing the storm waves to erode the jointing and pluck out patches of stone.
2. The city council (Cape Town) had no dedicated coastal engineering department and, at various times, allocated the maintenance of the wall to various other departments, notably, at times, roads and, later, amenities.

Phase 1 of the work of renovating of the wall commenced in 2011 with construction taking place largely in 2013.

### *14.3.2.2 Balustrades*

The original concept for the balustrades was for concrete stanchions with hand-railing of steel tubing passing through the stanchions. This concept has been retained in the renovation of the wall.

The original stanchions were of reinforced concrete and were subject to severe corrosion. In areas of severe wave attack and overtopping, the corrosion was particularly severe and was and still is accompanied by abrasion of the surface of the stanchions.

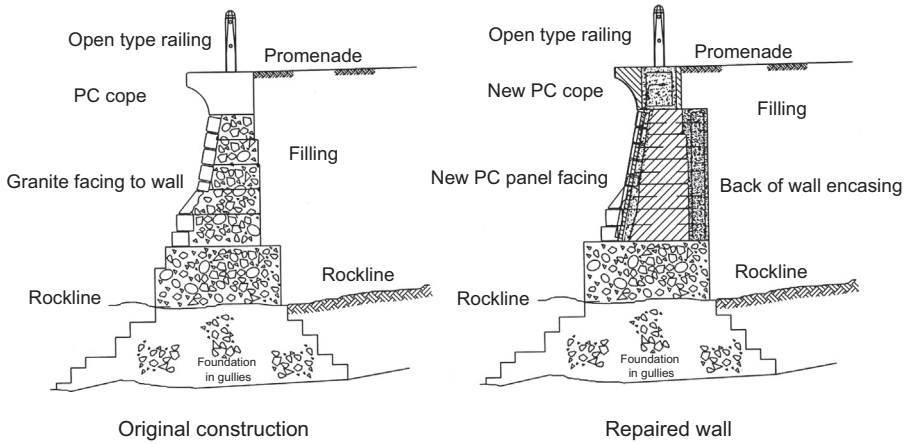



**Figure 14.24** Sea Point Seawall: original construction and repaired wall. Courtesy Ingerop.

In its original form, this design solution was both simple and practical. The stanchions were treated as consumables to be replaced at intervals as they deteriorated. They were set in pockets in the cope with a weak grout and could be easily replaced. No special provision is made to control corrosion in either the mix design of the concrete or in the reinforcement. They were replaced as they deteriorated. Judging by minor changes in the detailing and the localities of the different types, the average life of a stanchion is probably around 20 years. There are places, relatively protected, where the stanchions look very old, possibly original.

Hand-railing was supplied by $\phi$50 galvanised steel water pipe, also treated as a consumable.

The system is best described as 'low tech' and works very well.

For the renovated wall, the concrete stanchions were retained, but the steel reinforcement was eliminated, and polypropylene fibre reinforcement was mixed into the 40 MPa concrete. The galvanised steel hand-railing has been replaced by stainless-steel tubes filled with grout to prevent them being sawn off by vandals (see Fig. 14.25).



**Figure 14.25** New, fibre reinforced concrete stanchion.
Courtesy Ingerop.



**Figure 14.26** Exposed existing wall.
Courtesy Ingerop.



**Figure 14.27** Back of seawall showing buttresses and shutter board marks.
Courtesy Ingerop.

### *14.3.2.3 Original wall structure*

The actual construction and condition of the original wall is shown in Fig. 14.26. This shows remnants of the original granite facing with fresh pointing and regions of facing patched with a random selection of recycled stone. More significant though is the exposure of the interior of the original concrete. It is packed with 'plums' of waste rock as a displacer, a means of economising on cement, a practice common in the late 19th to early 20th centuries for mass concrete work.

In general, the contact between the base pour and the rock was found to be watertight, that is, free from leakage through the wall. However, in many cases, the contact between successive lifts of concrete was often poor and allowed ingress of seawater. Presumably, this was at partial to full tide and particularly severe under impact pressures from breaking waves. Fig. 14.28 is a close-up of such a section of wall.

The cope units were precast with a large central gap both to cast in the units and to provide pockets for the stanchions. These units were of 40 MPa concrete, with a 50:50 Portland cement/slag blend as the binder.

Restoration of the front of the wall was by precast reinforced concrete panels, 50 MPa with a 50:50 Portland cement/slag blend, preformed to a facing of faux stone. '*L*' dowels were grouted into the existing wall to mate with reinforcement protruding from the back of the panels, and the gap of 200−300 mm between the panels and the wall was filled with infill concrete, 40 MPa with pure Portland cement as binder.

It will be interesting to see how the faces of the precast panels stand up to the attack of the sea as compared to the original granite facing, pointing notwithstanding.

### 14.3.3 Coastal buildings and small structures

Building works close to the sea rarely take account of the special needs of reinforced concrete construction in this environmental exposure zone. Work is usually done according to the local trade practices as applied in the wider hinterland far from the



**Figure 14.28** Back of leaky wall.
Courtesy Ingerop.



**Figure 14.29** New precast cope units placed ready for casting in. Courtesy Ingerop.



**Figure 14.30** New precast facing and cope units. Courtesy Ingerop.

sea. Early deterioration of reinforced concrete building works close to the seashore is very common and contrasts strongly with associated brick and mortar work, which is usually quite durable.

#### *14.3.3.1 Hout Bay (Cape Peninsula)*

The structure in question is a workshop, about 100 m from the quayside, which in turn is about 400 m across the harbour to the breakwater. The dominant, dry, summer south-easterly wind blows across this reach, often at gale-force strength, onto the building (Evans, 2015).

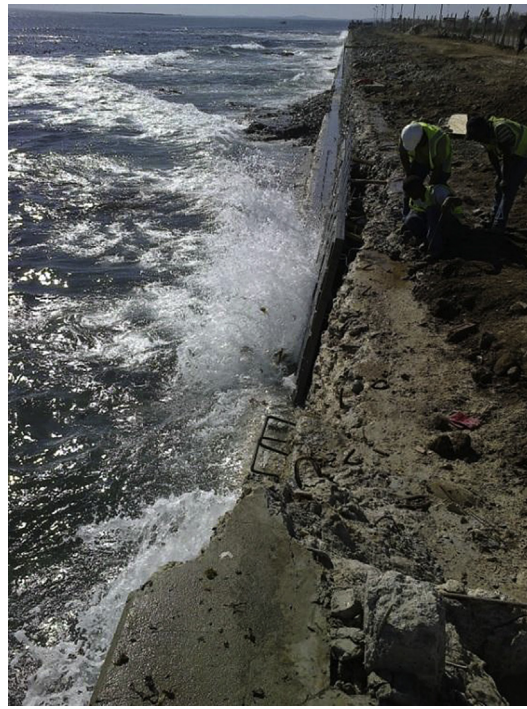


**Figure 14.31** Sea Point Seawall: working conditions for placing re-facing panels. Courtesy Ingerop.



**Figure 14.32** Restored promenade. Courtesy Ingerop.

The structure was a design/build project constructed in 1981−82 as a workshop with offices above by the building division of a large construction company. The design, however, is explicitly nonmarine. The resulting corrosion in the columns is the result of a combination of inadequate design/construction and the very severe exposure to wind driven saline aerosols; see Fig. 14.11. This case is a good example of the importance of identifying the exposure conditions in which a structure must operate and designing accordingly. It is notable that the steel cladding used elsewhere on the structure is as much impacted as the reinforced concrete work; see Fig. 14.33. Of course, construction quality in order to realise the needed durability is equally important.

#### *14.3.3.2 Walkway columns at water's edge: Grand-Baie, Mauritius*

The provenance of these columns is unknown. However, except during the rare event of a cyclone, the sea conditions inside the bay at the site are best described as 'placid'. Nevertheless, Fig. 14.34 shows severe deterioration of the reinforced concrete columns, and it seems to reveal inadequate cover to some of the steel. The concrete materials are also likely to have been ineffectual in arresting ingress of chlorides, even in this relatively mild exposure. The condition of these walkway columns simply reflects inappropriate local trade practice − in effect, normal building practice as used universally in the interior of the island.

### *14.3.4 Guano Island landing stage*

The offshore islands along the West Coast of Southern Africa between Cape Town and Walvis Bay are rich in guano. The original guano deposits were worked and cleared during the 1840s. Subsequently the islands were and still are scraped every year for



**Figure 14.33** Hout Bay workshop.
Photo 2015.



**Figure 14.34** Walkway columns, Mauritius.
Photo 2008.

their annual deposit of guano, and landing stages are needed for this activity. The style of construction generally used, as shown in Fig. 14.36, seems to have originated in the late 19th to early 20th century. It consists of a circular concrete casing in which is embedded sections of scrap railway line as reinforcing. There are signs on some of the islands of multiple rebuilding of these landing stages. The most recent work appears to have been done in the 1950s and 1960s. Fig. 14.35 is a good example of one of these landing stages: the landing stage on Meeuw Island in Saldanha Bay.

The provenance of these structures is almost entirely unknown except for rumours that the later structures were built by a blacksmith from the fishing village of Gans Bay.

### *14.3.5 Quays and jetties (wharfs and piers) in the South African and Namibian fishing harbours*

The structures discussed here are those primarily intended for the berthing of ships and boats. They are constructed over water and are structurally closely related to bridge engineering. Durability issues and construction techniques arising from these structures are often reciprocally relevant to bridge work in tidewater.

Note on provenance of structures: the structures in the fishing harbours were largely constructed by a dedicated engineering department of the erstwhile Fisheries Development Corporation. Unfortunately, as a result of bureaucratic shuffling of public service offices, the corporation together with the engineering department was closed. As a result, much of the provenance of the older structures has been lost or is unavailable. Details given here for the structures, such as they are, are from the personal records or recollections of the author (Mackie, 1999, 2008b).

Note on cement and reinforced concrete used: the 1960s in Southern Africa was a period of relatively intense marine construction. In response, one of the Cape Town



**Figure 14.35** Guano Island landing stage.
Photo ca. 1983.

cement manufacturers developed a synthetic pozzolanic cement using a burnt shale as the pozzolan. It was named 'Cemarine' and was intended for this activity. A significant number of the reinforced concrete marine structures in the commercial ports, in the small harbours, and in at least one freeway bridge were constructed during this period using this cement.

Note on design standards used: at the time, these quay and jetty structures were designed to British Standard CP 114 (1957), using the elastic method with 50-mm nominal steel cover. After 1970, its use was ameliorated in the fishing harbours by British Standard CP 2007 (1960) treating all faces as wet faces. The object of this latter was to introduce crack control by limiting tensile stress in the concrete and thereby improve the impermeability of the concrete.

By the early 1970s, the marine construction activity levels and use of Cemarine had dropped, prices increased, and the use of this cement and its manufacture ceased. The reinforced concrete structures for the 2000-ton Syncrolift shiplift in Walvis Bay built in 1972−73 were the last of these structures to use Cemarine cement. Thereafter, marine structures in small harbours were designed to the newly issued CP 110 (1972) (and its successors) using ordinary Portland cement (OPC), which from a durability perspective was unfortunate, given the inherent lack of resistance to chloride ingress of OPC.

Notwithstanding these points, and although these structures date to between the mid-1960s and the late 1980s, it is surprising that there is not more corrosion evident. In general, these structures have shown adequate durability. Even at that stage, however, although the state of the art was not as well developed as it is today, concrete

durability was taken very seriously both in design and in on-site quality assurance. Mix designs were done by the local laboratories of the Portland Cement Institute of South Africa (now closed) on behalf of the contractors. Minimum cement contents were always specified for the various mixes, as was the practice then using prescriptive specifications. There was always an engineer's representative resident on site, either an engineer for larger projects or otherwise a technician. A client-owned concrete cube test machine was always provided in the site representative's office. Doubtless, the presence on site of competent personnel went a long way to ensuring high-quality construction.

### *14.3.5.1 Typical fishing industry berthing structures*

These are typically column, usually pile, beam and slab structures, all in reinforced concrete, with raking piles or columns to absorb berthing impacts, together with cope aprons to carry the fenders. Typical examples are given in Figs 14.36 and 14.37.

Columns and piles were almost inevitably of precast concrete. Some piles were in reinforced concrete, while others were prestressed. Reinforced concrete decks were often cast in situ, but various ingenious methods were devised to use precast elements for this component. Sometimes, these elements were used to serve as both permanent shutters and part of the permanent structure; sometimes they formed the whole of the deck structure and acted as staging as construction progressed.

It is common to use precast beam units as a permanent soffit shutter to the berthing aprons. Generally, precast elements are favoured in that there is better quality control in their manufacture as compared to casting in situ in or over the sea. It is also, generally speaking, easier to place precast elements than to cast concrete in situ, either in or over water.



**Figure 14.36** Typical quay structure, built ca. 1968. Photo 2008.



**Figure 14.37** Typical jetty structure, built ca. 1968.
Photo 2008.

Concrete strengths were generally about 25 MPa for reinforced concrete and 42 MPa for prestressed concrete.

### *14.3.5.2 Deck and cope*

Given that throughout Southern Africa the spring tide range is generally about 2 m, that is, a spring high tide to about +2.0 m LAT and spring low tide to 0.00 LAT, it is practical to build fixed berthing structures for most craft from 10 to 75 m in length, such as fishing vessels, offshore oil service vessels, etc., instead of using floating berthing structures. Since these structures have a relatively low freeboard, their decks (typically of reinforced concrete) are often wetted by offloading of wet fish or nets, wind splash or spray, washing down with sea water and many other causes. As a consequence, they typically show quite intense reinforcement corrosion, often worst nearest the cope. These features are shown in Figs 14.38 and 14.39.

### *14.3.5.3 Enclosed deck soffits*

In many cases, reinforced concrete quays and jetties (wharfs and piers) are built with berthing aprons that extend to well below mean tide level to support the fendering. The enclosed spaces within these structures contain unique microclimates. The concrete surfaces are protected from direct sunshine, and the enclosures maintain a virtually constant 100% relative humidity. Generally, the interior surfaces of these structures are free from overt signs of corrosion. This is well illustrated in Fig. 14.40, which shows the underside of a deck element to the shiplift support jetties in Walvis Bay Harbour on the west coast of Namibia. Despite its relative age (33 years at the time of photographing), there are no signs of corrosion or corrosion damage on the deck soffit. In addition, the concrete is in a uniform and constantly saturated state. Thus, the absence of corrosion is



**Figure 14.38** Corrosion in quay deck, built 1968 (misguided attempt at repair in 1978).



**Figure 14.39** Corrosion in cope, built ca. 1968.
Photo 2008.



**Figure 14.40** Deck soffit, Walvis Bay, built 1972, free of corrosion.
Photo 2005.

an indication that the other essential element for corrosion, oxygen, is not available in sufficient quantities at the steel to sustain active corrosion. Therefore, soffits of these structures act more like fully submerged structures than exposed structures.

#### 14.3.5.4 Sheet pile bulkheads

Concrete sheet piles, both reinforced and prestressed, have sometimes been used for bulkheads, for quay walls or for vertical breakwaters. They have generally given good service. Fig. 14.41 shows the sheet pile wall of the North Mole to Hout Bay Harbour built in the mid-1960s. This photo taken at spring low tide shows the full tide range. The upper and lower bounds of the balanoid zone show clearly. The concrete shows no signs of corrosion (aside from a small spot, probably a construction error).

### 14.3.6 Simonstown Municipal jetty, Cape Peninsula

This is arguably the oldest marine reinforced concrete structure in Southern Africa, built ca. 1920 (Mackie, 2010).

The deck and supporting grillage of horizontal beams are of conventional reinforced concrete construction. The substructure, however, has been built in the style of a framed and braced structure. A general arrangement drawing of the jetty is given in Fig. 14.42.



**Figure 14.41** Sheet pile wall of North Mole, Hout Bay. Photo 2015.

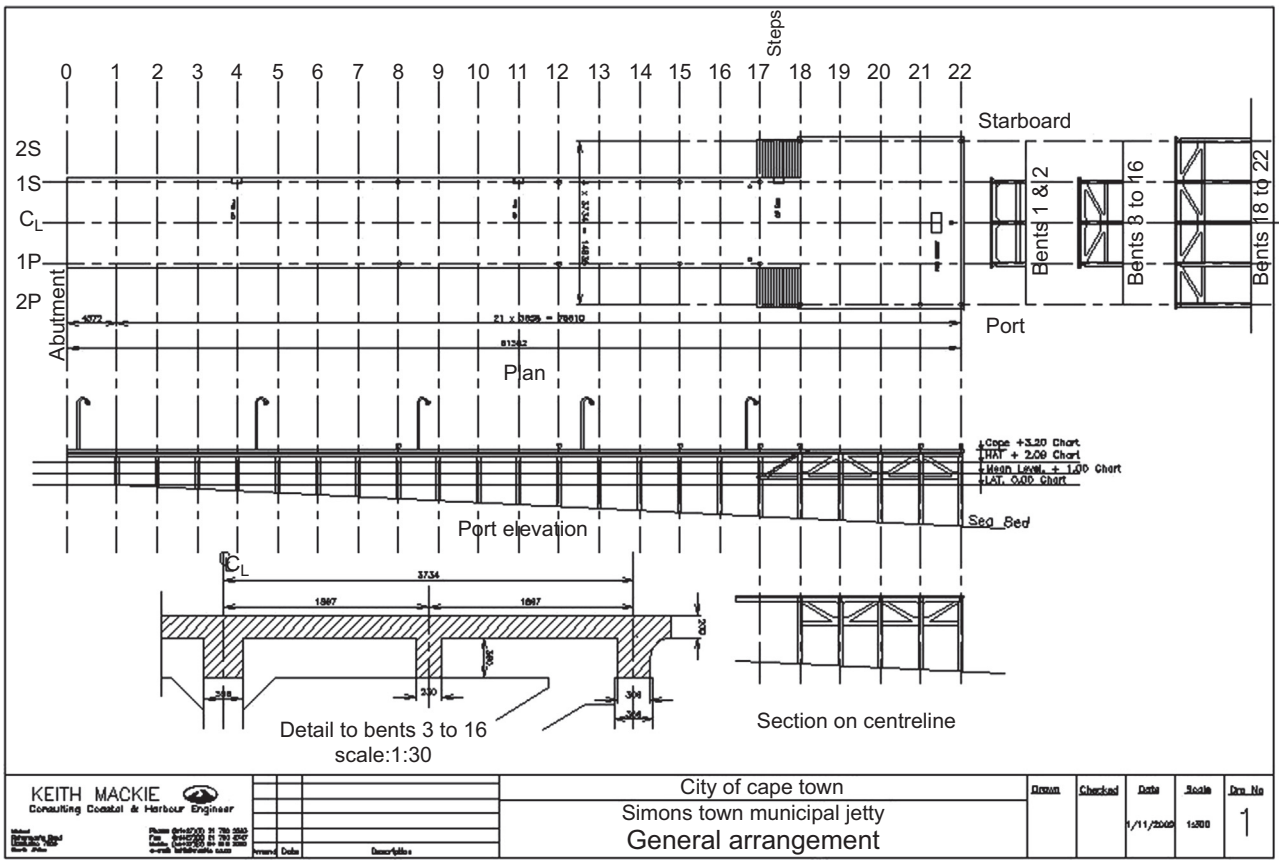



**Figure 14.42** Simonstown jetty general arrangement.

The design and construction of the original structure had several redeeming features, which meant that it was still in a repairable state after more than 75 years of service. These include fairly good and consistent cover depths being achieved in the structure at roughly 2 in., well-compacted concrete, and older cement probably better able to bind chlorides. Another feature of the jetty is the relatively sheltered location, which is not typical for such structures.

Tests on the original concrete in 1996 gave a strength of 25−35 MPa for the columns and raking members. Carbonation was minimal for such an old structure, of the order of only 10 mm, due to the high humidity and moist conditions preventing ingress of carbon dioxide into the concrete. However, chlorides had penetrated to the reinforcement, and much of it had been reduced to 50% of original cross-sectional area. In fact, chloride penetration was so deep that extrapolations of measured chloride profiles would have meant it was impossible to break back to uncontaminated concrete in most structural elements exposed to tidal or splash action.

Being such an old structure, the reinforcing was round, mild steel rod, while the concrete would have been batched by volume and mixed and placed by hand. Almost certainly, the cement would have been a 'plain' cement, probably rich in $C_2S$ and fairly coarsely ground. This would have given fairly low strength initially, but considerable reserves of both strength, density and impenetrability with time, as evidenced by the aforementioned strengths.

A patch repair system had been implemented in 1989 by exposing the corroded reinforcement, cleaning it, and giving it a zinc-rich primer coat, and then patching with patented cementitious grouts. However, this repair system was not successful, not least because contaminated concrete in the vicinity of the rebar had not been cut out properly. This points to a frequent and fundamental misunderstanding of repair of chloride-induced corrosion damage, where no amount of breaking out and substrate preparation can prevent the immediate formation of incipient anodes at the repair interface.

Therefore, a comprehensive restoration project was implemented in 1996 based on the following:

- cutting out and removal of all cracked and spalled concrete
- removal and replacement of severely corroded individual steel rods
- retrofitting of an impressed current CP system
- shotcreting the substructure to reinstate the concrete and cover the CP system

The shotcrete, for making good the cover and restoring some of the structural integrity of the structure, used a relatively small aggregate size (13-mm max) and contained silica fume as a cement extender, both to assist in 'grab' of the mix onto the substrate and for durability reasons. In general, strengths of this sprayed concrete were in excess of 50 MPa.

The CP system required regular monitoring. Unfortunately, shortly after the restoration was completed, the owner (the Simonstown municipality) was absorbed into the Cape Town City Authority. All records were transferred, and the CP monitoring contract lapsed. However, even before this, the CP cables had been cut by electrical

contractors installing lighting, and theft of submerged zinc anodes had occurred. The end result was that regular monitoring and possible remedial actions were not undertaken.

Figs 14.43 and 14.44 show photographs of the jetty in 2009, some 13 years after the comprehensive repairs of 1996. The repaired sections with a relatively smooth surface (shotcrete) can be clearly seen. Unfortunately, there is some evidence of ongoing



**Figure 14.43** Simonstown jetty landward end.
Photo 2009.



**Figure 14.44** Simonstown jetty seaward end.
Photo 2009.

corrosion in some of the elements, doubtless because the needed CP system was not properly operated. There had been no attempt to remove all contaminated concrete in 1996, only the spalled and corrosion-damaged concrete. Therefore, there would have been considerable portions of the structure that would have retained chloride contaminated concrete, and this has largely caused the corrosion seen in the figures.

### 14.3.7 Port Nolloth jetty, West Coast of South Africa

This structure was apparently built in 1946–47 and designed to carry narrow-gauge (ca. 600 mm) steam locomotives and a 10-ton rail-mounted crane. It is carried on reinforced concrete piles driven to bedrock with transverse pile caps to carry the deck slab. The structure has raised cope walls to contain about a metre depth of fill above the slab. This fill carries the rail track and distributes the locomotive loads to the support structure below.

Given the level of concrete technology at the time and the age of the structure, its survival to the present, some 70 years, is quite amazing. Notwithstanding the comments in Section 3.5.3 (enclosed deck soffits), the exposed deck soffits of this structure are now showing quite severe signs of corrosion. However, the upper surfaces under the fill have been completely protected by the fill and show no signs of corrosion (Fig. 14.49). The exposed faces of the fender aprons and the pile cap beams are showing extensive corrosion. See Figs 14.46–14.49.

Note: the soffit in Figs 14.47 and 14.48 does not form a fully enclosed space, having a downstand fender apron on only one side.

Given the extensive corrosion to the existing structure, a notable feature is the wide variability in the intensity of corrosion over different parts of the structure. Fig. 14.46 (see also Fig. 14.19) shows significant corrosion of the outer face of the cope wall. This is the landward side. Although the presence of a large vessel



**Figure 14.45** Port Nolloth jetty.
Photo 2009.



**Figure 14.46** Port Nolloth jetty landward apron.
Photo 2009.



**Figure 14.47** Port Nolloth jetty: typical soffit and beam (pile cap).
Photo 2009.

made it difficult to inspect the seaward side, the levels of corrosion to the cope wall face did appear to significantly less than the landward side. It is germane to ask whether this is the result of differential exposure to the prevailing winds – unlikely since they would be dominant on the seaward side – or is it an artifact of sheltering by the vessels berthed on that side? As a further possibility, is there any substantial difference in the quality of the concrete and the construction on one side as opposed to the other? In the absence of a proper investigation, it is difficult to answer these questions. However, it does illustrate a point made earlier, that of the importance of understanding microclimates or micro-exposure zones of marine structures when it comes to design. The soffit and beam corrosion shown in Figs 14.48 and 14.49 also varies widely between different panels.



**Figure 14.48** Port Nolloth jetty: typical beam end.
Photo 2009.



**Figure 14.49** Port Nolloth jetty: upper surface of deck and upstand beam exposed in inspection pit. The rust spot on the right appears to be the result of a steel drain hole through the slab.
Photo 2009.

### *14.3.8 Lamberts Bay diamond quay, West Coast of South Africa*

This structure was built relatively recently, in 1998, the design taking into account the issues discussed earlier together with research results available at the time with respect to concrete strength and cover and the use of hot-dip galvanised reinforcement and precast elements in those areas particularly prone to corrosion. Cement extenders were not used.

The function of this quay is the offloading of gravel concentrates from inshore diamond dredgers working the waters to the immediate north of Lamberts Bay. Initially

the requirement was for small craft of 6−10 m length overall, about 10−20 tons displacement, and laden with man-handled sacks of gravel, but this grew to vessels of 18−23 m length overall, about 100−150 tons displacement laden with 1 $m^3$ 'sugar sacks', each holding about 1.5 tons. Provision had to be made in the deck design for a hydraulic truck-type crane to handle these bags. Fortunately, it was possible to incorporate these changes during the design stage.

The cope level was set to the standard +3.00 LAT with a small slope seaward to keep water from ponding on the deck. The front of the quay is supported on precast columns set on the sea bed. The rear of the deck is monolithic with a dwarf wall founded on the rock revetment at + 2.00 LAT. A photo of the completed jetty is shown in Fig. 14.50.

The columns and the cope soffits were precast in 45 MPa concrete. The reinforcement to these precast elements and to the upper cope to the deck was all hot-dip galvanised. The deck and the dwarf wall were both cast in 40 MPa concrete, and the reinforcement to these elements was not galvanised. Only high-tensile deformed reinforcing bars were used. Aspects of these features and the construction are shown in Figs 14.51−14.54.

### 14.3.9 Small dry docking facilities (Mackie and Deane, 2006; Mackie, 2015)

Note on terminology used: 'slipway', the term used here, also called 'patent slip', is British usage for a cradle on wheels on rails that runs down into the sea to dry dock vessels, usually small vessels up to 2000-ton displacement. The equivalent American usage is 'marine railway'.

Also in British usage, particularly among yachtsmen, the term 'slipway' is used to describe a ramp for launching small vessels on road trailers. To avoid confusion, the American usage of 'boat ramp' is used here.



**Figure 14.50** Completed jetty at Lamberts Bay.
Photo 1998.



**Figure 14.51** Precast cope soffits.
Photo 1998.



**Figure 14.52** Precast columns in place, Lamberts Bay. Note corbels to column to receive precast cope.
Photo 1998.



**Figure 14.53** Casting of deck, in situ, Lamberts Bay.
Photo 1998.



**Figure 14.54** Underside of quay: deck and back wall, Lamberts Bay.
Photo 1998.

### 14.3.9.1 Boat ramps

Good practice requires that the ramp extend to a depth of −1.00 LAT; in Southern Africa, the section through the tidal zone down to this depth is usually constructed of precast, reinforced concrete slabs. Durability issues generally relate to abrasive wear on the slab surfaces. Good practice is to form herringbone grooves in the slab to assist with wheel traction. Design detailing is important in retaining effective grooving despite wear. Fig. 14.55 shows the boat ramp at Hout Bay in the Cape Peninsula, which has been in good use since it was constructed in 1976.

However, there is significant wear on these slabs, and the grooving has disappeared. The original grooving had been made by drawing a rubber tined rake across the surface of the green concrete. These were initially very effective in that the windrow was sharp and irregular, but it was poorly compacted. These windrows lacked any significant strength and were soon worn away. The grooves themselves were too shallow to be effective.

Another example of a boat ramp is that at Witsand on the Cape south coast, built in 2004. This is illustrated in Figs 14.56−14.58.

Concrete of 45 MPa was used for both precast and in situ elements, without any further precautions beyond the normal requirements for curing, nor were any special additives used. The project was considered too small and remote to justify more complex requirements. Only high-tensile deformed bars were used for reinforcement, and all bars were hot-dip galvanised.

Deep wear-resistant trapezoidal grooving was formed in the slab surfaces. Formers for the grooves were fixed to the soffit shutter, and the panels were cast upside down.



**Figure 14.55** Hout Bay boat ramp.
Photo 2012.



**Figure 14.56** Witsand boat ramp approach.
Photo 2005.



**Figure 14.57** Witsand boat ramp showing grooving.
Photo 2005.

Generally, boat ramps should be built in protected water, both to eliminate damaging wave attack on the ramp structure and to provide calm operating conditions. In this case, although the ramp faces into the prevailing storms, the offshore bathymetry provides significant reduction in wave attack (see Fig. 14.58), making the ramp possible. However, special design procedures were still needed to avoid having the ramp broken up by the waves. These included increased slab thickness/weight, chaining the corners of the slabs together and containing the slabs with boundary walls.



**Figure 14.58** Witsand boat ramp under storm attack.
Photo 2005.

### *14.3.9.2 Slipways and shiplifts*

The main issues with slipways and shiplifts are wear and mechanical damage. Shipyards are hard places for concrete: they are places of rough work, heavy tools and heavy parts and equipment. Corrosion often starts at sites where the cover to the reinforcement has been spalled off by mechanical damage.

Fig. 14.59 shows deterioration of a heavily trafficked deck of the concrete pontoon to a floating dock in Walvis Bay. The dock was built in the Baltic pre-1990, and despite the shallow cover, there seems to be no significant corrosion to the exposed reinforcement. Fig. 14.60 shows the cope to the Walvis Bay shiplift abutting the lift platform and seems to show a combination of mechanical damage and concomitant reinforcement corrosion.

Where flat bottom rails are used, it is common to set them in trenches cast in the ways beams. Once the rail has been set, it is encased by filling the trench with concrete with only the railhead protruding. This concrete infill continues to support the head even as the web corrodes.

Strictly, a slipway is a machine, and the ways beams (the rail support beams) are as much part of the machine as the bed is part of a lathe. The core issue is the construction of reinforced concrete ways beams underwater to support the rails to the required tolerances. Methods of construction are a whole subject in itself. The general trend is in situ construction in the dry in a coffer dam or in situ above water and precast elements below water.

Usually the reinforced concrete ways in the infralittoral zone are permanently immersed, while those in the supralittoral zone are buried with only the rail-bearing top surface exposed. Commonly, only the parts of the ways in the tidal zone are exposed. Fortunately, these are commonly only exposed below the zone



**Figure 14.59** Walvis Bay floating dock deck deteriorated from heavy traffic. Photo 2014.



**Figure 14.60** Shiplift mechanical damage. Photo 2014.

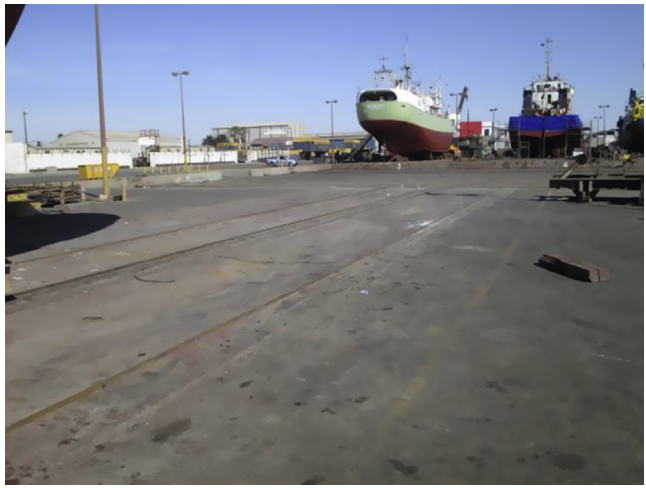


**Figure 14.61** Rails in the shipyard in Walvis Bay encased in trenches in the concrete substructure.
Photo 2012.



**Figure 14.62** Port Elizabeth slipway ways. (Note the way the photographer has carefully posed the photo, positioning the engineer, foreman, charge hand and labourers according to rank.)
Construction photo, 1945.

of AHWC. Generally, corrosion does not appear to be critical with these structures (see Figs 14.63 and 14.64).

Fig. 14.62 shows a 1200-ton lifting capacity slipway. It must be the ultimate in provision for durability, according to military specifications. This was a World War II military project completed in 1945. The ways beams were built in the dry inside a coffer dam. Interestingly, the design capacity was only 1200 tons, but a subsequent check by the author, assuming 25 MPa concrete and making a rough estimate of the scantlings,



**Figure 14.63** Port Elizabeth Slipway in the tidal zone. Photo 2012.

indicates a load capacity equal to the keel block loading of a Panamax freighter with a light displacement of 20,000 tons! By 2015, the facility had been de-rated to 400 tons because of the condition of the cradles and rails. The ways structure appears to retain its full design capacity.

The original ways structure to the Port Elizabeth slipway in the tidal zone (Fig. 14.63) still appears to be sound. Compared to Fig. 14.62, the rail appears to be a replacement fixed on top of the original rail, without removing the original, and then propped with grout. This grout, used to level and support the rails, is now spalling away where it protrudes from the sides to form a coping to the main structure. Note the debonding of the grout from the original concrete.

The St Helena slipway, shown in Fig. 14.64, was constructed in 1971. The ways beams were constructed as precast concrete trough sections with a central trench. This can be seen in the bottom left-hand corner of the photo. The rails were set in these and then grouted in. The ways have since been re-railed by removing the original rails, filling in the trench and laying the new rails on top.

The section of the ways shown is in the tidal zone and subject to the most intense corrosion, but they appear to be performing well. The concrete probably had an original 28-day strength of 30 MPa and would have used 'Cemarine' cement but no other additives.

## 14.4 Ancillary durability issues

Not all durability issues in marine structures are corrosion related. Circumstances do arise that can lead to such other attacks on the structural integrity of facilities. These need to be kept in mind in the design stages. Some examples are given next.



**Figure 14.64** St Helena Bay slipway rail support beams.
Photo 2012.



**Figure 14.65** Cover spalling through excessive localised loading to the soffit of Walvis Bay shiplift jetty.
Photo ca. 2010.

### *14.4.1 Walvis Bay shiplift jetties: punching shear*

The use of mobile cranes — particularly when they are used without supervision and do not use adequate dunnage under the outrigger pads — can result in the spalling of the cover to the reinforcement in the deck soffit through excessive localised stresses due to punching shear or localised bending under the pad position. This is illustrated in Fig. 14.65, showing such failure to an underside soffit of a deck slab at Walvis Bay shiplift support jetties. The failures appeared at about the time the first 100-ton mobile crane arrived on the site. In this case, a structure that ordinarily

would have been durable has been severely compromised by structural overload and misuse. However, this also illustrates the close interrelation between durability and structural integrity.

### 14.4.2 Wind-induced surface ablation

On the West Coast of Southern Africa, the dominant wind blows offshore. At harbours, it blows across the harbour basins onto the breakwaters and other structures in these regions. Surface ablation of the cement paste matrix of the concrete elements to these structures is common. A number of such cases are illustrated in Figs 14.66–14.68.

#### 14.4.2.1 St Helena Bay breakwater armour block surface ablation

The breakwater armour blocks shown in Fig. 14.66 were cast and placed around 1967. Concrete strength of the tetrapods would have been about 25–30 MPa.

#### 14.4.2.2 St Helena Bay slipway side slip altar or dwarf wall

This wall was originally built as part of the slipway in 1970 and is adjacent to the breakwater, in protected water but again windward of the harbour basin. Concrete strength was probably about 30 MPa. It rapidly began to exhibited severe surface ablation. It was repaired around 1990 by cutting out the old, damaged concrete to expose



**Figure 14.66** Surface ablation to tetrapod armour unit to breakwater, St Helena Bay. Photo 2010.



**Figure 14.67** Surface ablation to dwarf wall, St Helena Bay slipway. Photo 2010.



**Figure 14.68** Close-up of ablated surface shown in Fig. 14.66. Photo 2010.

the reinforcement and reconstructing that portion. The repair then began to exhibit the same surface ablation as shown on the photo taken in 2010.

Note the severe erosion of the matrix shown in the close-up in Fig. 14.68 of the wall, leaving coarse aggregate standing proud. Rough depth of erosion is about 10 mm after about 20 years of exposure.

Again, at the time the wall was built, there was no awareness of the unique nature of the problem as an explicit phenomenon and of any precautions to avoid it – an attitude that persisted to the time of the repair.

The preliminary proposition is that this is an essentially arid region phenomenon. Generally, both the concrete and the ambient wind are dry. If the wind does spray droplets of seawater onto the concrete, these are absorbed into the concrete. Thereafter the dry wind will draw out and evaporate the water, leaving the salt to crystallise under the surface and ablate the surface layer. This proposal has yet to be formally demonstrated.

### 14.4.3 Hydraulic erosion of concrete surfaces by wave action

Wave impact against concrete structures and overtopping can result in the degradation of the concrete surfaces. In many cases, the culprit will be the stagnation pressures of the very high-velocity water jets from the wave break impinging on the structure and penetrating cracks in the concrete surface. In some cases, this effect may be exacerbated by other factors such as the surface ablation effect (see Section 4.2).

#### 14.4.3.1 Original cope to sea point seawall

(See Section 3.2 for a full discussion of this structure.)

It is probable that the eroding surface shown in Fig. 14.69 is a mortar screed placed much more recently to repair the previously eroded top surface of the cope.

#### 14.4.3.2 Hout Bay breakwater cap

The section of the breakwater shown in Fig. 14.70 was constructed in the mid-1960s. There seem to be two factors at work here: wave overtopping erosion in the centre of the picture, and cracking and spalling probably due to settlement movement of this block of the breakwater cap. The random placing of the outer armour blocks may have created a local embayment that exacerbates the overtopping locally. However, it may also be the long-term results of a random construction incident in this panel of the breakwater cap.

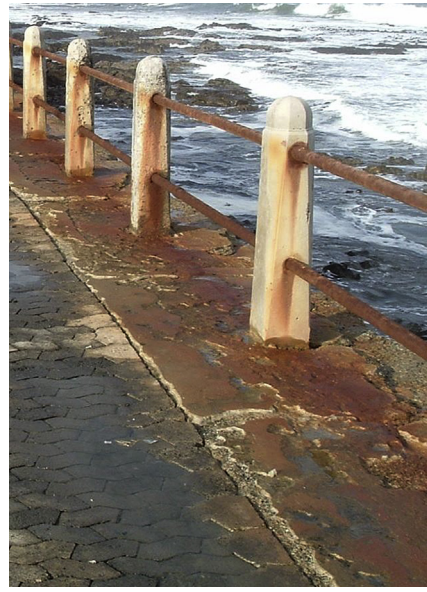


**Figure 14.69** Original cope to Sea Point seawall.
Photo ca. 2013.



**Figure 14.70** Hout Bay breakwater cap.
Photo 2015.



**Figure 14.71** Port Alfred Harbour breakwater splash wall.
Photo 1990.

### *14.4.3.3 Port Alfred Harbour breakwater splash wall*

This structure, shown in Fig. 14.71, was built in the latter part of the 19th century and largely abandoned in the early 20th century with little real maintenance subsequently. The provenance of the splash wall, beyond these comments is unknown (Methven, 1901).

Comments on the Hout Bay breakwater cap apply equally to the condition of this splash wall.

### 14.4.4 Abrasion of marine structures subject to wave action

Unbroken waves, even in relatively clear water, usually contain at least a small quantity of suspended sand particles. Inshore, the breaking or broken waves can lift gravel and even cobbles. These can all abrade concrete surfaces as the wave strikes an immersed structure.

#### 14.4.4.1 Effect of unbroken waves: New Swakopmund jetty

This structure was originally built in 1913−14 in steel and abandoned the following year. Recently, in 2010, it was reconstructed in reinforced concrete. Already (2014) it is showing preliminary signs of wave abrasion on the columns (see Fig. 14.72 and 14.73).

The town engineer has commented that there is a high sulphur content to the waters off this coast that may exacerbate the situation (Duvenhage, 2015). This is the result of biological activity on the Walvis Bay—Swakopmund coast of Namibia. At intervals, the sea bottom goes anaerobic and releases a plume of hydrogen sulphide into the water column (Copenhagen, 1953). On occasions, these eruptions can be sufficiently severe to compromise electronic equipment on this coast.

Fig. 14.73 shows the top of the balanoid zone at the water's edge; the rest is the littorina zone with limpets instead of periwinkles. The circled region is effectively free of organisms and shows the early onset of abrasion and the exposure of the aggregate.

#### 14.4.4.2 Cobble bombardment

Perhaps the best documented case of cobble bombardment was the 'bombing' of the Royal Air Force helicopter base at Chesil Beach, Chiswell, United Kingdom, in 1979.



**Figure 14.72** Reconstructed Swakopmund jetty ca. 2010. Photo 2014.



**Figure 14.73** Close-up of column abrasion of Swakopmund jetty in Fig. 14.72. Photo 2014.

Unusually long storm waves hurled cobbles over the back beach cobble dunes fronting the base. The base had to be hurriedly evacuated for the duration of the storm. When this kind of bombardment is directed against concrete sea defences, the effect can be very destructive (Draper and Bownass, 1982; Draper, 1982).

Sections of the Sea Point Seawall on the Atlantic seaboard of Cape Town are also exposed to this form of attack, in this case from the regular winter storms (see Fig. 14.23). The section in question is fronted by a beach of cobbles of ca.



**Figure 14.74** Undermining of Sea Point seawall concrete foundation plinth. Photo 1995.



**Figure 14.75** Use of sacrificial concrete blocks to protect foundation plinth. Photo 1995.

75 mm. Storm wave attack hurls these cobbles of hard stone at the concrete foundation plinth to the wall and systematically erodes it. The granite stonework to the wall above the plinth seems fairly resistant to this attack (see Fig. 14.74).

The only practical solution to protecting the lower concrete plinth has been to use large, sacrificial concrete blocks; see Fig. 14.75. However, given the severity of the wave exposure at the site, these blocks must be sized to resist movement by the storm waves.

## 14.5 Conclusions

Many of the reinforced concrete structures discussed in this chapter, despite their age and the fact that they were often constructed in what at the time were remote sites without the benefits of modern technology, have given relatively good performance. Although in some cases, others have not. In conclusion, there are five main lessons to be drawn from this survey:

1. The complexity of the behaviour of the sea, particularly at the seashore and the concomitant complexity of the nature of the interaction between the sea and structures on the seashore or in the sea must be taken into account in designing marine reinforced concrete structures.
2. An understanding of the behaviour of marine bio-organisms that inhabit the seashore can provide useful information about the long-term interaction between the sea and structures.
3. There are more ways that the sea can interact with a structure than simply the corrosion of reinforcement. These ways also need to be understood by designers and constructors of marine concrete structures.
4. A commitment to concrete durability in both the design office and in quality assurance on site with respect to good practice and common sense is essential for good durability of concrete structures on the seashore or in the sea, notwithstanding the application of the latest technology.
5. Competent and ongoing maintenance of these structures is essential to their continuing serviceability.

## References

Anon., 1984. New Moorings for World's Largest Yachts: Construction in Southern Africa.
Callaghan, B.G., 1988. Atmospheric Corrosion Testing in Southern Africa. Scientia Publishers, CSIR, 75 pp.
Copenhagen, W.J., 1953. The periodic mortality of fish in the Walvis region. A phenomenon within the Benguela Current. Investigational Report, vol. 14. Division of Sea Fisheries of South Africa, Cape Town, South Africa.
CP 110, 1972. The Structural Use of Concrete. British Standards Institution, London.
CP 114, 1957. The Structural Use of Reinforced Concrete in Buildings. British Standards Institution, London.
CP 2007, 1960. Design and Construction of Reinforced and Prestressed Concrete Structures for the Storage of Water and Other Aqueous Liquids. British Standards Institution, London.
Draper, L., Bownass, T.M., 1982. Unusual waves on European coasts, February 1979. In: Proceedings of 18th International Conference on Coastal Engineering, ASCE, Cape Town 1982.
Draper, L., 1982. Personal discussions with Draper on his paper during the conference given in Draper and Bomnass, 1982, above.
Duvenhage, D., 2015. Town Engineer. Personal Communication, Swakopmund.
Evans, K., 2015. Personal Communication. As the First Owner, Evans Had Commissioned the Construction of the Building.
Gates, T. (Engineer), 2015. Personal Communications, Sea Point Sea Wall Project.
Gliek, J., 1987. Chaos: Making a New Science. Cardinal, London.
Gowans, B.J.M., 1990. Marina design for South African harbours and dams. The Civil Engineer in South Africa 32 (2).
Griffiths, C., 2015. Marine Biologist. University of Cape Town, Personal communication.
Mackie, K.P., Deane, R.F., 2006. Issues in dry docking: economics, shiplifts, slipways and keel blocks. In: Proceedings of 31st PIANC International Navigation Congress, Lisbon, 2006.
Mackie, K.P., 1993. The anomalous nature of the South African coast and its implications for the coastal environment. SAICE Annual Congress, Durban, 1993, reprinted in Sea Changes No 16(1994).
Mackie, K.P., 1999. The debacle of the South African fishing harbours − a case study. In: Mocke, G.P. (Ed.), Proceedings of Fifth International Conference on Coastal and Port Engineering in Developing Countries. Cape Town.
Mackie, K.P., 2008a. Accelerated high water corrosion. In: Alexander, M.G., Beushausen, H., Dehn, F., Moyo, P. (Eds.), Proceedings of 2nd International Conference on Concrete Repair, Rehabilitation and Retrofitting (ICCRRR). Cape Town.
Mackie, K.P., 2008b. The fishing harbours of the Western cape, a study in extinction. SAICE Civil Engineering 16 (2), 16−27.
Mackie, K.P., 2010. Simonstown Municipal Jetty, Structural Assessment. City of Cape Town.
Mackie, K.P., 2012. Manual of Basic Coastal and Harbour Engineering. Private publication.
Mackie, K.P., 2014. Fixing the high-water mark. In: Funke, N., Claassen, M., Meissner, R., Nortje, K. (Eds.), Reflections on the State of Research and Technology in South Africa's Marine and Maritime Sectors. CSIR, Pretoria, pp. 43−52.
Mackie, K.P., 2015. Dry Dock Manual. Private publication.
Methven, C.W., 1901. Report on Port Alfred Harbour. Port Alfred Municipality.

PIANC, 2005. Accelerated Low Water Corrosion. MarCom Working Group, p. 44. November 2015. http://www.pianc.us/workinggroups/docs_wg/marcom-wg44.pdf.
Stephenson, T.A., Stephenson, A., 1949. The universal features of zonation between tide-marks on rocky coasts. Journal of Ecology 37, 289−305.
Verboom, A., 2015. Botanist. University of Cape Town, Personal communication.

# Concrete durability of the new Panama Canal: background and aspects of testing

15

C. Andrade [1], N. Rebolledo [1], F. Tavares [1], R. Pérez [2], M. Baz [2]
[1]Institute of Construction Science "Eduardo Torroja"-IETcc-CSIC, Spain; [2]GUPC: Grupo Unidos por el Canal (Sacyr)

## 15.1 Introduction: background, brief details, locality

Since it was built 100 years ago, the Panama Canal, with an approximate length of 80 km, has provided a route for passenger and freight traffic, which is of cardinal importance for world trade. It was opened on 15 August 1914, and it has dramatically shortened the distance between the Atlantic and Pacific Oceans.

Lake Gatun, enlarged for the sake of construction of the canal, has the present locks for the Atlantic side. This lake was enlarged during the original construction to facilitate navigation inside the country. The Pacific side has the Pedro Miguel and the Miraflores locks. Fig. 15.1 shows the construction of the old canal.

Before the present canal was built by North American companies, there had been an attempt by French companies at the end of 19th century to build it. This had failed because they tried to keep the canal at sea level throughout the crossing. As Lake Gatun is 26 m above sea level, this was impossible. The North American solution consisted in building three locks on each of the ocean sides to reach the lake level as indicated in Fig. 15.2.

Two parallel chambers were built to allow the simultaneous passing of two ships. The Pacific side of the canal has two locks at Miraflores and one lock at Pedro Miguel. The Atlantic side has three locks in Lake Gatun. The maximum size of ships



**Figure 15.1** View of the construction of old Panama Canal at the beginning of the 20th century. https://en.wikipedia.org/wiki/Panama_Canal

**Marine Concrete Structures.** http://dx.doi.org/10.1016/B978-0-08-100081-6.00015-5
Copyright © 2016 Elsevier Ltd. All rights reserved.

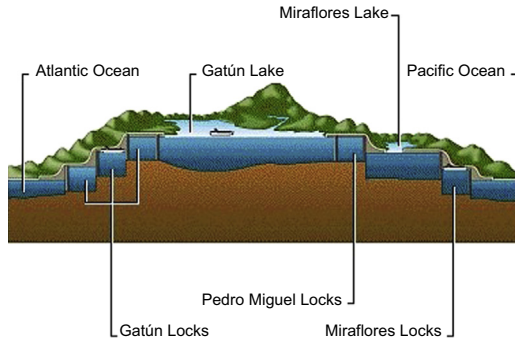



**Figure 15.2** Profile of the height of Lake Gatun and the need to build locks for navigation.

is 294.1 m in length, 32.3 m in width, and up to 12 m in ship draft (such ships are called Panamax).

From the 1930s, the need to enlarge the width of the canal due to the increasing demand of wider and heavier ships was identified. Continuous technological and industrial developments permitted more powerful engines and therefore larger ships. The solution was to construct a third set of locks by making a lane parallel to the existing one. This was started by the United States in 1939, but World War II suspended the initiative in 1942.

After the present canal was returned to the Panama Government at the end of the 20th century, the Panama Canal Authority (ACP) initiated studies for understanding the growing demand for transport through the canal. The studies considered the need for lanes allowing larger ships. Table 15.1 gives dimensions for the new larger ships, called Pospanamax, and comparisons of both types of ships. Other requirements were water recovery due to limitations of the water renewal of Lake Gatun.

In 2006, a tender for the construction of the third and fourth lanes of the new locks was issued, and finally awarded to the consortium Grupo Unidos por el Canal (GUPC), a joint venture by Impregilo (Italy), Sacyr (Spain), Jan de Nul (Belgium) and CUSA (Panama). The solution they offered consisted mainly in the building of three locks with chambers of 9 m each and the corresponding side water saving basins, where the water is recycled with a savings of up to 60% of the water used. This recycling prevents the chambers from delivering salt water to Lake Gatun. Completion of construction was scheduled for 2014 to celebrate the centenary of the old canal. This was not achieved, and the aim is now to complete the work by early 2016.

## 15.2 Details of the structures: structural form, layout, extent and complexity

In all, the work entailed casting around 5 Mt of concrete (five million tons), representing at the time the world's largest concrete work production on a single site. The amounts of the main materials used are given in Table 15.2, and the main elements

**Table 15.1 Dimensions and statistics of present and new locks on the Panama Canal**

| | | Present locks | New locks |
|---|---|---|---|
| **Lock dimensions** | Length | 305 m | 427 m |
| | Width | 33.5 m | 55 m |
| | Draft | 12.8 m | 18.3 m |
| **Maximum capacity of ship type** | | **Panamax** | **Pospanamax** |
| Length | | 294.1 m | 366 m |
| Sleeve | | 32.3 m | 49 m |
| Draft | | 12.4 m | 15.2 m |
| Maximum load | | 4500 TEU | 12,600 TEU |
| **Number of lanes** | | **2** | **1** |
| **Pools for water recycling** | | None | 3 |
| **Recovering of water** | | 0% | Up to 60% |
| **Locks** | | Hinged | Slides |

**Table 15.2 Amounts of materials used in the construction of the new Panama Canal**

| Activity | Amount |
|---|---|
| Dredge | 7,100,000 $m^3$ |
| Excavation | 52,000,000 $m^3$ |
| Filling material | 24,000,000 $m^3$ |
| Filter material | 700,000 $m^3$ |
| Concrete | 4,700,000 $m^3$ |
| Cement | 1,600,000 tons |
| Reinforcing steel | 192,000 tons |
| Steel in dates | 71,000 tons |
| Buildings (floor area) | 40,000 $m^2$ |

designed are shown in Fig. 15.3. Fig. 15.4 depicts the views on one of the gates, which were built in Italy and shipped to the Atlantic side and then transported to place through the existing Canal.

Two concrete plants were installed on each working site. A view of the Pacific site is shown in Fig. 15.5. Due to the need to control the concrete temperature during

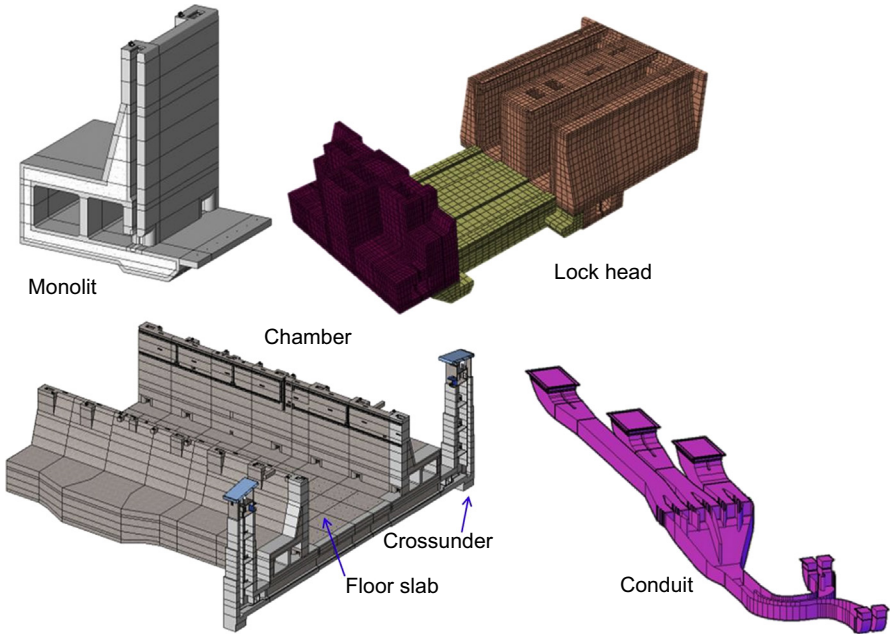



**Figure 15.3** Layout of the main concrete elements being built.



**Figure 15.4** The steel gates that will control the lock chambers. There are 16 gates which measure 57.6 m in width, they are 33 m high and have a weight of around 4.200 ton. Left: http://eandt.theiet.org/news/2013/aug/panama-gates.cfm and right: http://www.dredgingtoday.com/2013/08/21/panama-canal-expansion-massive-new-gates-arrive/.

setting, a refrigeration plant was built to produce ice that was mixed with the water. The production capacities of the plants are given in Table 15.3.

The aggregate-comprised basalt quarried from the site quarry and processed in crushing plants is shown in Fig. 15.6 The granulometric curves are shown in



**Figure 15.5** View of the Pacific concrete plant with the silos and the refrigeration plant producing ice that was used with the mixing water to control the setting temperature.

**Table 15.3 Concrete production plant and capacities**

| Transport and distribution of concrete | Nominal capacity | Atlantic site | Pacific site |
|---|---|---|---|
| Concrete mixing plant | 540 $m^3$/h | 1 | 1 |
| Baby tower belts Rotec | 120 $m^3$/h | 4 | 4 |
| Tele belts Putzmeister Tb 130 | 130 $m^3$/h | 6 | 5 |
| Tele belts Putzmeister Tb 200 | 200 $m^3$/h | – | 1 |
| Cretec crane, Rotec 24 × 200 | 150 $m^3$/h | 1 | 1 |
| Concrete pumps, Putzmeister BSF 58 | 60 $m^3$/h | – | 3 |
| Concrete pumps, Schwing S52 | 60 $m^3$/h | 3 | – |
| Trucks, Maxon and Gicalia | 9 $m^3$ | 38 | 38 |

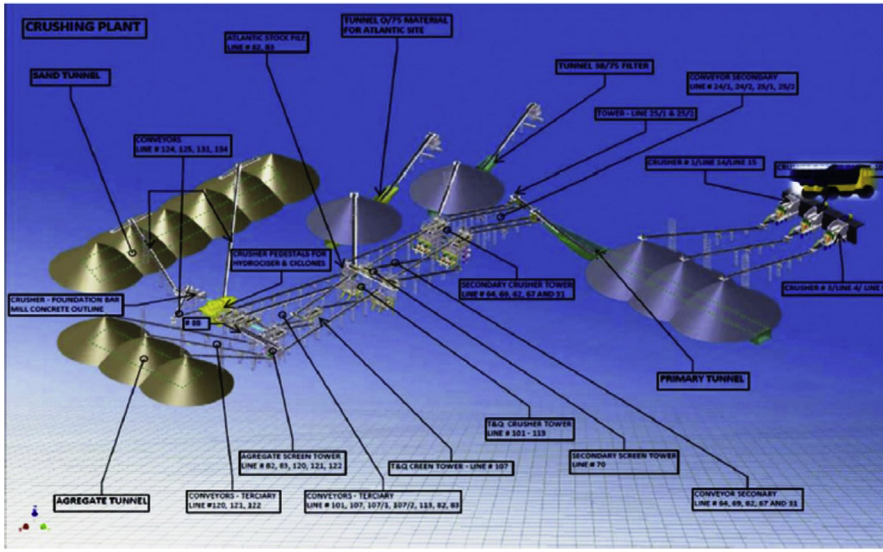



**Figure 15.6** Organisation of crushing plant of aggregates.

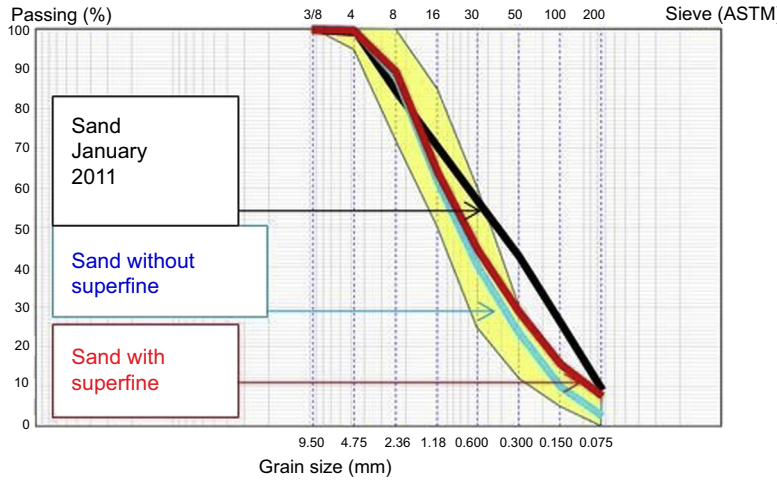



**Figure 15.7** Granulometric curves of the finer fractions of aggregates.

**Table 15.4 Capacities of concrete and aggregate plants**

| Industrial plants | Capacity | Atlantic | Pacific |
|---|---|---|---|
| Aggregate: primary crushing plant | 3300 ton/h | – | 1 |
| Aggregate: secondary, tertiary and quaternary crushers | 1300 ton/h | 1 | 1 |
| Barge for aggregate transport | 8000 ton | – | – |
| Truck for aggregate transport | 30 ton | – | 23 |
| Plant for cutting and bending of reinforcement | 400 ton/day | 1 | 1 |
| Silos for cement and pozzolan | 9000 $m^3$ | 1 | 1 |

Fig. 15.7. The aggregate was not as sound as expected and gave a much higher amount of 'superfine' sand than anticipated. This meant that at the beginning of the work, the grading needed to be corrected, which resulted in an important amount of waste material. Later this superfine fraction, after verifying its pozzolanic activity, was maintained to improve chloride resistance. Other machinery used is given in Table 15.4.

Aspects of the working sites for the Pacific and Atlantic locks are shown in Fig. 15.8. The organisation of the construction work was very complex due to the huge scale of construction at both sites. The length of each site is around 2 km.



**Figure 15.8** Views of the working sites of the new locks: left, Atlantic site; right, Pacific site.

## 15.3 Environment (salinity) of the marine concrete structures

The salinity of water in the lock nearer the sea (ie, the lower chamber) is completely different from that of the lock adjacent to Lake Gatun, which contains fresh water (ie, the upper chamber). The salinities are given in Table 15.5. These values can be compared to typical seawater salinities of around 35 g/L, although this varies widely in different oceans.

## 15.4 Concrete design philosophy and basis

Although the concrete on the existing canal is not reinforced, the design for the new structure has called for reinforcing steel as an anti-seismic precaution. Two kinds of concrete were specified: marine and standard concrete. The marine concrete, which is that placed in the external surfaces of the elements, had requirements that were more stringent. The concrete had to be cast on site and be capable of being pumped (Fig. 15.9, left). The maximum *w*/*c* ratio allowed was 0.4.

**Table 15.5 Salinities in the different lock chambers**

| Location | Chamber | Salinity (g/L) | Classification |
|---|---|---|---|
| Pacific side | Upper chamber + lock head 1 | 0.6 | Low |
| | Middle chamber + lock head 2 | 4.6 | Moderate |
| | Lower chamber + lock head 3 | 19.2 | High |
| | Wing walls + lock head 4 | 30.0 | Extra high |
| | Approach structures | 34.0 | – |
| Atlantic side | Upper chamber + lock head 1 | 0.6 | Low |
| | Middle chamber + lock head 2 | 3.8 | Moderate |
| | Lower chamber + lock head 3 | 16.2 | High |
| | Wing walls + lock head 4 | 27.6 | Extra high |
| | Approach structures | 32.0 | – |



**Figure 15.9** Left: pumping concrete; right: special system for curing during 7 days.

The specification of the ACP required a 100-year service life for the marine concrete in all members and also to have a maximum of 1000-C criterion as set out in ASTM C1202 (ASTM 1202, 2010). For the 100-year service life, there was no indication given on how to demonstrate this, but calculations regarding chloride penetration were required. Cover depths larger than 75 mm were requested. Additionally, temperature control requirements were prescribed in order to have temperatures no higher than 60°C in the centre of the elements, thus avoiding thermal cracking. Curing times of 7 days were also prescribed (Fig. 15.9, right).

As mentioned, for the thermal control of the mixes during casting, ice was incorporated into the mixing water, and temperature control was exercised using thermocouples in the fresh and hardening concrete, together with theoretical studies at the element size (Fig. 15.10).

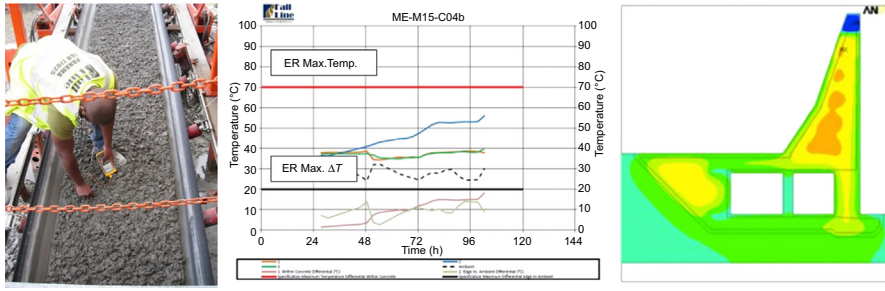



**Figure 15.10** Left: measuring temperature of the concrete mix in the conveyor belt. Middle: typical temperatures measured by the thermocouples embedded in the concrete. Right: simulation program of the temperatures in the monolith element.

## 15.5 Particular aspects considered relating to durability

The requirements prescribed for assuring 100-year service life were, in summary, the following:

- for all concretes without distinction of lock or place:
  - a maximum of 1000 coulombs in ASTM C1202 with no indication on the age of fulfilment (ASTM 1202, 2010; Andrade, 1993; Andrade and Tavares, 2012)
  - minimum of 100 years to corrosion initiation. A model was suggested to be used and accepted by GUPC (Andrade and Whiting, 1996; Tuutti, 1982; Baroghel-Bouny et al., 2010; Saetta et al., 1993; Sagüés, 2003; Mangat and Molloy, 1994; Gulikers, 2004; Andrade, 2004; Andrade et al., 2014, 2011; ASTM C1543-10a, Pr-UNE)
  - low shrinkage cracking (maximum temperature of 70°C in the cast concrete in the early stages of hydration, and less than 20°C difference in the interior of the concrete)

Figs 15.11 and 15.12 show details of the concrete specifications, taken directly from the documents.

The limitations that were identified with respect to these requirements were these:

1. The deterioration mechanism for which there was a coulomb limitation was not defined. This criterion was linked with 'permeability' and 'durability' requirements.
   a. No tests directly related to chlorides were prescribed.
   b. No age was specified for the conformity. Any 'ageing' of the concrete was not taken into account.
2. The characteristics or basis for the 100-year life calculation were not specified.
3. No link was established between the coulomb limitation and the 100-year service life requirement.
4. There was no mention of a test relating to the calculation method.
5. No tolerance of the 1000 C was specified. No mention was made of whether this was a mean or characteristic value.
6. No tolerance or accepted deviation on the life time was given.
7. The same concrete quality was required for all salinities in spite of the fact that they were completely different. Two chambers did not contain waters with chlorides sufficient to induce depassivation.

**1.04 Design criteria/system description and performance:**

A. **Structural marine concrete:** This subparagraph covers the requirements for structural marine concrete. Included in this Subparagraph are lock walls, approach structures, lock heads, lock floors, water-saving basins and conduits, and crossunders.

1. The concrete shall have a design life of 100 years.

2. The concrete shall conform to recommendations of ACI 201.2R and ACI 222.R. mass concrete shall conform to recommendations of ACI 207.IR. Use low heat and sulphate resisting concrete mixtures where required.

A16 3. (Reserved) A16

4. A5 The A5 use of fly ash or ground granulated blast-furnace slag in the mixture is encouraged. Consideration shall be given to heat dissipation, permeability, setting time, strength gain, curing time, A5 especially A5 for mass concrete placements.

5. Where concrete elements retain water, such as at water conduits, water-saving basins, etc, the concrete elements shall conform to applicable requirements for water-retaining concrete structures.

6. A5 Minimum concrete cover at reinforcing bars shall be 75 mm at marine concrete structures unless approved by the employer's representative. A5

**Figure 15.11** Section of the concrete specification relating to durability.

7. **Required characteristics of concrete mixtures:**

| | |
|---|---|
| Minimum compressive strength A5 based on cylinder tests A5 | A5 as required by design A5 |
| Maximum water-cementitious materials ratio | A5 0.40 A5 |
| A5 Permeability: maximum total charge passed per ASTM C1202 A5 | A5 1000 coulombs A5 |

a. The mixture proportions shall be developed by the contractor to produce the design strength A5 and durability A5 required, and to provide durability, workability, and mixture consistency to facilitate placement and consolidation into the forms and around reinforcement, without segregation or bleeding.

b. A5 Permeability testing shall be in accordance with ASTM C1202. Perform tests on five samples and report the average passed charge. Discard any tests that vary from the average by more than 30 percent and recalculate the average of the remaining tests. A5

c. A5 Concrete shrinkage shall be tested in accordance with ASTM C 157,

**Figure 15.12** Required characteristic of concrete mixes related to durability.

## 15.6 Construction aspects

Construction work on the new canal started in January 2011, with a laboratory in charge of verifying compliance with the 1000-C electrical charge and calculating the 100-year service life. The demonstration of the durability of 100 years was one reason why the present authors were incorporated into the working team of GUPC in May 2011. After conducting initial trials with different mixes, in May 2011 the GUPC consortium contacted some of the authors of this chapter to study the possibility of using alternative approaches to ensure compliance with the specifications. The IETcc[1] suggested the following:

1. different prime materials and batching to manufacture a series of alternative concrete mixes
2. the testing of natural chloride diffusion (ponding tests) and continuous monitoring by measuring electrical resistivity over time
3. the use of LIFEPRED, a numerical model developed at IETcc for calculating service life based on Fick's law (Andrade and Tavares, 2012)

This chapter describes and comments on the working program developed by IETcc and GUPC as an alternative and complementary specification to illustrate the fulfilment of the required durability in the concrete mixes prepared.

## 15.7 Experimental program developed between GUPC and IETcc

In view of the limitations in the main specification already identified, it was decided to undertake additional testing and analyses to complement the specification and to fulfil the performance requirements. A summary of this work is given in Table 15.6.

The results from the experimental program are illustrated using eight concrete mixes: four from the Atlantic site (A3, A11, A50, A56) and four from the Pacific site (P3, P11, P50, P56), representative of the over 50 mixes studied. The mix compositions are listed in Table 15.7.

Cement type CEM II (ASTM) was used, with additions such as natural pozzolans and silica fume. A 'superfine' fraction of sand with pozzolanic properties was also used, although for batching purposes, it was regarded as an aggregate rather than a mineral addition. The *w/c* ratio was of the order of 0.3. The 15 × 30 cm cylindrical specimens studied were prepared at an actual plant in Panama, where they were cured in a humidity chamber for 28 days and later sealed in water-tight packaging for continued curing. They were then shipped to Madrid, where they arrived 38 days after casting.

Upon receipt, three specimens of each composition were prepared as illustrated in Fig. 15.1 and tested as follows (Fig. 15.13). A 10-cm disk was cut off specimen 1, on which resistivity was monitored at the top, while actual chloride penetration from a

[1] El Instituto de Ciencias de la Construcción Eduardo Torroja (IETcc), Madrid, Spain.

**Table 15.6 Summary of the tests performed to complement those required in the main concrete specification**

| Test type | Objective |
|---|---|
| ASTM 1202 | To fulfil concrete specification |
| Time to depassivation (LIFEPRED program) | To fulfil concrete specification |
| Resistivity | To substitute for ASTM C1202 and to calculate ageing factors |
| Natural chloride diffusion (ponding) | To complement ASTM C1202 and the resistivity tests |
| Multi-regime migration test (abandoned soon) | To substitute natural diffusion (not possible) |
| ASTM water-penetrable porosity | To complement the specification |
| Mercury intrusion porosimetry | To complement the specification |

sodium chloride solution pond was measured at the bottom (ASTM C1543). Ten-centimetre disks were cut off specimens 2 and 3, and a central core measuring 7.5 cm in diameter was removed from the top of the specimen. A 2-cm wafer was cut off the sample for the multi-regime trials (not discussed here), and other samples were removed from the remaining crown to test for voids volume (ASTM C642) and mercury intrusion porosimetry (MIP). Chloride penetration was also measured by bottom ponding (ASTM C1543) in specimens 2 and 3.

- **Mercury intrusion porosimetry**
  Porosity (pores ranging from 400 to 0.01 μm) was measured on a Micromeritics PORE-SIZER mercury intrusion porosimeter following the procedure described in ASTM D4404. The 1-$cm^3$ sample used in the test was extracted from the inside of a concrete wafer taken from the middle third of the specimen.
- **Electrical resistivity: four-point test**
  Concrete resistivity can be determined in a number of ways: here the Wenner four-point test, described in Spanish standard UNE 83988-2, was chosen. The tips of four evenly spaced electrodes were moistened to ensure good contact and applied to the concrete surface. Alternating current (of up to 50 μA at a high frequency) was applied between the outer electrodes while measuring the change in the difference in potential between the inner electrodes. Resistivity depends on voltage, current and distance between electrodes (Fig. 15.14).

  In a quasi-infinite medium, resistivity ($\rho_a$) can be found with Eq. [15.1]:

$$\rho_a = R \cdot 2 \cdot \pi \cdot a \qquad [15.1]$$

  where $R$ is electrical resistance, $a$ is the distance between the electrodes, and the factor $2\pi a$ is the so-called geometric proportionality factor. Since the specimens used were finite, a 'form factor' has to multiply Eq. [15.1], whose value in the present case was 0.714.

**Table 15.7 Composition of four concrete mixes from each site (out of the more than 60 studied)**

| Plant | | Atlantic site | | | | Pacific site | | | |
|---|---|---|---|---|---|---|---|---|---|
| GUPC code | | SMC-A3 | SMC-A11 | SMC-A50 | SMC-A56 | SMC-P3 | SMC-P11 | SMC-P50 | SMC-P56 |
| | | 5796 | 1372 | 5777 | 6850 | 823 | 5067 | 9153 | 5481 |
| Mix | | 375 (23PN 0SF) | 375 (15PN 5SF) | 330 (12.5PN 5.8SF) | 332 (13.0PN 0.0SF) | 375 (23PN 0SF) | 375 (15PN 5SF) | 330 (12.5PN 5.8SF) | 332 (13.0PN 0.0SF) |
| Cement | Type | Panama CEM II | Panama CEM II | Panama CEM II | Panama CEM II | CEMEX CEM II | CEMEX CEM II | CEMEX CEM II | CEMEX CEM II |
| Pozzolan | $kg/m^3$ | 288.75 | 300 | 264 | 289 | 288.75 | 300 | 264 | 289 |
| | $kg/m^3$ | 86.38 | 56.3 | 47 | 43 | 86.87 | 56.3 | 46 | 43 |
| Silica fume | $kg/m^3$ | – | 18.8 | 19 | 0 | – | 18.8 | 19.5 | 0 |
| Total binder | $kg/m^3$ | 375 | 375 | 330 | 332 | 375 | 375 | 328 | 332 |
| w/c ratio | – | 0.30 | 0.29 | 0.34 | 0.34 | 0.35 | 0.30 | 0.29 | 0.34 |
| Admixture | $kg/m^3$ | 4.5 | 4.5 | 2.63 | 1.99 | 4.31 | 4.5 | 2.3 | 2.63 |
| Superfine sand | $kg/m^3$ | – | – | 49 | 49 | – | – | 66 | 44 |
| Fine sand (0–4.75 mm) | $kg/m^3$ | 567.5 + 206.25 = 773.75 | 573 + 211 = 784 | 686 | 716 | 522.5 + 217.5 = 740.0 | 535 + 220 = 755 | 688 | 703 |
| Coarse aggregate (4.75–19 mm) | $kg/m^3$ | 676.25 | 705 | 707 | 693 | 691.25 | 684 | 712 | 701 |
| Coarse aggregate (19–37.5 mm) | $kg/m^3$ | 620 | 644 | 647 | 633 | 630 | 628 | 649 | 641 |
| Slump | mm | 80 | 110 | 120 | 100 | 110 | 75 | 100 | 95 |
| Air (%) | % | 1.6 | 1.9 | 1.6 | 1 | 2.2 | 2 | 1.6 | 1.1 |
| Unit weight | $kg/m^3$ | 2539 | 2532 | 2508 | 2548 | 2597 | 2534 | 2525 | 2570 |
| 28-day strength | MPa | 50.1<br>49.5 | 57.8<br>58.1 | 52.1<br>51.5 | 42.6<br>41.3 | 53<br>53.8 | 61.4<br>61.0 | 44.7<br>48.4 | 45.3<br>44.5 |
| 90-day strength | MPa | 52.2<br>55.0 | 68.4<br>66.3 | 58.4<br>57.8 | 56.6<br>56.4 | 54.8<br>– | 78.3 | 58.1<br>60.1 | 60.5<br>61.2 |

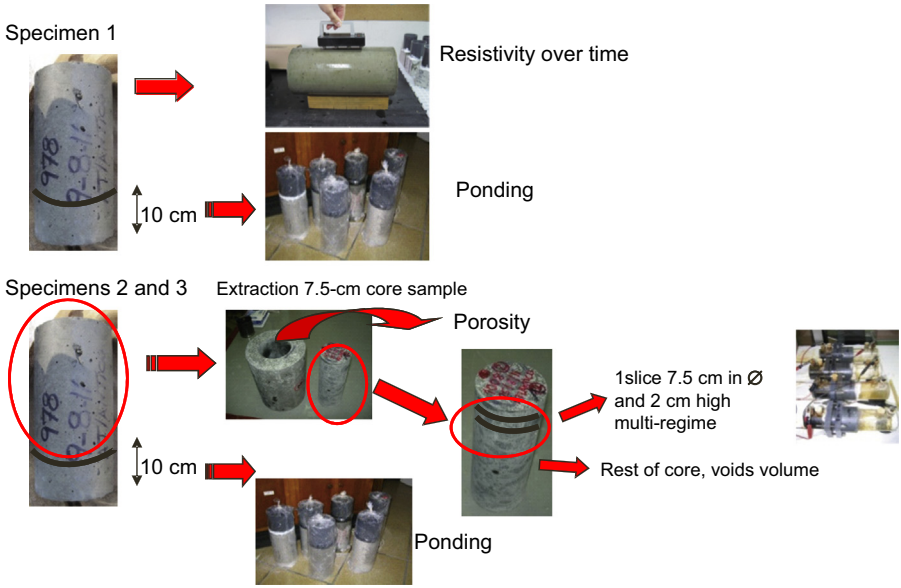



**Figure 15.13** Sample preparations for testing.

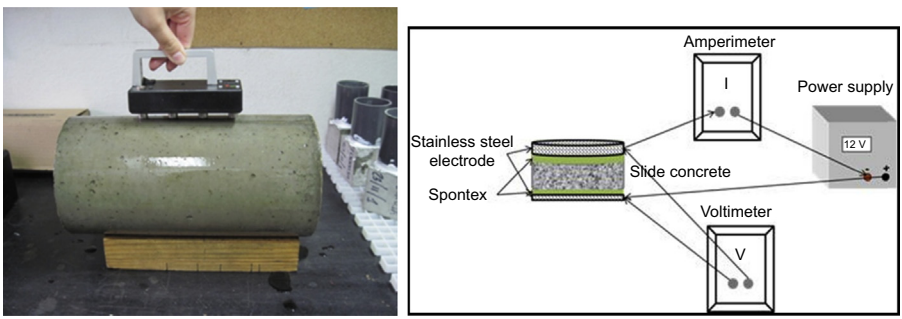



**Figure 15.14** Resistivity measured with a four-point resistivity meter.
ASTM 1202, 2010. Standard Test Method for Electrical Indication of Concrete'sAbility to Resist Chloride Ion Penetration (Annual Book of ASTM Standards) and ASTM C1543-10a. Standard Test Method for Determining the Penetration of Chloride Ion into Concrete by Ponding.

- **Determination of chloride penetration (natural diffusion coefficient) with ponding**
  The test was conducted as laid down in ASTM C1543. A section of pipe was sealed to the top of the specimen with silicone and filled with a 30-g/L solution of NaCl. The entire specimen assembly was then covered with plastic film to prevent evaporation of the solution from the side faces of the specimen (Fig. 15.15).

  The specimens were ponded for 90 days, during which time samples were tested to obtain the chloride profile by milling 2 mm off the surface of the specimen at a time. The samples obtained were analysed for the total chloride content as per Spanish standard (UNE 83986-I and II).



**Figure 15.15** Ponding to determine chloride penetration (natural diffusion coefficient).

The nonsteady-state diffusion coefficient and the chloride concentration on the concrete surface were calculated by applying Fick's second law of diffusion (Eq. [15.2]):

$$C_x = C_s \cdot \left(1 - \text{erf}\left[\frac{x}{2\sqrt{D_{ns} \cdot t}}\right]\right) \qquad [15.2]$$

where $C_x$ is the chloride concentration at depth $x$ and time $t$ (dry wt% of the sample), $C_s$ is the chloride surface concentration (dry wt% of the sample), $D_{ns}$ is the nonsteady-state diffusion coefficient ($cm^2/s$), erf is the Gauss error function and $t$ is test time in seconds.

## 15.8 LIFEPRED model for calculating service life (Andrade and Tavares, 2012)

The LIFEPRED model is based on the numerical solution to Fick's second law. One-, two- and three-dimensional versions were developed, although the 3-D version is not discussed here. Unlike other models that assume a semi-infinite medium, LIFEPRED assumes a finite medium due to the presence of reinforcing steel. This characteristic induces substantial variations in the results if the cover is small, because the chloride accumulates on the bar surface. The program can also handle data on variations in temperature and environmental humidity. Either a characteristic 'age' factor or several 'age' factors can be entered and the ceiling concentration can be visualised separately. The user interface, with very few data entry screens, is highly intuitive.

The operating sequence is as follows: (1) generation of geometry and bar position (Fig. 15.16); (2) determination of geometry mesh size (Fig. 15.16); (3) data entry: material characteristics; (4) data entry: surface concentration, age factor and temperature (Fig. 15.17); (5) processing and (6) delivery of results in graphic form (Fig. 15.18).

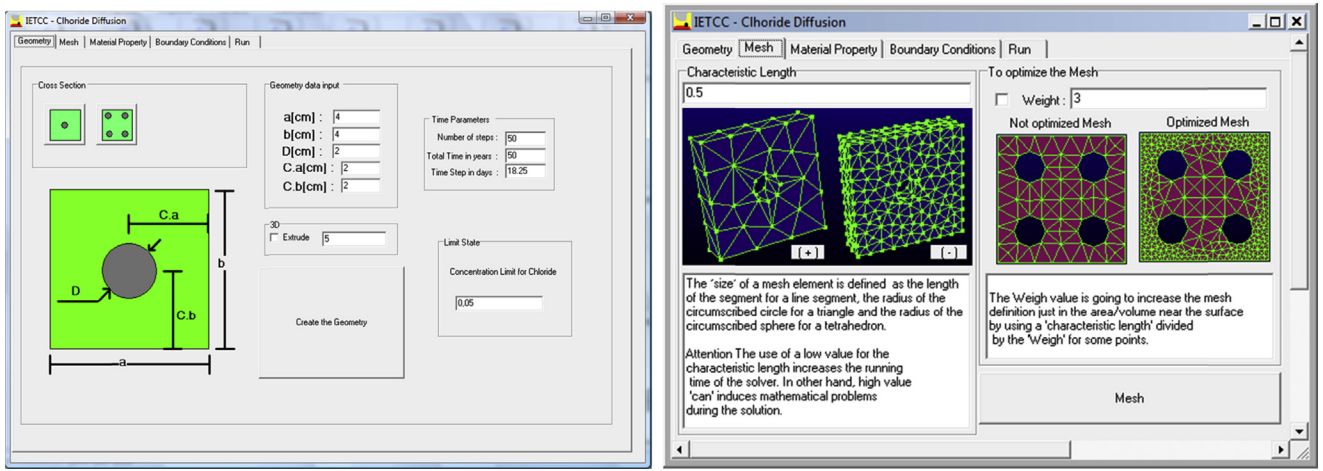



**Figure 15.16** LIFEPRED Model: left, geometry; right, mesh.

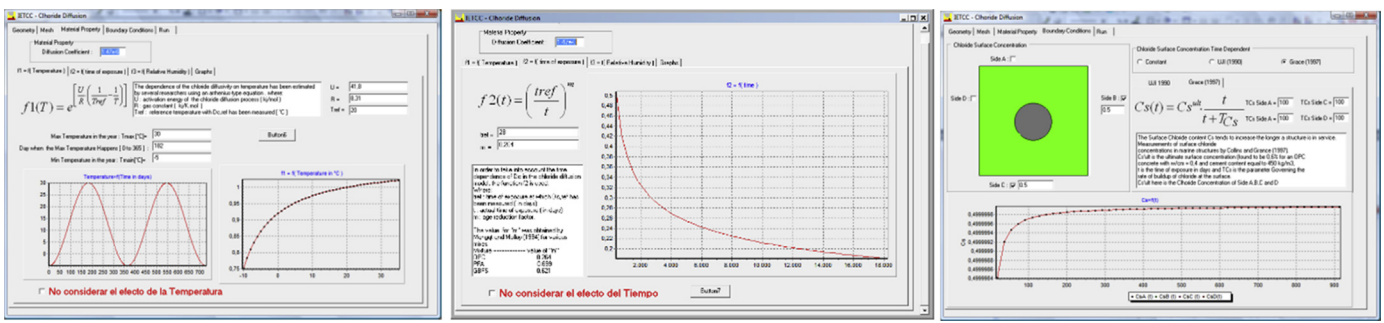



**Figure 15.17** LIFEPRED Model: operating conditions of temperature variations, age factors and surface concentrations.

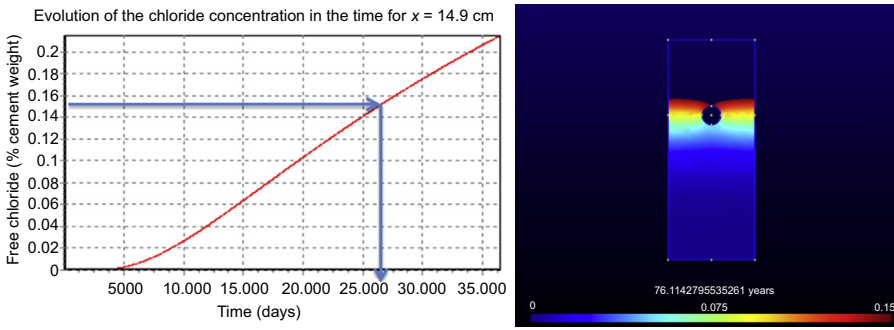



**Figure 15.18** LIFEPRED Model: one- and two-dimensional results.

## 15.9 Resistivity-based model (Andrade, 2004; Andrade et al., 2014, 2011)

A model was developed to calculate the service life from resistivity, based on the 28-day value in water-saturated conditions. The model was also able to calculate the corrosion propagation period. For the present purposes, only the time to reinforcement depassivation (ie, the first term in Eq. [15.3]) was used:

$$t_l = t_i + t_p = \frac{x^2 \cdot \rho_{ef} \cdot \left(\frac{t_a}{t_0}\right)^q \cdot r_{Cl,CO_2}}{F_{Cl,CO_2}} + \frac{P_{corr} \cdot \xi \cdot \rho_m \cdot \left(\frac{t_a}{t_0}\right)^q}{k_{corr}} \qquad [15.3]$$

where $x$ = cover depth, $\rho_{ef}$ = effective or nominal resistivity; $\rho_m$ = mean resistivity in the specific climate; $r_{Cl,CO_2}$ = chloride-cement paste reaction factor; $F_{Cl,CO_2}$ = environmental factor that depends on the chloride content in the environment; $q$ = age factor governed by progressive cement hydration; $P_{corr}$ = depth of corrosion in the reinforcement bar; $\xi$ = environmental factor that depends on climate and $k_{corr}$ = constant that relates resistivity to corrosion rate.

In addition to the resistivity value in water-saturated 28-day concrete, service life calculations with this model call for (1) periodic resistivity readings to find the age factor, $q$; (2) calculation of the chloride reaction factor from the multi-regime test and (3) identification of the environmental factor to be applied.

Factor $q$ is the age factor or variation in resistivity due to cement hydration reactions over time. It can be calculated graphically as shown in Fig. 15.19: the slope of the curve obtained by plotting the log of the inverse of resistivity against the log of time is $-q$.

Since, as noted earlier, resistivity is an indirect indication of porosity, the delay in chloride diffusion due to the reaction between the ion and the hydrated phases in the cement must be computed separately. This calculation can be performed in a number of ways: here Eq. [15.4] is used.

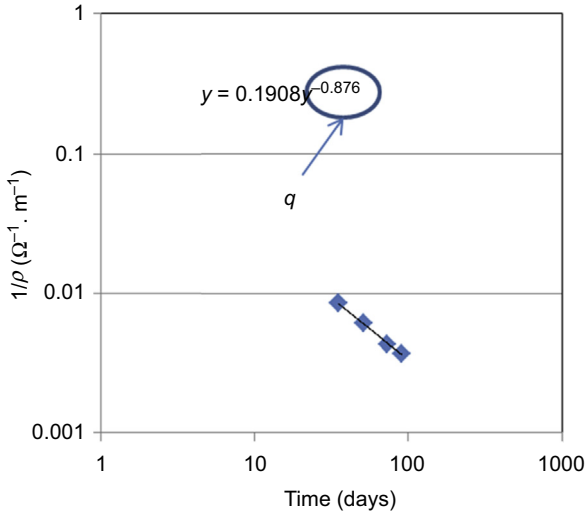



**Figure 15.19** Electrical resistivity plot to find the age factor, $q$. Example for mix 330 (16.5 PN; 3.5 SF).

$$r = \frac{D_s}{D_{ns} \cdot \varepsilon} \qquad [15.4]$$

where $D_s$ is the (unreacted) steady-state diffusion coefficient and $D_{ns}$ the nonsteady-state coefficient. $D_{ns}$ is multiplied by porosity, $\varepsilon$, for while the two coefficients are expressed in the same unit, they refer to different volumes (pore solution or total sample).

### 15.9.1 Tests on the old canal

To verify the diffusion coefficient in the concrete of the old canal, a total of 18 cores were drilled from different zones (Fig. 15.20). The zones were 'Miraflores' upper and lower chambers, and 'Pedro Miguel' East wall. The cores were shipped to the laboratory at IETcc in Madrid, carefully wrapped in wet black tissue and placed inside shielded plastic bags, all in a wooden box.

The cores were immediately cut in slices and ground to avoid any further change in the concentration profiles due to storage out of the structure. The procedure and techniques used for the characterisation of the cores were the following:

1. Chloride profiles in accordance with ASTM C1152 were made by grinding from the surface to approximately 300 mm in depth. Immediately after the powder samples were collected, they were individually sealed in properly identified plastic bags and sent to the chemical laboratory for chloride analysis.
2. From the collected powders: chloride concentration was analysed for the total chloride content as per Spanish standard UNE 83986. X-ray diffraction and thermal differential analysis ATD/TG was also performed.




**Figure 15.20** Drilling of cores: the aspect as received, and grinding machine to prepare the powder for chloride analysis.

3. From the profiles obtained, Eq. [15.2] was fitted to obtain the diffusion coefficient values.
4. In the inner part, one 40-mm-thick slice was cut to measure the electrical resistivity using the 'direct method' (UNE 83988-1) as indicated in Fig. 15.14, right.
5. From the innermost parts, samples were taken for mercury porosimetry (MIP), X-ray powder diffraction, differential thermogravimetric analysis and natural diffusion test (ASTM C1543).

## 15.10 Results

### *15.10.1 Tests in the old canal*

Figs 15.21 and 15.22 present the chloride profiles determined on the different cores. In the graphs, the zero coordinate on the *x*-axis corresponds to the exposed surface of the concrete core. The profiles, as expected due to the different salinity, are different in the upper and in the lower chambers. The profiles show an external part almost without chlorides, likely due to leaching of the cement paste, and a maximum chloride concentration at some point inside the concrete. The peak value is around 0.1% by dry sample mass in the upper chamber and around 0.3% for the lower chamber. In the case of the Pedro Miguel Chamber, the maximum is very low, lower than the theoretical chloride threshold for steel corrosion, and the profile is almost flat. This is due to the low salinity of the zones due to the fact that they are near the interior lakes. The chloride content may be that of the cement used, or it may be due to the low contamination in

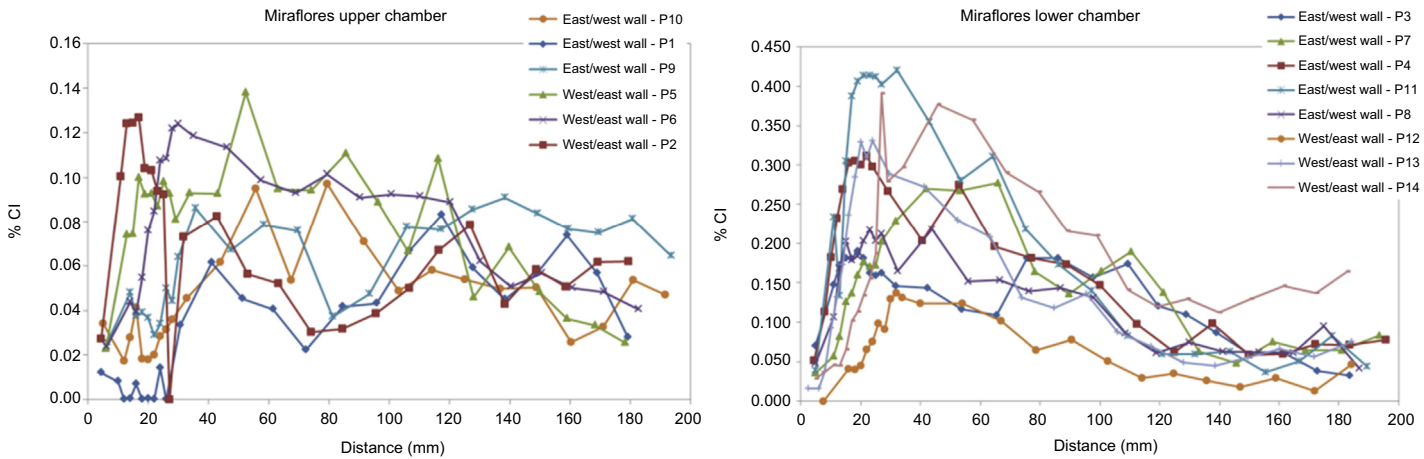



**Figure 15.21** Chloride profiles measured on cores extracted from the Miraflores upper and lower chambers.

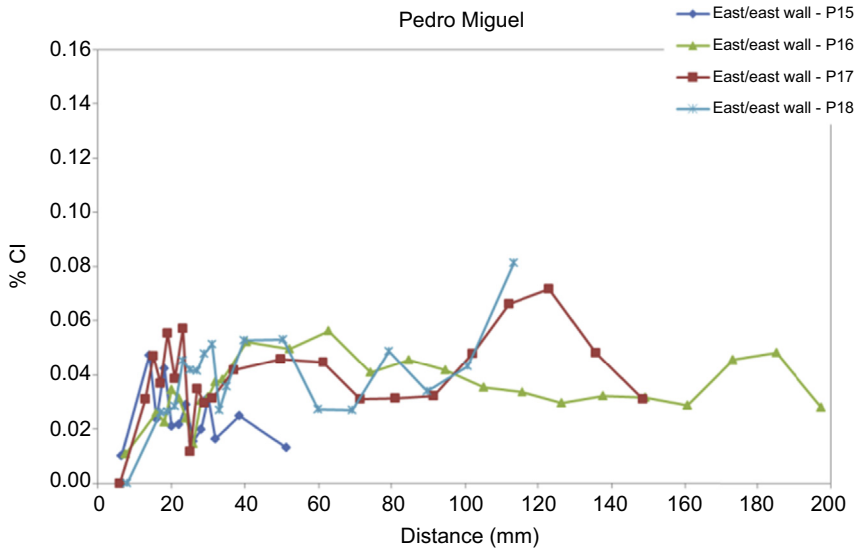



**Figure 15.22** Chloride profiles measured on cores extracted from the Pedro Miguel chamber.

chlorides of the interior lakes with the passing of the ships. Only in the lower chamber near the sea is the salinity more significant.

The chloride profiles obtained from the cores have been fitted to Fick's second law equation to obtain the apparent chloride diffusion coefficient, $D_{ap}$, and the chloride concentration of the maximum $C_s$ (in % of dry sample mass). Table 15.8 gives the values of both parameters. The $D_{ap}$ value results are a bit higher in the upper chamber (around 4E-12 $m^2/s$) than in the lower (around 2E-12 $m^2/s$), which seems contradictory, but it is a mathematical consequence of Eq. [15.2] in which the $D$ depends on the ratio between the surface and the internal chloride concentrations.

For resistivity measurements, Fig. 15.23 shows that the values are above 450 Ω m (45 kΩ cm), which are very high considering that the mixes have a relatively low aggregate content (only 30−35%), that is, they have a higher volumetric fraction of paste than modern concretes.

The MIP results in Fig. 15.24 show the total porosity (% by volume of concrete sample). The values are the mean of three samples from the same core. The values are relatively high and compatible with the high paste content of the concrete, but not in accordance with the high resistivity values.

### 15.10.2 Tests on concrete mixes for the new canal

Fig. 15.25 shows the MIP values for the mixes studied. Each data point is the mean for three samples. With the exception of P50, all had values of under 10%, denoting low porosity. These values were later entered in LIFEPRED to find the service life.

**Table 15.8 Nonsteady-state chloride diffusion coefficients, concrete from old canal**

| Coring place | Core | $C_s$[a] (% dry mass concrete) | $D_{ap}$ ($m^2/s$) |
|---|---|---|---|
| Miraflores upper chamber east | 10 | 0.161 | 2.55E-12 |
| Miraflores upper chamber west | 5 | 0.130 | 4.98E-12 |
| Miraflores upper chamber west | 6 | 0.141 | 5.48E-12 |
| Miraflores upper chamber west | 2 | 0.095 | 4.82E-12 |
| Miraflores lower chamber east | 3 | 0.253 | 3.23E-12 |
| Miraflores lower chamber east | 7 | 0.426 | 2.00E-12 |
| Miraflores lower chamber east | 4 | 0.340 | 2.47E-12 |
| Miraflores lower chamber east | 11 | 0.588 | 1.44E-12 |
| Miraflores lower chamber east | 8 | 0.256 | 2.81E-12 |
| Miraflores lower chamber west | 14 | 0.441 | 2.693E-12 |
| Miraflores lower chamber west | 12 | 0.190 | 1.451E-12 |
| Miraflores lower chamber west | 13 | 0.391 | 1.430E-12 |
| Pedro Miguel | 16 | 0.067 | 5.475E-12 |

[a]Value represents maximum chloride concentration in the profile.

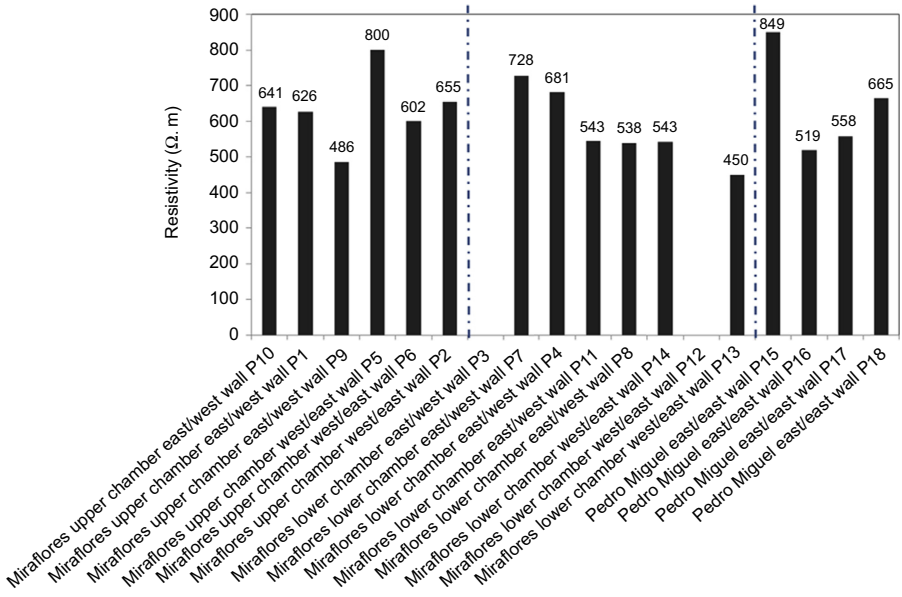



**Figure 15.23** Electrical resistivity.

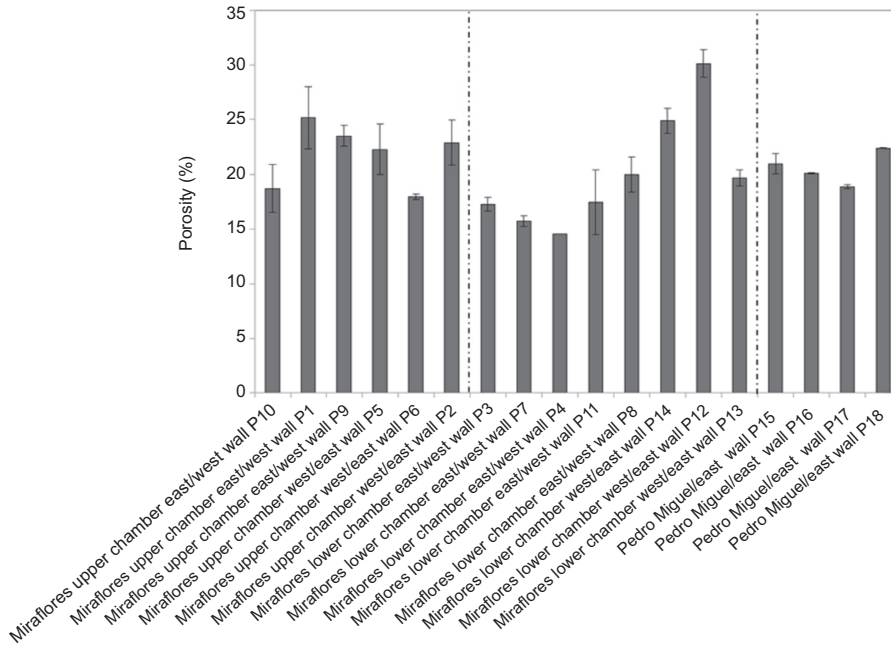



**Figure 15.24** Total porosity (% in volume) by mercury porosimetry.

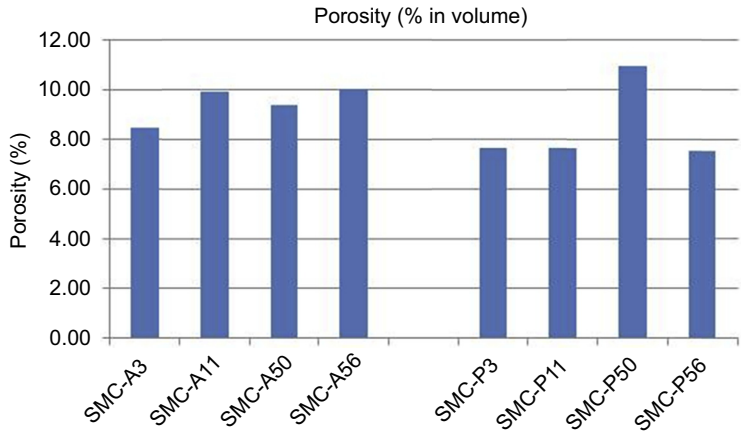



**Figure 15.25** Mercury intrusion porosimetry values for the mixes studied, new canal.

The resistivity values over time are shown in Fig. 15.26, while Table 15.9 gives the age factors obtained from the 38- and 120-day data. The 38- and 120-day diffusion coefficients are shown in Fig. 15.6 for all the mixes; for mixes A3 and P3, tests were conducted on the 14-month materials only. The values of the apparent diffusion coefficient are given in Fig. 15.27 after 38 and 120 days.

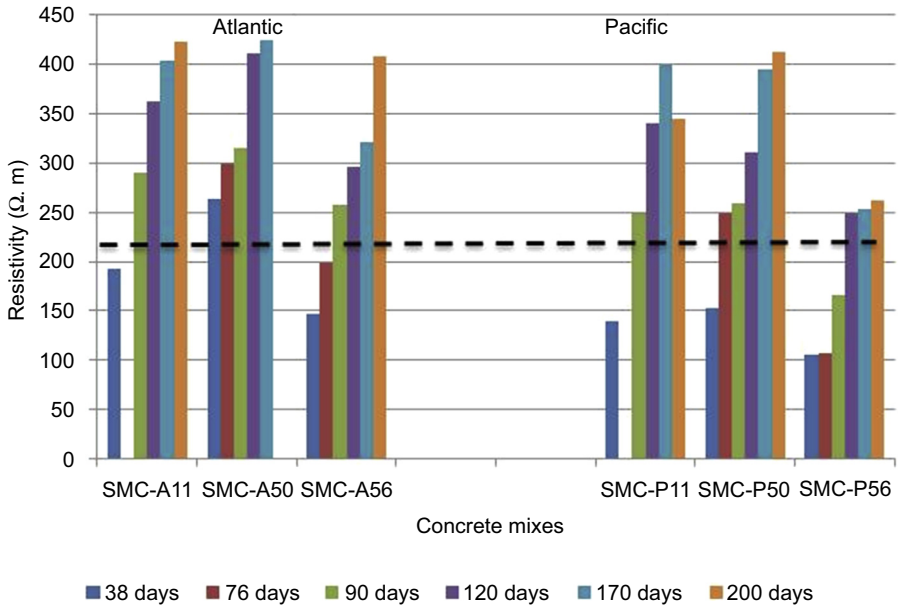



**Figure 15.26** Resistivity values up to 200 days.

**Table 15.9 Age factor values found from variations in resistivity over time**

| 38- and 120-day resistivity age factor | | | | | |
|---|---|---|---|---|---|
| SMC-A11 | SMC-P11 | SMC-A50 | SMC-P50 | SMC-A56 | SMC-P56 |
| 0.492 | 0.584 | 0.349 | 0.609 | 0.629 | 0.718 |

## 15.11 Analysis of results

As noted earlier, further to the specifications, the only requirements to be met by the concrete were a 1000-C limit at an undetermined age, and proof of a 100-year service life by application of a computer model. The two requirements were independent of one another and had to be confirmed simultaneously, subject to the condition that a 100-year service life could not be inferred from compliance with a maximum electrical charge of 1000 coulombs.

The different approaches proposed to prove these two requirements were as follows:

- Based on the equivalence between electrical charge in coulombs determined as per ASTM C1202 and resistivity, the proposal entailed replacing continuous mix monitoring for the former with resistivity measurement, which as a nondestructive method can be used to monitor one and the same specimen over time.

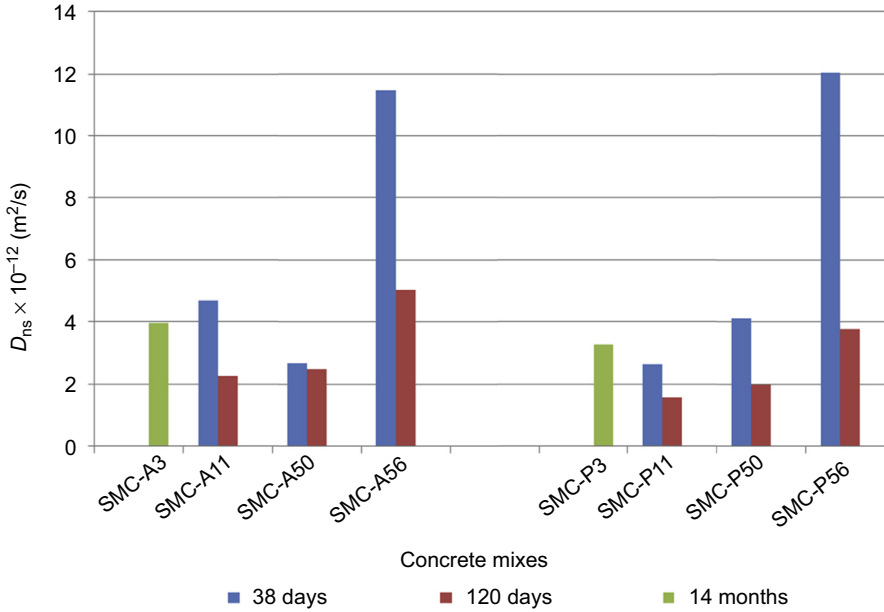



**Figure 15.27** Diffusion coefficients at 38- and 120-days for all mixes; A3 and P3 tested after 14 months only.

- Natural diffusion measured in ponded specimens, not initially envisaged, was proposed as the source of actual chloride penetration to be entered in a model based on Fick's law of diffusion (LIFEPRED program).
- Last, in light of the relationship between resistivity and apparent diffusion coefficients, the resistivity age factor was confirmed to be equivalent to actual penetration measurements at several ages for service life calculation purposes, and to yield very similar values, generally speaking. For the sake of being conservative, this age factor was agreed to be registered until 120 days from which it was considered constant, that is, not decreasing any more.

### 15.11.1 Relationship between electrical charge, resistivity and diffusion coefficient

The comparisons made showed that resistivity is a parameter appropriate for monitoring concrete durability in the laboratory and to be confirmed in situ due to its 'equivalence' to or good correlations with charge passed (in coulombs) and diffusion coefficients as illustrated in Fig. 15.28. The relationships between the electrical charge in coulombs defined in ASTM C1202 and resistivity is graphed in Fig. 15.28 for one of the samples. The regression coefficient was generally high for the equation fitted to the data:

$$\rho(\Omega\ \mathrm{m}) = \frac{200,000}{Q(\mathrm{coulombs})}$$

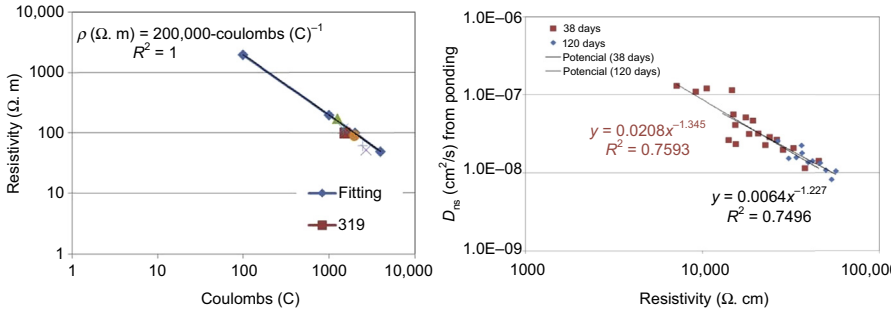



**Figure 15.28** Left: relationship between electrical charge in coulombs and resistivity; and right: relationship between resistivity and the 38- and 120-day apparent diffusion coefficients.

The relationship obtained for the apparent diffusion coefficient, $D_{ns}$, shown on the right in Fig. 15.28, derives from Einstein's equation that relates diffusivity to conductivity (Andrade and Tavares, 2012; Andrade and Whiting, 1996; Tuutti, 1982; Baroghel-Bouny et al., 2010; Saetta et al., 1993; Sagüés, 2003; Mangat and Molloy, 1994; Gulikers, 2004; Andrade, 2004; Andrade et al., 2011, 2014; ASTM C1543-10a; Pr-UNE). The regression coefficient was likewise acceptable in this case. Note that while the basic Einstein relationship gives a slope of $-1$, the slope obtained here was $<-1$ because the parameter used was the apparent coefficient, in which allowance is made for the chloride reaction. As reported in a prior study (Andrade and Tavares, 2012), the effective coefficient yields a slope of $-1$, confirming the applicability of this basic law. The difference between the slopes for a given $y$-intercept can be used to compute the reaction factor $r$ required for the resistivity model, although that parameter was calculated here with Eq. [15.4].

### 15.11.2 Confirmation of the use of the resistivity age factor

The feasibility of using the age factor obtained from the variation in resistivity was shown by comparison with the 120-day diffusion coefficient found from the ponding trials. The findings for the two calculation methods are shown in Fig. 15.29. As noted, mixes A3 and P3 were only tested at a later age of 14 months. For the others, with the exception of mix P50 whose 120-day value proved to be anomalously high, the values found with the two methods were very similar in each mix. No 120-day results were available for mix A56.

### 15.11.3 Calculation of service life with LIFEPRED compared to the resistivity model findings

The values found with the LIFEPRED program for the mixes studied are shown in Fig. 15.30. Three cover depths were analysed: 100, 125 and 150 mm. Fig. 15.30 shows only the data for the two chambers with 'high' or 'extra-high' salinity levels, regarded as detrimental (Table 15.5). The cover depth required to comply with the independent

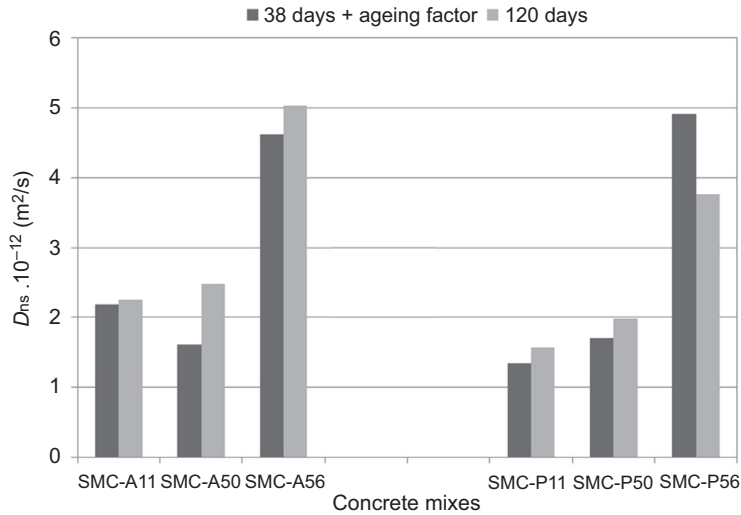



**Figure 15.29** Apparent diffusion coefficient values calculated as the mean 38-day value extrapolated using the resistivity age factor (Table 15.3) and as the 120-day value obtained from ponding.

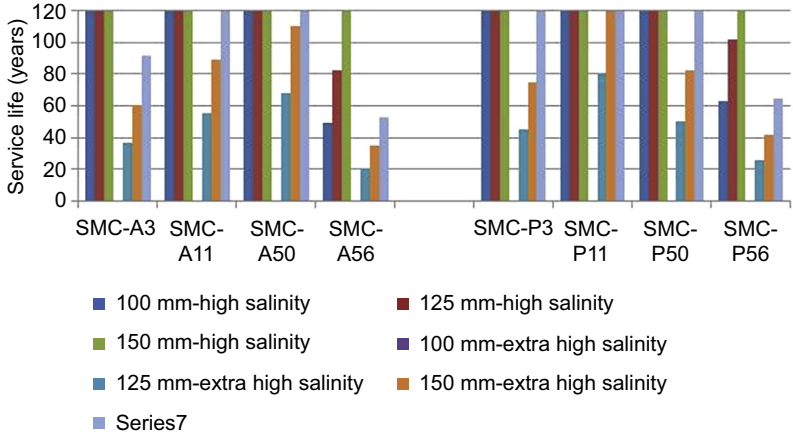



**Figure 15.30** Service lives of concrete calculated with the LIFEPRED program for high and extra-high salinity locks with three cover depths.

1000-C ceiling (equivalent to 200 Ω m) could be found for each chamber or salinity level on the grounds of these calculations.

Service life was also computed with the resistivity model (Eq. [15.3]) using only the initiation period, for the limit state defined by the ACP, which was the absence of corrosion after 100 years. As the hypothetical cases in Fig. 15.31 show, very similar results were found with the two models, which alternately and indistinctly delivered

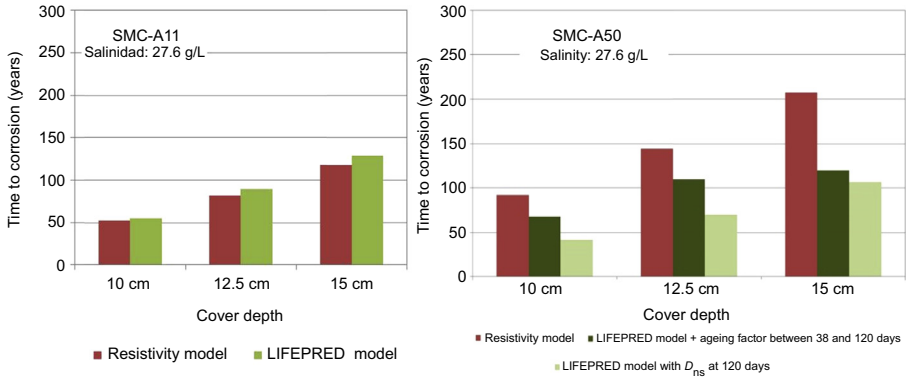



**Figure 15.31** Left: comparison of the LIFEPRED and resistivity models for mix A11; right: comparison for mix A50 of resistivity model to LIFEPRED using the ageing factor between 38 and 120 days and LIFEPRED using the $D_{ns}$ value obtained from ponding at 120 days.

the more conservative prediction. The explanation is to be found in the predictive component of the resistivity model, which is based on the square root of time, therefore respecting the quadratic relationship between distance travelled and time.

## 15.12 Conclusions

As a preliminary consideration it is important to emphasise that at present there are no available test results of 100-year concretes. The experience of calibrating short-term tests with long-term performance is limited to the last 20−30 years during which specific tests have been specified. The requirement of 100 years of service life is 'nominal' as no experience is available to certify it.

The main lesson learnt from the work program developed is the need to better define the concrete specification related to durability in marine environments. The requirement of a concrete with '100-year life' should be accompanied with the following:

- The identification of the deterioration processes. Durability is too general.
  - Define the type of time-explicit model and associate a test type to it.
  - The parameters of the models have to be explicitly and unambiguously obtained.
  - The models should reproduce local exposure classes.
- If a test type is required, definition of the threshold value, and tolerances and actions when nonconformity occurs, has to be precise.
- The concrete age of compliance verification should be defined.

Another important lesson learnt is the need to use local materials because transport adds huge costs to the work. The concrete has to be easy to handle, and the use of multiple materials or the shortage in their supply may be inconvenient compared to using local materials with proven properties.

With respect to the concrete mixes studied, the conclusions that can be drawn are these:

1. The concrete mixes adopted have shown in excess of a 100-year life in the predictions.
2. The resistivity enables the relationship between charge (coulombs) of ASTM C1202 test (1000 coulomb is equivalent to 200 Ω m) and the apparent diffusion coefficient, which allows relating the two basic durability requirements of the Concrete Specification in new Panama Canal: the charge passed and the service life.
3. The resistivity is able to mimic the ageing factor of the chloride $D_{ns}$.
4. Reasonable equivalence between prediction of the LIFEPRED program and the resistivity model were found.
5. The monitoring of concrete quality through the resistivity results is much easier due to the nondestructive character of the measurement.

## Acknowledgements

The authors gratefully acknowledge the assistance received from GUPC and CICP, a private company, in conducting the study. They are also grateful to ACP for the opportunity to discuss the new approaches to service life calculations. Funding was provided by the Spanish Ministry of Education and Science (now Ministry of the Economy and Competitiveness) for the Consolider SEDUREC project of 'Safety and Durability of Construction Structures' under which some of the basic work to develop LIFEPRED was performed.

## References

ASTM 1202, 2010. Standard Test Method for Electrical Indication of Concrete's Ability to Resist Chloride Ion Penetration. Annual Book of ASTM Standards.

Andrade, C., 1993. Calculation of chloride diffusion-coefficients in concrete from ionic migration measurements. Cement and Concrete Research 23 (3), 724−742.

Andrade, C., Tavares, F., 2012. LIFEPRED. Service Life Prediction Program.

Andrade, C., Whiting, D., October 1996. A comparison of chloride ion diffusion coefficients derived from concentration gradients and non-steady state accelerated ionic migration. Materials and Structures, RILEM 29, 476−484.

Andrade, C., 2004. Calculation of initiation and propagation periods of service-life of reinforcements by using the electrical resistivity. In: International Symposium on Advances in Concrete Through Science and Eng., RILEM Symposium, March 22−24, Evanston (Illinois, USA).

Andrade, C., d'Andrea, R., Rebolledo, N., 2014. Chloride ion penetration in concrete: the reaction factor in the electrical resistivity model. Cement & Concrete Composites 47, 41−46.

Andrade, C., Castellote, M., d'Andrea, R., 2011. Measurement of ageing effect of chloride diffusion coefficients in cementitious matrices. Journal of Nuclear Materials 412, 209−216.

ASTM C1543-10a. Standard Test Method for Determining the Penetration of Chloride Ion into Concrete by Ponding.

Baroghel-Bouny, V., Wang, X., Thiéry, M., October 2010. Prediction of chloride binding isotherms by analytical model or numerical inverse analysis. In: Proceedings of the 2nd Symposium on Service Life Design for Infrastructures. (DBMC Service Life). Delft University of Technology.

Gulikers, J., 2004. Critical evaluation of service life models applied on an existing marine concrete structure. In: NORECON Seminar 2004: Repair and Maintenance of Concrete Structures, Copenhagen April 19−20, 2004.

Mangat, P.S., Molloy, B.T., 1994. Predicting of long term chloride concentration in concrete. Materials and Structures 27, 338−346.

Pr-UNE 83988-1 and II Test Methods for Concrete Durability. Determination of the Electrical Resistivity. Direct Method and Four Points or Wenner Method.

Saetta, A., Scotta, R., Vitaliani, R., 1993. Analysis of chloride diffusion into partially saturated concrete24. ACI Materials Journal 90, 441−451.

Sagüés, A.A., October 2003. Modeling the effects of corrosion on the lifetime of extended reinforced concrete structures. Corrosion 854−866.

Tuutti, K., 1982. Corrosion of Steel in Concrete. Swedish Cement and Concrete Institute (CBI), Stockholm, pp. 4−82.

# Durability design of new concrete infrastructure for future development of Singapore City

16

*O.E. Gjørv*
Formerly of Norwegian University of Science and Technology - NTNU, Trondheim, Norway

**'In Memoriam' Prof. Odd E. Gjørv**



The editor and publisher of this book note with great sadness that Prof. Odd E. Gjørv, author of chapter 16, passed away in February 2016 before this book could be published. Prof Gjorv was Professor Emeritus and former head of the Department of Building Materials at the Norwegian University of Science and Technology (NTNU), Trondheim, Norway. He was a member of the Norwegian Academy of Technical Sciences since 1979, and was engaged in a large number of international professional societies and activities for construction materials. He published more than 400 scientific papers and several books in the field of concrete technology. His research mainly involved advanced concrete materials and concrete construction, as well as durability and service life of major concrete infrastructure.

We are grateful for the opportunity to publish this chapter written by Prof Gjorv in honour and memory of him.

## 16.1 Introduction

Singapore is a modern city with a large number of new, spectacular high-rise buildings (Fig. 16.1). However, with a population of more than 5 million located on a small island of only about 700 $km^2$, the city has an extremely limited land area; therefore, the creation of additional space has become an important strategic issue (Fig. 16.2). Traditional methods for space creation include constructing high-rise buildings, excavating underground caverns or placing sand fill along the coasts. But Singapore has nearly reached the limits for new high-rise construction, and creating underground

**Marine Concrete Structures.** http://dx.doi.org/10.1016/B978-0-08-100081-6.00016-7
Copyright © 2016 Elsevier Ltd. All rights reserved.



**Figure 16.1** Singapore has a large number of new spectacular high-rise buildings, some illustrated here.



**Figure 16.2** Singapore is located on a small island with an extremely limited land area for its high population, and the creation of additional space has become an important strategic issue. Figure shows planners discussing this problem.

caverns and placing sand fill are expensive alternatives. A new approach – capturing underwater space – was proposed in a new government-supported research program at Nanyang Technological University in Singapore. This approach comprises constructing offshore concrete structures extending from the seabed to above sea level. The upper surfaces of these structures would provide 'new land', and the volumes captured below sea level could be used for storage capacity or other industrial purposes, thereby freeing up land currently being used for these applications.

For such important concrete infrastructure, the structures would need the highest possible durability, reliability and service lives, so a comprehensive 5-year research program on marine concrete construction was started in 2011. While many different deterioration processes can affect the durability of concrete structures in the marine environment, extensive experience demonstrates that chloride-induced corrosion of embedded steel poses the most critical and greatest threat to the structures (Gjørv, 2014). This is particularly the case for concrete structures located in a tropical climate such as that in Singapore.

As part of the research program, a proper basis for the durability design of the concrete structures had to be established; for this design, the probability-based DURACON Model (Gjørv, 2014; PIANC Norway/NAHE, 2009) was adopted. In the following, the basis for this design is briefly outlined and discussed; reference to Chapter 7 is also given. A brief outline of an experimental program is further given, selected results from which are used as input to some durability analyses to demonstrate how future offshore concrete structures with very low probabilities of corrosion in the given environment could be produced.

## 16.2 Durability design

### *16.2.1 General*

Upon completion of new concrete structures, the achieved construction quality generally shows a high scatter and variability, and in a severe environment, any weaknesses and deficiencies will soon be revealed, whatever durability specifications and materials have been applied (Gjørv, 2014). To a certain extent, a probability approach to the durability design can accommodate high scatter and variability.

However, a numerical approach to the durability design alone is insufficient for ensuring the durability. Since much of the observed durability problems on concrete structures in severe environments can be ascribed to absence of proper concrete quality assurance and poorly achieved construction quality, greater control and improvements in durability also require the specification of performance-based durability requirements that can be verified and controlled during concrete construction to achieve quality assurance. For new major concrete infrastructure, documentation of achieved construction quality and compliance with the durability specification should be essential parts of any rational approach to a more controlled and increased durability. For a more controlled and increased service life, regular condition assessment and preventive maintenance of the structures are also essential.

In recent years, a rapid international development of models and procedures for probability-based durability design has taken place (Gjørv, 2014; CIRIA C674, 2010). In many countries, such design has been applied to a number of new important concrete structures. In 2000, guidelines for probability-based durability design of concrete structures from the European research program DuraCrete were introduced (DuraCrete, 2000). During the following years when practical experience with these guidelines to new marine concrete structures in Norwegian harbors was gained, these guidelines were further developed for more practical and appropriate implementation, but the basic principles remained essentially the same (NAHE, 2004). Lessons learned from further practical experience with these guidelines to new commercial projects were later incorporated into subsequent revised editions and denoted the DURACON Model (Gjørv, 2014; PIANC Norway/NAHE, 2009). At the same time, the model was expanded to provide the basis for concrete quality control and quality assurance during concrete construction, which upon completion of the concrete construction also would give documentation of achieved construction quality and compliance with the

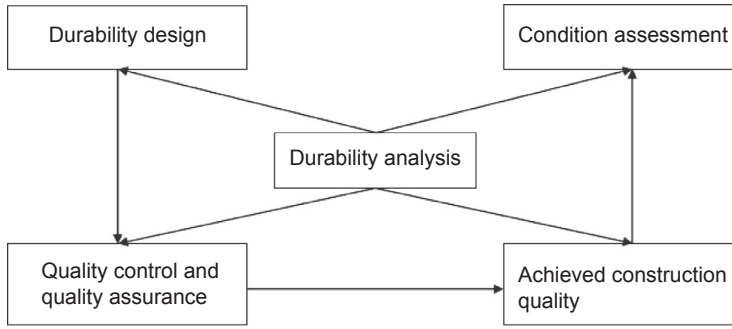



**Figure 16.3** The DURACON Model as a basis for durability design, quality assurance and operation of new major concrete infrastructure in severe environments (Gjørv, 2014; PIANC Norway/NAHE, 2009).

durability specification. The model also provided the basis for control of future chloride ingress as part of the regular condition assessment and preventive maintenance during operation of the concrete structures (Fig. 16.3).

In the DURACON Model, the overall durability requirement is based on the specification of a certain *service period* before the probability for onset of steel corrosion exceeds an upper level of 10%, which is in accordance with current standards for reliability of structures. To calculate the probability of corrosion, durability analyses are carried out, providing a basis for selecting proper combinations of concrete quality and concrete cover that would meet the required durability or *service period* for the given concrete structure in the given environment.

### 16.2.2 Durability analysis

In principle, the probability of corrosion can be calculated by use of several mathematical methods and available software. Based on current experience with durability design of concrete structures in chloride-containing environments, however, a simple combination of a modified Fick's second law of diffusion and a Monte-Carlo simulation was adopted as a basis for the calculation (Ferreira, 2004; Ferreira et al., 2004). Although such a combined calculation can also be carried out in different ways, a special software (DURACON) for this calculation was developed, for which proper information about the following input parameters is needed:

- environmental loading
  - chloride loading ($C_S$)
  - age at chloride loading ($t'$)
  - temperature ($T$)
- concrete quality
  - chloride diffusivity ($D$)
  - time dependence factor ($\alpha$)
  - critical chloride content ($C_{CR}$)
- concrete cover ($X_C$)

All the procedures and methods for determining and selecting these input parameters are described and discussed in more detail elsewhere (Gjørv, 2014), where the link to a free downloading of the DURACON software is also given. It should be noted, however, that in the DURACON Model, the concrete quality is characterized by the chloride diffusivity ($D$) according to the rapid chloride migration (RCM) method (AASHTO TP 64-03, 2003). Since the RCM method does not require any precuring of the concrete, it can be carried out very rapidly, independent of concrete age. Because the method provides a very strongly accelerated test, however, this chloride diffusivity should only be considered as a simple relative index. Although this index does not reflect the long-term capacity of the concrete for chloride binding, it reflects both the porosity and permeability of the concrete as well as the ion mobility in the pore solution of the concrete. Hence, it also reflects both the concrete mixture's resistance to chloride ingress as well as its general durability properties. Using the 28-day chloride diffusivity ($D_{28}$) as an input parameter to the durability design can be compared to using the 28-day compressive strength as an input parameter to the structural design; both parameters are actually relatively simple indices that can be used to establish that a concrete mixture is fit for purpose. However, it should be noted that the 28-day chloride diffusivity is a much more sensitive concrete quality parameter than the 28-day compressive strength.

For major concrete infrastructure where high durability and service life are of special importance, at least a 100-year *service period* should be specified before the probability of corrosion exceeds 10%. For increased *service periods* of more than 100 years, however, the calculation of corrosion probability gradually becomes less reliable. For service periods of up to 150 years, therefore, the corrosion probability should be kept as low as possible and not exceeding 10%, but in addition, some further protective measures such as partly use of stainless-steel or noncorrosive reinforcement should also preferably be specified. For service periods of more than 150 years, however, any calculation of corrosion probability is no longer considered valid. For such long service periods, the corrosion probability should still be kept as low as possible and not exceeding 10% for a 150-year service periods, but in addition, one or more additional protective measures such as partial use of stainless-steel or noncorrosive reinforcement should *always* be specified. If the risk for early age chloride exposure during concrete construction before the concrete has gained sufficient maturity and density is high, special precautions or protective measures should also be applied (Gjørv, 2014; PIANC Norway/NAHE, 2009).

As a result of the aforementioned durability design, requirements to both concrete quality ($D_{28}$) and concrete cover ($X_C$) are established, and this provides the basis for the regular quality control and quality assurance during concrete construction, the procedures for which are described and discussed in more detail elsewhere (Gjørv, 2014; PIANC Norway/NAHE, 2009). Upon completion of the concrete construction, a new durability analysis is then carried out with the obtained average values and standard deviations of both the 28-day chloride diffusivity and the concrete cover as new input parameters. For this durability analysis, all the other originally assumed input parameters, which may have been somewhat difficult to select during durability design, are now kept the same. Therefore, this documentation primarily reflects the results

obtained from the regular quality control of the 28-day chloride diffusivity and the concrete cover during concrete construction, including the scatter and variability observed. As a result, documentation of achieved construction quality and compliance with the durability specification is obtained.

During operation of the concrete structures, further calculations of corrosion probability are carried out as a basis for the regular condition assessment and preventive maintenance of the structures. In this case, the calculations are based on the apparent chloride diffusivities ($D_a$) obtained from the observed rates of chloride ingress in combination with site data on the concrete cover ($X_C$); before this probability of corrosion becomes too high, appropriate protective measure should be implemented (Gjørv, 2014; PIANC Norway/NAHE, 2009).

To provide a certain basis for selecting proper combinations of concrete quality based on constituent materials locally available and concrete cover that would give a probability of corrosion as low as possible for future offshore concrete structures in the harbor region of Singapore City, an experimental program was undertaken as briefly described in the following.

## 16.3 Experimental work

### 16.3.1 Concrete mixtures

Based on preliminary investigations of concrete mixtures with various types of binder systems, four concrete mixtures were selected for more detailed investigations (Table 16.1). As a reference, one of the exploratory mixtures was based on a pure Portland cement (PC), while the other mixtures were produced by replacing portions of the

**Table 16.1 Concrete mixtures (ASTM C1202-10, 2010)**

| Mixture | A | B | C | D |
|---|---|---|---|---|
| *w/b* | 0.28 | | 0.25 | |
| *a/b* | 3.35 | | 2.85 | |
| PC replacement with slag, % | 0 | 30 | 0 | 30 |
| PC replacement with USF, % | 0 | 0 | 10 | 10 |
| Total binder per unit volume, kg/m$^3$ | 523 | 518 | 585 | 580 |
| Coarse aggregate/fine aggregate | 1 | | | |
| HRWRA dosage, % of binder weight | 1 | 1 | 1.5 | 1.5 |
| Aggregate content, % by total batch weight | 72 | 72 | 69 | 69 |

*a/b*, aggregate/binder ratio; *HRWRA*, high-range water-reducing admixture; *PC*, Portland cement; *USF*, un-densified silica fume; *w/b*, water/binder ratio.

PC with various combinations of very finely ground granulated blast-furnace slag (FGGBS) and un-densified silica fume (USF). Although the primary objective of the experimental investigation was to develop a concrete with very high resistance to chloride ingress, some other properties of the concrete were also investigated. The following four concrete mixtures were produced:

- Mixture A was the reference mixture, with only ASTM C150 Type I PC as the binder. Mixture A had a water/binder ratio (*w*/*b*) of 0.28 and an aggregate/binder ratio (*a*/*b*) of 3.35.
- Mixture B was based on Mixture A, with a 30% replacement of the PC with the blast-furnace slag (FGGBS). Mixture B was also produced with *w*/*b* of 0.28 and *a*/*b* of 3.35.
- Mixture C was based on Mixture A, with a 10% replacement of the PC with USF. Mixture C was produced with a *w*/*b* of 0.25 and *a*/*b* of 2.85.
- Mixture D was based on Mixture A, with 30% and 10% replacements of the PC with slag (FGGBS) and USF, respectively. Mixture D was produced with a *w*/*b* of 0.25 and *a*/*b* of 2.85.

In these mixtures, the PC and the blast-furnace slag had surface areas based on Blain of 360 and 870 $m^2$/kg and BET of 1500 and 5000 $m^2$/kg, respectively, while the USF had a BET surface area of about 20,000 $m^2$/kg. All mixtures were produced with a high-range water-reducing admixture (HRWRA) based on polycarboxylic-ether, and they were locally available fine and coarse aggregates with a maximum size of 20 mm.

From the concrete mixtures shown in Table 16.1, more than 100 concrete specimens were produced, mainly consisting of 100-mm cubes and 100 $\Phi \times 200$-mm cylinders. All concrete specimens were water cured at 25°C until time of testing. Both the chloride diffusivity (RCM) and the cube compressive strength were tested for all concrete mixtures. Since the rapid chloride permeability (RCP) according to ASTM C1202-10 (ASTM C1202-10, 2010) is a more internationally known and established test method for characterizing the durability properties of concrete, a simulated testing of RCP was also carried out in combination with the RCM testing; these two methods are very similar in testing conditions. For the RCM testing, the total charge passing through the concrete for the first 6 h was recorded with readings every 30 min.

### 16.3.2 Concrete properties

From Table 16.2, it can be seen that the combined inclusion of both FGGBS and USF (Mix D) significantly reduced the chloride diffusivity compared to that of the other mixtures; both the early age and the ultimate chloride diffusivity of the concrete were reduced. For concrete construction work in marine environments, also high early age resistance to chloride ingress may be important if the risk for early age exposure before the concrete has gained sufficient maturity and density is high.

After three days of water curing, mixes B, C, and D reached chloride diffusivities of 2.6, 1.9 and $1.7 \times 10^{-12}$ $m^2$/s, respectively, compared to $10.2 \times 10^{-12}$ $m^2$/s for the reference mixture (Mix A). For the same mixtures, 28-day chloride diffusivities of 1.0, 0.2 and $0.1 \times 10^{-12}$ $m^2$/s, respectively, were obtained, while the reference concrete

**Table 16.2 Chloride diffusivity (RCM) and chloride permeability (RCP) (ASTM C1202-10, 2010)**

| Mix | Age (days) | RCM ($D \times 10^{-12}$ m$^2$/s) | RCP (coulombs) |
|---|---|---|---|
| A | 3 | 10.2 | 2704 |
| | 28 | 7.9 | 2487 |
| | 56 | 6.0 | 2094 |
| | 90 | 3.8 | 1741 |
| B | 3 | 2.6 | 1233 |
| | 28 | 1.0 | 472 |
| | 56 | 0.7 | 470 |
| | 90 | 0.5 | 345 |
| C | 3 | 1.9 | 821 |
| | 28 | 0.2 | 196 |
| | 56 | 0.1 | 118 |
| | 90 | 0.04 | 54 |
| D | 3 | 1.7 | 876 |
| | 28 | 0.1 | 117 |
| | 56 | 0.07 | 98 |
| | 90 | 0.01 | 47 |

achieved $7.9 \times 10^{-12}$ m$^2$/s. Somewhat depending on the binder system, it may take a long time before a final value of the chloride diffusivity is reached. After 90 days of water curing, however, mixes B, C and D showed chloride diffusivities of 0.5, 0.04 and $0.01 \times 10^{-12}$ m$^2$/s, compared to $3.8 \times 10^{-12}$ m$^2$/s for the reference concrete (Mix A). Therefore, all the results for mixes B, C and D reflect a very high resistance to chloride ingress.

Since the chloride diffusivity based on the RCM method was carried out by use of the same electrical potential (60 V) and the same preconditioning of the test specimens as that in the RCP method, both of these test methods were carried out in parallel on the same concrete specimens. After 28 days of curing, the total amount of charge passed during the first 6 h was 2478, 472, 196 and 117 coulombs for mixes A, B, C and D, respectively, while after 90 days, the charge passed was 1741, 345, 54 and 47 coulombs, respectively (Table 16.2). It should be noted that the applied sodium chloride concentration for the RCM testing is 10%, while it is 3% for the RCP testing. However, the present results indicate that also the RCP of both mixes C and D reached negligible values, indicating very good durability with very high resistance to chloride ingress.

The compressive strength of the various types of concrete was also very good. Thus, after 3 days of water curing, mixes A and B showed compressive strengths of 76.5 and 94.5 MPa, respectively, while mixes C and D showed compressive strengths of 82.5 and 110.5 MPa, respectively. After 28 days, the compressive strengths of mixes A, B, C and D were 91.5, 110.0, 120.5 and 135.0 MPa, respectively. The inclusion of FGGBS and USF had significantly increased both the early age and the ultimate compressive strength of the concrete. Also the workability of the fresh concrete mixtures was very good, showing rheological properties similar to that of self-consolidating concrete. Further information about the experimental investigations is given elsewhere (Teng et al., 2014, 2016).

## 16.4 Probability of corrosion

### 16.4.1 General

As a first step of durability design, some durability analyses were carried out to determine how the aforementioned four concrete mixes A to D (Table 16.2) of differing qualities, in combination with a nominal concrete cover of 70 mm, would influence the probability of corrosion for a *service period* of up to 150 years.

### 16.4.2 Effect of concrete quality

Based on the obtained values of the 28-day chloride diffusivity ($D_{28}$) and a nominal concrete cover of 70 mm ($X_C$), calculations of corrosion probability were carried out; estimated input parameters both for the time dependence of the chloride diffusivity ($\alpha$) and the critical chloride content ($C_{CR}$) are shown in Table 16.3. For the other input parameters to the calculations, estimated average values with standard deviation both for chloride loading $C_S$ (5.5; 1.4%), age at chloride loading $t'$ (28 days), and

**Table 16.3 Input parameters for analyzing the effect of concrete quality**

| Concrete | Input parameter | | | |
|---|---|---|---|---|
| | $D_{28}$ ($m^2/s \times 10^{-12}$) | $\alpha$ | $C_{CR}$ (% by wt of binder) | $X_C$ (mm) |
| Mix A | N[a](7.9; 1.9) | N(0.5; 0.1) | N(0.4; 0.1) | N(70; 7) |
| Mix B | N(1.0; 0.25) | | | |
| Mix C | N(0.2; 0.05) | | | |
| Mix D | N(0.1; 0.025) | | | |

[a]Normal distribution with average value and standard deviation.

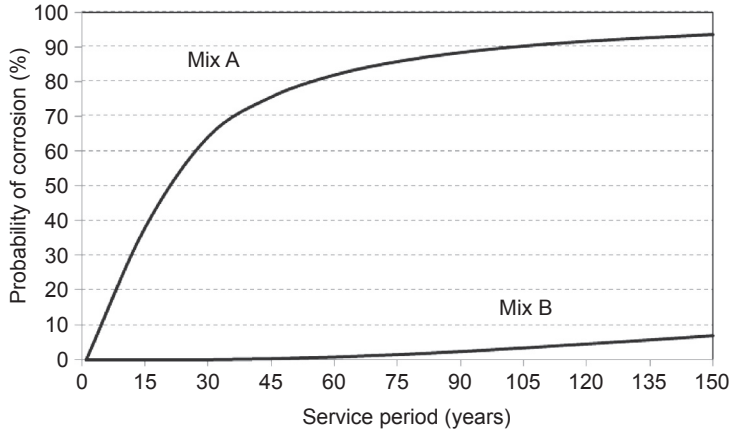



**Figure 16.4** Effect of concrete quality on the probability of corrosion.

temperature $T$ (30°C) were selected. For all input parameters, a normal distribution was assumed.

As a result of these calculations, all the concrete mixtures B to D would meet the required 150-year service period before 10% probability of corrosion would be reached. Although the reference concrete (Mix A) also had a very low water/binder ratio and thus would generally be considered very durable, Fig. 16.4 demonstrates that this concrete distinctly failed to meet the required durability. For the concrete of Mix B, approximately 7% probability of corrosion would be reached, while for the two other types of concrete (mixes C and D), the 28-day chloride diffusivities were so low that it was not possible to quantify or detect any probability of corrosion for a 150-year service period.

For evaluation of these results (Fig. 16.4), it should be noted that the obtained *service periods* should not be considered to reflect any service life of the given concrete structures. Nor should the *service periods* be considered as any real time until start of corrosion. As discussed in Chapter 7, these calculations of corrosion probability were only used as a simple engineering tool for quantifying and comparing the combined effect of various concrete qualities and concrete covers to obtain a best possible durability of the future concrete structures in the given environment. Thus, both concrete mixes C and D, and may be also Mix B in combination with a nominal concrete cover of 70 mm, would be proper selections for production of the future concrete structures.

It may be argued that the aforementioned durability analyses were only based on the obtained 28-day chloride diffusivities of the various concrete mixtures, while a further reduction of the chloride diffusivity for the various concrete mixtures would develop somewhat differently. Therefore, some additional durability analyses based on the chloride diffusivities obtained after longer curing periods of up to 90 days were also carried out, but none significantly changed the relative basis for comparing the effect of the various types of concrete.

**Table 16.4 Input parameters for analyzing the effect of concrete cover (Mix A)**

| Input parameter | Average value | Standard deviation | Comments |
|---|---|---|---|
| $D_{28}$ | 7.9 | 1.9 | Chloride diffusivity ($m^2/s \times 10^{-12}$) |
| $\alpha$ | 0.5 | 0.1 | Time dependence factor |
| $C_{CR}$ | 0.4 | 0.1 | Critical chloride content (% by wt of binder) |
| $X_C$ | 70 | 7 | Nominal concrete cover (mm) |
| | 90 | 7 | |
| | 120 | 7 | |

### 16.4.3 Effect of concrete cover

To find out whether an increased concrete cover beyond 70 mm would make it possible to also use the reference concrete mixture (Mix A) and still meet the required durability, some further durability analyses based on 90- and 120-mm concrete cover were also carried out (Table 16.4). These analyses were only carried out for the reference concrete mixture (Mix A), while holding all the other input parameters from the previous analyses constant. From Fig. 16.5 it can be seen, however, that even an increased cover depth of up to 120 mm would not meet the required durability for this type of concrete; the probability of corrosion would still reach approximately 50% for a service period of up to 150 years.

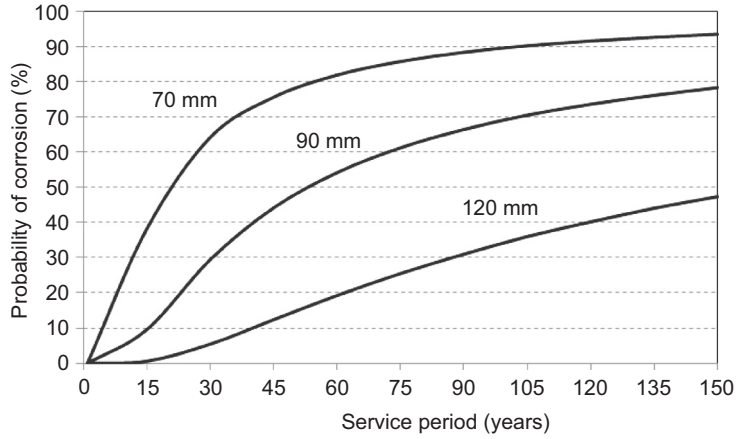



**Figure 16.5** Effect of concrete cover on the probability of corrosion (Mix A).

## 16.5 Discussion of results

As already emphasized, it should be noted that the aforementioned calculations of corrosion probability should not be considered as any prediction of service life. Nor should the s*ervice periods* be considered as any real time until start of corrosion. Based on all assumptions and simplifications in these calculations of corrosion probability, the durability analyses were only carried out to provide a certain basis for quantifying and comparing the effect of various technical solutions for the durability of the future concrete structures in the given environment.

Even for s*ervice periods* of more than 150 years, both concrete mixes C and D, and possibly also Mix B in combination with a nominal concrete cover of 70 mm, would be proper selections for production of the future concrete structures. For combinations of increased concrete covers of more than 70 mm or use of additional protective measures such as replacement of the outer layer of the rebar system with stainless-steel or noncorrosive reinforcement, even higher durability with lower risk of corrosion for the future offshore concrete structures would then be obtained.

As also already emphasized, much of the durability problems typically observed on marine concrete structures can be ascribed to lack of proper quality assurance during concrete construction and poorly achieved construction quality. As a result of this durability design, however, performance-based durability requirements are established, which provide a proper basis for concrete quality control and quality assurance during concrete construction. This would also be of greatest importance for ensuring a best possible durability of the future offshore concrete structures in Singapore City.

The application of the DURACON Model to a number of new commercial projects in recent years has shown that the required documentation of achieved construction quality and compliance with the durability specification has been very important for obtaining a best possible construction quality and durability of the structures (Gjørv, 2010, 2014, 2015). This was clearly demonstrated during the new city development on Tjuvholmen in the harbor region of Oslo City, which was carried out during the period 2005 to 2010; this project includes a number of business and apartment buildings on top of concrete substructures in seawater, providing up to four levels of submerged parking (Fig. 16.6).

The Tjuvholmen project was carried out by two different contractors, one of which applied the DURACON Model as a basis for the contract, while the other mainly based the contract on the prescriptive durability specifications according to the then-current European Concrete Standards with some additional protective measures. As a result, it was typically observed that the performance-based durability specification distinctly clarified the responsibility of the contractor for the quality of the construction process. During concrete construction, any unacceptable deviations from the performance-based requirements for concrete quality and concrete cover could be detected and corrected for. The required documentation of compliance to the durability specification clearly resulted in improved workmanship during concrete construction with reduced scatter and variability of achieved construction quality.

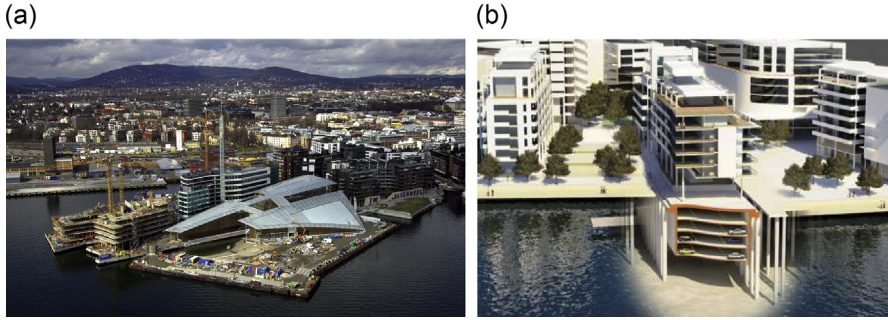



**Figure 16.6** The new city development on Tjuvholmen in the harbor region of Oslo City includes a number of business and apartment buildings on top of concrete substructures in seawater, providing up to four levels of submerged parking, illustrated in this figure (Gjørv, 2015). Photo (a) courtesy of Terje Løchen and (b) Contractor B

However, for all the other concrete structures where only the prescriptive durability requirements were applied, it was not possible to provide any documentation of compliance with the durability specification. These concrete structures typically showed a higher scatter and variability of achieved construction quality (Gjørv, 2015). For one of the structures, a severe segregation of the self-consolidating concrete also took place during concrete construction. Separate investigations based on extensive concrete coring of this particular structure clearly demonstrated that the durability properties of the segregated concrete were distinctly reduced, but it was not possible to provide any documentation of increased *w*/*b* ratio of the segregated concrete beyond what was specified as a basis for the contract. Also, since the in-place compressive strength of the segregated concrete was just high enough to be acceptable according to the current concrete standard, the owner had to accept the reduced durability of this particular structure; it was very difficult to argue against a contract only based on some prescriptive durability requirements that could not be verified and controlled during concrete construction.

## 16.6 Conclusions

As a basis for durability design and execution of new major concrete infrastructure in severe environments such as the marine environment, all minimum requirements in existing concrete codes and practice for ensuring the durability must be strictly fulfilled. Although chloride-induced corrosion represents the biggest challenge to the durability of concrete structures in such environments, there are also a number of other deterioration processes that need proper attention; in particular, a proper control of early age cracking during concrete construction needs special attention.

Over the last decade, however, there has been a rapid international development of new knowledge and experience on durability and service life of new concrete structures for severe environments, while current concrete codes and practice for concrete

durability have typically shown a very slow upgrading. Thus, it took more than 30 years for the existing European Concrete Standards to reach the same strict durability specifications for concrete structures in marine environments as those specified for the first offshore concrete structures produced for the oil and gas industry in the North Sea in the early 1970s (FIP, 1973). Although the required service life for the offshore concrete structures in the North Sea was much shorter than what was typically required for other marine concrete structures, the international oil and gas industry was much more demanding for obtaining a more safe and regular operation of their installations. After more than 40 years of experience, the offshore concrete structures in the North Sea have typically shown much better durability than that of other marine concrete structures produced during the same period. However, the offshore concrete structures in the North Sea also typically showed a high scatter and variability of achieved construction quality (Gjørv, 2014), and for some of these concrete structures, very costly durability problems have occurred that could be ascribed to lack of proper quality assurance during concrete construction and poor achievement of construction quality.

To obtain a more controlled and increased durability of new major concrete infrastructure beyond what is possible based only on existing concrete codes and standards, additional procedures for durability design, such as those described in this chapter, for future offshore concrete structures in Singapore City should be applied. Based on the durability design and experimental investigations as briefly described and discussed in the present chapter, it appears that very durable offshore concrete structures for a future development of Singapore City can be produced.

## References

AASHTO TP 64-03, 2003. Predicting Chloride Penetration of Hydraulic Cement Concrete by the Rapid Migration Procedure. American Association of State Highway and Transportation Officials, Washington, DC.

ASTM C1202-10, 2010. Electrical Indication of Concrete's Ability to Resist Chloride Ion Penetration. ASTM International, West Conshohocken.

CIRIA C674, 2010. The Use of Concrete in Maritime Engineering − A Guide to Good Practice. CIRIA Classic House, London.

DuraCrete, 2000. DuraCrete − General Guidelines for Durability Design and Redesign, the European Union Brite EuRam III Research Project: Probabilistic Performance Based Durability Design of Concrete Structures. Document BE95-1347/R15. CUR, Gauda.

Ferreira, R.M., 2004. Probability-based Durability Design of Concrete Structure in Marine Environment (Ph.D. thesis). University of Minho, Guimarães.

Ferreira, R.M., Gjørv, O.E., Jalali, S., 2004. Software for probability-based durability design of concrete structures. In: Oh, B.H., Sakai, K., Gjørv, O.E., Banthia, N. (Eds.), Proceedings from 4th International Conference on Concrete Under Severe Conditions − Environment and Loading. Seoul National University and Korea Concrete Institute, Seoul, pp. 1015−1024.

FIP, 1973. Recommendations for the Design and Construction of Concrete Sea Structures. Fédération Internationale de la Précontrainte, London, ISBN 0-7210-0932-8.

Gjørv, O.E., 2014. Durability Design of Concrete Structures in Severe Environments, second ed. Taylor & Francis, CRC Press, London and New York. Also published in Chinese by Press of China Building Materials Industry, Beijing (2015) and in Portuguese by Oficina de Textos, Sao Paulo (2015).

Gjørv, O.E., 2010. Durability design and quality assurance of concrete infrastructure − performance-based programs boost service life. Concrete International 32 (9), 29−36.

Gjørv, O.E., 2015. Quality control for concrete durability − a case study provides comparisons of work performed under performance and prescriptive specifications. Concrete International 37 (11), 52−57.

NAHE, 2004. Durable Concrete Structures − Part 1: Recommended Specifications for New Concrete Harbour Structures, Part 2: Practical Guidelines for Durability Design and Concrete Quality Assurance. Norwegian Association for Harbour Engineers (NAHE), TEKNA, Oslo (in Norwegian).

PIANC Norway/NAHE, 2009. Durable Concrete Structures − Part 1: Recommended Specifications for New Concrete Harbor Structures, Part 2: Practical Guidelines for Durability Design and Concrete Quality Assurance, third ed. Norwegian Association for Harbor Engineers (NAHE), TEKNA, Oslo (in Norwegian).

Teng, S., Divsholi, B.S., Lim, T.Y.D., Gjørv, O.E., 2014. Concrete with very high resistance to chloride ingress. Concrete International 36 (5), 30−36.

Teng, S., Divsholi, B.S., Lim, T.Y.D., Gjørv, O.E., 2016. Durability of very high strength concrete with supplementary cementitious materials for the marine environment. ACI Materials Journal 113 (01), 95−103.

# Index

'*Note*: Page numbers followed by "f" indicate figures, "t" indicate tables.'


**A**
AAR. *See* Alkali-aggregate reaction (AAR)
Abegweit Passage, 201
Abrasion resistance, 156
Accelerated low water corrosion (ALWC), 384
Accropode™, 50, 50f
Aggregates, 161
Alkali-aggregate reaction (AAR), 156
Alkali-silica reaction (ASR), 74, 289
Al Raha Eastern Precinct island walls, 221
Al Sowwah Quay Wall, 219
Alternative reinforcement
  corrosion-resistant steel, 162–163
  epoxy-coated steels, 162
  nonferrous reinforcement, 163
Amsterdam Ordnance Datum (AOD), 322
Anchor walls, 32–33, 32f
Ancillary durability issues
  hydraulic erosion, of concrete surfaces, 421–422
  marine structures subject to wave action, 423–425
  Walvis Bay shiplift jetties, 418–419
  wind-induced surface ablation, 419–420
Anti-washout admixtures, 9–10, 75–76, 161
AOD. *See* Amsterdam Ordnance Datum (AOD)
Appropriate binders/cements
  non-Portland cements, 160
  Portland cement, types, 157
  supplementary cementing materials, 157–160
Arabian Gulf region
  allowable crack widths, 230, 231f
  alternative reinforcement, 222–223
  challenges of designing, 216–218
  concrete cover, 227–230
  concrete mixture design, 227, 228t
  concrete quality monitoring
    compressive strength test results, 235–236
    initial surface absorption test results, 237
    petrographic tests, 234
    rapid chloride permeability test, 233–234, 233f, 235f
    water absorption test results, 236
    water permeability test results, 237
  constructing marine concrete structures, 216–218
  construction methodology
    Al Raha, Western precinct, islands, 223, 223f
    concrete batching plant, 223, 224f
    lifting frame and 250-ton crawler crane, 225, 225f
    L-wall placement, 226, 226f
    precast units lifting, casting beds and storage, 224, 224f–225f
    stone foundation bed, 225–226, 226f
  corrosion protection systems, 222–223
  diaphragm walls, 220f
    Al Raha Eastern Precinct island walls, 221
    Al Sowwah Quay Wall, 219
    precast fascia panel installation, 220f, 221
  Dubai Dry Docks, 216
  quality assurance procedure, 230–232
  ready-mixed concrete, 215–216
  reinforced in situ and precast concrete, 218–219
  risk assessments and service-life predictions, 227–230
  typical marina developments, 218
  unreinforced block wall *vs.* reinforced concrete L-wall, 221–222, 222f
  unreinforced precast concrete, 218, 219f
Australian standards, 72

**B**
Bagnold explosion, 379, 379f
Blockwork walls
  Berth, Durban, 19, 20f
  Durban Container Terminal, 19, 21f
  Port of Maputo Harbour, 19
  Victoria Basin, Cape Town, 18, 18f–19f
Boat ramps/slipways
  boat ramp surface V-grooves, 45f
  longitudinal section, 44f
  Mossel Bay harbour slipway, 45f
  trailer launched small craft, Victoria & Alfred Waterfront, 44f
Breakwater armour units, 49f–50f, 106–108
BS 6349 codes, 71

**C**
Caisson walls
  dry dock construction, 20, 23f
  Durban Berths D to G, 22, 24f–25f
  Richards Bay Coal Terminal, 20, 22f–23f
  Saldanha Bay, 22, 23f
Calcium nitrite inhibitor (CNI), 161
Canal, Victoria & Alfred Waterfront (V&AW), 252–257, 254f–255f
  aquarium deck cross-section, 253f
  aquarium deck under construction, 253f
  canal jetty cross-section, 257f
  canal wall under construction, 256f
  layout, 254f
  portion, residential area, 254f
  typical canal wall cross-section, 256f
Cantilever walls, 25–27, 28f
Carbonation model, 348–349, 349t, 350f
Carbon steel, 76
Cathodic protection, 359
Chemical admixtures
  anti-washout admixtures, 161
  corrosion inhibitors, 161
Chloride diffusivity, 353, 354t
Chloride-induced corrosion, 289
Chloride ingress
  design parameters, 346–347, 347t
  design results, 347, 348f
  Fick's second law, 346
CIRIA, 11
Clad carbon steel, 77
Coastal, 1
Coastal jetties
  Durban beach groynes, 52, 53f
  u'Shaka Marine World intake jetty, 52, 53f
  wave impacts, 52, 52f
Coastal protection structures, Netherlands
  Delta Project, 322–323, 323f
  Eastern Scheldt Storm Surge Barrier
    condition assessment and survey, 331–336
    description, 323, 324f
    durability design, 324–331
  Kleine Sluis/Small Lock, 321, 322f
Coastal structures, 46
  breakwater armour units, 49f–50f
  breakwater cap, 51
  breakwaters/revetments, 47–52, 48f
  bridges, 53
  caisson breakwater, 51–52, 51f
  coastal jetties
    Durban beach groynes, 52, 53f
    u'Shaka Marine World intake jetty, 52, 53f
    wave impacts, 52, 52f
  hydraulic coastal structures, 54–56
  intake and outfalls, 59–60
  lighthouses, 59, 59f
  oil production platforms, 57
  pump stations, 60–61
  seawalls, 46–47, 46f–47f
  submarine pipelines, 53–54, 54f–55f
Cold marine environments, 177–178
Common midpoint (CMP) method, 354
Concrete testing program, 231–232
Confederation Bridge, 208–209
  Abegweit Passage, 201
  concrete mix design, 209–210
  design considerations
    design compressive strength, 206
    freeze-thaw resistance, 206–207
    materials, 207–208
    prefabrication, 203
    weight limitations, 202–203, 202f–203f
  field performance, 211–212, 212f–213f
  financial considerations, 202
  ice shield, in winter, 201, 201f
  ice shields, 210–211

Prince Edward Island (PEI) and New Brunswick, Canada, 199, 200f
Core-loc®, 50, 50f
Corrosion inhibitors, 75, 161
Corrosion-resistant steel, 162–163
Counterfort walls
Richards Bay, 24–25, 27f
Saldanha Bay, 24, 26f
typical precast counterfort unit, 22, 26f
Crack control, 83
flexural crack checks, 86–87, 86t
minimum reinforcement, 87
shrinkage crack checks, 84–86
significance of cracking, 83
Cubipod, 50, 50f

**D**

Danish strait crossings
asset management, 316–317
concrete durability issues, 287–289
Femern Bælt Tunnel
description, 310–312
design, 312–313
execution, 314
inspection and maintenance, 314
materials, 313–314
Lillebælt Bridge
description, 290
design, 291
execution, 292
inspection and maintenance, 292–293
materials, 291–292
location map, islands and straits, 287, 288f
Øresund Link
description, 302–303
design, 303–305
execution, 305–309
inspection and maintenance, 309–310
materials, 305
ownership and financing, 315–316
Storebælt Link
description, 293–294
design, 294–296
execution, 297–300
inspection and maintenance, 300–301
materials, 296–297
Delta Project, 322–323, 323f
Desirable properties, 151
abrasion resistance, 156
alkali-aggregate reaction (AAR), 156
chloride resistance
convection, 153
diffusion, 153
migration, 154
permeation, 153
exposure class, 152–153
freeze-thaw resistance, 154–155
structure type, 152–153
sulphate resistance, 155–156
Diaphragm walls, 30–31, 31f, 220f
Al Raha Eastern Precinct island walls, 221
Al Sowwah Quay Wall, 219
precast fascia panel installation, 220f, 221
Dry docks/ship lifts, 42, 43f
Dubai Dry Docks, 216
Duplex and Lean Duplex stainless steels, 77
Durability limits states (DLS), 344
DURACON Model, 462, 462f, 470
Durban Bluff, 389
Durban Harbour entrance
layout, 272f
north groyne, 273
sand bypass hopper, 273–275
south breakwater, 271–272
Durban Maydon Wharf 12, 276f
concrete components, 276–278
plan view, 276f
Durban Point Yacht Club (DPYC), 387–389

**E**

East Bridge, Storebælt Link, 293, 295–296
Eastern Scheldt Storm Surge Barrier
condition assessment and survey, 331–336
description, 323, 324f
durability design, 324–325
chloride content, predicted development, 327, 328f
conceptual two-stage model, 326, 326f
exposure conditions, 325
piers under construction, 330, 331f
predicted corrosion rates, 328–329, 329f
reinforcement corrosion, initiation and propagation stage, 329–330, 330f
East Tunnel, Storebælt Link, 293–295
Engineer procure construct (EPC), 116

Epoxy-coated carbon steel, 76–77
Epoxy-coated rebars, 359
Epoxy-coated reinforcement (ECR), 162
Eurocodes, 71
Extending service life, 167–168

**F**
Femern Bælt Tunnel
  description, 310–312
  design, 312–313
  execution, 314
  inspection and maintenance, 314
  materials, 313–314
Fibre-reinforced plastics (FRP), 79
Freeze-thaw resistance, 154–155
Frost damage, 289
Full probabilistic method, 358t
  atmospheric zone, bridge elements, 363–364
  failure probability of concrete elements, 359–362, 362f
  immersed tube tunnel, 365
  immersed zones, bridge elements, 364–365
  protection measures, 359–362, 360t–361t
  splash and tidal zones, bridge elements, 364

**G**
Grade 304 and 316 stainless steel, 77
Grade 3CR12 stainless steel, 77
Granger Bay shoreline protection, 242, 244f
  casting yard, 244f
  revetment cross-section, 243f
  25-ton dolosse, 243, 243f
  typical dolosse packing, 245f
Guano Island landing stage, 396–397

**H**
High-density polyethylene (HDPE), 53–54
High-range water-reducing admixture (HRWRA), 465
HLV *Svanen* catamaran, 202–203, 202f
Hong Kong–Zhuai-Macau (HZM) sea link project, 365
  artificial islands, 339–341, 342f
  constitutive elements, concrete structures, 339–341, 343t
  design philosophy, 344, 345t
  durability assessment, 356–357
    assessment model, 357
    construction options, 357–359
    full probabilistic method, 359–365
  durability design
    carbonation model, 348–349, 349t, 350f
    chloride ingress, 346–347
    requirements, 344–346, 345t, 350–352
  general overview, 339, 340f
  immersed tunnel tube segments, 339–341, 341f
  life-cycle management, 366
    inspection and monitoring, 366, 367f
    strategy, 367–368, 368f
  non-navigable bridge spans, 339–341, 340f
  quality control
    chloride diffusivity, 353, 354t
    concrete cover thickness, 354–355, 355t
    durability, 352–353
    NDT measurements, 355–356
    nondestructive tests (NDT), 352
Hot dip galvanised carbon steel, 76
Hydraulic coastal structures
  ship and boat locks, 54–56, 56f
  surge barriers, 56, 57f–58f
HZM. *See* Hong Kong-Zhuai-Macau (HZM) sea link project

**I**
In situ tests, marine concretes, 167, 167f

**J**
Japan Society of Civil Engineers (JSCE), 72
Jetties/wharves
  deck on piles, 38f
    caisson/blockwork pier substructure, 39f
    cargo handling, Maydon Wharf, Durban, 38f
    dry bulk jetty, Richards Bay, 36f
    precast units, wharf construction, 36f
    Saldanha Bay iron ore export jetty, 39f–40f
    small craft jetty, Mossel Bay, 34f
    typical fully decked jetty, 34f
    typical fully decked wharf, 35f
    wharf structure, Mossel Bay, 36f
  marine construction methodologies, 123–124, 123f–124f

skeletal jetties, 37–42
V&A Waterfront, 33, 33f

**L**
Lamberts Bay diamond quay, West Coast of South Africa, 408–409
LIFEPRED model, 443, 444f–445f
Lillebælt Bridge
description, 290
design, 291
execution, 292
inspection and maintenance, 292–293
materials, 291–292
L-wall, 221–223, 222f

**M**
Marine, 1
Marine concrete structure design/specification, 69–71, 95–96, 108–109
Australian standards, 72
blockwork wall units, 98
breakwater armour units, 106–108
BS 6349, 71
caisson units, 98
cathodic protection, 110–111
chloride content, 108
construction joints, 109–110
counterfort units, 98–99
cover spacers, 108, 109f
curing, 110
Eurocodes, 71
grout, 80–81
indicative design working life categories, 68, 68t
Japanese guidelines, 72
materials
aggregates, 74–75
cements, 73–74
concrete admixtures and surface treatments, 75–76
extenders, 73–74
fibres, in concrete, 79
reinforcement, 76–79
microenvironments, exposure conditions, 66, 67f, 67t
piles, 99–100, 99f, 101f
plain concrete marine structure components, 80, 80t
prescriptive *vs.* performance-based specifications, 68–69, 70t
reinforced concrete marine structures
codes of practice, 87–95
durability design, 81–87
strength design, 87
South African standards, 72–73
steel corrosion, 65
superstructure units
beams, 103–104, 105f–106f
fender cope units, 106, 107f
pile caps and headstocks, 100–102, 102f–103f
slabs, 104–106, 106f
USA standards, 72
Marine construction structures/methodologies
available resources
materials, 117
personnel, 119
plant and equipment, 117–119, 119f
boat ramps and slipways, 128, 128f
breakwaters, 124–126, 125f–127f
computer modelling and software, 132, 132f
design, 116–117, 118f
dry docks and ship lifts, 127
fundamental requirements
Little Bay bridge, US., 6–8, 8f
materials selection and concrete specifications, 9–10
Storebælt East Bridge, Norway, 6–8, 8f
structural selection and form, 10–11
jetties/wharves, 123–124, 123f–124f
location, 116
materials, 130
monitoring technology, 131
quay walls
block wall, 120
caisson wall, 120–121
cantilever walls, 122
counterfort cantilever precast unit, transit, 121, 122f
counterfort walls, 121
gantry, precast element placement, 121, 122f

Marine construction structures/methodologies (*Continued*)
specialised barge-mounted piling rig, 122, 123f
typical stone spreader arrangement, 120, 121f
renewable energy, 131
tolerances, 130
types. *See* Coastal structures; Port structures; Sea water-retaining structures
underwater concrete construction, 128−130, 129f
Marine environment, 5f, 6
chemical mechanisms, deterioration
cementitious composites, 141−142, 141t
chloride profiles, 143, 143f
Fick's second law, 143
gypsum, 142
seawater composition, 141, 141t
defined, 4
durability requirements, different codes, 146t−147t
importance of concrete, 2−3, 2f
loading, 4
marine exposure classes, 5−6, 7t
marine exposure zones, 139−140
physical mechanisms, deterioration, 144
steel corrosion, 144−145
transport process and movement, salts, 4−5, 5f
transport processes
absorption, 138−139
capillary suction, 139
different exposure conditions, 137−139, 138f
permeation, 139
Marine exposure classes, 5−6, 7t
Marine exposure environments, 180
categorisation, 177
cold marine environments, 177−178
hot and dry marine environments, 178−179
hot and wet marine environments, 179−180
moist marine environments, 179−180
temperate marine environments, 178
concrete mix composition and quality, 189−190
cracking effect, 190−191
dominant mechanism, deterioration, 183−189
marine sites, 184t−187t
caged concrete specimens, 181−182, 182f
medium-sized beam specimens, 182, 183f
small-sized beam specimens, 182, 183f
spatial variability, deterioration, 191
variability, 172, 176−177
freeze-thaw cycles, 175−176
pH and aggressive species concentration, 172−173
precipitation and fresh water inflow, 173
suspended solid particles, in seawater, 174−175, 175f
temperature and relative humidity, 173
wettingedrying cycles and time duration, 173
wind intensity and direction, 174, 174f
Maritime, 1
Mercury intrusion porosimetry, 440
Mix design/proportioning
performance approach, 164−165
prescriptive approach, 163−164

**N**

New Lillebælt Bridge, 290f, 292
New Marina Basin, 245f
aquarium deck, 252, 253f
cut edge lining, 248−250, 249f
east jetty, 250−252, 251f−252f
North Wharf, 250, 250f−251f
residential edge wall
completed section, 248f
concrete durability requirements, 248t
construction, 247f
cross-section, 247f
New Panama Canal
concrete design philosophy and basis, 435−436, 436f−437f
construction aspects, 439
construction, old Panama Canal, 429, 429f
dimensions and statistics, 430, 431t
environment/salinity, 435, 436t
experimental program, GUPC and IETcc

chloride penetration, 442–443
composition of four concrete mixes, 439, 441t
electrical resistivity, 440
mercury intrusion porosimetry, 440
ponding to determine chloride penetration, 443f
resistivity measurement, 442f
sample preparations, 442f
test and objective, 439, 440t
Lake Gatun, 429, 430f
LIFEPRED model, 443, 444f–445f
location, 429
locks, present canal, 429–430
new locks with side water saving basins, 430
old canal test
age factor values, 451, 452t
chloride profiles, 447–449, 448f–449f
diffusion coefficients, 38- and 120-days, 451, 453f
electrical resistivity, 449, 450f
mercury intrusion porosimetry values, 451f
non-steady-state chloride diffusion coefficients, 449, 450t
resistivity values, 200 days, 451, 452f
total porosity, mercury porosimetry, 449, 451f
particular aspects, 437, 438f
resistivity-based model, 445
electrical resistivity plot, 445, 446f
old canal, test, 446–447, 447f
result analysis, 452
diffusion coefficient, 453–454
electrical charge and resistivity, 453–454
LIFEPRED vs, resistivity model findings, 454–456
resistivity age factor, 454
ship size comparison, 430
structure details
concrete and aggregate plants, 434t
concrete production plant and capacities, 433t
crushing plant of aggregates, 433f
granulometric curves, 434f
main concrete elements, layout, 432f
materials used, in construction, 431t
new locks, working sites, 435f
Pacific concrete plant, 433f
steel gates, lock chambers, 432f
New Sprogø, 293
Ngqura Harbour, Eastern Cape
breakwaters
caissons, 260–263
rubble mound breakwaters, 258–260, 259f–260f
layout, 257, 258f
quay walls
completion, 268f
cross-section, 267f
end of construction, 267f
typical plan view, 268f
sand bypass jetty
completed jetty, underside, 271f
location, 269f
plan and elevation, 270f
typical jetty cross-section, 270f
Nonferrous reinforcement, 163
Non-steady-state diffusion (NSSD), 350–352
Non-steady-state migration (NSSM), 350–352
North Wharf, 250, 250f–251f

**O**

Oil production platforms, 57
Ordinary Portland cement (OPC), 398
Øresund Link
description, 302–303
design, 303–305
execution, 305–309
inspection and maintenance, 309–310
materials, 305

**P**

Panama Canal. *See* New Panama Canal
Panamax, 429–430
Petrographic tests, 234
Plasticizers/superplasticizers, 75
Pore filling admixtures, 75
Portland cement (PC), 3
Port Nolloth jetty, West Coast of South Africa, 406f

Port Nolloth jetty, West Coast of South Africa (*Continued*)
landward apron, 407f
typical beam end, 408f
typical soffit and beam, 407f
upper surface of deck and upstand beam, 408f
Port structures
boat ramps/slipways, 42–46
dry docks/ship lifts, 42, 43f
jetties/wharves
deck on piles, 33–37
skeletal jetties, 37–42
V&A Waterfront, 33, 33f
quay walls, 17–18
blockwork walls, 18–20
caisson walls, 20–22
cantilever walls, 25–27, 28f
counterfort walls, 22–25
sheet pile walls, 27–33
Precast sheet piles, 27–30, 28f–30f
Prefabrication, Confederation Bridge, 206f
footing components, 203, 204f
general view, precasting site, 203, 204f
precast elements, 203, 205f
*Svanen* lifting, 203, 205f

**Q**

Quay walls, 17–18
blockwork walls, 18–20
caisson walls, 20–22
cantilever walls, 25–27, 28f
counterfort walls, 22–25
marine construction methodologies
block wall, 120
caisson wall, 120–121
cantilever walls, 122
counterfort cantilever precast unit, transit, 121, 122f
counterfort walls, 121
gantry, precast element placement, 121, 122f
specialised barge-mounted piling rig, 122, 123f
typical stone spreader arrangement, 120, 121f
Ngqura Harbour, Eastern Cape
completion, 268f
cross-section, 267f
end of construction, 267f
typical plan view, 268f
sheet pile walls, 27–33

**R**

Rapid chloride migration (RCM) method, 350–352, 463
Rapid chloride permeability test (RCPT), 166
Rapid index tests, 166–167, 166f
Reducing environmental footprint, 168
Reinforced concrete marine structures
codes of practice
Australian durability design requirements, 89, 89t–91t
South African durability design requirements, 94–95, 95t–97t
USA durability design requirements, 87–88, 87t–88t
durability design
concrete mix and cover, 81–83, 82t
crack control, 83–87
strength design (ULS), 87
Rupert's Bay Wharf, St Helena Island
breakwater, 281–283
development, 278
quay wall, 278–281

**S**

Sand bypass jetty, Ngqura Harbour
completed jetty, underside, 271f
location, 269f
plan and elevation, 270f
typical jetty cross-section, 270f
SANRAL. *See* South African National Roads Agency Limited (SANRAL)
Sea Point Seawall, Cape Town
balustrades, 390–391
history, 389–390
original wall structure
back of leaky wall, 393f
buttresses and shutter board marks, 392f
exposed existing wall, 392f
Seashore, Southern Africa
sea level, 380–381
shoreline stability
groin showing accretion and erosion, 382, 382f

summer beach, 381, 381f
winter beach, 381, 382f
tides
genesis, 373, 373f
Southern African coastline, 371f, 373
structural element, percentage of time, 374, 375f
tidal parameters, in standard, 374, 376f
waves
effect of water depth, 375, 377f
generic wave form, 375, 376f
wave shoaling
Bagnold explosion, 379, 379f
clapotis reflection, 378, 379f
plunging breaker and surf, 378, 378f
spilling breakers, 377, 378f
transitions, 377
wind-whipped spray, 379–380, 380f
zonation
accelerated low water corrosion (ALWC), 384
biological tide level zones, 383, 384f
jetty cope wall and pile cap ends, 386f
marine growth, concrete pile, 385f
steel exhibiting, ALWC, 385f
Sea water-retaining structures
aquarium tanks, 61, 62f
sand bypass hoppers, 62–63
tidal pools, 63
Serviceability limit state (SLS), 71
Shark Rock Pier, 285
Sheet pile walls, 27
anchor walls, 32–33, 32f
concrete components, 31, 32f
diaphragm walls, 30–31, 31f
precast sheet piles, 27–30, 28f–30f
Shoreline stability
groin showing accretion and erosion, 382, 382f
summer beach, 381, 381f
winter beach, 381, 382f
Silane impregnation, 359
Simonstown Municipal jetty, Cape Peninsula
general arrangement, 402, 403f
landward end, 405–406, 405f
seaward end, 405–406, 405f
Singapore City, 460f
durability design
durability analysis, 462–464
general, 461–462, 462f
experimental work
concrete mixtures, 464–465, 464t
concrete properties, 465–467, 466t
probability of corrosion
effect of concrete cover, 469
effect of concrete quality, 467–468, 467t, 468f
general, 466t, 467
Skeletal jetties
computer-generated model, 37–40, 40f
liquid bulk jetty, 40, 41f
LNG jetty at Quintero, Chile, 40, 41f
Small dry docking facilities
boat ramps, 412–413
slipways and shiplifts, 414–417
Small harbours, South African coast
ancillary durability issues
hydraulic erosion of concrete surfaces, 421–422
marine structures subject to wave action, 423–425
Walvis Bay shiplift jetties, 418–419
wind-induced surface ablation, 419–420
coastal buildings and small structures, 393–396
Durban Point Yacht Club (DPYC), 387–389
Guano Island landing stage, 396–397
Lamberts Bay diamond quay, West Coast of South Africa
casting of deck, in situ, 411f
completed jetty, 409f
precast columns in place, 410f
precast cope soffits, 410f
underside of quay, 411f
Port Nolloth jetty, West Coast of South Africa, 406f
landward apron, 407f
typical beam end, 408f
typical soffit and beam, 407f
upper surface of deck and upstand beam, 408f

Small harbours, South African coast (*Continued*)
quays and jetties
deck and cope, 400
enclosed deck soffits, 400–402
ordinary Portland cement (OPC), 398
sheet pile bulkheads, 402
typical fishing industry berthing structures, 399–400
Sea Point Seawall, Cape Town
balustrades, 390–391
history, 389–390
original wall structure, 392–393
seashore
sea level, 380–381
shoreline stability, 381–383
tides, 373–374
waves, 374–375
wave shoaling, 377–380
zonation, 383–387
Simonstown Municipal jetty, Cape Peninsula
general arrangement, 402, 403f
landward end, 405–406, 405f
seaward end, 405–406, 405f
small dry docking facilities
boat ramps, 412–413
slipways and shiplifts, 414–417
South African National Roads Agency Limited (SANRAL), 69, 95
South African standards, 72–73
Southern African marine structures
commercial ports, 284–285
Durban Harbour entrance
layout, 272f
north groyne, 273
sand bypass hopper, 273–275
south breakwater, 271–272
Durban Maydon Wharf 12, 276f
concrete components, 276–278
plan view, 276f
Durban seafront groynes, 286
Ngqura Harbour, Eastern Cape
breakwaters, 258–263
layout, 257, 258f
quay walls, 264–269
sand bypass jetty, 269
Rupert's Bay Wharf, St Helena Island
breakwater, 281–283
development, 278
quay wall, 278–281
Shark Rock Pier, 285
Victoria and Alfred Waterfront (V&AW) development
aerial photograph, 241, 242f
canal, 252–257
Granger Bay shoreline protection, 242–244
new Marina Basin, 244–252
SRC. *See* Sulphate-resisting cements (SRC)
Stainless steel, 77–79, 78t–79t
Stainless steel reinforcement (SSR), 162–163
Steel corrosion, 65, 144–145
Storebælt Link
description, 293–294
design, 294–296
execution, 297–300
inspection and maintenance, 300–301
materials, 296–297
Strait Crossing Development Inc. (SCDI), 202
Submarine pipelines, 53–54, 54f–55f
Sulphate-resisting cements (SRC), 74
Superstructure units
beams, 103–104, 105f–106f
fender cope units, 106, 107f
pile caps and headstocks, 100–102, 102f–103f
slabs, 104–106, 106f
Supplementary cementing materials (SCM), 3, 154, 157–160

**T**

Temperate marine environments, 178
Tjuvholmen project, 470, 471f
30-ton dolos, 50, 50f
Torrent Permeability Tester (TPT), 355
Traditional durability tests, 165

**U**

Ultimate limit state (ULS), 71
Un-densified silica fume (USF), 465
Unreinforced precast concrete, 218, 219f
USA standards, 72

**V**

Victoria and Alfred Waterfront (V&AW) development
aerial photograph, 241, 242f

canal, 252−257
Granger Bay shoreline protection, 242−244
new Marina Basin, 244−252

**W**
Wave shoaling
Bagnold explosion, 379, 379f
clapotis reflection, 378, 379f
plunging breaker and surf, 378, 378f
spilling breakers, 377, 378f
transitions, 377
wind-whipped spray, 379−380, 380f
West Bridge, 293−294